15.6 DECREASE IN REACTOR COOLANT INVENTORY

Events that result in a decrease in reactor coolant inventory, as discussed in this section, are as follows:

a. Inadvertent opening of a pressurizer safety or relief valve (Section 15.6.1)

b. Break in instrument line or other lines from the reactor coolant pressure boundary that penetrate the containment (Section 15.6.2)

c. Steam generator tube rupture (SGTR) (Section 15.6.3)

d. Spectrum of boiling water reactor (BWR) steam system piping failures outside of the containment (Section 15.6.4 - Not applicable to St. Lucie Unit 2)

e. Loss-of-coolant accident (LOCA) resulting from a spectrum of postulated piping breaks within the reactor coolant pressure boundary (Section 15.6.5)

15.6.1 INADVERTENT OPENING OF A PRESSURIZER SAFETY OR RELIEF VALVE

15.6.1.1 Accident Description

An accidental depressurization of the reactor coolant system could occur as a result of one of the following: an inadvertent opening of both of the pressurizer Power Operated Relief Valves (PORVs), an inadvertent opening of a single Pressurizer Safety Valve (PSV), or a malfunction of the pressurizer spray system. Since a PSV is sized to relieve approximately half the steam flow rate of a PORV, and the pressurizer spray system, even if fully open, cannot depressurize the RCS at the rate of two open PORVs, the most severe core conditions are associated with an inadvertent opening of both of the PORVs. It is assumed that a mechanical failure, spurious actuation signal, or unanticipated operator action will cause the opening of both PORVs. Initially the event results in a rapidly decreasing RCS pressure which could reach the hot leg saturation pressure if a reactor trip did not occur. The pressure continues to decrease throughout the transient. The effect of the pressure decrease is to decrease power via the moderator density feedback. Pressurizer level increases initially due to expansion caused by depressurization and then decreases following reactor trip. In the event analyzed for pressurizer overfill, the pressurizer level decreases initially post-trip. However, since the transient time is extended, safety injection is actuated and the pressurizer level begins to increase. This has the potential to result in overfill and liquid discharge through the stuck open valves.

The reactor core is protected against fuel damage by the Thermal Margin/Low Pressure (TM/LP) Trip function.

An inadvertent opening of both of the pressurizer relief valves is classified as an ANS Condition II event, a fault of moderate frequency. It should be noted that a stuck open PSV is considered a more serious Condition III event. However, in the case of St. Lucie Unit 2, the relief capacity of a PORV far exceeds that of a PSV. Thus, the assumption of the opening of both PORVs, and demonstration that the more restrictive Condition II acceptance criteria are met removes the PSV scenario from concern.

15.6.1.2 Method of Analysis

The accidental depressurization transient is analyzed by employing the detailed digital computer code RETRAN (References 15.6.1-1 and 15.6.1-3). The code simulates the neutron kinetics, RCS, pressurizer, pressurizer relief and safety valves, pressurizer spray, steam generator, and steam generator safety valves. The code computes pertinent plant variables including temperatures, pressures, and power level.

This accident is analyzed with the revised thermal design procedure described in Reference 15.6.1-2.

Two cases are analyzed. One for thermal margin and Departure from Nuclear Boiling (DNB) concerns and one for time to pressurizer overfill.

Plant characteristics and initial conditions are discussed in Table 15.0-27. In order to give conservative results in calculating the Departure from Nucleate Boiling Ratio (DNBR) during the transient, the following assumptions for the DNB case are made:

1. The initial reactor power and RCS temperature are assumed to be at their nominal values, the initial RCS flow rate is assumed at a value consistent with the minimum measured flow rate and the initial RCS pressure is assumed at a value consistent with minimum value allowed by the plant technical specifications. Uncertainties in initial conditions are statistically included in the calculation of the DNBR limit as described in Reference 15.6.1-2.

2. A least negative moderator temperature coefficient of reactivity is assumed. The spatial effect of void due to local or subcooled boiling is not considered in the analysis with respect to reactivity feedback or core power shape.

3. A least negative Doppler power coefficient is assumed such that the resultant amount of negative feedback is conservatively low in order to maximize any power increase due to moderator reactivity feedback.

The pressurizer overfill case is analyzed to determine the minimum time to fill the pressurizer after an inadvertent PORV opening. To produce conservative results for the overfill analysis, the DNB case input parameters were modified to bias the transient for overfill via sensitivity studies. These input changes include:

- Actuation of two charging pumps at the time of SIAS

- One open PORV is used to depressurize the system

- Sensitivity cases showed a low Tavg, maximum reactivity feedback, maximum UA, and maximum SGTP produce the most limiting results

Plant systems and equipment which are necessary to mitigate the effects of the accident are discussed in Section 15.0.11.

The automatic rod control system is not modeled as it is disabled at the plant. The reactor protection system functions to trip the reactor on the appropriate signal. No single active failure will prevent the reactor protection system from functioning properly.

AREVA DNB Analysis

The analysis was performed with the approved non-LOCA methodology given in Reference 15.6.1-4, as supplemented in Section 2.7 of Reference 15.6.1-5. For this event, the S-RELAP5 code was used to model the key system components and calculate the neutron power, fuel thermal response, surface heat transport, fluid conditions (such as coolant flow rates, temperatures, and pressures), and an estimated time of MDNBR. The core fluid boundary conditions and average rod surface heat flux were then input to the XCOBRA-IIIC code (Reference 15.6.1-6), which was used to calculate the MDNBR using the HTP CHF correlation (Reference 15.6.1-7).

A single calculation was performed at BOC full-power conditions, TS maximum core inlet temperature, and TS minimum RCS flow rate. This produced the minimum margin to the DNB limit. A conservative moderator density reactivity feedback was used, based on the TS HZP most-positive MTC.

The key input parameters and their values used in the analysis of this event were consistent with, or conservative relative to, the approved Reference 15.6.1-4 methodology, as supplemented in Section 2.7 of Reference 15.6.1-5. See Table 15.0-27 for key input parameter values.

- Reactor Protection System Trips and Delays – The RPS trip setpoints and response times were conservatively biased to delay actuation of the trip function. In addition, rod insertion was delayed to account for CEA holding coil release delay time. The analysis did not credit the variable portion of the TM/LP function; it conservatively credited only the Low Pressurizer Pressure floor setpoint.

- Pressurizer PORVs Flow Rate – A conservative pressurizer PORVs flow rate was assumed for this analysis. The value was based on two valves opening, and the flow rate was biased 1% higher than the maximum flow rates, to maximize the depressurization of the RCS and the potential pressure undershoot of the RPS trip setpoint.

- Gap Conductance – The fuel-to-cladding gap conductance was set to a conservative BOC value, to be consistent with the time-in-cycle for the reactivity coefficients. The value accounts for the effects of fuel TCD.

15.6.1.3 Results

DNB Case:

The system response to an inadvertent opening of both PORVs is shown in Figures 15.6.1-1 through 15.6.1-4. Figure 15.6.1-1 illustrates the nuclear power transient following the depressurization. Nuclear power remains relatively constant while pressurizer pressure decreases from the initial value until reactor trip occurs on the floor of the TM/LP Trip. The pressure transient and average coolant temperature transient following the accident are given in Figures 15.6.1-2 and 15.6.1-3, respectively. The DNBR decreases initially, but increases rapidly following the trip, as shown in Figure 15.6.1-4. The DNBR remains above the limit value throughout the transient.

The calculated sequence of events for the inadvertent opening of both PORVs is shown in Table 15.6.1-1.

Pressurizer Overfill Case:

The system response to an inadvertent opening of a single PORV is shown in Figures 15.6.1-5 through 15.6.1-8. Figure 15.6.1-5 illustrates that core power decreases slightly initially until the TM/LP reactor trip. Figure 15.6.1-6 presents the pressurizer pressure for the pressurizer overfill case. Figure 15.6.1-7 and 15.6.1-8 present pressurizer mixture volume and liquid level.

The calculated sequence of events for the pressurizer overfill case is shown in Table 15.6.1-2.

AREVA DNB Analysis

The sequence of events is shown in Table 15.6.1-3. The result is given in Table 15.6.1-4. The MDNBR was calculated to be above the 95/95 limit for the HTP CHF correlation.

The system responses are shown in Figure 15.6.1-9 through Figure 15.6.1-15. Figure 15.6.1-9 shows the PORVs flow rate as a function of time. Figure 15.6.1-10 shows the pressurizer pressure. Figure 15.6.1-11 through Figure 15.6.1-15 show the pressurizer liquid level, reactivity feedback, reactor power, core power based on rod surface heat flux, and RCS loop temperatures, respectively.

15.6.1.4 Conclusions

The results of the DNB analysis show that the TM/LP reactor protection system signal provides adequate protection against the accidental depressurization of the RCS. No fuel or clad damage is predicted for this accident. All acceptance criteria are satisfied.

The pressurizer overfill case shows that the minimum time to pressurizer overfill and for operators to respond prior to the pressurizer filing is 174 seconds.

15.6.1.5 References

15.6.1-1 WCAP-14882-P-A, Rev. 0, “RETRAN-02 Modeling and Qualification for Westinghouse Pressurized Water Reactor Non-LOCA Safety Analyses,” April 1999.

15.6.1-2 WCAP-11397-P-A, "Revised Thermal Design Procedure," April 1989.

15.6.1-3 EPRI NP-1850-CCM, Rev. 6, “RETRAN-02 – A Program for Transient Thermal Hydraulic Analysis of Complex Fluid Flow Systems,” December 1995.

15.6.1-4 EMF-2310(P)(A) Revision 1, SRP Chapter 15 Non-LOCA Methodology for Pressurized Water Reactors, Framatome ANP, Inc., May 2004.

15.6.1-5 ANP-3347P, St. Lucie Unit 2 Fuel Transition Chapter 15 Non LOCA Summary Report, AREVA Inc., November 2014.

15.6.1-6 XN-NF-82-21(P)(A) Revision 1, Application of Exxon Nuclear Company PWR Thermal Margin Methodology to Mixed Core Configurations, Exxon Nuclear Company, August 1983.

15.6.1-7 EMF-92-153(P)(A) Revision 1, HTP: Departure From Nucleate Boiling Correlation for High Thermal Performance Fuel, Siemens Power Corporation, January 2005.

15.6.2 BREAK IN INSTRUMENT LINE OR OTHER LINES FROM THE REACTOR COOLANT PRESSURE BOUNDARY THAT PENETRATE THE CONTAINMENT

15.6.2.1 Accident Description

A Small Primary Line Break Outside Containment Event may result from a break in a letdown line, instrument line, or sample line. The double-ended break of the letdown line outside containment upstream of the outside containment isolation valve was selected for this analysis since it is the largest line and results in the largest release of reactor coolant to the environment.

The Small Primary Line Break Outside Containment Event was analyzed to ensure that the resulting site boundary doses are within the guidelines established for design basis accidents.

15.6.2.2 Acceptance Criteria

The primary line break event does not directly challenge peak linear heat rate, peak RCS pressure, or peak secondary pressure criteria; and is bounded by the inadvertent opening of a pressurizer relief valve event with respect to RCS depressurization rate and approach to the DNB criteria. This event is analyzed to calculate the maximum mass release due to a break in either a small primary instrument or letdown line to be used as input to a dose analysis.

15.6.2.3 Method of Analysis

The Small Primary Line Break Outside Containment Event was initiated from the conditions presented in Table 15.6.2-1. The conditions and assumptions were selected to maximize the radiological release. The assumptions used in the dose consequence analysis are presented in Table 15.6.2-4. Initial primary coolant activity was assumed to be at the Technical Specification maximum of 1.0 μCi/gm. An iodine activity spike coincident with rapid reactor coolant system depressurization was assumed to occur upon reactor trip or pressurizer emptying, whichever occurred sooner. An iodine activity spiking factor of 500 was used. To maximize the leak rate from the letdown line, critical flow from the break was assumed.

To further ensure conservative results, a ten minute delay in the automatic closing of the letdown isolation valve upon Safety Injection Actuation Signal (SIAS) was assumed in the dose calculations. This assumption, in conjunction with using the largest break size, results in more adverse doses than those obtained using smaller break sizes.

The single active failure of an isolation valve was considered in the analysis. The letdown line includes two isolation valves in series situated outside containment. Hence, failure of one isolation valve does not make the consequences of the event more adverse.

15.6.2.4 Radiological Analysis

15.6.2.4.1 Background

This event is a rupture of a primary coolant letdown line outside of containment. The dose assessment for this event is comprised of two separate release paths. The first path represents the leakage from the double ended rupture of the letdown line in the auxiliary building outside of containment with a direct release to the environment via the plant stack. The second path represents the release through the secondary side steam relief following the turbine trip and

subsequent plant cooldown. The St. Lucie Unit 2 AST dose analysis methodology is presented in NAI-1101-044, “AST Licensing Technical Report for St. Lucie Unit 2”.

15.6.2.4.2 Compliance with RG 1.183 Regulatory Positions

Since Regulatory Guide 1.183 does not provide any direct guidance regarding analysis of a Letdown Line Rupture, Standard Review Plan (SRP) Section 15.6.2 is used as the primary source of guidance for this analysis. In accordance with SRP 15.6.2, this analysis assumes an accident- generated or concurrent iodine spike in combination with the maximum leakage of primary fluid through the SG tubes into the secondary side. The RG 1.183 guidance provided for other events is applied to this event as applicable and appropriate.

The Letdown Line Rupture event dose consequence analysis is performed consistent with the guidance provided in RG 1.183, as discussed below:

1. Regulatory Position 5.6 of Appendix A - For ECCS leakage into the Reactor Auxiliary Building, the form of the released iodine is 97% elemental and 3% organic.

2. Regulatory Position 2.2 of Appendix E - This guidance is used to define the concurrent iodine spike of 500 times the release rate corresponding to the iodine concentration at the equilibrium value (1.0 µCi/gm DE I-131).

3. Regulatory Position 3 of Appendix E - The activity released from the fuel is assumed to be released instantaneously and homogeneously through the primary coolant.

4. Regulatory Position 5.1 of Appendix E - The primary-to-secondary leak rate is apportioned between the SGs as specified by TS 6.8.4.l (0.5 gpm total, 0.25 gpm to any one SG). Thus, the tube leakage is apportioned equally between the two SGs.

5. Regulatory Position 5.2 of Appendix E - The density used in converting volumetric leak rates to mass leak rates is based upon RCS conditions, consistent with the plant design basis.

6. Regulatory Position 5.3 of Appendix E - The primary-to-secondary leakage is assumed to continue until after shutdown cooling has been placed in service and the temperature of the RCS is less than 212°F.

7. Regulatory Position 5.4 of Appendix E - All noble gas radionuclides released from the primary system are assumed to be released to the environment without reduction or mitigation.

8. Regulatory Position 5.5.1 of Appendix E - Both steam generators are used for plant cooldown. A portion of the primary-to-secondary leakage is assumed to flash to vapor based on the thermodynamic conditions in the reactor and secondary immediately following plant trip when tube uncovery is postulated. The primary-to-secondary leakage is assumed to mix with the secondary water without flashing during periods of total tube submergence.

9. Appendix E, Regulatory Position 5.5.2 - The portion of leakage that immediately flashes to vapor is assumed to rise through the bulk water of the SG, enter the steam

space, and be immediately released to the environment with no mitigation; i.e., no reduction for scrubbing within the SG bulk water is credited.

10. Appendix E, Regulatory Position 5.5.3 - All of the SG tube leakage flow that does not flash is assumed to mix with the bulk water.

11. Regulatory Position 5.5.4 of Appendix E - The radioactivity within the bulk water is assumed to become vapor at a rate that is a function of the steaming rate and the partition coefficient. A partition coefficient of 100 is assumed for the iodine. The retention of particulate radionuclides in the SGs is limited by the moisture carryover from the SG. The same partition coefficient of 100, as used for iodine, is assumed for other particulate radionuclides. This assumption is consistent with the SG carryover rate of less than 1%.

12. Regulatory Position 5.6 of Appendix E - Steam generator tube bundle uncovery in the SGs is postulated for up to 45 minutes following a reactor trip for St. Lucie Unit 2. During this period, the fraction of primary-to-secondary leakage which flashes to vapor is assumed to rise through the bulk water of the SG into the steam space and is assumed to be immediately released to the environment with no mitigation. The flashing fraction is based on the thermodynamic conditions in the reactor and secondary coolant. The leakage which does not flash is assumed to mix with the bulk water in the steam generator. A conservative uncovery time of 60 seconds was assumed in the analysis.

15.6.2.4.3 Other Assumptions

1. The initial RCS activity is assumed to be at the TS 3.4.8 limit of 1.0 μCi/gm Dose Equivalent I-131 and 518.9 μCi/gm DE Xe-133 gross activity. The initial SG activity is assumed to be at the TS 3.7.1.4 limit of 0.1 μCi/gm Dose Equivalent I-131.

2. The steam mass release values for the intact SG are provided in Table 15.6.2-5.

3. The RCS fluid density used to convert the primary-to-secondary leakage from a volumetric flowrate to a mass flow rate is consistent with the RCS cooldown rate applied in the generation of the secondary steam releases. The high initial cooldown rate conservatively maximizes the fluid density. The SG tube leakage mass flow rate is provided in Table 15.6.2-6.

4. For the purposes of determining the iodine concentrations, the SG mass is assumed to remain constant throughout the event. However, it is also assumed that operator action is taken to restore secondary water level above the top of the tubes within a conservative time of one hour following a reactor trip.

15.6.2.4.4 Methodology

This event is a rupture of a primary coolant letdown line outside of containment. The leakage from the double ended rupture of the letdown line in the Reactor Auxiliary Building is released directly to the environment via the plant stack. Additional release also occurs as a result of secondary side steam relief following the turbine trip and subsequent plant cooldown. Input assumptions used in the dose consequence analysis of the letdown line break are provided in Table 15.6.2-4. Since RG 1.183 does not provide any direct guidance regarding analysis of a

Letdown Line Rupture, Standard Review Plan (SRP) Section 15.6.2 is used as the primary source of guidance for this analysis.

In accordance with SRP 15.6.2, this analysis assumes an accident-generated or concurrent iodine spike. The RCS activity is initially assumed to be 1.0 μCi/gm DE I-131 as allowed by TS 3.4.8. Iodine is released from the fuel into the RCS at a rate of 500 times the iodine equilibrium release rate for a period of 8 hours. Parameters used in the determination of the iodine equilibrium release rate are provided in Table 15.6.2-7. The iodine activities and the appearance rates are shown in Table 15.6.2-8.

The Letdown Line Rupture flow rate is modeled as 94,300 lbm over 1800 seconds with a flashing fraction of 6% as computed using the RG 1.183 guidance from position 5.4 of Appendix A for ECCS leakage. All of the activity in the flashed fluid is assumed to be released directly to the environment. Additional activity, based on the proposed primary-to-secondary leakage limits, is released via steaming from the ADVs until the RCS is cooled to 212°F.

For this event, the Control Room ventilation system cycles through three modes of operation:

- Initially the ventilation system is assumed to be operating in normal mode. The air flow distribution during this mode is 1000 cfm of unfiltered fresh air and an assumed value of 395 cfm of unfiltered inleakage.

- After the start of the event, the Control Room is isolated due to a high radiation reading in the Control Room ventilation system. A 30-second delay is applied to account for diesel generator start time, damper actuation time, instrument delay, and detector response time. After isolation, the air flow distribution consists of 0 cfm of makeup flow from the outside, 395 cfm of unfiltered inleakage, and 1760 cfm of filtered recirculation flow.

- At 1.5 hours into the event, the operators are assumed to initiate makeup flow from the outside to the Control Room. During this operational mode, the air flow distribution consists of up to 504 cfm of filtered makeup flow, 395 cfm of unfiltered inleakage, and 1256 cfm of filtered recirculation flow.

The Control Room ventilation filter efficiencies that are applied to the filtered makeup and recirculation flows are 99% for particulate, and 95% for elemental iodine, and organic iodine.

15.6.2.4.5 Radiological Consequences

The Control Room atmospheric dispersion factors (χ/Qs) used for this event are based on the postulated release locations and the operational mode of the control room ventilation system. The release-receptor point locations are chosen to minimize the distance from the release point to the Control Room air intake.

When the Control Room Ventilation System is in normal mode, the most limiting χ/Q corresponds to the worst air intake to the control room. When the ventilation system is isolated at 30 seconds, the limiting χ/Q corresponds to the midpoint between the two air intakes. The operators are assumed to reopen the most favorable air intake at 1.5 hours. Development of control room atmospheric dispersion factors is discussed in Appendix 2.5D. The χ/Q values for the various combinations of release points and receptor locations applicable to this event are presented in Table 15.6.2-9.

For the EAB dose analysis, the χ/Q factor for the zero to two-hour time interval is assumed for all time periods. Using the zero to two-hour χ/Q factor provides a more conservative determination of the EAB dose, because the χ/Q factor for this time period is higher than for any other time period. The LPZ dose is determined using the χ/Q factors for the appropriate time intervals. These χ/Q factors are provided in Appendix 2.5C.

RG 1.183 does not provide any direct guidance for the acceptance criteria for this event. However, the SRP states that the acceptance criteria is “a small fraction” of the 10 CFR 100 values which is further described as 10% of the limit. In applying the AST methodology to the letdown line break that same 10% interpretation is applied to the 10 CFR Part 50.67 limits for the LPZ and EAB dose. The acceptable dose limit for the Control Room (CR) is that specified in 10 CFR 50.67. For a Letdown Line Rupture, these limits are interpreted as:

Area	**Dose Criteria**
EAB	2.5 rem TEDE (for the worst two hour period)
LPZ	2.5 rem TEDE (for 30 days)
Control Room	5 rem TEDE (for 30 days)

The radiological consequences of the Letdown Line Rupture event are analyzed using the RADTRAD-NAI code and the inputs and assumptions previously discussed. As shown in Table 15.6.2-3, the radiological consequences of the Letdown Line Rupture event are all within the appropriate acceptance criteria.

15.6.2.5 Conclusions

The results of a Small Primary Line Break Outside Containment Event show that the radiological consequences are a fraction of the guidelines established for design basis accidents. Letdown flow is released to the auxiliary building, resulting in a slow decrease in RCS pressure and pressurizer level. Activity escaping to the auxiliary building is vented to the atmosphere. A reactor trip occurs on low pressurizer pressure SIAS and letdown line isolation occur post reactor trip, prior to operator action. At 1800 seconds, the operator is assumed to initiate plant cooldown, resulting in further release of activity. The sequence of events is provided in Table 16.6.2-2.

The primary pressure in the Low Tavg case remains higher throughout the transient resulting in more break flow out of the primary system. This causes the Low Tavg case to be slightly more limiting than the High Tavg case. Figures 15.6.2-1 through 15.6.2-5 show the NSSS response for power, letdown line break flow, integrated letdown line break flow, RCS temperatures and RCS pressures for the limiting case. This event is bounded by UFSAR event 15.6.1 (Inadvertent Opening of a Pressurizer Safety or Relief Valve) relative to the DNBR SAFDL and is analyzed mainly for RCS mass release input to the dose analysis, which is not affected by the fuel transition.

15.6.2.6 References

15.6.2-1 B.T. Moroney to J. A. Stall, “St. Lucie Plant, Unit No.2 – Issuance of Amendment Regarding Change in Reload Methodology and Increase in Steam Generator Tube Plugging Limit (TAC NO. MC1566),” dated January 31, 2005.

15.6.3 STEAM GENERATOR TUBE RUPTURE (SGTR)

15.6.3.1 Introduction

The Steam Generator Tube Rupture (SGTR) with a Concurrent Loss of Offsite Power event was evaluated to account for the plant conditions consistent with Extended Power Uprate (EPU).

15.6.3.2 Input Assumptions

Two cases were analyzed for the SGTR event. One case was analyzed for steam releases while the other was analyzed for steam generator margin to overfill (MTO). The SGTR event analyzed for steam releases assumes the initial conditions in Table 15.6.3-1. In addition, the following assumptions were made:

1. While the reactor is operating at full power prior to trip, the steam mixture containing reactor coolant fission products passes through the turbine and the condenser.

2. Following the reactor and turbine trip, all fission product activity that is released is via the MSSVs until operator action at 2700 seconds.

Within forty-five minutes (2700 seconds) after the tube rupture occurs, the operator identifies the problem and isolates the affected steam generator. At this time, plant cooldown is initiated using the unaffected steam generator atmospheric dump valves (ADVs).

This analysis assumes that following the SGTR, the RCS pressure drops until reaching the TM/LP low pressurizer pressure trip setpoint, thus preventing violation of the DNBR specified acceptable fuel design limit (SAFDL). Crediting the earliest trip maximizes the offsite doses. Offsite power is assumed to be lost at time of trip. The RCS continues to depressurize and the pressurizer empties.

Subsequent to reactor trip, stored and fission product decay heat is dissipated by the reactor coolant and main steam systems. In the absence of forced reactor coolant flow (due to a loss of offsite power), convective heat transfer is supported by natural circulation. The increasing steam generator pressure results in steam release to atmosphere via the MSSVs. At 2700 seconds, the operators are assumed to isolate the affected steam generator and initiate plant cooldown through the unaffected steam generator atmospheric dump valves. With the availability of stand-by power, auxiliary feedwater (AFW) is automatically initiated on a low steam generator water level signal. To maximize the offsite dose results this analysis conservatively assumes that the emergency feedwater will be unavailable until 2700 seconds and the normal feedwater flow ramps down immediately following loss of offsite power.

Table 15.6.3-1 documents the input parameters used in the SGTR with LOOP event analyzed for steam releases.

The SGTR case analyzed for SG MTO is based on the 2700 second steam release case with the initial conditions presented in Table 15.6.3-1 and the following additional assumptions:

1. Upon reaching the AFAS reset point, the TDAFW valve fails open, delivering maximum AFW flow to the affected SG for 15 minutes, maximizing liquid inventory.

2. No ADV operation.

15.6.3.3 Acceptance Criteria

The SGTR event was analyzed to assure that the following dose criteria are not exceeded:

- With an assumed pre-accident iodine spike in the reactor coolant and with the highest worth control rod assumed to stick in the fully withdrawn position on scram, the calculated doses do not exceed the values of Regulatory Guide 1.183, and

- With an equilibrium iodine concentration corresponding to full power operation and an assumed accident generated iodine spike, the calculated doses do not exceed 10% of Regulatory Guide 1.183 limits.

Steam generator or RCS pressure limits are not challenged by SGTR and the TM/LP trip assures the DNBR SAFDL is met for SGTR.

15.6.3.4 Description of Analysis/Evaluation And Results

This thermal-hydraulic response of the transient was simulated using the RETRAN computer code.

Table 15.6.3-4 provides the radiological exposure for the SGTR event.

Table 15.6.3-3 contains the sequence of events for the SGTR Event with a Loss of Offsite Power.

Figures 15.6.3-1 through 15.6.3-13 show the NSSS response for the system parameters important in dose calculation.

Table 15.6.3-2 provides the sequence of events for the SGTR MTO analysis. Figures 15.6.3-14 through 15.6.3-18 show the NSSS response for the SGTR MTO analysis.

15.6.3.5 SGTR Radiological Analysis

15.6.3.5.1 Background

This event is assumed to be caused by the instantaneous rupture of a Steam Generator tube that relieves to the lower pressure secondary system. No fuel melt or clad breach is postulated for the St. Lucie Unit No. 2 SGTR event. The St. Lucie 2 AST dose analysis methodology is presented in Section 15.0.15.

15.6.3.5.2 Compliance with RG 1.183 Regulatory Positions

The revised SGTR dose consequence analysis is consistent with the guidance provided in RG 1.183, Appendix F, "Assumptions for Evaluating the Radiological Consequences of a PWR Steam Generator Tube Rupture Accident," as discussed below:

1. Regulatory Position 1 - The total core inventory of the radionuclide groups utilized for determining the source term for this event is based on RG 1.1.83, Regulatory Position 3.1. No fuel damage is postulated to occur for the St. Lucie Unit No. 2 SGTR event.

2. Regulatory Position 2 - No fuel damage is postulated to occur for the St. Lucie Unit No. 2 SGTR event. Two cases of iodine spiking are assumed.

3. Regulatory Position 2.1 - One case assumes a reactor transient prior to the postulated SGTR that raises the primary coolant iodine concentration to the maximum allowed by TS 3.4.8, Fig. 3.4-1 value of 60.0 µCi/gm DE I-131. This is the pre-accident spike case.

4. Regulatory Position 2.2 - One case assumes the transient associated with the SGTR causes an iodine spike. The spiking model assumes the primary coolant activity is initially at the TS 3.4.8 value of 1.0 µCi/gm DE I-131. Iodine is assumed to be released from the fuel into the RCS at a rate of 335 times the iodine equilibrium release rate for a period of 8 hours. This is the accident-induced (concurrent) spike case.

5. Regulatory Position 3 - The activity released from the fuel is assumed to be released instantaneously and homogeneously through the primary coolant.

6. Regulatory Position 4 - Iodine releases from the steam generators to the environment are assumed to be 97% elemental and 3% organic.

7. Regulatory Position 5.1 - The primary-to-secondary leak rate is apportioned equally between the two SGs.

8. Regulatory Position 5.2 - The density used in converting volumetric leak rates to mass leak rates is based upon RCS conditions, consistent with the plant design basis.

9. Regulatory Position 5.3 - The primary-to-secondary leak rate is assumed to continue until after shutdown cooling has been placed in service and the temperature of the RCS is less than 212°F. An input assumption for the termination of the affected SG activity release states that the affected SG is isolated within 45 minutes by operator action. This isolation terminates releases from the affected SG, while primary-to-secondary leakage continues to provide activity for release from the unaffected SG. EC282511

10. Regulatory Position 5.4 - The release of fission products from the secondary system is evaluated with the assumption of a coincident loss of offsite power (LOOP).

11. Regulatory Position 5.5 - All noble gases released from the primary system are assumed to be released to the environment without reduction or mitigation.

12. Regulatory Position 5.6 - Regulatory Position 5.6 refers to Appendix E, Regulatory Positions 5.5 and 5.6. The iodine transport model for release from the steam generators is as follows:

    - Appendix E, Regulatory Position 5.5.1 - A portion of the primary-to-secondary ruptured tube flow through the SGTR is assumed to flash to vapor based on the thermodynamic conditions in the reactor and secondary. For the unaffected steam generator used for plant cooldown, flashing is considered immediately following plant trip when tube uncovery is postulated. The primary-to-secondary

leakage is assumed to mix with the secondary water without flashing during periods of total tube submergence.

- Appendix E, Regulatory Position 5.5.2 - The portion of leakage that immediately flashes to vapor is assumed to rise through the bulk water of the SG, enter the steam space, and be immediately released to the environment with no mitigation; i.e., no reduction for scrubbing within the SG bulk water is credited.

- Appendix E, Regulatory Position 5.5.3 - All of the SG tube leakage and ruptured tube flow that does not flash is assumed to mix with the bulk water.

- Appendix E, Regulatory Position 5.5.4 - The radioactivity within the bulk water is assumed to become vapor at a rate that is a function of the steaming rate and the partition coefficient. A partition coefficient of 100 is assumed for the iodine. The retention of particulate radionuclides in the SGs is limited by the moisture carryover from the SGs. The same partition coefficient of 100, as used for iodine, is assumed for other particulate radionuclides. This assumption is consistent with the SG carryover rate of less than 1%.

- Appendix E, Regulatory Position 5.6 - Steam generator tube bundle uncovery in the intact SG is postulated for up to 45 minutes following a reactor trip for St. Lucie Unit 2. During this period, the fraction of primary-to-secondary leakage which flashes to vapor is assumed to rise through the bulk water of the SG into the steam space and is assumed to be immediately released to the environment with no mitigation. The flashing fraction is based on the thermodynamic conditions in the reactor and secondary coolant. The leakage which does not flash is assumed to mix with the bulk water in the steam generator. A conservative uncovery time of 60 minutes was assumed in the analysis.

15.6.3.5.3 Other Assumptions

1. This evaluation assumes that the RCS mass remains constant throughout the event.

2. For the purposes of determining the iodine concentrations, the SG mass is assumed to remain constant throughout the event. However, it is also assumed that operator action is taken to restore water level above the top of the tubes in the unaffected steam generator within a conservative time of one hour following a reactor trip.

3. Data used to calculate the iodine equilibrium appearance rates are provided in Table 15.6.3-8, “Iodine Equilibrium Appearance Assumptions.” The iodine spike activity appearance rates are provided in Table 15.3.6-9.

15.6.3.5.4 Methodology

Input assumptions used in the dose consequence analysis of the SGTR event are provided in Table 15.6.3-5. This event is assumed to be caused by the instantaneous rupture of a steam generator tube releasing primary coolant to the lower pressure secondary system. In the unlikely event of a concurrent loss of power, the loss of circulating water through the condenser would result in the loss of condenser vacuum thereby causing steam relief directly to the atmosphere from the ADVs or MSSVs. This direct steam relief continues until the faulted steam generator is isolated. The isolation is assumed to require 45 minutes. EC282511

A thermal-hydraulic analysis is performed to determine a conservative maximum break flow, break flashing flow, and steam release inventory through the faulted SG relief valves. Additional activity, based on the primary-to-secondary leakage limits, is released via the unaffected SG ADVs until the RCS is cooled to 212°F.

As stated in Section 15.6.3.5.1, no fuel melt or clad breach is postulated for the SGTR event.

Consistent with RG 1.183 Appendix F, Regulatory Position 2, if no, or minimal, fuel damage is postulated for the limiting event, the activity release is assumed for two cases of iodine spiking: (1) maximum pre-accident iodine spike, and (2) maximum accident-induced, or concurrent, iodine spike.

For the case of a pre-accident iodine spike, a reactor transient is assumed to have occurred prior to the postulated SGTR event. The primary coolant iodine concentration is increased to the maximum value of 60 μCi/gm DE I-131 permitted by TS 3.4.8 (see Table 15.6.3-7). Primary coolant is released into the ruptured SG by the tube rupture and by a fraction of the total primary-to-secondary leakage. Activity is released to the environment from the ruptured SG via direct flashing of a fraction of the released primary coolant from the tube rupture and also via steaming from the ruptured SG ADVs until the ruptured steam generator is isolated at 45 minutes. The unaffected SG is used to cool down the plant during the SGTR event. Primary-to-secondary tube leakage is also postulated into the intact SG. Activity is released via steaming from the unaffected SG ADVs until the RCS is cooled below 212°F. These release assumptions are consistent with the requirements of RG 1.183. EC282511

For the case of the accident-induced spike, the postulated SGTR event induces an iodine spike. The RCS activity is initially assumed to be 1.0 μCi/gm DE I-131 as allowed by TS 3.4.8. Iodine is released from the fuel into the RCS at a rate of 335 times the iodine equilibrium release rate for a period of 8 hours. Parameters used in the determination of the iodine equilibrium releak rate are provided in Table 15.6.3-8. The iodine activities and appearance rates for the accident induced (concurrent) iodine spike case are presented in Table 15.6.3-9. All other release assumptions for this case are identical to those for the pre-accident spike case.

For this event, the Control Room ventilation system cycles through three modes of operation:

- Initially the ventilation system is assumed to be operating in normal mode. The air flow distribution during this mode is 1000 cfm of unfiltered fresh air and an assumed value of 395 cfm of unfiltered inleakage.

- After the start of the event, the Control Room is isolated due to a high radiation reading in the Control Room ventilation system. For this event, it is conservatively assumed that the CR isolation signal is delayed until the release from the ADVs is initiated at 284 seconds. An additional 30-second delay is applied to account for the diesel generator start time, fan start and damper actuation time. After isolation, the air flow distribution consists of 0 cfm of makeup flow from the outside, 395 cfm of unfiltered inleakage, and 1760 cfm of filtered recirculation flow.

- At 1.5 hours into the event, the operators are assumed to initiate makeup flow from the outside to the control room. During this operational mode, the air flow distribution consists of 504 cfm of filtered makeup flow, 395 cfm of unfiltered inleakage, and 1256 cfm of filtered recirculation flow.

- The Control Room ventilation filter efficiencies that are applied to the filtered makeup and recirculation flows are 99% for particulate, elemental iodine, and organic iodine.

15.6.3.5.5 Radiological Consequences

The Control Room atmospheric dispersion factors (χ/Qs) used for this event are based on the postulated release locations and the operational mode of the control room ventilation system. The release-receptor point locations are chosen to minimize the distance from the release point to the Control Room air intake.

For the SGTR event, releases are assumed to occur from the condenser prior to reactor trip, and from the ADV that produces the most limiting χ/Qs following reactor trip. When the Control Room Ventilation System is in normal mode, the most limiting χ/Q corresponds to the worst air intake to the control room. When the ventilation system is isolated, the limiting χ/Q corresponds to the midpoint between the two control room air intakes. The operators are assumed to reopen the most favorable air intake at 1.5 hours. Development of control room atmospheric dispersion factors is discussed in Appendix 2.5D. The χ/Qs for the SGTR releases are summarized in Table 15.6.3-10.

For the EAB dose analysis, the χ/Q factor for the zero to two-hour time interval is assumed for all time periods. Using the zero to two-hour χ/Q factor provides a more conservative determination of the EAB dose, because the χ/Q factor for this time period is higher than for any other time period. The LPZ dose is determined using the χ/Q factors for the appropriate time intervals. These χ/Q factors are provided in Appendix 2.5C.

The radiological consequences of the SGTR Accident are analyzed using the RADTRAD-NAI code and the inputs/assumptions previously discussed. Two activity release cases corresponding to the RCS maximum pre-accident iodine spike and the accident-induced iodine spike, based on TS 3.4.8 limits, are analyzed. As shown in Table 15.6.3-4, the radiological consequences of the St. Lucie Unit 2 SGTR event for EAB dose, LPZ dose, and Control Room dose are all within the appropriate regulatory acceptance criteria. The transient analysis for this event provides input to a subsequent radiological analysis. Key parameters for this event include system related parameters such as the break flow rate and mass release from the affected steam generator MSSVs and ADVs. The change in fuel design parameters has no significant effect on this event. Therefore, this event does not require a reanalysis due to the fuel transition.

15.6.3.5.6 Conclusions

The radiological releases calculated for the SGTR Event with a concurrent loss of offsite power are provided in Table 15.6.3-4. Primary and secondary system pressures are well below upset pressure limits thus assuring the integrity of these systems.

15.6.4 SPECTRUM OF BOILING WATER REACTOR (BWR) STEAM SYSTEM PIPING FAILURES OUTSIDE OF THE CONTAINMENT (NOT APPLICABLE TO ST. LUCIE UNIT 2)

This section is not applicable to St. Lucie Unit 2, even with the transition to AREVA fuel.

15.6.5 LOSS-OF-COOLANT ACCIDENTS

15.6.5.1 Accident Description

A Loss-of-Coolant Accident (LOCA) is defined in 10 CFR 50.46(c)(1) as a hypothetical accident that would result from the loss of reactor coolant, at a rate in excess of the capability of the reactor coolant makeup system, from breaks in pipes in the reactor coolant pressure boundary up to and including a break equivalent in size to the double-ended rupture of the largest pipe in the reactor coolant system.

Two distinct LOCA analyses are presented in Section 15.6.5, namely, the Emergency Core Cooling System (ECCS) performance analysis and the radiological analysis. The ECCS performance analysis consists of a large break LOCA analysis (Section 15.6.5.2), a small break LOCA analysis (Section 15.6.5.3), and a post-LOCA long term cooling analysis (Section 15.6.5.4). The LOCA radiological analysis is described in Section 15.6.5.5.

The transition to AREVA's HTP 16x16 fuel design is supported by additional analysis. Section 15.6.5.2.5 presents the ECCS performance analysis with the AREVA Realistic Large Break LOCA methodology and Section 15.6.5.3.5 presents the AREVA Appendix K analysis for SBLOCA. These sections are added to the unchanged existing sections describing the Westinghouse analysis while the two fuel designs are coresident in the core.

For the ECCS performance analysis, a large break LOCA is defined as a pipe break with a total break area equal to or greater than 1.0 ft^2. As identified in Section 15.0.6.4, a large break LOCA is classified as an ANS Condition IV plant condition, i.e., a limiting fault. Likewise, a small break LOCA is defined as a pipe break with a total break area that is less than 1.0 ft^2. As identified in Section 15.0.6.3, a small break LOCA is classified as an ANS Condition III plant condition, i.e., an infrequent fault.

The acceptance criteria for ECCS performance analyses are specified in Paragraph (b) of 10 CFR 50.46 (Reference 15.6.5-1). They are as follows.

Criterion 1: <u>Peak Cladding Temperature</u>: The calculated maximum fuel element cladding temperature shall not exceed 2200°F.

Criterion 2: <u>Maximum Cladding Oxidation</u>: The calculated total oxidation of the cladding shall nowhere exceed 0.17 times the total cladding thickness before oxidation.

Criterion 3: <u>Maximum Hydrogen Generation</u>: The calculated total amount of hydrogen generated from the chemical reaction of the cladding with water or steam shall not exceed 0.01 times the hypothetical amount that would be generated if all of the metal in the cladding cylinders surrounding the fuel, excluding the cladding surrounding the plenum volume, were to react.

Criterion 4: <u>Coolable Geometry</u>: Calculated changes in core geometry shall be such that the core remains amenable to cooling.

Criterion 5: <u>Long-Term Cooling</u>: After any calculated successful initial operation of the ECCS, the calculated core temperature shall be maintained at an acceptably low value and decay heat shall be removed for the extended period of time required by the long-lived radioactivity remaining in the core.

Additionally, ECCS performance must be calculated in accordance with an acceptable evaluation model and must be calculated for a number of postulated LOCAs of different sizes, locations, and other properties sufficient to provide assurance that the most severe postulated LOCAs are calculated. The evaluation model may either be a realistic evaluation model as described in 10 CFR 50.46(a)(1)(i) or must conform to the required and acceptable features of Appendix K ECCS Evaluation Models (Reference 15.6.5-2). The evaluation models used to perform the St. Lucie Unit 2 ECCS performance analysis are Appendix K evaluation models.

15.6.5.2 Large Break LOCA

15.6.5.2.1 Method of Analysis

The large break LOCA ECCS performance analysis used the 1999 EM version of the Westinghouse large break LOCA evaluation model for Combustion Engineering designed Pressurized Water Reactors (PWRs) (Reference 15.6.5-3).

Several computer codes are used in the 1999 EM. The computer codes are described in the references cited below with additional descriptive information provided in the 1999 EM topical report (Reference 15.6.5-3, Supplement 4-P-A). The CEFLASH-4A computer code (Reference 15.6.5-4) is used to perform the blowdown hydraulic analysis of the reactor coolant system (RCS) and the COMPERC-II computer code (Reference 15.6.5-5) is used to perform the RCS refill/reflood hydraulic analysis and to calculate the minimum containment pressure. It is also used in conjunction with the methodology described in Reference 15.6.5-6 to calculate the FLECHT-based reflood heat transfer coefficients used in the hot rod heatup analysis. The HCROSS (Reference 15.6.5-7) and PARCH (Reference 15.6.5-8) computer codes are used to calculate steam cooling heat transfer coefficients. The hot rod heatup analysis, which calculates the peak cladding temperature and maximum cladding oxidation, is performed with the STRIKIN-II computer code (Reference 15.6.5-9). Core-wide cladding oxidation is calculated using the COMZIRC computer code (Appendix C of Supplement 1 of Reference 15.6.5-5). The 1999 EM uses the models for ZIRLO® cladding that are described in Section 6 of Reference 15.6.5-10. The initial steady state fuel rod conditions used in the large break LOCA analysis are determined using the FATES3B computer code (Reference 15.6.5-11).

The Safety Evaluation Reports for the evaluation model and computer code topical reports that comprise 1999 EM are documented in References 15.6.5-12 through 15.6.5-20.

The limiting initial fuel rod conditions used in the large break LOCA analysis (i.e., the conditions that result in the highest calculated peak cladding temperature) were determined by performing burnup dependent calculations with STRIKIN-II using initial fuel rod conditions calculated by FATES3B. The calculations included the analysis of both UO_2 fuel rods and gadolinia burnable absorber fuel rods and ZIRLO® cladding.

The analysis included a study to determine the most limiting single failure of ECCS equipment. The study analyzed no failure, failure of an emergency diesel generator, and failure of a low pressure safety injection (LPSI) pump. Maximum safety injection pump flow rates were used in the no failure case; minimum safety injection pump flow rates were used in the emergency diesel generator and LPSI pump failure cases. The pumps were actuated on a safety injection actuation signal (SIAS) generated by low pressurizer pressure with a startup delay of 30 seconds. The most limiting single failure (i.e., the failure that resulted in the highest calculated peak cladding temperature) was no failure of ECCS equipment. No failure is the worst condition because it maximizes the amount of safety injection that spills into the containment. This acts to

minimize containment pressure, which in turn minimizes the rate at which the core is reflooded. The failure of either an emergency diesel generator or a LPSI pump is not the most damaging failure because, in both cases, there is sufficient safety injection pump flow to keep the reactor vessel downcomer filled to the cold leg nozzles. This maintains the same driving force for reflooding the core as for no failure, but results in less spillage into the containment. A study was also performed to investigate the impact of variations in safety injection tank (SIT) temperature, pressure, and water volume and refueling water tank temperature on peak cladding temperature. The combination of minimum temperature, minimum pressure and maximum water volume for the SITs and minimum refueling water tank temperature was determined to result in the highest peak cladding temperature.

A spectrum of guillotine breaks in the reactor coolant pump discharge leg was analyzed. As described in Section 3.4 of Reference 15.6.5-3, Supplement 4-P-A, the discharge leg is the most limiting break location and a guillotine break is more limiting than a slot break. In particular, the 1.0, 0.8, 0.6, and 0.4 Double-Ended Guillotine breaks in the reactor coolant Pump Discharge leg (DEG/PD) were analyzed. The 0.6 DEG/PD break was determined to be the limiting large break LOCA (i.e., the break that results in the highest calculated peak cladding temperature).

15.6.5.2.2 Input Parameters and Initial Conditions

Important core, RCS, ECCS, and containment design data used in the large break LOCA analysis are listed in Table 15.6.5-1. The fuel rod conditions listed in Table 15.6.5-1 are for the hot rod burnup that produced the highest calculated peak cladding temperature. Plant design data for the containment (e.g., data for the containment initial conditions, containment volume, containment heat removal systems, and containment passive heat sinks) were selected to minimize the transient containment pressure. The Large Break LOCA analysis has been modified to represent Extended Power Uprate (EPU conditions, Replacement Steam Generators (RSG) with up to 10% tube plugging per generator and Radial Enrichment Zoning (REZ) fuel loading pattern core design.

15.6.5.2.3 Results

Table 15.6.5-2 lists the peak cladding temperature and oxidation percentages for the spectrum of large break LOCAs. Times of interest are listed in Table 15.6.5-3. The variables listed in Table 15.6.5-4 are plotted as a function of time for each break size in Figures 15.6.5-1 through 15.6.5-27 and Figures 15.6.5-39 through 15.6.5-47. The additional variables listed in Table 15.6.5-5 are plotted for the 0.6 DEG/PD break, the limiting large break LOCA, in Figures 15.6.5-28 through 15.6.5-38. The results demonstrate conformance to the ECCS acceptance criteria as summarized below.

Parameter	Criterion	Result
Peak Cladding Temperature	≤2200°F	2087°F
Maximum Cladding Oxidation	≤17%	14.48%
Maximum Core-Wide Oxidation	≤1%	<1%
Coolable Geometry	Yes	Yes

15.6.5.2.4 Conclusions

The results of the St. Lucie Unit 2 large break LOCA ECCS performance analysis demonstrate conformance to Criteria 1 through 4 of the ECCS acceptance criteria of 10 CFR 50.46(b) for a rated core power of 3020 MWt (3030 MWt including a 0.3% power measurement uncertainty) and a peak linear heat generation rate of 12.5 kW/ft. The results are applicable to St. Lucie Unit 2 with Extended Power Uprate (EPU) conditions, Radial Enrichment Zoning (REZ) and Replacement Steam Generators (RSG) with up to 10% tube plugging in each steam generator, a tube plugging differential between the two steam generators of up to 360 tubes, and a minimum RCS flow rate of 375,000 gpm.

15.6.5.2.5 Transition to AREVA HTP Fuel

The analysis supports operation beginning with the introduction of AREVA's HTP 16X16 fuel design using standard UO_2 fuel with 2%, 4%, 6% and 8% Gd_2O_3 and M5 cladding and Zirc-4 structural materials, unless changes in the Technical Specifications, Core Operating Limits Report, core design, fuel design, plant hardware, or plant operation invalidate the results presented herein. The analysis was performed in compliance with AREVA's NRC-approved Realistic Large Break LOCA (RLBLOCA) EM (Reference 15.6.5-34) with exceptions noted in Reference 15.6.5-35. Analysis results confirm the 10CFR50.46 (b) (Reference 15.6.5-1) acceptance criteria 1 through 4 presented in Section 15.6.5.1 are met and serve as the basis for operation of the St Lucie Nuclear Plant Unit 2 with AREVA fuel. The long term cooling criterion is addressed in Section 15.6.5.4.

15.6.5.2.5.1 AREVA Method of Analysis

The non-parametric statistical methods inherent in the AREVA RLBLOCA methodology provide for the consideration of a full spectrum of break sizes, break configuration (guillotine or split break), axial shapes, and plant operational parameters. A conservative loss of a diesel single failure assumption is applied in which one LPSI pump injects into the broken cold leg and intact cold leg of the broken loop, and one HPSI pump injects into all four cold legs. Regardless of the failure assumption, all containment pressure-reducing systems are assumed fully functional. The effects of Gadolinia-bearing fuel rods and peak fuel rod exposures are considered.

The RLBLOCA methodology is documented in Reference 15.6.5-34. The methodology follows the Code Scaling, Applicability, and Uncertainty (CSAU) evaluation approach (Reference 15.6.5-36). This method outlines an approach for defining and qualifying a best-estimate thermal-hydraulic code and quantifies the uncertainties in a LOCA analysis.

The RLBLOCA methodology consists of the following computer codes:

- RODEX3A (Reference 15.6.5-37) for computation of the initial fuel stored energy, fission gas release, and fuel-cladding gap conductance.
- S-RELAP5 (Reference 15.6.5-38) for the system calculation (includes ICECON for containment response).
- AUTORLBLOCA_TRN for generation of ranged parameter values, transient input, transient runs, and general output documentation.

The governing two-fluid (plus non-condensables) model with conservation equations for mass, energy, and momentum transfer is used. The reactor core is modeled in S-RELAP5 with heat generation rates determined from reactor kinetics equations (point kinetics) with reactivity feedback, and with actinide and decay heating.

The two-fluid formulation uses a separate set of conservation equations and constitutive relations for each phase. The effects of one phase on the other are accounted for by interfacial friction, and heat and mass transfer interaction terms in the equations. The conservation equations have the same form for each phase; only the constitutive relations and physical properties differ.

The modeling of plant components is performed by following guidelines developed to ensure accurate accounting for physical dimensions and that the dominant phenomena expected during the LBLOCA event are captured. The basic building blocks for modeling are hydraulic volumes for fluid paths and heat structures for heat transfer. In addition, special purpose components exist to represent specific components such as the RCPs or the steam generator separators. All geometries are modeled at the resolution necessary to best resolve the flow field and the phenomena being modeled within practical computational limitations.

A typical calculation using S-RELAP5 begins with the establishment of a steady-state initial condition with all loops intact. The input parameters and initial conditions for this steady-state calculation are chosen to reflect plant technical specifications or to match measured data. Additionally, the RODEX3A code provides initial conditions for the S-RELAP5 fuel models.

Following the establishment of an acceptable steady-state condition, the transient calculation is initiated by introducing a break into one of the loops. The evolution of the transient through blowdown, refill and reflood is computed continuously using S-RELAP5. Containment pressure is also calculated by S-RELAP5 using containment models derived from ICECON (Reference 15.6.5-39), which is based on the CONTEMPT-LT code (Reference 15.6.5-40).

The methods used in the application of S-RELAP5 to the LBLOCA are described in Reference 15.6.5-34. A detailed assessment of this computer code was made through comparisons to experimental data, many benchmarks with cladding temperatures ranging from 1,700 °F (or less) to above 2,200 °F.

These assessments were used to develop quantitative estimates of the ability of the code to predict key physical phenomena in a PWR LBLOCA. Various models—for example, the core heat transfer, the decay heat model and the fuel cladding oxidation correlation—are defined based on code-to-data comparisons and are, hence, plant-independent.

The RV internals are modeled in detail based on St Lucie Unit 2 specific inputs. Nodes and connectivity, flow areas, resistances and heat structures are all accurately modeled. The location of the hot assembly/hot pin(s) is unrestricted; however, the channel is always modeled to restrict appreciable upper plenum liquid fallback.

15.6.5.2.5.2 Input Parameters and Initial Conditions

The best-estimate methodology combines all the uncertainties related to the code and plant parameters, and estimates the PCT at a high probability level. The steps taken to derive the PCT uncertainty estimate are summarized below:

1. Base Plant Input File Development

   First, base RODEX3A and S-RELAP5 input files for the plant (including the containment input file) are developed. Code input development guidelines are applied to ensure that model nodalization is consistent with the model nodalization used in the code validation.

2. Sampled Case Development

   The non-parametric statistical approach requires that many “sampled” cases be created and processed. For every set of input created, each “key LOCA parameter” is randomly sampled over a range established through code uncertainty assessment or expected operating limits (provided by plant technical specifications or data). Those parameters considered "key LOCA parameters" are listed in Table 15.6.5-18. This list includes both parameters related to LOCA phenomena (based on the PIRT provided in Reference 15.6.5-34) and to plant operating parameters.

3. Determination of Adequacy of ECCS

   The RLBLOCA methodology uses a non-parametric statistical approach to determine values of PCT at the 95 percent probability level. Total oxidation and total hydrogen are based on the limiting PCT case. The adequacy of the ECCS is demonstrated when these results satisfy the criteria set forth in Section 15.6.5.1.

The S-RELAP5 model explicitly describes the RCS, RV, pressurizer, and ECCS. The ECCS includes a SIT path and a LPSI/HPSI path per RCS loop. The HPSI and LPSI feed into the SIT line that connects to each cold leg pipe downstream of the RCP discharge. The ECCS pumped injection is modeled as a table of flow versus backpressure. This model also describes the secondary-side steam generator that is instantaneously isolated (closed MSIV and feedwater trip) at the time of the break. A steam generator tube plugging level of 20 percent per steam generator was assumed.

As described in the AREVA RLBLOCA methodology, many parameters associated with LBLOCA phenomenological uncertainties and plant operation ranges are sampled. A summary of those parameters is given in Table 15.6.5-18. The LBLOCA phenomenological uncertainties are provided in Reference 15.6.5-34. Values for process or operational parameters, including ranges of sampled process parameters, and fuel design parameters used in the analysis are given in Table 15.6.5-19 and Table 15.6.5-20. Plant data are analyzed to develop uncertainties for the process parameters sampled in the analysis. Table 15.6.5-20 presents a summary of the uncertainties used in the analysis. Where applicable, the sampled parameter ranges are based on technical specification limits or supporting plant calculations that provide more bounding values.

Containment heat sink data is given in Table 15.6.5-21. In accordance with Reference 15.6.5-34, the condensing heat transfer coefficient is intended to be closer to a best-estimate instead of a bounding high value. The initial conditions and boundary conditions are given in Table 15.6.5-22. The building spray is modeled at maximum heat removal capacity. All spray flow is delivered to the containment.

15.6.5.2.5.3 Results

Two case sets of 59 transient calculations were performed sampling the parameters listed in Table 15.6.5-18. For each case set, PCT was calculated for a UO_2 rod, and for Gadolinia-bearing rods with concentrations of 2, 4, 6 and 8 w/o Gd_2O_3, for both fresh and once-burned exposure. The limiting case set, that contained the PCT, was the set with no offsite power available. The limiting PCT (1732°F) occurred in Case 57 for the fresh UO_2 rod. The major parameters for the limiting transient are presented in Table 15.6.5-23. Table 15.6.4-24 lists the event times for the limiting case. The fraction of total hydrogen generated was not directly calculated; however, it is conservatively bounded by the calculated total percent oxidation, which is well below the 1 percent limit. The best-estimate PCT case is Case 30, which corresponded to the median case out of the 59-case set with no offsite power available. The nominal PCT was 1496°F, for an 8% Gd_2O_3 once-burned rod. This result can be used to quantify the relative conservatism in the limiting case result. In this analysis, it was 236°F.

The case results, event times and analysis plots for the limiting PCT case are shown in Table 15.6.5-23, Table 15.6.5-24, and in Figure 15.6.5-79 through Figure 15.6.5-95. Figure 15.6.5-79 shows linear scatter plots of the key parameters sampled for the 59 calculations. Parameter labels appear to the left of each individual plot. These figures show the parameter ranges used in the analysis. Figure 15.6.5-80 and Figure 15.6.5-81 show the time of PCT and break size versus PCT scatter plots for the 59 calculations, respectively. Figure 15.6.5-82 and Figure 15.6.5-83 show the maximum oxidation and total oxidation versus PCT scatter plots for the 59 calculations, respectively. Key parameters for the limiting PCT case are shown in Figure 15.6.5-84 through Figure 15.6.5-94. Figure 15.6.5-84 is the plot of PCT independent of elevation; this figure shows that the transient exhibits a sustained and stable quench. A comparison of PCT results from both case sets is shown in Figure 15.6.5-95.

15.6.5.2.5.4 Conclusions

Analysis results show that the limiting LOOP case has a PCT of 1732°F, and a maximum oxidation thickness and hydrogen generation that fall well within regulatory requirements.

The analysis supports operation at a nominal power level of 3029.06 MWt (including 0.3% uncertainty), a steam generator tube plugging level of up to 20 percent in all steam generators, a total LHR of 13.0 kW/ft, a total peaking factor (F_Q) up to a value of 2.504, and a nuclear enthalpy rise factor ($F_{\Delta H}$ or F_r^T) up to a value of 1.81 (including 6% uncertainty and 3.5% allowance for control rod insertion effect on an F_r^T of 1.65) with no axial or burnup dependent power peaking limit. Peak rod average exposures of up to 62,000 MWd/MTU are supported, with the analysis considering both fresh and once-burned fuel assemblies as potentially limiting.

For large break LOCA, the 10CFR50.46 (b) (Reference 15.6.5-1) criteria 1 through 4 presented in Section 15.6.5.1 are met and operation of St Lucie Unit 2 with AREVA supplied 16x16 M5 clad fuel is justified. Criterion 5 (Post-LOCA Long-Term Cooling) is addressed in Section 15.6.5.4.

15.6.5.3 Small Break LOCA

15.6.5.3.1 Method of Analysis

The small break LOCA ECCS performance analysis used the Supplement 2 version (referred to as the S2M or Supplement 2 Model) of the Westinghouse small break LOCA evaluation model for Combustion Engineering designed PWRs (Reference 15.6.5-21).

In the S2M evaluation model, the CEFLASH-4AS computer program (Reference 15.6.5-22) is used to perform the hydraulic analysis of the RCS until the time the SITs begin to inject. After injection from the SITs begins, the COMPERC-II computer program (Reference 15.6.5-5) is used to perform the hydraulic analysis. The hot rod cladding temperature and maximum cladding oxidation are calculated by the STRIKIN-II computer program (Reference 15.6.5-9) during the initial period of forced convection heat transfer and by the PARCH computer program (Reference 15.6.5-8) during the subsequent period of pool boiling heat transfer. Core-wide cladding oxidation is conservatively represented as the rod-average cladding oxidation of the hot rod. The S2M uses the models for ZIRLO® cladding that are described in Section 6 of Reference 15.6.5-10. The initial steady state fuel rod conditions used in the small break LOCA analysis are determined using the FATES3B computer program (Reference 15.6.5-11).

The Safety Evaluation Reports for the evaluation model and computer code topical reports that comprise S2M are documented in References 15.6.5-23 and 15.6.5-24 as well as several of the Safety Evaluation Reports identified in Section 15.6.5.2.1.

The COMPERC-II computer code was not run for this analysis because flow from the SITs was not credited for the limiting break size even if the RCS was calculated to depressurize below the minimum SIT gas pressure. Table 15.6.5-9 identifies when SIT injection would have begun if it were credited.

The break spectrum analysis was performed for the fuel rod conditions at the burnup that results in the maximum initial stored energy in the fuel. In addition, the rod internal pressure was adjusted to cause cladding rupture to occur at the time that resulted in the highest peak cladding temperature and oxidation. The calculations included the analysis of both UO_2 fuel rods and gadolinia burnable absorber fuel rods and ZIRLO® cladding.

The analysis was performed using the failure of an emergency diesel generator as the most limiting single failure of the ECCS. This failure causes the loss of both a high pressure safety injection (HPSI) pump and a LPSI pump and results in a minimum of safety injection water being available to cool the core. Based on this failure and the design of the St. Lucie Unit 2 ECCS, 75% of the flow from one HPSI pump is credited in the small break LOCA analysis. The LPSI pumps are not explicitly credited in the small break LOCA analysis since the RCS pressure never decreases below the LPSI pump shutoff head during the portion of the transient that is analyzed. However, 50% of the flow from one LPSI pump is available to cool the core given a failure of an emergency diesel generator and a break in the reactor coolant pump discharge leg.

In addition to the SIS flows, injection flow from a single charging pump is credited in the small break analysis for St. Lucie 2 at Extended Power Uprate (EPU) conditions. Charging flow is supplied through the charging system piping which meets the requirements for a seismic Category 1 structure (Table 3.2-1). Injection is into two cold legs in opposing loops (Figure 5.1-1). The charging pump is automatically started and loaded (Table 8.3-2) after a

safety injection actuation signal and a loss of offsite power. The analysis is based on a value of 35 gpm for the injection flow rate of one charging pump, a charging flow split of 40% to the intact injection loop and 60% to the break, and a charging pump response time of 330.0 seconds (see Table 15.6.5-6).

A spectrum of three break sizes in the reactor coolant pump discharge leg was analyzed. The reactor coolant pump discharge leg is the limiting break location because it maximizes the amount of spillage from the ECCS. In particular, the 0.04, 0.05, and 0.06 ft^2/PD breaks were analyzed. The 0.05 ft^2/PD break was determined to be the limiting small break LOCA (i.e., the break that results in the highest calculated peak cladding temperature). The 0.04, 0.05, and 0.06 ft^2/PD breaks are at the upper end of the range of break sizes for which the hot rod cladding heatup transient is terminated solely by injection from a HPSI pump. It is within this range of break sizes that the limiting small break LOCA resides. Smaller breaks are too small to experience as much core uncovery as these breaks. For larger breaks, injection from the SITs and a HPSI pump recovers the core and terminates the heatup of the cladding before the cladding temperature approaches the peak cladding temperature of the limiting small break LOCA.

15.6.5.3.2 Input Parameters and Initial Conditions

Important core, RCS, and ECCS design data used for Extended Power Uprate (EPU) conditions in the small break LOCA analysis are listed in Tables 15.6.5-6 and 15.6.5-7.

15.6.5.3.3 Results

Table 15.6.5-8 lists the peak cladding temperature and oxidation percentages for the spectrum of small break LOCAs. Times of interest are listed in Table 15.6.5-9. The variables listed in Table 15.6.5-10 are plotted as a function of time for each break size in Figures 15.6.5-48 through 15.6.5-71. The results for the 0.05 ft^2/PD break, the limiting small break LOCA, demonstrate conformance to the ECCS acceptance criteria as summarized below.

Parameter	Criterion	Result
Peak Cladding Temperature	≤2200°F	1903°F
Maximum Cladding Oxidation	≤17%	9.21%
Maximum Core-Wide Oxidation	≤1%	<0.94%
Coolable Geometry	Yes	Yes

15.6.5.3.4 Conclusions

The results for Extended Power Uprate (EPU) conditions of the St. Lucie Unit 2 small break LOCA ECCS performance analysis demonstrate conformance to Criteria 1 through 4 of the ECCS acceptance criteria of 10 CFR 50.46(b) for a rated core power of 3020 MWt (3030 MWt including a 0.3% power measurement uncertainty) and a peak linear heat generation rate of 13.0 kW/ft. The results are applicable to St. Lucie Unit 2 with up to 10% tube plugging in each steam generator of the Replacement Steam Generator design, a tube plugging differential between the two steam generators of up to 360 tubes and a minimum RCS flow rate of 375,000 gpm.

15.6.5.3.5 Transition to AREVA HTP Fuel

The analysis supports operation beginning with the introduction of AREVA's HTP 16X16 fuel design using standard UO_2 fuel M5 cladding and Zirc-4 structural materials, unless changes in the Technical Specifications, Core Operating Limits Report, core design, fuel design, plant hardware, or plant operation invalidate the results presented herein. The analysis was performed in compliance with AREVA's NRC-approved Small Break LOCA (SBLOCA) EM (Reference 15.6.5-41). Analysis results confirm the 10CFR50.46 (b) (Reference 15.6.5-1) acceptance criteria 1 through 4 presented in Section 15.6.5.1 are met and serve as the basis for operation of the St Lucie Nuclear Plant Unit 2 with AREVA fuel. The long-term cooling criterion is addressed in Section 15.6.5.4.

15.6.5.3.5.1 AREVA Method of Analysis

The AREVA SBLOCA methodology is an Appendix K ECCS Evaluation Model (Reference 15.6.5-2). A spectrum of cold leg break sizes was considered, ranging from 2.0-inch diameter (0.022 ft^2) to 9.49-inch diameter (0.491ft^2). In addition, a sensitivity study was performed to consider breaks in attached ECCS piping. A conservative loss of an emergency diesel generator single-failure assumption is applied in which one LPSI pump injects into the broken cold leg and intact cold leg of the broken loop, and one HPSI pump injects into all four cold legs. The charging system was modeled to deliver 60% of the available flow from a single charging pump to the broken cold leg and 40% of the flow to an intact cold leg. The single-failure assumption also disables a motor-driven AFW pump, and the turbine-driven AFW pump was not modeled.

The SBLOCA methodology consists of the following computer codes:

- RODEX2-2A (Reference 15.6.5-42) for computation of the initial fuel stored energy, fission gas release, and fuel-cladding gap conductance.

- S-RELAP5 (Reference 15.6.5-38) for the system calculation.

The governing two-fluid (plus non-condensables) model with conservation equations for mass, energy, and momentum transfer is used. The reactor core is modeled in S-RELAP5 with heat generation rates determined from reactor kinetics equations (point kinetics) with reactivity feedback, and with actinide and decay heating.

The two-fluid formulation uses a separate set of conservation equations and constitutive relations for each phase. The effects of one phase on the other are accounted for by interfacial friction, and heat and mass transfer interaction terms in the equations. The conservation equations have the same form for each phase; only the constitutive relations and physical properties differ.

15.6.5.3.5.2 Input Parameters and Initial Conditions

The steps taken to derive the Appendix K PCT estimate are summarized below:

1. Base Plant Input File Development

   First, base RODEX2-2A and S-RELAP5 input files for the plant are developed. Code input development guidelines are applied to ensure that model nodalization is

consistent with the model nodalization used in the code validation. System parameters and initial conditions are listed in Table 15.6.5-25. The HPSI and LPSI flow rates are shown in Tables 15.6.5-26 and 15.6.5-27, respectively.

2. Break Spectrum Case Development

   A spectrum of break sizes is calculated ranging from 2.0-inch diameter (0.022 ft^2) to 9.49-inch diameter (0.491ft^2). Each case is identical except for the size of the break. The 9.49-inch (0.491ft^2) break corresponds to 10% of the cold leg area, which is the limit of applicability for the methodology.

3. Determination of Adequacy of ECCS

   The adequacy of the ECCS is demonstrated when the PCT and oxidation results satisfy the criteria set forth in Section 15.6.5.1 for all break sizes.

The S-RELAP5 model explicitly describes the RCS, RV, pressurizer, and ECCS. The ECCS includes a SIT path and a LPSI/HPSI path per RCS loop. The HPSI and LPSI feed into the SIT line that connects to each cold leg pipe downstream of the RCP discharge. The ECCS pumped injection is modeled as a table of flow versus backpressure. This model also includes the secondary-side of the steam generator and steam lines with safety valves. Offsite power is assumed to be lost coincident with a reactor trip on low pressurizer pressure. The turbine model and main feedwater injection are isolated at reactor trip but steam is relieved through the safety valves until the primary system depressurizes below that of the secondary. AFW is available to maintain steam generator level after an appropriate delay. A symmetric steam generator tube plugging level of 20 percent per steam generator was assumed.

The containment response is not modeled in the SBLOCA calculation.

15.6.5.3.5.3 Results

The limiting peak cladding temperature (PCT) is 2057°F for a 2.70-inch diameter (0.040 ft^2) cold leg pump discharge break. The total maximum local oxidation is less than 12.0%, including a pre-transient oxidation of 2.3925% and transient maximum oxidation of less than 9.0%. The maximum core-wide oxidation is less than 0.3%. The results of the analysis demonstrate the adequacy of the ECCS to support the criteria given in 10 CFR 50.46(b).

In addition to the break spectrum analysis, a sensitivity study was performed to consider a break in an attached pipe. The break in an attached piping sensitivity study was performed with a 10.126-inch diameter (double-ended guillotine) break in the safety injection tank (SIT) line. The PCT calculated for this case was 1445ºF. The SIT line break results are non-limiting compared to the break spectrum results.

The results for the break spectrum calculations are presented in Table 15.6.5-28. Time sequence evolution for each break size analysis is reported in Table 15.6.5-29. The limiting break size was determined to be a 2.70 inch diameter (0.040-ft2) break. Figures 15.6.5-96 through 15.6.5-111 show the behavior of significant parameters for the 2.70 inch break.

The primary pressure decreased immediately after break initiation (Figure 15.6.5-97). When the primary pressure reached the low pressurizer pressure trip setpoint at 28 seconds the reactor is tripped (Figure 15.6.5-96). Within approximately 1 second after reactor trip, reactor SCRAM

occurs, which occurs coincident with the loss of offsite power, causing turbine to trip, RCP trip and MFW pump trip (Figure 15.6.5-101 and Figure 15.6.5-102). As MFW to the SGs is ramped down and steam flow to the main steam isolation valves (MSIVs) are closed, the pressure in the SGs increase for approximately 10 seconds until MSSV inlet reaches the lowest opening pressure setpoint. This provides core heat removal in the early stages of the transient.

The primary system depressurization continues at a relatively fast rate for the first 200 seconds. Significant inventory is lost out the break until the break transitions from expelling liquid to steam at approximately 600 seconds (Figure 15.6.5-98 and Figure 15.6.5-99). Around this time, the broken leg loop seal begins to clear and the remaining intact loops remain plugged (Figure 15.6.5-100).

Prior to loop seal clearing, the core uncovers below top of active fuel (Figure 15.6.5-110). Since there is no loop flow, a large amount of steam is generated and accumulated in the core by the decay heat power until enough pressure is built to clear the loop seal in the broken leg at 604 seconds into the transient. This causes an abrupt level drop in the downcomer region and a small core level recovery. As the broken leg clears, the plant then enters a fairly slow boil-off phase where mass is lost out the break, and the primary system continues to empty.

From approximately 1000 to 1400 seconds, the primary side pressure is only slightly higher than the secondary side pressure (Figure 15.6.5-97), limiting the primary side heat removal. Broken loop steam generator AFW is initiated at approximately 934 seconds (Figure 15.6.5-103), providing an increasing SG level (Figure 15.6.5-104). However, the small pressure difference between the primary and secondary side limits the AFW's ability to remove heat from the primary side. At approximately 1500 seconds, the primary pressure reduces below the secondary side pressure, ending heat removal by the secondary side.

The charging system injects at 368 seconds. HPSI becomes available at 68 seconds into the transient but does not begin to inject water into the primary system cold legs until 668 seconds into the transient (Figure 15.6.5-106). However, HPSI flow does not provide sufficient inventory at this time to offset the large amount of RCS inventory lost out the break. As effective cooling is lost in the core, the fuel rods begin to heat up at approximately 1350 seconds (Figure 15.6.5-111). Hot rod rupture occurs at 1921 seconds. The fuel continues to heat up until the maximum PCT of 2057°F is reached at 2125 seconds. SIT injection begins just prior to reaching the PCT at 2118 seconds, providing sufficient cooling to turn the PCT over. The PCT occurs at approximately 4 inches below the top of active fuel.

For this break size, charging flow (Figure 15.6.5-105), HPSI flow (Figure 15.6.5-106), and SIT injection (Figure 15.6.5-108) were active at the time of PCT. Although LPSI is available, it did not inject (Figure 15.6.5-107) due to the slow primary system depressurization. The continued supply of charging and HPSI supports an increasing reactor vessel inventory (Figure 15.6.5-109) through event termination.

15.6.5.3.5.4 Conclusions

Analysis results show that the limiting break size has a PCT of 2057°F, and a maximum oxidation thickness and hydrogen generation that fall well within regulatory requirements.

The analysis supports plant operation at a core power level of 3029.06 MWt (including measurement uncertainty), a peak linear heat rate (LHR) of 13.0 kW/ft, a radial peaking factor of

1.65 (1.81 including uncertainty and an augmentation factor) and a steam generator tube plugging level of 20% in each generator.

For small break LOCA, the 10CFR50.46 (b) (Reference 15.6.5-1) criteria 1 through 4 presented in Section 15.6.5.1 are met and operation of St Lucie Unit 2 with AREVA supplied 16x16 M5 clad fuel is justified. Criterion 5 (Post-LOCA Long-Term Cooling) is addressed in Section 15.6.5.4.

15.6.5.4 Post-LOCA Long-Term Cooling

15.6.5.4.1 Method of Analysis

The post-LOCA long-term cooling analysis used the Westinghouse post-LOCA long-term cooling evaluation model for Combustion Engineering designed PWRs, CENPD-254-P-A (Reference 15.6.5-25). The Safety Evaluation Report documenting NRC acceptance of CENPD-254-P-A is contained in Reference 15.6.5-26.

However, in a leter dated August 1, 2005 (Reference 15.6.5-31), the NRC identified concerns regarding the CENPD-254-P-A LTC evaluation model. The letter states the following:

> *"Until the NRC staff's concerns are sufficiently resolved, the staff will not approve the use of TR CENPD-254-P for license applications."*

Based on discussions with the NRC staff, the issues identified in Reference 15.6.5-31 must be addressed to the staff's satisfaction for any plant change that impacts the LTC analysis and that requires NRC approval before implementation (e.g., a change that requires a license amendment, such as an EPU.) This understanding was confirmed by the NRC in a letter dated November 23, 2005 (Reference 15.6.5-32), wherein the following is stated:

> *"Until a supplement to TR CENPD-254-P is issued addressing the staff concerns, the following four items will also need to be addressed by licensees on a plant-specific basis in any future submittals regarding post-LOCA LTC."*

As alluded to above, the NRC identified four items that must be addressed by licensees on a plant-specific basis in license submittals that are made prior to the ultimate resolution of the concerns identified in Reference 15.6.5-31. The following are the four items identified in Reference 15.6.5-32.

1. The mixing volume must be justified; its calculation must account for void fraction.

2. The calculation of the mixing volume must account for the loop pressure drop between the core and the break.

3. The boric acid solubility limit must be justified, especially if crediting containment pressures greater than 14.7 psia or chemical additives in the sump water.

4. A decay heat multiplier of 1.2 must be used for all times if an Appendix K evaluation model is used.

The modifications to the CENPD-254-P-A methodology to address Items 1, 2, and 3 were previously included in the boric acid precipitation analysis that was performed in support of the

Waterford 3 Extended Power Uprate (EPU). The Waterford 3 EPU boric acid precipitation analysis also credited mixing of the charging flow with the safety injection flow prior to the flows entering the mixing volume.

The methodology used in the Waterford 3 EPU boric acid precipitation analysis has since become known as the “Waterford approach.” It has been recognized by the NRC (Reference 15.6.5-33) as an acceptable interim methodology for performing boric acid precipitation analyses prior to the establishment of a new methodology that addresses the issues identified in Reference 15.6.5-31.

The long-term cooling analysis consists of two separate analyses, namely, a boric acid precipitation analysis and a decay heat removal analysis. These two analyses are referred to as the large break analysis and the small break analysis in CENPD-254-P-A.

The purpose of the boric acid precipitation analysis is to demonstrate that for the limiting break, i.e., a large cold leg break, the maximum boric acid concentration in the core remains below the solubility limit, thereby preventing the precipitation of boric acid in the core. If boric acid was to precipitate in the core region, the precipitate could prevent water from remaining in contact with the fuel cladding and, consequently, result in the core temperature not being maintained at an acceptably low value. For the limiting break, boric acid precipitation is prevented by initiating simultaneous hot and cold leg injection.

The boric acid precipitation analysis used a boric acid concentration of 27.6 wt% as the solubility limit of boric acid. This is the solubility limit of boric acid in saturated water at atmospheric pressure. Atmospheric pressure is a conservative minimum value for the core pressure following a large break LOCA.

The St. Lucie Unit 2 boric acid precipitation analysis documented in this design analysis for EPU uses the CENPD-254-P-A post-LOCA boric acid precipitation analysis methodology as modified by the Waterford approach. This analysis was performed with the BORON computer code (Reference 15.6.5-25, Appendix C). In addition, it uses a decay heat multiplier of 1.2 for all times. Thus, the methodology used for this design analysis addresses the four items identified in Reference 15.6.5-32.

The purpose of the decay heat removal analysis is to demonstrate that, regardless of break size, the core remains covered with two-phase liquid in the long-term, thereby ensuring that the core temperature is maintained at an acceptably low value. If the break is small enough for the RCS to refill, the RCS is cooled down via the steam generators to the shutdown cooling entry temperature and shutdown cooling is initiated. Decay heat is then removed by the shutdown cooling system. For breaks that are too large for the RCS to refill, the break flow is sufficient to remove decay heat from the RCS in the long-term and simultaneous hot and cold leg injection prevents the precipitation of boric acid in the core. In the analysis, the selection of the initiating shutdown cooling versus maintaining simultaneous hot and cold leg injection is based on the RCS inventory at a specified time. In actual operation, the selection can be made much sooner based on indications of RCS pressure, subcooling, and inventory.

The decay heat removal analysis for EPU was performed with the CELDA, NATFLOW, and CEPAC computer codes (Reference 15.6.5-25, Appendices A, B, and D).

The decay heat removal portion of the long term cooling plan for St. Lucie Unit 2 relies on the RCS inventory results from CELDA to show an acceptable plan. In other words, the analysis methodology can show acceptable results by demonstrating both of the following two criteria:

1. The break is small enough such that the RCS has refilled and the SDC entry temperature has been met, and thus the SDC system is used to remove decay heat and prevent boric acid precipitation (small breaks), or

2. Breaks that do not meet this requirement are large enough for the break flow and simultaneous H/C side injection to remove decay heat and prevent boric acid precipitation in the long-term (large breaks).

This analytical approach is consistent with LOCA emergency operating procedures and the underlying philosophy of CENPD-254-P-A, namely, that it can be analytically demonstrated that decay heat can be removed in the long-term for any size LOCA and that the operator can correctly identify and initiate an appropriate means of long-term decay heat removal.

The worst single failure modeled in the analysis is the failure of an emergency diesel generator. The failure of an emergency diesel generator results in the following:

- One HPSI pump is operable.

- One LPSI pump is operable. Operation of the LPSI pump is automatically terminated upon generation of a Recirculation Actuation Signal.

- One motor-driven and the steam-driven auxiliary feedwater pumps are operable.

15.6.5.4.2 Input Parameters and Initial Conditions

Important plant design data used in the post-LOCA long-term cooling analysis for EPU are listed in Table 15.6.5-11.

15.6.5.4.3 Results

The post-LOCA boric acid precipitation analysis for EPU determined that a minimum flow rate of 250 gpm from a HPSI pump to the hot legs and 273 gpm from a HPSI pump to the cold legs of the RCS, initiated between four and six hours post-LOCA, prevents boric acid precipitation and maintains decay heat removal. The analysis also determined that the potential for entrainment of the hot leg injection by the steam flowing in the hot legs ends prior to two hours post-LOCA.

Figure 15.6.5-72 compares the core boiloff rate with the minimum hot leg injection flow rate of 250 gpm. It shows that the initiation of 250 gpm of hot and cold leg injection at six hours post-LOCA provides a substantial and time-increasing flushing flow through the core.
Figure 15.6.5-73 presents the core boric acid concentration as a function of time for the limiting break. It shows that without simultaneous hot and cold leg injection, the boric acid concentration in the core exceeds the solubility limit at approximately 7.1 hours post-LOCA. When 250 gpm of hot leg injection and 273 gpm of cold leg injection is initiated at six hours post-LOCA, the maximum boric acid concentration in the core is 26.3 wt%, a margin of 1.3 wt% to the solubility limit of 27.6 wt%. Figure 15.6.5-73 also shows that a flushing flow rate of 25 gpm started by six hours post-LOCA is sufficient to prevent the core boric acid concentration from reaching the solubility limit.

The decay heat removal analysis shows that, regardless of break size, decay heat can be removed for the long-term and that in doing so, the core remains covered with two-phase liquid, thereby ensuring that core temperatures are maintained at acceptably low values. The analysis identified a decision time of 16 hours. At the decision time, for breaks as large as 0.036 ft^2, the RCS has refilled and shutdown cooling may be used as the long-term decay heat removal method. For breaks as small as 0.013 ft^2, decay heat may be removed in the long-term by simultaneous hot and cold leg injection. The overlap in these two break ranges ensures that an appropriate long-term decay heat removal method is possible.

Figure 15.6.5-75 is a plot of break area versus RCS refill time. Figure 15.6.5-76 is a plot of RCS pressure at the decision time of 16 hours post-LOCA versus break area. Figure 15.6.5-77 tabulates break size and RCS pressure at the decision time. It also indicates the range of break sizes that are large breaks (i.e., simultaneous hot and cold leg injection is acceptable for long-term decay heat removal) and the range of break sizes that are small breaks (i.e., shutdown cooling is acceptable for long-term decay heat removal).

15.6.5.4.4 Conclusions

The results of the St. Lucie Unit 2 post-LOCA long-term cooling analysis for EPU demonstrate conformance to Criterion 5 of the ECCS acceptance criteria of 10 CFR 50.46(b) for a rated core power of 3030 MWt (3020 MWt including a 0.3% power measurement uncertainty). The results are applicable to St. Lucie Unit 2 with up to 10% tube plugging in each steam generator of the Replacement Steam Generator design, a tube plugging differential between the two steam generators of up to 360 tubes and a minimum RCS flow rate of 375,000 gpm.

15.6.5.5 Radiological Consequences

15.6.5.5.1 Background

This event is assumed to be caused by an abrupt failure of the main reactor coolant pipe and the ECCS fails to prevent the core from experiencing significant degradation (i.e., melting). This sequence cannot occur unless there are multiple failures, and thus goes beyond the typical design basis accident that considers a single active failure. Activity is released from the containment and from there, released to the environment by means of containment leakage and leakage from the ECCS. The St. Lucie Unit 2 AST dose analysis methodology is presented in NAI-1101-044, “AST Licensing Technical Report for St. Lucie Unit 2”.

15.6.5.5.2 Compliance with RG 1.183 Regulatory Positions

The revised LOCA dose consequence analysis is consistent with the guidance provided in RG 1.183, Appendix A, "Assumptions for Evaluating the Radiological Consequences of a LWR Loss-of-Coolant Accident," as discussed below:

1. Regulatory Position 1 - The total core inventory of the radionuclide groups utilized for determining the source term for this event is based on RG 1.183, Regulatory Position 3.1, at 100.3% of core thermal power and is provided in Table 15.0-32. The core inventory release fractions for the gap release and early in-vessel damage phases of the LOCA are consistent with Regulatory Position 3.2 and Table 2 of RG 1.183.

2. Regulatory Position 2 - The sump pH is controlled at a value greater than 7.0 per UFSAR Figure 6.5-8. Therefore, the chemical form of the radioiodine released to the

containment is assumed to be 95% cesium iodide (CsI), 4.85% elemental iodine, and 0.15% organic iodide. With the exception of elemental and organic iodine and noble gases, fission products are assumed to be in particulate form.

3. Regulatory Position 3.1 - The activity released from the fuel is assumed to mix instantaneously and homogeneously throughout the free air volume of the containment. The release into the containment is assumed to terminate at the end of the early in-vessel phase.

4. Regulatory Position 3.2 - Reduction of the airborne radioactivity in the containment by natural deposition is credited. A natural deposition removal coefficient for elemental iodine is calculated per SRP 6.5.2 as 2.89 hr-1. A natural deposition removal coefficient of 0.1 hr-1 is assumed for all aerosols in the unsprayed region of containment as well as in the sprayed region after spray is terminated at 8 hours. No removal of organic iodine by natural deposition is assumed.

5. Regulatory Position 3.3 - Containment spray provides coverage to 85% of the containment. Therefore, the St. Lucie Unit 2 containment building atmosphere is not considered to be a single, well-mixed volume. A mixing rate of two turnovers of the unsprayed region per hour is assumed. The maximum decontamination factor (DF) for the elemental iodine spray removal coefficient is 200 based on the maximum airborne elemental iodine concentration in the containment. Based upon the conservatively assumed elemental iodine removal rate of 20 hr-1, the DF of 200 is computed to occur at 3.07 hours. In addition, the particulate iodine removal rate is reduced by a factor of 10 when a DF of 50 is reached. Based upon the calculated iodine aerosol removal rate of 6.52 hr-1, the DF of 50 is conservatively computed to occur at 2.64 hours.

6. Regulatory Position 3.4 - Reduction in airborne radioactivity in the containment by filter recirculation systems is not assumed in this analysis.

7. Regulatory Position 3.5 - This position relates to suppression pool scrubbing in BWRs, which is not applicable to St. Lucie Unit No. 2.

8. Regulatory Position 3.6 - This position relates to activity retention in ice condensers, which is not applicable to St. Lucie Unit No. 2.

9. Regulatory Position 3.7 - A containment leak rate of 0.5% per day of the containment air is assumed for the first 24 hours. After 24 hours, the containment leak rate is reduced to 0.25% per day of the containment air.

10. Regulatory Position 3.8 - 100% of the radionuclide inventory of the RCS is released instantaneously at the beginning of the event. The containment purge flow is 2500 cfm through the eight-inch line and is assumed to be isolated after 30 seconds. No filters are credited.

11. Regulatory Position 4.1 - Leakage from containment collected by the secondary containment is processed by ESF filters prior to an assumed ground level release.

12. Regulatory Position 4.2 - Leakage into the secondary containment is assumed to be released directly to the environment as a ground level release prior to drawdown of the secondary containment at 310 seconds.

13. Regulatory Position 4.3 - SBVS is credited as being capable of maintaining the Shield Building Annulus at a negative pressure with respect to the outside environment considering the effect of high windspeeds and LOCA heat effects on the annulus as described in Section 6.2. No exfiltration through the concrete wall of the Shield Building is expected to occur.

14. Regulatory Position 4.4 - No credit is taken for dilution in the secondary containment volume.

15. Regulatory Position 4.5 - 9.6% of the primary containment leakage is assumed to bypass the secondary containment. This bypass leakage is released as a ground level release without credit for filtration.

16. Regulatory Position 4.6 - The SBVS is credited as meeting the requirements of RG 1.52 and Generic Letter 99-02. The filters in the SBVS ventilation system are credited at 99% efficiency for particulates and 95% for both elemental and organic iodine.

17. Regulatory Position 5.1 - Engineered Safety Feature (ESF) systems that recirculate water outside the primary containment are assumed to leak during their intended operation. With the exception of noble gases, all fission products released from the fuel to the containment are assumed to instantaneously and homogeneously mix in the containment sump water at the time of release from the core.

18. Regulatory Position 5.2 - Leakage from the ESF system is greater than two times the value identified in UFSAR Section 6.5.1.3 for pump seals and valve stems in the ECCS area. The leakage is assumed to start at the earliest time the recirculation flow occurs in these systems and continue for the 30-day duration. Backleakage to the RWT is also considered separately as two times 1 gpm, which is the bounding value based upon RCS leakage monitoring documented in the Control Room database. RWT leakage is assumed to begin at the start of recirculation and continue for the remainder of the 30-day duration.

19. Regulatory Position 5.3 - With the exception of iodine, all radioactive materials in the recirculating liquid are assumed to be retained in the liquid phase.

20. Regulatory Position 5.4 - A flashing fraction of 5.7% was calculated based upon the sump temperature at the time of recirculation. However, consistent with Regulatory Position 5.5, the flashing fraction for ECCS leakage is assumed to be 10%. This ECCS leakage enters the Reactor Auxiliary Building. For ECCS leakage back to the RWT, the analysis demonstrates that the temperature of the leaked fluid will cool below 212°F prior to release into the tank.

21. Regulatory Position 5.5 - The amount of iodine that becomes airborne is conservatively assumed to be 10% of the total iodine activity in the leaked fluid for the ECCS leakage entering the Reactor Auxiliary Building. For the ECCS leakage

back to the RWT, the sump and RWT pH history and temperature are used to evaluate the amount of iodine that enters the RWT air space.

22. Regulatory Position 5.6 - For ECCS leakage into the Reactor Auxiliary Building, the form of the released iodine is 97% elemental and 3% organic. An ECCS area ventilation system filter efficiency of 95% is assumed for both elemental and organic iodine. The ECCS area ventilation system meets the requirements of RG 1.52 and Generic Letter 99-02. There is no credit for hold-up or dilution in the Reactor Auxiliary Building. The temperature and pH history of the sump and RWT are considered in determining the radioiodine available for release and the chemical form. Credit is taken for dilution of the activity in the RWT.

23. Regulatory Position 6 - This position relates to MSIV leakage in BWRs, which is not applicable to St. Lucie Unit No. 2.

24. Regulatory Position 7 - Containment purge is not considered as a means of combustible gas or pressure control in this analysis; however, the effect of containment purge before isolation is considered.

15.6.5.5.3 Methodology

Input assumptions used in the dose consequence analysis of a LOCA are provided in Table 15.6.5-12. For the purposes of the LOCA analyses, a major LOCA is defined as a rupture of the RCS piping, including the double-ended rupture of the largest piping in the RCS, or of any line connected to that system up to the first closed valve. Should a major break occur, depressurization of the RCS results in a pressure decrease in the pressurizer. A reactor trip signal occurs when the pressurizer low-pressure trip setpoint is reached. A SIS signal is actuated when the appropriate setpoint (high containment pressure) is reached. The following measures will limit the consequences of the accident in two ways:

1. Reactor trip and borated water injection complement void formation in causing rapid reduction of power to a residual level corresponding to fission product decay heat, and

2. Injection of borated water provides heat transfer from the core and prevents excessive cladding temperatures.

<u>Release Inputs</u>

The core inventory of the radionuclide groups utilized for this event is based on RG 1.183, Regulatory Position 3.1, at 100.3% of core thermal power and is provided as Table 15.0-32. The source term represents end of cycle conditions assuming enveloping initial fuel enrichment and an average core burnup of 49,000 MWD/MTU.

From TS Surveillance Requirement 3.6.1.1, the initial leakage rate from containment is 0.5% of the containment air per day. Per RG 1.183, Regulatory Position 3.7, the primary containment leakage rate is reduced by 50% at 24 hours into the LOCA to 0.25% /day based on the post-LOCA primary containment pressure history. The majority of the leakage is released through the plant stack via the SBVS. 9.6% if the total leakage is assumed to bypass the SBVS filters and is modeled as a release from a feedwater line penetration.

The ESF leakage to the Reactor Auxiliary Building is assumed to be 1.08 gph, which is two times the current licensing basis value of 0.54 gph. The leakage is conservatively assumed to start at 20 minutes into the event and continue throughout the 30-day period. This portion of the analysis assumes that 10% of the total iodine is released from the leaked liquid. The form of the released iodine is 97% elemental and 3% organic. Dilution and holdup of the ECCS leakage in the Reactor Auxiliary Building are not credited.

The ECCS backleakage to the RWT is initially assumed to be 2 gpm based upon doubling the current bounding value of 1 gpm. This leakage is assumed to start at 22.3 minutes into the event when recirculation starts and continue throughout the 30-day period. Based on sump pH history, the iodine in the sump solution is assumed to all be nonvolatile. However, when introduced into the acidic solution of the RWT inventory, there is a potential for the particulate iodine to convert into the elemental form. The fraction of the total iodine in the RWT which becomes elemental is both a function of the RWT pH and the total iodine concentration. The amount of elemental iodine in the RWT fluid which then enters the RWT air space is a function of the temperature-dependent iodine partition coefficient.

The time-dependent concentration of the total iodine in the RWT (including stable iodine) was determined from the tank liquid volume and leak rate. This iodine concentration ranged from a minimum value of 0 at the beginning of the event to a maximum value of 4.088E-05 gm-atom/liter at 30 days. Based upon the backleakage of sump water, the RWT pH slowly increases from an initial value of 4.5 to a maximum pH of 4.9 at 30 days. Using the time-dependent RWT pH and the total iodine concentration in the RWT liquid space, the amount of iodine converted to the elemental form was determined using guidance provided in NUREG/CR-5950 (Reference 15.6.5-28). This RWT elemental iodine fraction ranged from 0 at the beginning of the event to a maximum of 0.193.

The elemental iodine in the liquid region of the RWT is assumed to become volatile and to partition between the liquid and vapor space in the RWT based upon the partition coefficient for elemental iodine as presented in NUREG/CR-5950. A GOTHIC model was used to determine the RWT temperature as a function of time which was then used to calculate the partition coefficient. The RWT is a vented tank; therefore, there will be no pressure transient in the air region that would affect the partition coefficient. Since no boiling occurs in the RWT, the release of the activity from the vapor space within the RWT is calculated based upon the displacement of air by the incoming leakage. The elemental iodine flow rate from the RWT is equal to the air flow rate times the elemental iodine concentration in the RWT vapor space.

For the organic iodine flow, the same approach was used with an organic iodine fraction of 0.0015 from RG 1.183 in combination with a partition coefficient of 1.0. The particulate portion of the leakage is assumed to be retained in the liquid phase of the RWT. Therefore, the total iodine flow is the sum of the elemental and organic iodine flow rates.

The time dependent iodine release rate presented in Table 15.6.5-14 is then applied to the entire iodine inventory (particulate, elemental and organic) in the containment sump. The iodine released via the RWT air vent to the environment was effectively set to 100% elemental (the control room filters have the same efficiency for all forms of iodine).

Containment purge is also assumed coincident with the beginning of the LOCA. Since the purge is isolated prior to the initial release of fission products from the core at 30 seconds, only the initial RCS activity (at an assumed 1.0 microcuries per gram DE I-131and 518.9 μCi/gm DE

Xe-133 gross activity) is available for release via this pathway. The release is conservatively modeled for 30 seconds at 2500 cfm until isolation occurs.

Transport Inputs

During the LOCA event, the initial containment purge is released through the plant stack with no filtration. Leakage into the secondary containment is assumed to be released directly to the environment as a ground level release prior to drawdown of the secondary containment at 310 seconds. Activity subsequently collected by the SBVS is assumed to be a filtered release from the plant stack with a filter efficiency of 99% for particulates and 95% for both elemental and organic iodine. The activity that bypasses the SBVS is released unfiltered to the environment via a ground level release from containment. ECCS leakage into the Reactor Auxiliary Building is modeled as a release via the Reactor Auxiliary Building. For this release path, the ECCS area ventilation system is credited with a particulate removal efficiency of 99% and elemental and organic iodine efficiencies of 95%. The activity from the RWT is modeled as an unfiltered ground level release from the RWT.

For this event, the Control Room ventilation system cycles through three modes of operation:

- Initially the ventilation system is assumed to be operating in normal mode. The air flow distribution during this mode is 1000 cfm of unfiltered fresh air and an assumed value of 395 cfm of unfiltered inleakage.

- After the start of the event, the Control Room is isolated due to a CIAS as a result of a high containment pressure signal. A 30-second delay is applied to account for the time to reach the signal, the diesel generator start time, damper actuation time. After isolation, the air flow distribution consists of 0 cfm of makeup flow from the outside, 395 cfm of unfiltered inleakage, and 1760 cfm of filtered recirculation flow.

- At 1.5 hours into the event, the operators are assumed to initiate makeup flow from the outside to the control room. During this operational mode, the air flow distribution consists of up to 504 cfm of filtered makeup flow, 395 cfm of unfiltered inleakage, and 1256 cfm of filtered recirculation flow.

- The Control Room ventilation filter efficiencies that are applied to the filtered makeup and recirculation flows are 99% for particulate, and 95% for elemental iodine, and organic iodine.

LOCA Removal Inputs

Reduction of the airborne radioactivity in the containment by natural deposition is credited. The natural deposition removal coefficient for elemental iodine is calculated per SRP 6.5.2 as 2.89 hr^{-1}. A natural deposition removal coefficient of 0.1 hr^{-1} is assumed for all aerosols in the unsprayed region and in the sprayed region after spray flow is secured at 8 hours. No removal of organic iodine by natural deposition is assumed.

Containment spray provides coverage to 85% of the containment. Therefore, the St. Lucie Unit 2 containment building atmosphere is not considered to be a single, well-mixed volume. A mixing rate of two turnovers of the unsprayed region per hour is assumed.

The elemental spray coefficient is limited to 20 hr^{-1} per SRP 6.5.2. This coefficient is reduced to 0 when an elemental decontamination factor (DF) of 200 is reached. Based upon the elemental iodine removal rate of 20 hr^{-1}, the DF of 200 is conservatively computed to occur at 3.07 hours. The particulate iodine removal rate is reduced by a factor of 10 when a DF of 50 is reached. Based upon the calculated iodine aerosol removal rate of 6.52 hr^{-1}, the DF of 50 is conservatively computed to occur at 2.643 hours.

15.6.5.5.4 Radiological Consequences

The Control Room atmospheric dispersion factors (χ/Qs) used for this event are based on the postulated release locations and the operational mode of the control room ventilation system. The release-receptor point locations are chosen to minimize the distance from the release point to the Control Room air intake.

When the Control Room Ventilation System is in normal mode, the most limiting χ/Q corresponds to the worst air intake to the control room. When the ventilation system is isolated at 30 seconds, the limiting χ/Q corresponds to the midpoint between the two control room air intakes. The operators are assumed to reopen the most favorable air intake at 1.5 hours. Development of control room atmospheric dispersion factors is discussed in Appendix 2.5D. The χ/Qs for the LOCA releases are summarized in Table 15.6.5-16.

For the EAB dose analysis, the χ/Q factor for the zero to two-hour time interval is assumed for all time periods. Using the zero to two-hour χ/Q factor provides a more conservative determination of the EAB dose, because the χ/Q factor for this time period is higher than for any other time period. The LPZ dose is determined using the χ/Q factors for the appropriate time intervals. These χ/Q factors are provided in Appendix 2.5C.

The radiological consequences of the design basis LOCA are analyzed using the RADTRAD-NAI code and the inputs/assumptions previously discussed. In addition, the MicroShield code, Version 5.05, Grove Engineering, is used to develop direct shine doses to the Control Room. MicroShield is a point kernel integration code used for general-purpose gamma shielding analysis.

The post accident doses are the result of five distinct activity releases:

Containment leakage via the SBVS.

Containment leakage which bypasses the SBVS.

ESF system leakage into the Reactor Auxiliary Building.

ESF system leakage into the RWT.

Containment Purge at event initiation.

The dose to the Control Room occupants includes terms for:

1. Contamination of the Control Room atmosphere by intake and infiltration of radioactive material from the containment and ESF.

2. External radioactive plume shine contribution from the containment and ESF leakage releases. This term takes credit for Control Room structural shielding.

3. A direct shine dose contribution from the Containment's contained accident activity. This term takes credit for both Containment and Control Room structural shielding.

4. A direct shine dose contribution from the activity collected on the Control Room ventilation filters.

As shown in Table 15.6.5-17, the sum of the results of all dose contributions for EAB dose, LPZ dose, and Control Room dose are all within the appropriate regulatory acceptance criteria.

15.6.5.6 References

15.6.5-1 Code of Federal Regulations, Title 10, Part 50, Section 50.46, "Acceptance Criteria for Emergency Core Cooling Systems for Light Water Nuclear Power Reactors".

15.6.5-2 Code of Federal Regulations, Title 10, Part 50, Appendix K, "ECCS Evaluation Models".

15.6.5-3 CENPD-132P, "Calculative Methods for the C-E Large Break LOCA Evaluation Model," August 1974.

CENPD-132P, Supplement 1, "Calculational Methods for the C-E Large Break LOCA Evaluation Model," February 1975.

CENPD-132-P, Supplement 2-P, "Calculational Methods for the C-E Large Break LOCA Evaluation Model," July 1975.

CENPD-132, Supplement 3-P-A, "Calculative Methods for the C-E Large Break LOCA Evaluation Model for the Analysis of C-E and W Designed NSSS," June 1985.

CENPD-132, Supplement 4-P-A, "Calculative Methods for the CE Nuclear Power Large Break LOCA Evaluation Model," March 2001.

15.6.5-4 CENPD-133P, "CEFLASH-4A, A FORTRAN-IV Digital Computer Program for Reactor Blowdown Analysis," August 1974.

CENPD-133P, Supplement 2, "CEFLASH-4A, A FORTRAN-IV Digital Computer Program for Reactor Blowdown Analysis (Modifications)," February 1975.

CENPD-133, Supplement 4-P, "CEFLASH-4A, A FORTRAN-IV Digital Computer Program for Reactor Blowdown Analysis," April 1977.

CENPD-133, Supplement 5-A, "CEFLASH-4A, A FORTRAN77 Digital Computer Program for Reactor Blowdown Analysis," June 1985.

15.6.5-5 CENPD-134 P, "COMPERC-II, A Program for Emergency-Refill-Reflood of the Core," August 1974.

CENPD-134 P, Supplement 1, "COMPERC-II, A Program for Emergency Refill-Reflood of the Core (Modifications)," February 1975.

CENPD-134, Supplement 2-A, "COMPERC-II, A Program for Emergency Refill-Reflood of the Core," June 1985.

15.6.5-6 CENPD-213-P, "Application of FLECHT Reflood Heat Transfer Coefficients to C-E's 16x16 Fuel Bundles," January 1976.

15.6.5-7 LD-81-095, Enclosure 1-P-A, "C-E ECCS Evaluation Model, Flow Blockage Analysis," December 1981.

15.6.5-8 CENPD-138P, "PARCH, A FORTRAN-IV Digital Program to Evaluate Pool Boiling, Axial Rod and Coolant Heatup," August 1974.

CENPD-138P, Supplement 1, "PARCH, A FORTRAN-IV Digital Program to Evaluate Pool Boiling, Axial Rod and Coolant Heatup (Modifications)," February 1975.

CENPD-138, Supplement 2-P, "PARCH, A FORTRAN-IV Digital Program to Evaluate Pool Boiling, Axial Rod and Coolant Heatup," January 1977.

15.6.5-9 CENPD-135P, "STRIKIN-II, A Cylindrical Geometry Fuel Rod Heat Transfer Program," August 1974.

CENPD-135P, Supplement 2, "STRIKIN-II, A Cylindrical Geometry Fuel Rod Heat Transfer Program (Modifications)," February 1975.

CENPD-135, Supplement 4-P, "STRIKIN-II, A Cylindrical Geometry Fuel Rod Heat Transfer Program," August 1976.

CENPD-135-P, Supplement 5, "STRIKIN-II, A Cylindrical Geometry Fuel Rod Heat Transfer Program," April, 1977.

15.6.5-10 CENPD-404-P-A, Rev. 0, "Implementation of ZIRLO™ Cladding Material in CE Nuclear Power Fuel Assembly Designs," November 2001.

15.6.5-11 CENPD-139-P-A, "C-E Fuel Evaluation Model," July 1974.

CEN-161(B)-P-A, "Improvements to Fuel Evaluation Model," August 1989.

CEN-161(B)-P, Supplement 1-P-A, "Improvements to Fuel Evaluation Model," January 1992.

15.6.5-12 O. D. Parr (NRC) to F. M. Stern (C-E), June 13, 1975.

15.6.5-13 O. D. Parr (NRC) to A. E. Scherer (C-E), December 9, 1975.

15.6.5-14 D.M. Crutchfield (NRC) to A. E. Scherer (C-E), "Safety Evaluation of Combustion Engineering ECCS Large Break Evaluation Model and Acceptance for Referencing of Related Licensing Topical Reports," July 31, 1986.

15.6.5-15 S. A. Richards (NRC) to P. W. Richardson (Westinghouse), "Safety Evaluation of Topical Report CENPD-132, Supplement 4, Revision 1, 'Calculative Methods for the CE Nuclear Power Large Break LOCA Evaluation Model' (TAC No. MA5660)," December 15, 2000.

15.6.5-16 K. Kniel (NRC) to A. E. Scherer (C-E), "Combustion Engineering Emergency Core Cooling System Evaluation Model," November 12, 1976.

15.6.5-17 R. L. Baer (NRC) to A. E. Scherer (C-E), "Evaluation of Topical Report CENPD-135 Supplement No. 5," September 6, 1978.

15.6.5-18 K. Kniel (NRC) to A. E. Scherer (C-E), "Evaluation of Topical Report CENPD-138, Supplement 2-P," April 10, 1978.

15.6.5-19 K. Kniel (NRC) to A. E. Scherer (C-E), August 2, 1976.

15.6.5-20 S.A. Richards (NRC) to P. W. Richardson (Westinghouse), “Safety Evaluation of Topical Report CENPD-404-P, Revision 0, ‘Implementation of ZIRLO Material Cladding in CE Nuclear Power Fuel Assembly Designs’ (TAC No. MB1035),” September 12, 2001.

15.6.5-21 CENPD-137P, “Calculative Methods for the C-E Small Break LOCA Evaluation Model,” August 1974.

CENPD-137, Supplement 1-P, “Calculative Methods for the C-E Small Break LOCA Evaluation Model,” January 1977.

CENPD-137, Supplement 2-P-A, “Calculative Methods for the ABB CE Small Break LOCA Evaluation Model,” April 1998.

15.6.5-22 CENPD-133P, Supplement 1, “CEFLASH-4AS, A Computer Program for the Reactor Blowdown Analysis of the Small Break Loss of Coolant Accident,” August, 1974. CENPD-133, Supplement 3-P, “CEFLASH-4AS, A Computer Program for the Reactor Blowdown Analysis of the Small Break Loss of Coolant Accident,” January 1977.

15.6.5-23 K. Kniel (NRC) to A. E. Scherer (C-E), “Evaluation of Topical Reports CENPD-133, Supplement 3-P and CENPD-137, Supplement 1-P,” September 27, 1977.

15.6.5-24 T.H. Essig (NRC) to I. C. Rickard (ABB), “Acceptance for Referencing of the Topical Report CENPD-137(P), Supplement 2, Calculative Methods for the C-E Small Break LOCA Evaluation Model (TAC No. M95687),” December 16, 1997.

15.6.5-25 CENPD-254-P-A, “Post-LOCA Long Term Cooling Evaluation Model,” June 1980.

15.6.5-26 R.L. Baer (NRC) to A. E. Scherer (C-E), “Staff Evaluation of Topical Report CENPD-254-P,” July 30, 1979.

15.6.5-27 USNRC Regulatory Guide 1.183, “Alternative Radiological Source Terms for Evaluating Design Basis Accidents at Nuclear Power Plants,” July 2000.

15.6.5-28 NUREG/CR-5950, “Iodine Evolution and pH Control”.

15.6.5-29 NRC Regulatory Issue Summary 2006-04, “Experience with Implementation of Alternate Source Terms,” March 7, 2006.

15.6.5-30 NAI-1101-044, “AST Licensing Technical Report for St. Lucie Unit 2” (part of NRC Submittal L-2007-087, “St. Lucie Unit 2 Proposed License Amendment Alternative Source Term and Conforming Amendment”).

15.6.5-31 NRC letter "Suspension of NRC Approval for use of Westinghouse Topical Report CENPD-254-P, 'Post-LOCA Long-Term Cooling Model,' Due to Discovery of Non-Conservative Modeling Assumptions During Calculations Audit," R.A. Gramm, August 1, 2005 (ADAMS No. ML051920310).

15.6.5-32 NRC letter "Clarification of NRC Letter Dated August 1, 2005, Suspension of NRC Approval of use of Westinghouse Topical Report CENPD-254-P, 'Post-LOCA Long-Term Cooling Model,' Due to Discovery of Non-Conservative Modeling Assumptions During Calculations Audit (TAC No. MB1365)," D.S. Collins, November 23, 2005 (ADAMS No. ML053220569).

15.6.5-33 S.E. Peters (NRC) to S.L. Rosenberg (NRC), "Summary of August 23, 2006 Meeting with the Pressurized Water Reactor Owners Group (PWROG) to Discuss the Status of Program to Establish Consistent Criteria for Post Loss-of-Coolant (LOCA) Calculations," October 3, 2006 (ADAMS No. ML062690017).

15.6.5-34 EMF-2103(P)(A) Revision 0, Realistic Large Break LOCA Methodology, Framatome ANP, Inc., April 2003.

15.6.5-35 ANP-3346NP Revision 0, St. Lucie Unit 2 Fuel Transition Realistic Large Break LOCA Summary Report, December 2014.

15.6.5-36 Technical Program Group, Quantifying Reactor Safety Margins, NUREG/CR-5249, EGG-2552, October 1989.

15.6.5-37 ANF-90-145(P)(A), "RODEX3 Fuel Rod Thermal-Mechanical Response Evaluation Model," April 1996.

15.6.5-38 EMF-2102(P)(A) Revision 0, S-RELAP5: Code Verification and Validation, Framatome ANP, Inc., August 2001.

15.6.5-39 XN-CC-39 (A) Revision 1, "ICECON: A Computer Program to Calculate Containment Back Pressure for LOCA Analysis (Including Ice Condenser Plants)," Exxon Nuclear Company, October 1978.

15.6.5-40 Wheat, Larry L., "CONTEMPT-LT A Computer Program for Predicting Containment Pressure-Temperature Response to a Loss-Of-Coolant-Accident," Aerojet Nuclear Company, TID-4500, ANCR-1219, June 1975.

15.6.5-41 EMF-2328(P)(A) Revision 0, PWR Small Break LOCA Evaluation Model, S-RELAP5 Based, March 2001.

15.6.5-42 XN-NF-81-58(P)(A) Revision 2, Supplements 1 and 2, RODEX2 FUEL Thermal-Mechanical Response Evaluation Model, Exxon Nuclear Company, March 1984.

15.6.5-43 ANF-81-58(P)(A) Revision 2, Supplements 3 and 4, RODEX2 FUEL Thermal-Mechanical Response Evaluation Model, Advanced Nuclear Fuels Corporation, June 1990.

Table 15.6.1-1 Time Sequence of Events Accidental Depressurization of the RCS DNB Case	
Event	**Time (seconds)***
Inadvertent Opening of Two PORVs	10.02
Low Pressurizer Pressure Reactor Trip Setpoint Reached	26.87
TMLP Trip Signal Obtained	27.63
Reactor Trip Signal	28.03
Rods Begin to Drop	28.77
Minimum DNBR Occurs	29.00

* The time sequence includes a 10 second steady state.

Table 15.6.1-2 Time Sequence of Events Accidental Depressurization of the RCS Pressurizer Overfill Case	
Event	**Time (seconds)***
Inadvertent Opening of a Single PORV	10.100
Low Pressurizer Pressure Reactor Trip Setpoint Reached	42.374
TMLP Trip Signal Obtained	42.744
Reactor Trip on TMLP	43.514
Safety Injection Signal	50.986
Safety Injection Initiation	71.000
Pressurizer Fills	184.00

* The time sequence includes a 10 second steady state.

Table 15.6.1-3 RCS Depressurization (AREVA DNB): Sequence of Events	
Event	Time (sec)
Two PORVs inadvertently open	0.00
Pressurizer pressure reaches Low Pressurizer Pressure trip setpoint	18.85
Reactor is scrammed on Low Pressurizer Pressure (including signal processing delay)	20.02
MDNBR occurs	20.45
CEA insertion begins	20.77

Table 15.6.1-4 RCS Depressurization (AREVA DNB): Result		
Criterion	Result	Limit
MDNBR	1.237	1.164

Table 15.6.2-1 Key Parameters Assumed for the Small Primary Line Break Outside Containment Event			
Parameter	**Units**	**Low Tavg Value**	**High Tavg Value**
Total RCS Power (Core Thermal Power + Pump Heat)	MWt	3050	3050
Initial Core Coolant Inlet Temperature	°F	532	554
Initial Reactor Coolant System Pressure	psia	2395	2395
Initial RCS Vessel Flow Rate	gpm	375,000	375,000
CEA Worth at Trip	%Δρ	-5.20	-5.20

Table 15.6.2-2
Sequence of Events
Small Primary Line Break Outside Containment Event

Parameter	Low Tavg Results*	High Tavg Results*
Letdown Line Break Occurs	0.0	0.0
TM/LP Low Pressure Trip Setpoint Reached	850.0	886.5
Reactor Trip Breakers Open	851.1	887.6
CEAs Begin to Drop	851.9	888.4
Secondary Safety Valves Open	869.1	891.4
Safety injection Actuation Signal Reached	859.9	894.5
Letdown Line Isolation Occurs	1459.1	1494.5
Operator Action Occurs	1800.0	1800.0

* Note the 20 second steady state period is subtracted.

Table 15.6.2-3

Letdown Line Rupture Dose Consequences

Case	EAB Dose (1) (rem TEDE)	LPZ Dose (2) (rem TEDE)	Control Room Dose (2) (rem TEDE)
Letdown Line Rupture	0.32	0.31	2.85
Acceptance Criteria	2.5 (3)	2.5 (3)	5 (4)

EC290539

(1) Worst 2-hour dose
(2) Integrated 30-day dose
(3) RG 1.183, Table 6
(4) 10 CFR 50.67

Table 15.6.2-4

Letdown Line Rupture – Inputs and Assumptions

Input/Assumption	Value
Core Power Level	3030 MW_{th} (3020 + 0.3%)
Initial RCS Equilibrium Activity	1.0 μCi/gm DE I-131 and 518.9 μCi/gm gross activity (Table 15.6.5-15)
Initial Secondary Side Equilibrium Iodine Activity	0.1 μCi/gm DE I-131 (Table 15.1.6-6)
Iodine spike Appearance Rate	500 times
Duration of Accident Initiated Spike	8 hrs
Steam Generator Tube Leakage	0.5 gpm (Table 15.6.2-6)
Time to Terminate SG Tube Leakage	12.4 hours
Secondary Side Mass Releases to Environment	Table 15.2.6-5
SG Tube Uncovery Following Reactor Trip Time to tube recovery Flashing Fraction	 1 hour 5 %
Steam Generator Secondary Side Partition Coefficient	Flashed tube flow – none Non-flashed tube flow – 100
Time to Reach 212 °F and Terminate Steam Release	12.4 hours
RCS mass	RCS Activity – 420,090 lb_m Concurrent Iodine spike – 386,354 lb_m
SG Secondary Side Mass	minimum – 128,390 lb_m -5% (per SG) Minimum used for primary-to-secondary leakage to maximize secondary nuclide concentration.
Letdown Line Rupture flow rate	94,300 lb_m over 1800 seconds
Letdown Line Flashing Fraction	6%

Table 15.6.2-4 (continued)

Letdown Line Rupture – Inputs and Assumptions

Input/Assumption	Value
Control Room Ventilation System Time of Control Room Ventilation System Isolation Time of Control Room Filtered Makeup Flow Control Room Unfiltered Inleakage	 30 seconds 1.5 hours 395 cfm
Chemical Form of Iodine Released	Particulate – 0% Elemental – 97% Organic – 3%
Atmospheric Dispersion Factors Offsite Onsite	Appendix 2.5C Tables 15.6.2-9
Breathing rates Offsite Control Room	RG 1.183, Section 4.1.3 RG 1.183, Section 4.2.6
CR Occupancy Factors	RG 1.183, Section 4.2.6

Table 15.6.2-5

Letdown Line Rupture Steam Release Rate

Time (hours)	Steam Release Rate (lb_m/min)
0.0	11473.7
0.5	5124.4
2.0	2690.3
8.0	2611.7
9.0	2478.3
10.0	2393.3
11.0	2301.7
12.00	2213.3
12.4	0.0

Table 15.6.2-6

Letdown Line Rupture Steam Generator Tube Leakage

Time (hours)	SG Tube Leakage (lb_m/min)
0	3.15
0.50	3.34
1.00	3.50
1.50	3.65
2.00	3.71
4.00	3.80
6.00	3.89
9.00	3.96
11.00	4.00
12.40	0.00

Table 15.6.2-7

Iodine Equilibrium Appearance Assumptions

Input Assumption	Value
Maximum Letdown Flow	150 gpm at 120°F, 650 psia
Maximum Identified RCS Leakage	10 gpm
Maximum Unidentified RCS Leakage	1 gpm
RCS Mass	386,354 lb_m
I-131 Removal Rate (Min $^{-1}$)	0.003430
I-132 Removal Rate (Min $^{-1}$)	0.008393
I-133 Removal Rate (Min $^{-1}$)	0.003925
I-134 Removal Rate (Min $^{-1}$)	0.016548
I-135 Removal Rate (Min $^{-1}$)	0.005117

Table 15.6.2-8

Concurrent Iodine Spike (500 x) Activity Appearance Rate

Nuclide	1 µCi/gm Appearance (Ci/min)	8 hour Production (Ci)
I-131	0.5064	1.215E+05
I-132	0.2484	5.962E+04
I-133	0.5994	1.439E+05
I-134	0.2240	5.377E+04
I-135	0.3527	8.465E+04

Table 15.6.2-9a

Control Room χ/Q (for releases from the steam generators)

Time (hours)	χ/Q (sec/m^3)
0	6.71E-03
0.00833	3.13E-03
1.5	1.89E-03
2	1.53E-03
8	6.02E-04
24	4.55E-04
96	3.89E-04
720	3.89E-04

Table 15.6.2-9b

Control Room χ/Q (for releases from the line break)

Time (hours)	χ/Q (sec/m^3)
0	4.80E-03
0.00833	5.06E-03
1.5	3.22E-03
2	2.67E-03
8	1.14E-03
24	8.62E-04
96	7.04E-04
720	7.04E-04

Table 15.6.3-1
Key Parameters Assumed For The Steam Generator Tube Rupture Event With a Loss of Offsite Power

Parameter	Units	Value
Total RCS Power (Core Thermal Power + Pump Heat)	MWt	3050
Initial Core Coolant Inlet Temperature	°F	554
Initial RCS Vessel Flow Rate	gpm	375,000
Number of SG Plugged Tubes	---	10%
Initial Steam Generator Pressure	psia	879
Steam Generator U-Tube Break Size	in^2	0.346
CEA Worth at Trip	$\%\Delta\rho$	-5.2
Initial Pressurizer Pressure	psia	2395

Table 15.6.3-2
Sequence of Events for the Steam Generator Tube Rupture Margin to Overfill Event

Time (sec)	Event	Setpoint/Value
0.1	Tube Rupture	---
282.2	TMLP Low Pressure Setpoint Reached	2122 psia
283.0	TMLP Signal for Reactor Trip	2122 psia
283.4	Reactor Trip Signal	---
284.1	CEA Release (0.74 sec delays)	---
285.1	Main Steam Safety Valves Open	970.0 psia
462.0	AFW Flow Initiated (Intact SG 120 sec delayed)	SG NR Level 25.5%
464.3	AFW Flow Initiated (Ruptured SG 120 sec delayed)	SG NR Level 25.5%
514.1	Pressurizer Empties	---
571.8	SIAS on Low Pressurizer Pressure	1578 psia*
871.3	AFAS Reset Setpoint Reached & TDAFW Continues	39.1% NR
871.6	SI Flow Begins (RCS Pressure Below Shutoff)	1454.8 psia (shutoff)
1771.3	TDAFW Flow Terminated (900 sec delayed)	SG Vol. 3189 ft^3
2660.9	Maximum SG Level Loop 1	6631 ft^3
2700	All Other Operation Action Begins	--

* The analysis is insensitive to this value since the pressure drops to below the SI shut-off head much later, and an earlier SIAS would not initiate HPSI earlier.

Table 15.6.3-3
Sequence of Events for the Steam Generator Tube Rupture With a Loss of Offsite Power

Time (sec)	Event	Setpoint / Value
0.0	Tube Rupture Occurs	---
284.0	Reactor Trip Signal on Floor of TM/LP, psia	2122
284.7	CEAs Begin to Drop	----
285.6	MSSVs open,* psia	970
287.6	Maximum SG Pressure, psia	1009.5
570.8	SIAS Generated on Low Pressurizer Pressure, psia	1578
657.3	Pressurizer Empties	----
868.2	HPSI Pumps Reach Full Speed	----
1189.5	Auxiliary Feedwater Flow Initiates on Low Steam Generator Level, % NRS	5%
2700	1. Operator Borates to Cold Shutdown Concentration	----
2700	2. Operator Isolates Affected SG by Closing MSIV	----
2700	3. Operator Activates ADVs (Intact SG) to Commence Cooldown of RCS	----
----	Steam Releases via Turbine to Condenser Prior to Trip (50.1% Affected SG/49.9% Intact SG), lbm	1,050,872
----	MSSVs Close, Affected/Intact SG Steam Releases, lbm (from Reactor Trip to 2700 seconds)	131,269 / 103,333
----	Affected SG Leakage Before Trip, lbm	17,190
----	Affected SG Leakage from Reactor Trip up to 2700 seconds, lbm	90,347
----	RCS to Affected SG Total Tube Leakage up to 2700 seconds, lbm	107,537
7200	Total Intact SG Steam Releases via ADV (from 2700 seconds to 2 hours), lbm	492,200**
28800	Total Intact SG Steam Releases via ADV (from 2 hours to 8 hours), lbm	911,300**

* MSSVs Cycle Until Operator Activates ADVs @ 2700 Sec

** Based on a 100°F cooldown rate to maximize the steam releases over the first two hour period.

Table 15.6.3-4 Radiological Exposures as a Result of a Steam Generator Tube Rupture Event With a Loss of Offsite Power

Case	EAB Dose (1) (rem TEDE)	LPZ Dose (2) (rem TEDE)	Control Room Dose (2) (rem TEDE)
SGTR pre-accident iodine spike	0.38	0.37	4.13
Acceptance Criteria (pre-accident iodine spike)	25 (3)	25 (3)	5 (4)
SGTR concurrent iodine spike	0.18	0.18	1.55
Acceptance Criteria (concurrent iodine spike)	2.5 (3)	2.5 (3)	5 (4)

EC290539

(1) Worst 2-hour dose

(2) Integrated 30-day dose

(3) RG 1.183, Table 6

(4) 10 CFR 50.67

Table 15.6.3-5
Steam Generator Tube Rupture (SGTR) Inputs and Assumptions

Input/Assumption	Value
Core Power Level	3030 MW_{th} (3020 + 0.3%)
Initial RCS Equilibrium Activity	1.0 µCi/gm DE I-131 and 518.9 µCi/gm DE Xe-133 gross activity (Table 15.6.5-15)
Initial Secondary Side Equilibrium Iodine Activity	0.1 µCi/gm DE I-131 (Table 15.1.6-6)
Maximum Pre-Accident Spike Iodine Concentration	60µCi/gm DE I-131
Maximum Equilibrium Iodine Concentration	1.0µCi/gm DE I-131
Iodine Spike Appearance Rate	335 times
Duration of Accident-Initiated Spike	8 hours
Integrated Break Flow and Steam Release	Table 15.6.3-6
Break Flow Flashing Fraction	Prior to Reactor Trip - 15.5% Following Reactor Trip – 6%
Time to Terminate Break Flow	45 minutes
Steam Generator Tube Leakage Rate	0.25 gpm per SG
Time to Terminate Tube Leakage	12.4 hours
Time to Re-cover Intact SG Tubes	1 hour
Steam Generator Secondary Side Partition Coefficients	Flashed tube flow – none Non-flashed tube flow – 100
Time to Reach 212 °F and Terminate Steam Release	12.4 hours
RCS Mass	Pre-accident Iodine spike – 422,090 lb_m Concurrent Iodine spike – 386,354 lb_m
SG Secondary Side Mass	minimum – 121,970.5 lb_m (per SG) Minimum used for primary-to-secondary leakage to maximize secondary nuclide concentration.
Atmospheric Dispersion Factors Offsite Onsite	 Appendix 2.5C Table 15.6.3-10
Control Room Ventilation System Time of Control Room Ventilation System Isolation Time of Control Room Filtered Makeup Flow Control Room Unfiltered Inleakage	 314 seconds 1.5 hours 395 cfm
Breathing Rates Offsite Control Room	 RG 1.183, Section 4.1.3 RG 1.183, Section 4.2.6
Control Room Occupancy Factor	RG 1.183 Section 4.2.6

Table 15.6.3-6
SGTR Integrated Mass Releases

Time (hours)	Break Flow in Ruptured SG (lb_m)	Steam Release from Ruptured SG (lb_m)	Steam Release from Unaffected SG (lb_m)
0 – 0.75	110,600	0 – 0.0789 hrs: 578,100 (via Condenser) 0.0789 – 0.75 hrs: 147,300 (via MSSV)	575,200 (via Condenser) 136,800 (via MSSVs)
0.75 – 2.0	0	0	377,100 (via ADVs)
2 – 8	N/A	N/A	971,600
8 – 12.42	N/A	N/A	723,700

Table 15.6.3-7 60 μCi/gm D.E. I-131 Activities

Isotope	Activity (μCi/gm)
I-131	50.6
I-132	10.1
I-133	52.3
I-134	4.6
I-135	23.6

Table 15.6.3-8
Iodine Equilibrium Appearance Assumptions

Input Assumption	Value
Maximum Letdown Flow	150 gpm at 120°F, 650 psia
Maximum Identified RCS Leakage	10 gpm
Maximum Unidentified RCS Leakage	1 gpm
RCS Mass	386,354 lb_m
I-131 Removal Rate (Min $^{-1}$)	0.003430
I-132 Removal Rate (Min $^{-1}$)	0.008393
I-133 Removal Rate (Min $^{-1}$)	0.003925
I-134 Removal Rate (Min $^{-1}$)	0.016548
I-135 Removal Rate (Min $^{-1}$)	0.005117

Table 15.6.3-9
Concurrent Iodine Spike (335x) Activity Appearance Rate

Nuclide	Iodine Spike Appearance (Ci/min)	8-hour Production (Ci)
I-131	169.6	8.14E+04
I-132	83.2	3.995E+04
I-133	200.8	9.638E+04
I-134	75.1	3.603E+04
I-135	118.2	5.672E+04

Table 15.6.3-10 Control Room χ/Q (for releases from the steam generators)

Time (hours)	χ/Q (sec/m^3)
0	3.02E-03
0.0789	6.71E-03
0.08722	3.13E-03
1.5	1.89E-03
2	1.53E-03
8	6.02E-04
24	4.55E-04
96	3.89E-04
720	3.89E-04

Table 15.6.5-1 Large Break LOCA ECCS Performance Analysis Input Parameters and Initial Conditions

Quantity	Value	Units
Reactor power level (100.3% of rated power)	3030	MWt
Peak linear heat generation rate (PLHGR) of the hot rod	12.5	kW/ft
PLHGR of the average rod in assembly with hot rod	11.7	kW/ft
Average linear heat generation rate (100.3% of rated)	5.204	kW/ft
Gap conductance at the PLHGR(1)	1555	BTU/hr-ft^2-°F
Fuel centerline temperature at the PLHGR(1)	3067	°F
Fuel average temperature at the PLHGR(1)	1974	°F
Hot rod gas pressure(1)	1014	psia
Moderator temperature coefficient at initial density	0.3×10^{-4}	$\Delta\rho$/°F
RCS flow rate (minimum)	144.3×10^6	lbm/hr
Core flow rate (minimum)	138.9×10^6	lbm/hr
RCS pressure (nominal)	2250	psia
Cold leg temperature (minimum)	532	°F
Hot leg temperature	587.4	°F
Number of plugged tubes per steam generator	900	—
Maximum asymmetry in number of plugged tubes between the two steam generators	360	—
Low pressurizer pressure SIAS setpoint (minimum)	1646	psia
Safety injection tank pressure (min/max)	485 / 665	psig
Safety injection tank water volume (min/max)	1388 / 1588	ft^3
Safety injection tank water temperature (min/max)	90/124.5	°F
LPSI+HPSI pump flow rate (min, 1 train/max, 2 trains)	2568 / 10,942	gpm
Containment pressure (minimum)	13.782	psia
Containment temperature (minimum)	90.0	°F
Containment humidity (maximum)	100.0	%
Containment net free volume (maximum)	2.6313×10^6	ft^3
Containment spray pump flow rate (maximum)	4500	gpm/pump
Refueling water tank temperature (min/max)	51/104	°F

(1) These quantities correspond to the rod average burnup of the hot rod (500 MWD/MTU) that yields the highest peak cladding temperature.

Table 15.6.5-2 Large Break LOCA ECCS Performance Analysis Results

Break Size (DEG/PD)	Peak Cladding Temperature (ºF)	Maximum Cladding Oxidation (%)	Maximum Core-Wide Oxidation (%)
1.0	2065	13.31	<1.0
0.8	2076	13.75	<1.0
0.6	2087	14.48	<1.0
0.4	2054	12.71	<1.0

Table 15.6.5-3 Large Break LOCA ECCS Performance Analysis Times of Interest (seconds after break)

Break Size (DEG/PD)	SITs Inject	Time of Annulus Downflow	Start of Reflood	SITs Empty	SI Pumps On	Hot Rod Rupture
1.0	11.86	22.79	38.64	113.61	36.59	58.42
0.8	13.35	24.30	39.77	115.14	36.62	56.82
0.6	15.78	27.00	41.85	117.62	36.69	55.01
0.4	20.61	32.47	46.07	123.07	36.88	76.42

Table 15.6.5-4 Large Break LOCA ECCS Performance Analysis Variables Plotted as a Function of Time for Each Break

Variable
Core Power
Pressure in Center Hot Assembly Node
Break Flow Rate
Hot Assembly Flow Rate (Below Hot Spot)
Hot Assembly Flow Rate (Above Hot Spot)
Hot Assembly Quality
Containment Pressure
Mass Added to Core During Reflood
Peak Cladding Temperature(1)

(1) The cladding temperature at the elevation of cladding rupture is also shown for the limiting break.

Table 15.6.5-5 Large Break LOCA ECCS Performance Analysis Variables Plotted as a Function of Time for the Limiting Break

Variable
Mid Annulus Flow Rate
Quality Above and Below the Core
Core Pressure Drop
Safety Injection Flow Rate into Intact Discharge Legs
Water Level in Downcomer During Reflood
Hot Spot Gap Conductance
Maximum Local Cladding Oxidation Percentage
Fuel Centerline, Fuel Average, Cladding, and Coolant Temperature at the Hot Spot
Hot Spot Heat Transfer Coefficient
Hot Rod Internal Gas Pressure
Core Bulk Channel Flow Rate

Table 15.6.5-6 Small Break LOCA ECCS Performance Analysis Input Parameters and Initial Conditions

Quantity	Value	Units
Reactor power level (100.3% of rated power)	3030	MWt
Peak linear heat generation rate	13.0	kW/ft
Axial shape index	-0.16	asiu
Moderator temperature coefficient at initial density	0.3×10^{-4}	$\Delta\rho/^{o}F$
RCS flow rate	375,000	gpm
RCS pressure	2250	psia
Cold leg temperature	554	^{o}F
Hot leg temperature	609	^{o}F
Number of plugged tubes per steam generator	900	—
MSSV first bank opening pressure	1030	psia
Low pressurizer pressure reactor trip setpoint	1810	psia
Low pressurizer pressure SIAS setpoint	1646	psia
HPSI pump flow rate	Table 15.6.5-7	gpm
Safety injection tank pressure	500	psia
Minimum charging pump flow (40% of one pump credited)	35	gpm
Maximum time delay for actuation of charging flow (with loss of offsite power)	330	second

Table 15.6.5-7 High Pressure Safety Injection Pump Minimum Delivered Flow to RCS (Assuming Failure of an Emergency Diesel Generator)

RCS Pressure (psia)	Flow Rate (gpm)
1212	0
1205	63.6
1198	76.8
1177	109.6
1104	194.4
1035	244.4
943	290.4
829	340.4
699	393.2
551	448.8
393	500.4
217	551.6
0	608.4

(1) The flow is assumed to be split equally to each of the four discharge legs.
(2) The flow to the broken discharge leg is assumed to spill out the break.

Table 15.6.5-8 Small Break LOCA ECCS Performance Analysis Results

Break Size	Peak Cladding Temperature (ºF)	Maximum Cladding Oxidation (%)	Maximum Core-Wide Cladding Oxidation (%)
0.04 ft^2/PD	1810	6.80	<0.72
0.05 ft^2/PD	1903	9.21	< 0.94
0.06 ft^2/PD	1839	3.44	<0.392

Table 15.6.5-9 Small Break LOCA ECCS Performance Analysis Times of Interest (seconds after break)

Break Size	HPSI Flow Delivered to RCS	LPSI Flow Delivered to RCS	SIT Flow Delivered to RCS	Peak Cladding Temperature Occurs
0.04 ft^2/PD	153	(1)	2489(2)	2085
0.05 ft^2/PD	117	(1)	1766(2)	1700
0.06 ft^2/PD	93	(1)	1397	1400

(1) Calculation completed before LPSI flow delivery to RCS begins.
(2) SIT injection calculated to begin but not credited in analysis.

Table 15.6.5-10 Small Break LOCA ECCS Performance Analysis Variables Plotted as a Function of Time for Each Break

Variable
Core Power
Inner Vessel Pressure
Break Flow Rate
Inner Vessel Inlet Flow Rate
Inner Vessel Two-Phase Mixture Level
Heat Transfer Coefficient at Hot Spot
Coolant Temperature at Hot Spot
Cladding Temperature at Hot Spot

Table 15.6.5-11 EPU Post-LOCA Long-Term Cooling Analysis Input Parameters and Initial Conditions

Quantity	Value	Units
Reactor power level (102% of rated power)	3030	MWt
Number of plugged tubes per steam generator	900	—
SG/RCS cooldown rate	75*	°F/hr
Shutdown cooling entry temperature	300	°F
RCS pressure measurement uncertainty	±90	psi
Number of atmospheric dump valves/SG	1	—
Atmospheric dump valve flow rate, at 55 psia	54,000	lbm/hr/valve
Condensate storage tank volume	276,200	gal
Reactor coolant system		
liquid mass	479,000	lbm
boron concentration	2200	ppm
Boric acid makeup tanks		
number	2	—
liquid volume (total)	19,950	gal
boric acid concentration	3.56	wt%
Refueling water tank		
liquid mass	4,325,565	lbm
boron concentration	2600	ppm
Safety injection tanks		
number	4	—
liquid volume per tank	1588	ft^3
boron concentration	2600	ppm
Charging pumps		
number	3	—
flow rate per pump	49	gpm
Flow rates for emptying the RWT		
HPSI pump flow rate	515	gpm
LPSI pump flow rate	2213	gpm
CS pump flow rate	2701	gpm

* Analysis conclusions were verified to be applicable for a cooldown rate of 50 ^{0}F/hr.

Table 15.6.5-12

Loss of Coolant Accident (LOCA) – Inputs and Assumptions

Input/Assumption	Value
Release Inputs:	
Core Power Level	3030 MW_{th} (3020 + 0.3%)
Core Average Fuel Burnup	49,000 MWD/MTU
Fuel Enrichment	1.5 – 5.05 w/o
Initial RCS Equilibrium Activity	1.0 μCi/gm DE I-131 and 518.9 μCi/gm DE Xe-133 gross activity (Table 15.6.5-15)
Core Fission Product Inventory	Table 15.0-32
Containment Leakage Rate 0 to 24 hours after 24 hours	 0.5% (by weight)/day 0.25% (by weight)/day
LOCA release phase timing and duration	Table 15.6.5-13
Core Inventory Release Fractions (gap release and early in-vessel damage phases)	RG 1.183, Sections 3.1 and 3.2
<u>ECCS Systems Leakage</u> Sump Volume (minimum) ECCS Leakage to RAB (2 times allowed value) Flashing Fraction Chemical form of the iodine in the sump water Release ECCS Area Filtration Efficiency	 57,683 ft^3 1.08 gph Calculated – 5.7% Used for dose determination – 10% 0% aerosol, 97% elemental, and 3.0% organic Elemental – 95% Organic – 95% Particulate – 99% (100% of the particulates are retained in the ECCS fluid)
RWT Back-leakage Sump Volume (at time of recirculation) ECCS Leakage to RWT (more than 2 times allowed value) Flashing Fraction (elemental Iodine assumed to be released into tank space based upon partition factor)	 57,683 ft^3 2 gpm 0 % based on temperature of fluid reaching RWT
Initial RWT Liquid Inventory (minimum)	65,350 gal
Release from RWT Vapor Space	Table 15.6.5-14
Containment Purge Release	2500 cfm for 30 seconds
Removal Inputs:	
Containment Particulate/Aerosol Natural Deposition (only credited in unsprayed regions)	0.1/hour
Containment Elemental Iodine Natural/Wall Deposition	2.89/hour
Containment Spray Region Volume	2,125,000 ft^3
Containment Unsprayed Region Volume	375,000 ft^3
Flowrate between sprayed and unsprayed volumes	12,500 cfm

Table 15.6.5-12 (continued)

Loss of Coolant Accident (LOCA) – Inputs and Assumptions

Input/Assumption	Value
Spray Removal Rates: Elemental Iodine Time to reach DF of 200 Particulate Iodine Time to reach DF of 50	 20/hour 3.07 hours 6.52/hour 2.64 hours
Spray Initiation Time Spray Termination Time	60 seconds (0.01667 hours) 8 hours
Control Room Ventilation System Time of automatic control room isolation Time of manual control room unisolation	 30 seconds 1.5 hrs
Secondary Containment Filter Efficiency	Particulate – 99% Elemental – 95% Organic – 95%
Secondary Containment Drawdown Time	310 seconds
Secondary Containment Bypass Fraction	9.6%
Containment Purge Filtration	0 %
Transport Inputs:	
Containment Release Secondary Containment release prior to drawdown	Nearest containment penetration to CR ventilation intake
Containment Release Secondary Containment release after drawdown	Plant stack
Containment Release Secondary Containment Bypass Leakage	Nearest containment penetration to CR ventilation intake
ECCS Leakage	ECCS exhaust louver
RWT Backleakage	RWT
Containment Purge	Plant Stack
Personnel Dose Conversion Inputs:	
Atmospheric Dispersion Factors Offsite Onsite	 Appendix 2.5C Table 15.6.5-16
Breathing Rates	RG 1.183 Sections 4.1.3 and 4.2.6
Control Room Occupancy Factor	RG 1.183 Section 4.2.6

Table 15.6.5-13*

LOCA Release Phases

Phase	Onset	Duration
Gap Release	30 seconds	0.5 hours
Early In-Vessel	0.5 hours	1.3 hours

* From RG 1.183, Table 4

Table 15.6.5-14

Release from RWT

Time (hours)	Release Rate (cfm)
0.0	0.0
0.37	5.485E-07
10.0	5.524E-06
25.0	3.235E-05
75.0	1.104E-04
125.0	2.026E-04
200.0	3.278E-04
300.0	4.659E-04
450.0	5.694E-04
600.0	6.223E-04

Table 15.6.5-15
Reactor Coolant Source Term

Nuclide	RCS Activity µCi/gm	Nuclide	RCS Activity µCi/gm
Co-58	4.394E-02	Ba-139	4.800E-04
Co-60	8.256E-02	Ba-140	7.124E-03
Kr-85	4.160E+01	La-140	3.299E-03
Kr-85m	1.268E+00	La-141	2.646E-04
Kr-87	7.574E-01	La-142	7.483E-05
Kr-88	2.247E+00	Ce-141	1.147E-03
Rb-86	3.403E-02	Ce-143	6.485E-04
Sr-89	5.691E-03	Ce-144	9.815E-04
Sr-90	5.459E-04	Pr-143	1.031E-03
Sr-91	1.526E-03	Nd-147	4.302E-04
Sr-92	6.105E-04	Kr-83m	3.826E-01
Y-90	7.799E-04	Xe-138	5.168E-01
Y-91	3.327E-02	Xe-131m	3.022E+00
Y-92	7.402E-04	Xe-133m	3.479E+00
Y-93	4.706E-04	Xe-135m	8.553E-01
Zr-95	1.159E-03	Cs-138	9.667E-01
Zr-97	5.170E-04	Cs-134m	1.179E-01
Nb-95	1.187E-03	Rb-88	2.326E+00
Mo-99	5.111E+00	Rb-89	1.022E-01
Tc-99m	3.885E+00	Sb-124	1.910E-03
Ru-103	1.359E-03	Sb-125	1.277E-02
Ru-105	1.934E-04	Sb-126	9.173E-04
Ru-106	7.973E-04	Te-131	1.741E-02
Rh-105	7.047E-04	Te-134	2.280E-02
Sb-127	5.187E-02	Te-125m	2.828E-03
Sb-129	2.918E-02	Te-133m	1.326E-02
Te-127	5.496E-02	Ba-141	1.009E-04
Te-127m	8.677E-03	Rh-103m	1.350E-03
Te-129	4.558E-02	Nb-97	8.889E-05
Te-129m	2.486E-02	Nb-95m	8.343E-06
Te-131m	4.273E-02	Pm-147	1.069E-04
Te-132	5.233E-01	Pm-148	1.866E-04
I-131	8.425E-01	Pm-149	3.485E-04
I-132	1.689E-01	Pm-151	1.021E-04
I-133	8.713E-01	Pm-148m	2556E-05

Table 15.6.5-15
Reactor Coolant Source Term (continued)

Nuclide	RCS Activity µCi/gm	Nuclide	RCS Activity µCi/gm
I-134	7.726E-02	Pr-144	9.816E-04
I-135	3.933E-01	Y-94	1.528E-05
Xe-133	2.381E+02	Y-91m	8.872E-04
Xe-135	9.235E+00	Br-82	6.096E-02
Cs-134	6.972E+00	Br-83	1.214E-01
Cs-136	1.543E+00	Br-84	5.002E-02
Cs-137	2.899E+00		

Table 15.6.5-16a

Control Room χ/Q (SBVS Bypass Leakage)

Time (hours)	χ/Q (sec/m^3)
0	7.29E-03
0.00833	3.33E-03
1.5	1.95E-03
2	1.57E-03
8	6.56E-04
24	4.75E-04
96	3.99E-04
720	3.99E-04

Table 15.6.5-16b

Control Room χ/Q (SBVS Leakage and Containment Purge)

Time (hours)	χ/Q (sec/m^3)
0	2.39E-03
0.00833	3.96E-03
1.5	6.70E-04
2	4.58E-04
8	2.02E-04
24	1.40E-04
96	1.13E-04
720	1.13E-04

Table 15.6.5-16c

Control Room χ/Q (ECCS Leakage)

Time (hours)	χ/Q (sec/m^3)
0	4.80E-03
0.00833	5.06E-03
1.5	3.22E-03
2	2.67E-03
8	1.14E-03
24	8.62E-04
96	7.04E-04
720	7.04E-04

Table 15.6.5-16d

Control Room χ/Q (RWT Leakage)

Time (hours)	χ/Q (sec/m^3)
0	1.37E-03
0.00833	1.34E-03
1.5	1.04E-03
2	8.49E-04
8	3.64E-04
24	2.73E-04
96	2.32E-04
720	2.32E-04

Table 15.6.5-17

LOCA Dose Consequences

Dose Contribution	TEDE Dose (rem) EAB(1) worst 2-hr	LPZ(2) 30 days	CR(2) 30 days
Containment Purge	2.1885E-03	2.1065E-03	3.1450E-02
Containment Leakage	1.2508E+00	2.6861E+00	4.2371E+00
ECCS Leakage	1.6024E-03	1.6290E-02	1.3128E-01
RWT Leakage	1.3477E-03	3.1463E-02	9.1111E-02
Shine Dose			0.15
Total	**1.26**	**2.74**	**4.64**
Acceptance Criteria	***25***	***25***	***5***

(1) Worst 2-hour dose
(2) Integrated 30-day dose

Table 15.6.5-18

Sampled RLBLOCA Parameters

Phenomenological	
	Time in cycle (peaking factors, axial shape, rod properties, burnup)
	Break type (guillotine versus split)
	Critical flow discharge coefficients (break)
	Critical flow discharge coefficients (surgeline)
	Initial upper head temperature
	Film boiling heat transfer
	Dispersed film boiling heat transfer
	Critical heat flux
	T_{min} (intersection of film and transition boiling)
	Initial stored energy
	Downcomer hot wall effects
	Condensation interphase heat transfer
	Metal-water reaction
Plant[1]	
	Offsite power availability[2]
	Break size
	Pressurizer pressure
	Pressurizer liquid level
	SIT pressure
	SIT liquid level
	SIT temperature (based on containment temperature)
	Containment temperature
	Containment volume
	Initial RCS flow rate
	Initial operating RCS temperature

1 Uncertainties for plant parameters are based on typical plant-specific data with the exception of “Offsite power availability,” which is a binary result that is specified by the analysis methodology.

2 Not sampled.

Table 15.6.5-19

Plant Operating Range Supported by the LOCA Analysis

	Event	Operating Range
1.0	Plant Physical Description	
	1.1 Fuel	
	a) Cladding outside diameter	0.382 in.
	b) Cladding inside diameter	0.332 in.
	c) Cladding thickness	0.025 in.
	d) Pellet outside diameter	0.3255 in.
	e) Pellet density	95.35 percent of theoretical
	f) Active fuel length	136.7 in.
	g) Gd_2O_3 concentrations	2, 4, 6, 8 w/o
	1.2 RCS	
	a) Flow resistance	Analysis
	b) Pressurizer location	Analysis assumes location giving most limiting PCT (broken loop)
	c) Hot assembly location	Anywhere in core
	d) Hot assembly type	16X16 AREVA HTP with M5 cladding and Zirc-4 structural materials
	e) SG tube plugging	20 percent [1]
2.0	Plant Initial Operating Conditions	
	2.1 Reactor Power	
	a) Nominal reactor power	3029.06 MWt [2]
	b) LHR	13.0 kW/ft [3]
	c) F_Q	2.504 [3]
	d) Fr	1.810 [4]
	2.2 Fluid Conditions	
	a) Loop flow	138.9 Mlbm/hr ≤ M ≤ 161.8 Mlbm/hr
	b) RCS Cold Leg temperature	535.0 °F ≤ T ≤ 554.0 °F
	c) Pressurizer pressure	2180 psia ≤ P ≤ 2320 psia
	d) Pressurizer level	60.0 percent ≤ L ≤ 71.0 percent

1 In the RLBLOCA analysis, only the maximum 20% tube plugging in each steam generator was analyzed.

2 Includes 0.3% uncertainty.

3 F_Q is based on LHR. F_Q is sampled for each case from a lower bound (a case-specific maximum peaking factor determined from the power history data), to an upper bound value of 2.504,

4 The radial power peaking for the hot rod is including 6% measurement uncertainty and 3.5% allowance for control rod insertion affect. This value is not sampled in the uncertainty analysis.
$Fr_{tech\ spec}$ *(1+ uncert_Fr) * (1+uncert_cr_insertion) = 1.65*(1.0+0.06)*(1+0.035)=1.810

Table 15.6.5-19 (Continued)

Plant Operating Range Supported by the LOCA Analysis (Continued)

	Event	Operating Range	
	e) SIT pressure	499.7 psia ≤ P ≤ 679.7 psia	
	f) SIT liquid volume	1388 ft^3 ≤ V ≤ 1588 ft^3	
	g) SIT temperature	80.5 °F ≤ T ≤ 124.5 °F (coupled with containment temperature)	
	h) SIT resistance fL/D	As-built piping configuration	
	i) Minimum ECCS boron	≥1800 ppm	
3.0	Accident Boundary Conditions		
	a) Break location	Cold leg pump discharge piping	
	b) Break type	Double-ended guillotine or split	
	c) Break size (each side, relative to cold leg pipe area)	0.299 ≤ A ≤ 1.0 full pipe area (split) 0.299 ≤ A ≤ 1.0 full pipe area (guillotine)	
	d) Worst single-failure	Loss of one emergency diesel generator	
	e) Offsite power	On or Off	
	f) ECCS pumped injection temperature	104 °F	
	g) HPSI pump delay	20.0 (w/ offsite power) 30.0 (w/o offsite power)	
	h) LPSI pump delay	20.0 (w/ offsite power) 30.0 (w/o offsite power)	
	i) Containment pressure	13.78 psia	
	j) Containment temperature	80.5 °F ≤ T ≤ 124.5 °F	
	k) Containment sprays delay	0 s	
	l) LPSI flow	Broken Loop	
		RCS press	flow
		psia	gpm
		0.0	1267.2
		12.4	1200.0
		59.9	880.0
		94.3	560.0
		117.9	240.0
		125.5	0.0
		Intact Loop 1	
		RCS press	flow
		psia	gpm
		0.0	1267.2
		12.4	1200.0
		59.9	880.0
		94.3	560.0
		117.9	240.0
		125.5	0.0
		Intact Loop 2	
		RCS press	flow
		psia	gpm
		0.0	0.0
		12.4	0.0
		59.9	0.0
		94.3	0.0
		117.9	0.0
		125.5	0.0

Table 15.6.5-19 (Continued)

Plant Operating Range Supported by the LOCA Analysis (Continued)

	Event	Operating Range	
		Intact Loop 3	
		RCS press	flow
		psia	gpm
		0.0	0.0
		12.4	0.0
		59.9	0.0
		94.3	0.0
		117.9	0.0
		125.5	0.0
	m) HPSI flow	For each Loop,	
		RCS press	flow
		psia	gpm
		0.0	129.8
		12.4	129.3
		59.9	127.7
		94.3	126.4
		117.9	125.5
		125.5	125.2
		148.1	124.3
		307.6	116.9
		476.6	106.3
		603.7	95.6
		708.4	85.0
		800.7	74.4
		883.3	63.8
		954.3	53.1
		1009.7	42.5
		1045.8	31.9
		1062.6	10.6
		1063.1	0.0

Table 15.6.5-20

Statistical Distributions Used for Process Parameters[1]

Parameter	Operational Uncertainty Distribution	Parameter Range
Pressurizer Pressure (psia)	Uniform	2180 – 2320
Pressurizer Liquid Level (percent)	Uniform	60.0 – 71.0
SIT Liquid Volume (ft^3)	Uniform	1388 – 1588
SIT Pressure (psia)	Uniform	499.7 – 679.7
Containment Temperature (°F)	Uniform	80.5 – 124.5
Containment Volume (ft^3)	Uniform	2.493E+6 – 2.631E+6
Initial RCS Flow Rate (Mlbm/hr)	Uniform	138.9 – 161.8
Initial RCS Operating Temperature (Tcold) (°F)	Uniform	535.0 – 554.0
RWST Temperature for ECCS (°F)	Point	104
Offsite Power Availability[2]	Binary	0,1
Delay for Containment Spray (s)	Point	0
LPSI Pump Delay (s)	Point	20.0 (w/ offsite power) 30.0 (w/o offsite power)
HPSI Pump Delay (s)	Point	20.0 (w/ offsite power) 30.0 (w/o offsite power)

1 Note that core power and decay heat are not sampled.

2 This is not a sampled parameter. One set of 59 cases is run with LOOP and one set of 59 cases is run with No-LOOP.

Table 15.6.5-21

Passive Heat Sinks in Containment

Heat Sink	Area (ft^2)	Thickness (ft)	Material
Containment Primary Cylinder	58695	0.16	Carbon Steel
Containment Primary Dome	32340	0.08	Carbon Steel
Ground Floor	6020.0	2.0	Concrete
Shield Walls and Pads	67225.0	2.0	Concrete
Containment Sump	25093.0	3.0	Concrete
Stainless Steel – Embedded	8715.0	0.01563	Stainless Steel
Stainless Steel – piping and other comp.	16399.0	0.04249	Stainless Steel
Galvanized Steel – conduits and cable trays	165823.0	0.00924	Galvanized Steel
Structure and Misc. Exposed Steel	111802.0	0.06166	Carbon Steel

Material	Thermal Conductivity (BTU/hr-ft-°F)	Volumetric Heat Capacity (BTU/ft^3-°F)
Concrete	1.0	34.2
Carbon Steel	25.9	53.57
Stainless Steel	9.8	54.0
Galvanized Steel	64.0	40.6

Table 15.6.5-22

Containment Initial and Boundary Conditions

Containment Net Free Volume (ft^3)	2.493E+6 ft^3 – 2.631E+6 ft^3
Initial Conditions	
Containment Pressure (nominal)	13.78 psia
Containment Temperature	80.5 °F – 124.5 °F
Outside Temperature	26 °F
Humidity	1.0
Containment Spray	
Number of Pumps operating	2
Spray Flow Rate (Total, both pumps)	9,000 gpm
Minimum Spray Temperature	46 °F
Fastest Post-LOCA initiation of spray	0 s
Containment Fan Coolers	
Number of Fan Coolers Operating	4
Minimum Post Accident Initiation Time of Fan Coolers (sec)	0
Fan Cooler Capacity (1 Fan Cooler)	
Containment Temperature (F)	Heat Removal Rate (BTU/sec)
60	0
120	3167
200	14722
280	27639

Table 15.6.5-23

Summary of Results for the Limiting PCT Case

Case # 57 (offsite power unavailable)	Limiting Hot Rod (fresh UO_2 rod)
PCT	
Temperature	1732 °F
Time	105.6 s
Elevation	9.784 ft
Metal-Water Reaction[1]	
Percent Oxidation Maximum	2.2802%
Percent Total Oxidation	0.0139%

[1] These values are the oxidation calculated during the transient. A pre-transient oxidation of 1.057% was calculated for the fresh UO_2 rod, for a total of 3.337% maximum local oxidation.

Table 15.6.5-24

Calculated Event Times for the Limiting PCT Case

Event	Time (s)
Break Opened	0.0
RCP Trip	N/A
SIAS Issued	1.2
Start of Broken Loop SIT Injection	7.7
Start of Intact Loop SIT Injection (Loops 2, 3 and 4 respectively)	13.4, 13.5, and 13.3
Broken Loop LPSI Delivery Began	31.2
Intact Loop LPSI Delivery Began (Loops 2, 3 and 4 respectively)	31.2, N/A, and N/A
Broken Loop HPSI Delivery Began	31.2
Intact Loop HPSI Delivery Began (Loops 2, 3 and 4 respectively)	31.2, 31.2, and 31.2
Beginning of Core Recovery (Beginning of Reflood)	30.2
Broken Loop SIT Emptied	75.8
Intact Loop SITs Emptied (Loops 2, 3 and 4 respectively)	80.6, 75.4, and 76.2
PCT Occurred	105.6
Transient Calculation Terminated	551.9

Table 15.6.5-25

SBLOCA System Parameters and Initial Conditions

Reactor Power, MWt	3029.06[1]
Peak LHR, kW/ft	13.0
Radial Peaking Factor (1.65 plus uncertainty & augmentation factor)	1.81
RCS Flow Rate, gpm	370000
Pressurizer Pressure, psia	2250
Core Inlet Coolant Temperature, °F	554
SIT Pressure, psia	499.7
SIT Fluid Temperature, °F	124.5
Average SG Tube Plugging Level, %	20
SG Secondary Pressure, psia	846-849
MFW Temperature, °F	436
AFW Flow Rate per SG, gpm	255
AFW Temperature, °F	110
AFW Delay Time, sec	330
Low SG Level AFAS Setpoint, %	4
HPSI & LPSI Fluid Temperature, °F	104
Charging System Delay Time, sec	330
Reactor Trip - Low Pressurizer Pressure Setpoint, psia	1810
Reactor Trip Delay Time on Low Pressurizer Pressure, sec	1.15
SCRAM CEA Holding Coil Release Delay Time, sec	0.74
SIAS Activation Setpoint Pressure for Harsh Conditions, psia	1638
HPSI & LPSI Pump Delay Time on SIAS, sec	30
MSSV Lift Pressures and Tolerances	Nominal + 3% (Bank 1 Valves) Nominal + 2% (Bank 2 Valves)
Charging Flow Rate, gpm	21 (Loop 2B) 14 (Loop 1A)

[1] Includes 0.3% measurement uncertainty

Table 15.6.5-26

SBLOCA HPSI Flow Rate versus RCS Pressure

RCS Pressure (psia)	Loop 1A (gpm)	Loop 1B (gpm)	Loop 2A (gpm)	Loop 2B (gpm)
1063.1	0.0	0.0	0.0	0.0
1062.6	10.6	10.6	10.6	10.6
1062.0	21.3	21.3	21.3	21.3
1045.8	31.9	31.9	31.9	31.9
1009.7	42.5	42.5	42.5	42.5
954.3	53.1	53.1	53.1	53.1
883.3	63.8	63.8	63.8	63.8
800.7	74.4	74.4	74.4	74.4
708.4	85.0	85.0	85.0	85.0
603.7	95.6	95.6	95.6	95.6
476.6	106.3	106.3	106.3	106.3
307.6	116.9	116.9	116.9	116.9
148.1	124.3	124.3	124.3	124.3
125.5	125.2	125.2	125.2	125.2
117.9	125.5	125.5	125.5	125.5
94.3	126.4	126.4	126.4	126.4
59.9	127.7	127.7	127.7	127.7
12.4	129.3	129.3	129.3	129.3
0.0	129.8	129.8	129.8	129.8

Table 15.6.5-27

SBLOCA LPSI Flow Rate versus RCS Pressure

RCS Cold Leg Pressure (psia)	Intact Loop 1 1A (gpm)	Intact Loop 2 1B (gpm)	Intact Loop 3 2A (gpm)	Broken Loop 2B (gpm)
125.5	0.0	0.0	0.0	0.0
117.9	0.0	0.0	240.0	240.0
94.3	0.0	0.0	560.0	560.0
59.9	0.0	0.0	880.0	880.0
12.4	0.0	0.0	1200.0	1200.0
0.0	0.0	0.0	1267.2	1267.2

Table 15.6.5-28

Summary of SBLOCA Break Spectrum Results

Break diameter (in)	2.00	2.50	2.60	2.70	2.80	3.00
Break Area (ft^2)	0.022	0.034	0.037	0.040	0.043	0.049
Peak Clad Temperature (°F)	1708	1952	2030	2057	2003	1914
Time of PCT (sec)	3595	2575	2333	2125	1937	1617
Time of Rupture (sec)	--	2257	2079	1921	1775	1501
Transient Maximum Local Oxidation (%)	2.3898	7.5666	8.5535	8.9253	7.6124	5.1904
Total Local Maximum Oxidation (%)*	4.7823	9.9591	10.946	11.3178	10.0049	7.5829
Core Wide Oxidation (%)	0.1858	0.2440	0.2467	0.2353	0.1955	0.1248
PCT Elevation (ft)	11.02	11.02	11.02	11.02	11.02	11.02

Break diameter (in)	3.50	3.90	4.00	4.50	5.00	6.00
Break Area (ft^2)	0.067	0.083	0.087	0.110	0.136	0.196
Peak Clad Temperature (°F)	1731	1629	1461	1298	1067	1017
Time of PCT (sec)	1053	834	839	651	525	145
Time of Rupture (sec)	1025	--	--	--	--	--
Transient Maximum Local Oxidation (%)	1.4445	0.5044	0.2440	0.0734	0.0119	0.0065
Total Local Maximum Oxidation (%)*	3.837	2.8969	2.6365	2.4659	2.4044	2.399
Core Wide Oxidation (%)	0.0389	0.0177	0.0058	0.0012	0.0002	0.0001
PCT Elevation (ft)	10.77	10.52	10.52	10.27	10.27	10.02

Break diameter (in)	7.00	8.00	9.00	9.49
Break Area (ft^2)	0.267	0.349	0.442	0.491
Peak Clad Temperature (°F)	1078	1460	1451	1520
Time of PCT (sec)	128	170	155	136
Time of Rupture (sec)	--	--	--	--
Transient Maximum Local Oxidation (%)	0.0114	0.1545	0.1531	0.1800
Total Local Maximum Oxidation (%)*	2.4039	2.547	2.5456	2.5725
Core Wide Oxidation (%)	0.0002	0.0016	0.0020	0.0030
PCT Elevation (ft)	10.02	10.02	10.27	10.02

* Includes the pre-transient oxidation of 2.3925%.

Table 15.6.5-29

Sequence of Events for the SBLOCA Break Spectrum

Break diameter (in)	PCT (°F)	Break opens	Low PZR Pressure Trip	Reactor Scram, RCP and Turbine Trip	SIAS issued	HPSI available	LPSI available	Charging Flow Begins	HPSI Flow Begins	LPSI Flow Begins	Motor driven AFW on, Initial	Loop seal 1A clears	Loop seal 1B clears	Loop seal 2A clears	Loop seal 2B clears	Break uncovers	SIT injection begins	Minimum RV mass occurs	Hot Rod rupture occurs	PCT occurs	Time of core uncover	Non-condensible gas at the break
2.00	1708	0	50	52	63	93	93	394	1256	--	940	--	--	--	1070	1116	--	3260	--	3595	2292	--
2.50	1952	0	32	34	43	73	73	374	784	--	928	--	--	--	686	784	2582	2200	2257	2575	1476	--
2.60	2030	0	30	32	40	70	70	372	724	--	932	--	--	--	634	726	2328	2102	2079	2333	384	--
2.70	2057	0	28	29	38	68	68	368	668	--	934	--	--	--	604	670	2118	1956	1921	2125	352	--
2.80	2003	0	26	28	35	65	65	366	624	--	942	--	--	--	572	630	1930	1846	1775	1937	330	--
3.00	1914	0	22	24	32	62	62	362	550	--	1606	--	--	--	508	568	1602	1584	1501	1617	286	--
3.50	1731	0	17	19	25	55	55	356	416	--	--	--	--	--	378	404	1044	1042	1025	1053	208	--
3.90	1629	0	14	16	21	51	51	352	340	--	--	--	--	--	310	340	810	814	–	834	170	--
4.00	1461	0	13	15	21	51	51	352	322	--	--	404	--	--	296	306	824	828	--	839	158	--
4.50	1298	0	11	13	17	47	47	348	266	--	--	--	--	254	240	258	640	646	–	651	126	--
5.00	1067	0	10	12	15	45	45	346	220	--	--	--	--	206	196	220	512	516	--	525	102	--
6.00	1017	0	8	10	13	43	43	344	146	--	--	--	--	140	138	160	326	330	--	145	76	--
7.00	1078	0	8	10	12	42	42	342	104	1818	--	--	--	112	102	124	234	238	--	128	54	--
8.00	1460	0	8	9	11	41	41	342	68	940	--	102	102	--	80	106	164	166	--	170	48	1243
9.00	1451	0	7	9	11	41	41	342	52	198	--	68	74	70	60	84	132	134	--	155	40	724
9.49	1520	0	7	9	10	40	40	342	46	186	--	64	66	62	56	82	122	122	--	136	38	699

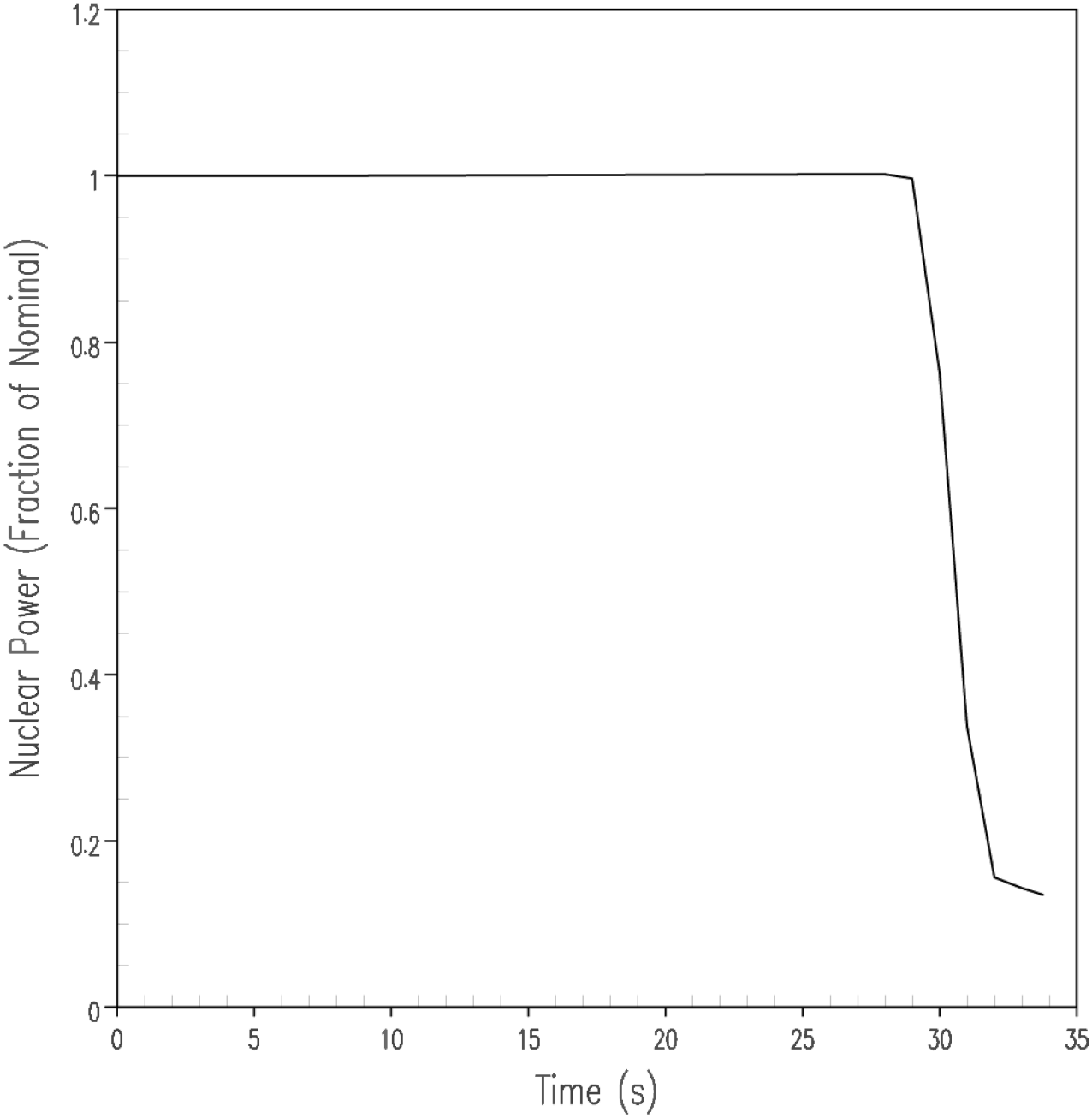

FLORIDA POWER & LIGHT COMPANY ST. LUCIE PLANT UNIT 2
FIGURE 15.6.1-1 Accidental Depressurization of the Reactor Coolant System Nuclear Power vs. Time

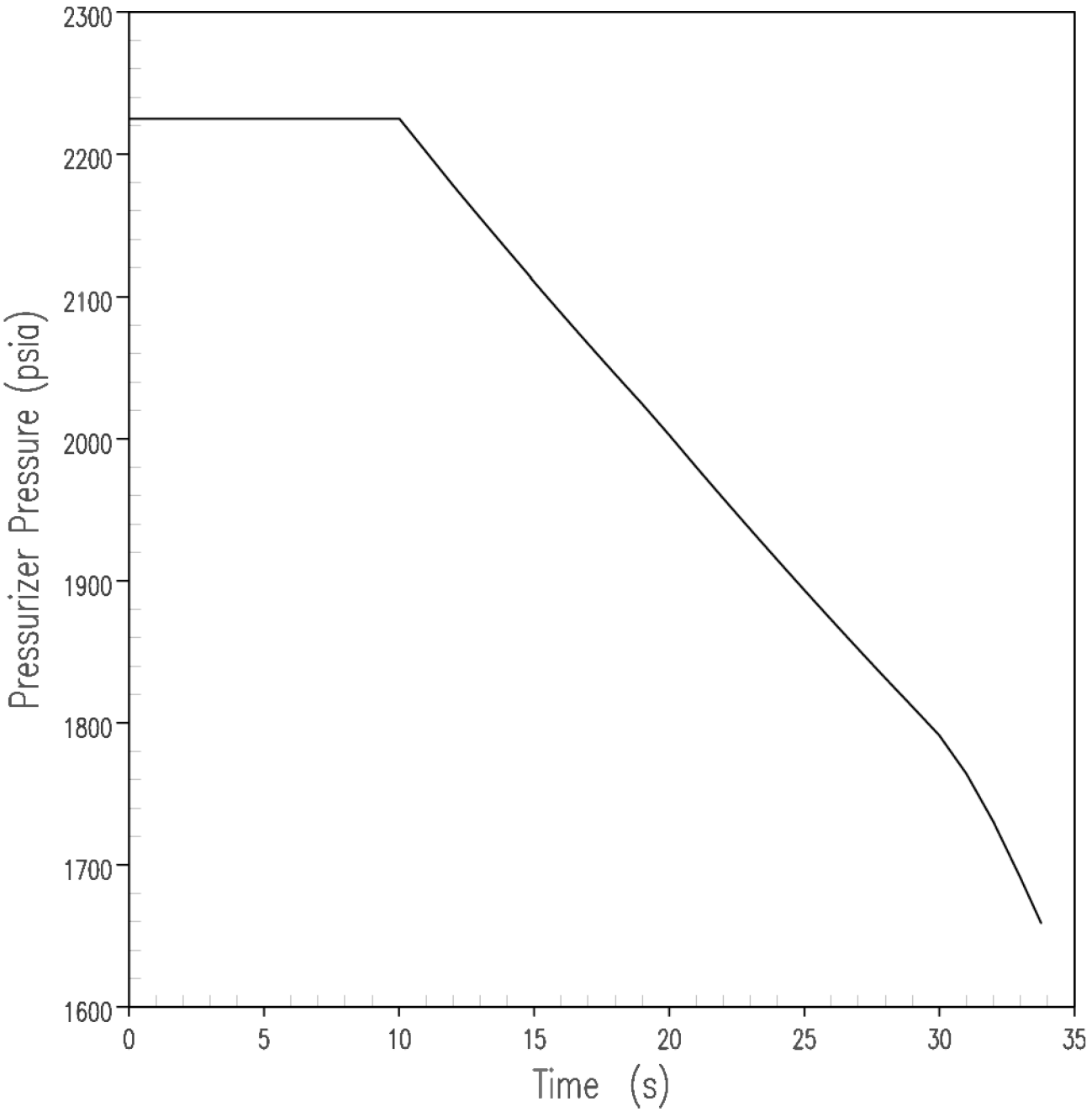

FLORIDA POWER & LIGHT COMPANY ST. LUCIE PLANT UNIT 2
FIGURE 15.6.1-2 Accidental Depressurization of the Reactor Coolant System Pressurizer Pressure vs. Time

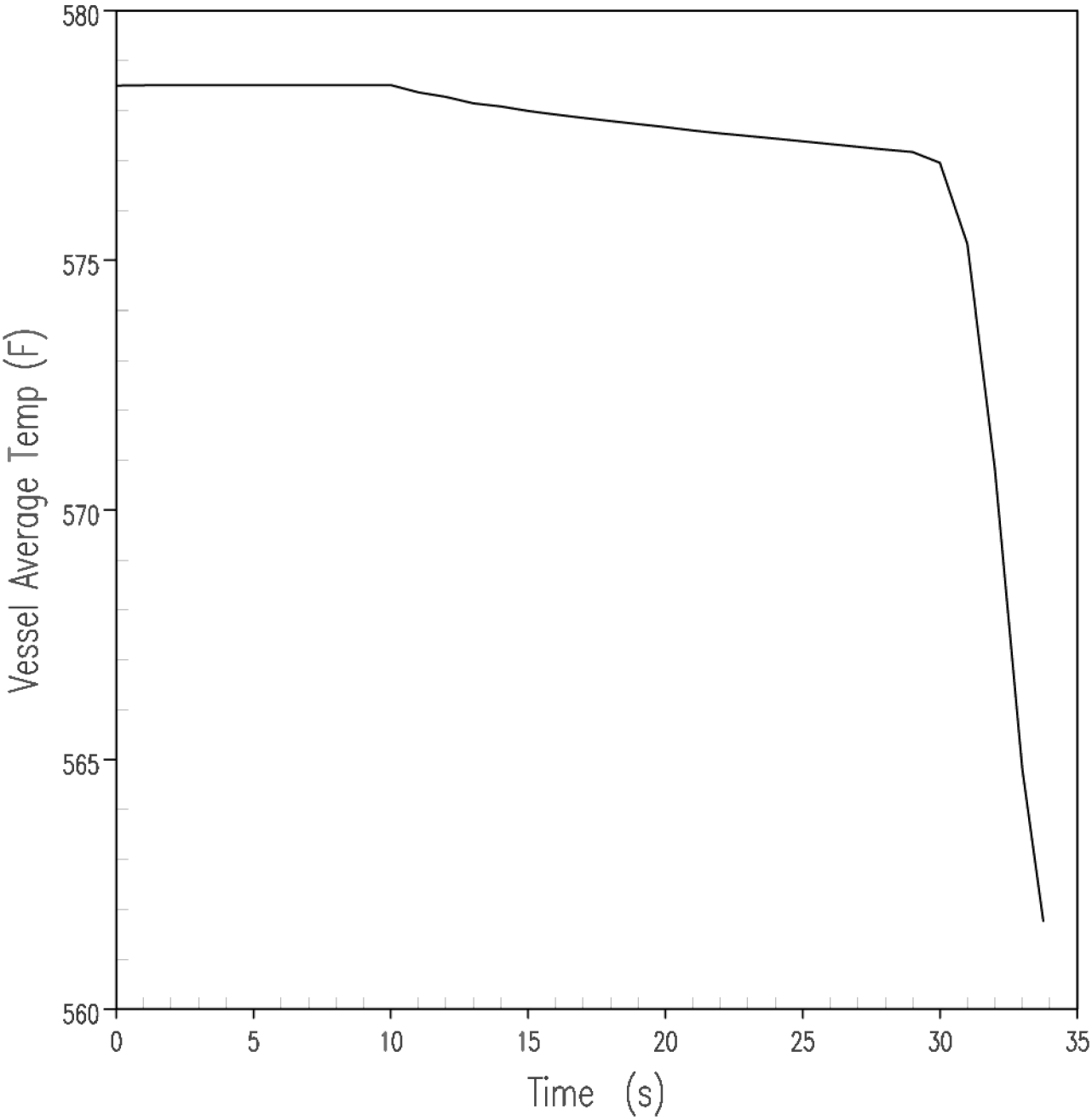

FLORIDA POWER & LIGHT COMPANY ST. LUCIE PLANT UNIT 2
FIGURE 15.6.1-3 Accidental Depressurization of the Reactor Coolant System Vessel Average Temperature vs. Time

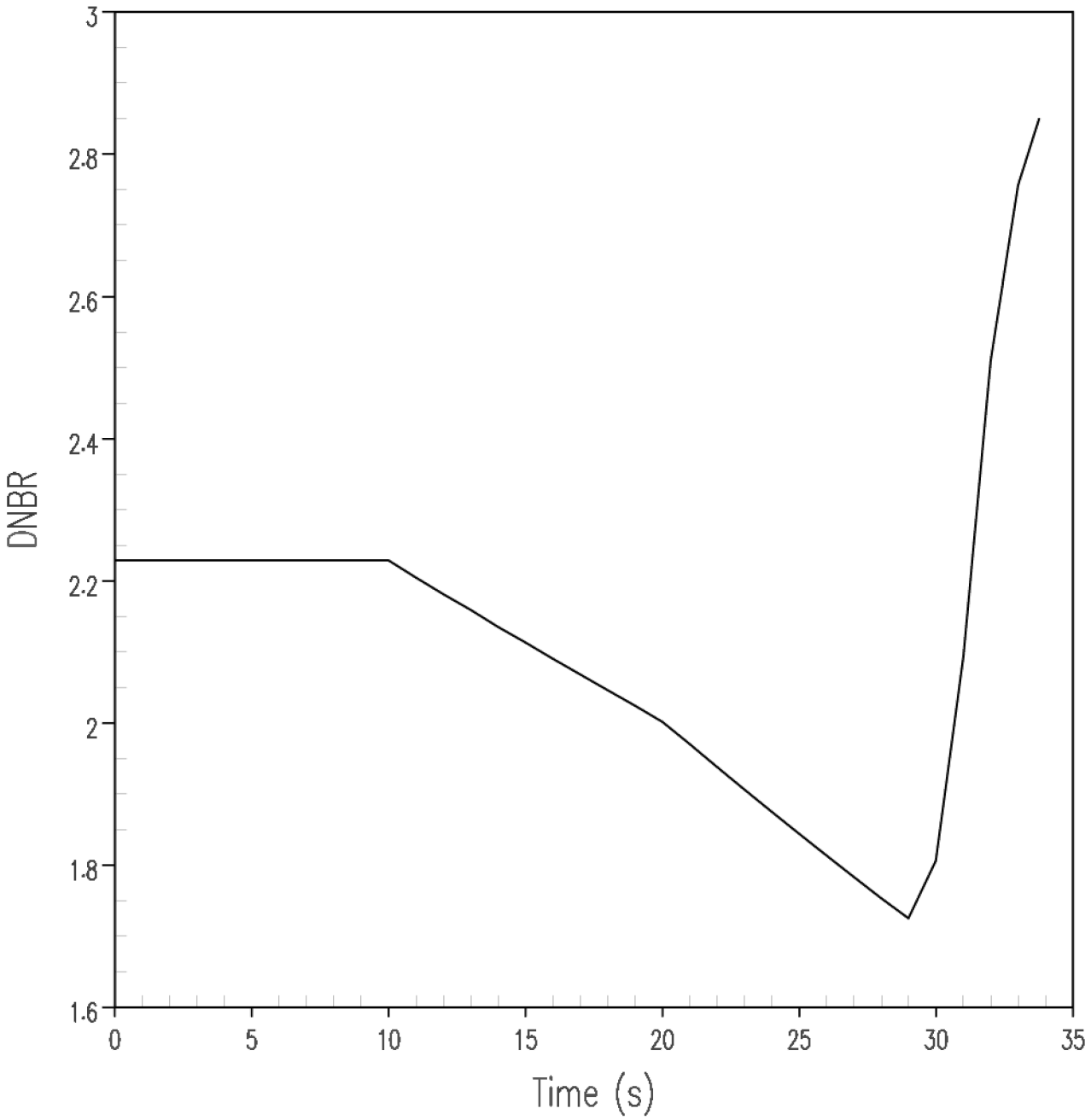

FLORIDA POWER & LIGHT COMPANY ST. LUCIE PLANT UNIT 2
FIGURE 15.6.1-4 Accidental Depressurization of the Reactor Coolant System DNBR vs. Time

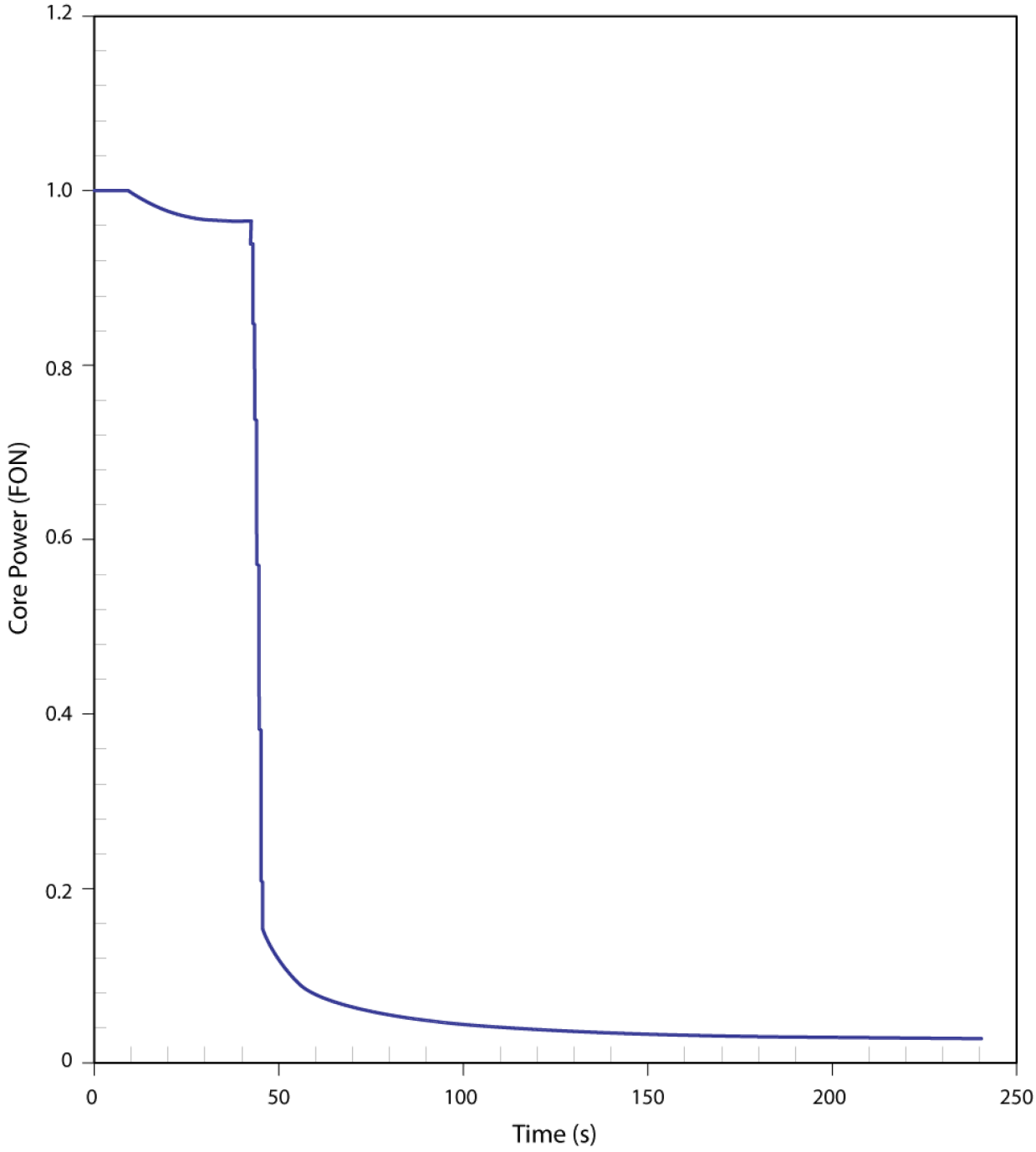

FLORIDA POWER & LIGHT COMPANY ST. LUCIE PLANT UNIT 2
FIGURE 15.6.1-5 Accidental Depressurization of the Reactor Coolant System Pressurizer Overfill Case Core Power vs. Time

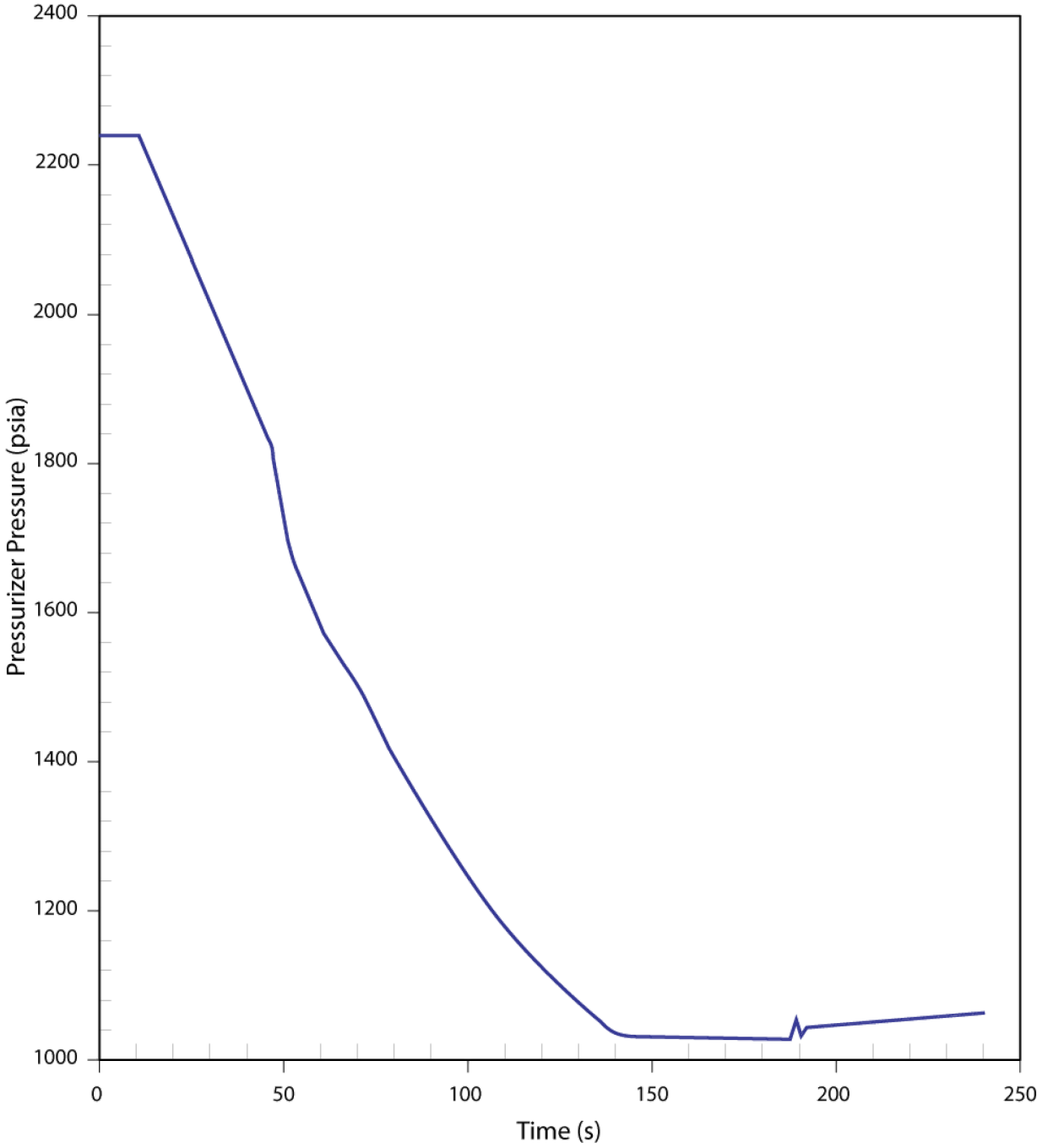

FLORIDA POWER & LIGHT COMPANY ST. LUCIE PLANT UNIT 2
FIGURE 15.6.1-6 Accidental Depressurization of the Reactor Coolant System Pressurizer Overfill Case Pressurizer Pressurer vs. Time

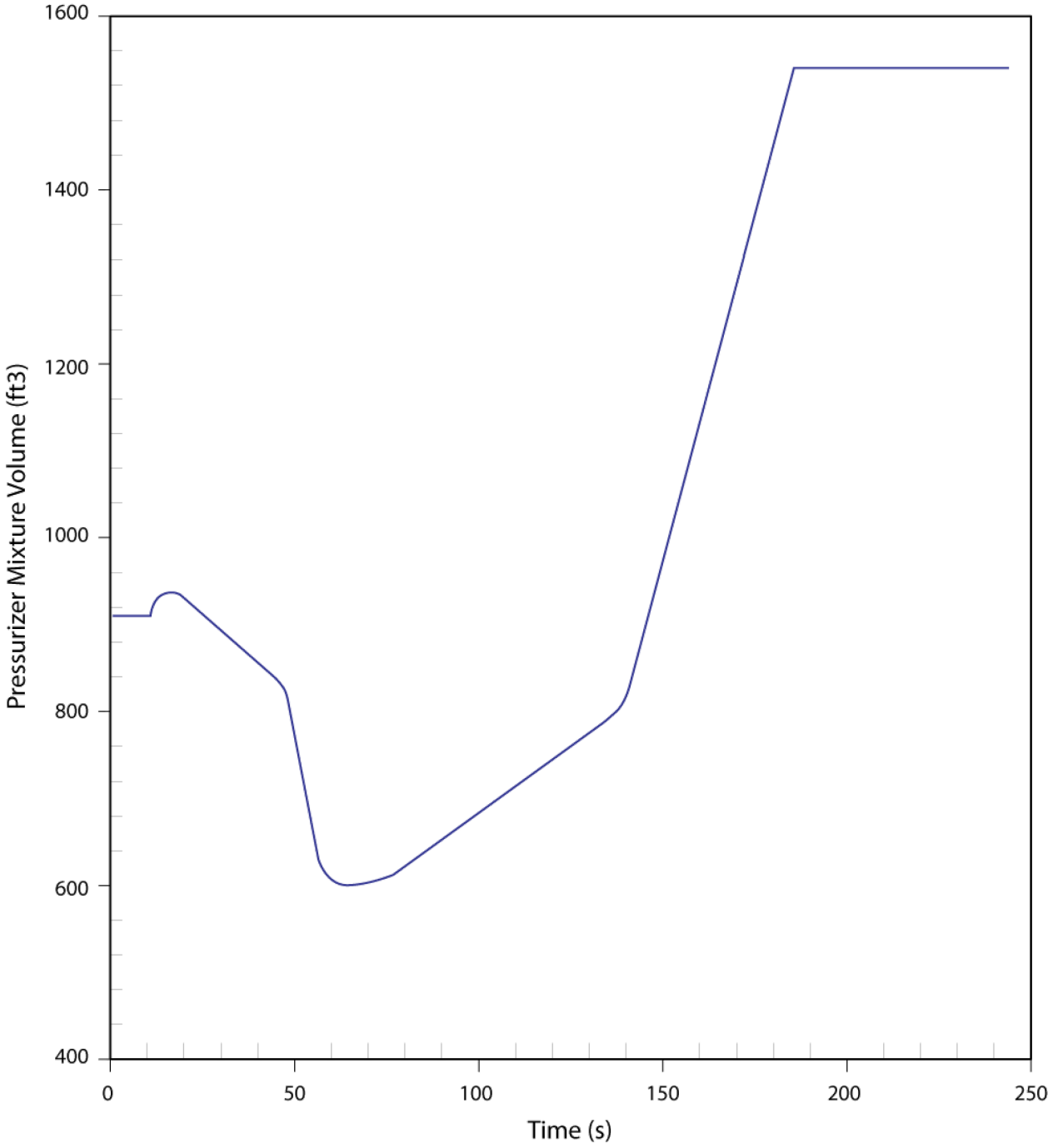

FLORIDA POWER & LIGHT COMPANY ST. LUCIE PLANT UNIT 2
FIGURE 15.6.1-7 Accidental Depressurization of the Reactor Coolant System Pressurizer Overfill Case Pressurizer Volume vs. Time

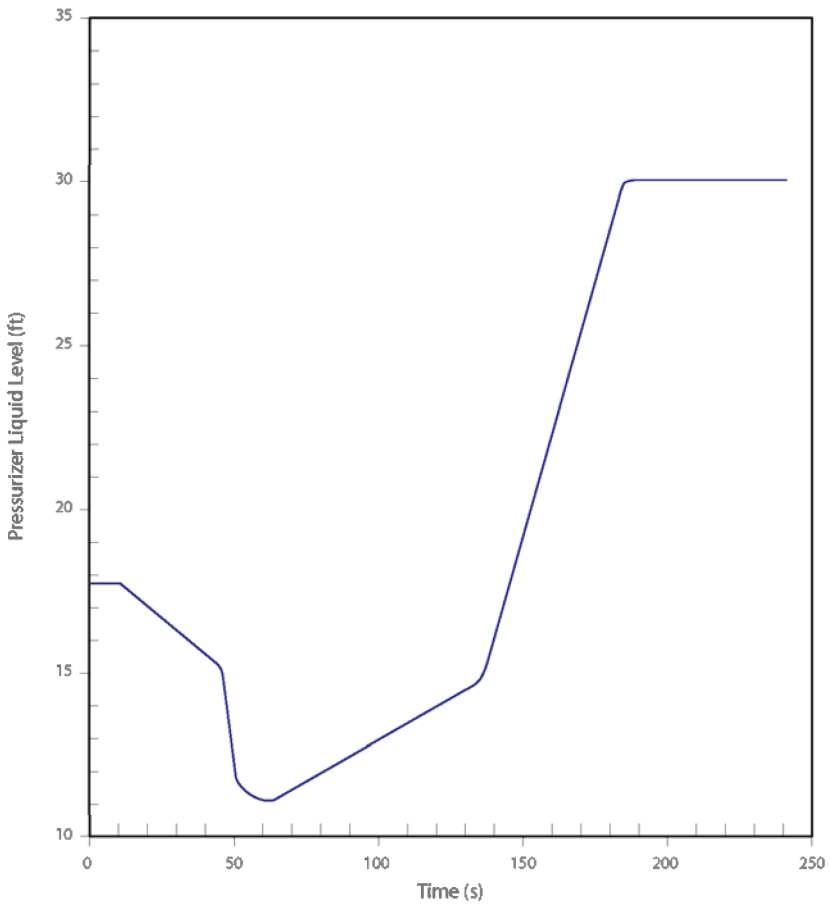

FLORIDA POWER & LIGHT COMPANY ST. LUCIE PLANT UNIT 2
FIGURE 15.6.1-8 Accidental Depressurization of the Reactor Coolant System Pressurizer Overfill Case Pressurizer Level vs. Time

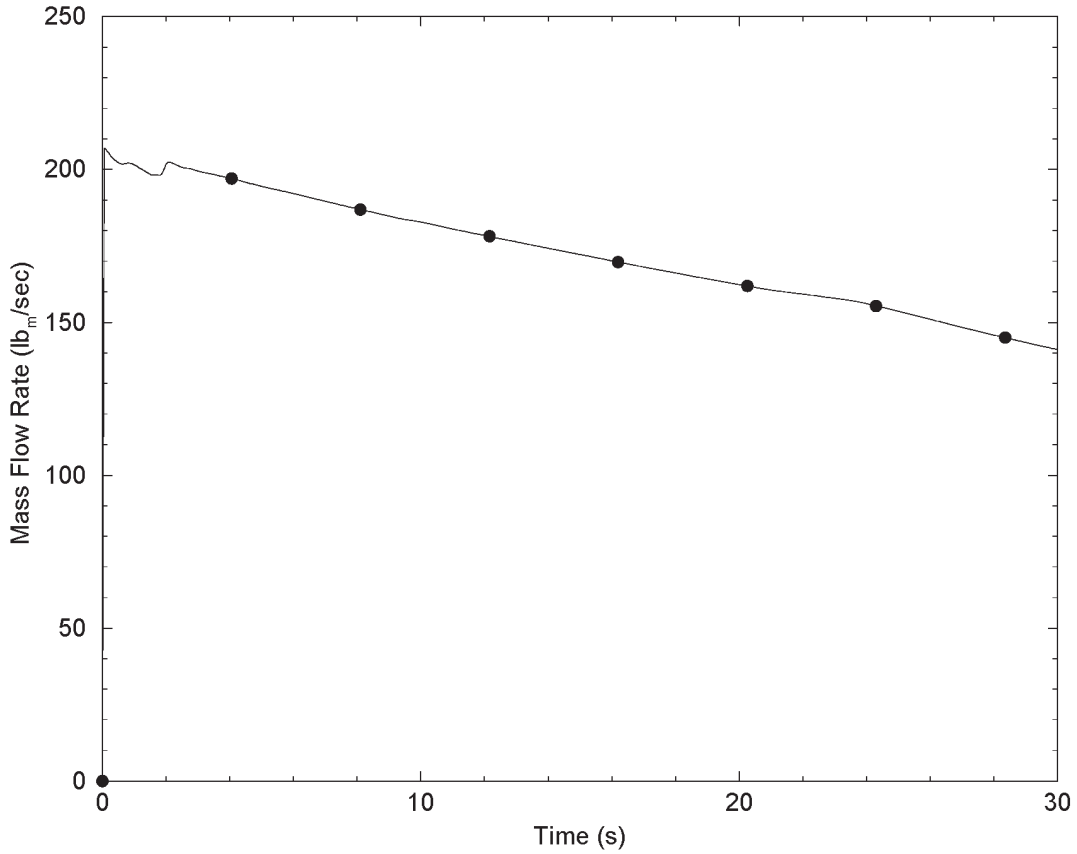

EC287528

FLORIDA POWER & LIGHT COMPANY
ST. LUCIE PLANT UNIT 2

Figure 15.6.1-9
RCS Depressurization (AREVA DNB):
Pressurizer PORVs Flow Rate vs. Time

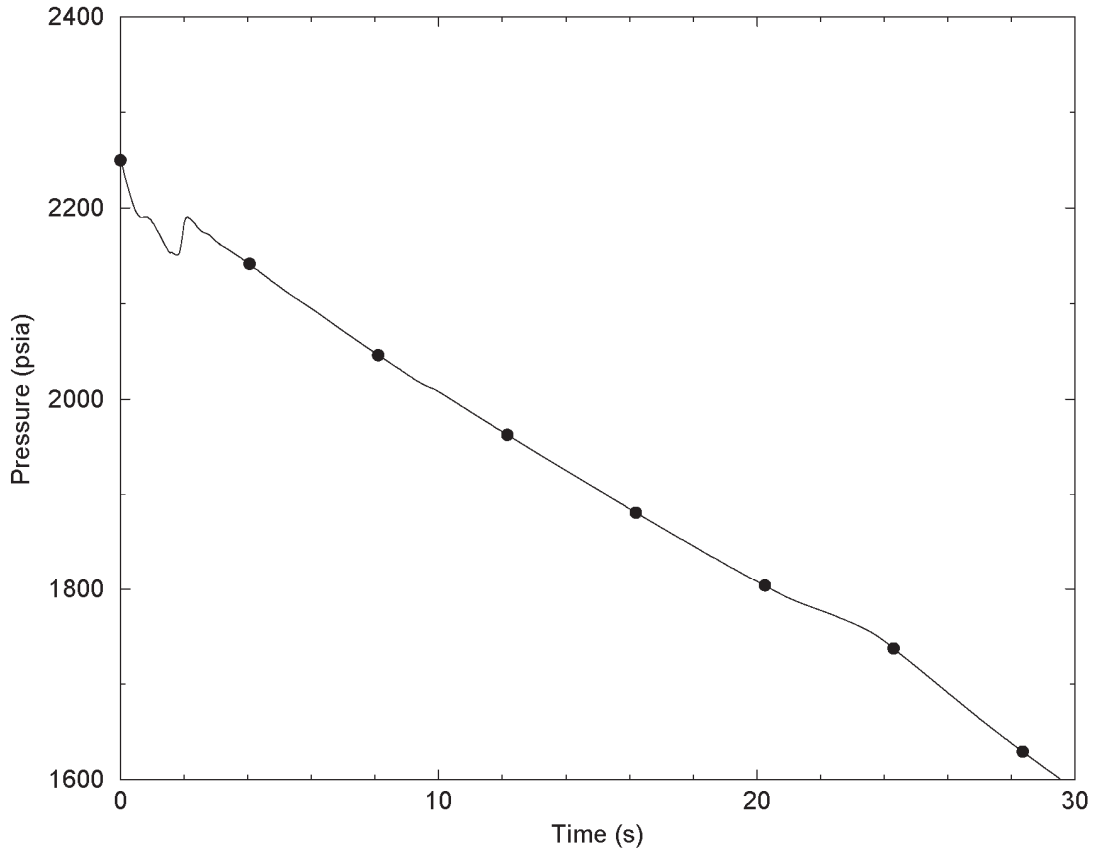

EC287528

FLORIDA POWER & LIGHT COMPANY
ST. LUCIE PLANT UNIT 2

Figure 15.6.1-10
RCS Depressurization (AREVA DNB):
Pressurizer Pressure vs. Time

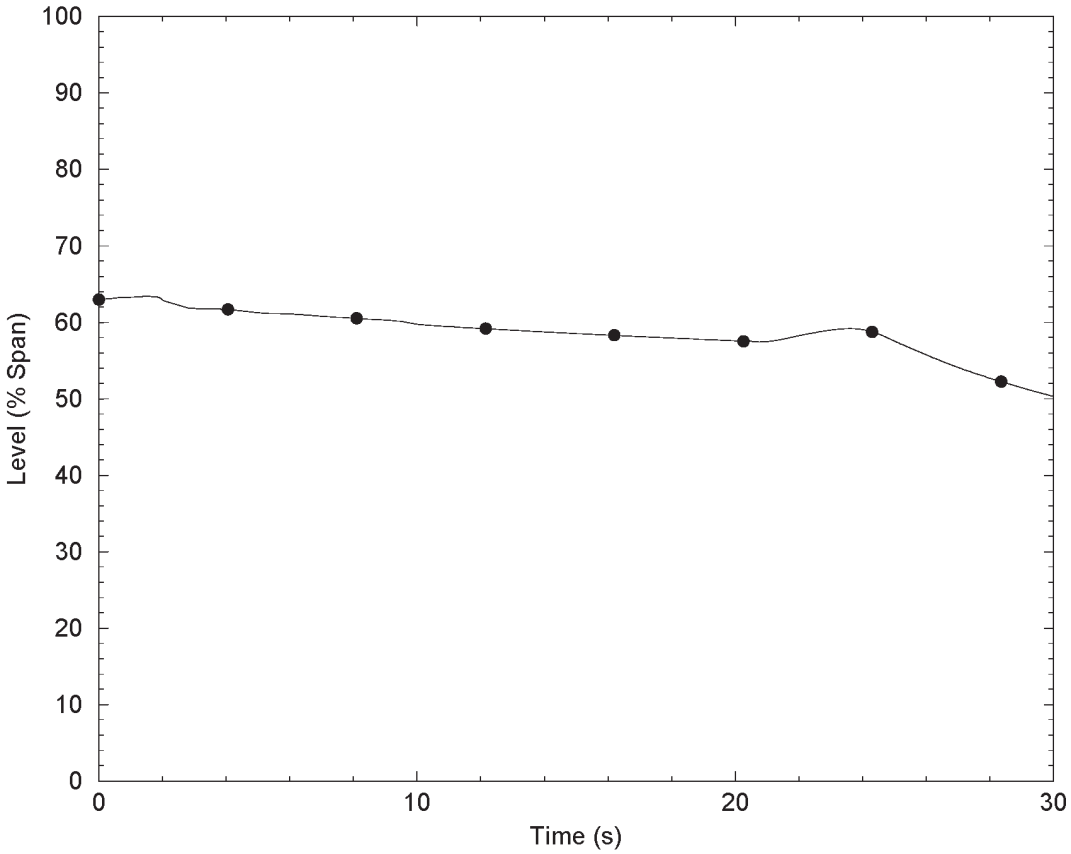

EC287528

FLORIDA POWER & LIGHT COMPANY
ST. LUCIE PLANT UNIT 2

Figure 15.6.1-11
RCS Depressurization (AREVA DNB):
Pressurizer Liquid Level vs. Time

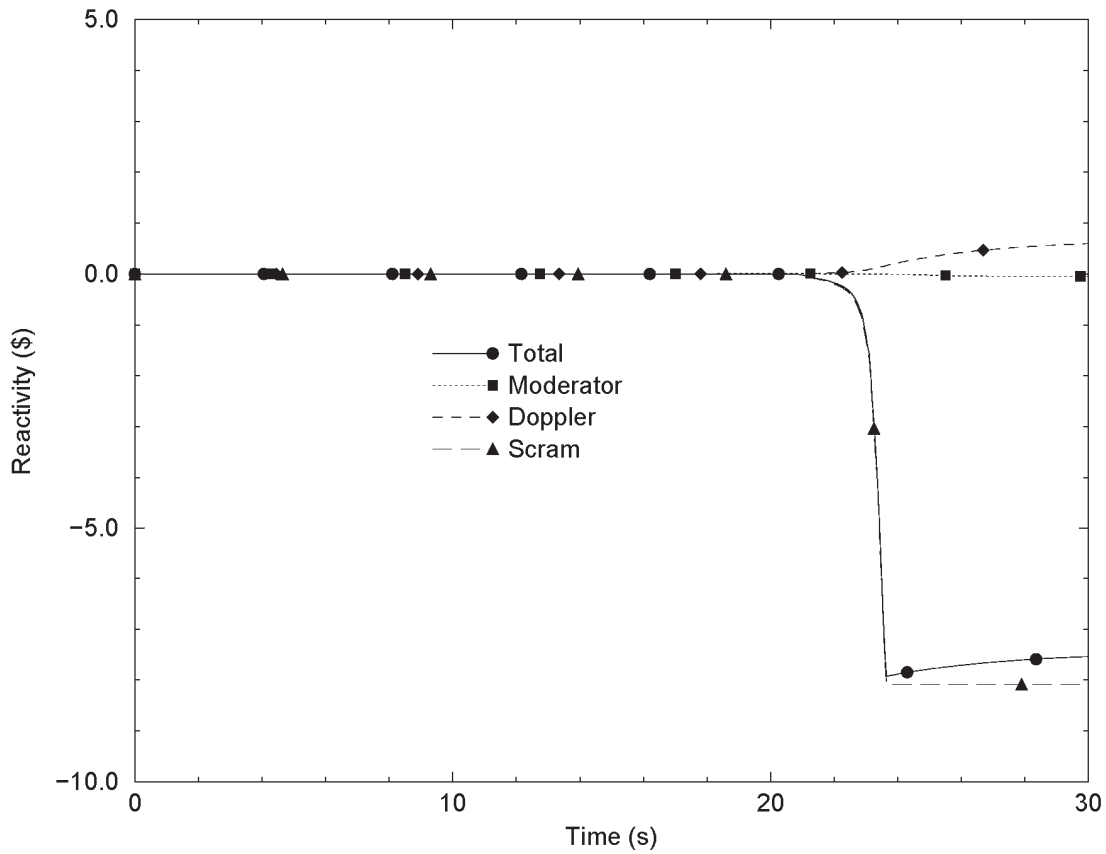

EC287528

FLORIDA POWER & LIGHT COMPANY
ST. LUCIE PLANT UNIT 2

Figure 15.6.1-12
RCS Depressurization (AREVA DNB):
Reactivity Feedback vs. Time

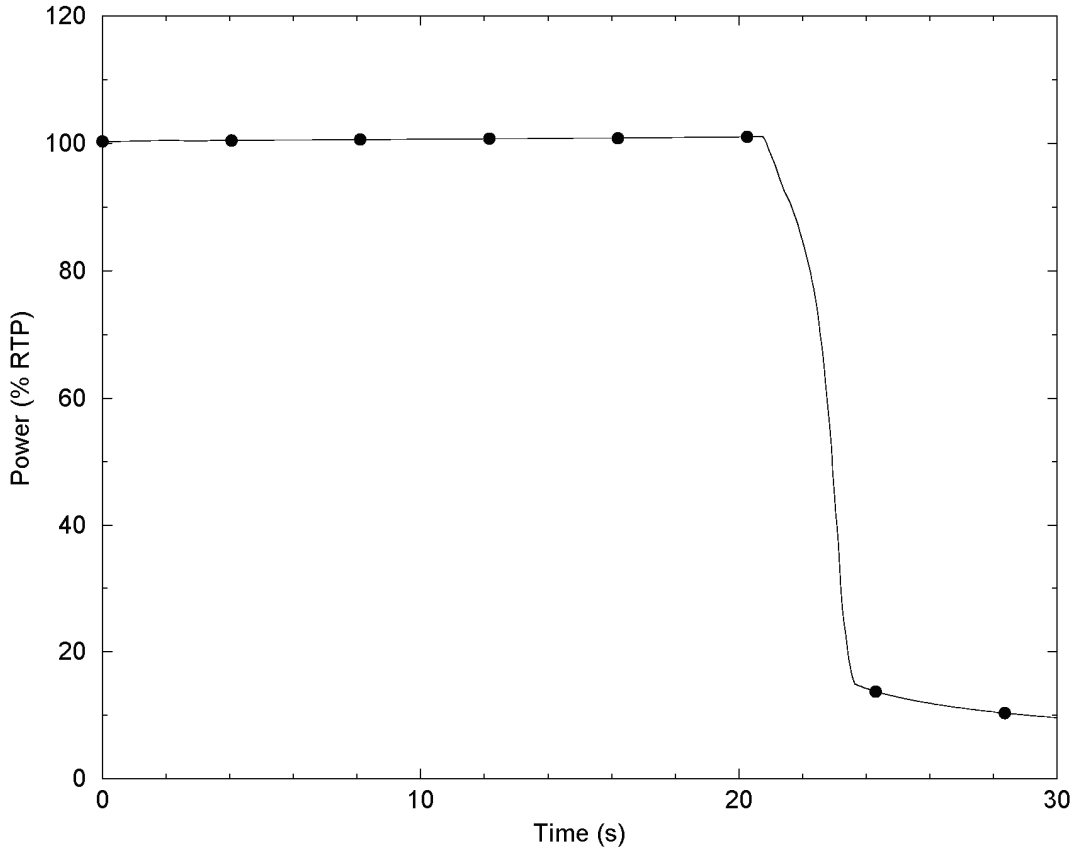

EC287528

FLORIDA POWER & LIGHT COMPANY
ST. LUCIE PLANT UNIT 2

Figure 15.6.1-13
RCS Depressurization (AREVA DNB):
Reactor Power vs. Time

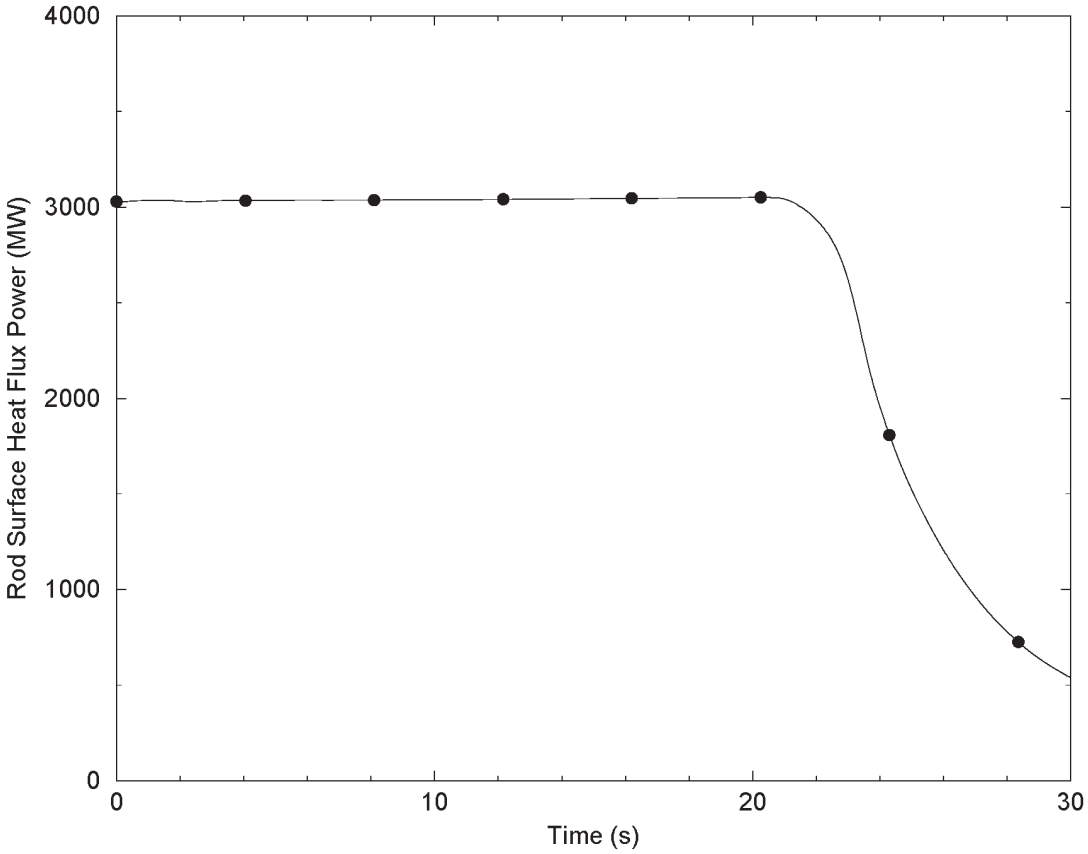

EC287528

FLORIDA POWER & LIGHT COMPANY
ST. LUCIE PLANT UNIT 2

Figure 15.6.1-14
RCS Depressurization (AREVA DNB):
Total Core Heat Flux Power vs. Time

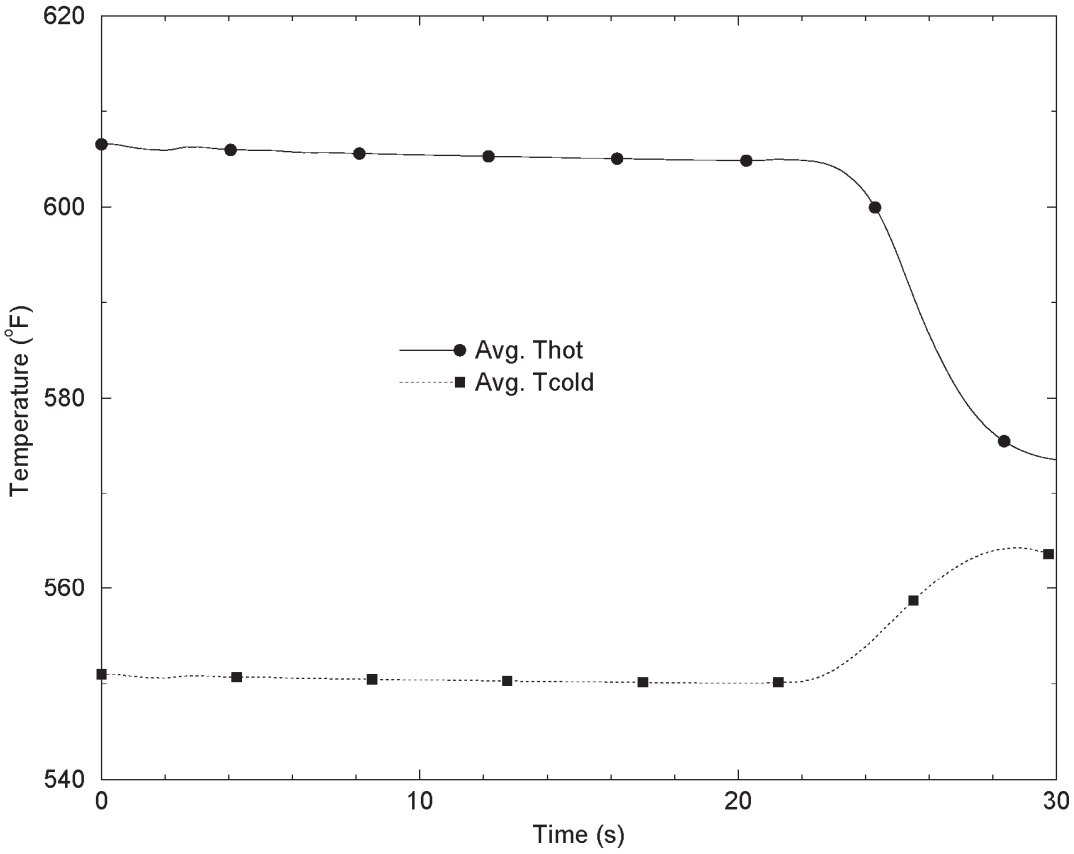

EC287528

FLORIDA POWER & LIGHT COMPANY
ST. LUCIE PLANT UNIT 2

Figure 15.6.1-15
RCS Depressurization (AREVA DNB):
RCS Loop Temperatures vs. Time

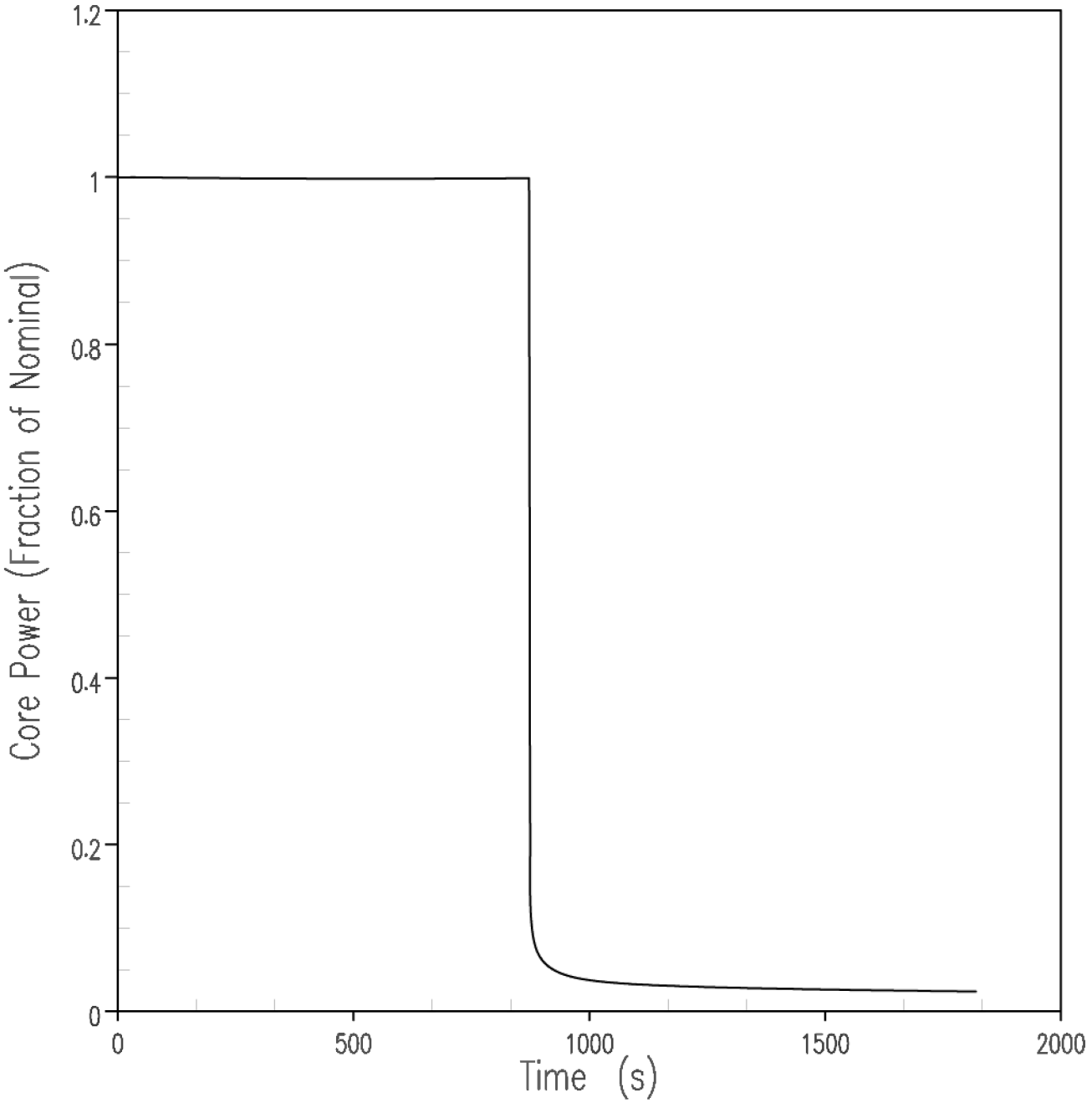

FLORIDA POWER & LIGHT COMPANY ST. LUCIE PLANT UNIT 2
FIGURE 15.6.2-1 Letdown Line Break Event Low Tavg Case Core Power vs. Time

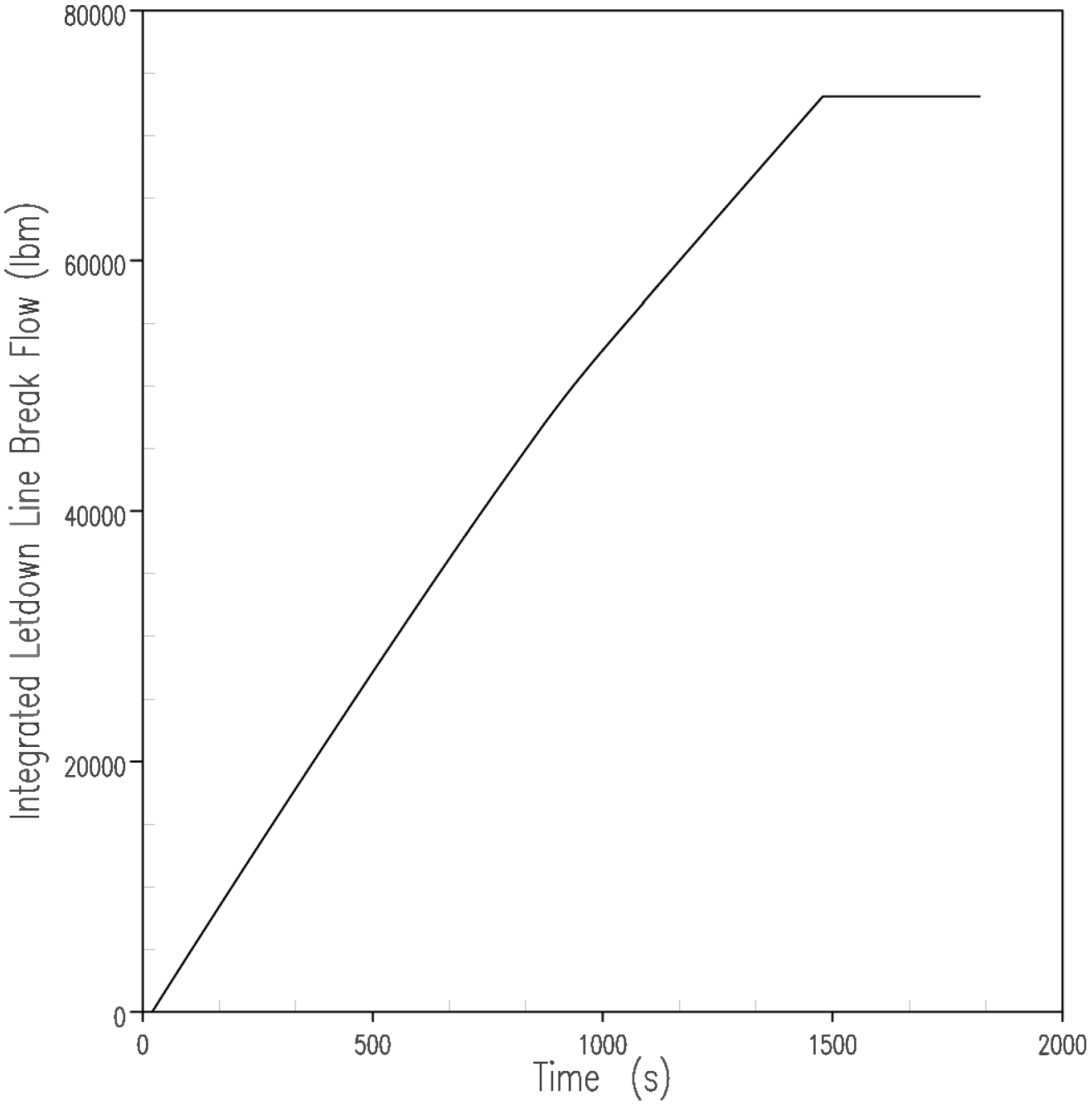

FLORIDA POWER & LIGHT COMPANY ST. LUCIE PLANT UNIT 2
FIGURE 15.6.2-2 Letdown Line Break Event Low Tavg Case Integrated Letdown Line Break Flow

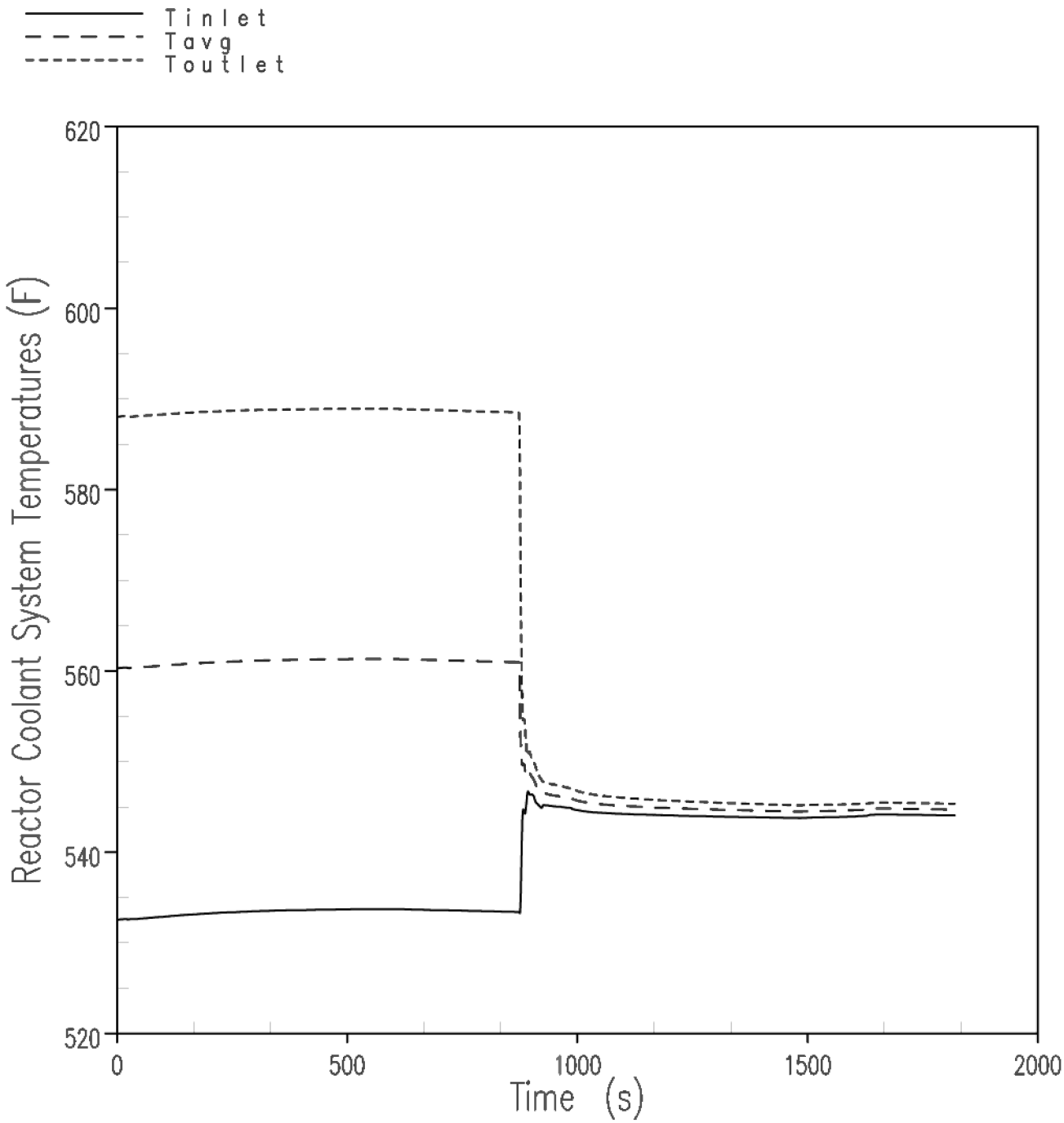

FLORIDA POWER & LIGHT COMPANY ST. LUCIE PLANT UNIT 2
FIGURE 15.6.2-3 Letdown Line Break Event Low Tavg Case RCS Temperatures vs. Time

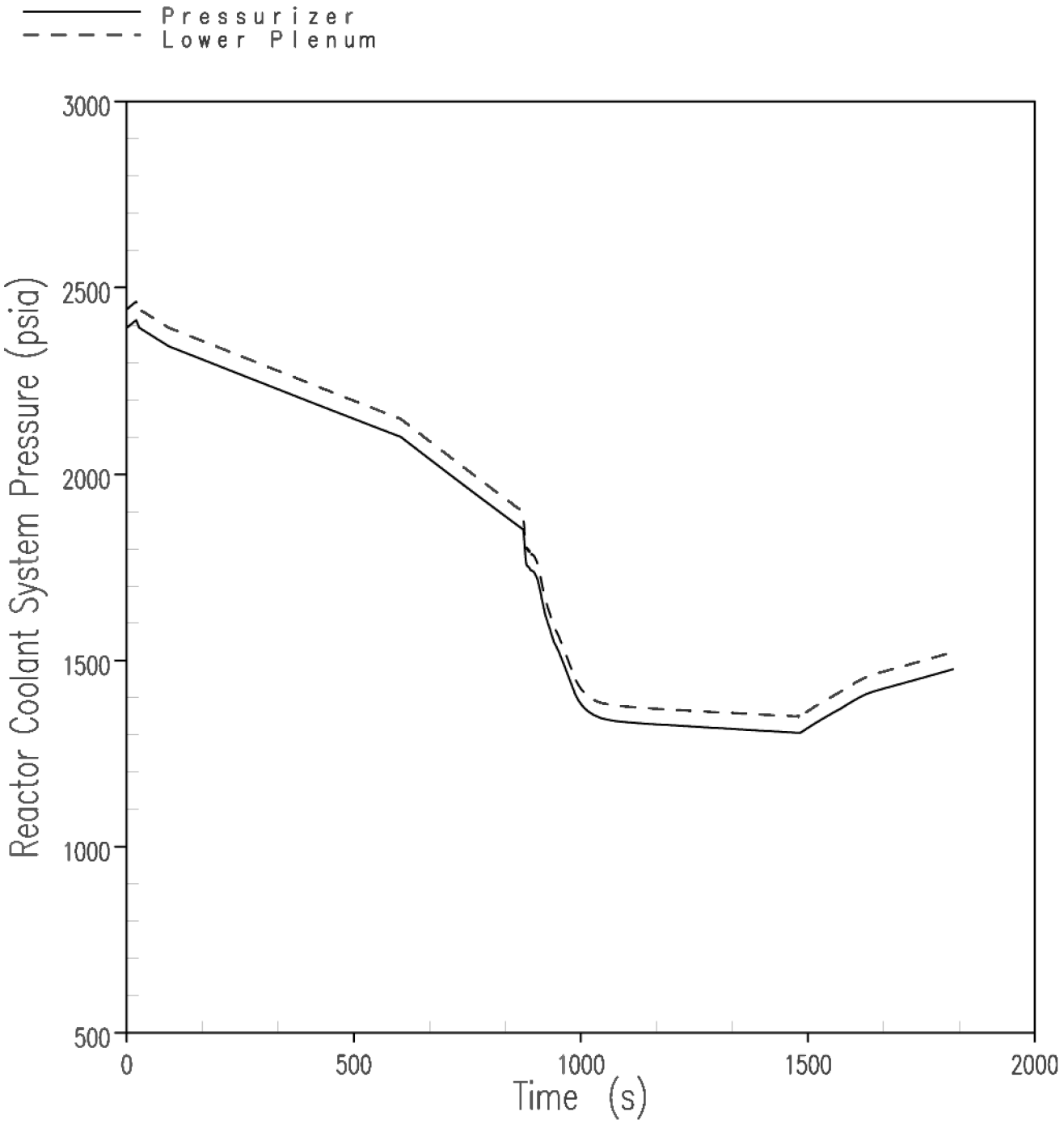

FLORIDA POWER & LIGHT COMPANY ST. LUCIE PLANT UNIT 2
FIGURE 15.6.2-4 Letdown Line Break Event Low Tavg Case RCS Pressure vs. Time

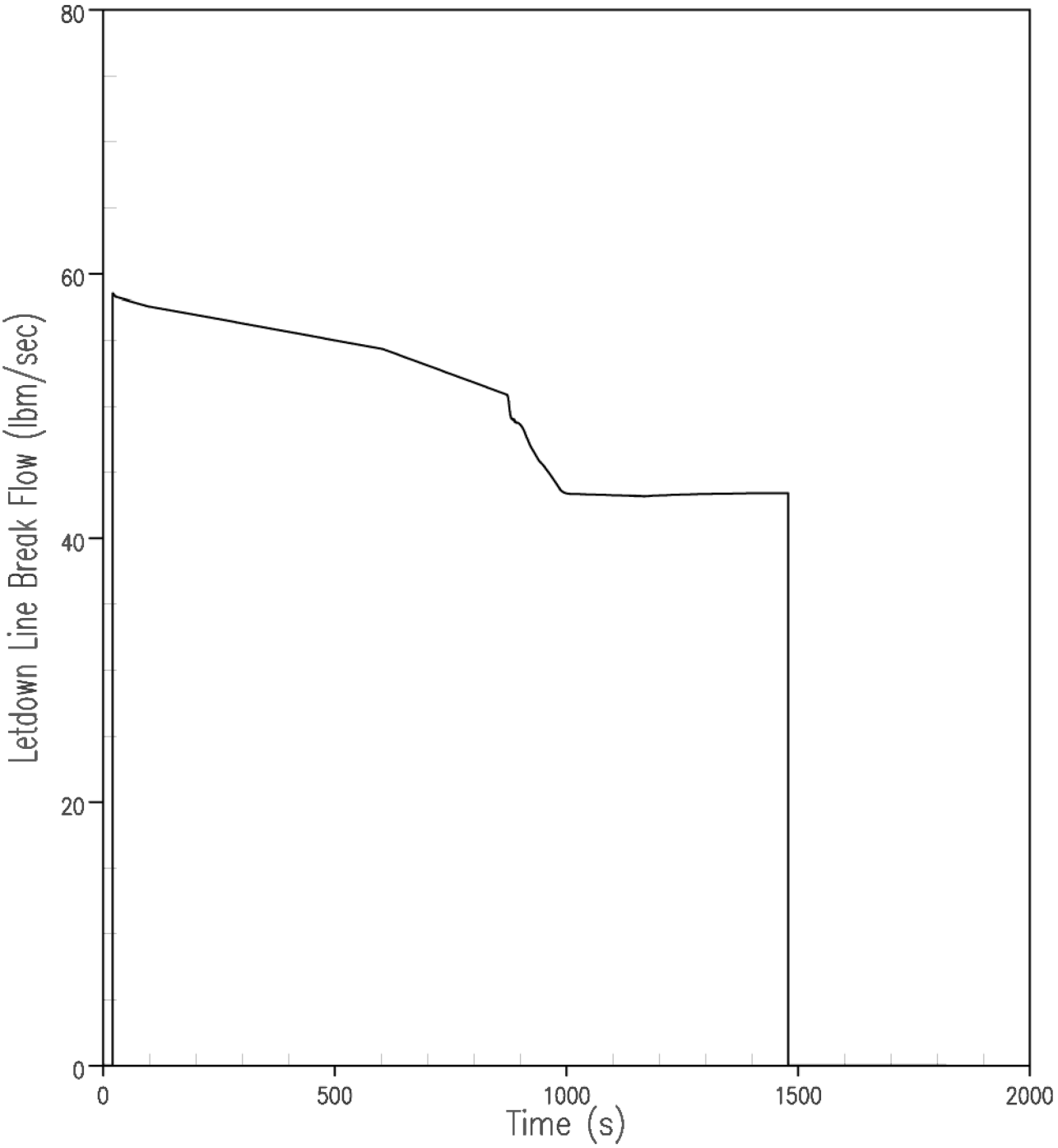

FLORIDA POWER & LIGHT COMPANY ST. LUCIE PLANT UNIT 2
FIGURE 15.6.2-5 Letdown Line Break Event Low Tavg Case Letdown Line Break Flow vs. Time

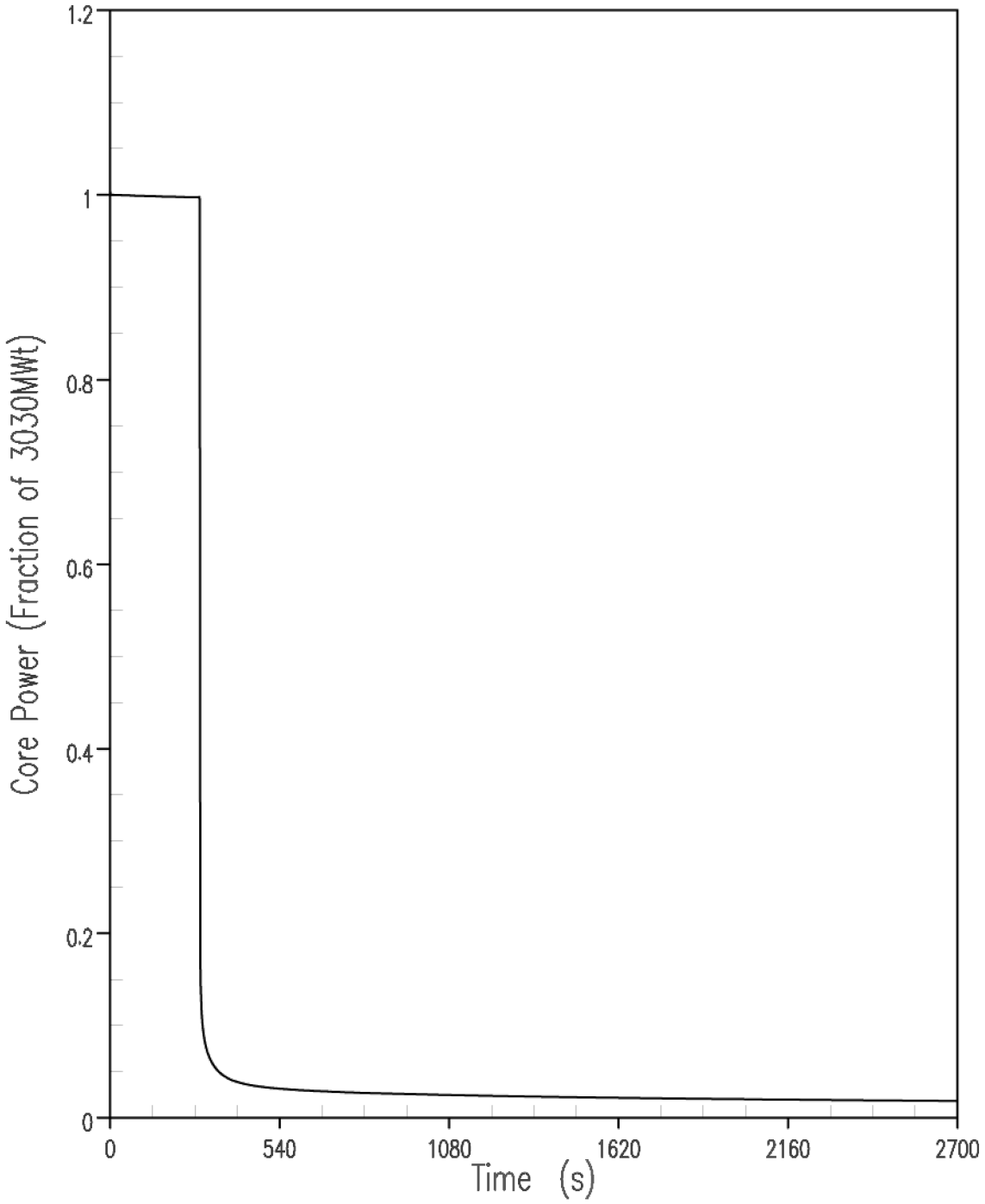

FLORIDA POWER & LIGHT COMPANY ST. LUCIE PLANT UNIT 2
FIGURE 15.6.3-1 SGTR with LOOP Core Power Flow vs. Time

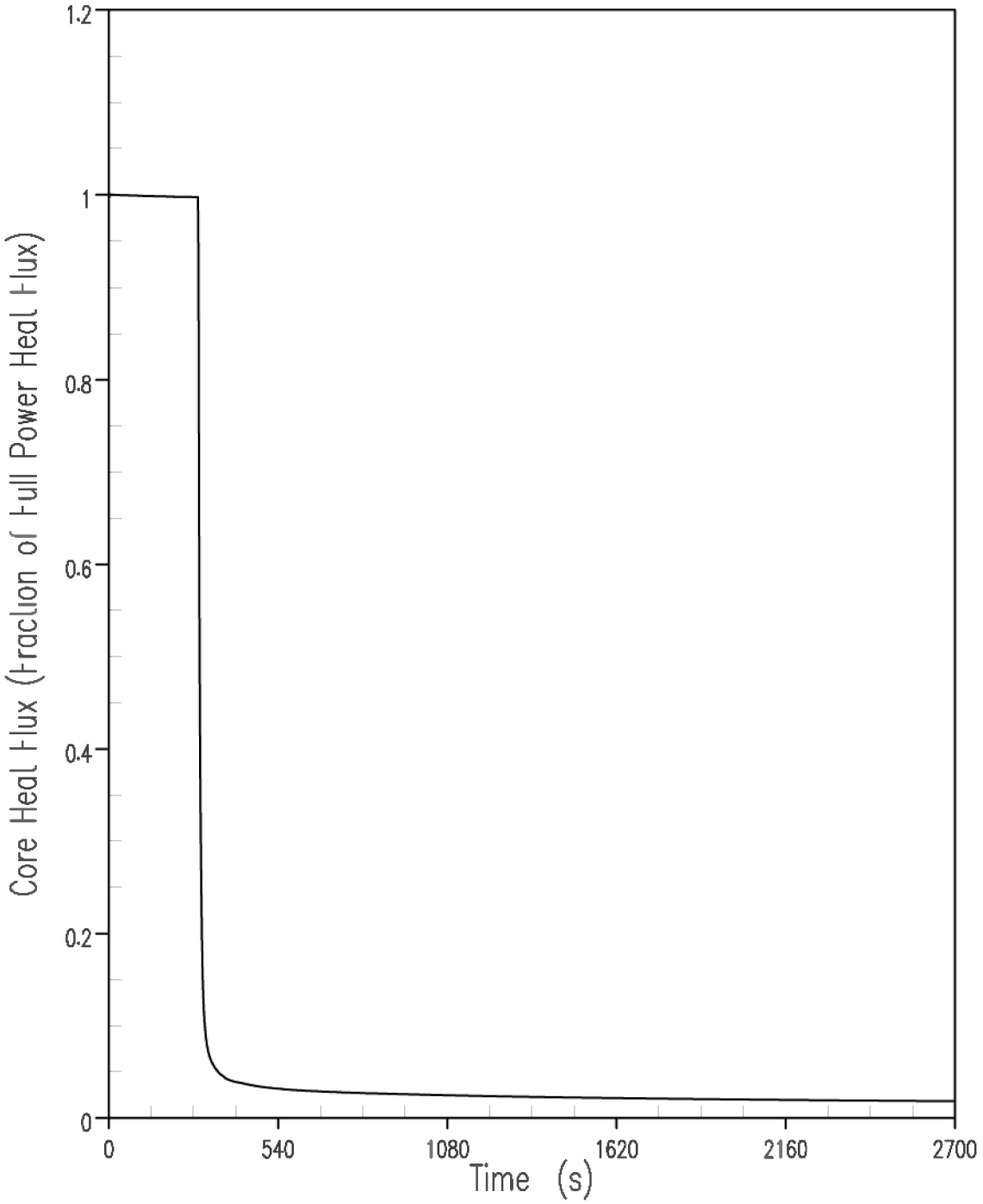

FLORIDA POWER & LIGHT COMPANY ST. LUCIE PLANT UNIT 2
FIGURE 15.6.3-2 SGTR with LOOP Core Heat Flux vs. Time

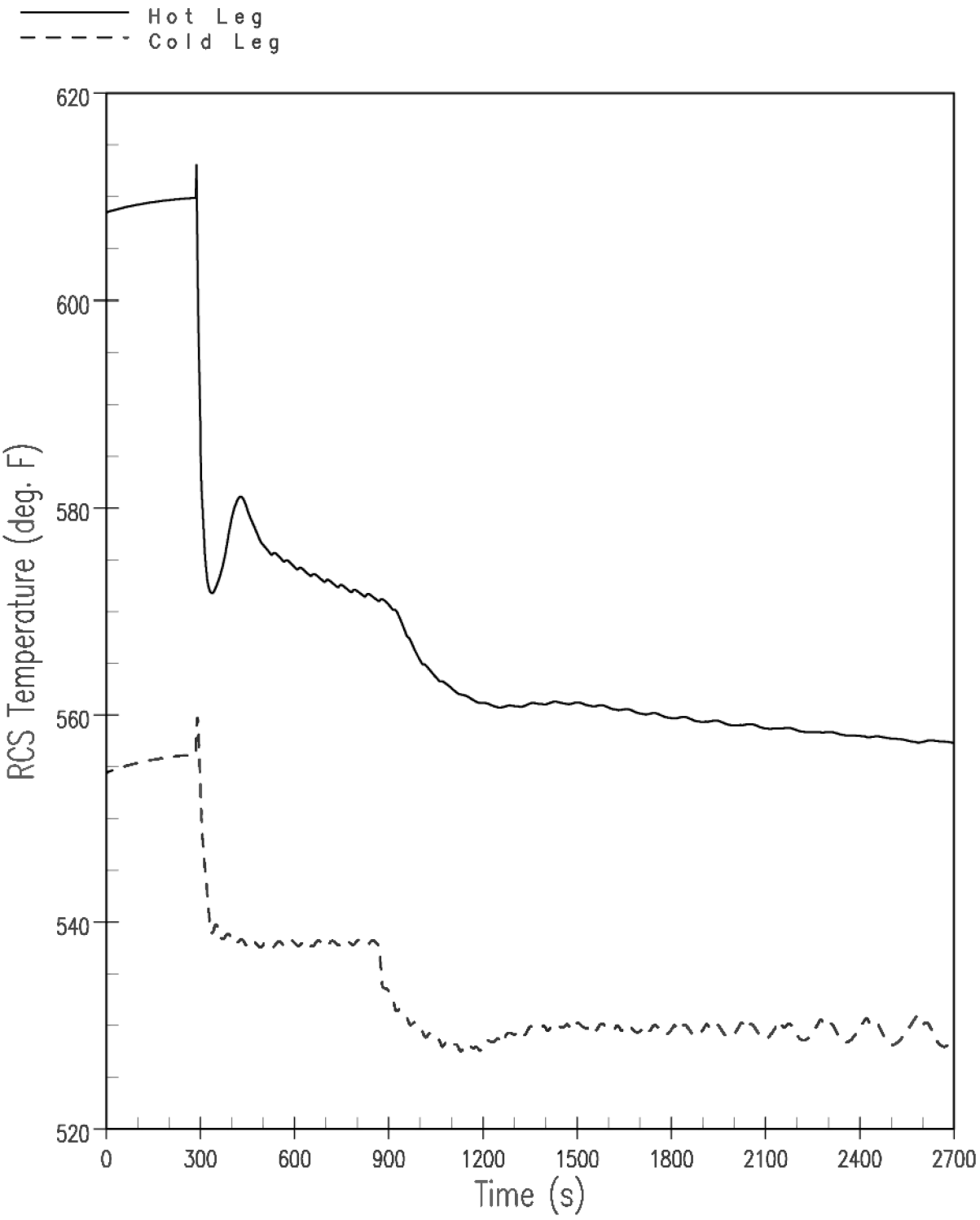

FLORIDA POWER & LIGHT COMPANY ST. LUCIE PLANT UNIT 2
FIGURE 15.6.3-3 SGTR with LOOP RCS Temperature vs. Time

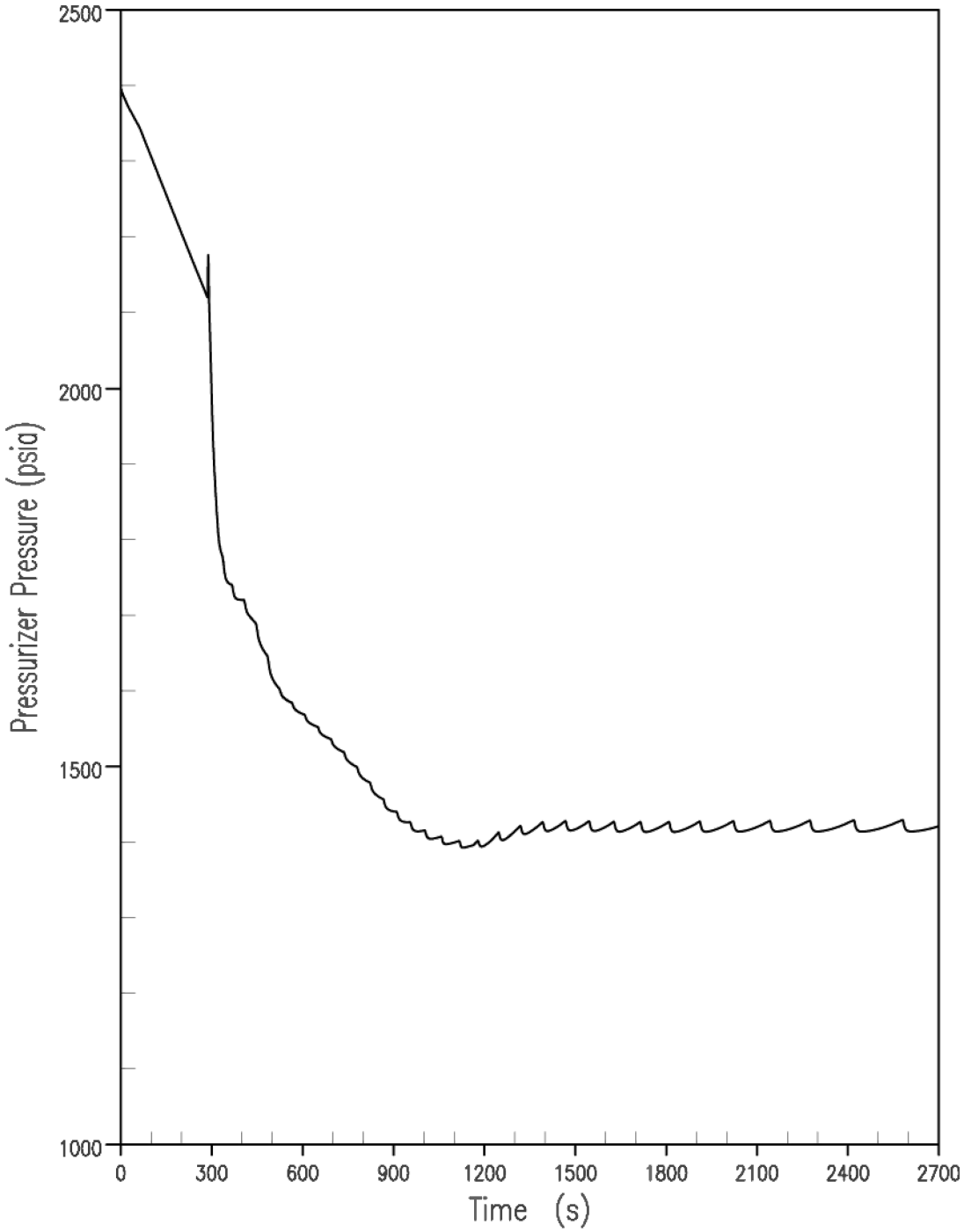

FLORIDA POWER & LIGHT COMPANY ST. LUCIE PLANT UNIT 2
FIGURE 15.6.3-4 SGTR with LOOP Pressurizer Pressure vs. Time

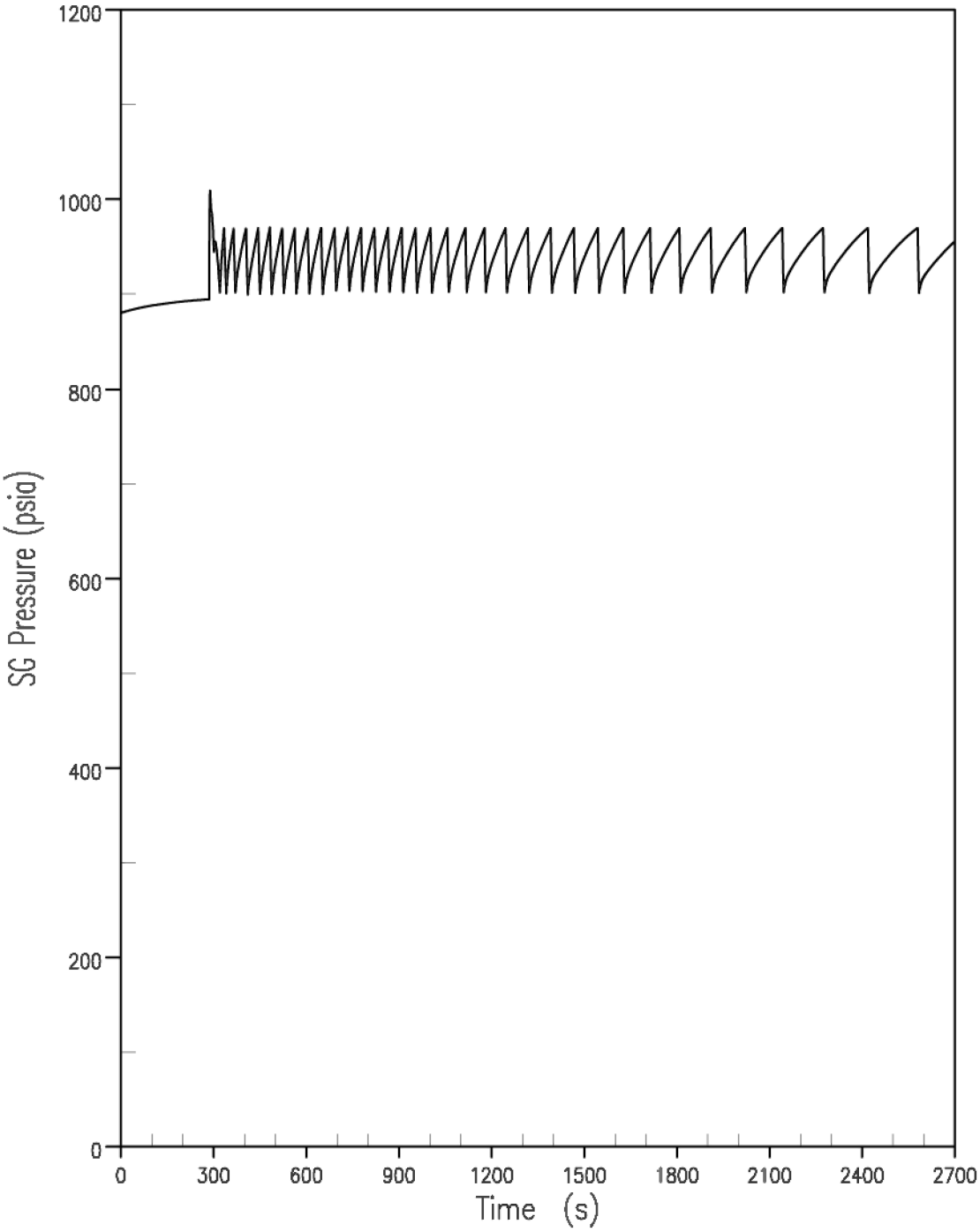

FLORIDA POWER & LIGHT COMPANY ST. LUCIE PLANT UNIT 2
FIGURE 15.6.3-5 SGTR with LOOP SG Pressure vs. Time

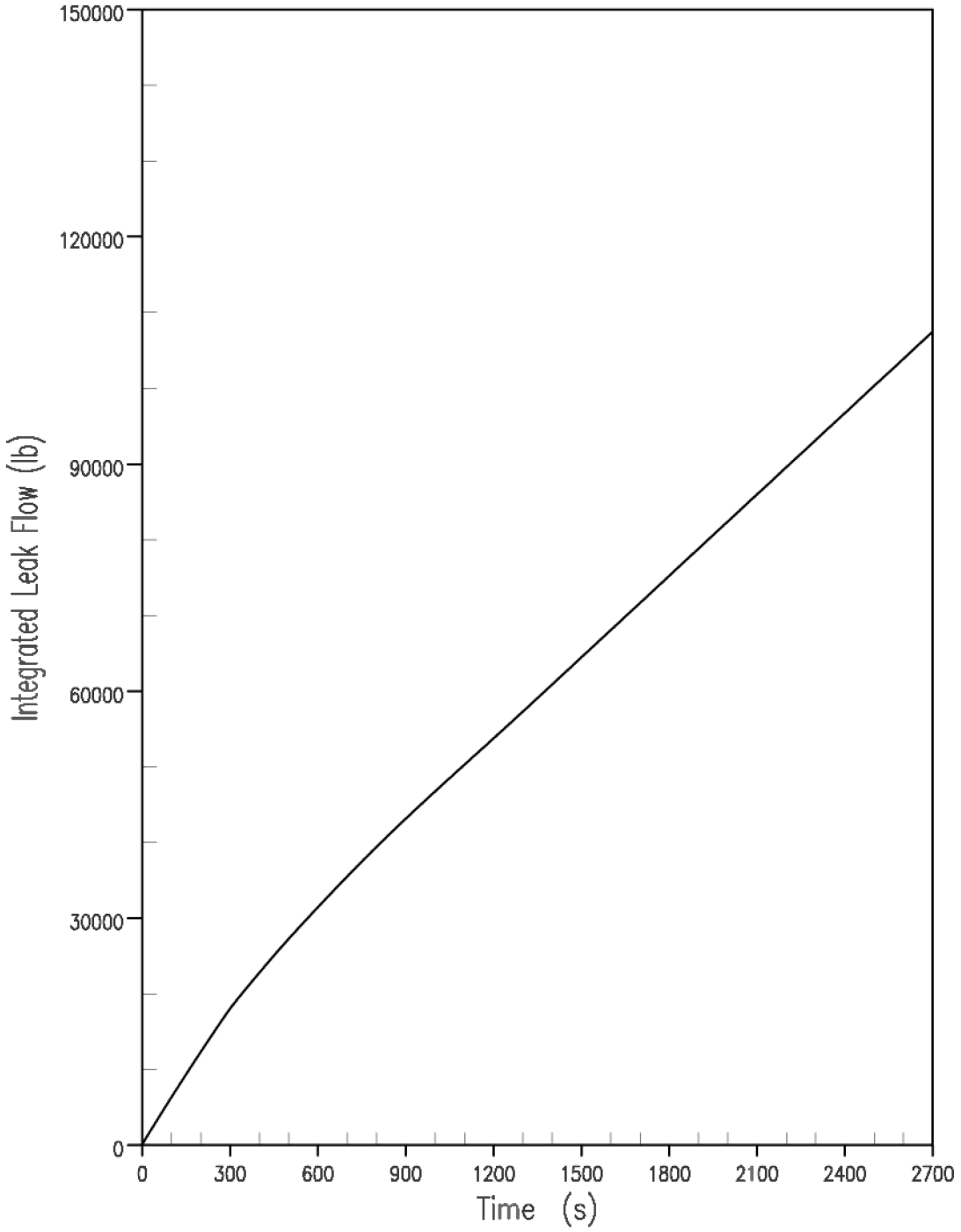

FLORIDA POWER & LIGHT COMPANY ST. LUCIE PLANT UNIT 2
FIGURE 15.6.3-6 SGTR with LOOP Integrated Break Flow vs. Time

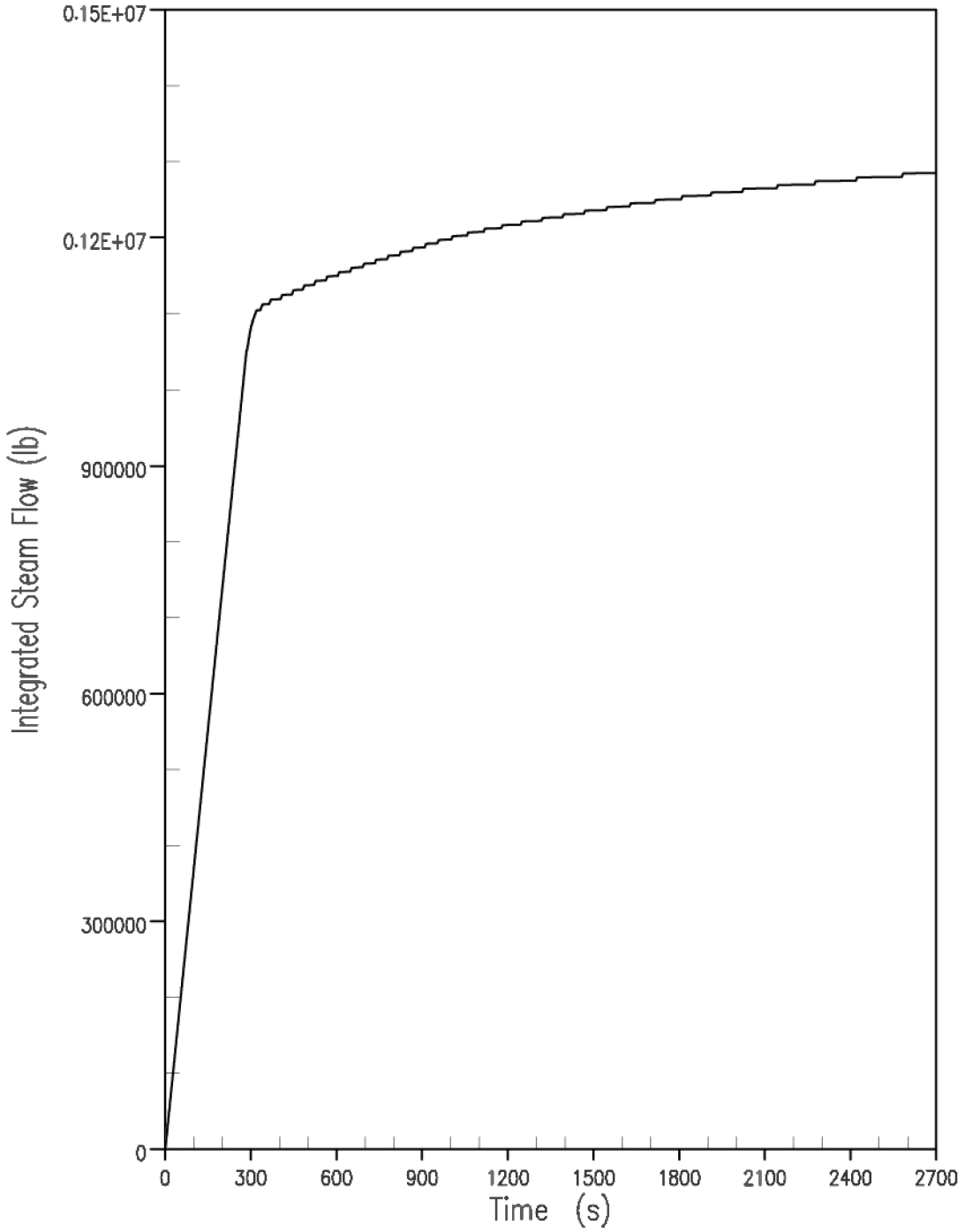

FLORIDA POWER & LIGHT COMPANY ST. LUCIE PLANT UNIT 2
FIGURE 15.6.3-7 SGTR with LOOP Integrated Steam Flow vs. Time

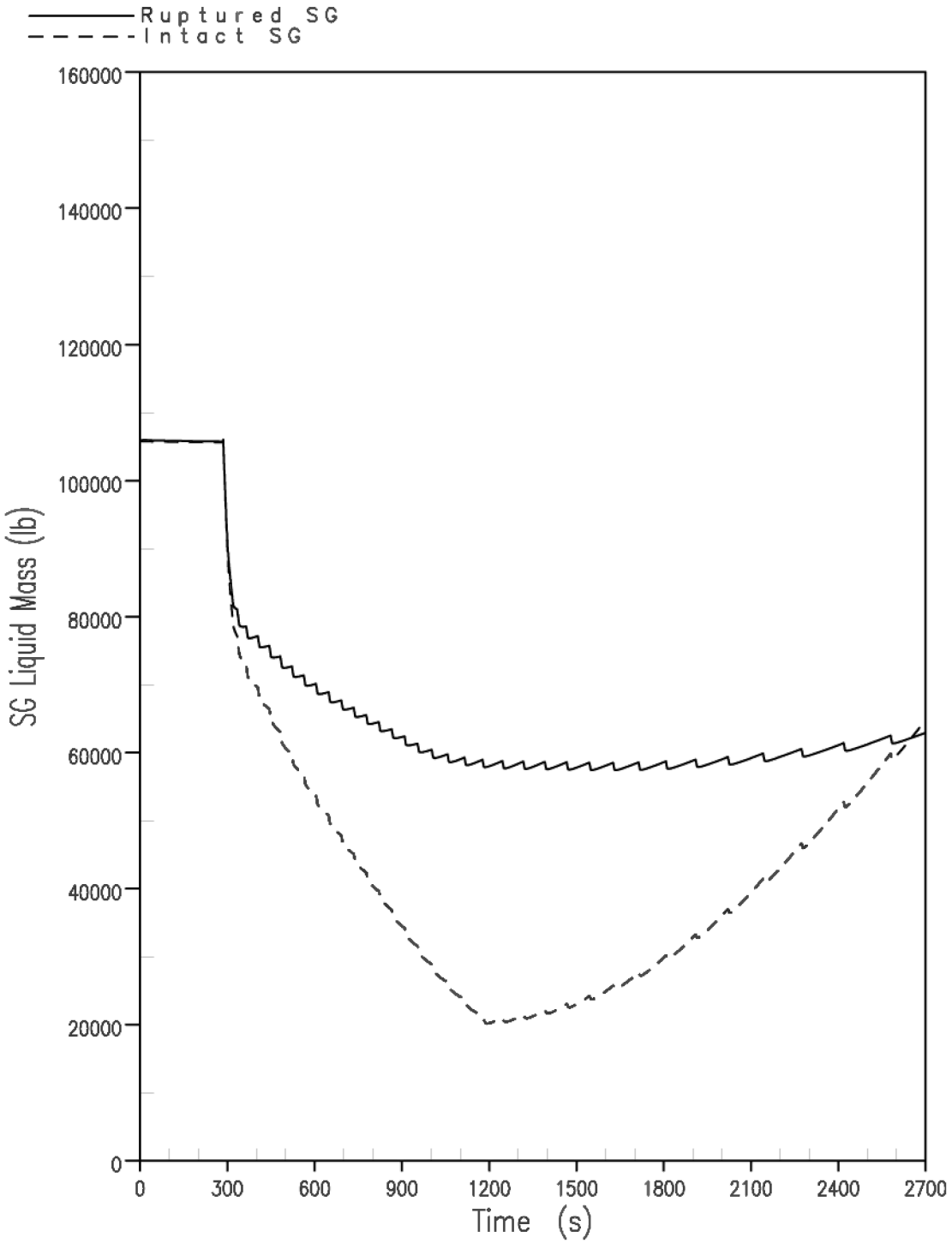

FLORIDA POWER & LIGHT COMPANY ST. LUCIE PLANT UNIT 2
FIGURE 15.6.3-8 SGTR with LOOP SG Liquid Mass vs. Time

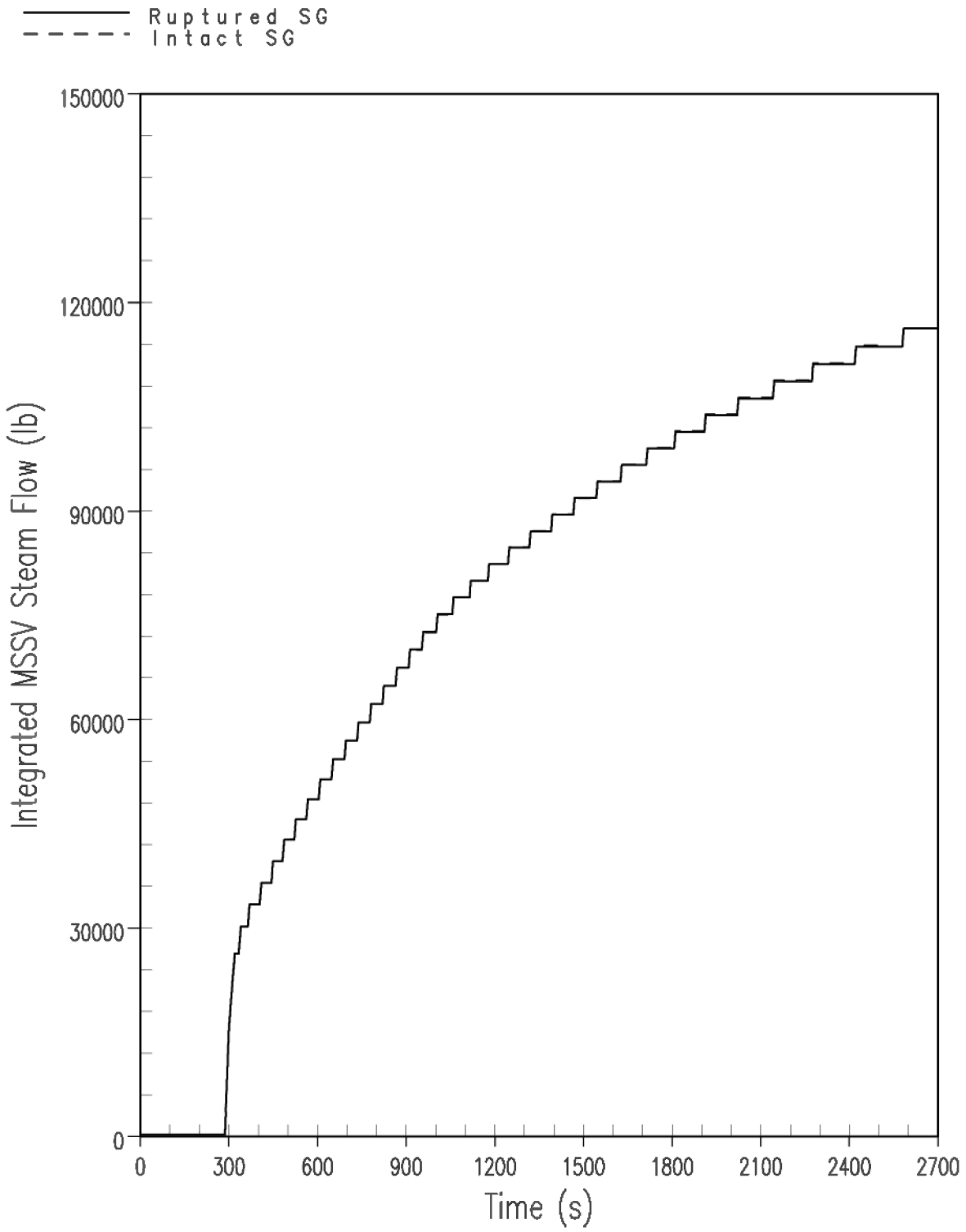

FLORIDA POWER & LIGHT COMPANY ST. LUCIE PLANT UNIT 2
FIGURE 15.6.3-9 SGTR with LOOP Integrated Steam Release vs. Time

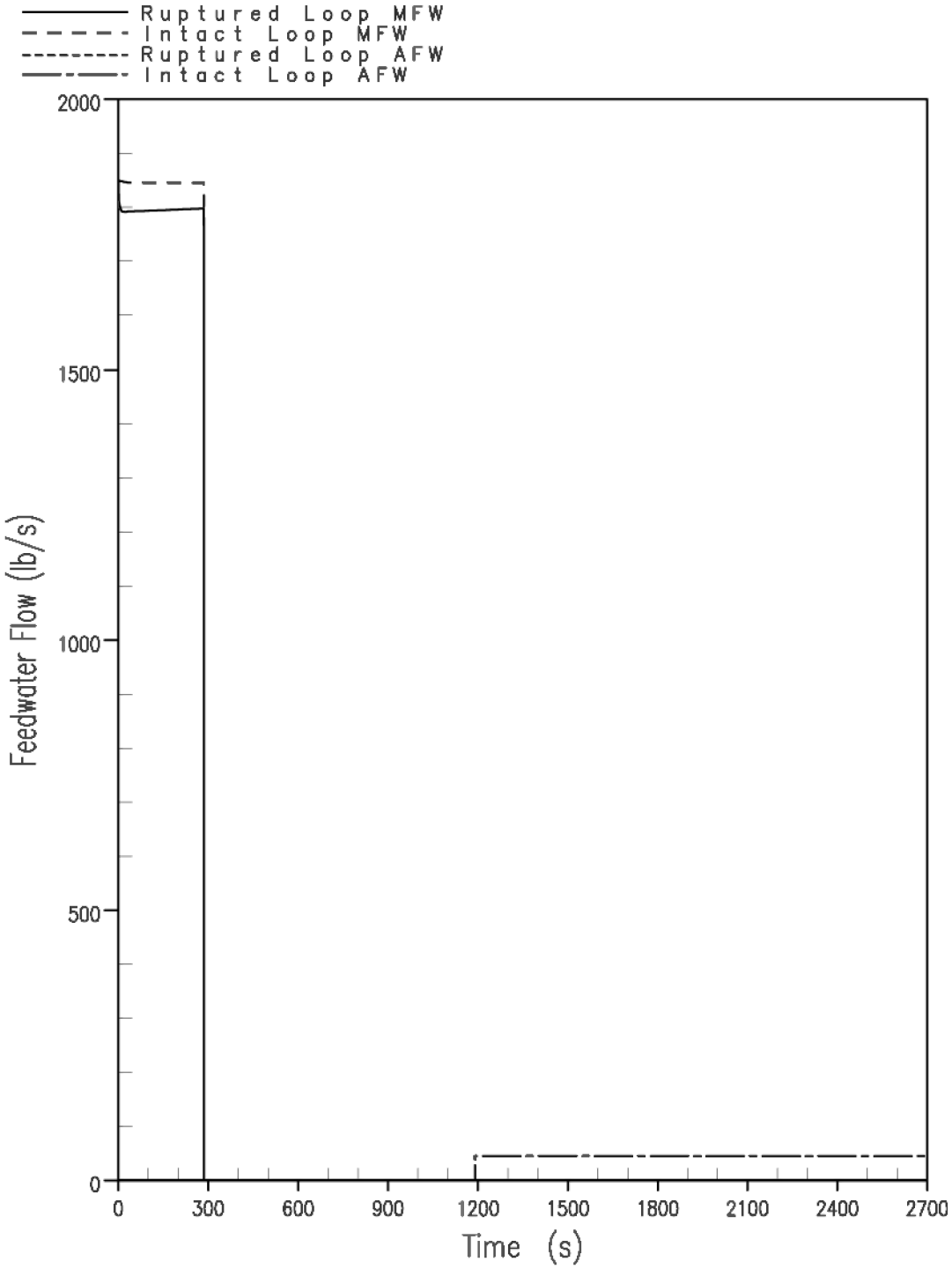

FLORIDA POWER & LIGHT COMPANY ST. LUCIE PLANT UNIT 2
FIGURE 15.6.3-10 SGTR with LOOP Main & Auxiliary Feedwater Flow vs. Time

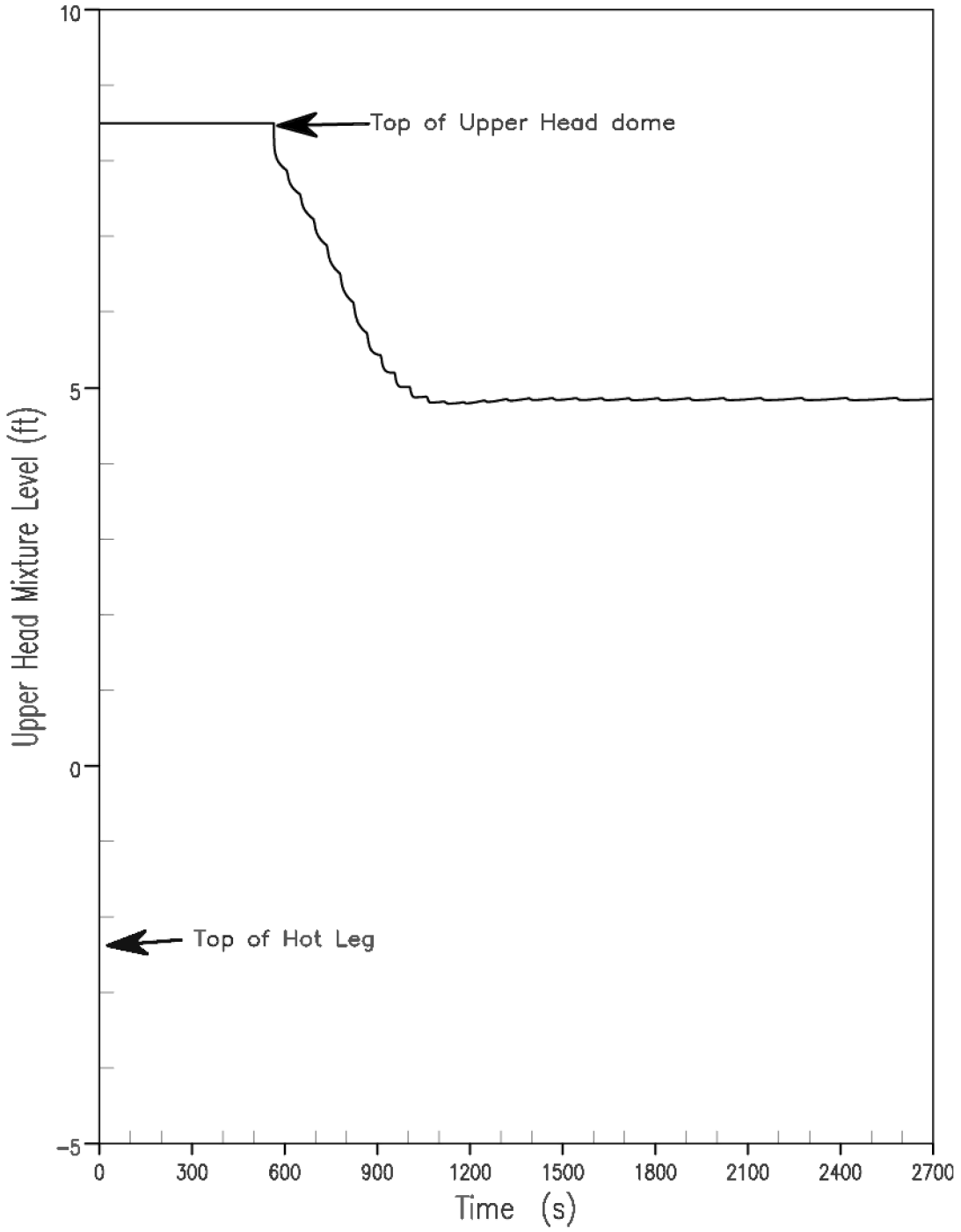

FLORIDA POWER & LIGHT COMPANY ST. LUCIE PLANT UNIT 2
FIGURE 15.6.3-11 SGTR with LOOP Vessel Upper Head Mixture vs. Time

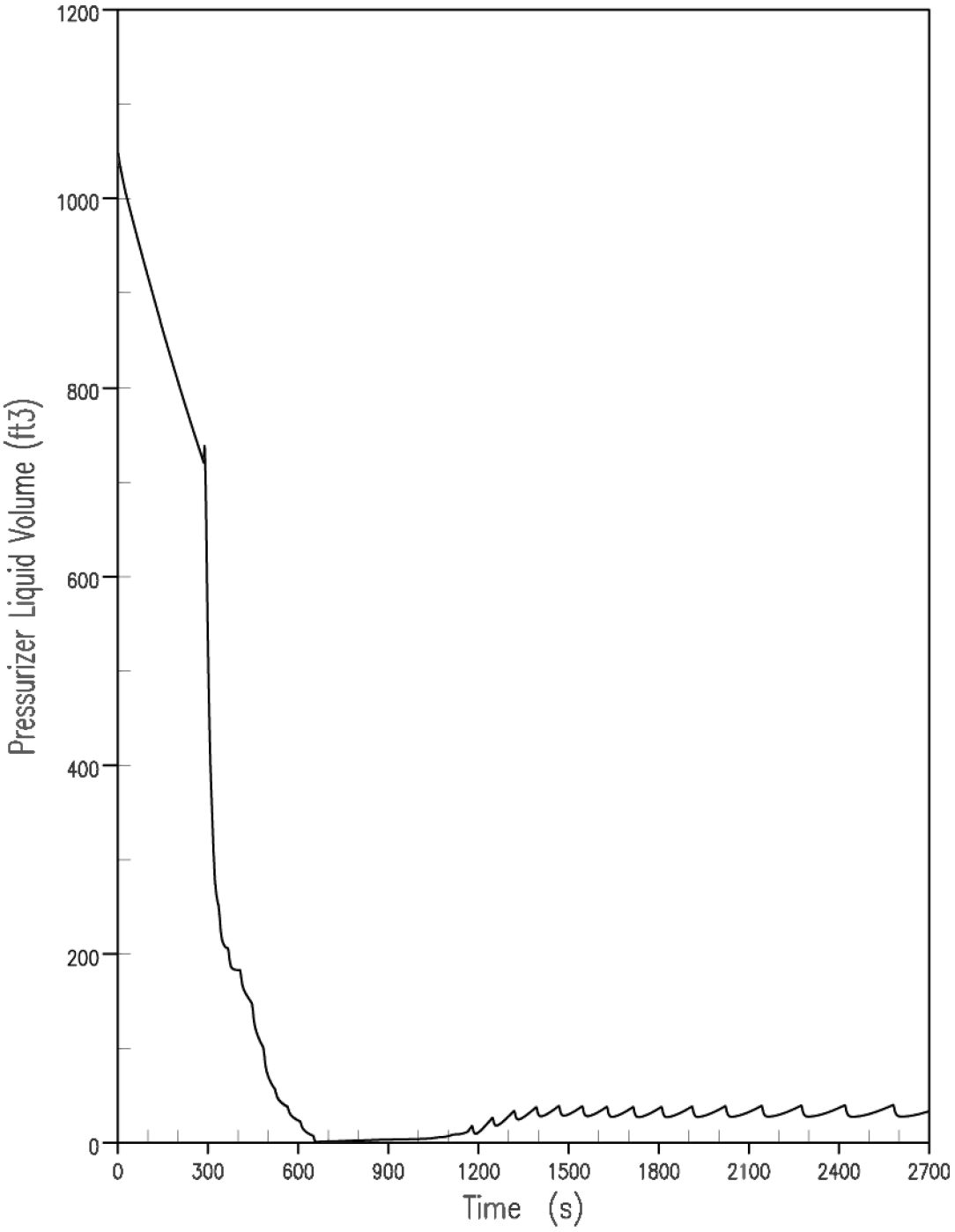

FLORIDA POWER & LIGHT COMPANY ST. LUCIE PLANT UNIT 2
FIGURE 15.6.3-12 SGTR with LOOP Pressurizer Water Volume vs. Time

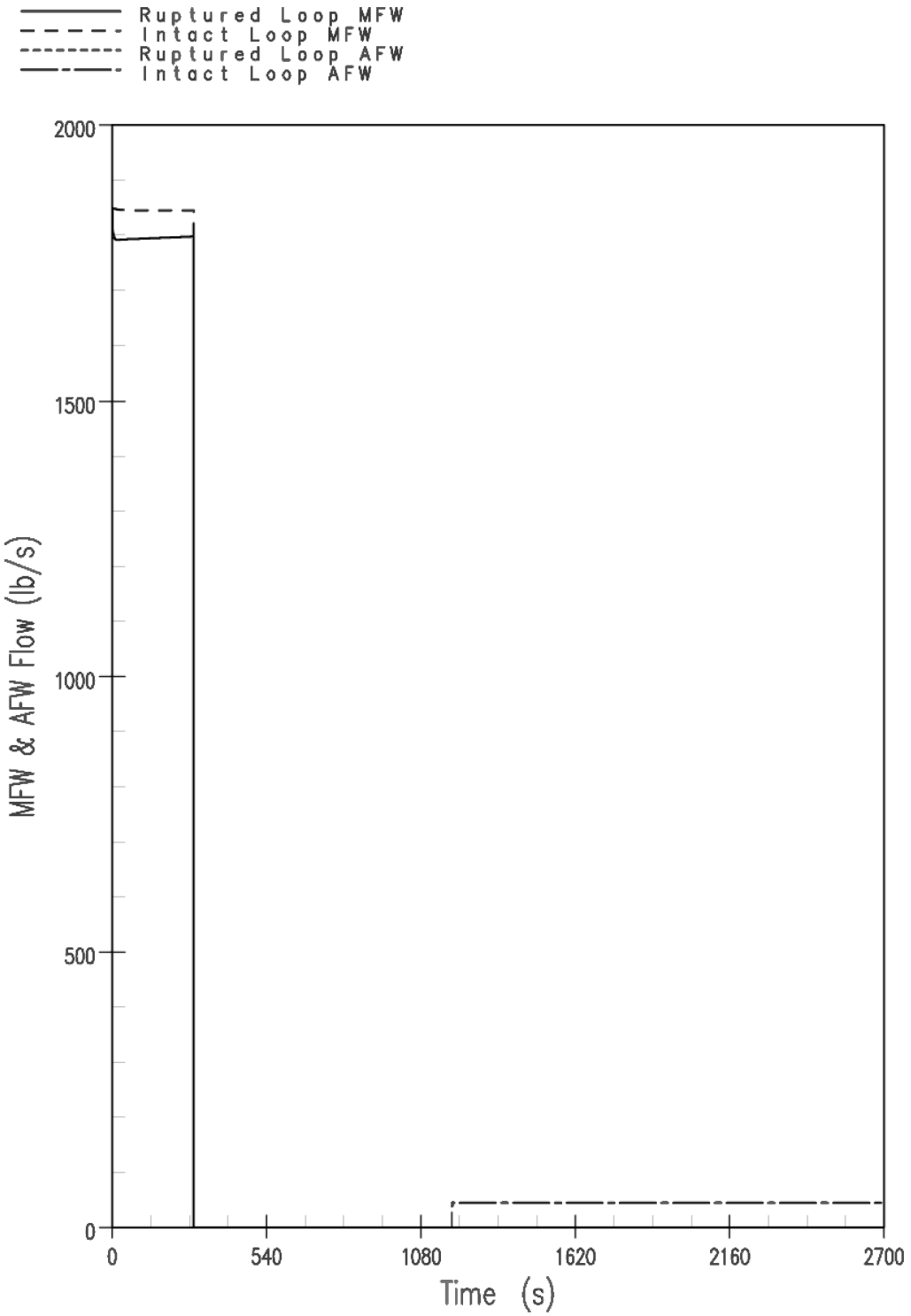

FLORIDA POWER & LIGHT COMPANY ST. LUCIE PLANT UNIT 2
FIGURE 15.6.3-13 SGTR with LOOP Main/Auxiliary Feedwater Flow vs. Time

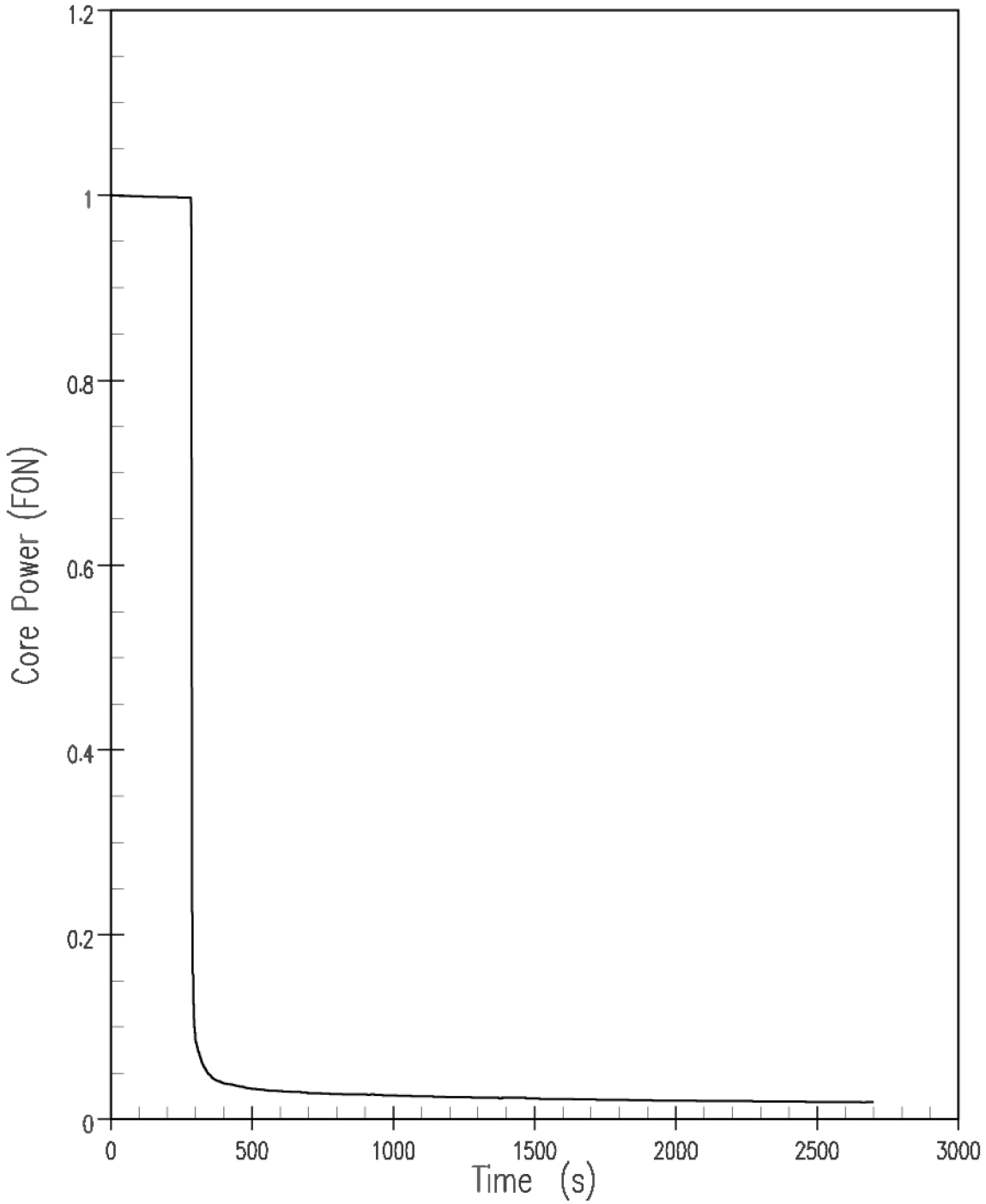

FLORIDA POWER & LIGHT COMPANY ST. LUCIE PLANT UNIT 2
FIGURE 15.6.3-14 SGTR for MTO Core Power vs. Time

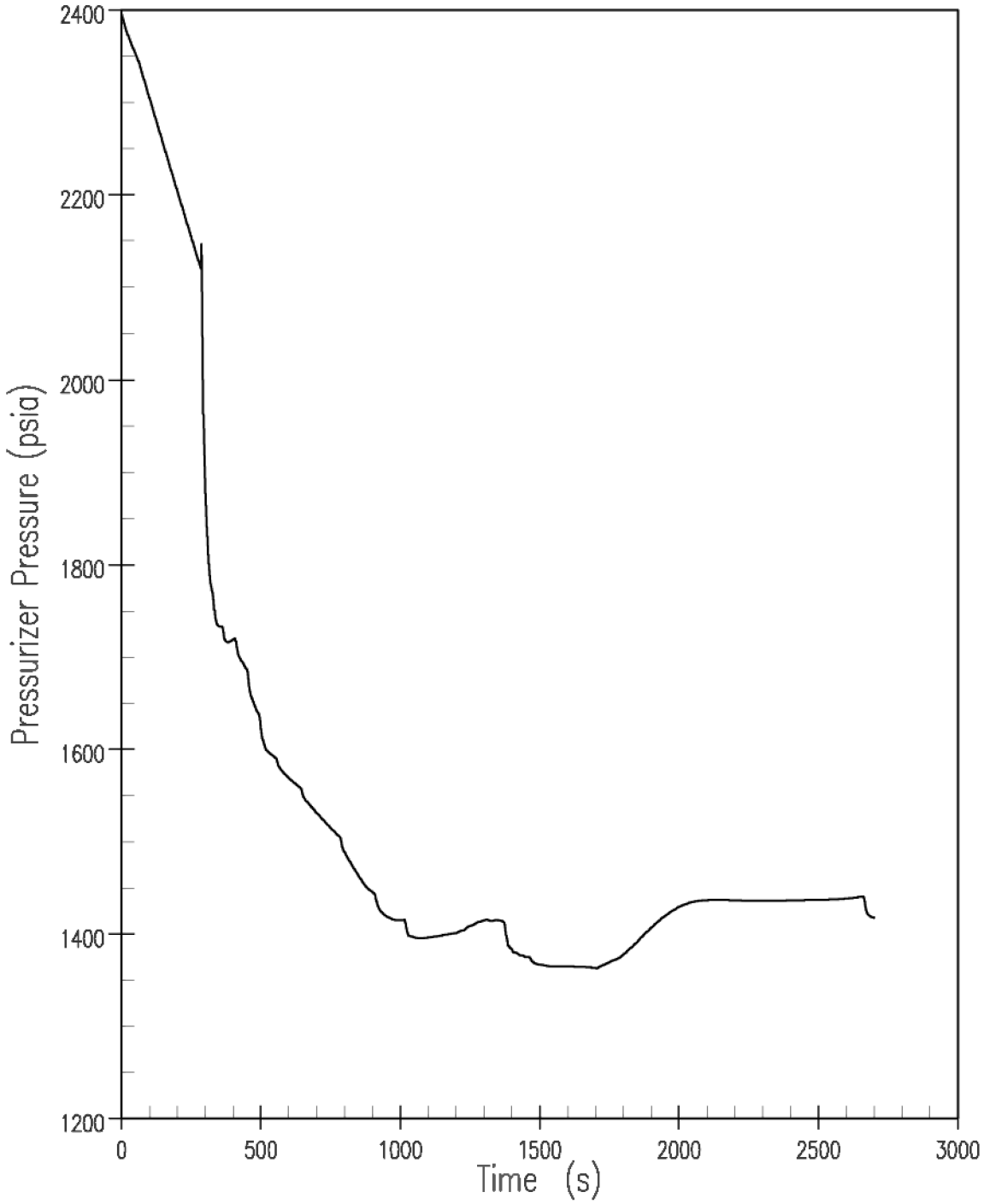

FLORIDA POWER & LIGHT COMPANY ST. LUCIE PLANT UNIT 2
FIGURE 15.6.3-15 SGTR for MTO Pressurizer Pressure vs. Time

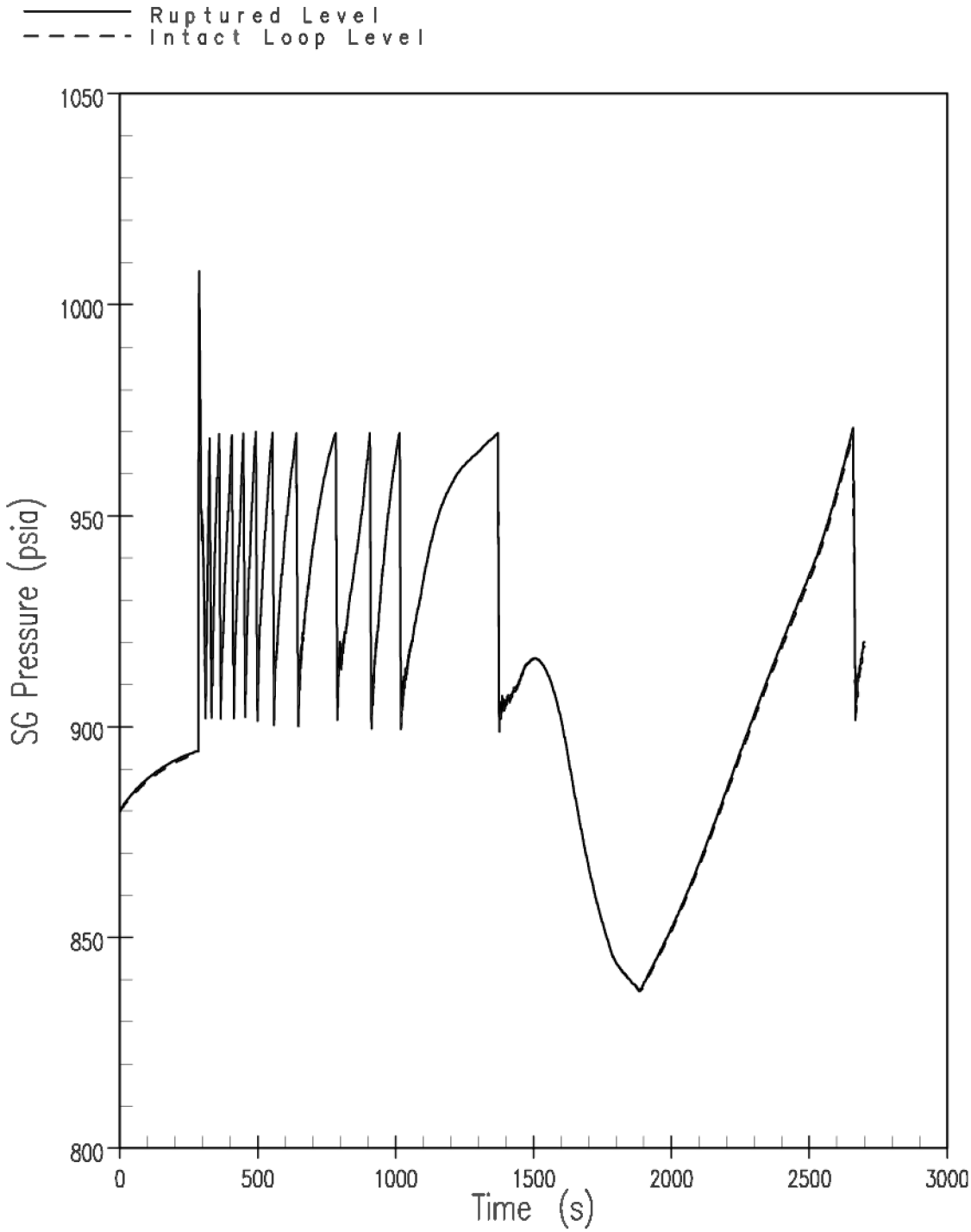

FLORIDA POWER & LIGHT COMPANY ST. LUCIE PLANT UNIT 2
FIGURE 15.6.3-16 SGTR for MTO Steam Generator Pressure vs. Time

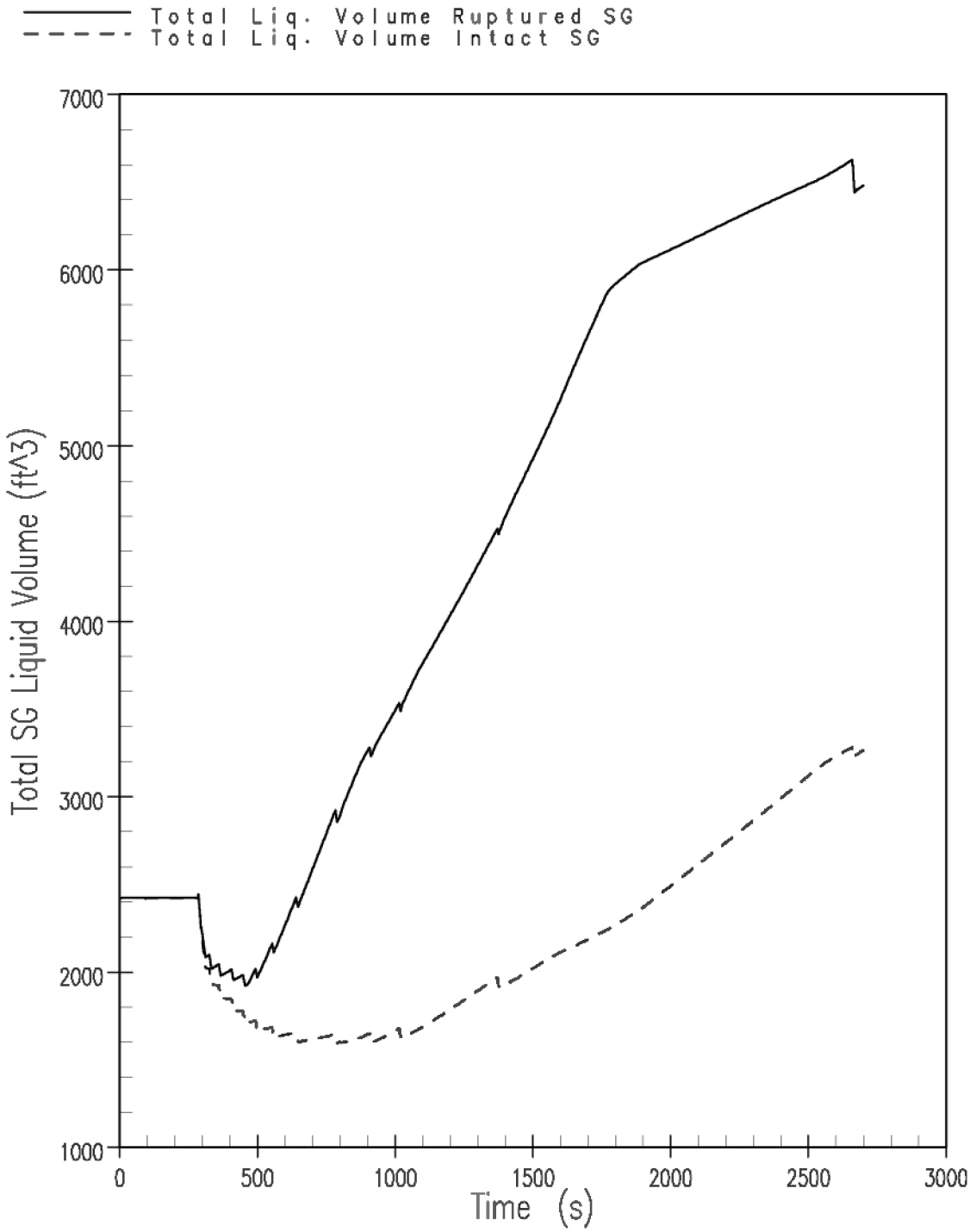

FLORIDA POWER & LIGHT COMPANY ST. LUCIE PLANT UNIT 2
FIGURE 15.6.3-17 SGTR for MTO Steam Generator Liquid Volume vs. Time

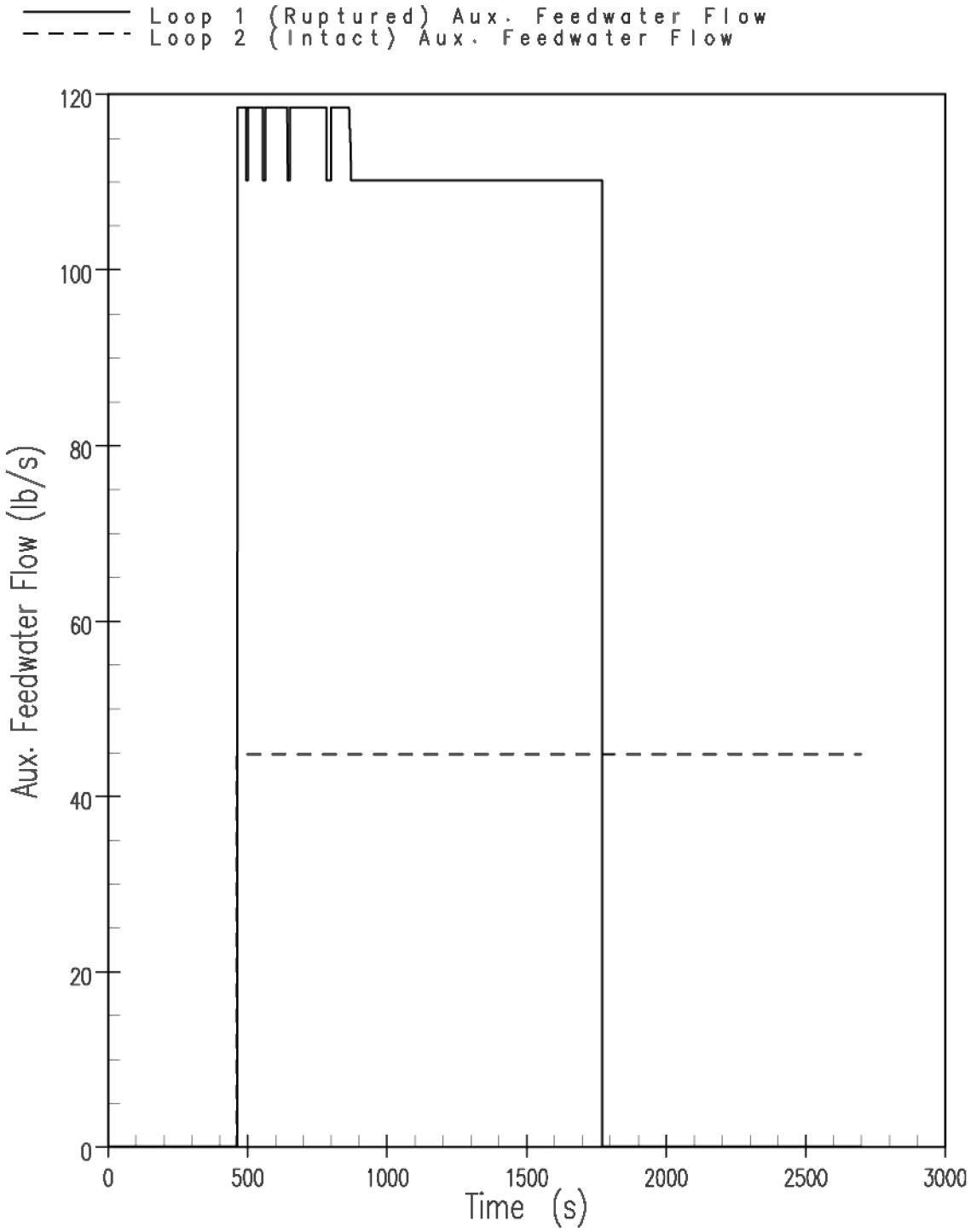

FLORIDA POWER & LIGHT COMPANY ST. LUCIE PLANT UNIT 2
FIGURE 15.6.3-18 SGTR for MTO Auxiliary Feedwater Flow vs. Time

Figure 15.6.5-1
Large Break LOCA ECCS Performance Analysis
1.0 DEG/PD Break
Core Power

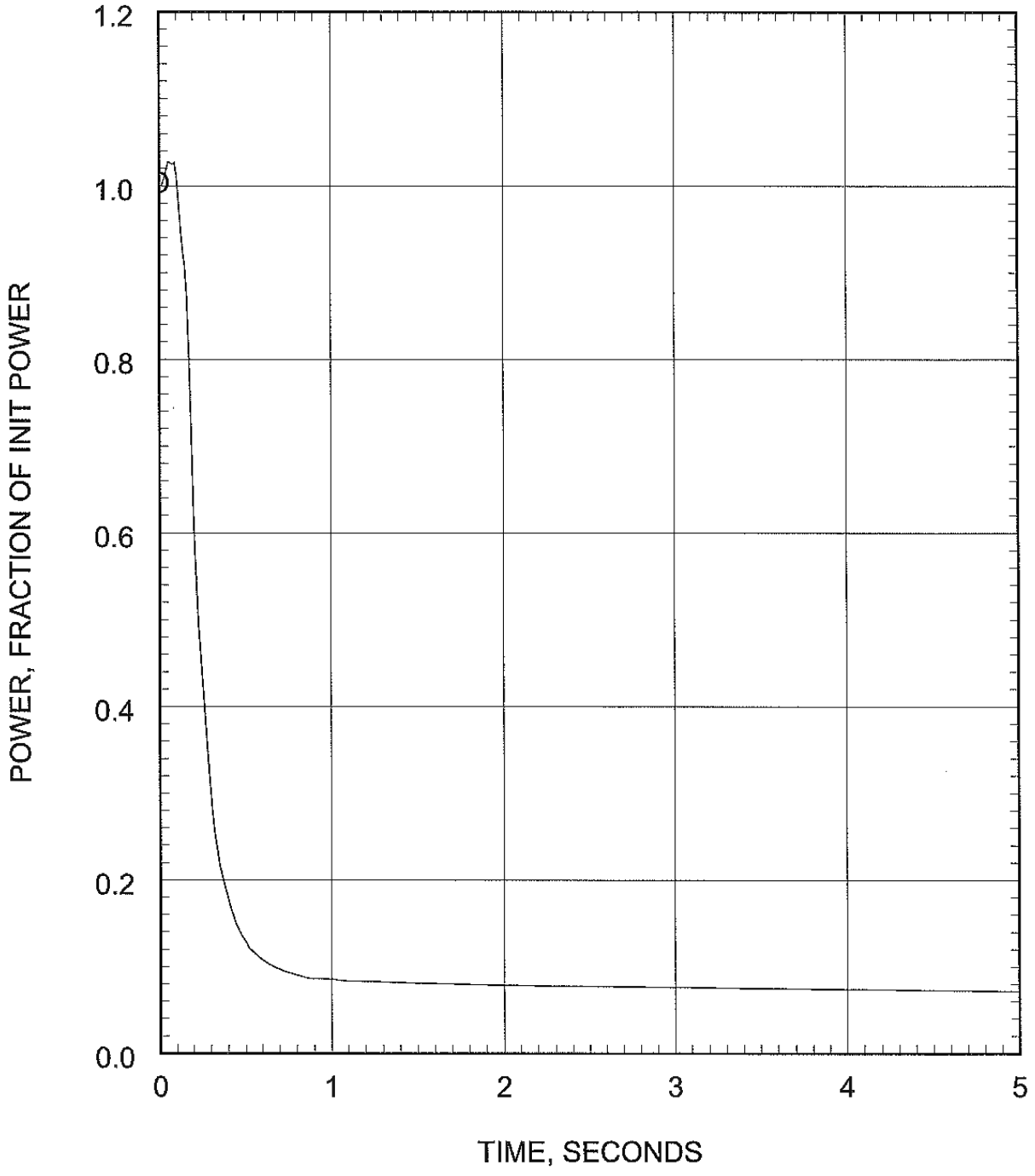

Figure 15.6.5-2
Large Break LOCA ECCS Performance Analysis
1.0 DEG/PD Break
Pressure in Center Hot Assembly Node

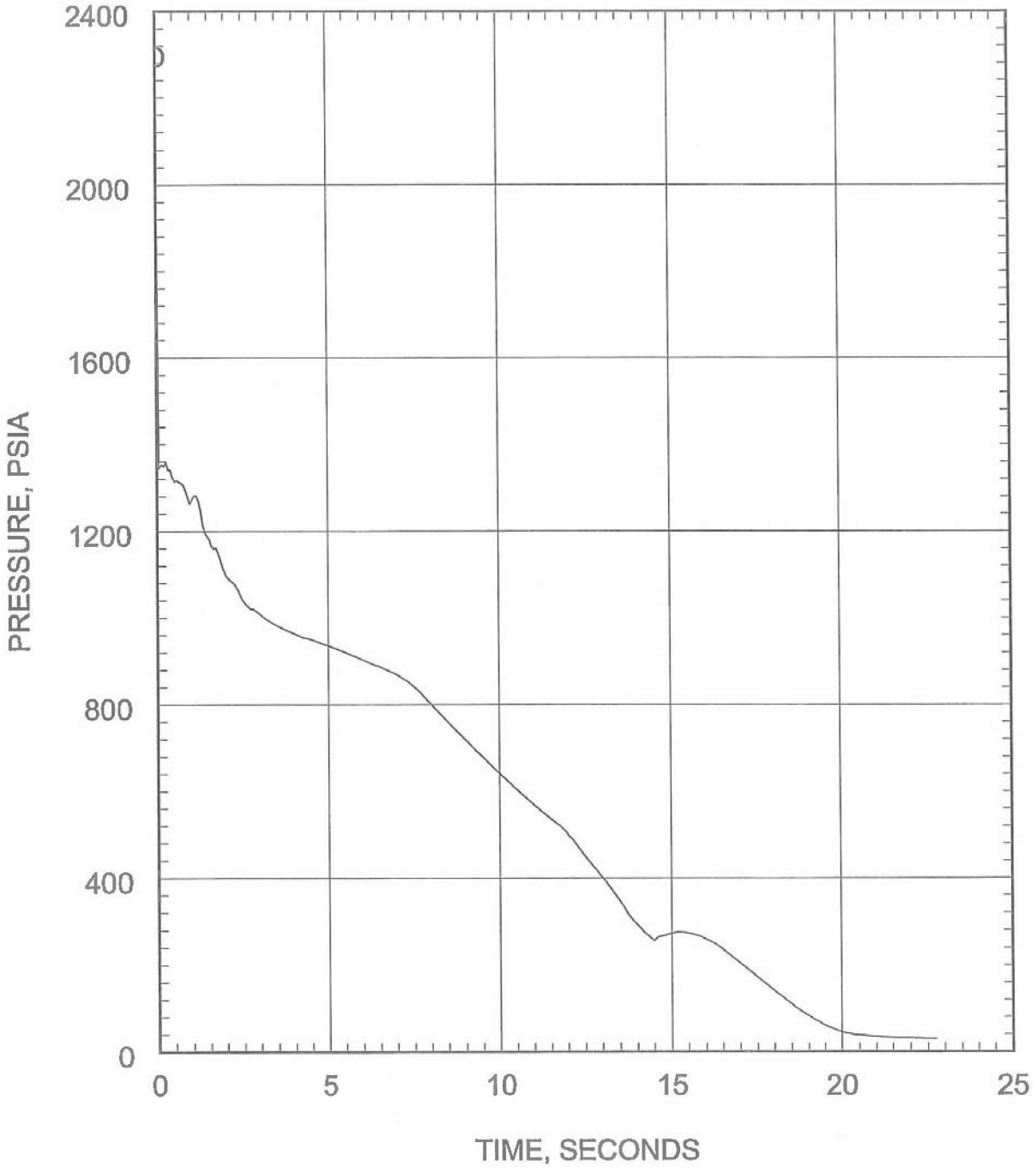

Figure 15.6.5-3
Large Break LOCA ECCS Performance Analysis
1.0 DEG/PD Break
Leak Flow Rate

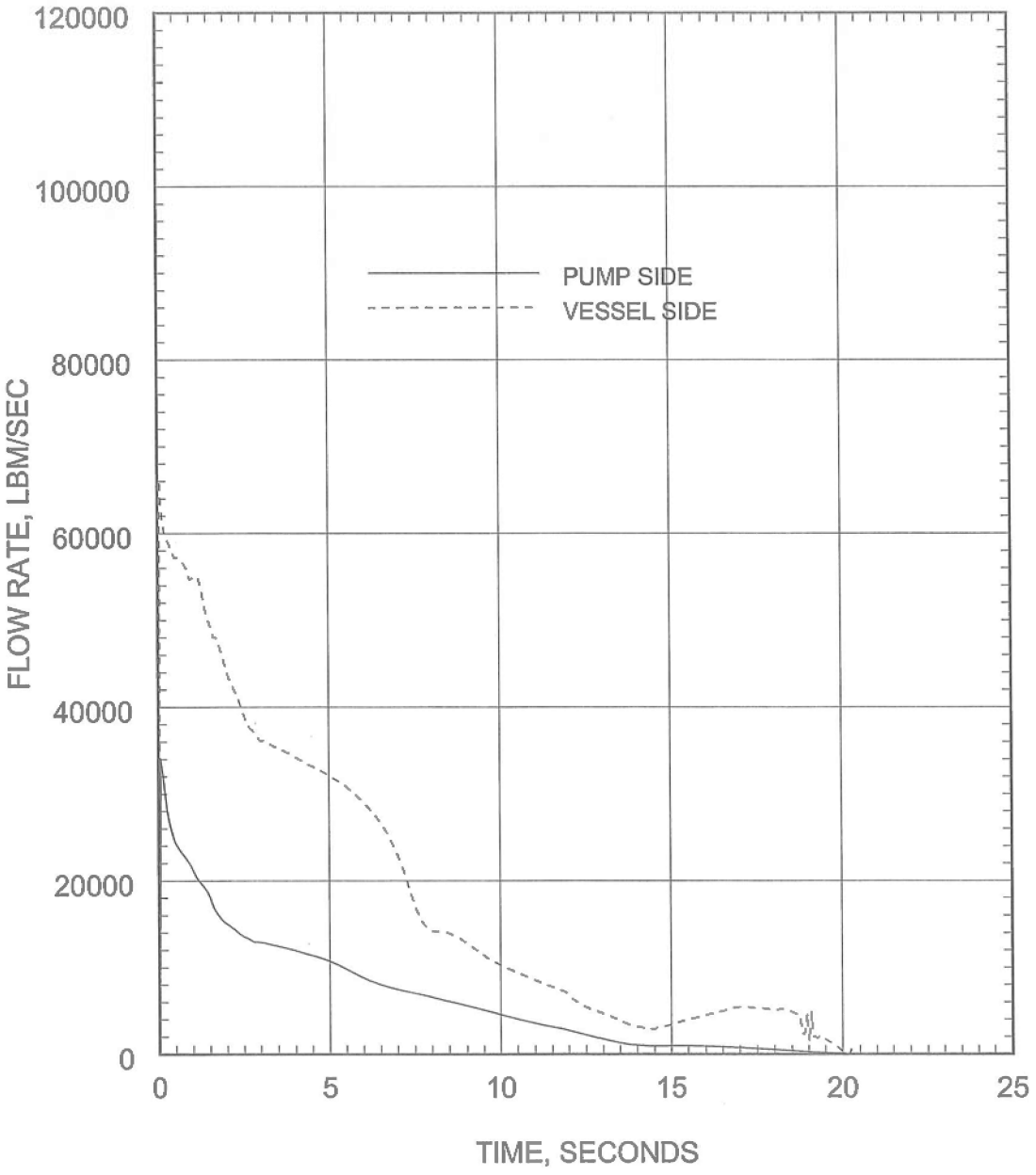

Figure 15.6.5-4
Large Break LOCA ECCS Performance Analysis
1.0 DEG/PD Break
Hot Assembly Flow Rate (Below Hot Spot)

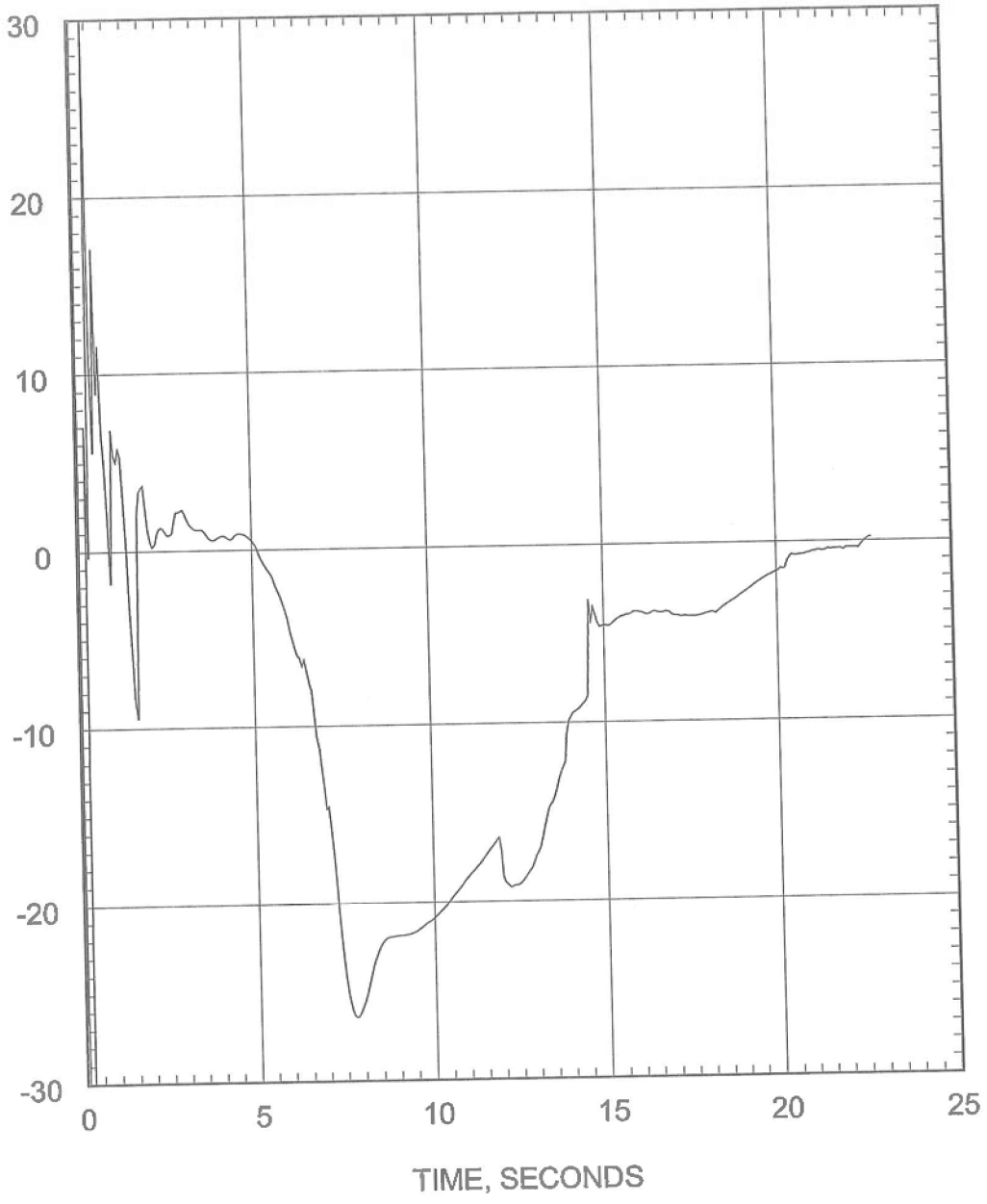

Figure 15.6.5-5
Large Break LOCA ECCS Performance Analysis
1.0 DEG/PD Break
Hot Assembly Flow Rate (Above Hot Spot)

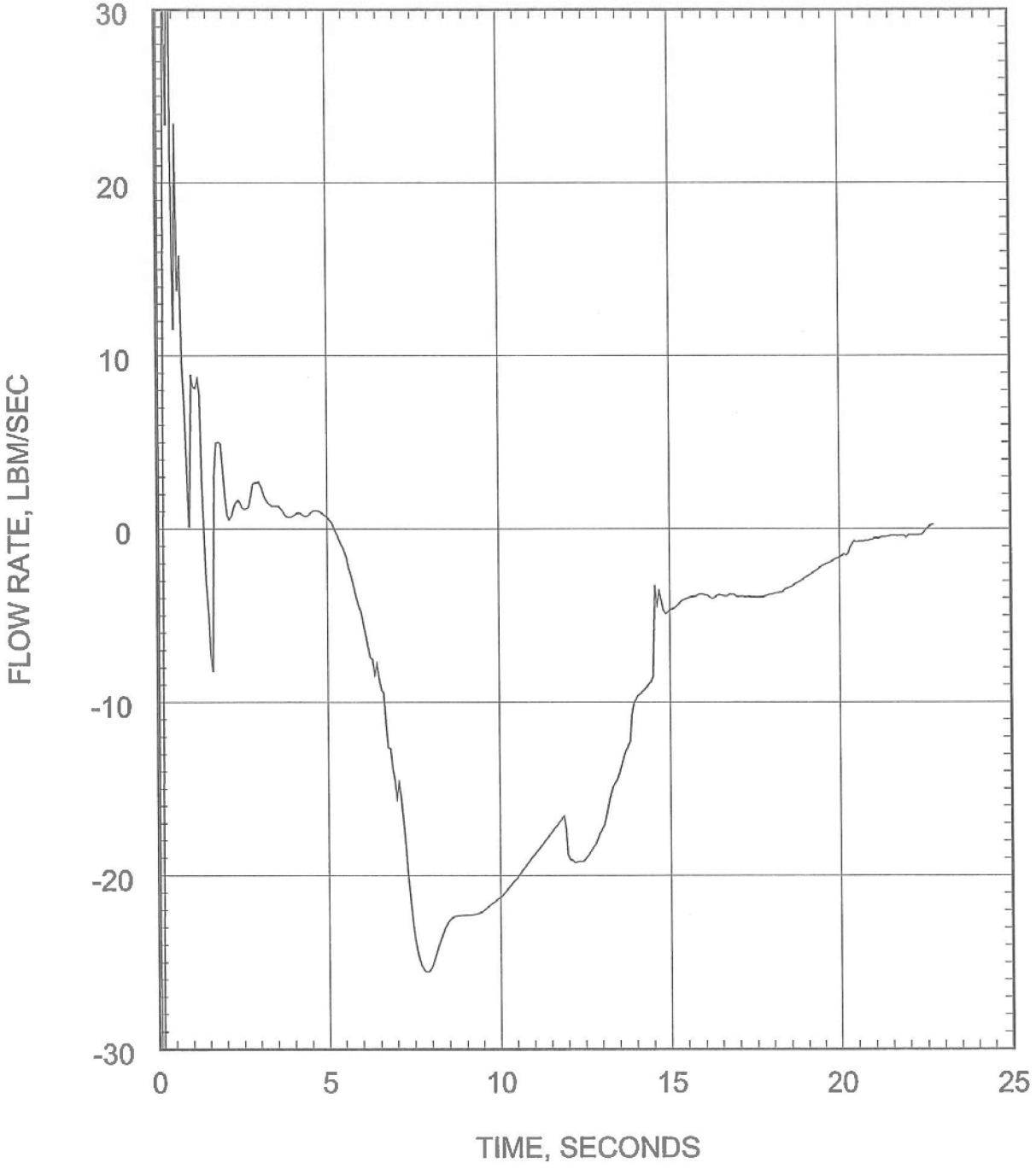

Figure 15.6.5-6
Large Break LOCA ECCS Performance Analysis
1.0 DEG/PD Break
Hot Assembly Quality

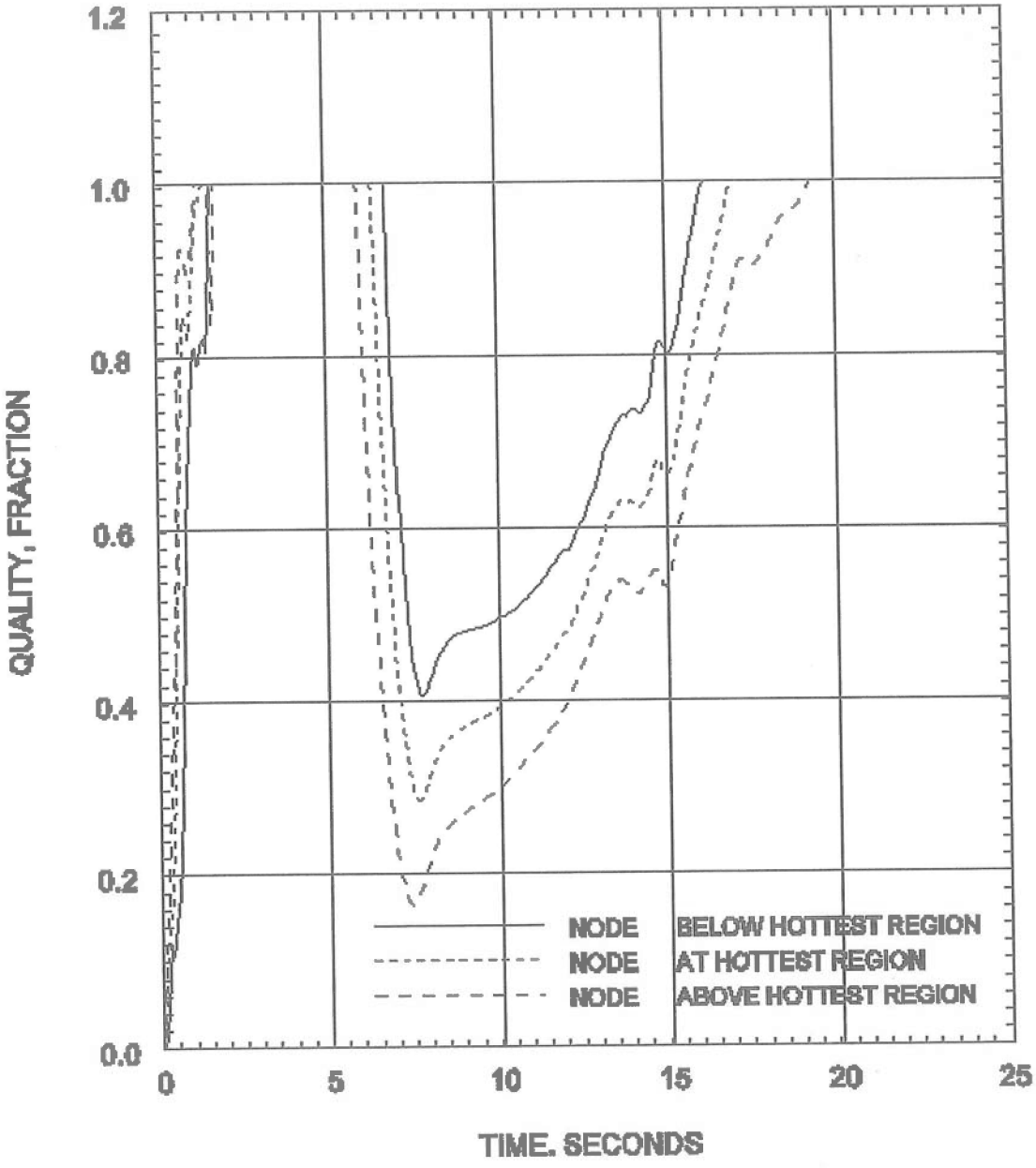

Figure 15.6.5-7
Large Break LOCA ECCS Performance Analysis
1.0 DEG/PD Break
Containment Pressure

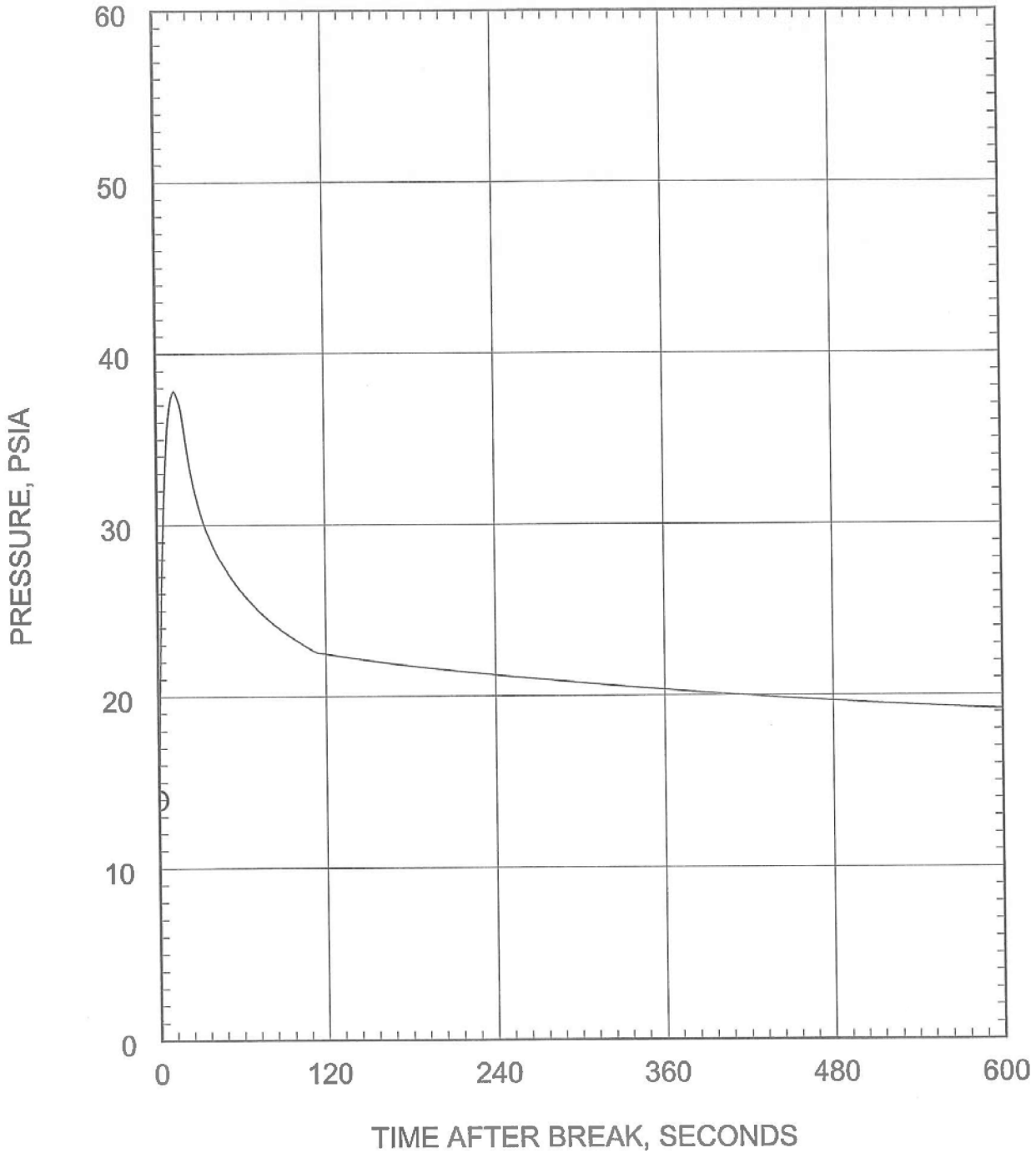

Figure 15.6.5-8
Large Break LOCA ECCS Performance Analysis
1.0 DEG/PD Break
Mass Added to Core During Reflood

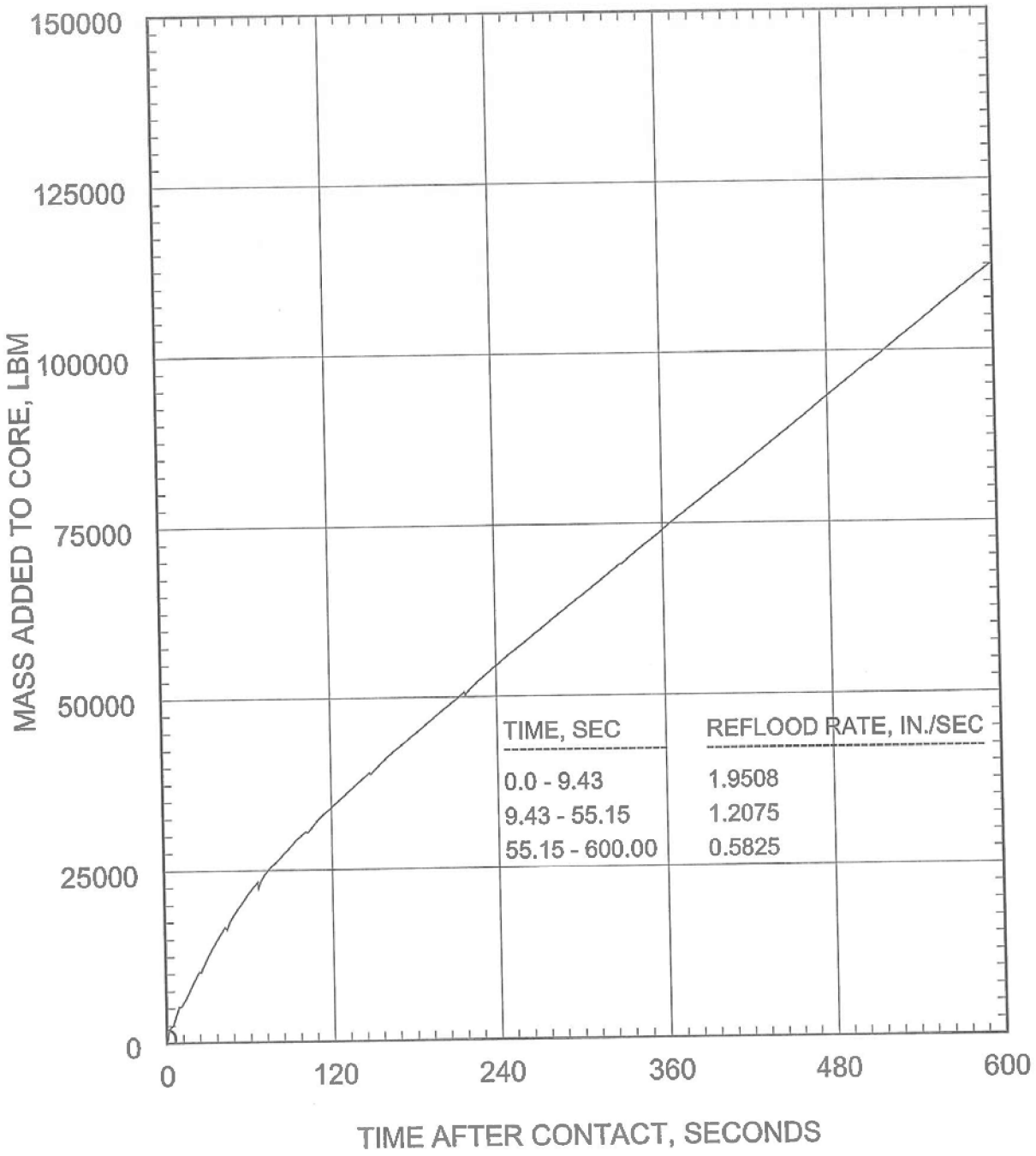

Figure 15.6.5-9
Large Break LOCA ECCS Performance Analysis
1.0 DEG/PD Break
Peak Cladding Temperature

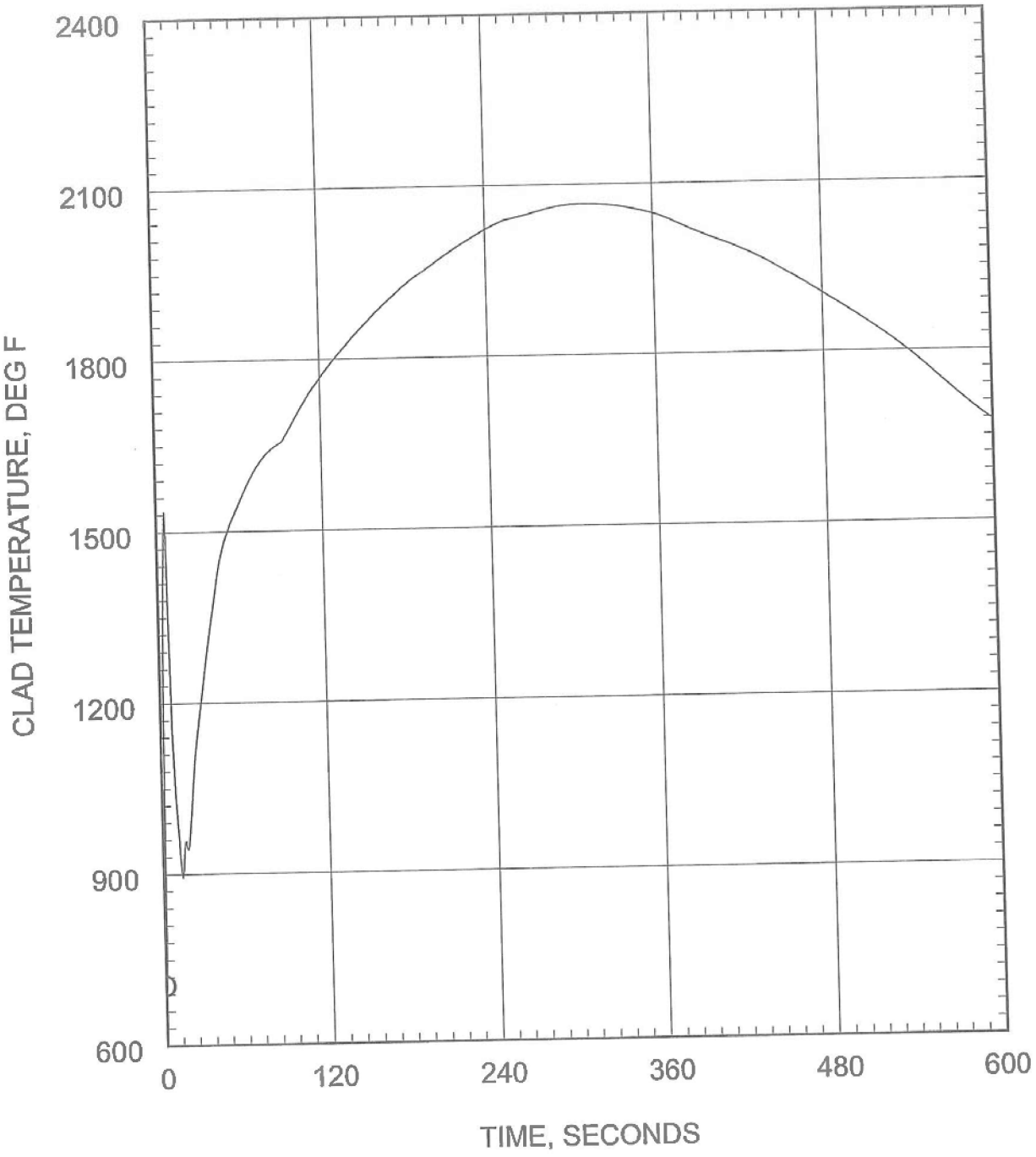

Figure 15.6.5-10
Large Break LOCA ECCS Performance Analysis
0.8 DEG/PD Break
Core Power

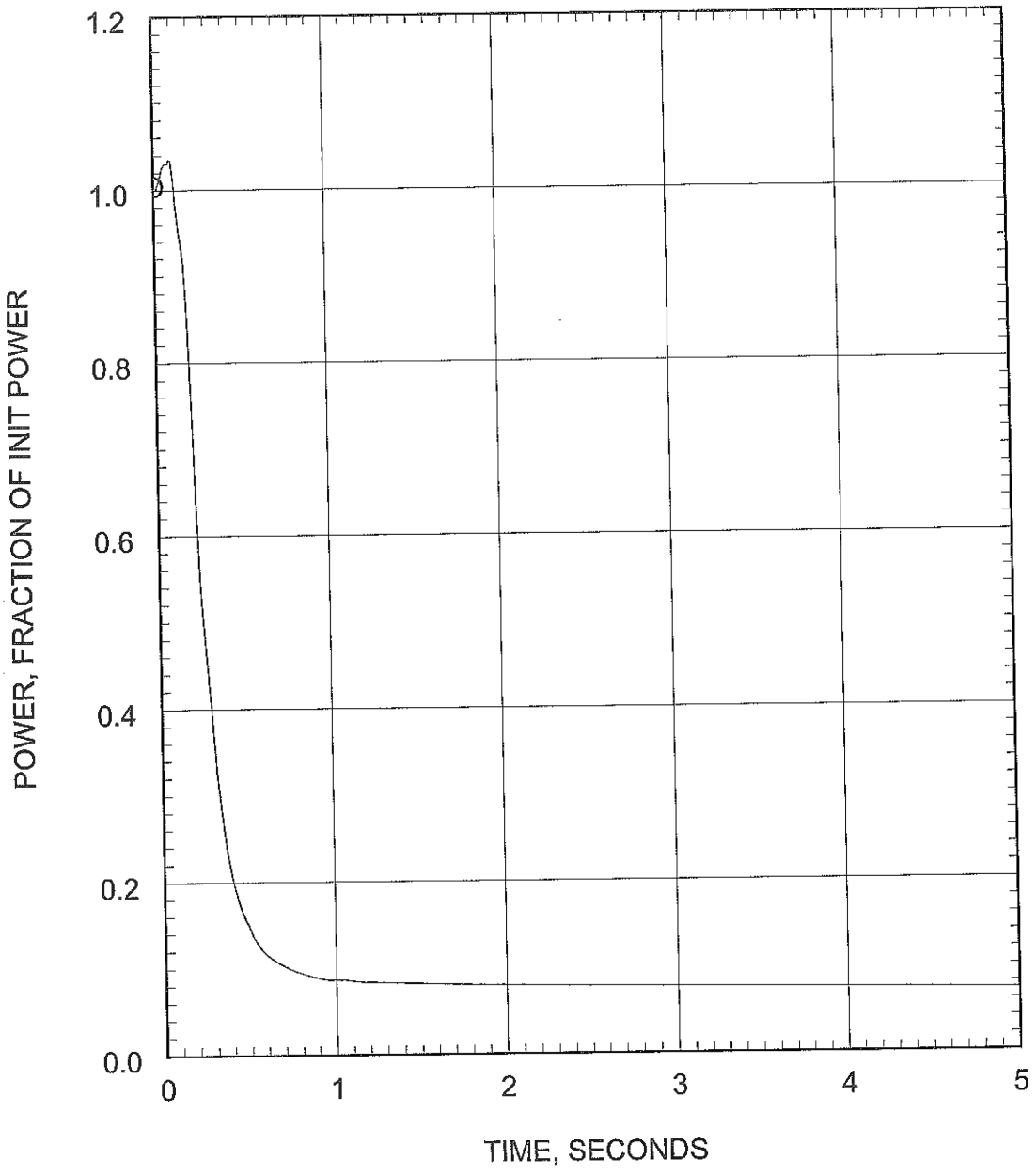

Figure 15.6.5-11
Large Break LOCA ECCS Performance Analysis
0.8 DEG/PD Break
Pressure in Center Hot Assembly Node

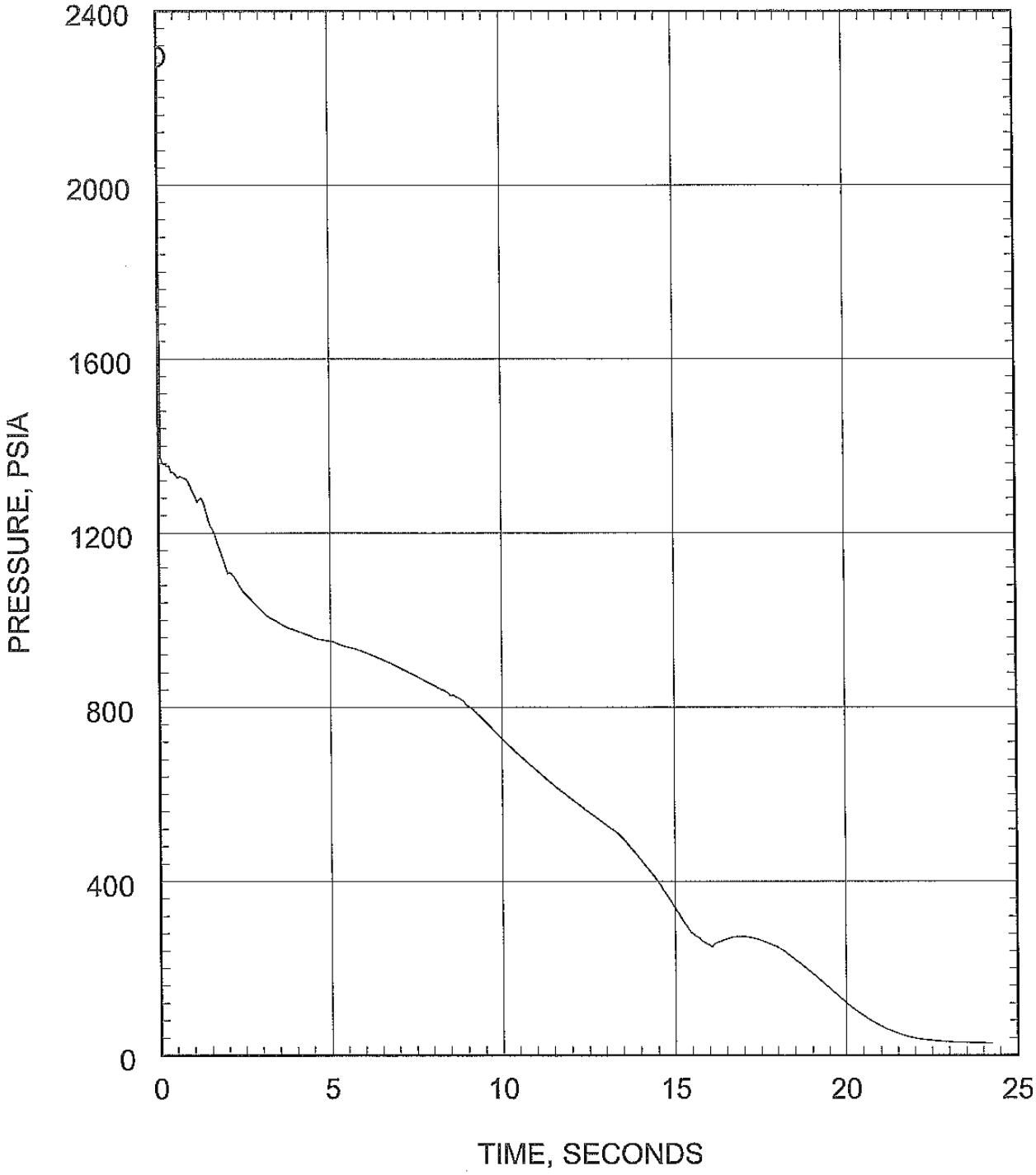

Figure 15.6.5-12
Large Break LOCA ECCS Performance Analysis
0.8 DEG/PD Break
Leak Flow Rate

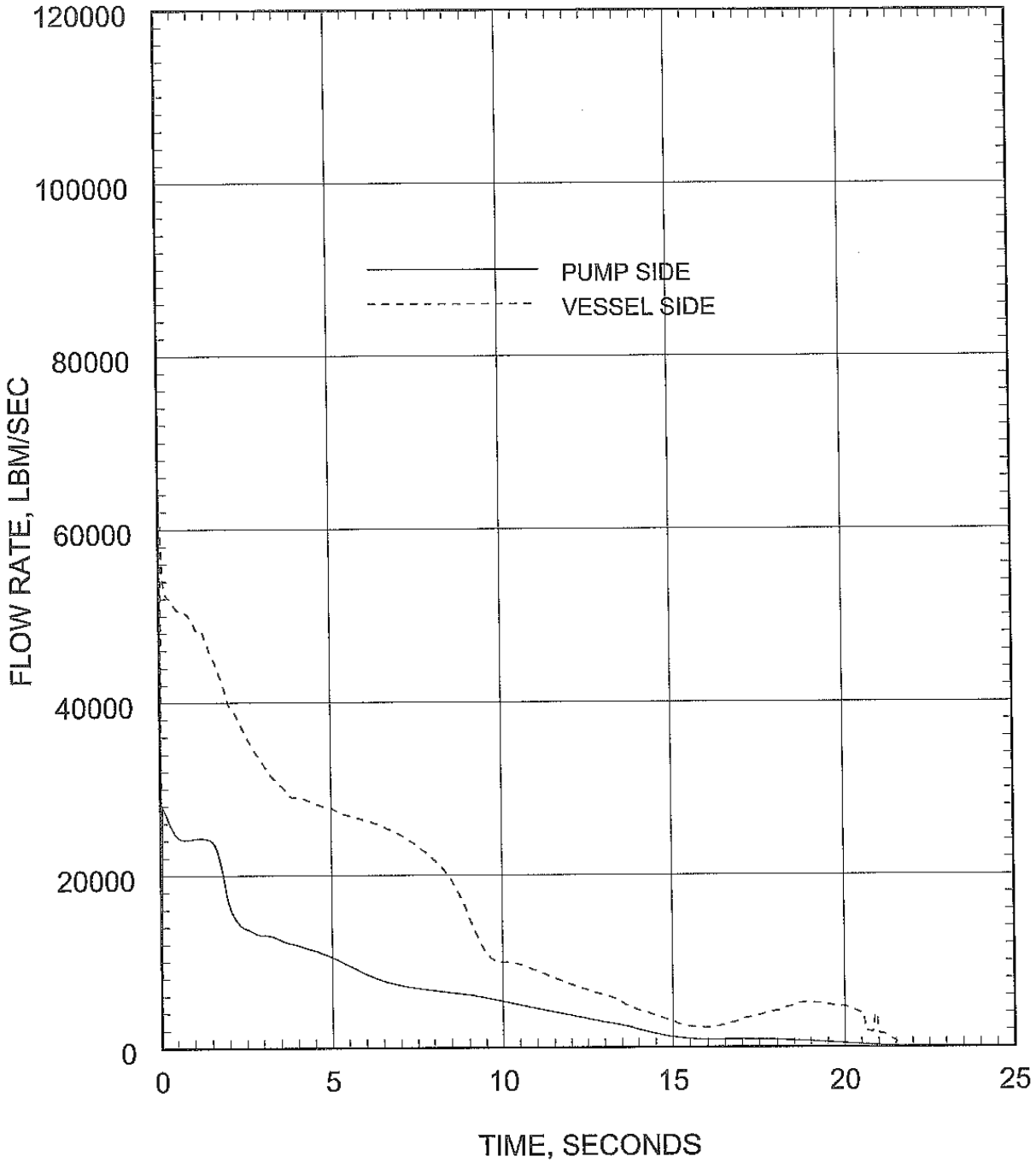

Figure 15.6.5-13
Large Break LOCA ECCS Performance Analysis
0.8 DEG/PD Break
Hot Assembly Flow Rate (Below Hot Spot)

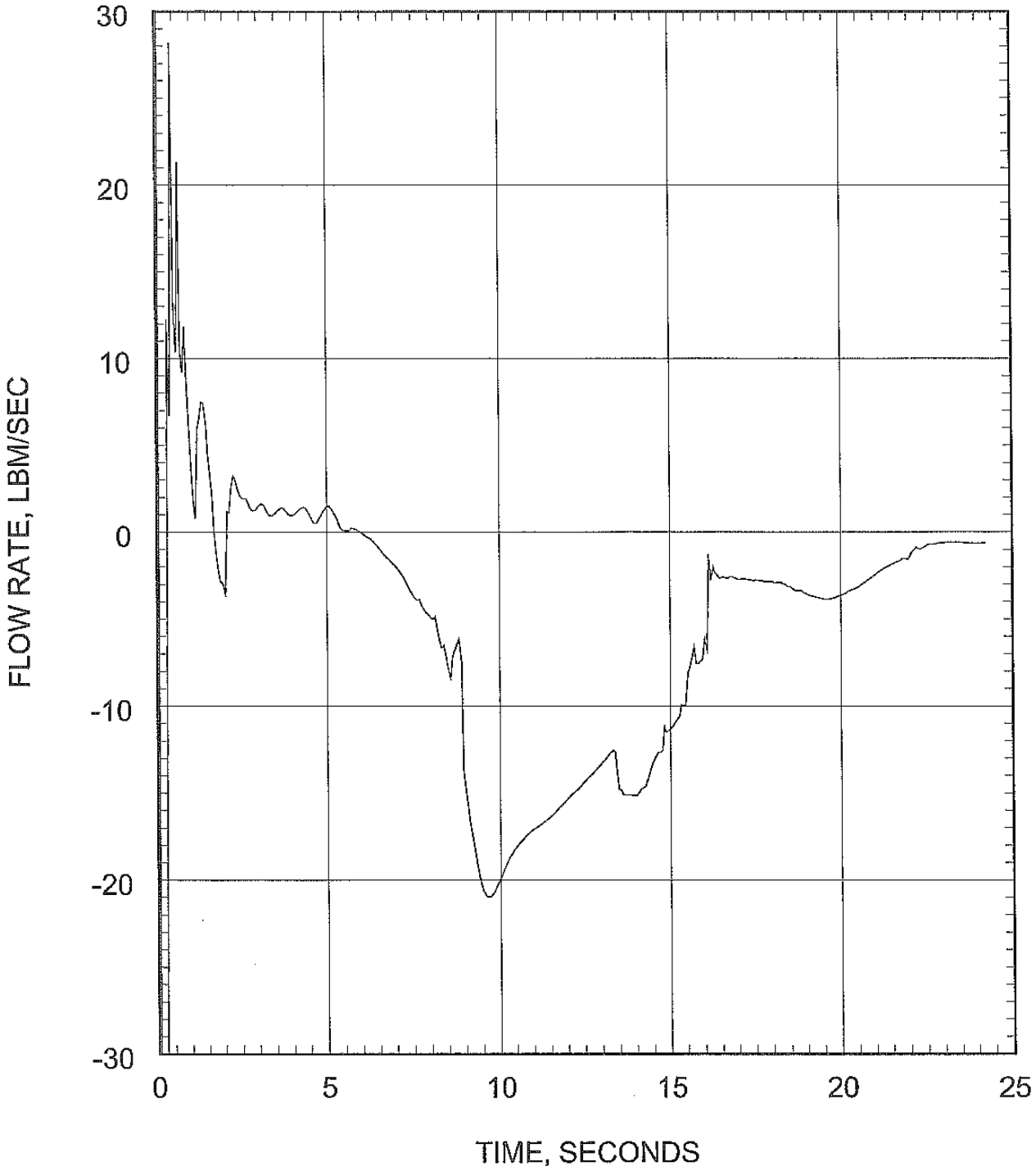

Figure 15.6.5-14
Large Break LOCA ECCS Performance Analysis
0.8 DEG/PD Break
Hot Assembly Flow Rate (Above Hot Spot)

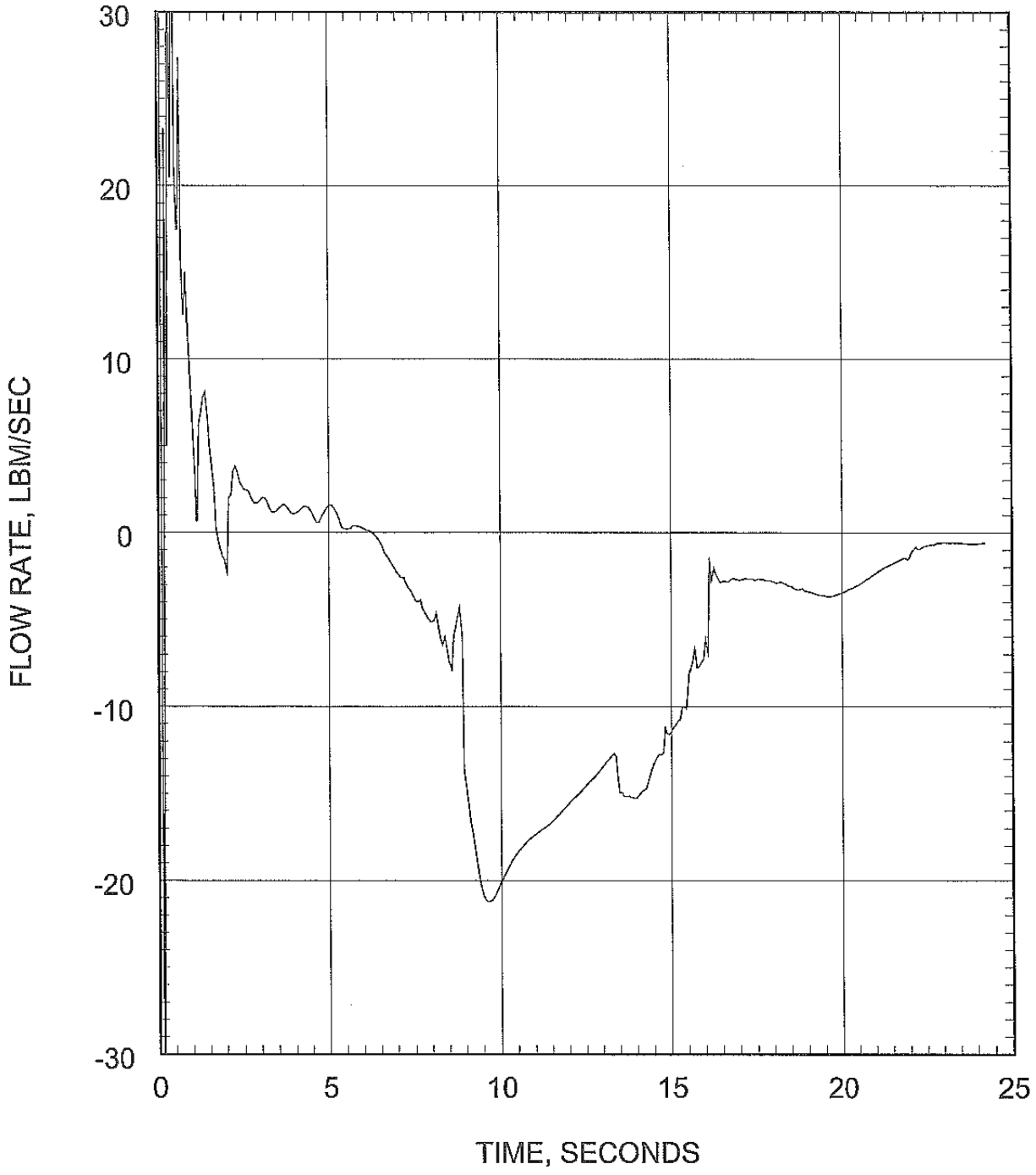

Figure 15.6.5-15
Large Break LOCA ECCS Performance Analysis
0.8 DEG/PD Break
Hot Assembly Quality

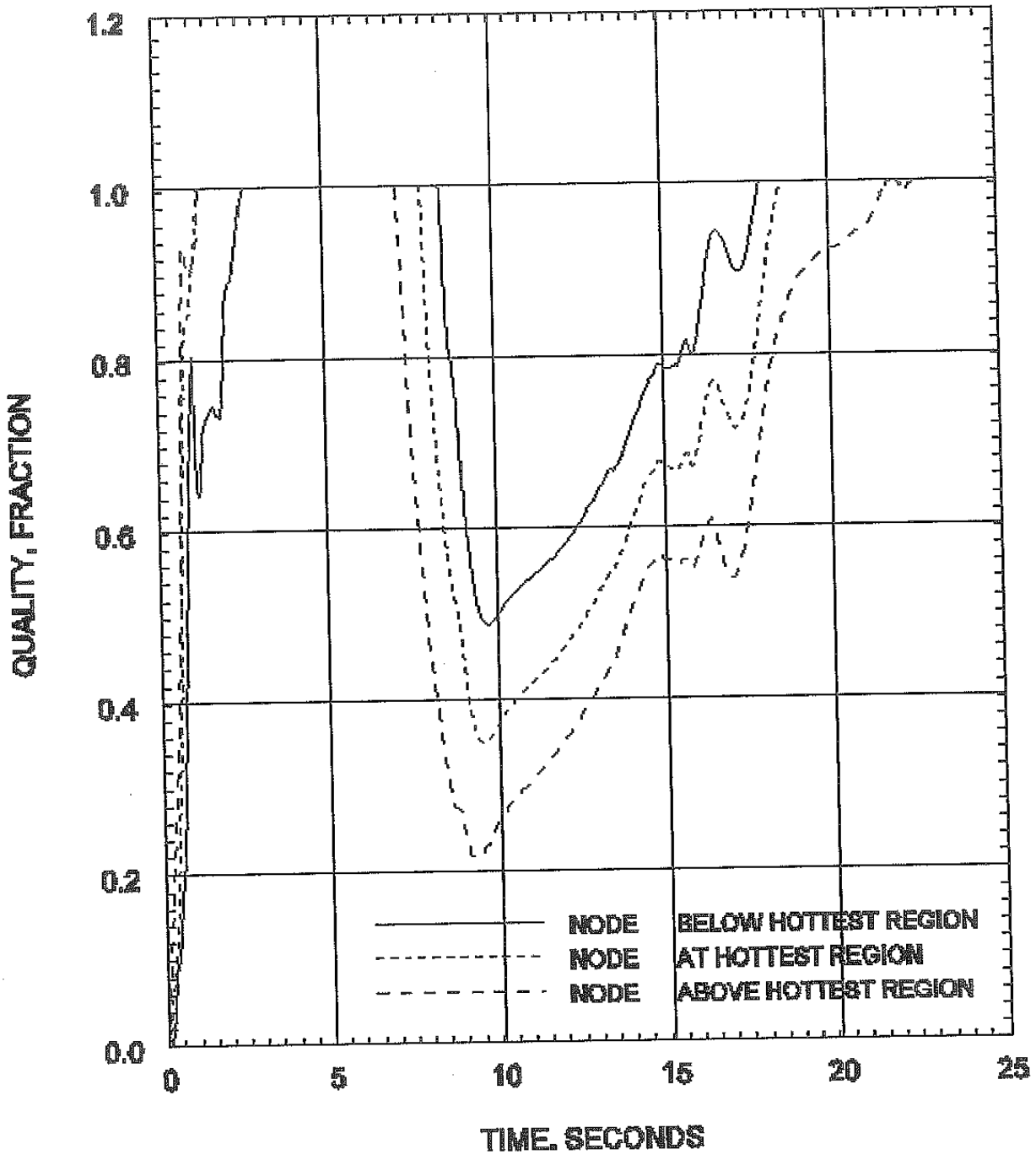

Figure 15.6.5-16
Large Break LOCA ECCS Performance Analysis
0.8 DEG/PD Break
Containment Pressure

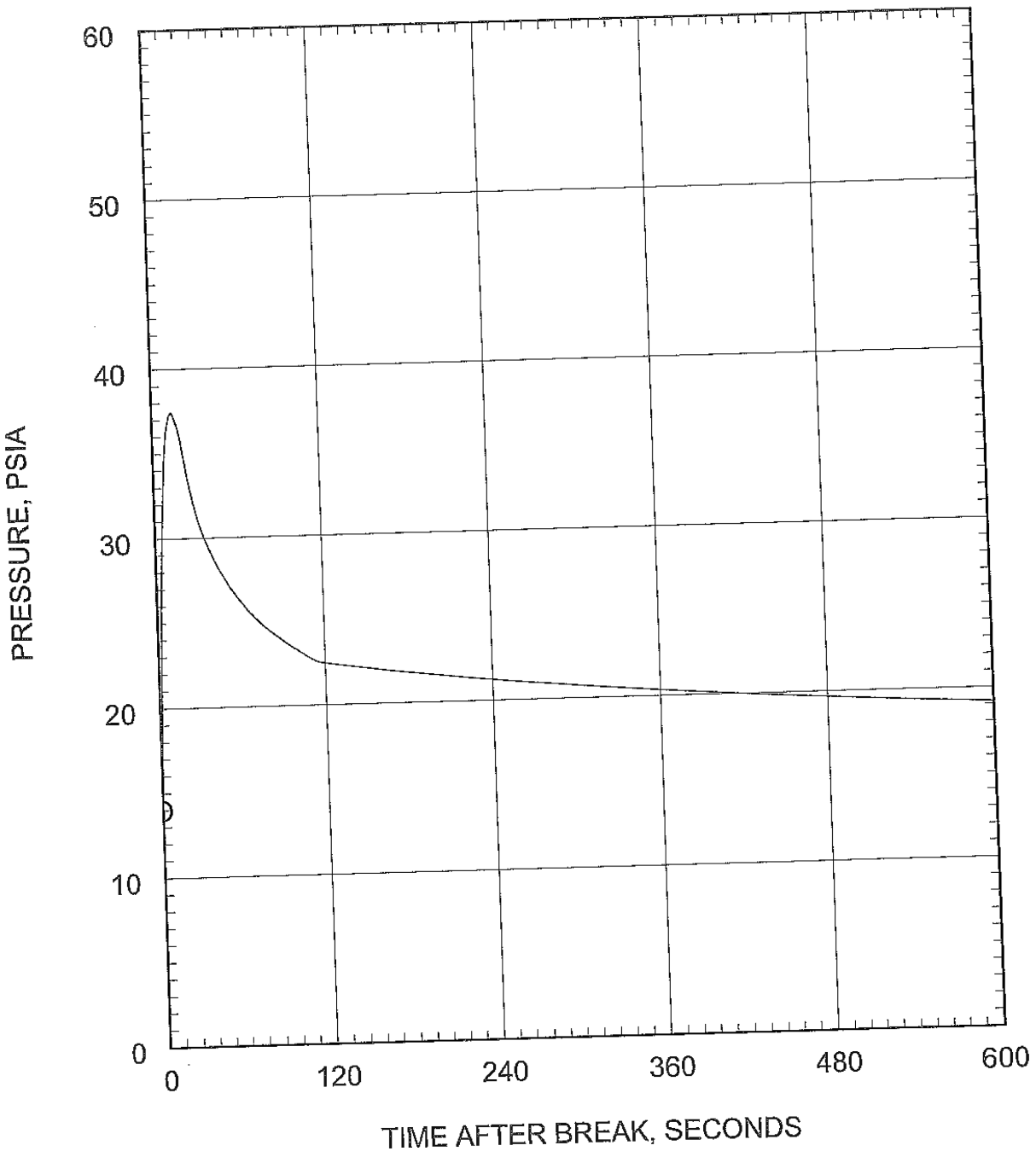

Figure 15.6.5-17
Large Break LOCA ECCS Performance Analysis
0.8 DEG/PD Break
Mass Added to Core During Reflood

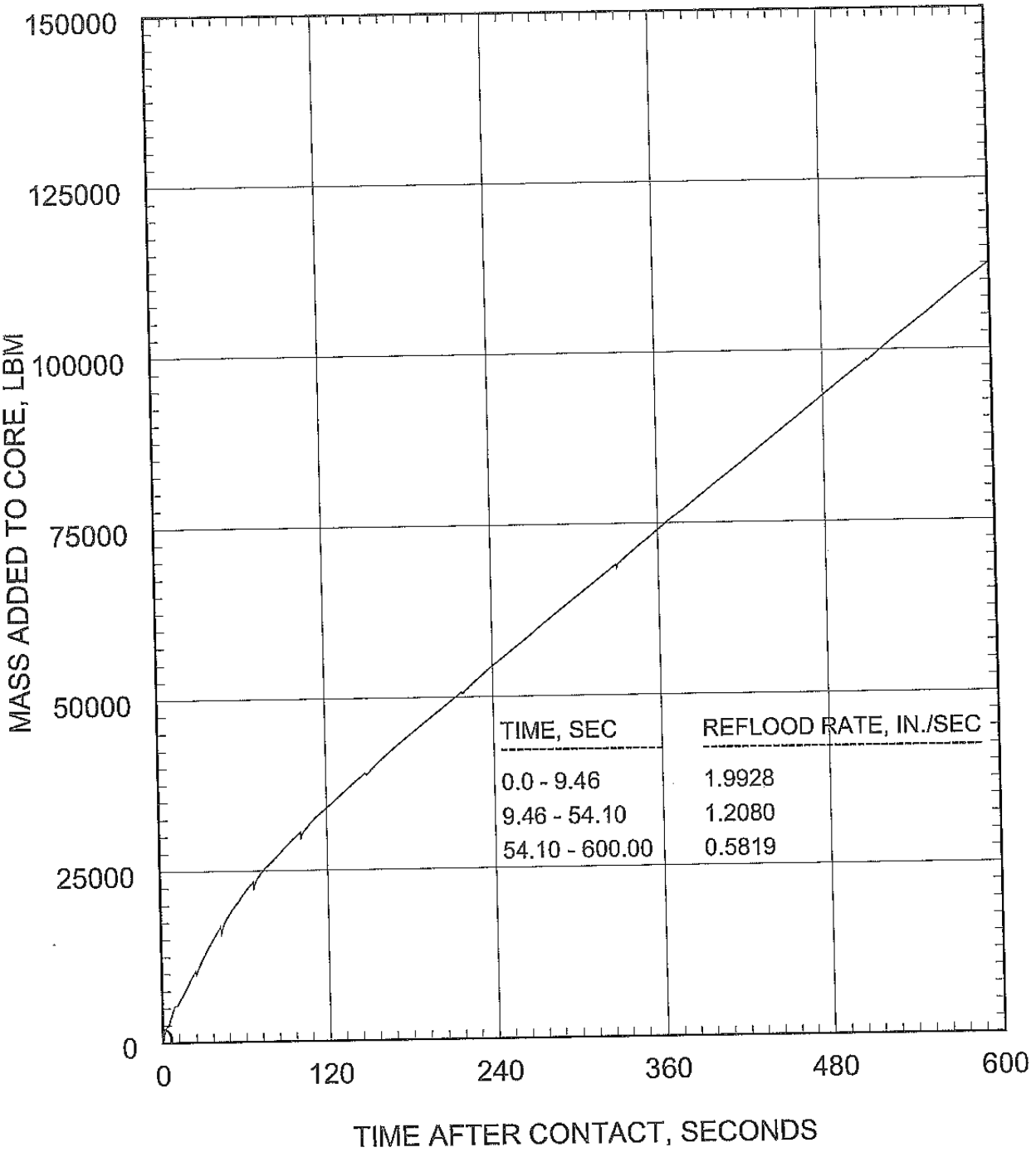

Figure 15.6.5-18
Large Break LOCA ECCS Performance Analysis
0.8 DEG/PD Break
Peak Cladding Temperature

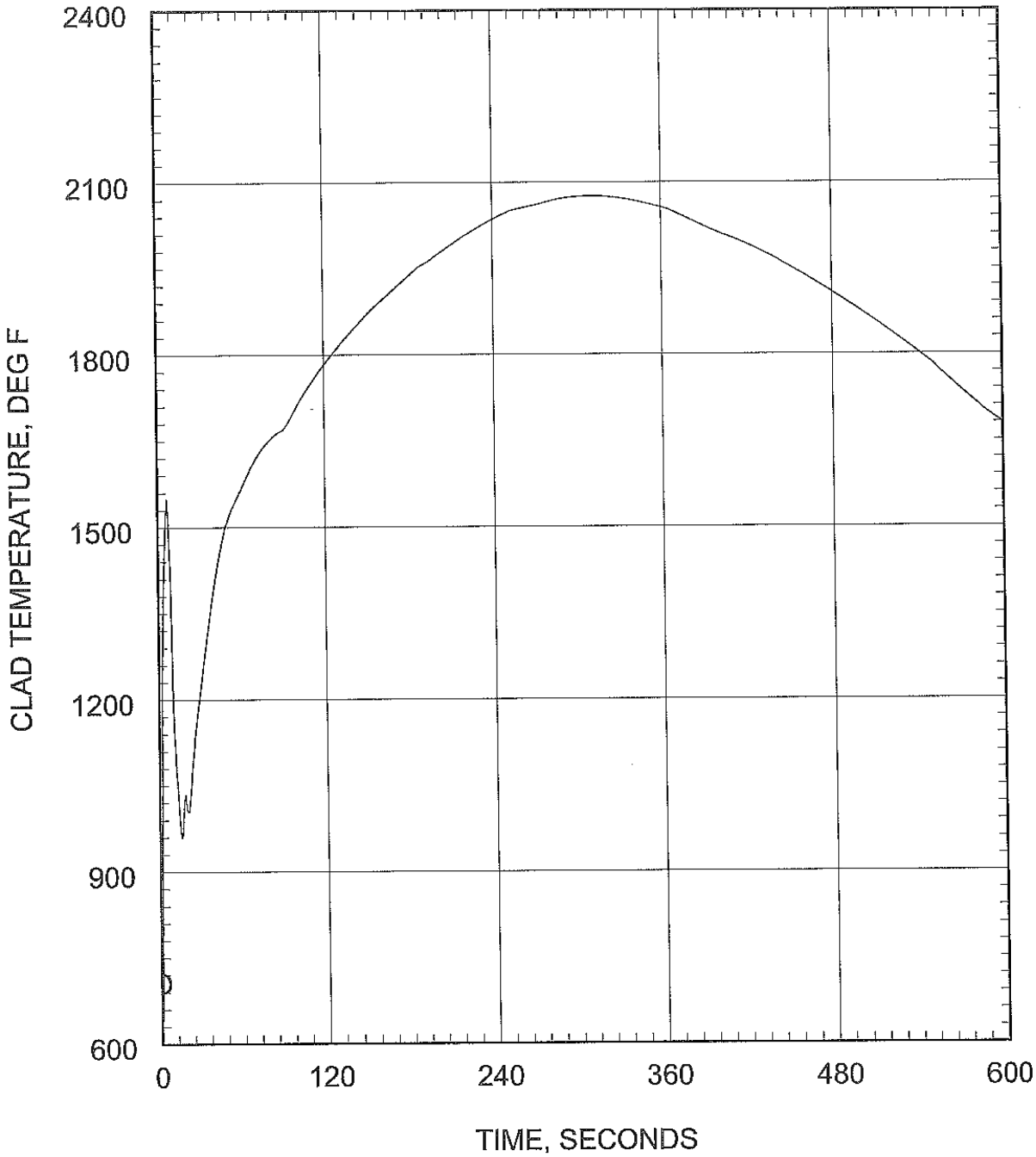

Figure 15.6.5-19
Large Break LOCA ECCS Performance Analysis
0.6 DEG/PD Break
Core Power

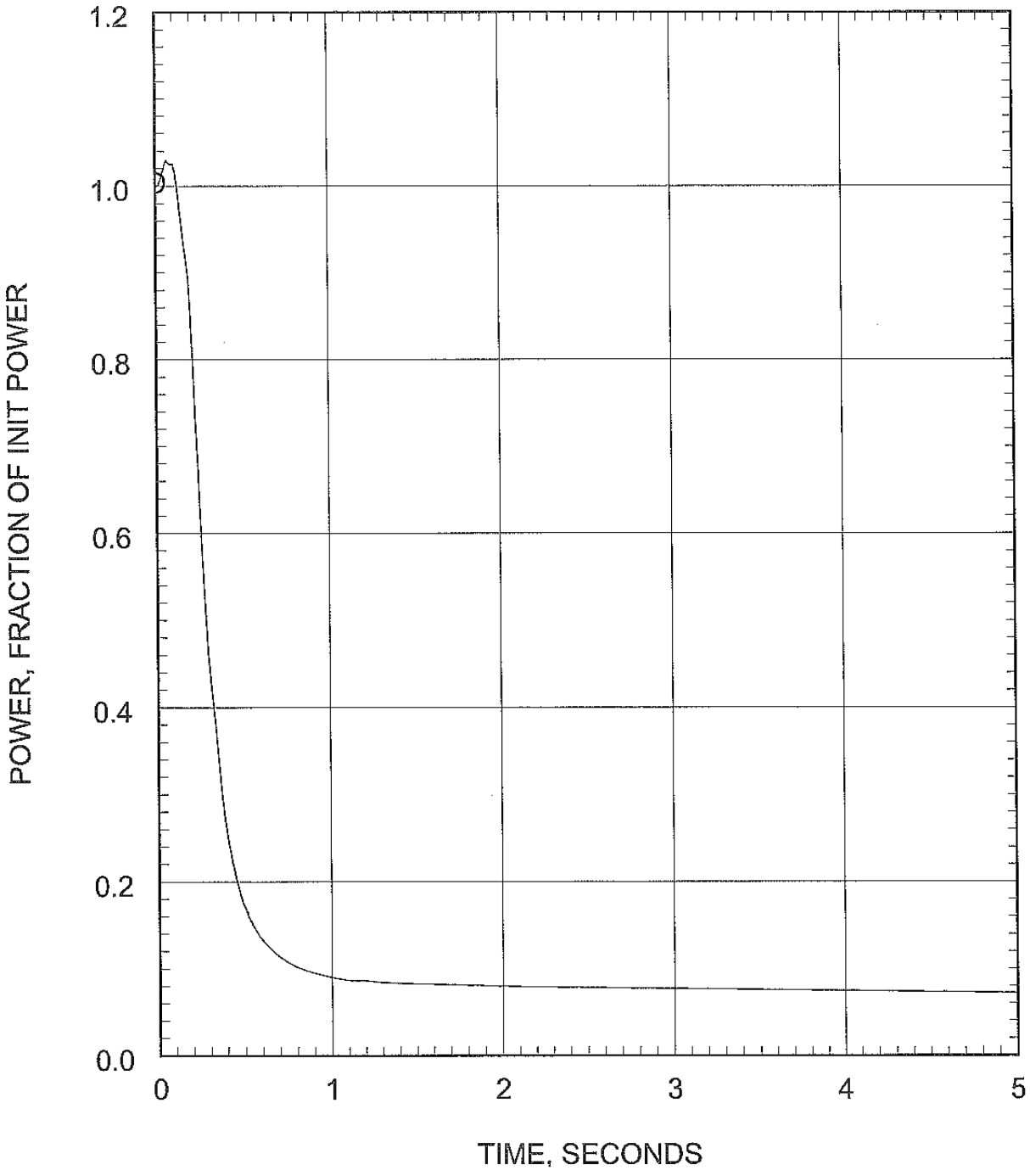

Figure 15.6.5-20
Large Break LOCA ECCS Performance Analysis
0.6 DEG/PD Break
Pressure in Center Hot Assembly Node

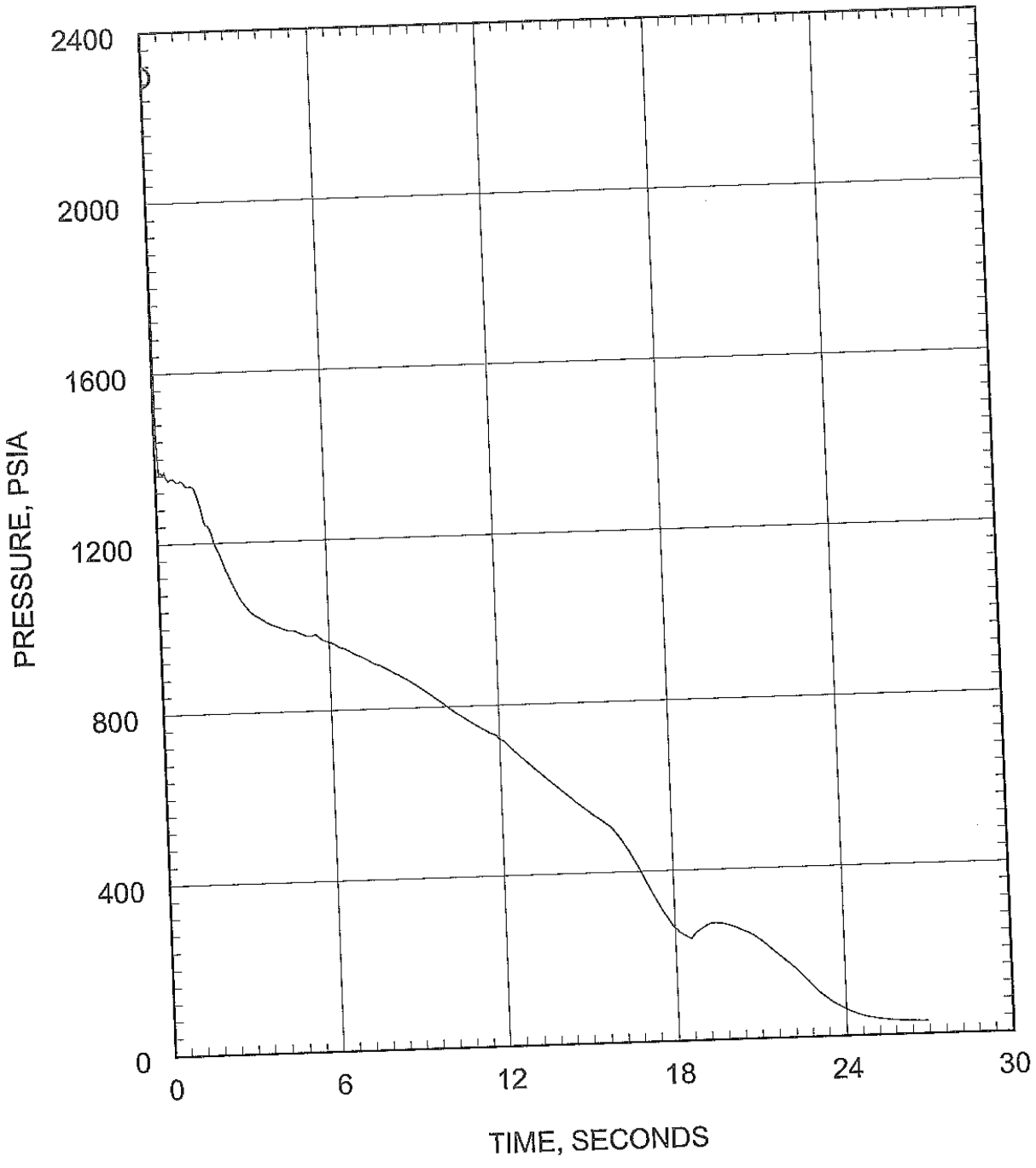

Figure 15.6.5-21
Large Break LOCA ECCS Performance Analysis
0.6 DEG/PD Break
Leak Flow Rate

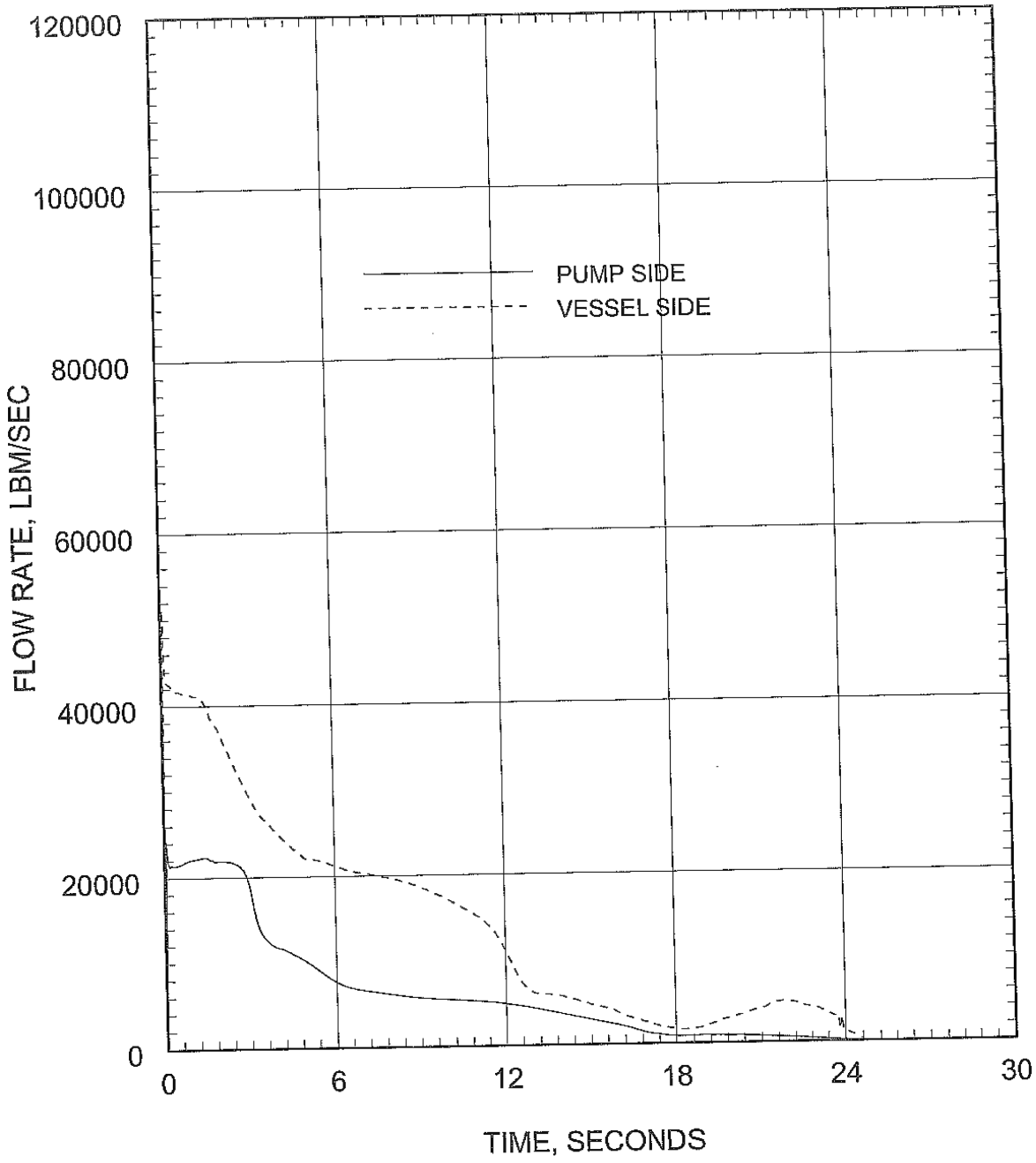

Figure 15.6.5-22
Large Break LOCA ECCS Performance Analysis
0.6 DEG/PD Break
Hot Assembly Flow Rate (Below Hot Spot)

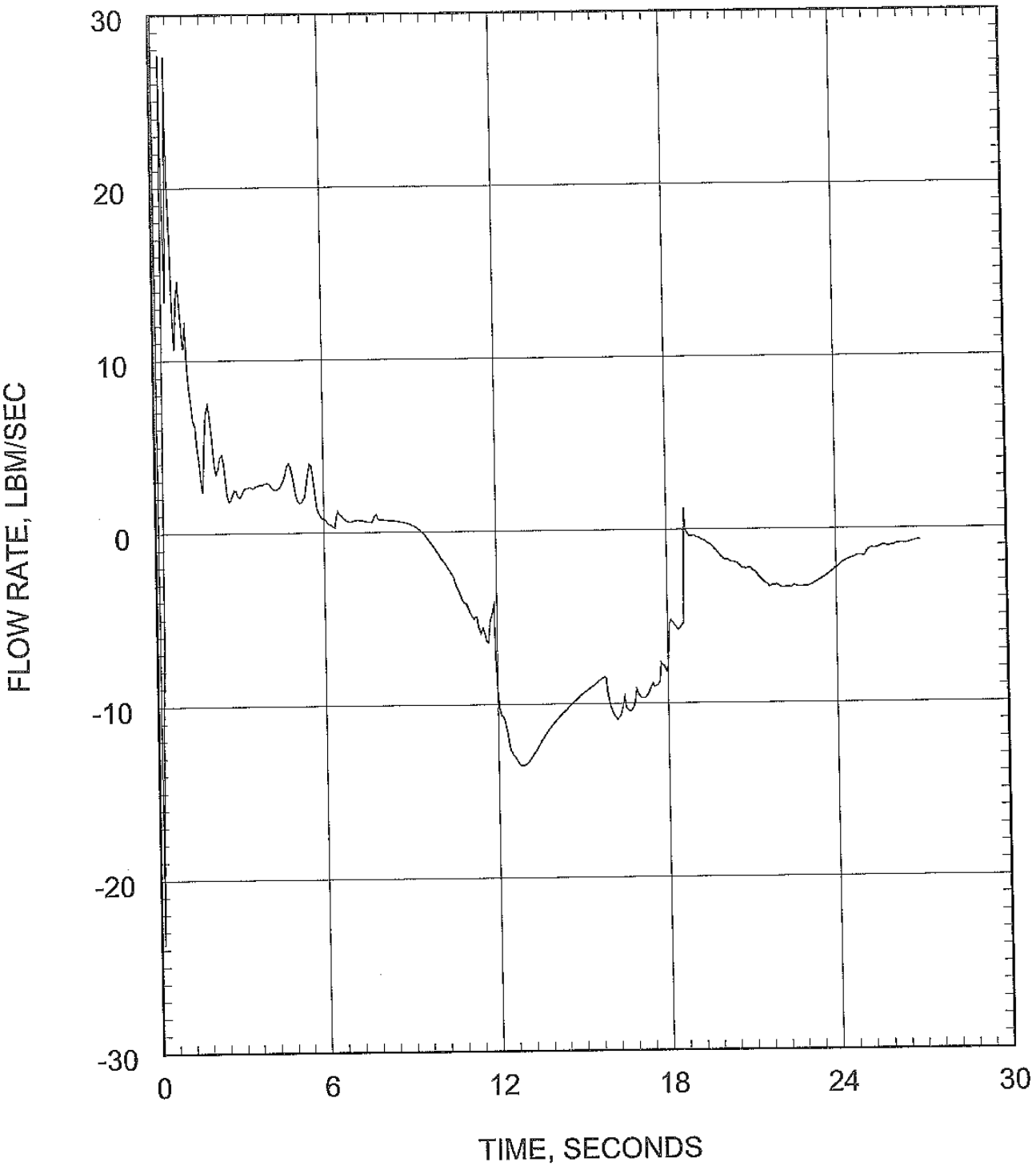

Figure 15.6.5-23
Large Break LOCA ECCS Performance Analysis
0.6 DEG/PD Break
Hot Assembly Flow Rate (Above Hot Spot)

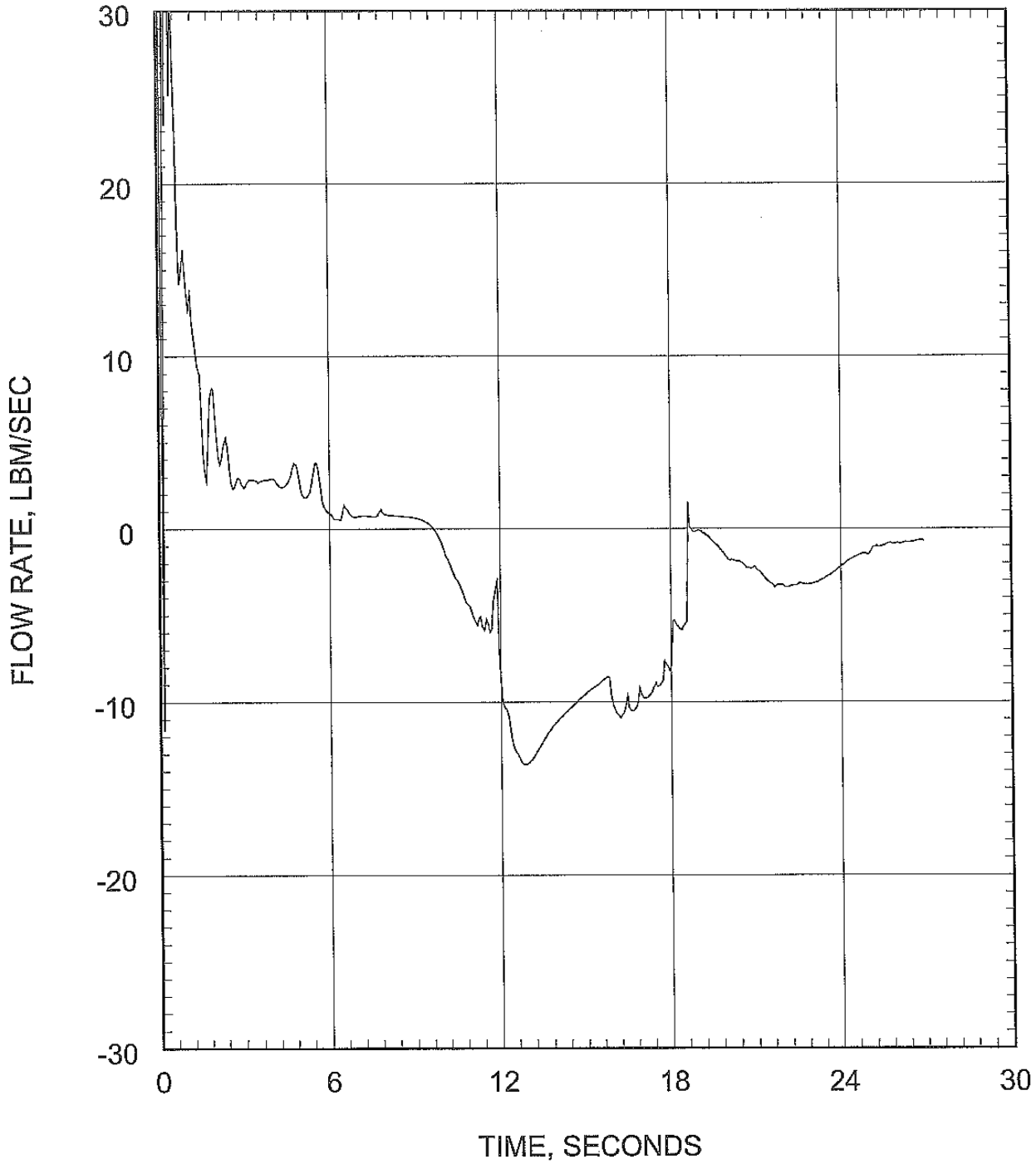

Figure 15.6.5-24
Large Break LOCA ECCS Performance Analysis
0.6 DEG/PD Break
Hot Assembly Quality

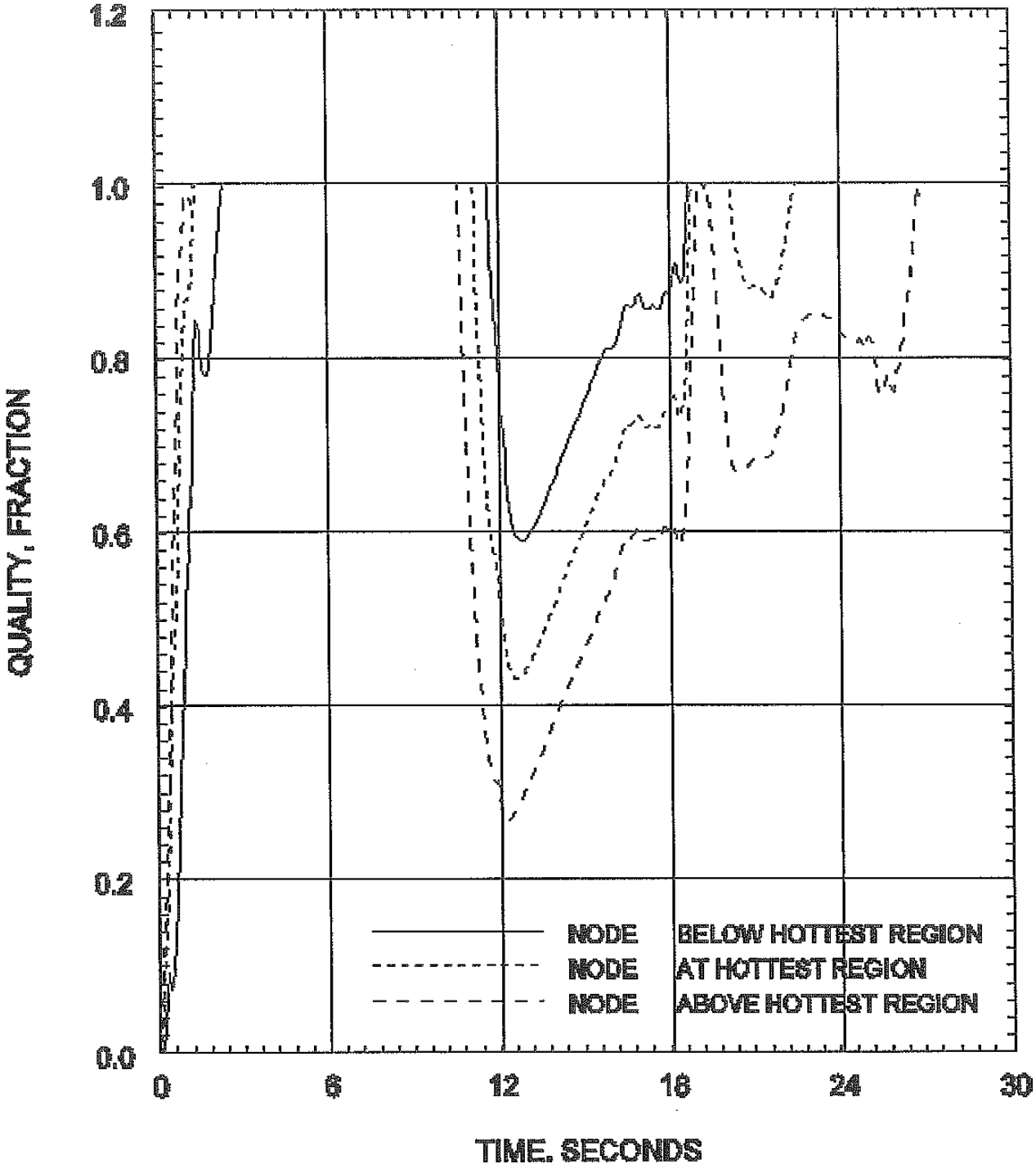

Figure 15.6.5-25
Large Break LOCA ECCS Performance Analysis
0.6 DEG/PD Break
Containment Pressure

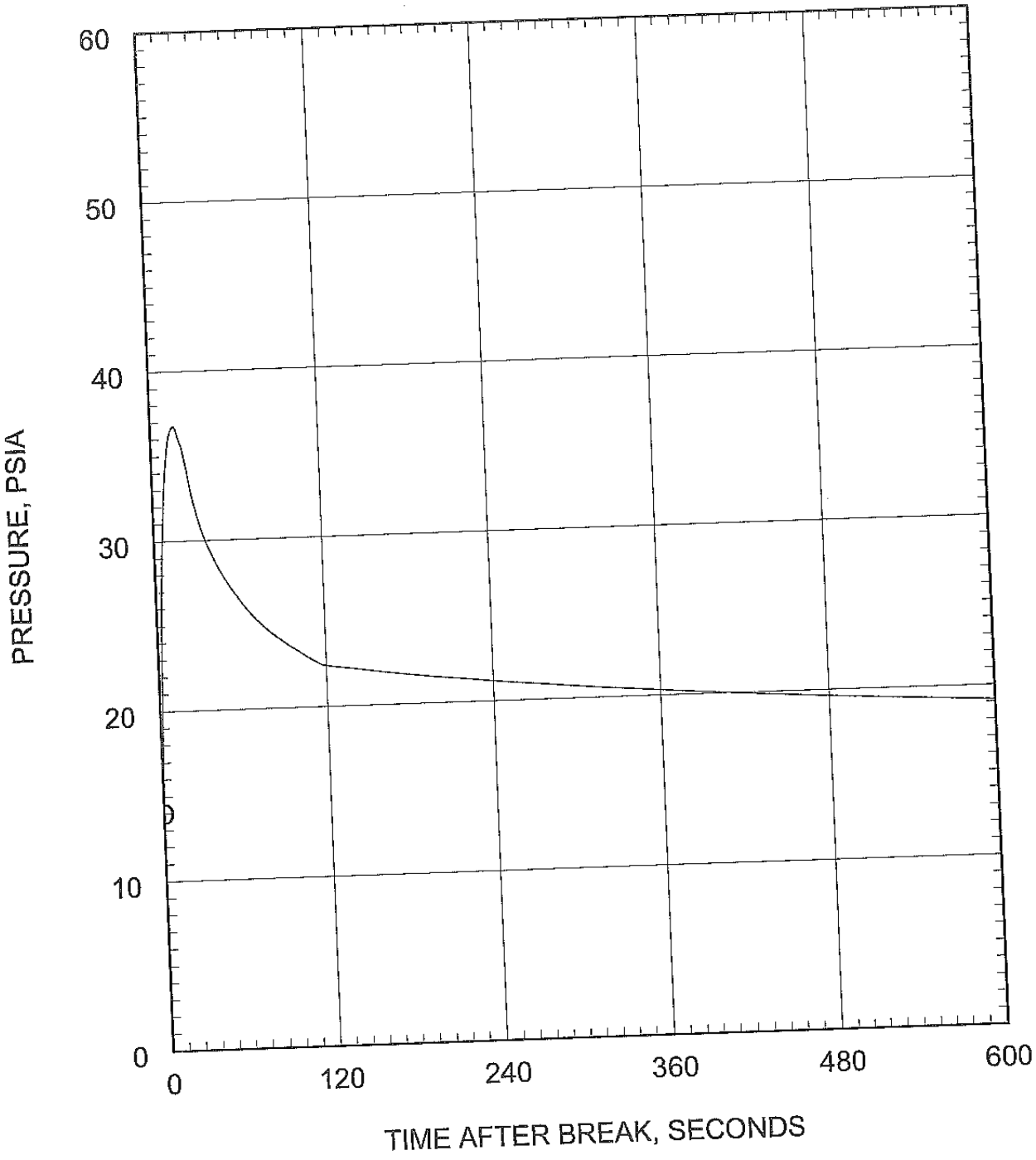

Figure 15.6.5-26
Large Break LOCA ECCS Performance Analysis
0.6 DEG/PD Break
Mass Added to Core During Reflood

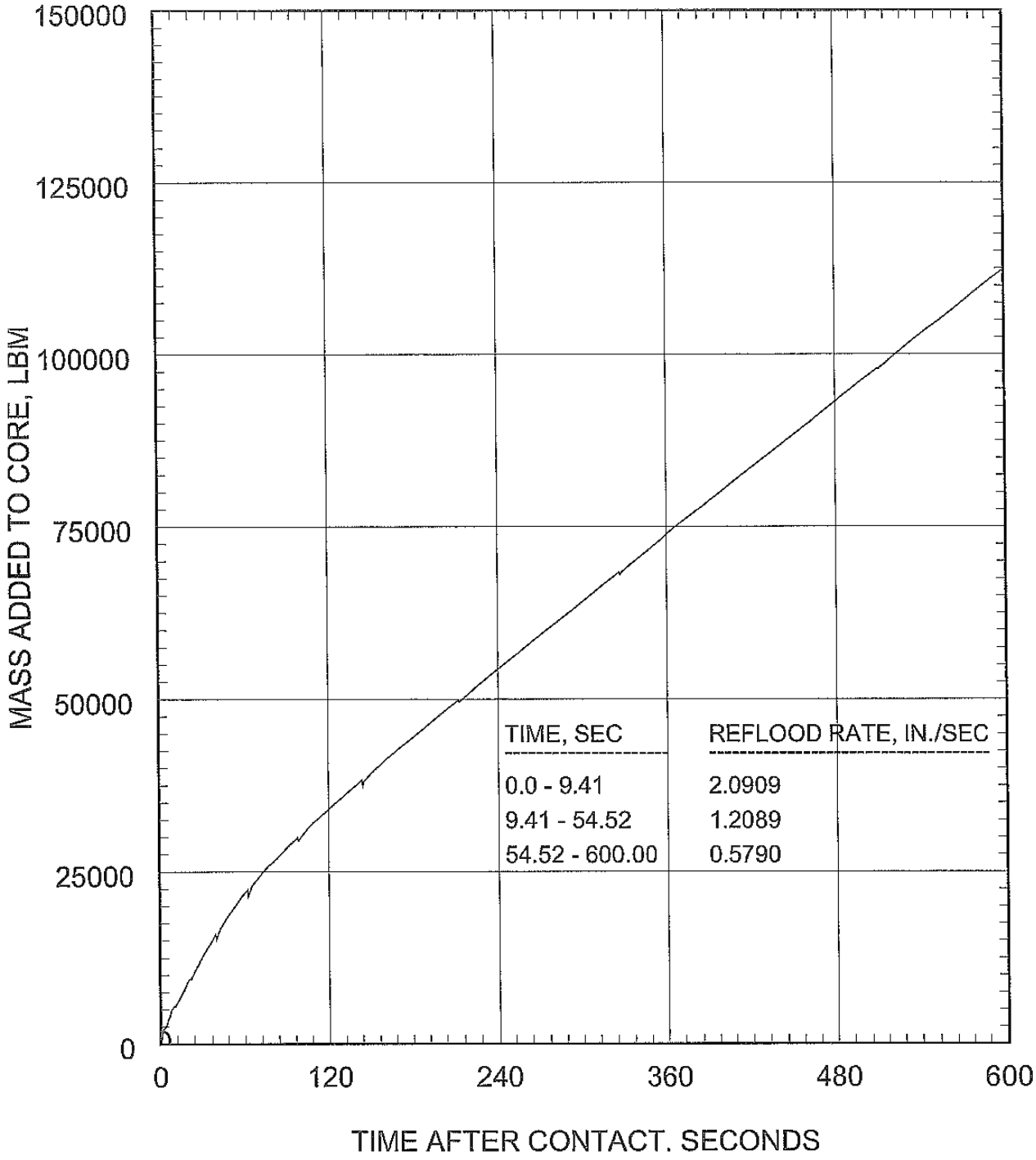

Figure 15.6.5-27
Large Break LOCA ECCS Performance Analysis
0.6 DEG/PO Break
Peak Cladding Temperature

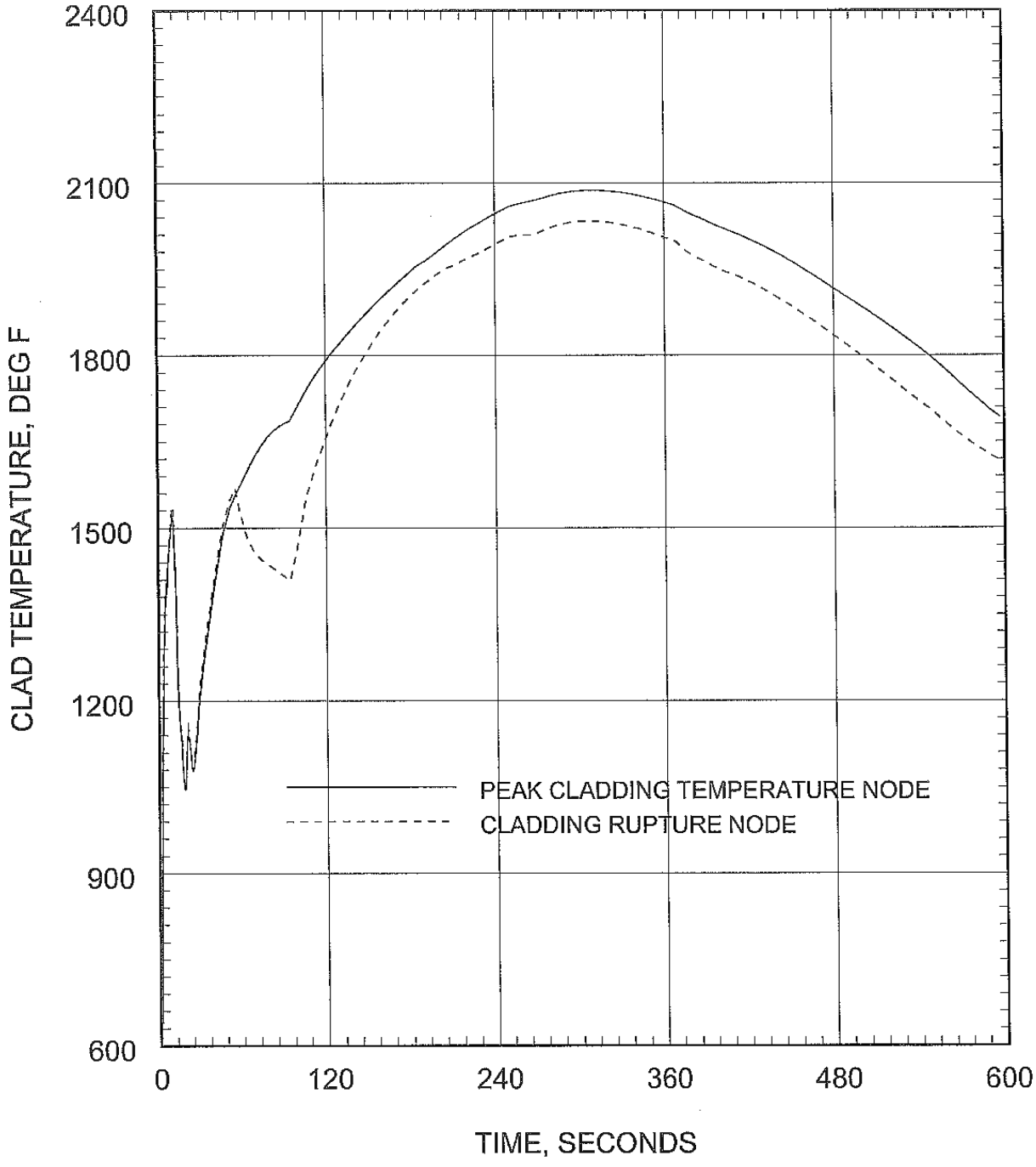

Figure 15.6.5-28
Large Break LOCA ECCS Performance Analysis
0.6 DEG/PO Break
Mid Annulus Flow Rate

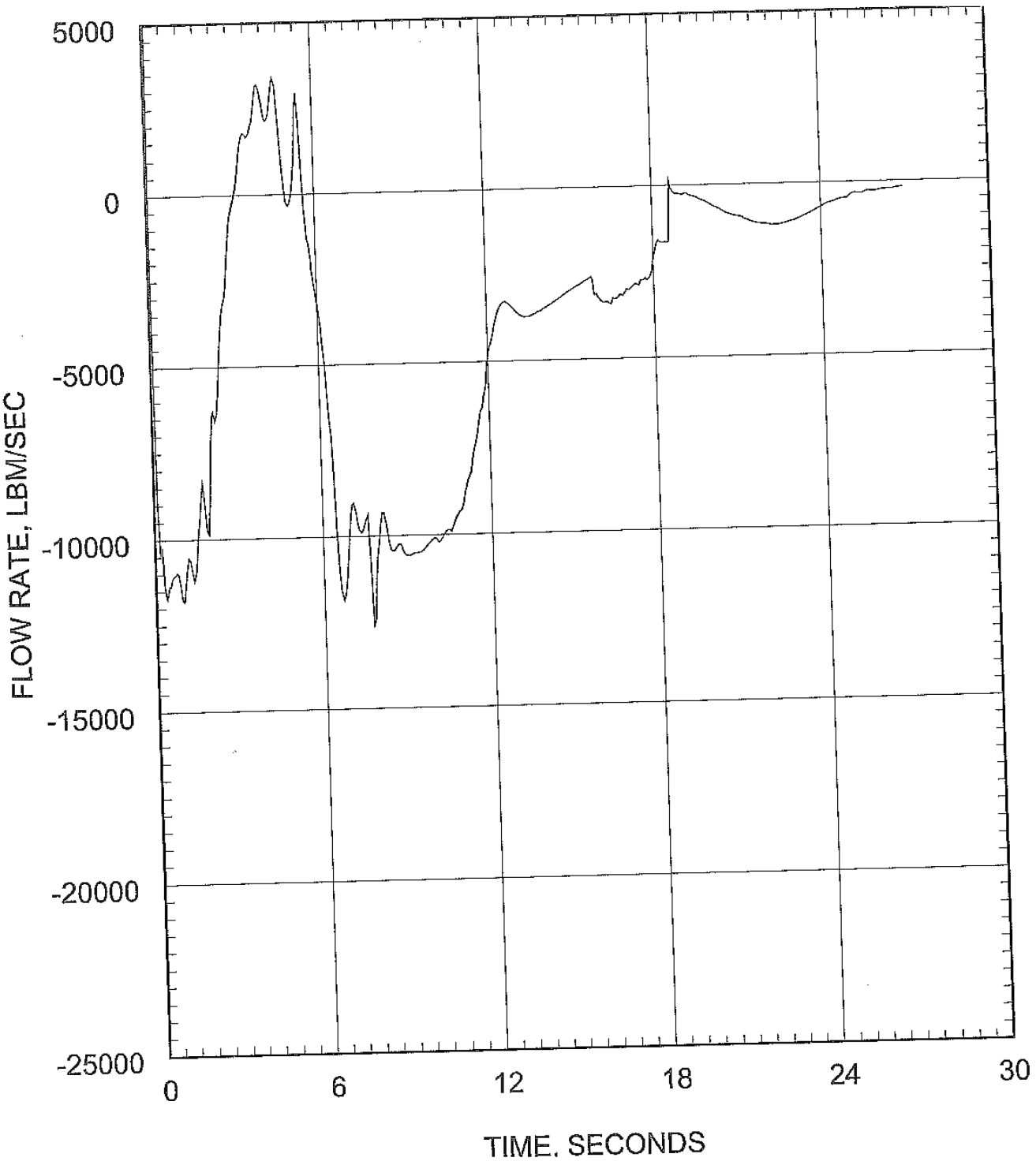

Figure 15.6.5-29
Large Break LOCA ECCS Performance Analysis
0.6 DEG/PD Break
Quality Above and Below the Core

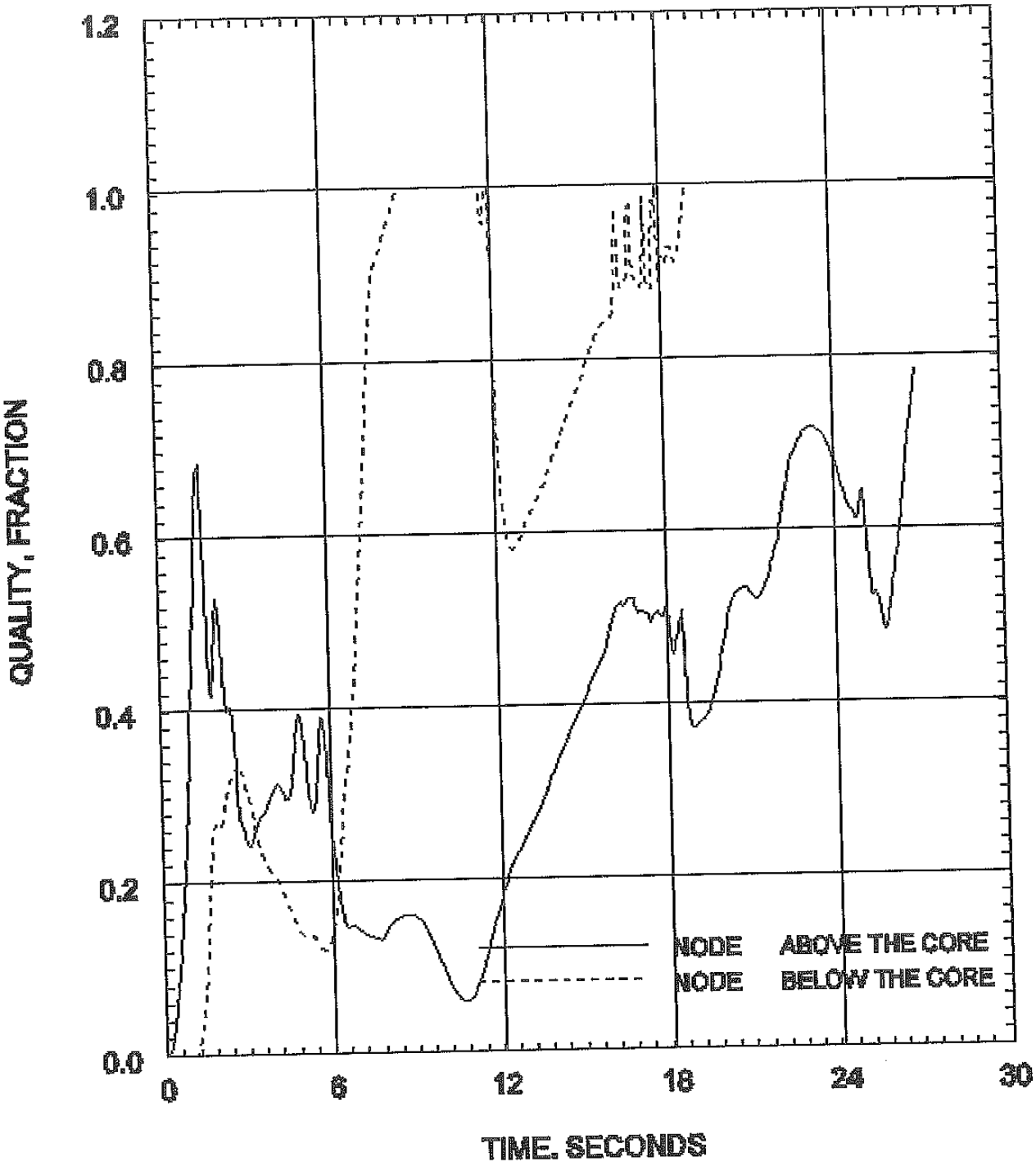

Figure 15.6.5-30
Large Break LOCA ECCS Performance Analysis
0.6 DEG/PD Break
Core Pressure Drop

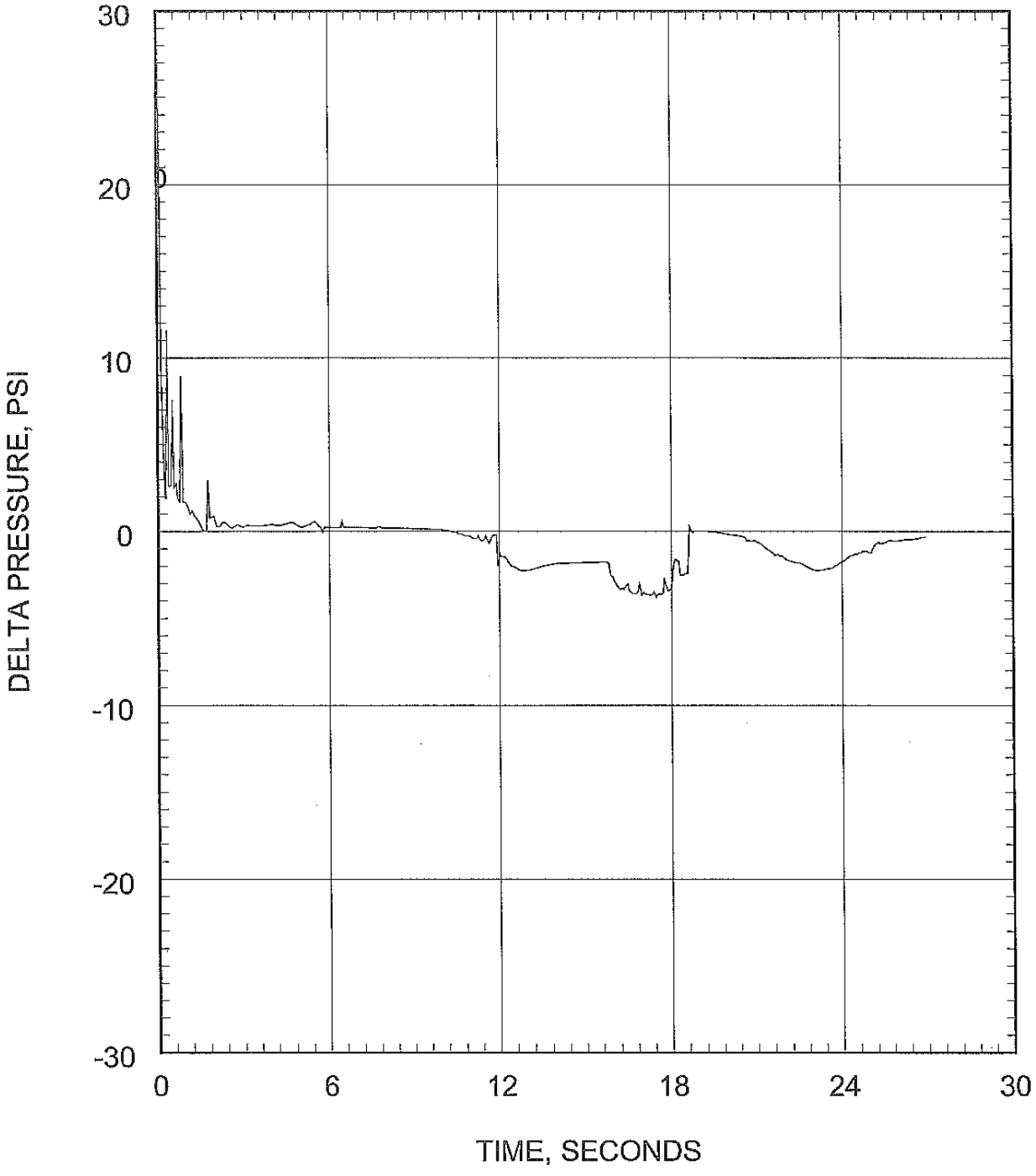

Figure 15.6.5-31
Large Break LOCA ECCS Performance Analysis
0.6 DEG/PD Break
Safety Injection Flow Rate Into Intact Discharge Legs

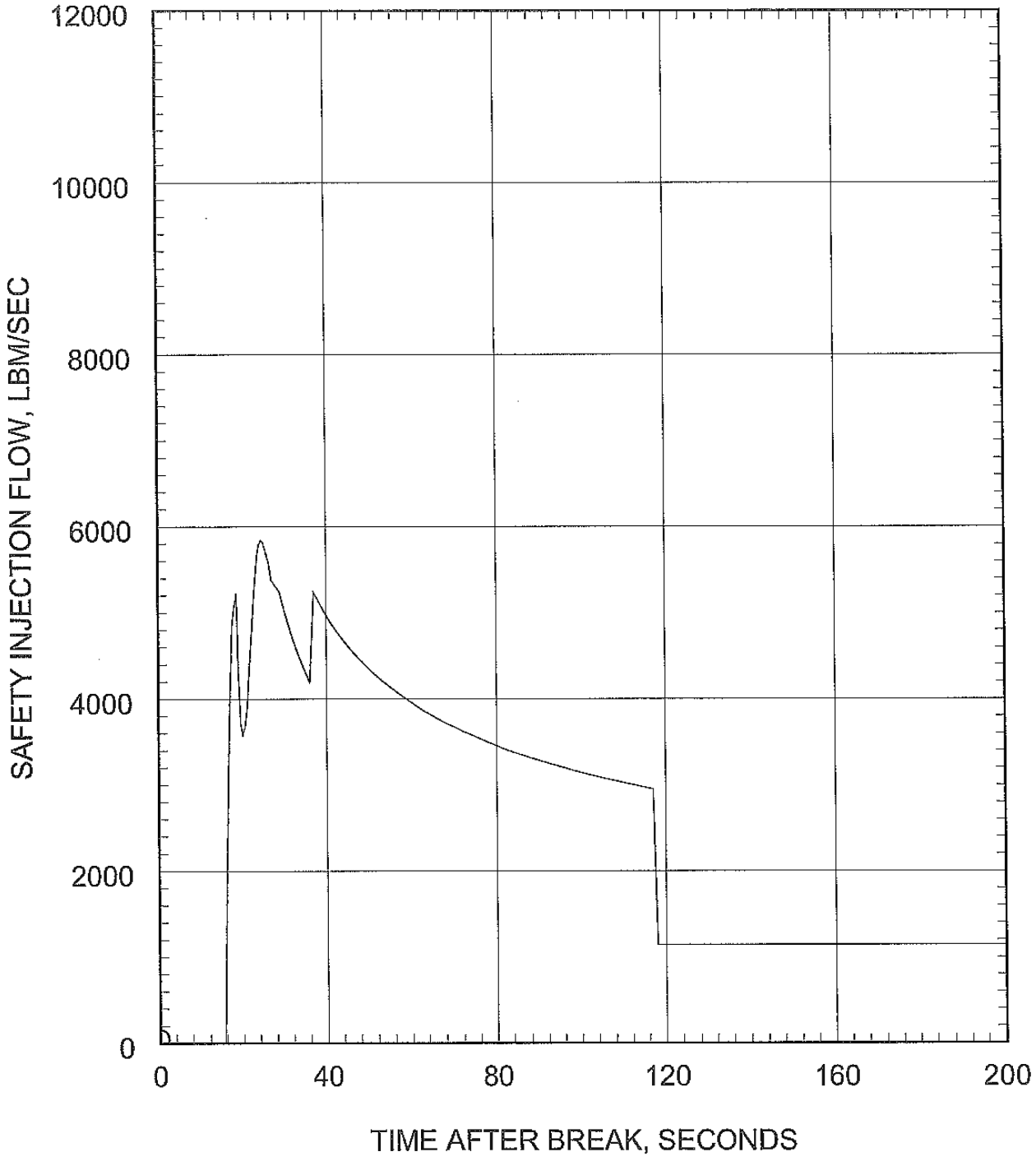

Figure 15.6.5-32
Large Break LOCA ECCS Performance Analysis
0.6 DEG/PD Break
Water Level in Downcomer During Reflood

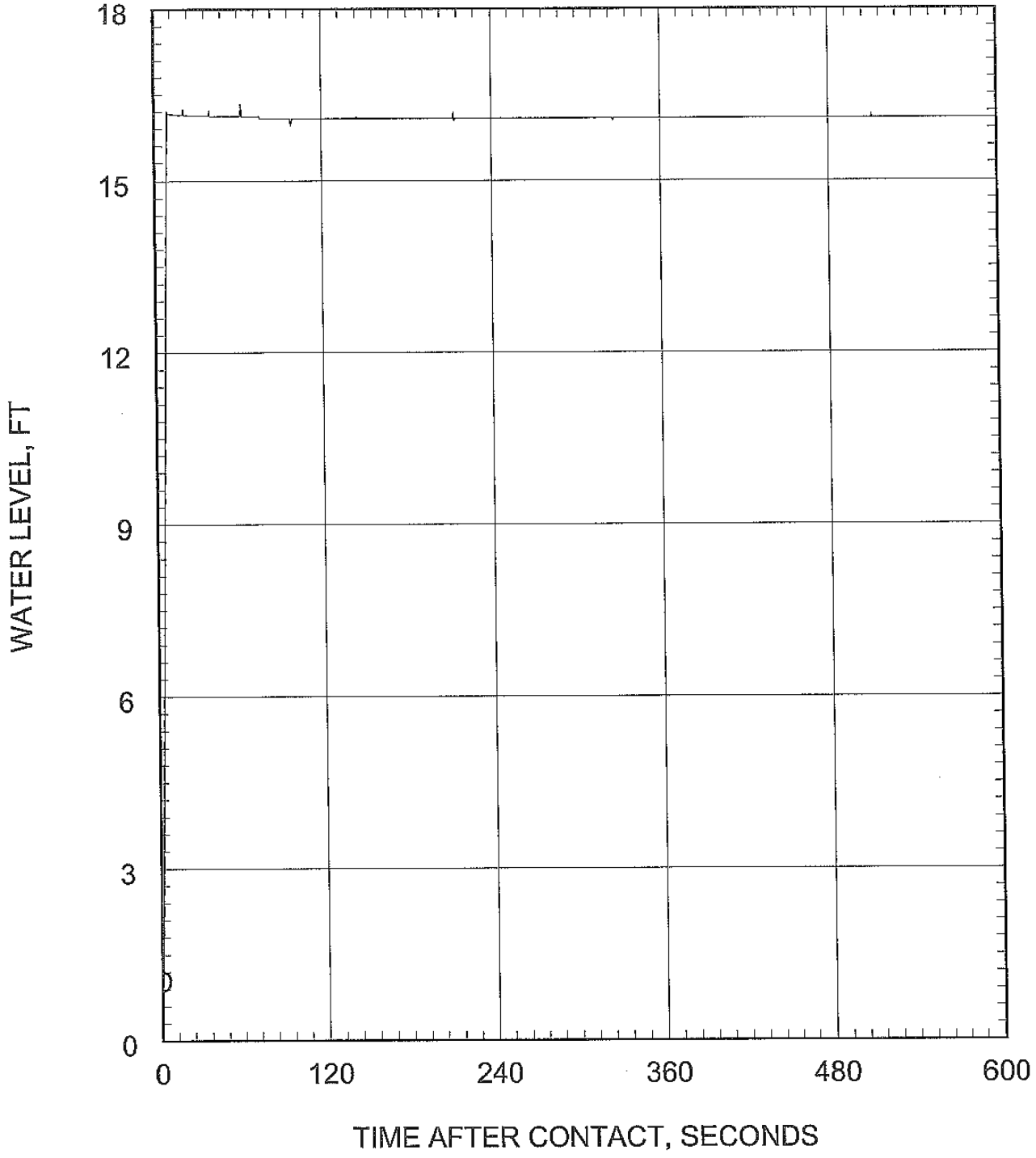

Figure 15.6.5-33
Large Break LOCA ECCS Performance Analysis
0.6 DEG/PD Break
Hot Spot Gap Conductance

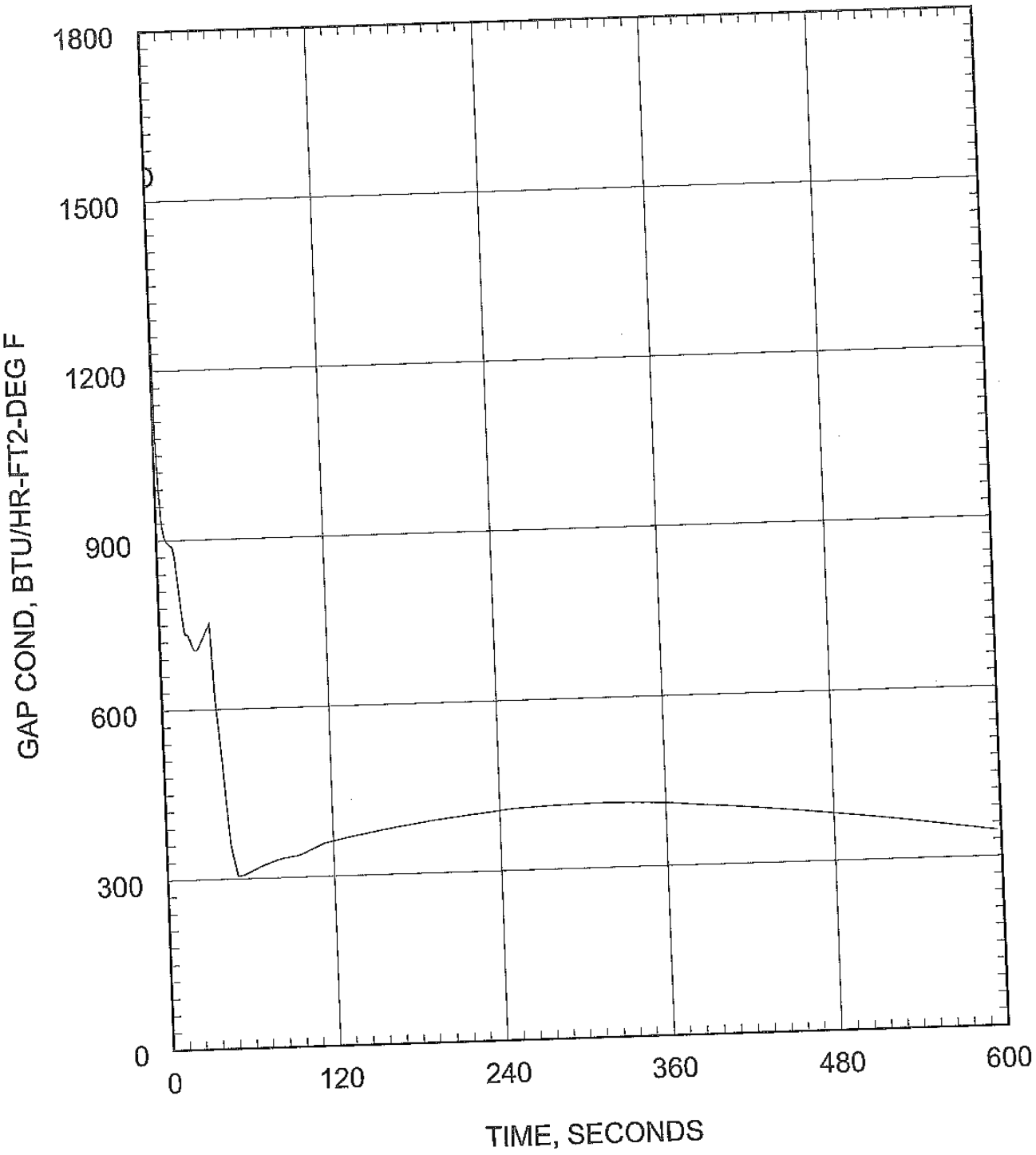

Figure 15.6.5-34
Large Break LOCA ECCS Performance Analysis
0.6 DEG/PD Break
Maximum Local Cladding Oxidation Percentage

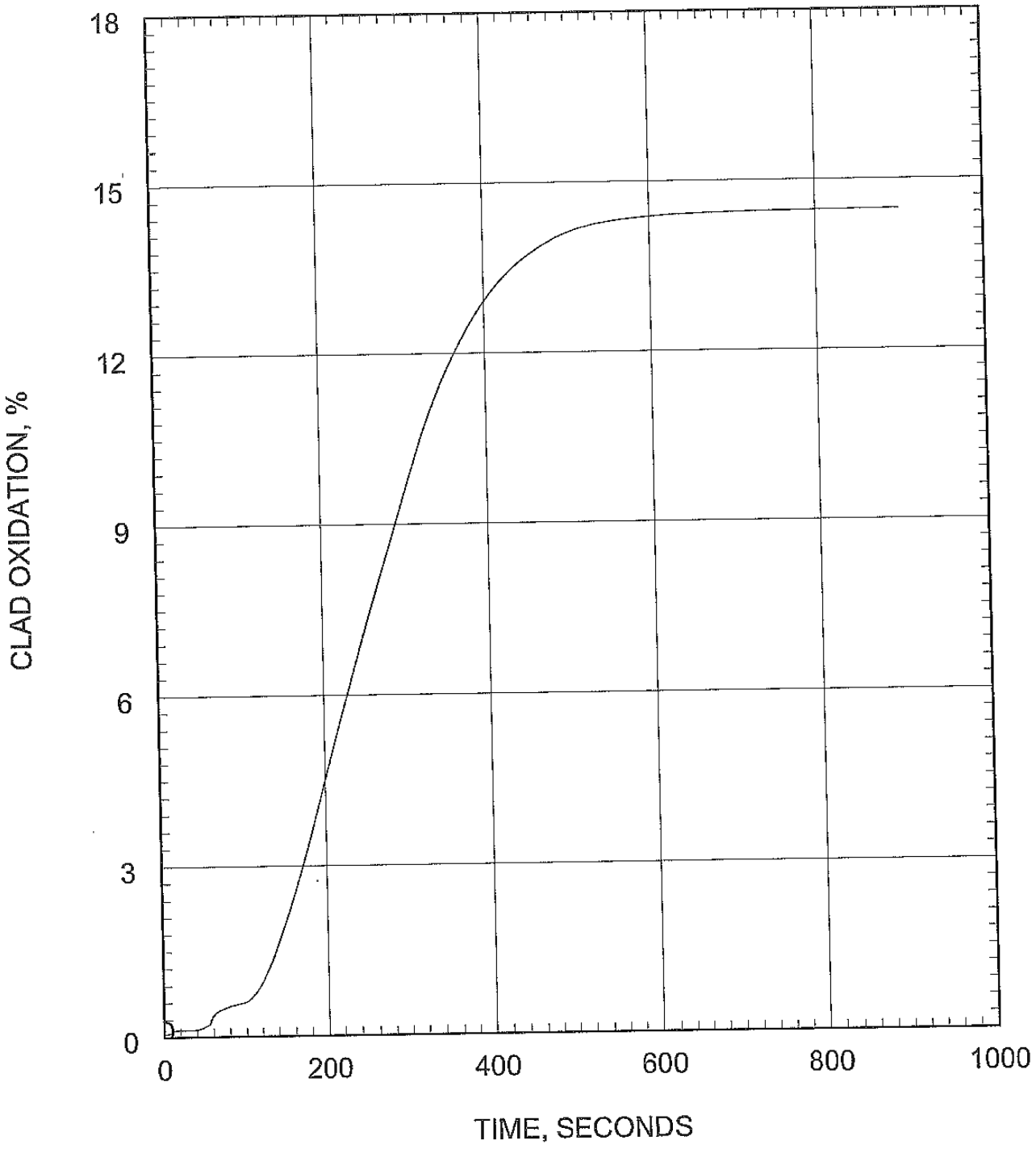

Figure 15.6.5-35
Large Break LOCA ECCS Performance Analysis
0.6 DEG/PD Break
Fuel Centerline, Fuel Average, Cladding and Coolant Temperature at the Hot Spot

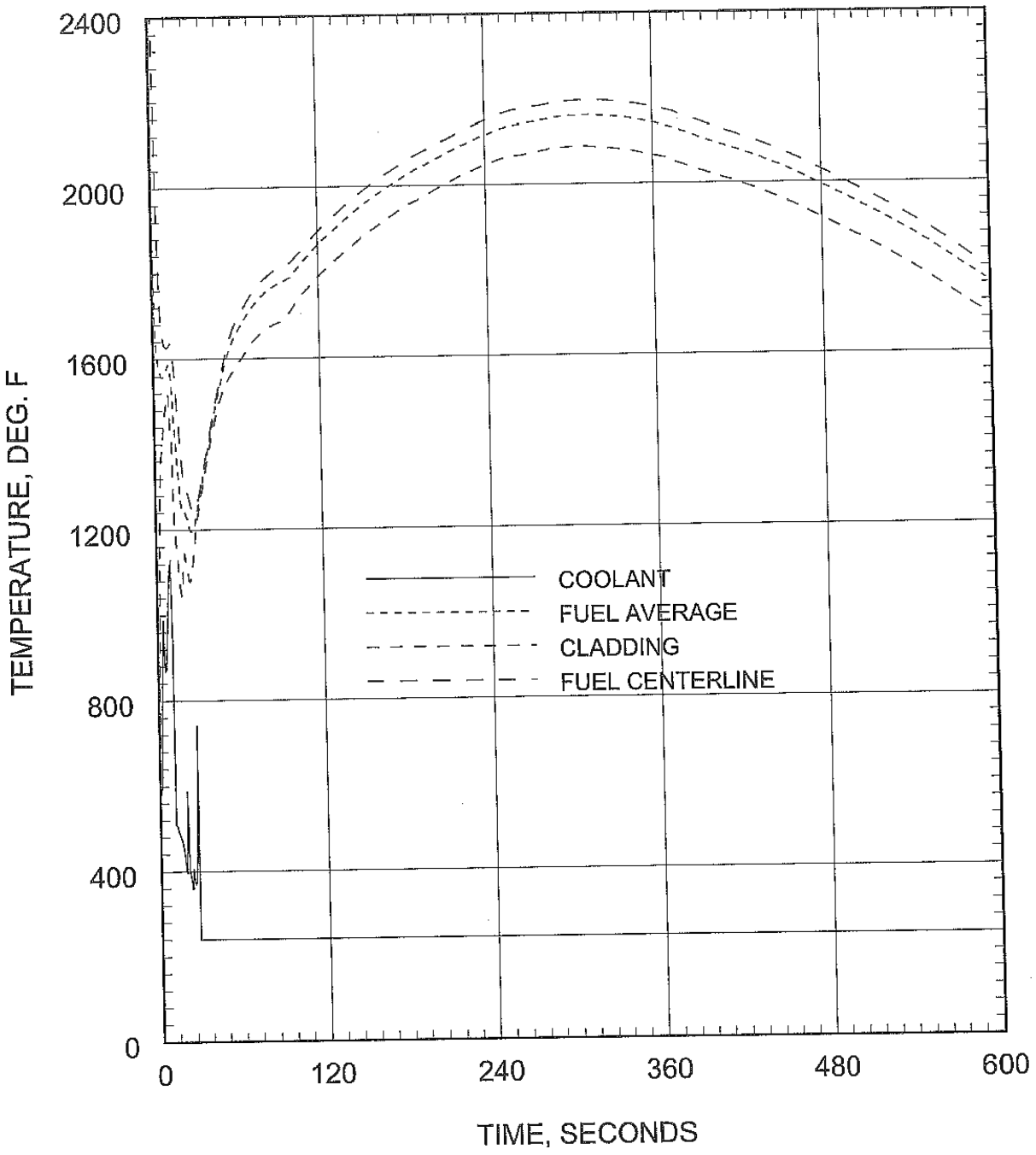

Figure 15.6.5-36
Large Break LOCA ECCS Performance Analysis
0.6 DEG/PD Break
Hot Spot Heat Transfer Coefficient

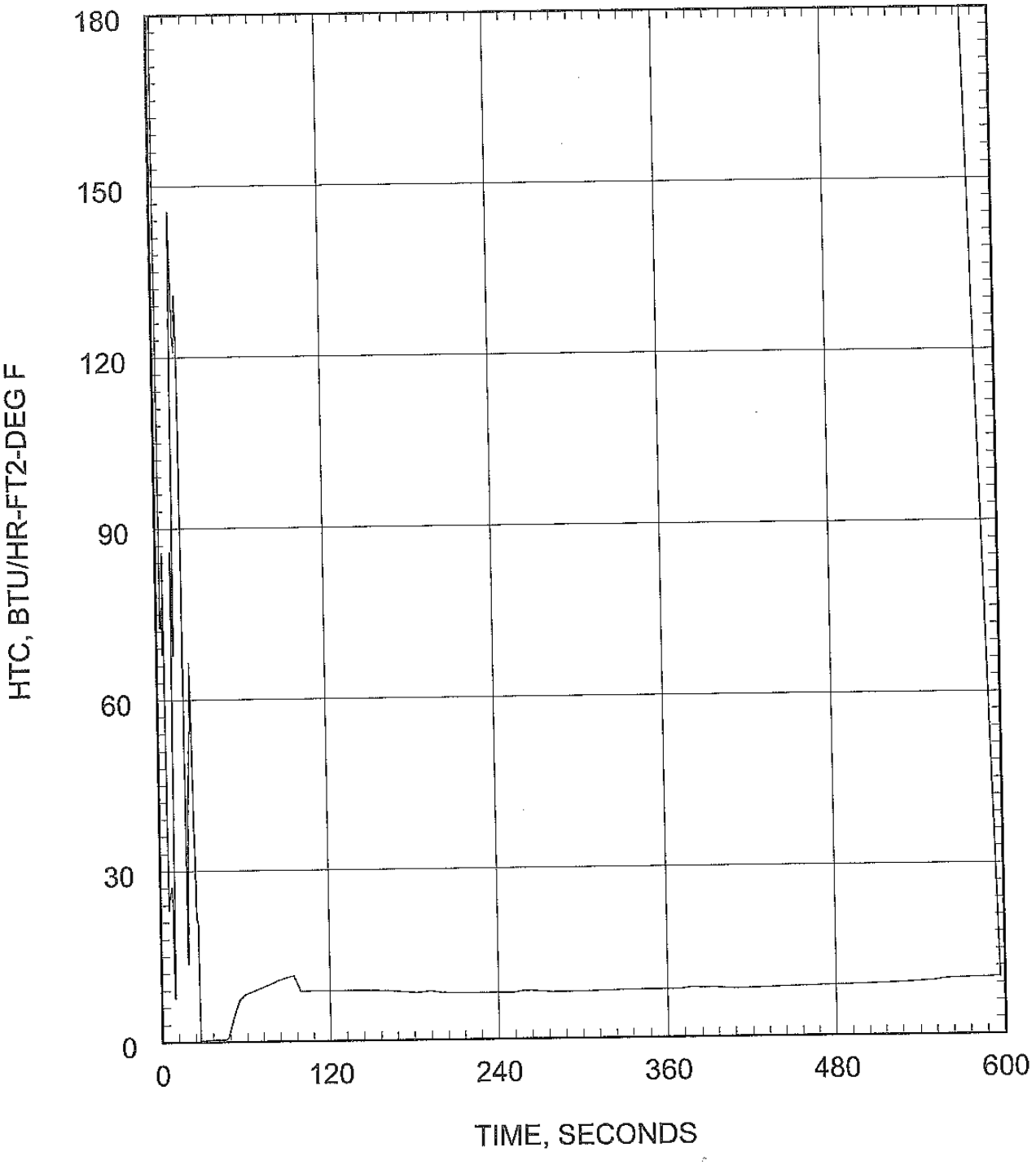

Figure 15.6.5-37
Large Break LOCA ECCS Performance Analysis
0.6 DEG/PD Break
Hot Rod Internal Gas Pressure

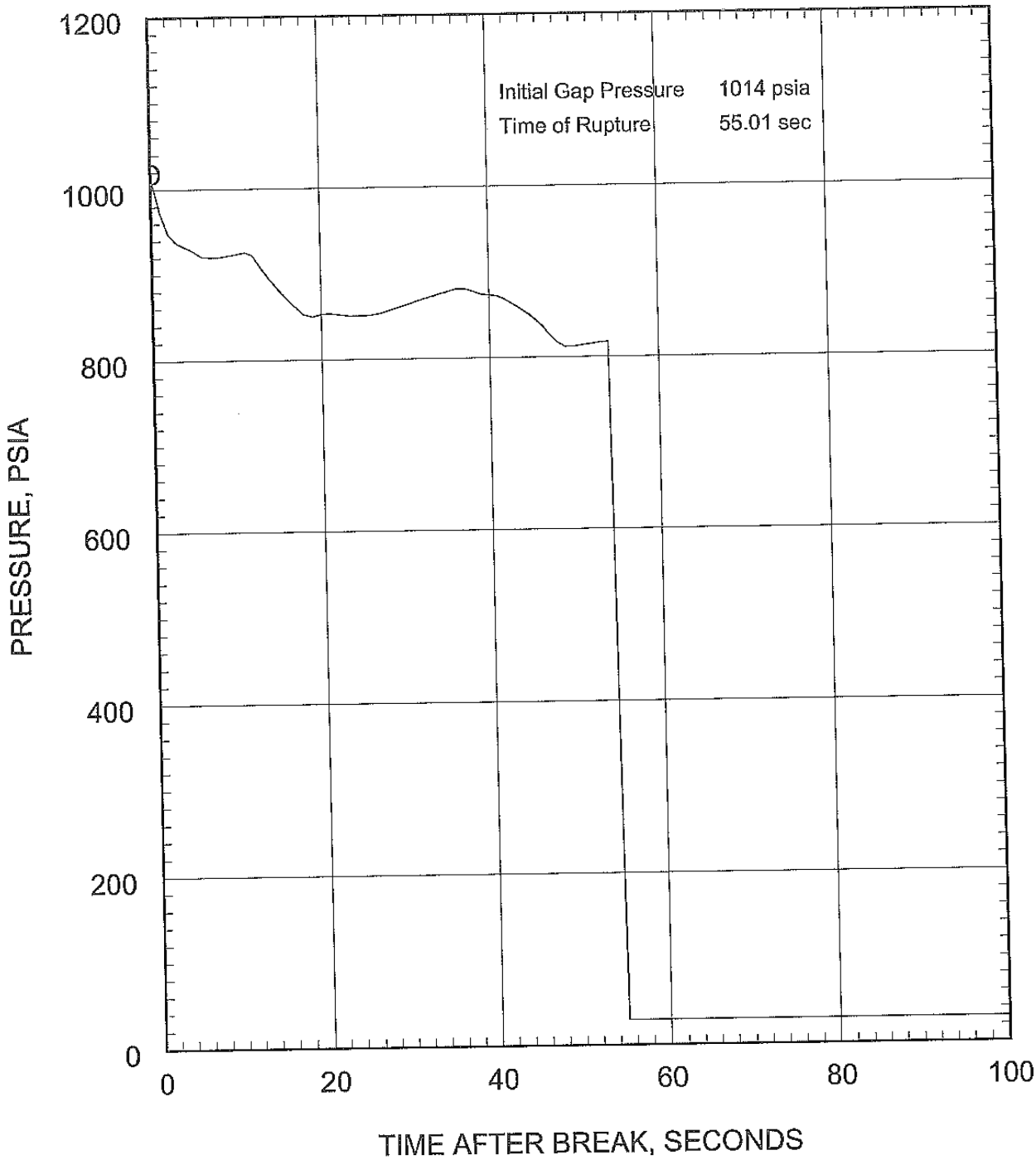

Figure 15.6.5-38
Large Break LOCA ECCS Performance Analysis
0.6 DEG/PD Break
Core Bulk Channel Flow Rate

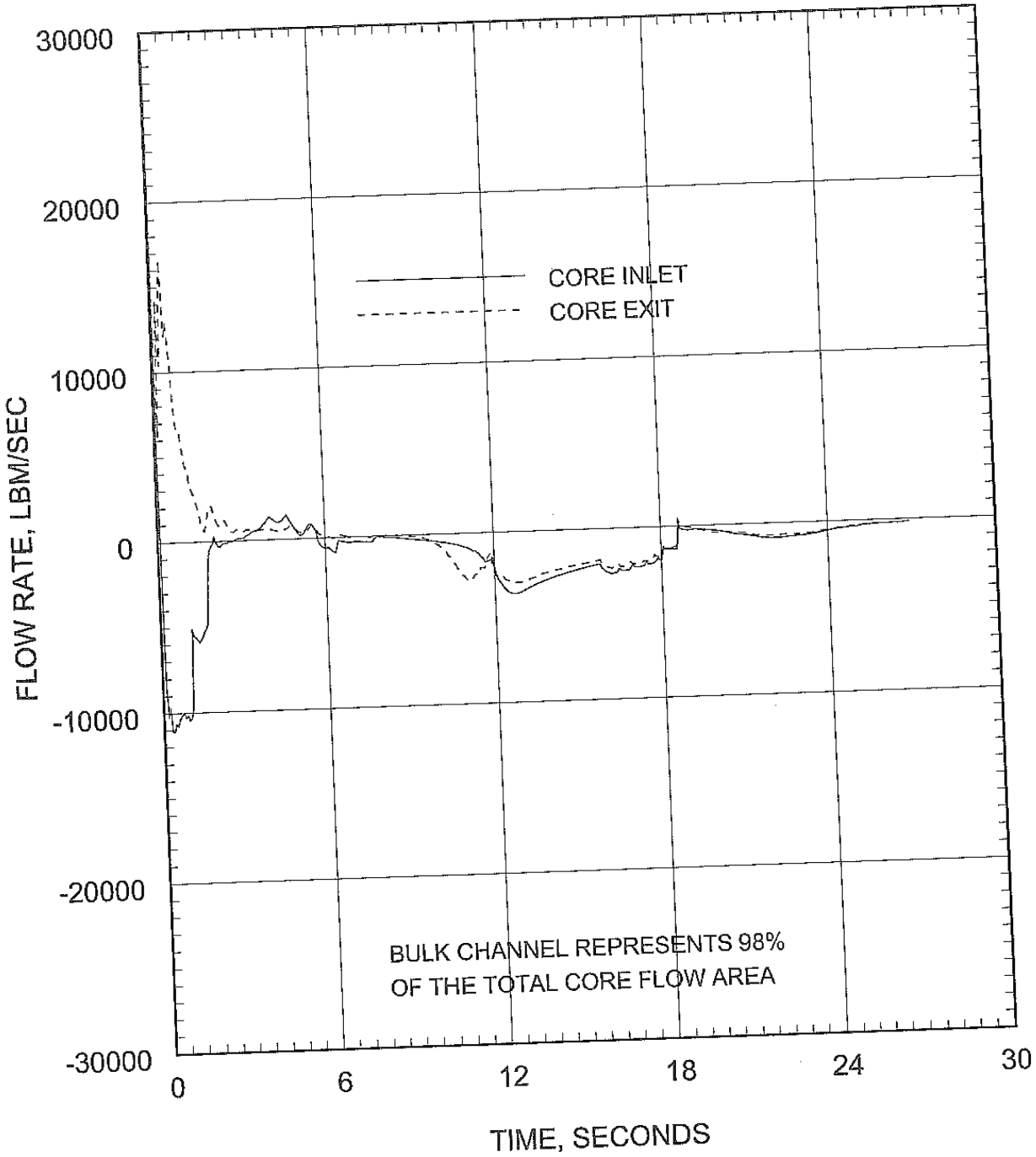

Figure 15.6.5-39
Large Break LOCA ECCS Performance Analysis
0.4 DEG/PD Break
Core Power

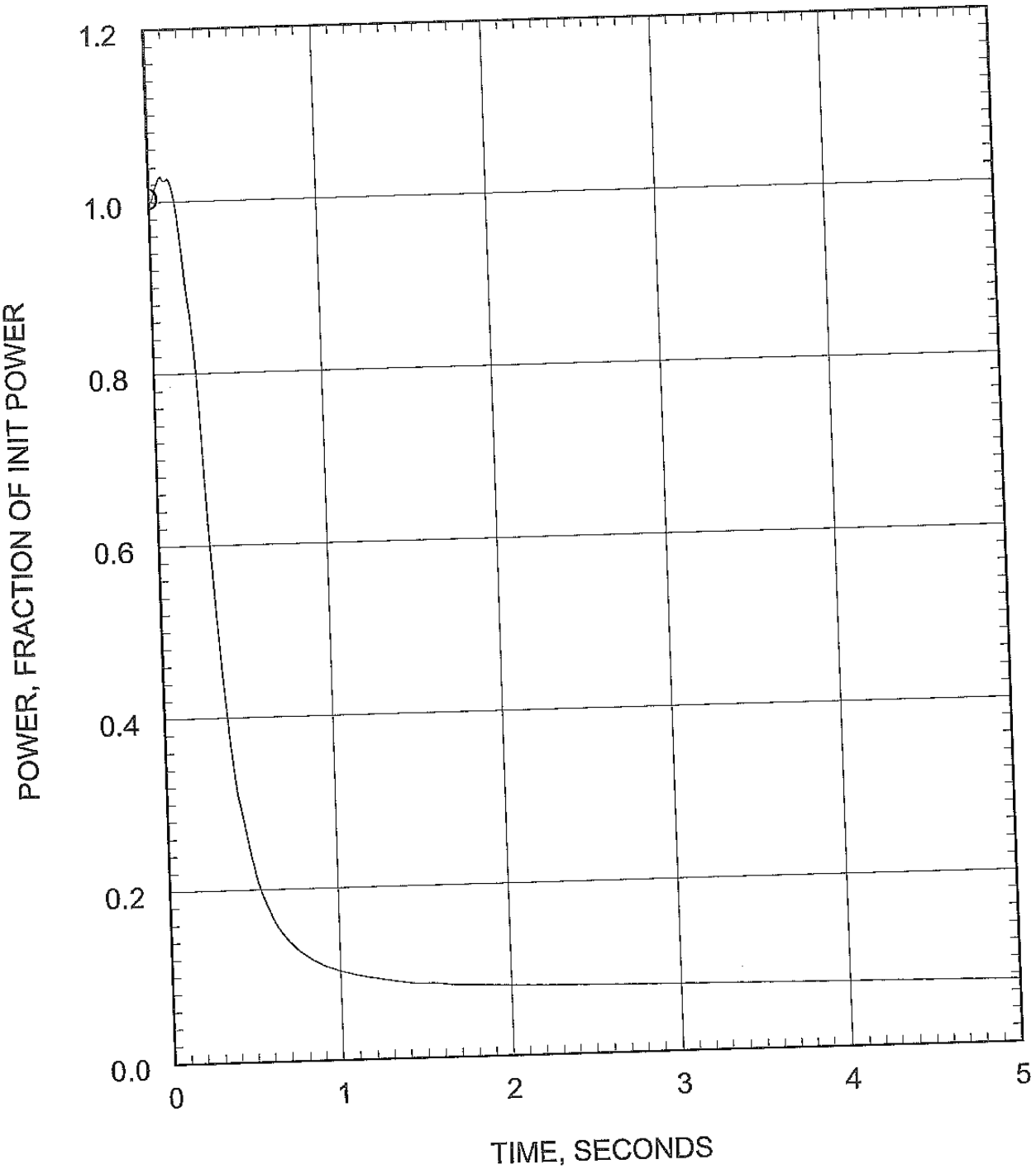

Figure 15.6.5-40
Large Break LOCA ECCS Performance Analysis
0.4 DEG/PD Break
Pressure in Center Hot Assembly Node

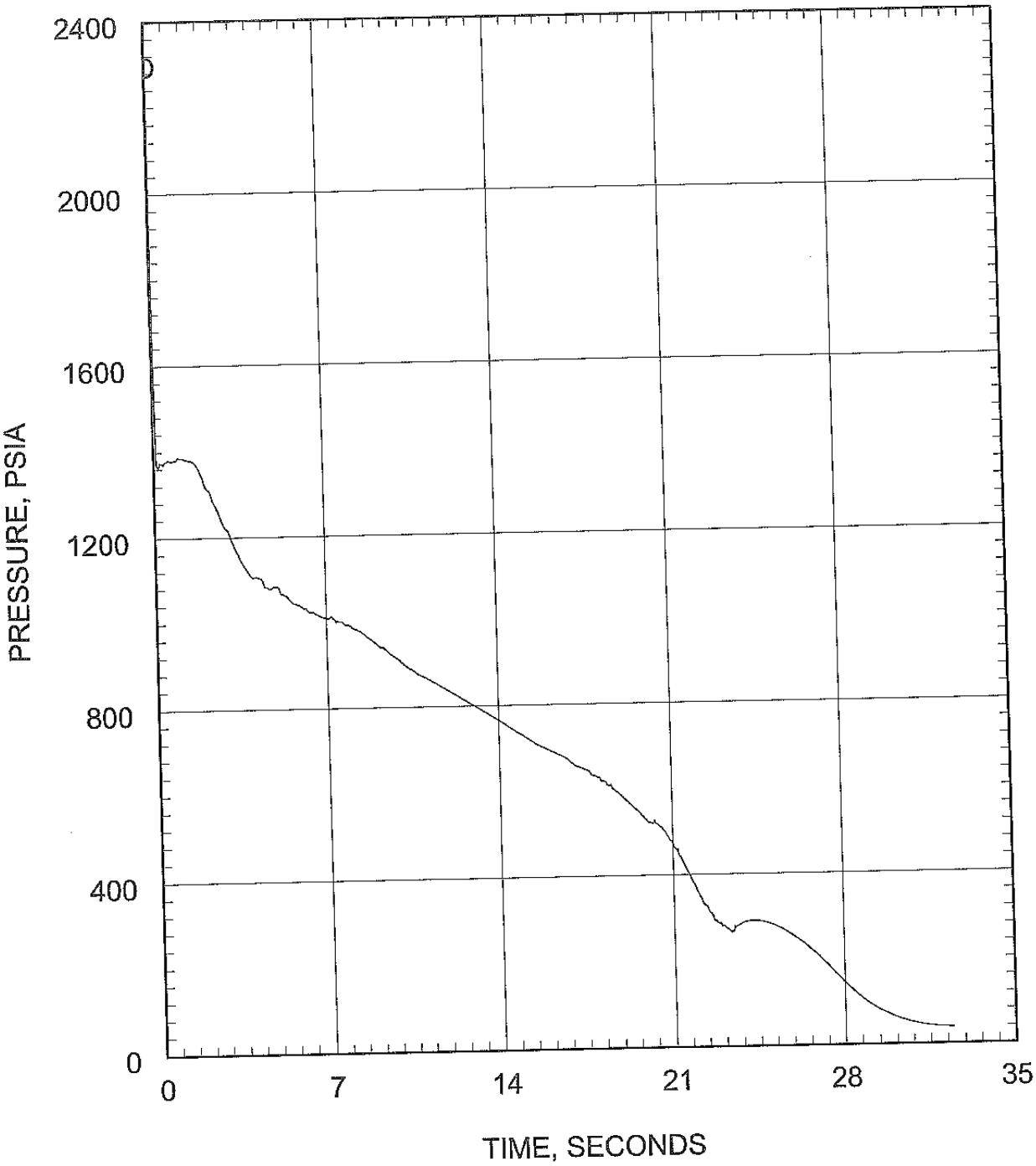

Figure 15.6.5-41
Large Break LOCA ECCS Performance Analysis
0.4 DEG/PO Break
Leak Flow Rate

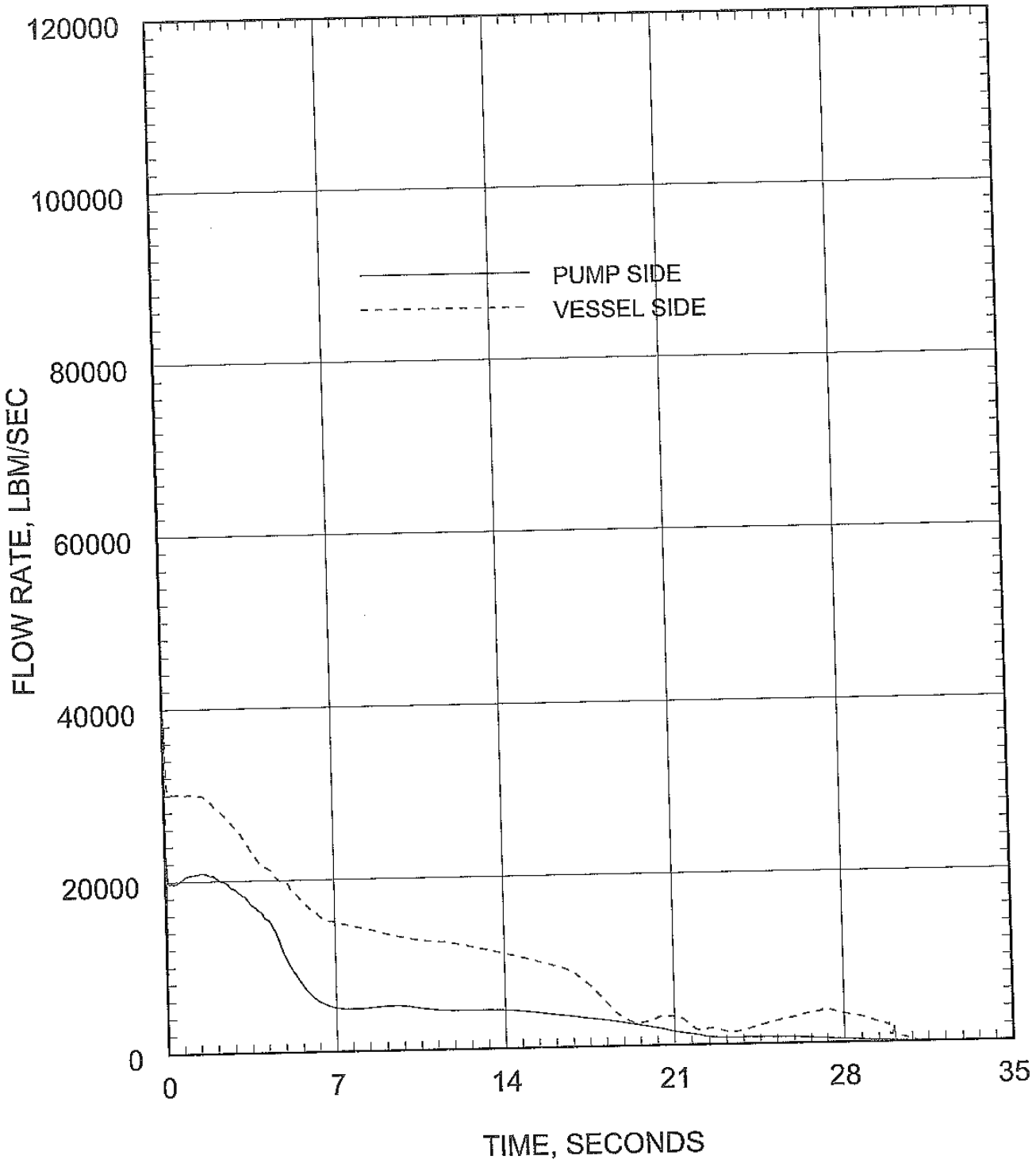

Figure 15.6.5-42
Large Break LOCA ECCS Performance Analysis
0.4 DEG/PD Break
Hot Assembly Flow Rate (Below Hot Spot)

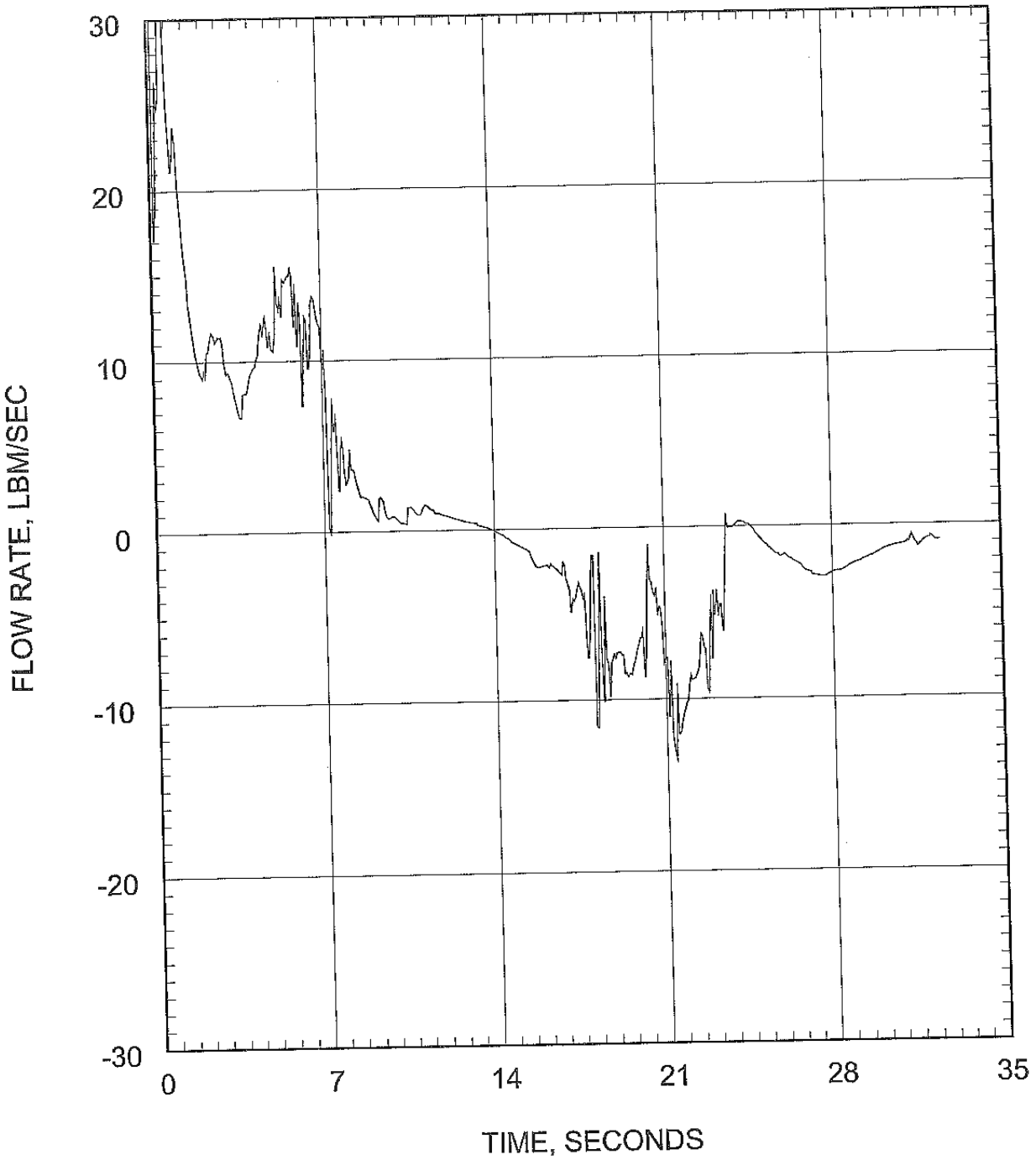

Figure 15.6.5-43
Large Break LOCA ECCS Performance Analysis
0.4 DEG/PD Break
Hot Assembly Flow Rate (Above Hot Spot)

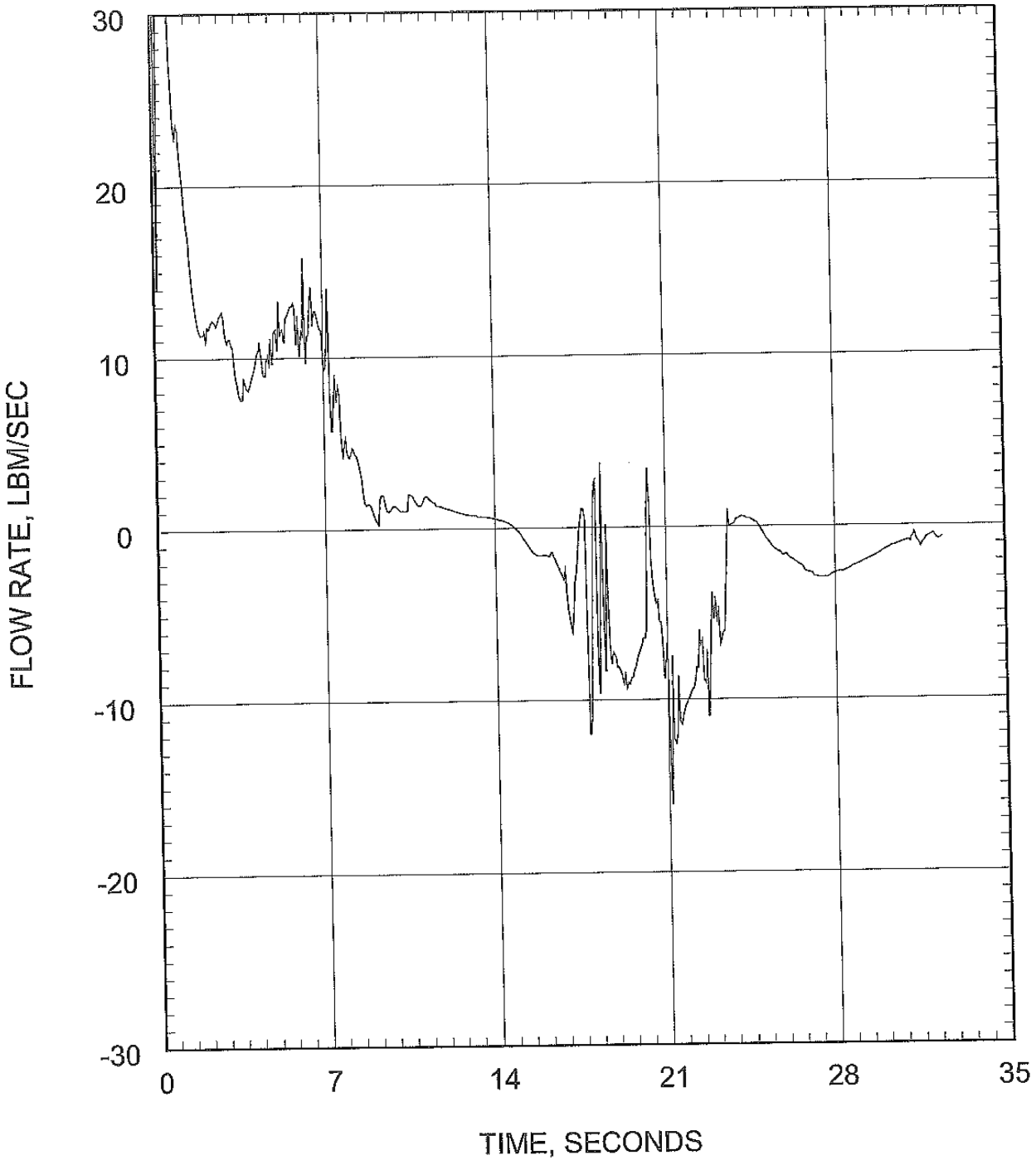

Figure 15.6.5-44
Large Break LOCA ECCS Performance Analysis
0.4 DEG/PD Break
Hot Assembly Quality

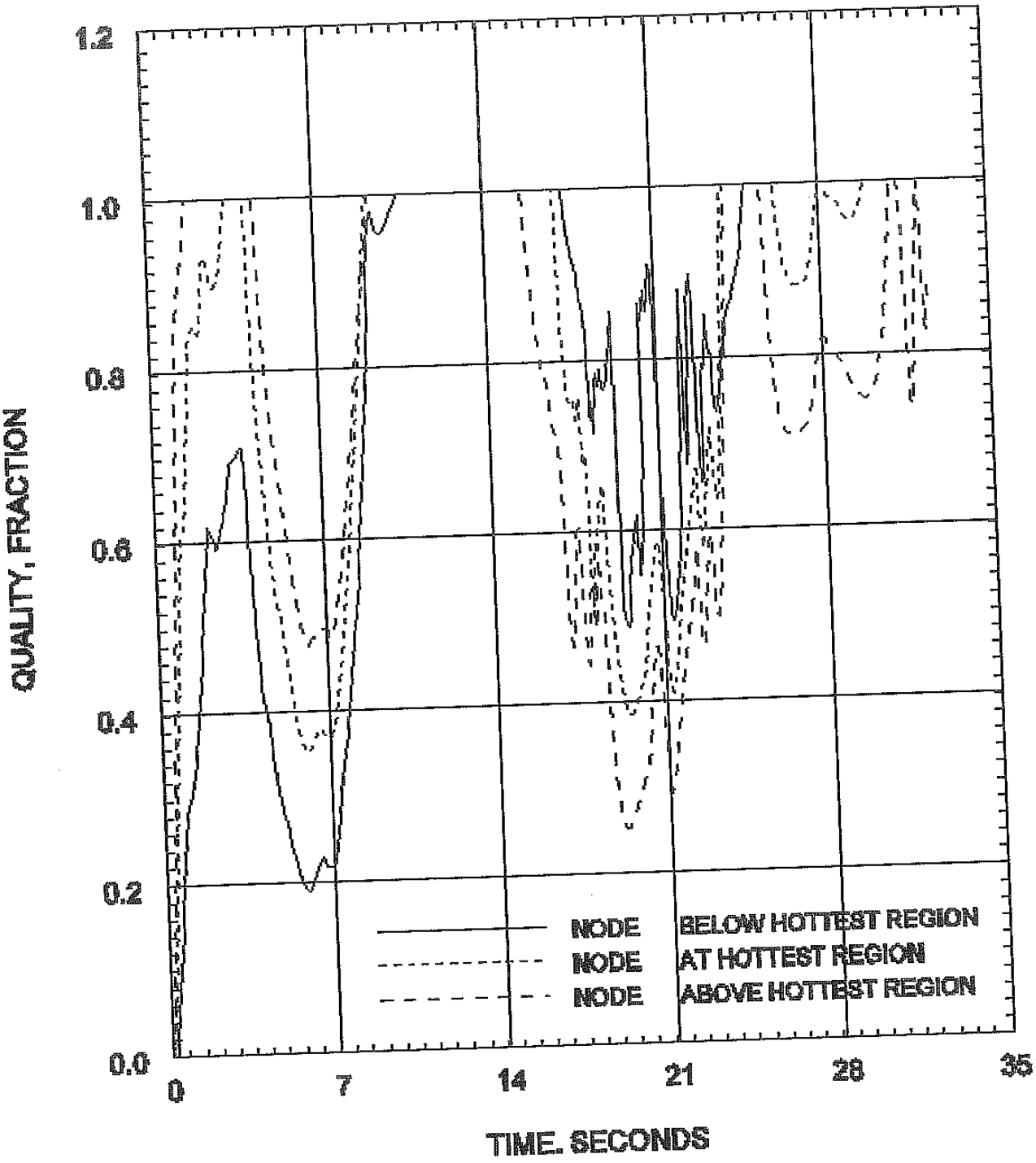

Figure 15.6.5-45
Large Break LOCA ECCS Performance Analysis
0.4 DEG/PD Break
Containment Pressure

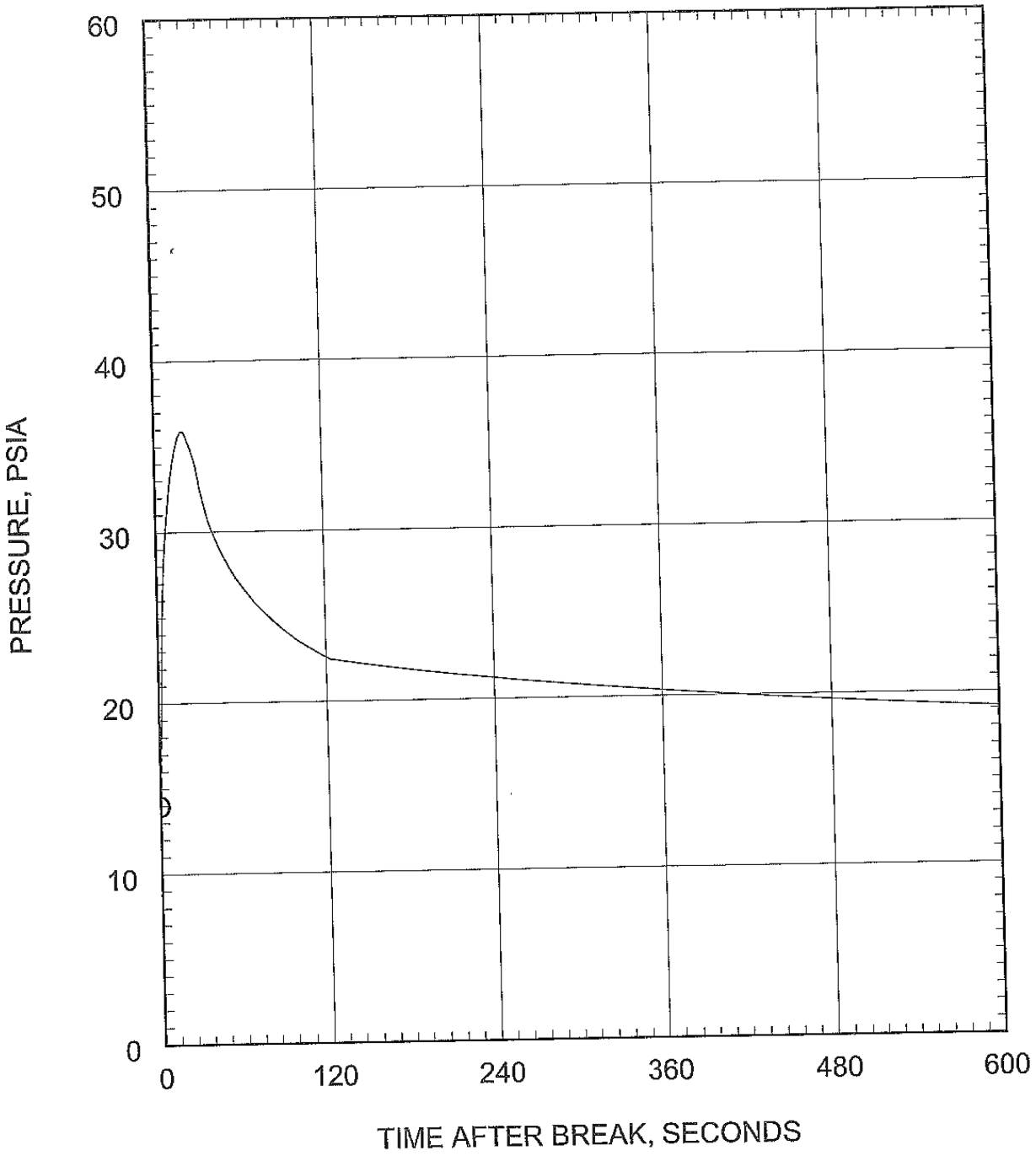

Figure 15.6.5-46
Large Break LOCA ECCS Performance Analysis
0.4 DEG/PD Break
Mass Added to Core During Reflood

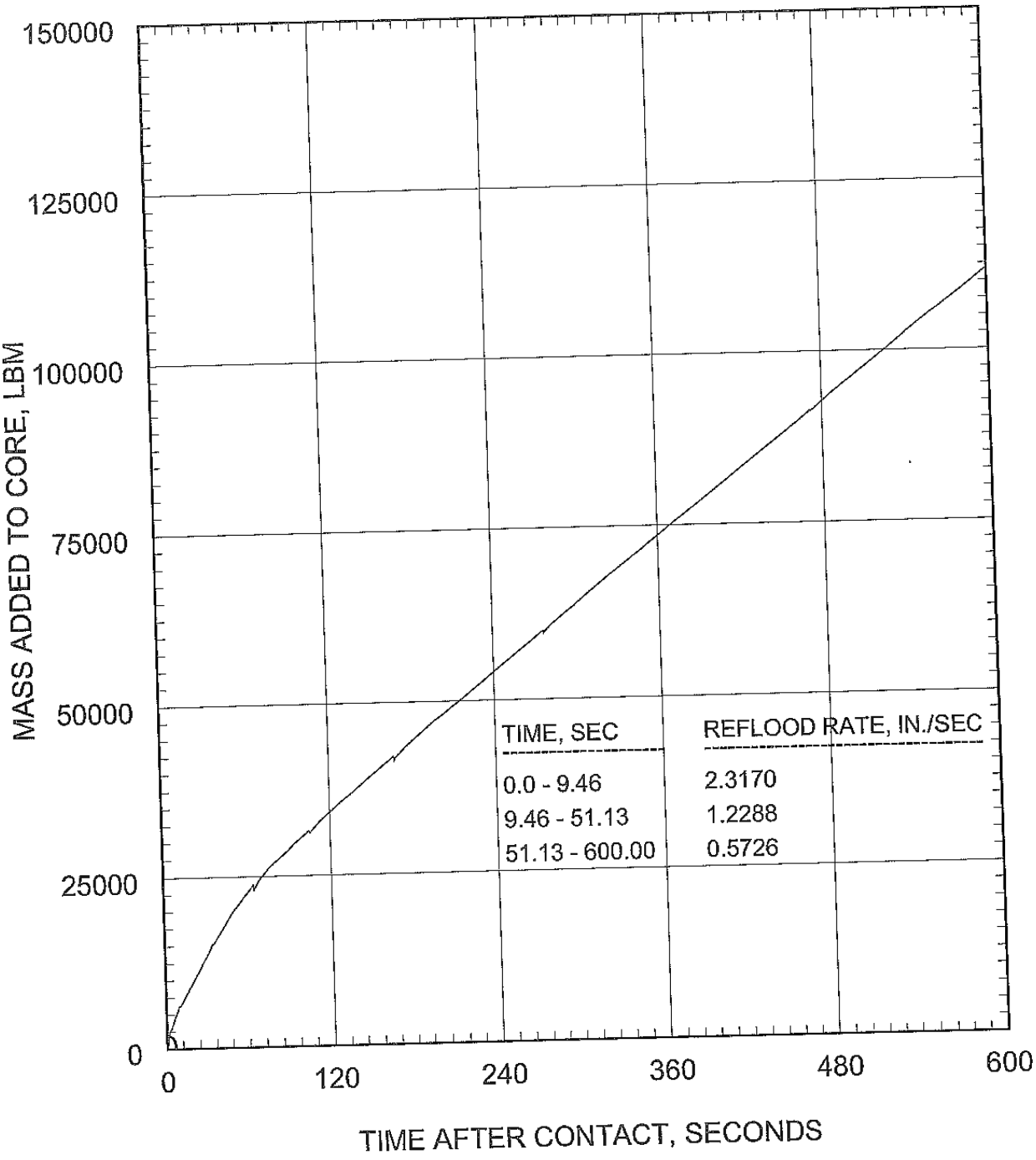

Figure 15.6.5-47
Large Break LOCA ECCS Performance Analysis
0.4 DEG/PD Break
Peak Cladding Temperature

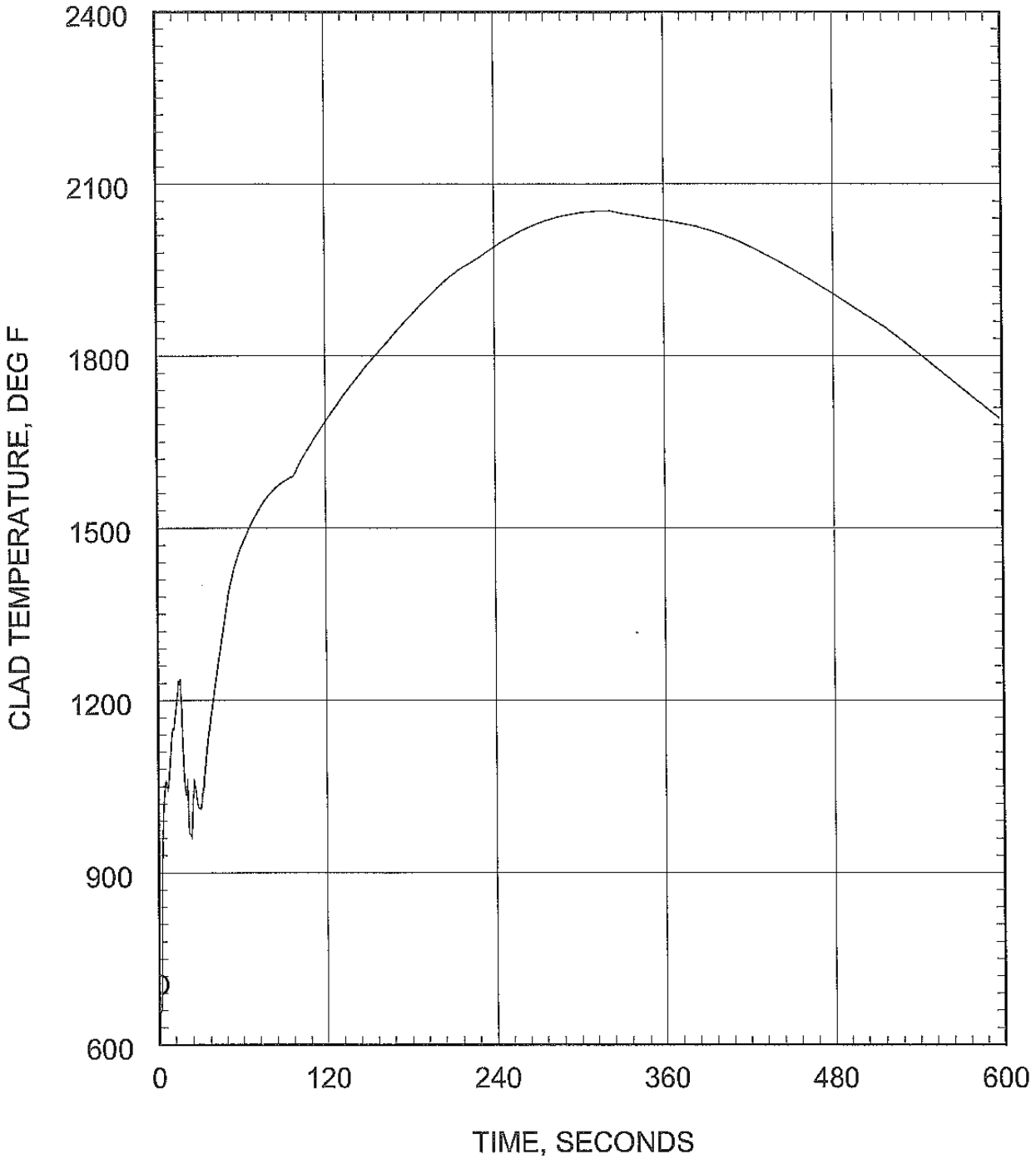

Figure 15.6.5-48
Small Break LOCA ECCS Performance Analysis
0.04 ft^2/PD Break
Core Power

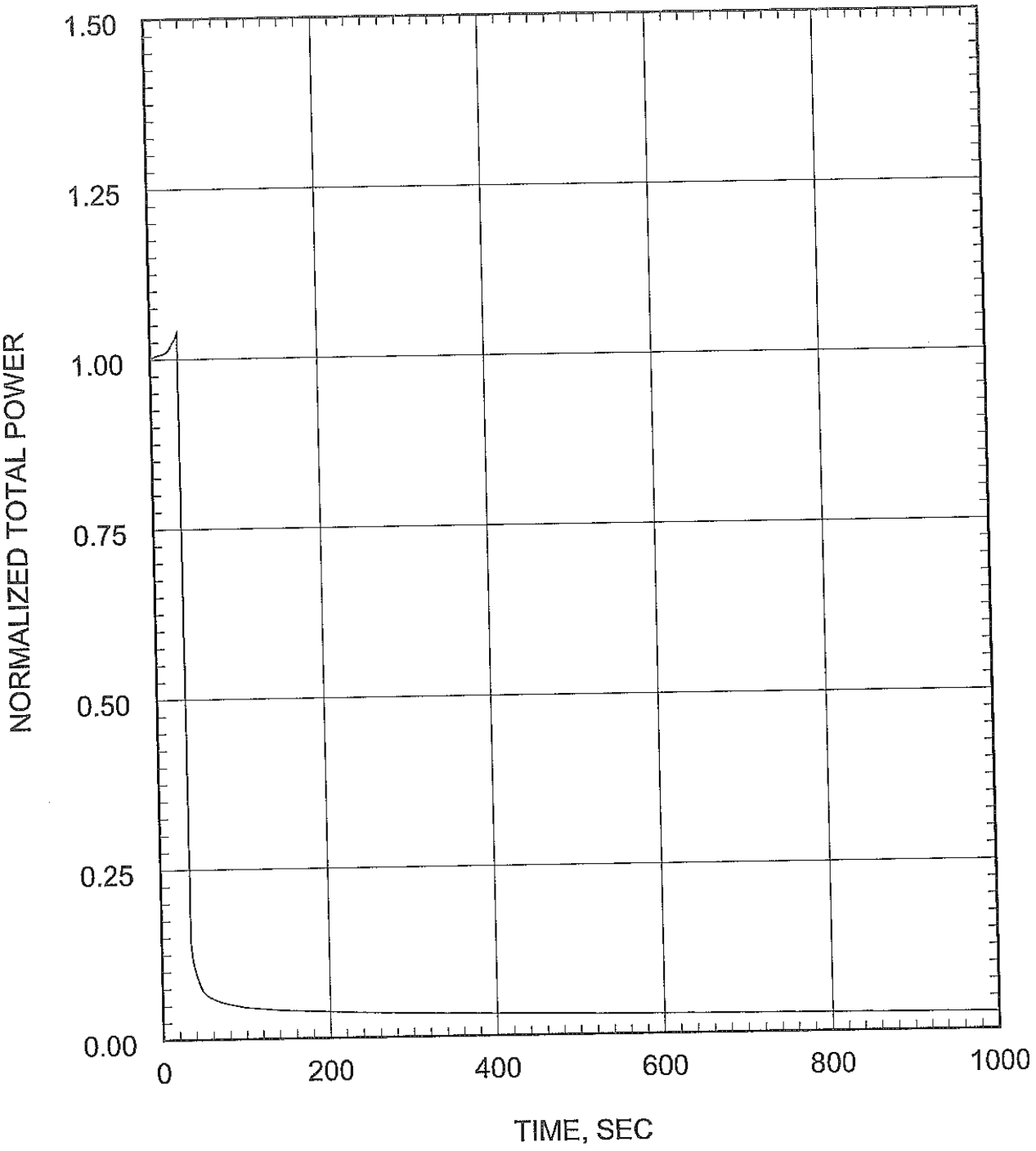

Figure 15.6.5-49
Small Break LOCA ECCS Performance Analysis
0.04 ft^2/PD Break
Inner Vessel Pressure

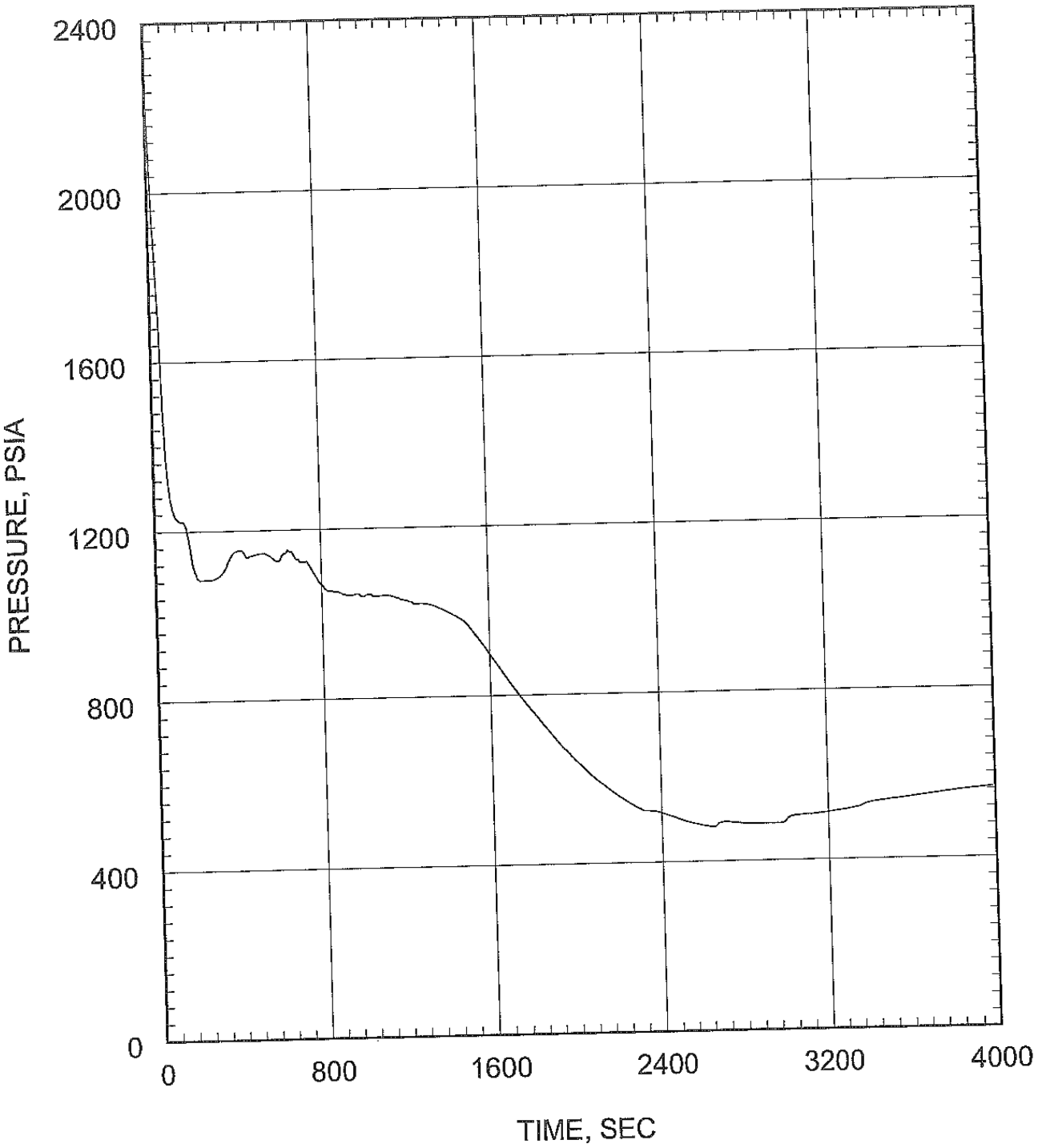

Figure 15.6.5-50
Small Break LOCA ECCS Performance Analysis
0.04 ft^2/PD Break
Break Flow Rate

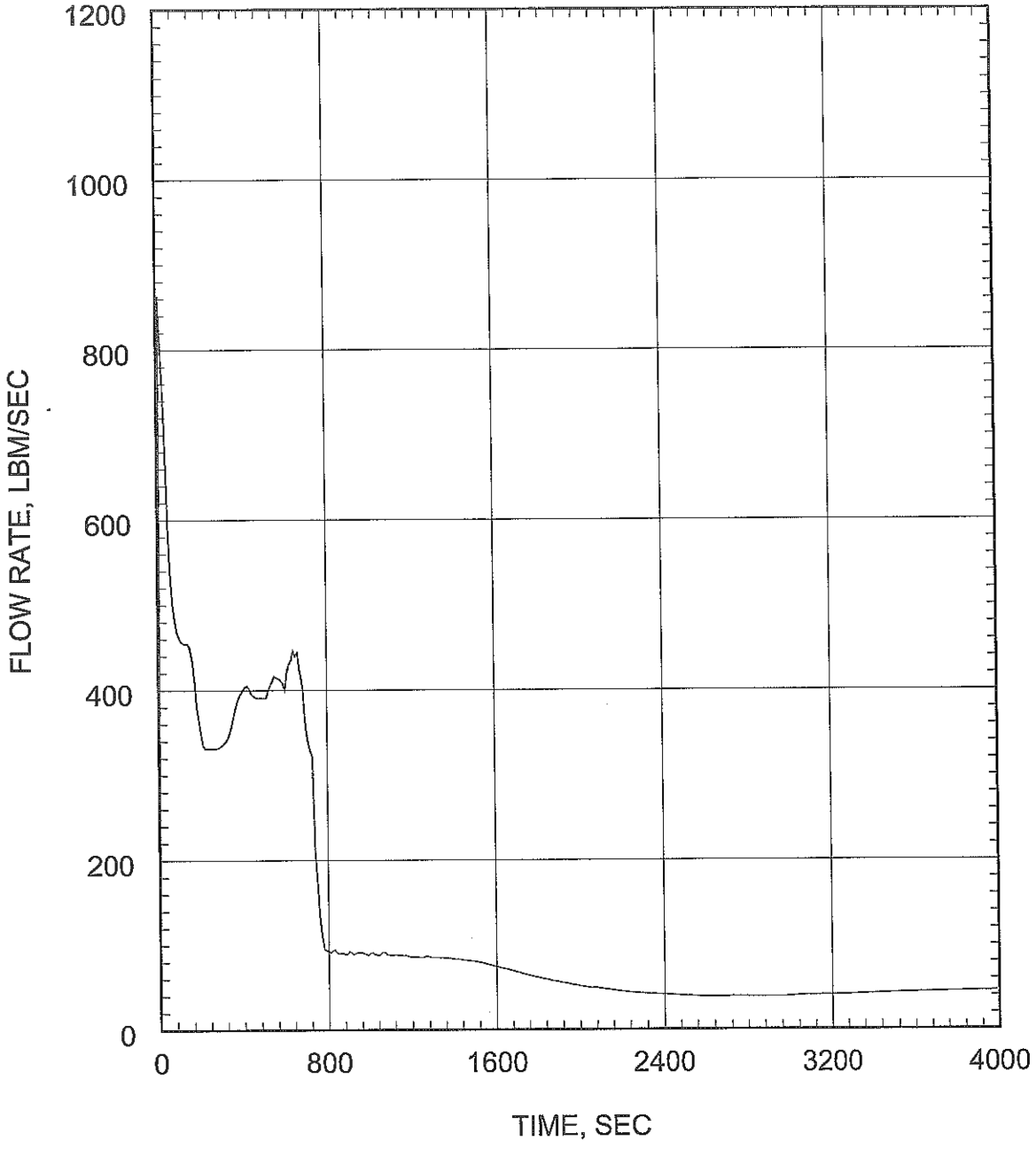

Figure 15.6.5-51
Small Break LOCA ECCS Performance Analysis
0.04 ft^2/PD Break
Inner Vessel Inlet Flow Rate

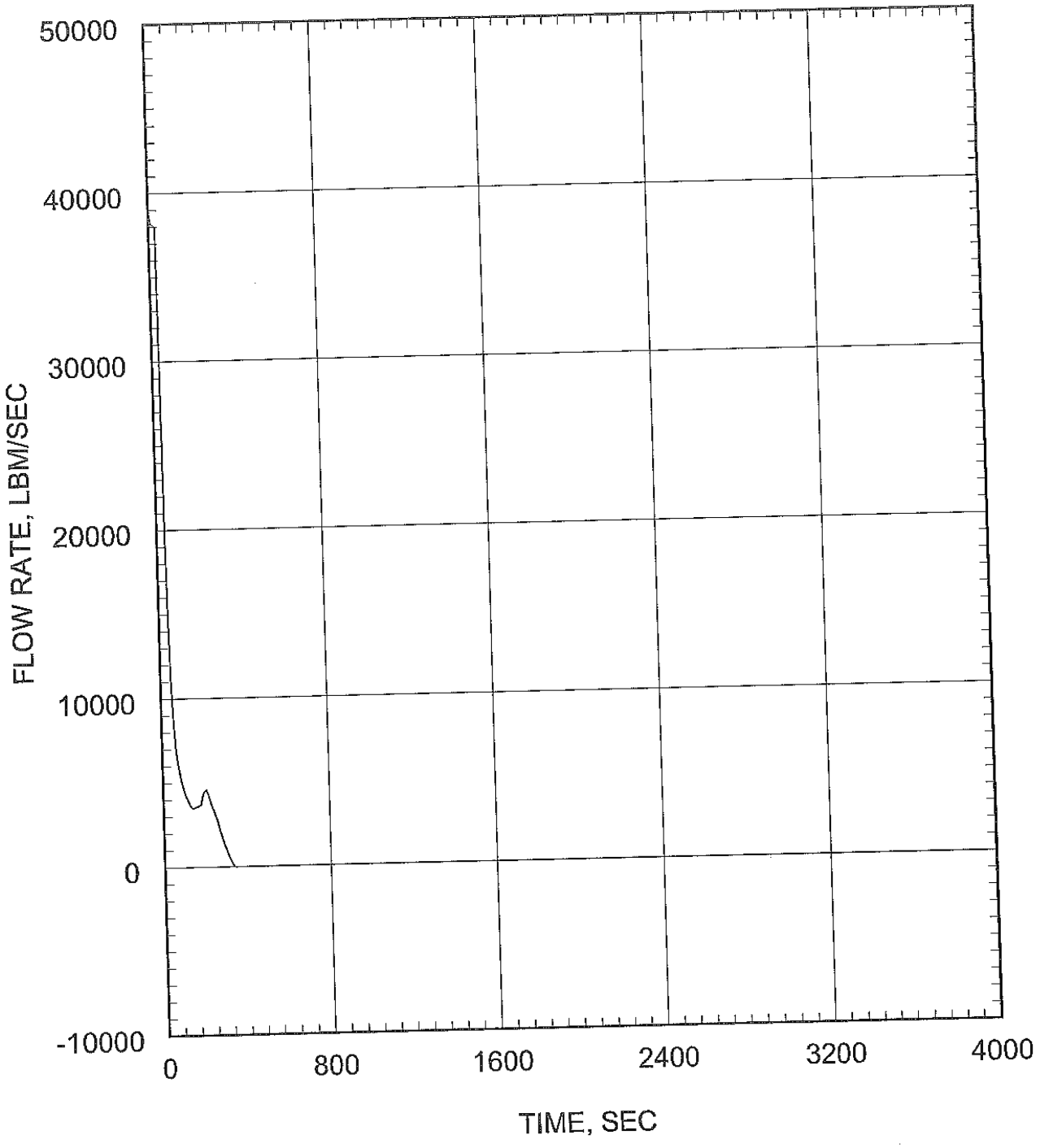

Figure 15.6.5-52
Small Break LOCA ECCS Performance Analysis
0.04 ft^2/PD Break
Inner Vessel Two-Phase Mixture Level

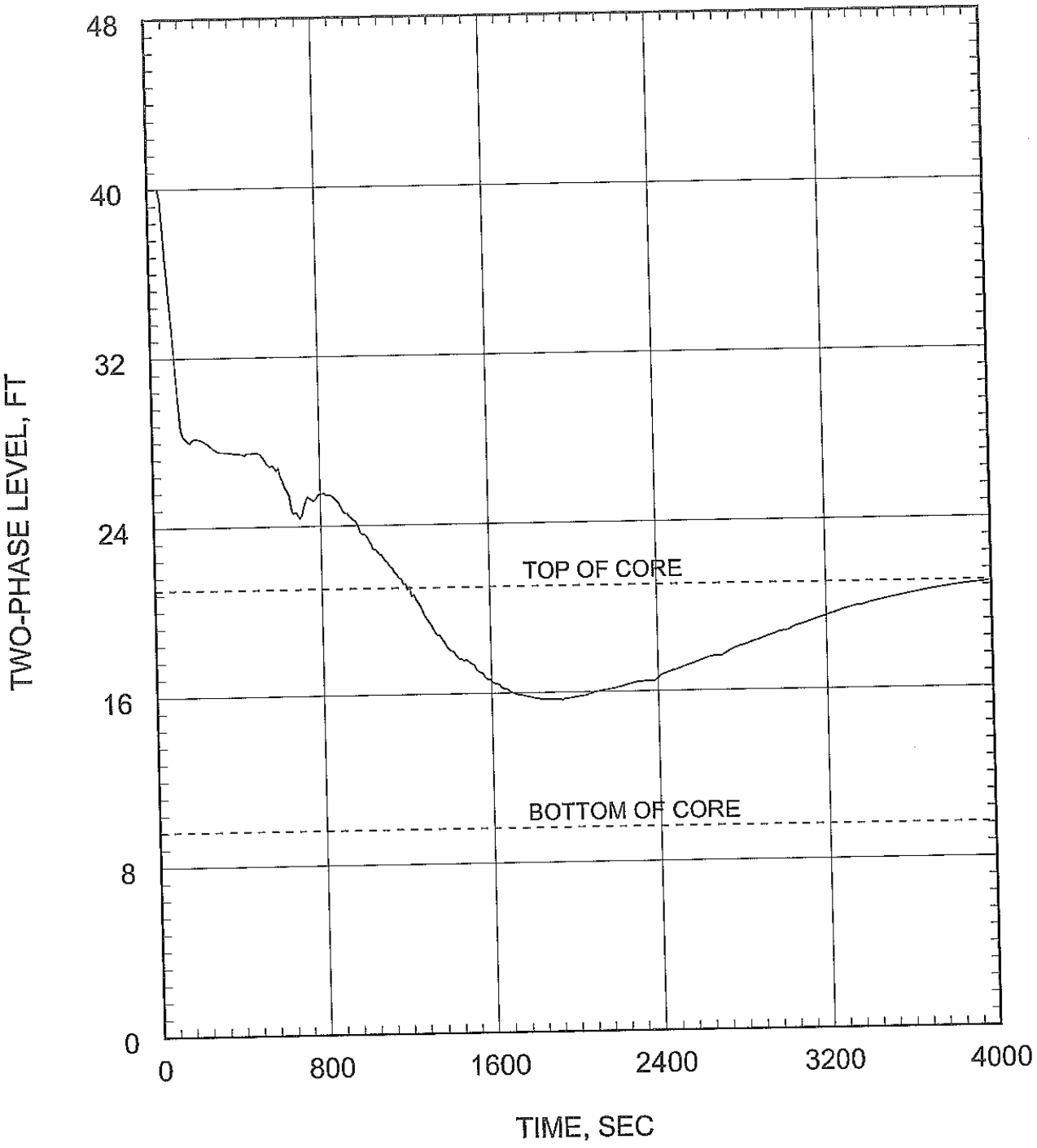

Figure 15.6.5-53
Small Break LOCA ECCS Performance Analysis
0.04 ft^2/PD Break
Heat Transfer Coefficient at Hot Spot

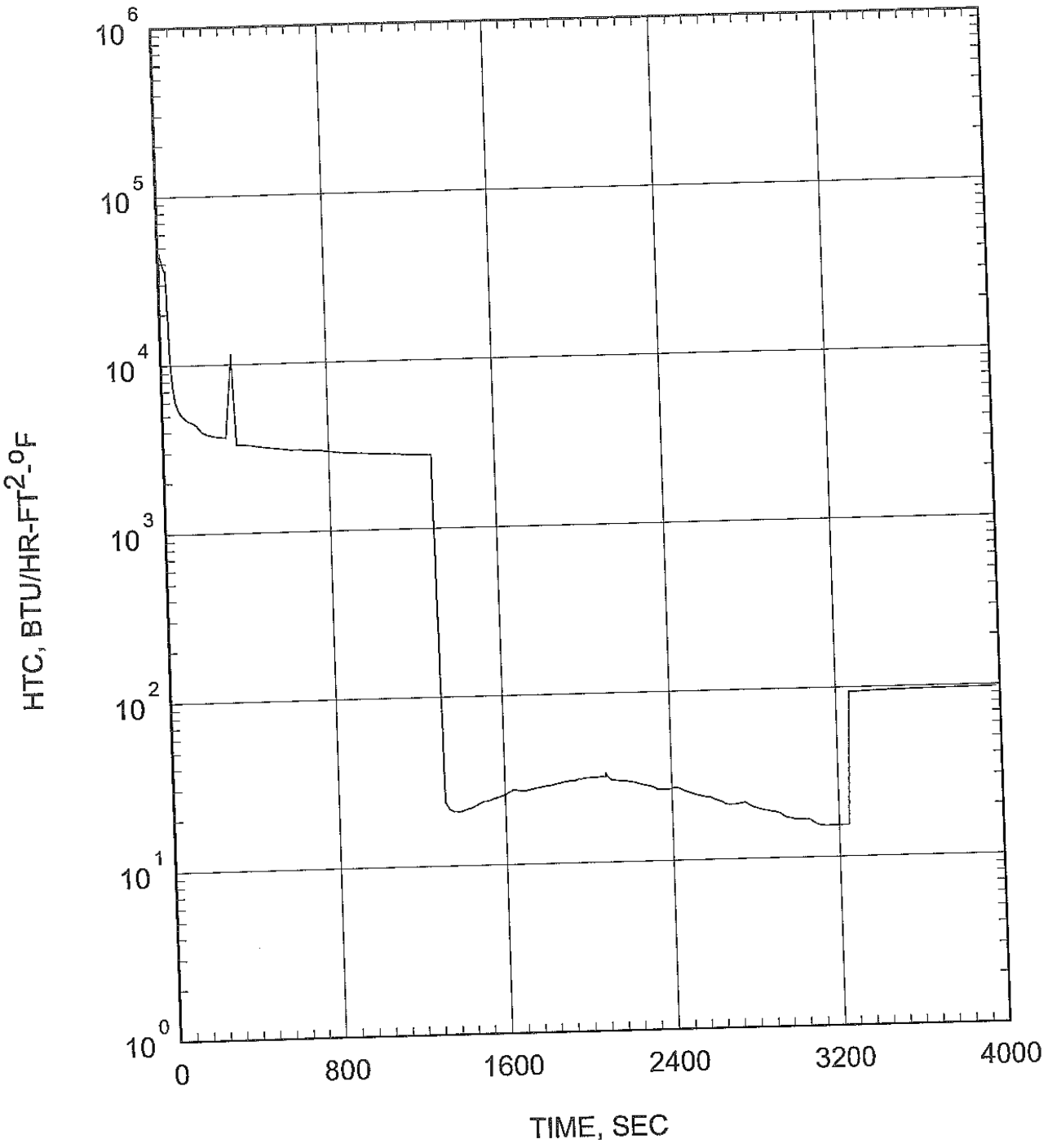

Figure 15.6.5-54
Small Break LOCA ECCS Performance Analysis
0.04 ft^2/PD Break
Coolant Temperature at Hot Spot

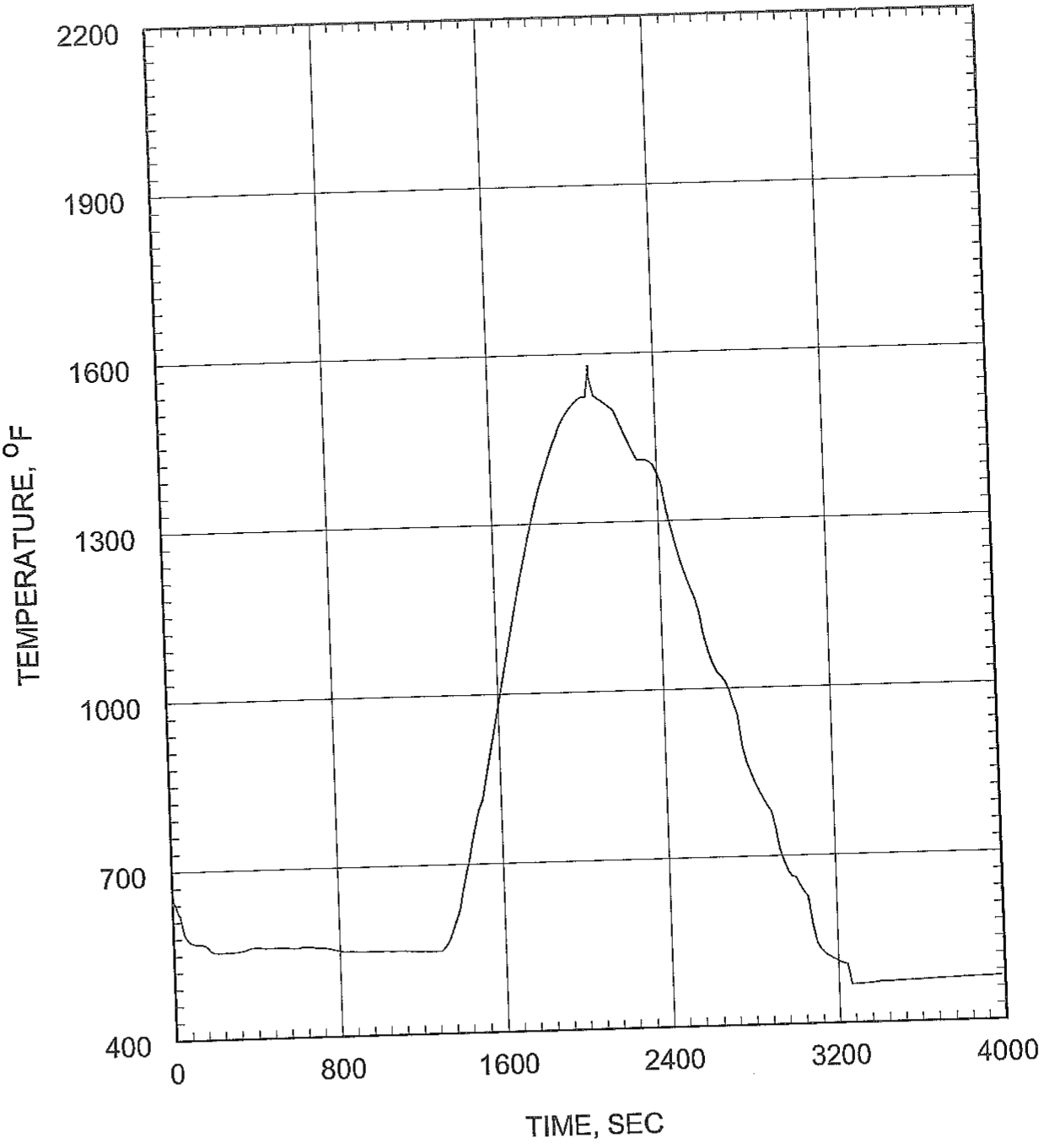

Figure 15.6.5-55
Small Break LOCA ECCS Performance Analysis
0.04 ft^2/PD Break
Cladding Temperature at Hot Spot

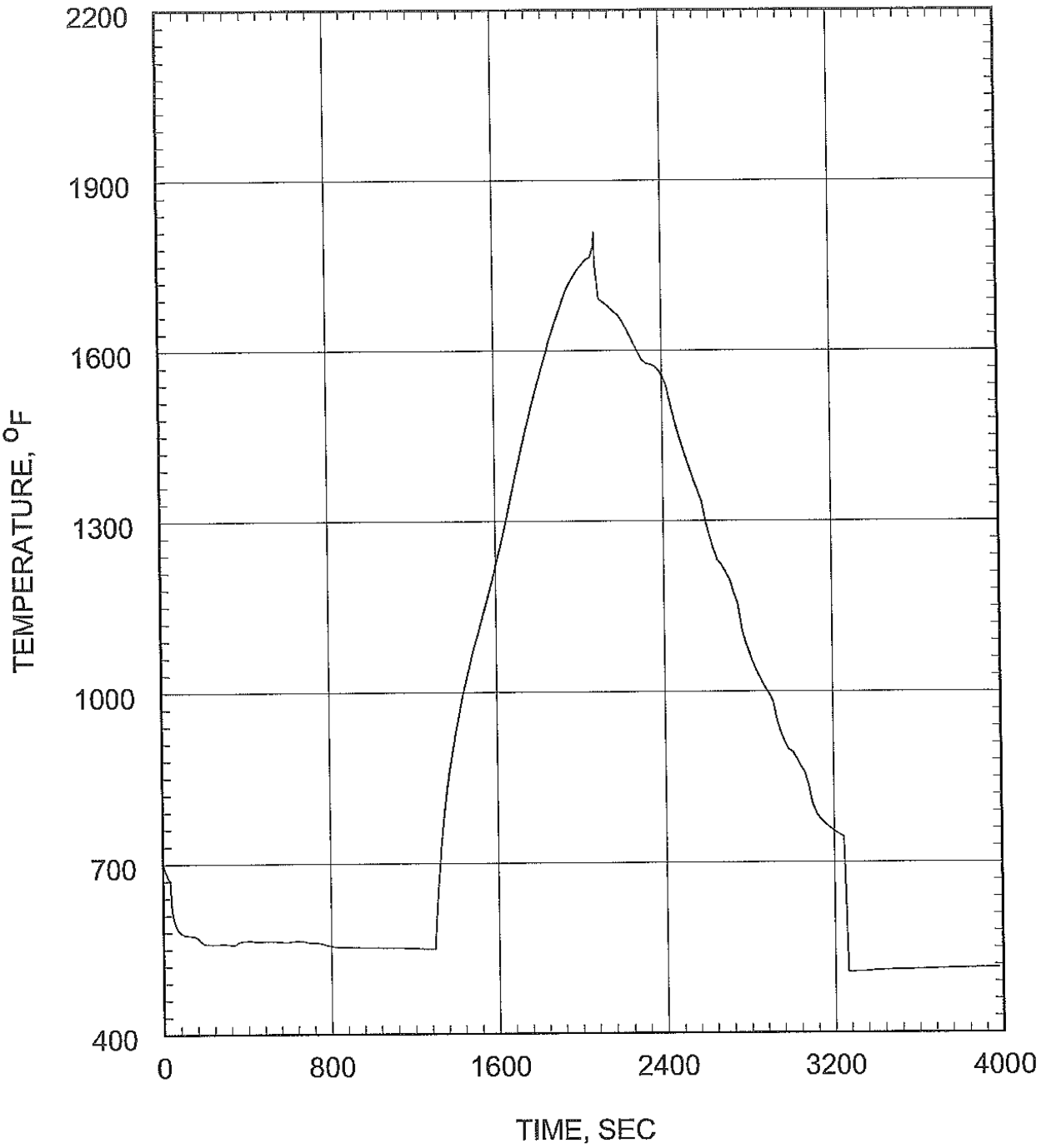

Figure 15.6.5-56
Small Break LOCA ECCS Performance Analysis
0.05 ft^2/PD Break
Core Power

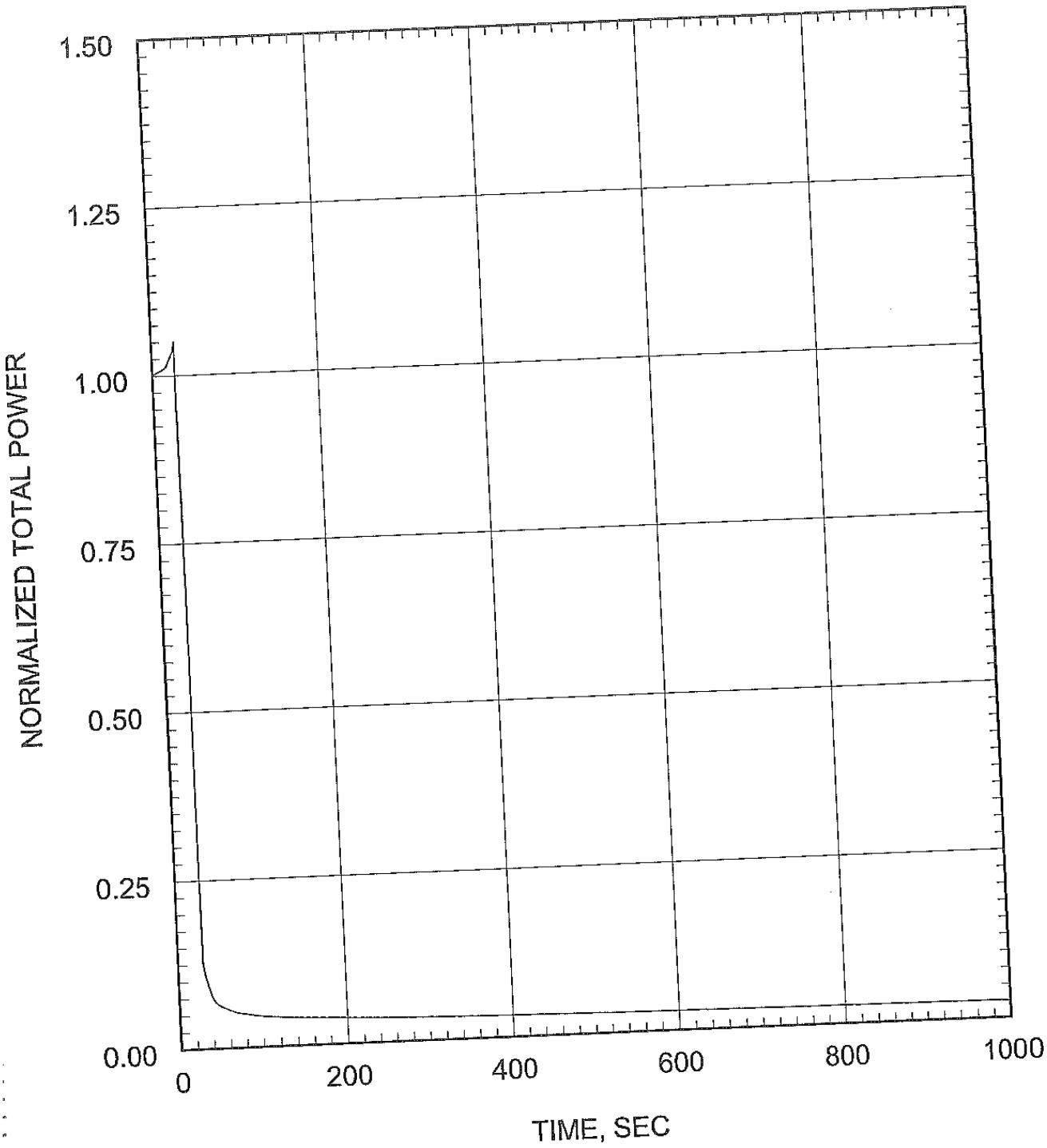

Figure 15.6.5-57
Small Break LOCA ECCS Performance Analysis
0.05 ft^2/PD Break
Inner Vessel Pressure

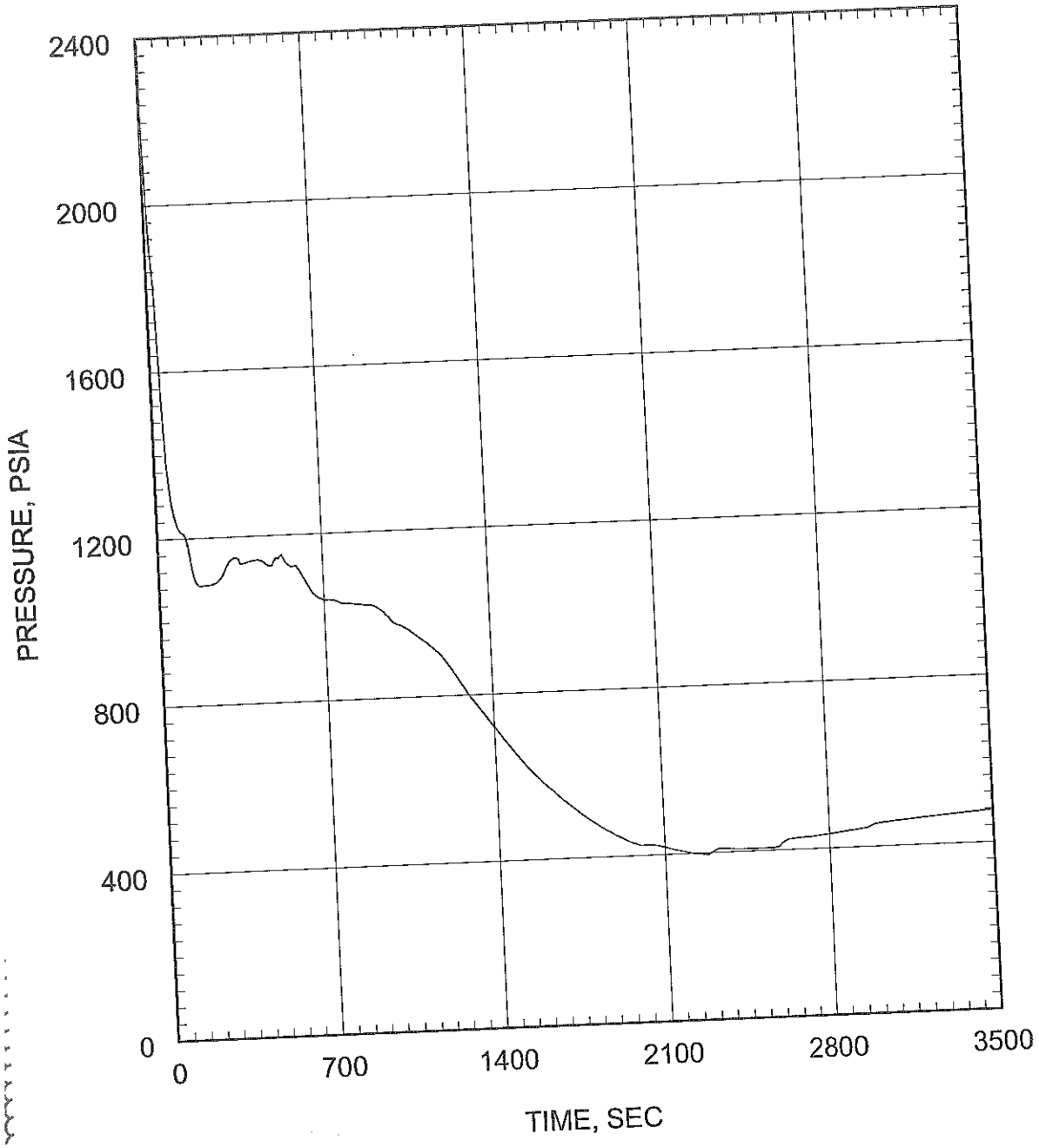

Figure 15.6.5-58
Small Break LOCA ECCS Performance Analysis
0.05 ft^2/PD Break
Break Flow Rate

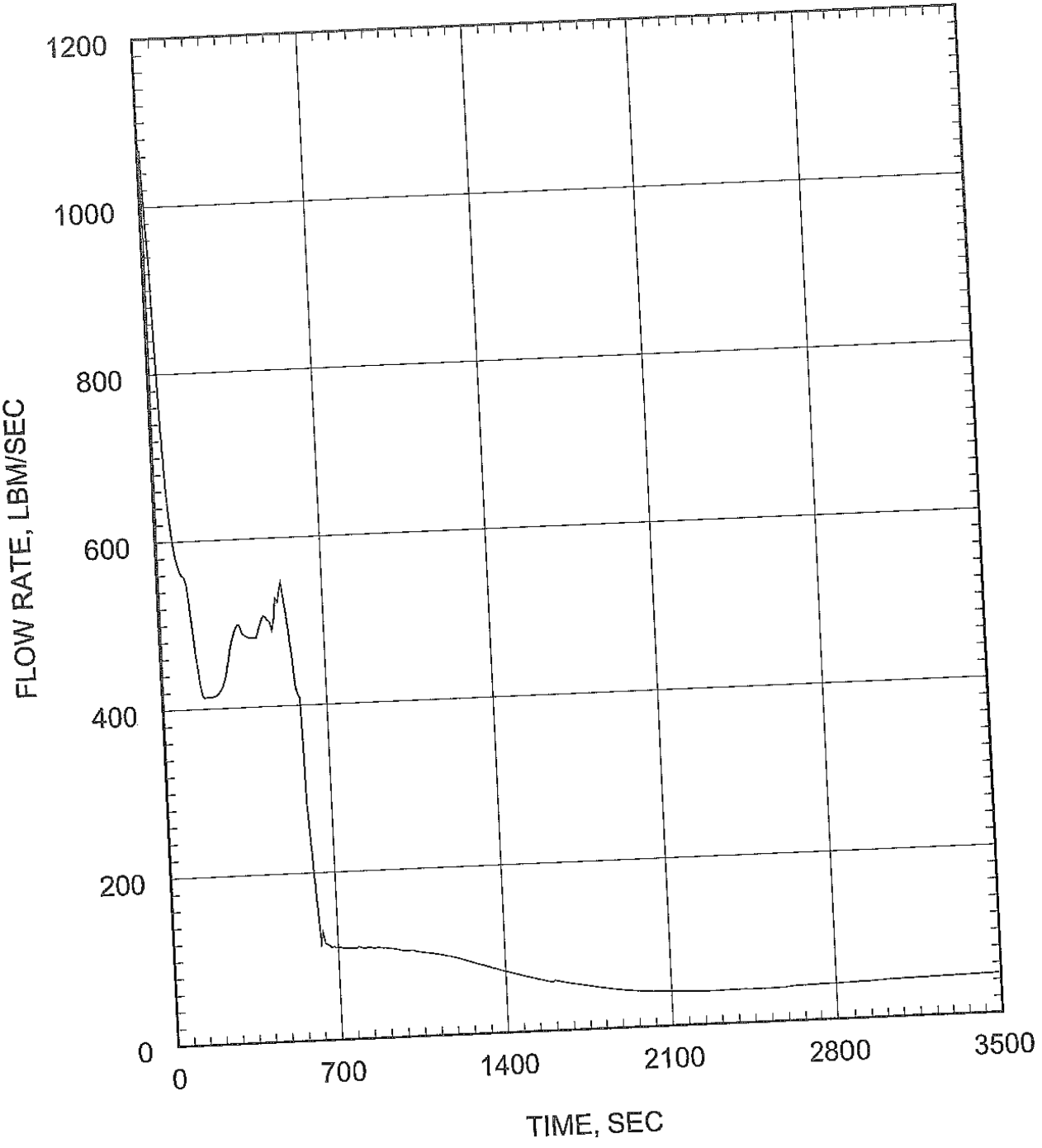

Figure 15.6.5-59
Small Break LOCA ECCS Performance Analysis
0.05 ft^2/PD Break
Inner Vessel Inlet Flow Rate

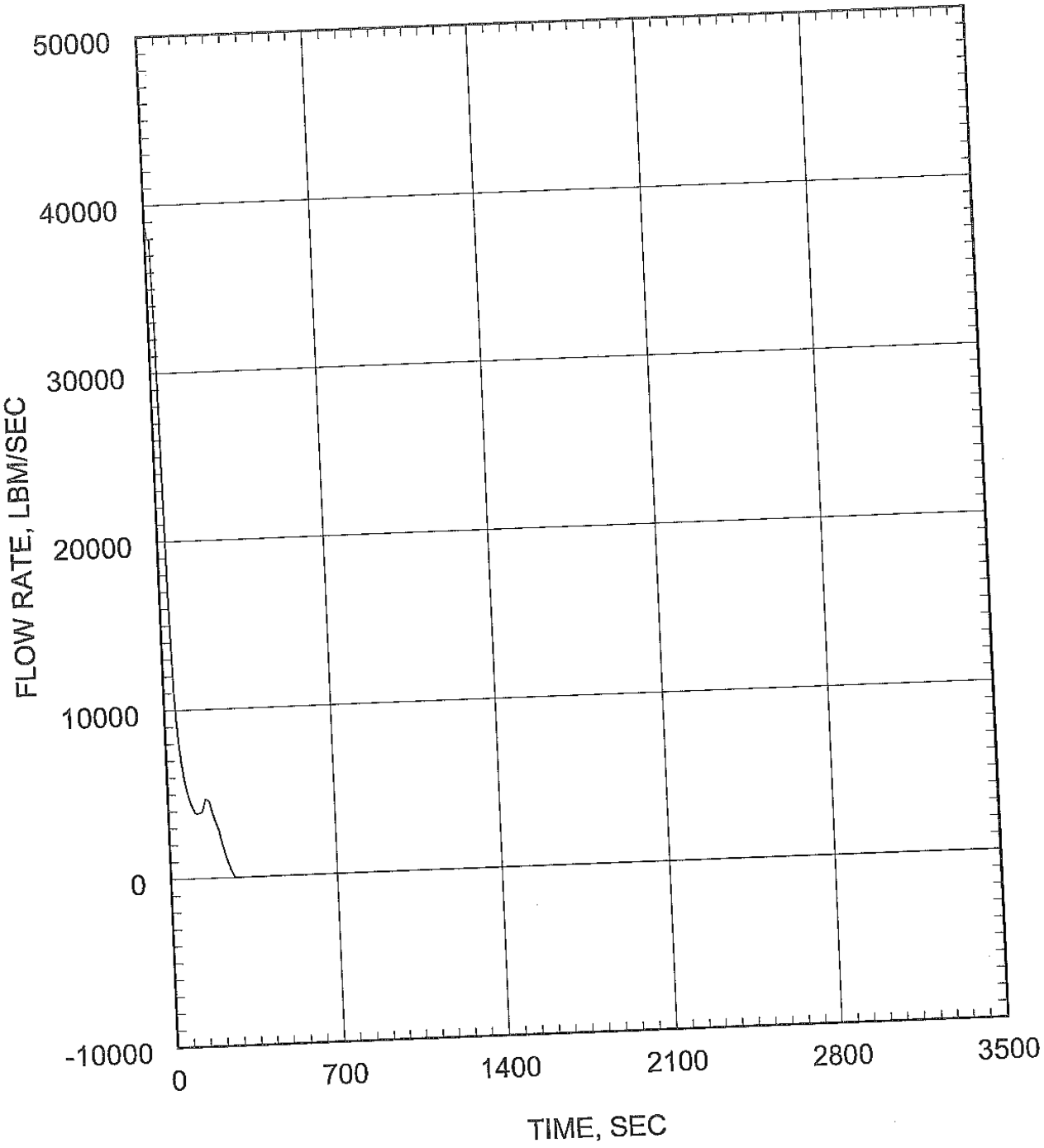

Figure 15.6.5-60
Small Break LOCA ECCS Performance Analysis
0.05 ft^2/PD Break
Inner Vessel Two-Phase Mixture Level

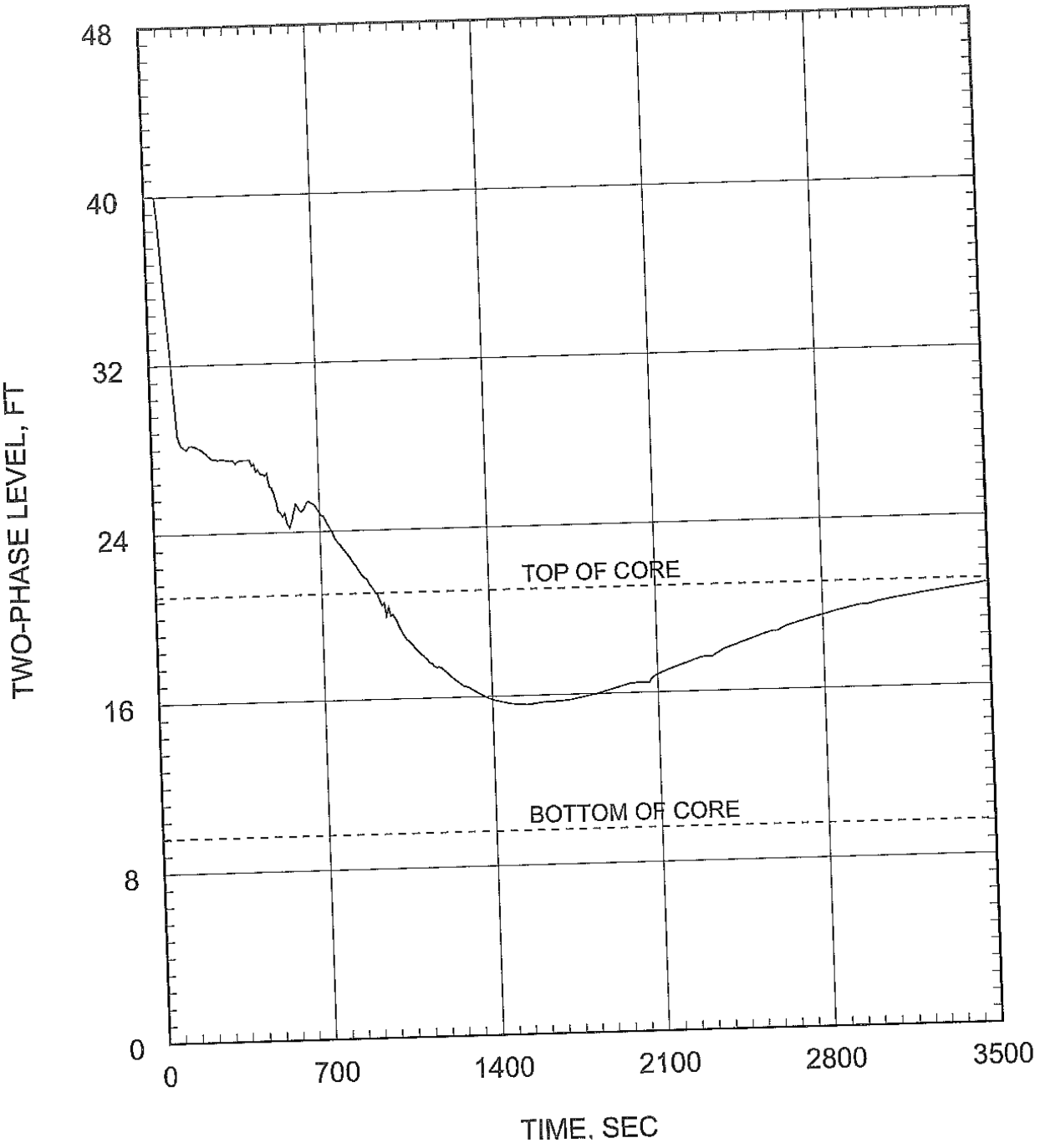

Figure 15.6.5-61
Small Break LOCA ECCS Performance Analysis
0.05 ft^2/PD Break
Heat Transfer Coefficient at Hot Spot

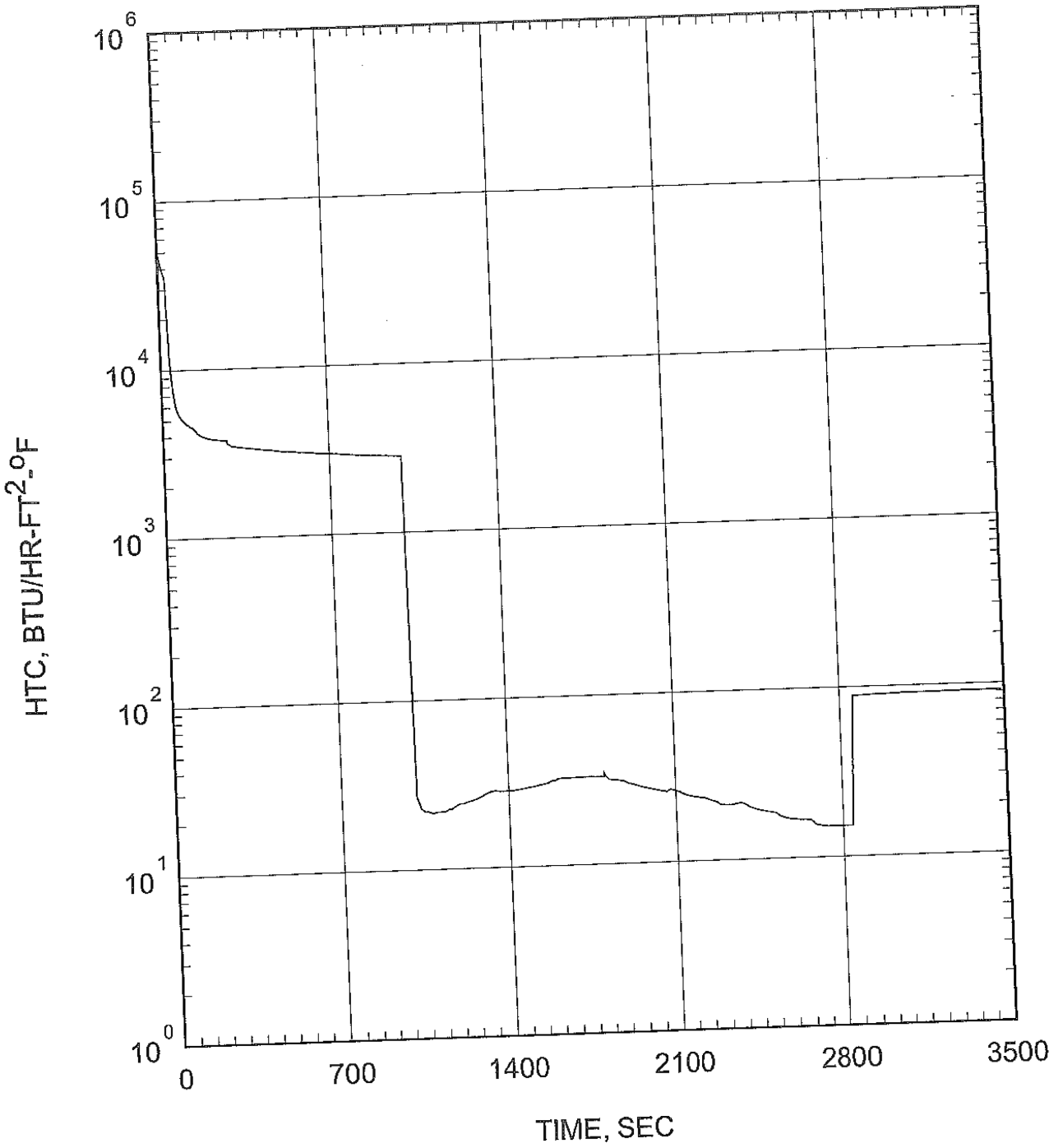

Figure 15.6.5-62
Small Break LOCA ECCS Performance Analysis
0.05 ft^2/PD Break
Coolant Temperature at Hot Spot

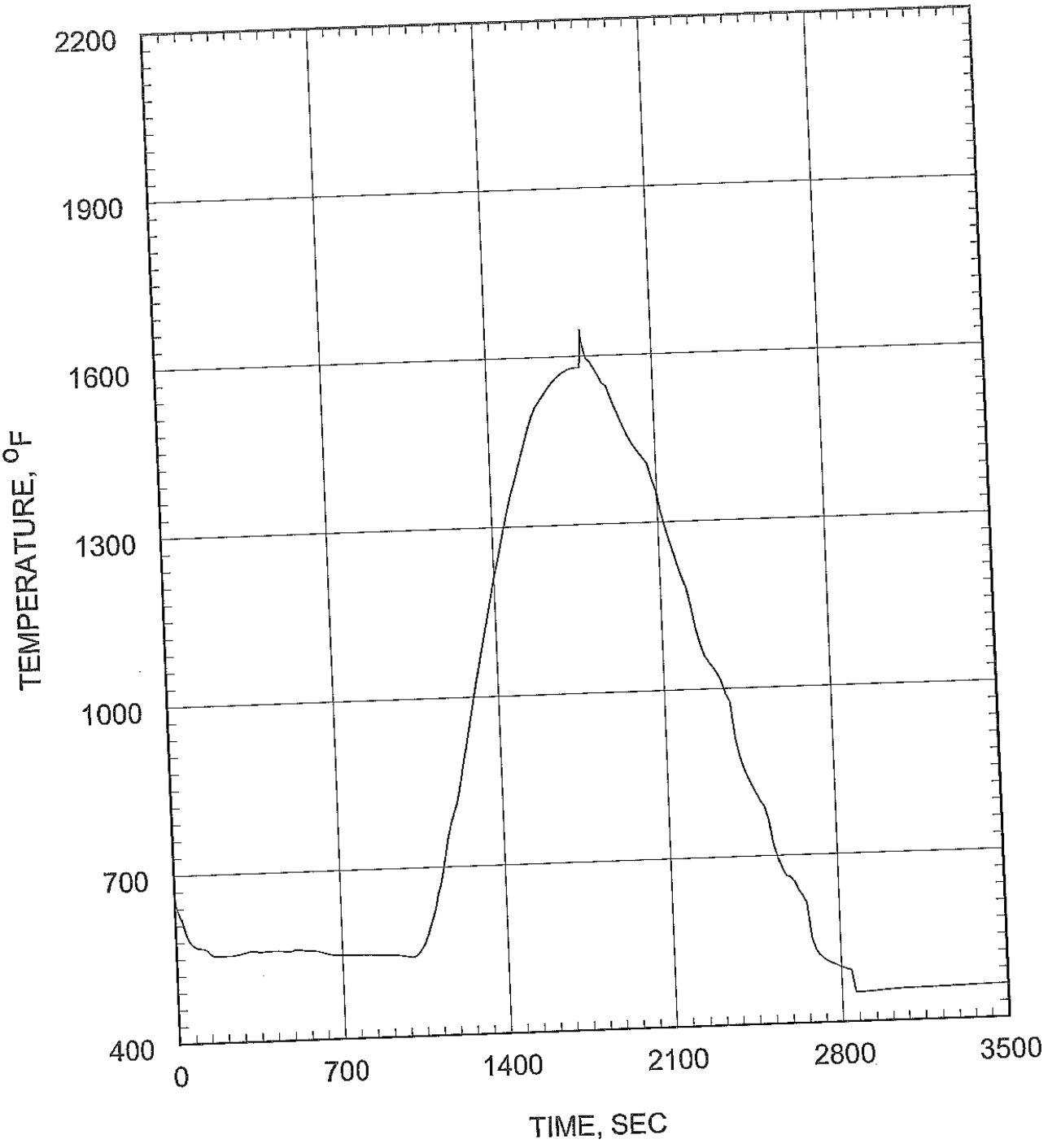

Figure 15.6.5-63
Small Break LOCA ECCS Performance Analysis
0.05 ft^2/PD Break
Cladding Temperature at Hot Spot

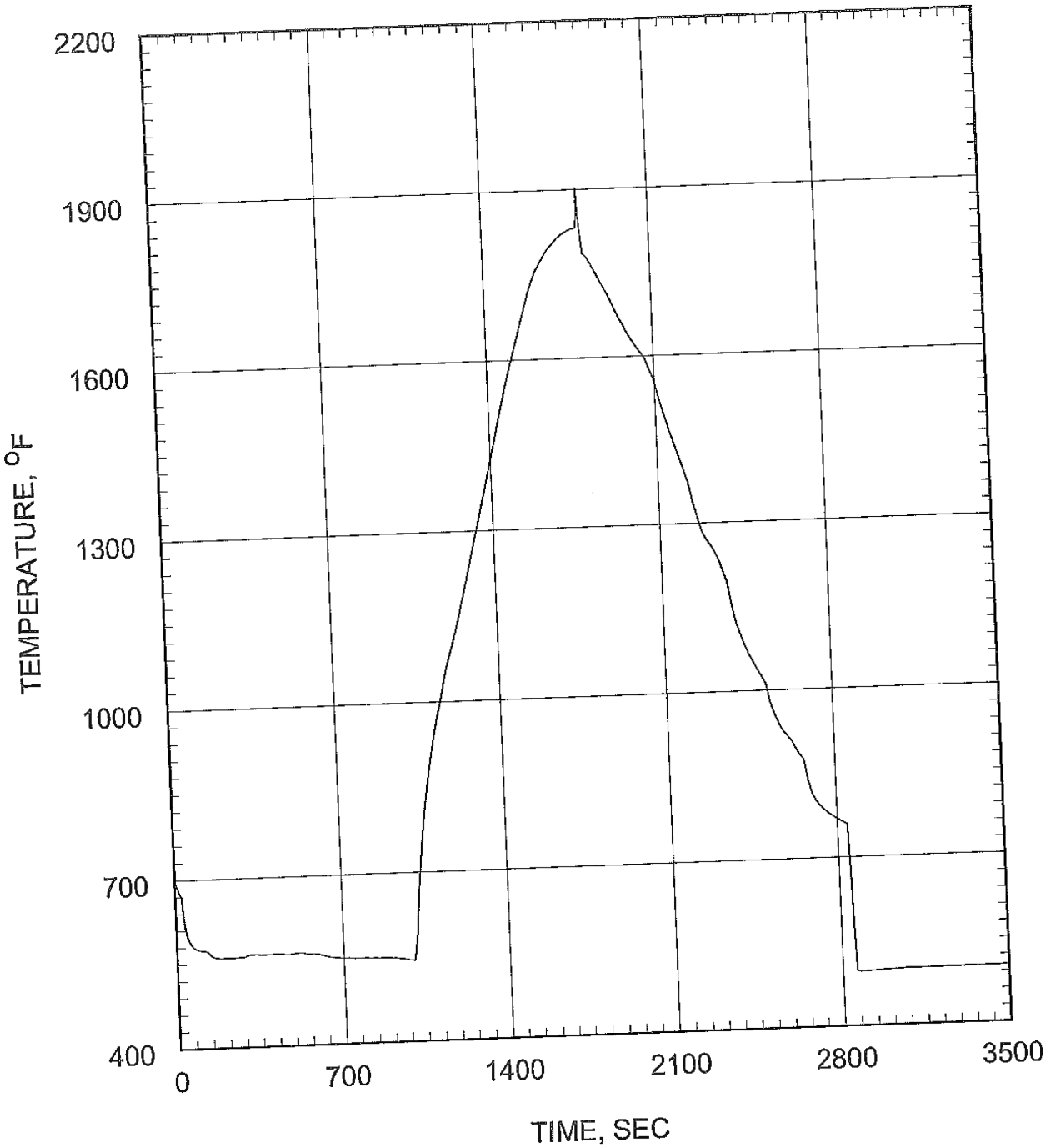

Figure 15.6.5-64
Small Break LOCA ECCS Performance Analysis
0.06 ft^2/PD Break
Core Power

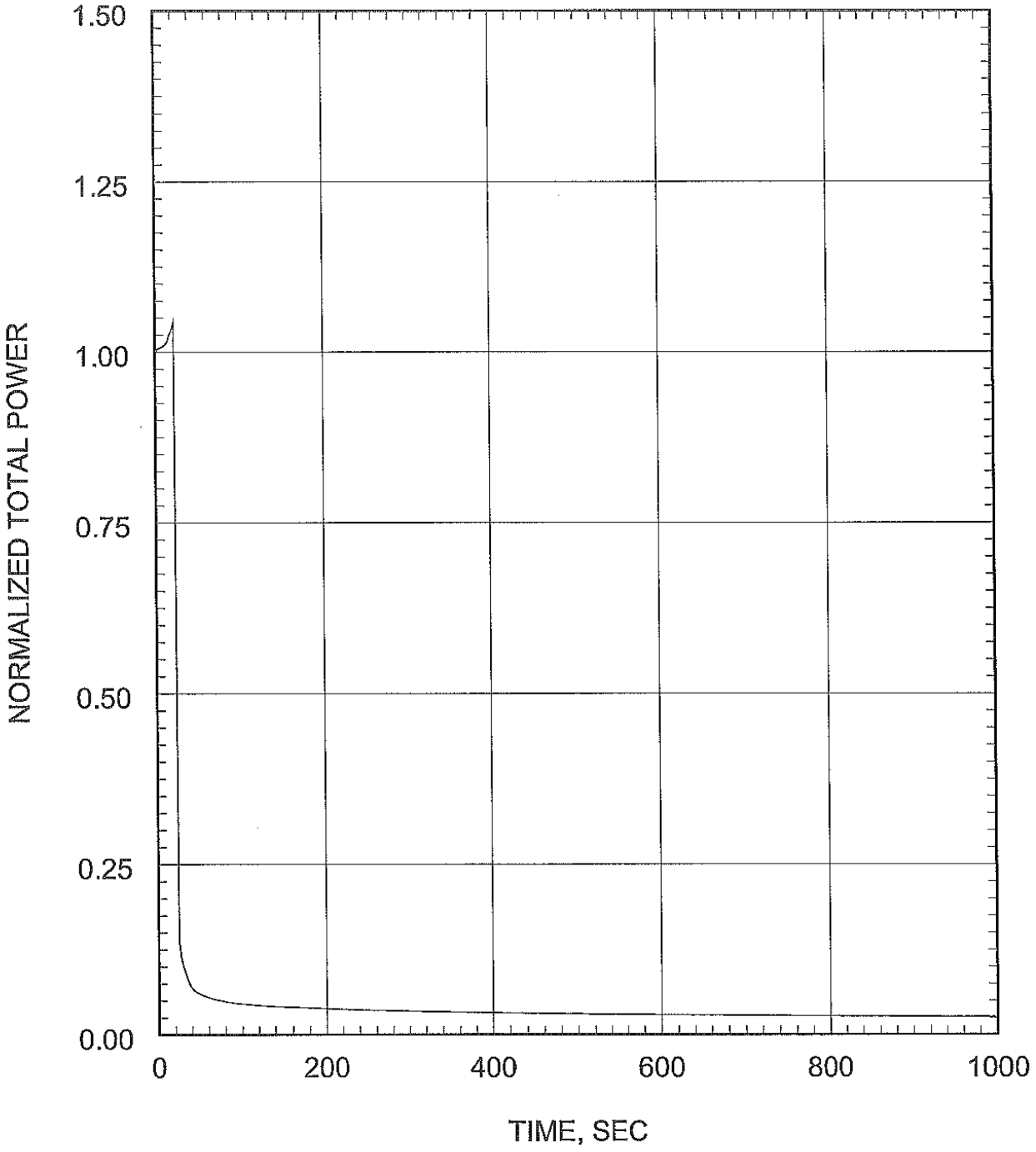

Figure 15.6.5-65
Small Break LOCA ECCS Performance Analysis
0.06 ft^2/PD Break
Inner Vessel Pressure

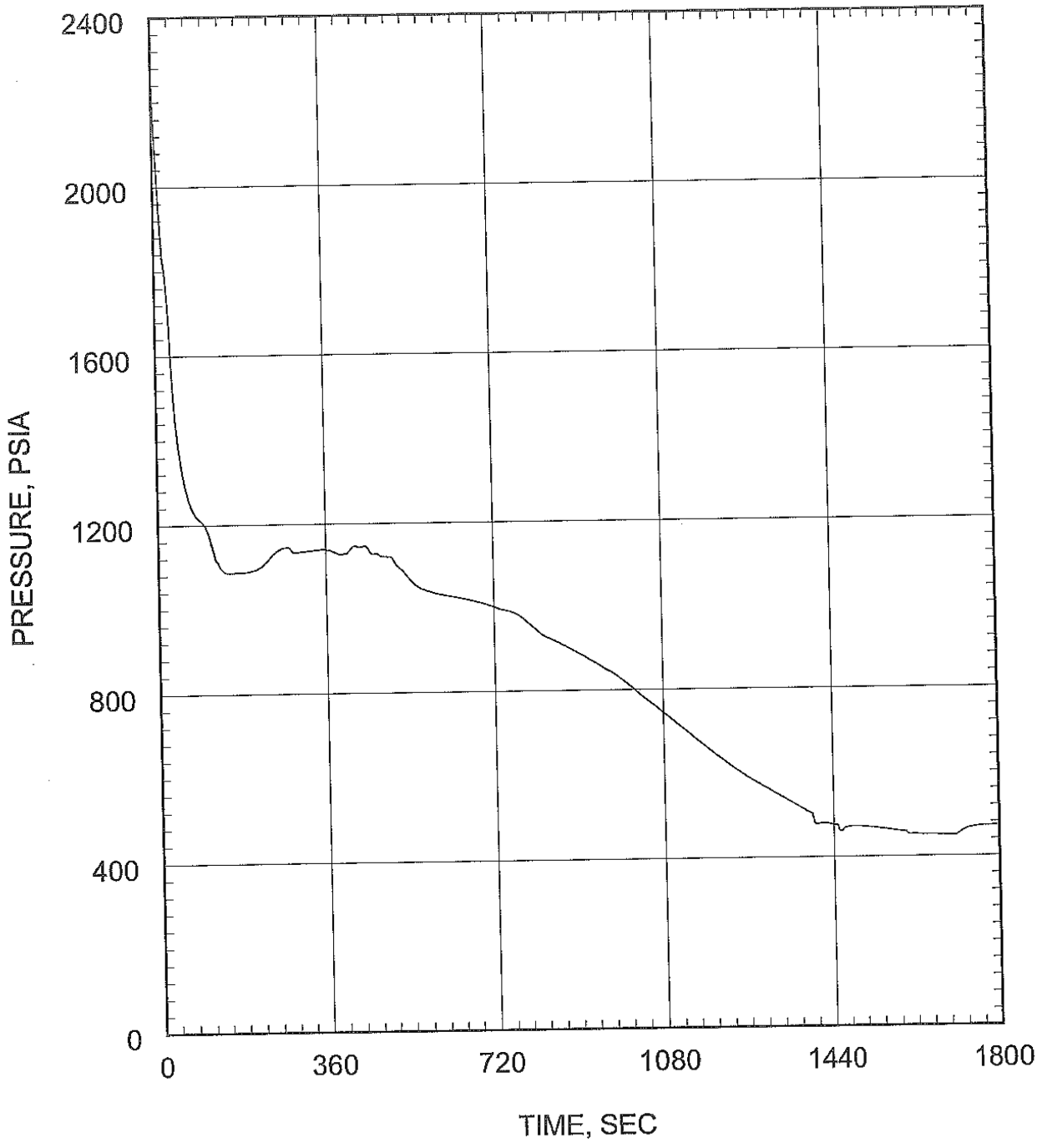

Figure 15.6.5-66
Small Break LOCA ECCS Performance Analysis
0.06 ft^2/PD Break
Break Flow Rate

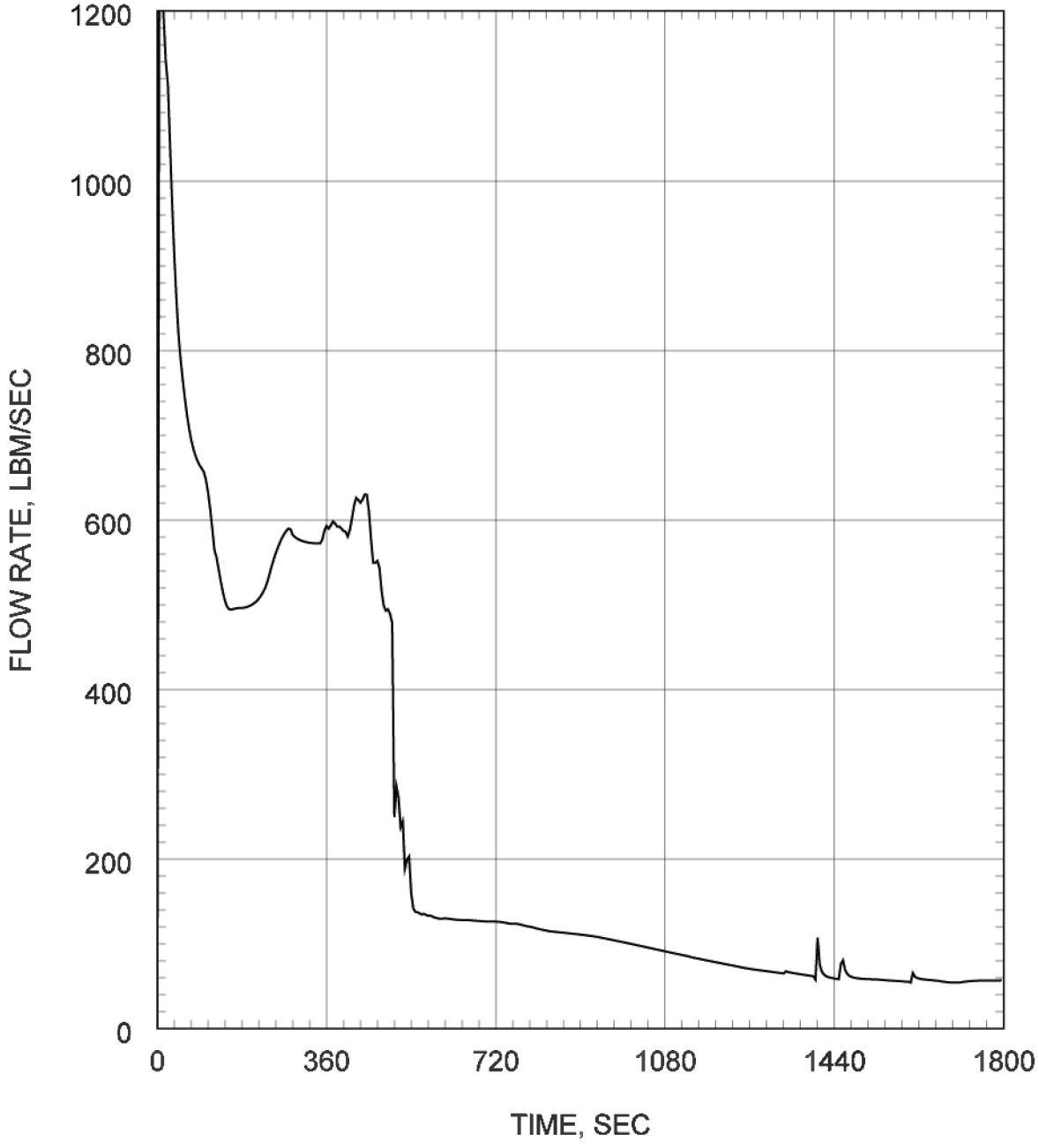

Figure 15.6.5-67
Small Break LOCA ECCS Performance Analysis
0.06 ft^2/PD Break
Inner Vessel Inlet Flow Rate

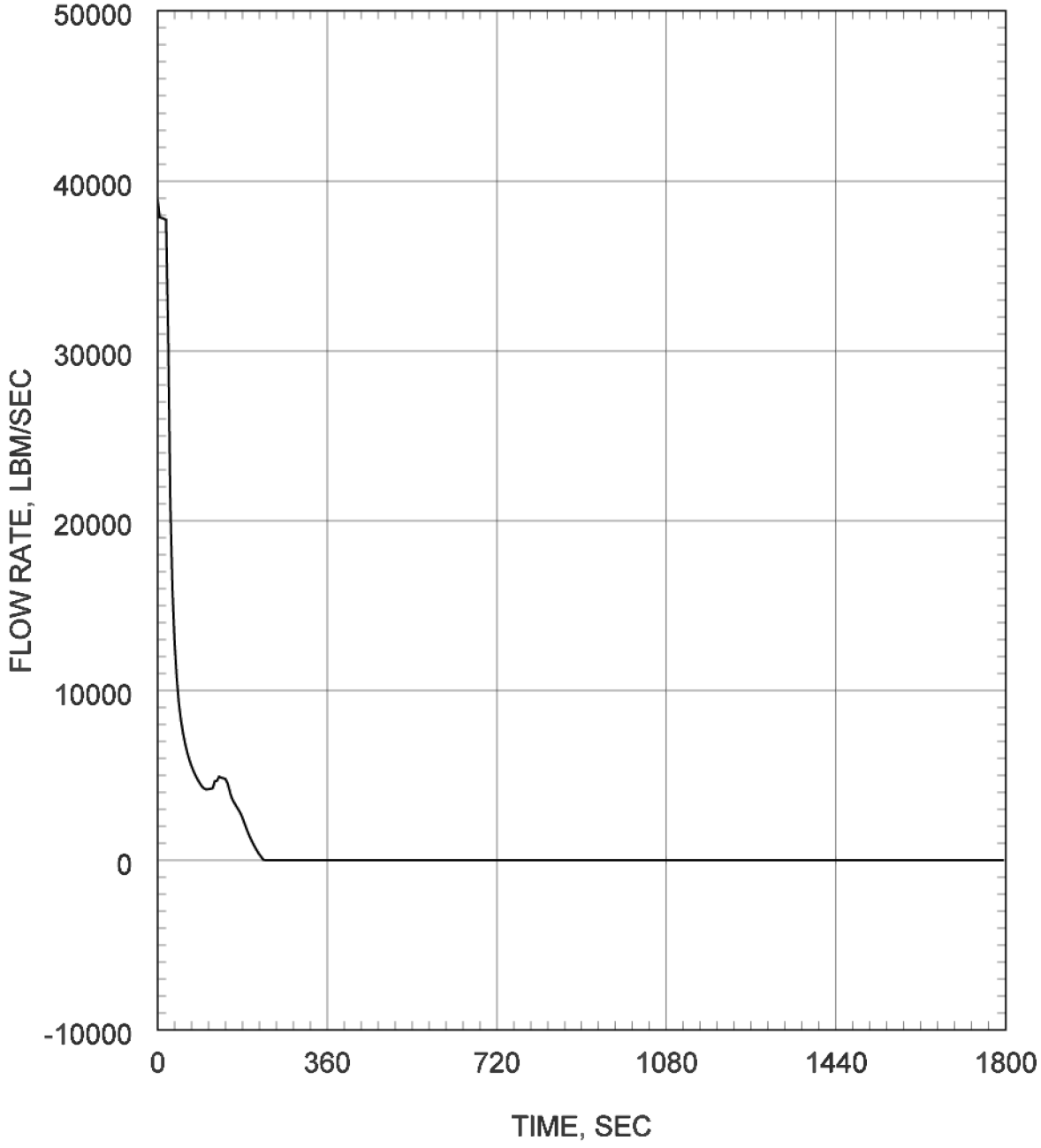

Figure 15.6.5-68
Small Break LOCA ECCS Performance Analysis
0.06 ft^2/PD Break
Inner Vessel Two-Phase Mixture Level

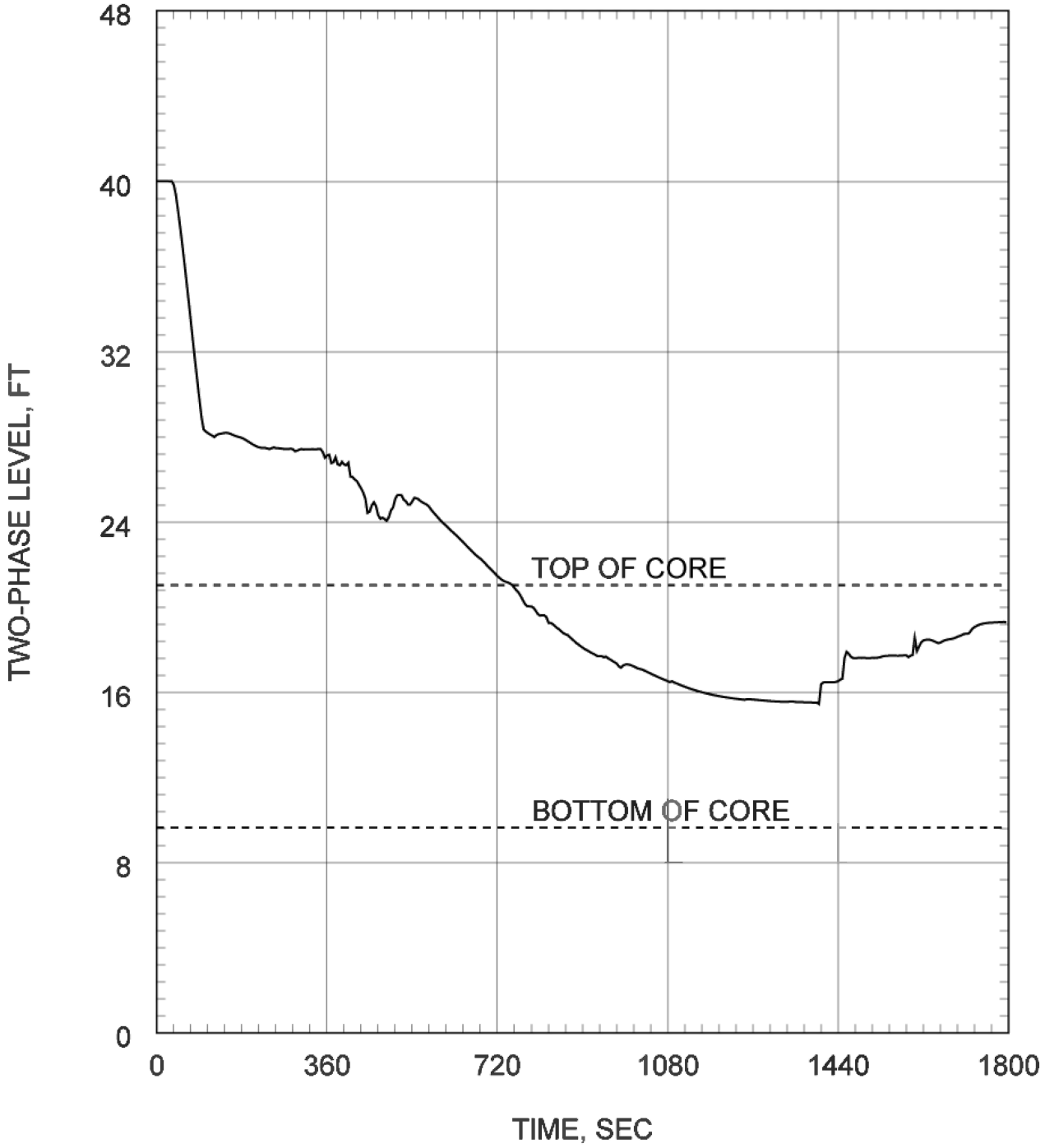

Figure 15.6.5-69
Small Break LOCA ECCS Performance Analysis
0.06 ft^2/PD Break
Heat Transfer Coefficient at Hot Spot

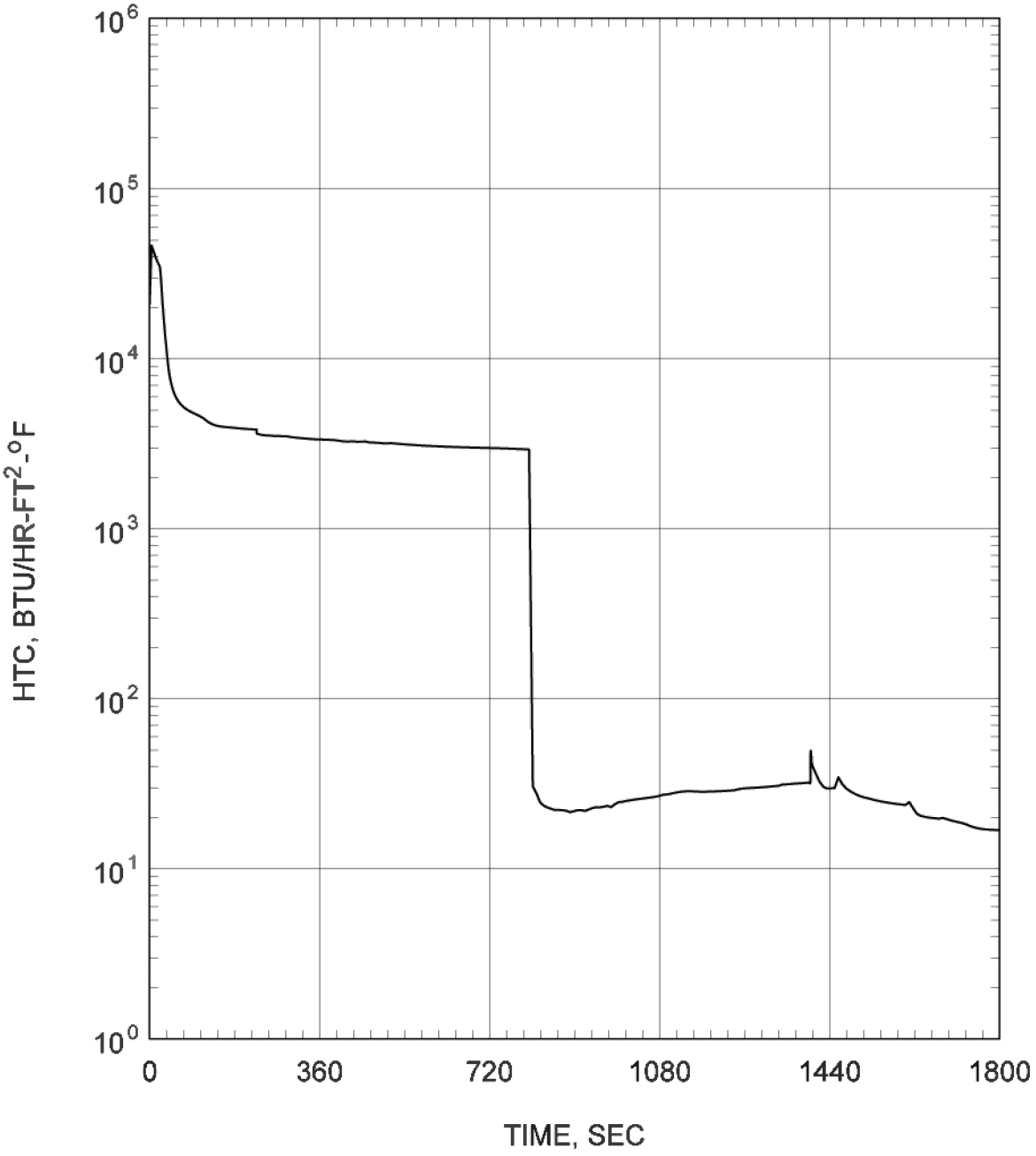

Figure 15.6.5-70
Small Break LOCA ECCS Performance Analysis
0.06 ft^2/PD Break
Coolant Temperature at Hot Spot

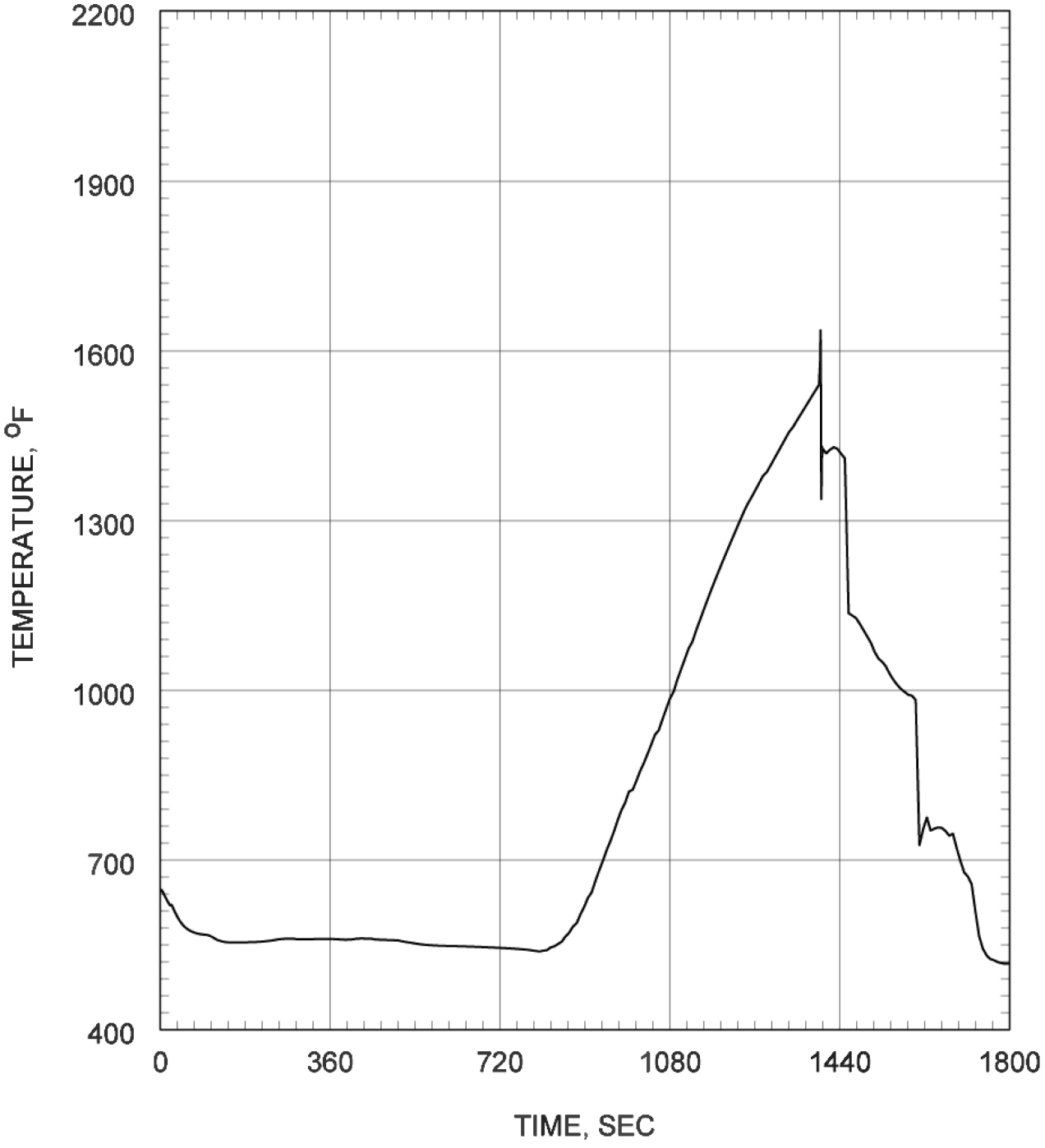

Figure 15.6.5-71
Small Break LOCA ECCS Performance Analysis
0.06 ft^2/PD Break
Cladding Temperature at Hot Spot

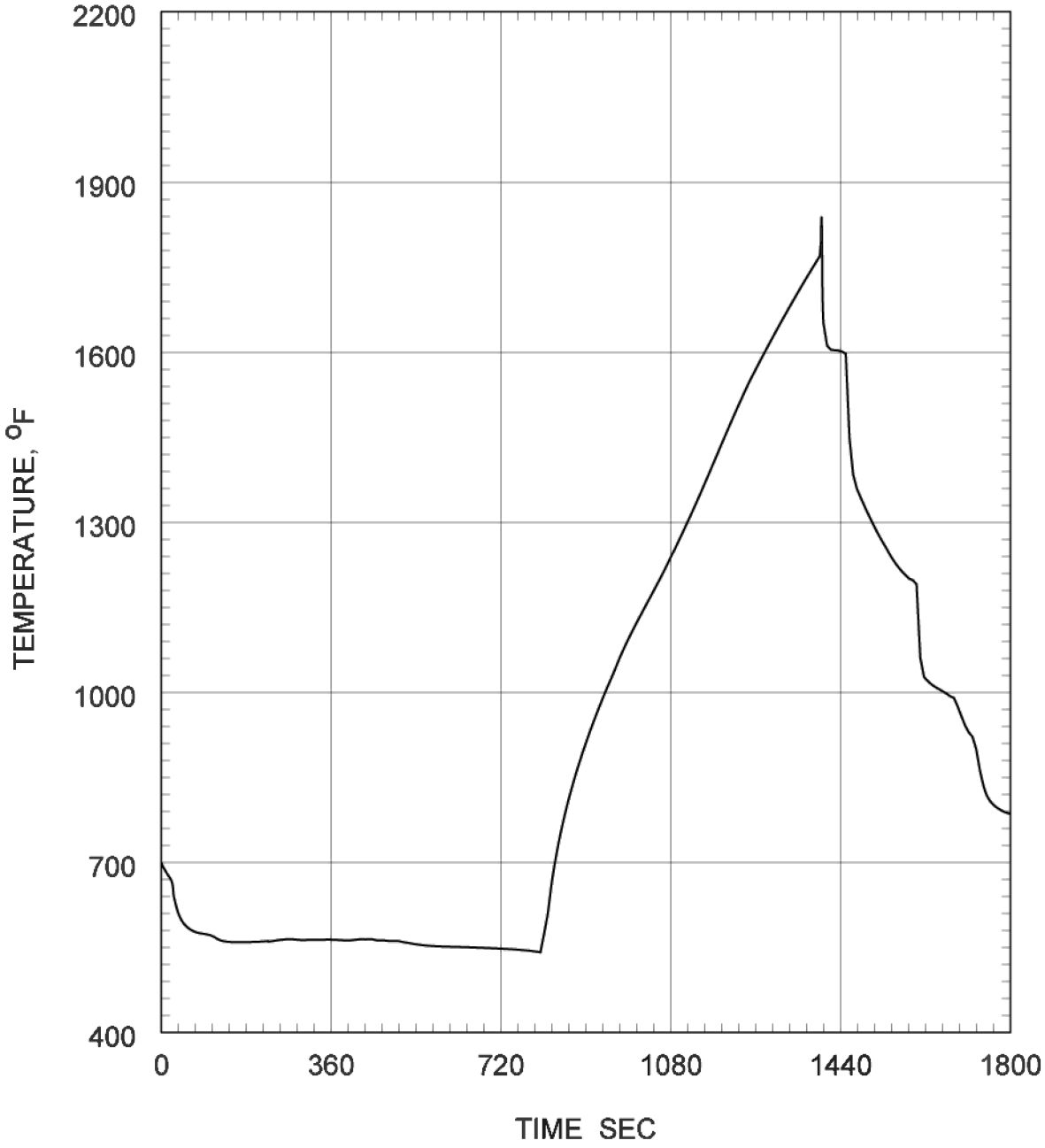

Figure 15.6.5-72
Long-Term Cooling Analysis
Comparison of Core Boiloff Rate and the Minimum
Simultaneous Hot and Cold Side Injection Flow Rate for EPU

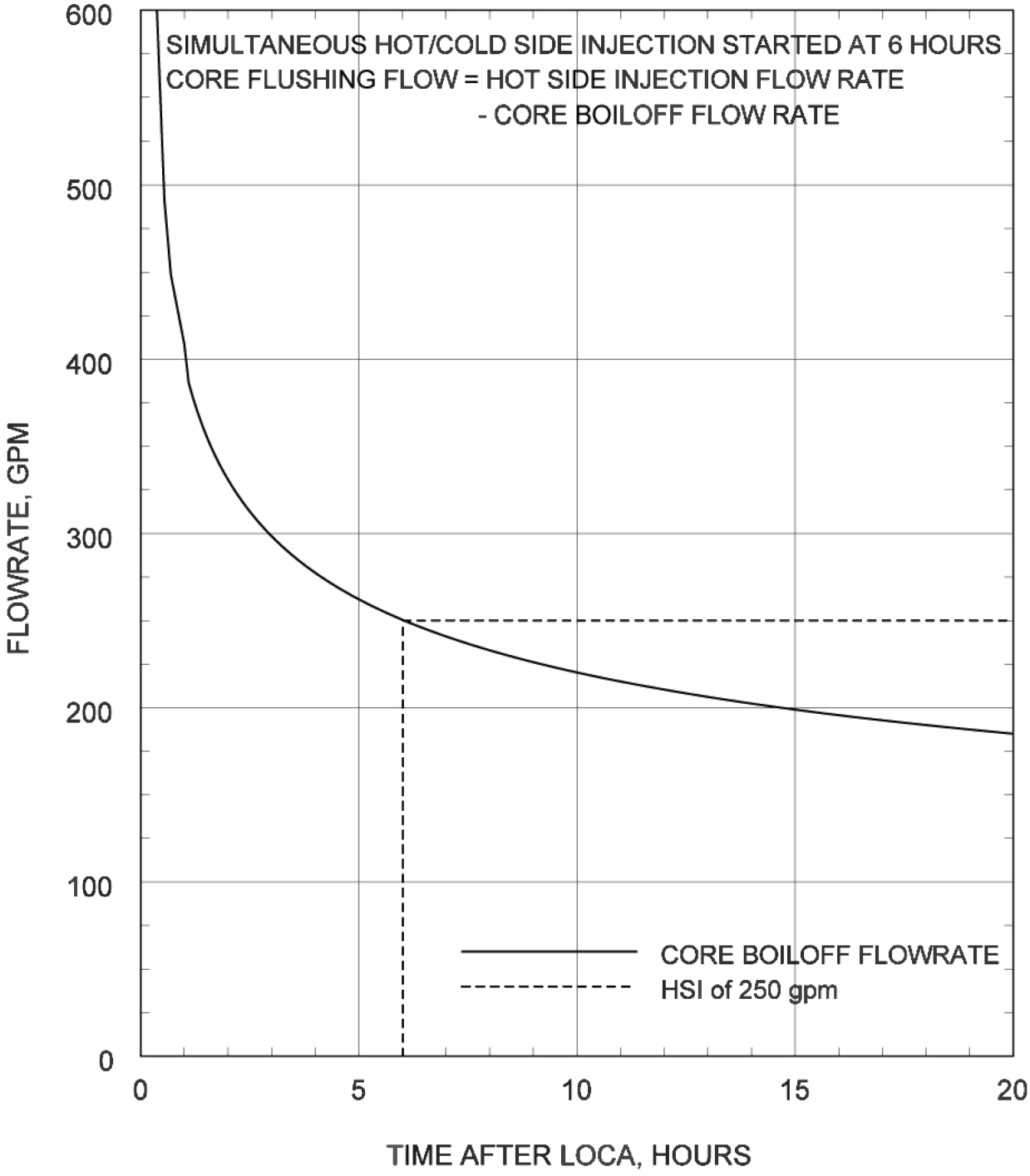

Figure 15.6.5-73
Long-Term Cooling Analysis
Boric Acid Concentration in the Core Versus Time for EPU

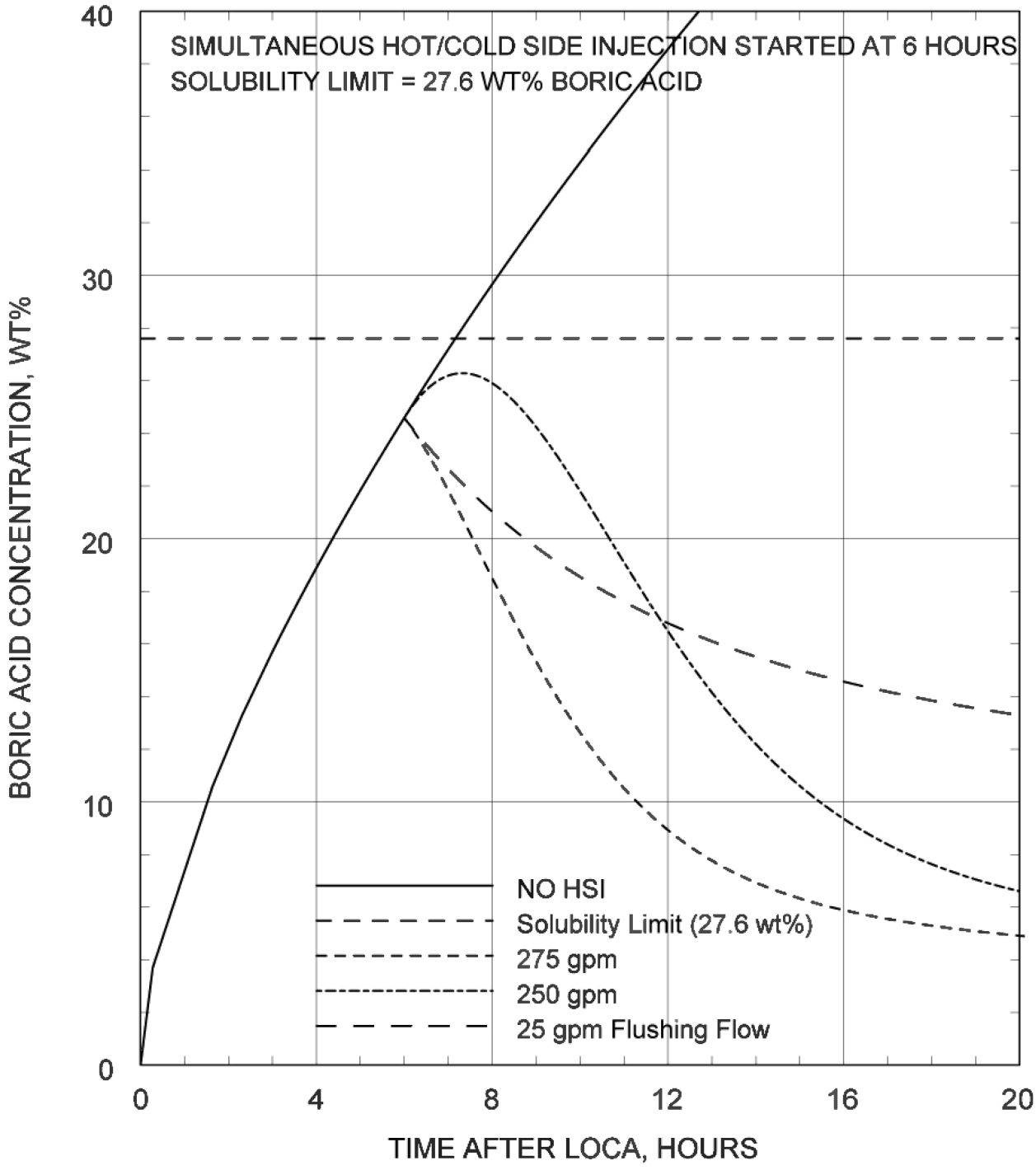

Figure 15.6.5-74 - Not Used

Figure 15.6.5-75
Long-Term Cooling Analysis
Break Area Versus RCS Refill Time for EPU

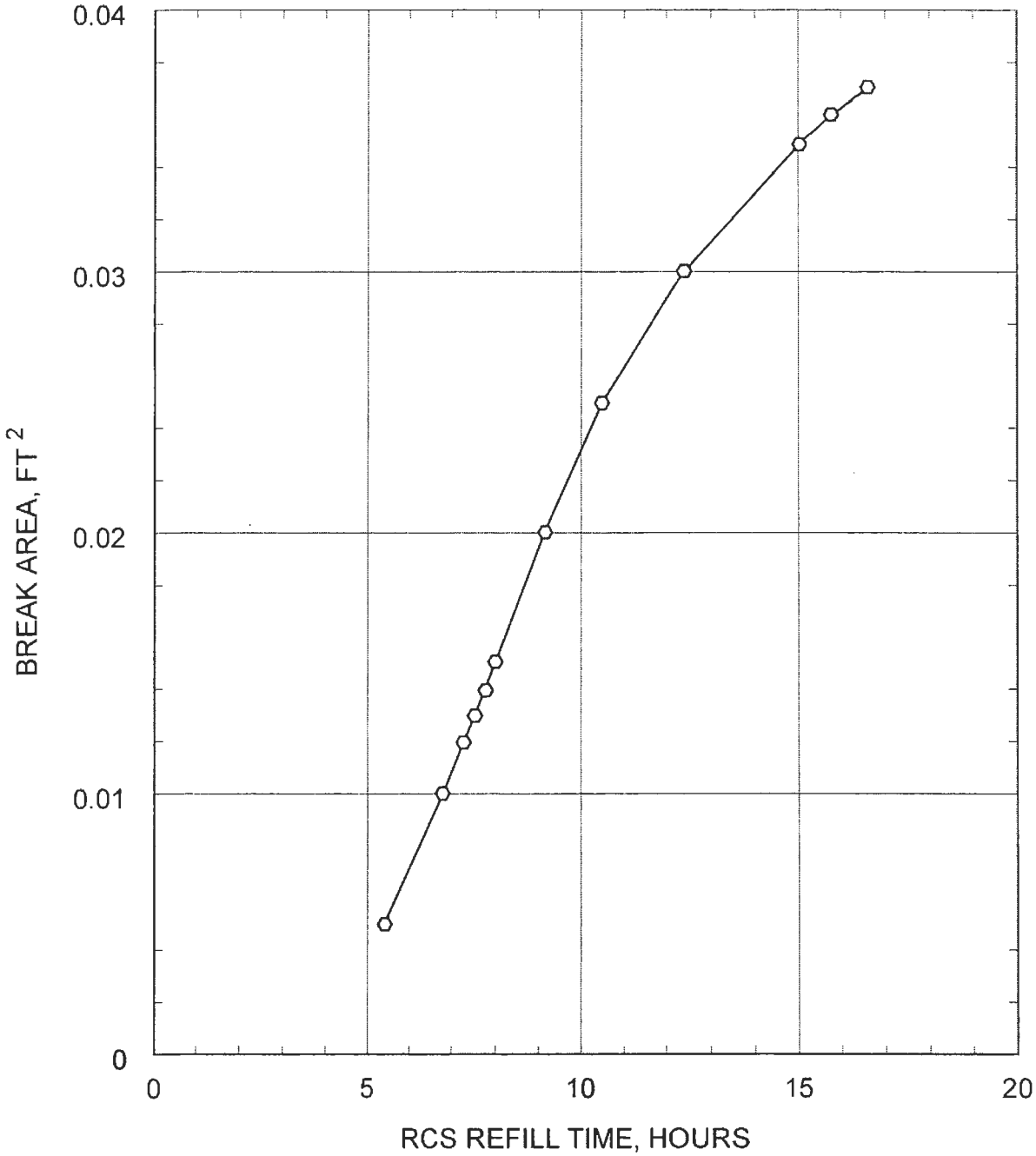

Figure 15.6.5-76
Long-Term Cooling Analysis
RCS Pressure at the Decision Time Versus Break Area at EPU

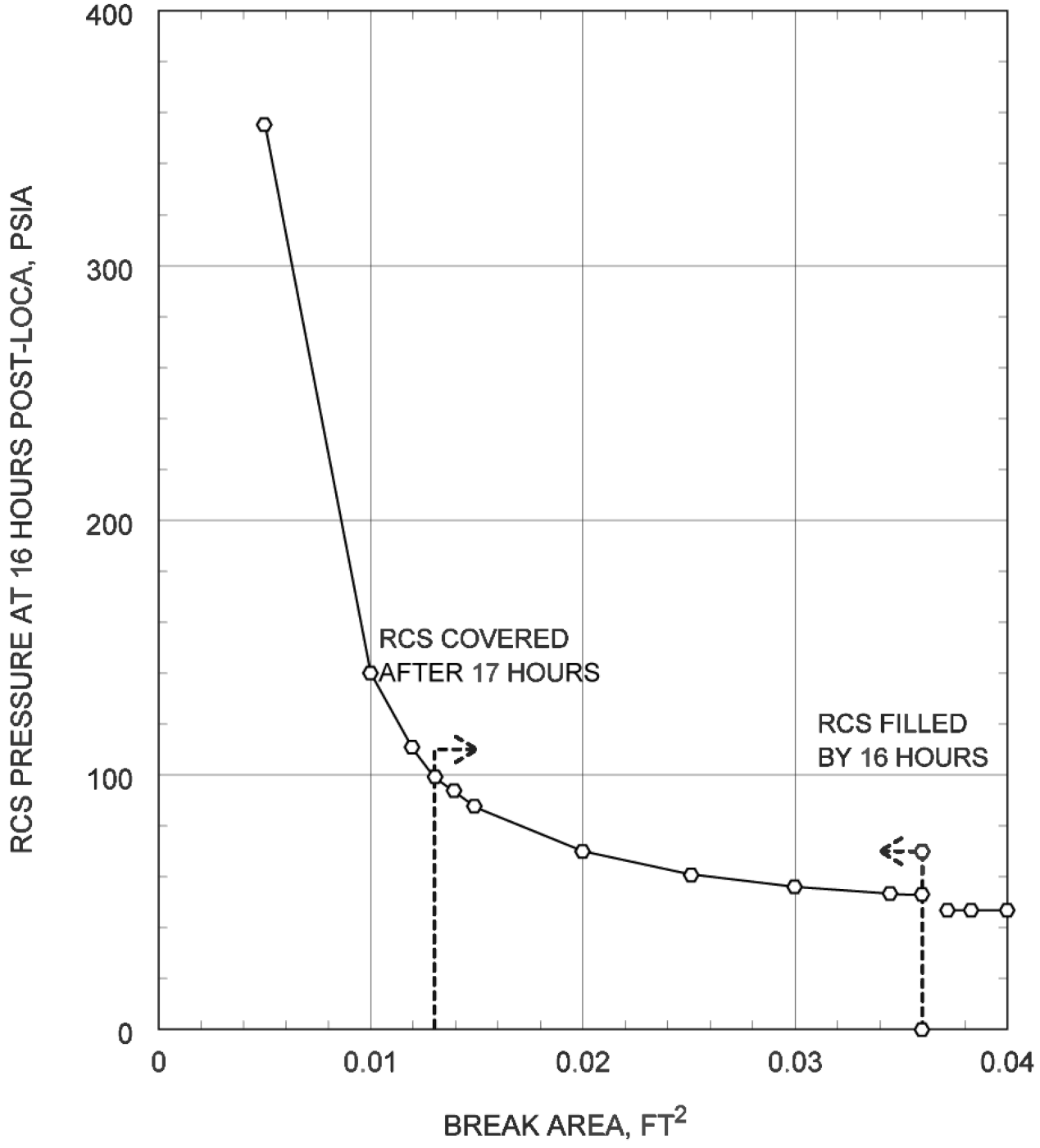

Figure 15.6.5-77
Long-Term Cooling Analysis
Overlap of Acceptable Procedures in Terms of Break Size for EPU

For break areas 0.013 ft^2 and larger, simultaneous hot/cold leg leg injection cools the core and flushes boric acid from the core.

For break areas 0.036 ft^2 and smaller, refill of the RCS disperses boric acid throughout the RCS and the SGs cool the RCS to the SDC entry temperature.

Break Size (ft^2)	RCS Pressure at 16 Hours Post-LOCA (psia)
0.040	47
0.038	47
0.037	47
0.036	53
0.035	53
0.030	56
0.025	61
0.020	70
0.015	87
0.014	93
0.013	99
0.012	110
0.010	140
0.005	356

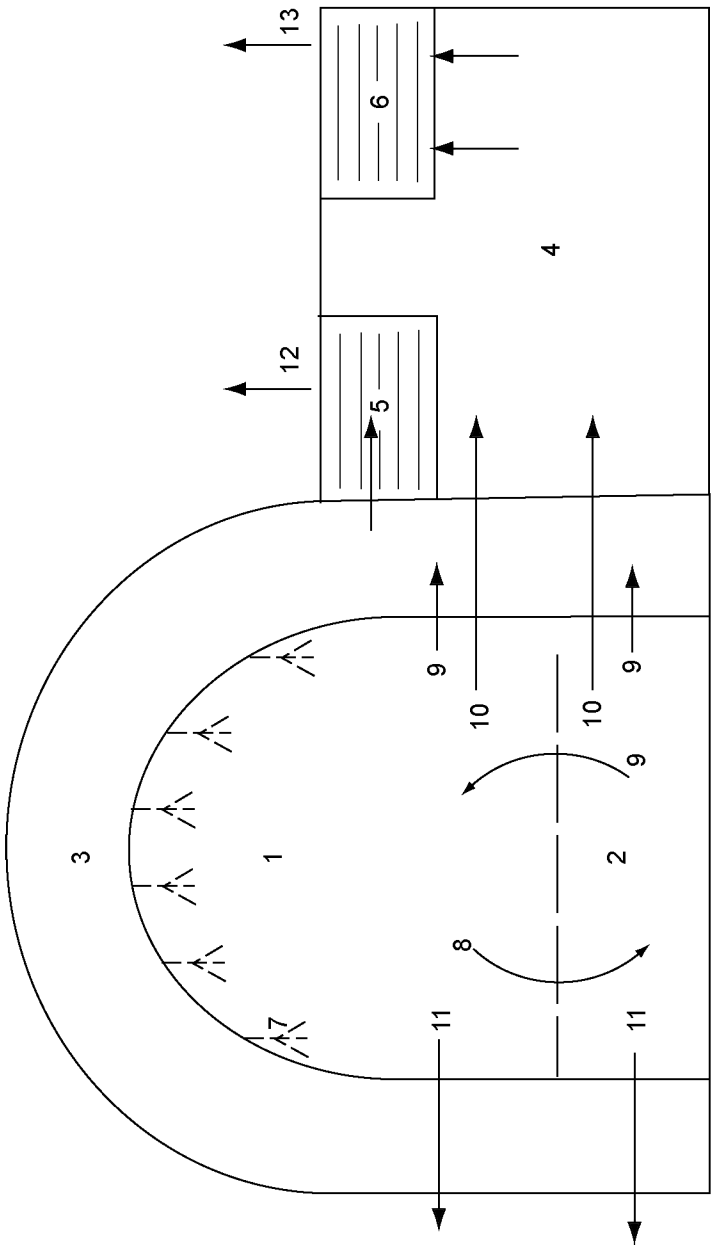

NOTES:

1. CONTAINMENT SPRAYED VOLUME
2. CONTAINMENT UNSPRAYED VOLUME
3. SHIELD BUILDING ANNULUS
4. NEGATIVE PRESSURE ARE OF THE REACTOR AUXILIARY BUILDING
5. SHIELD BUILDING VENTILATION SYSTEM
6. CONTROLLED VENTILATION SYSTEM
7. CONTAINMENT SPRAYS
8. AIR EXCHANGE BETWEEN REGIONS 1 AND 2
9. LEAKAGE INTO THE SHIELD BUILDING ANNULUS
10. LEAKAGE INTO THE NEGATIVE PRESSURE AREA OF THE REACTOR AUXILIARY BUILDING
11. BYPASS LEAKAGE
12. SHIELD BUILDING VENTILATION SYSTEM RELEASE
13. CONTROLLED VENTILATION AREA SYSTEM RELEASE

FLORIDA POWER & LIGHT COMPANY
ST. LUCIE PLANT UNIT 2

CONTAINMENT LEAKAGE DOSE MODEL

FIGURE 15.6.5-78

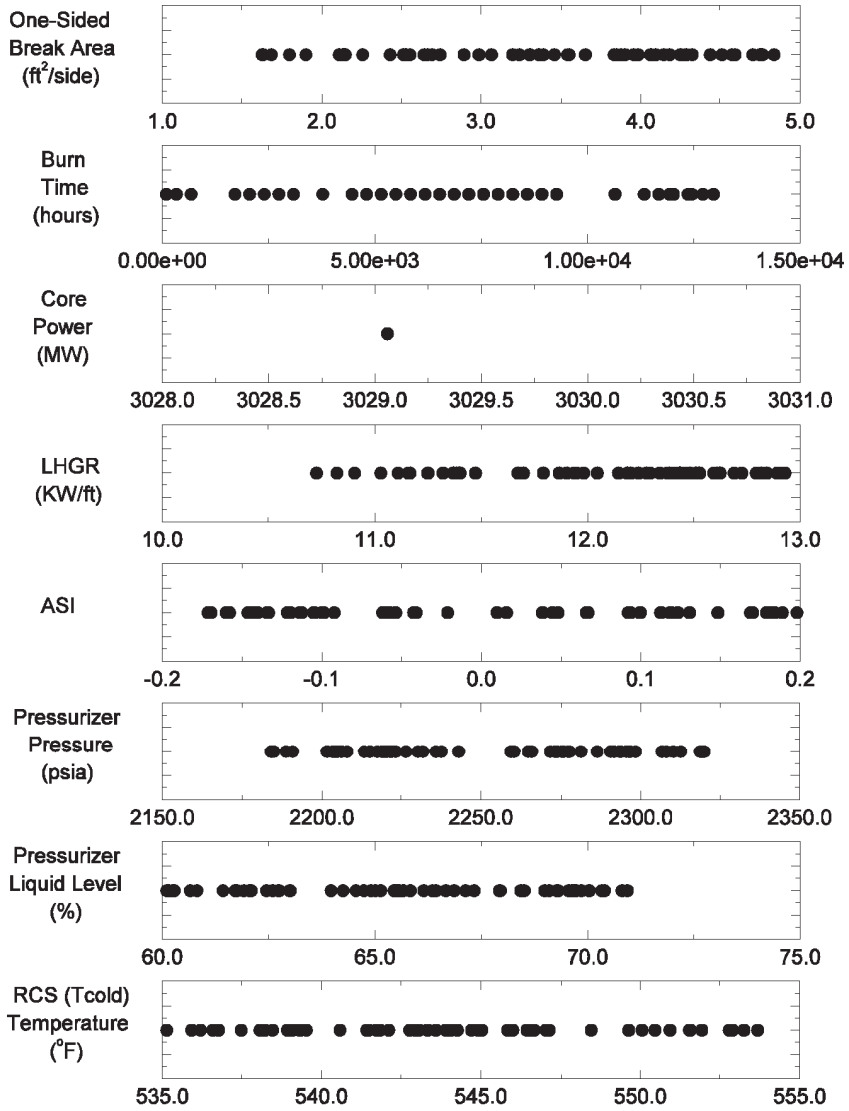

EC287528

FLORIDA POWER & LIGHT COMPANY
ST. LUCIE PLANT UNIT 2

Figure 15.6.5-79
Scatter Plot of Operational Parameters

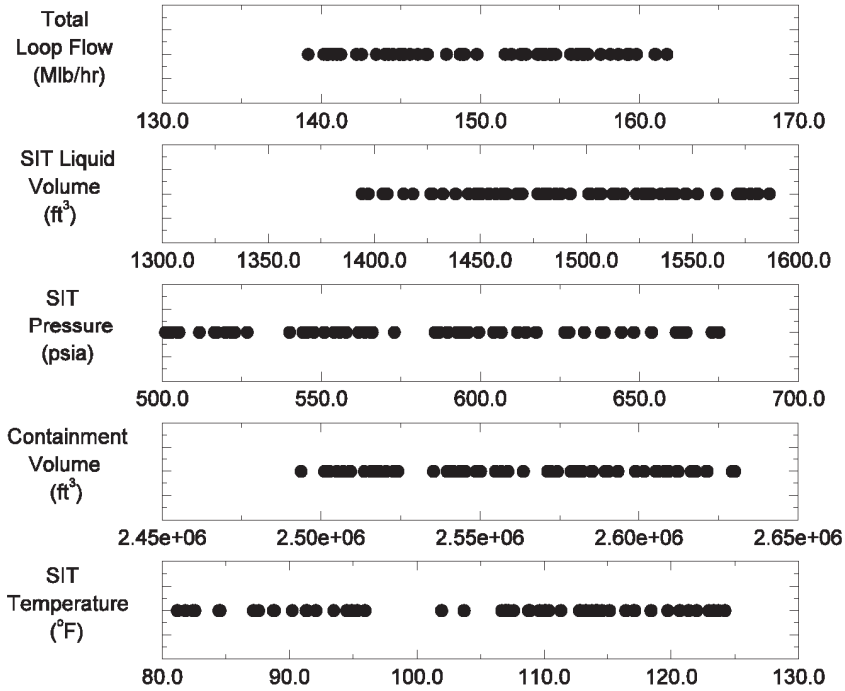

EC287528

FLORIDA POWER & LIGHT COMPANY
ST. LUCIE PLANT UNIT 2

Figure 15.6.5-79
Scatter Plot of Operational Parameters
(Continued)

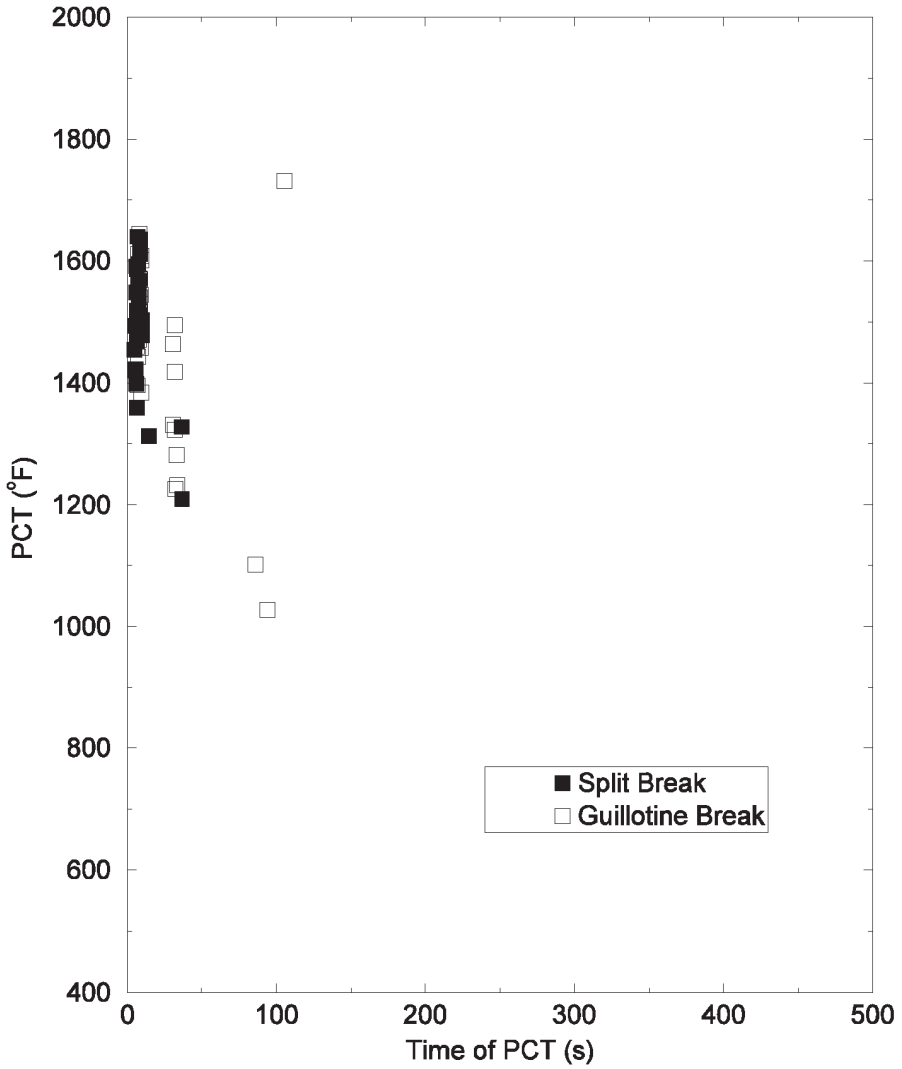

EC287528

FLORIDA POWER & LIGHT COMPANY
ST. LUCIE PLANT UNIT 2

Figure 15.6.5-80
PCT versus PCT Time Scatter Plot
from 59 Calculations

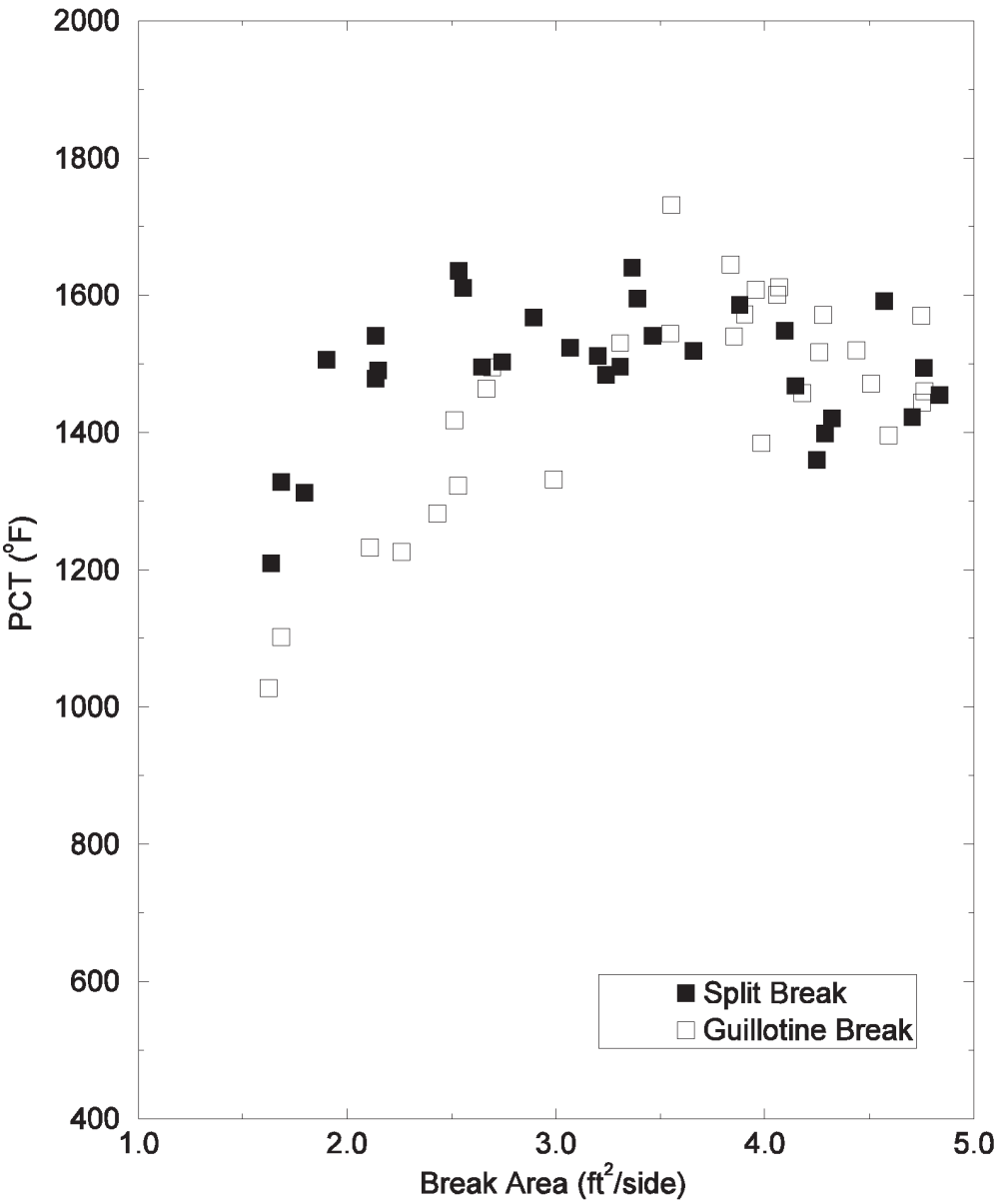

EC287528

FLORIDA POWER & LIGHT COMPANY
ST. LUCIE PLANT UNIT 2

Figure 15.6.5-81
PCT versus Break Size Scatter Plot
from 59 Calculations

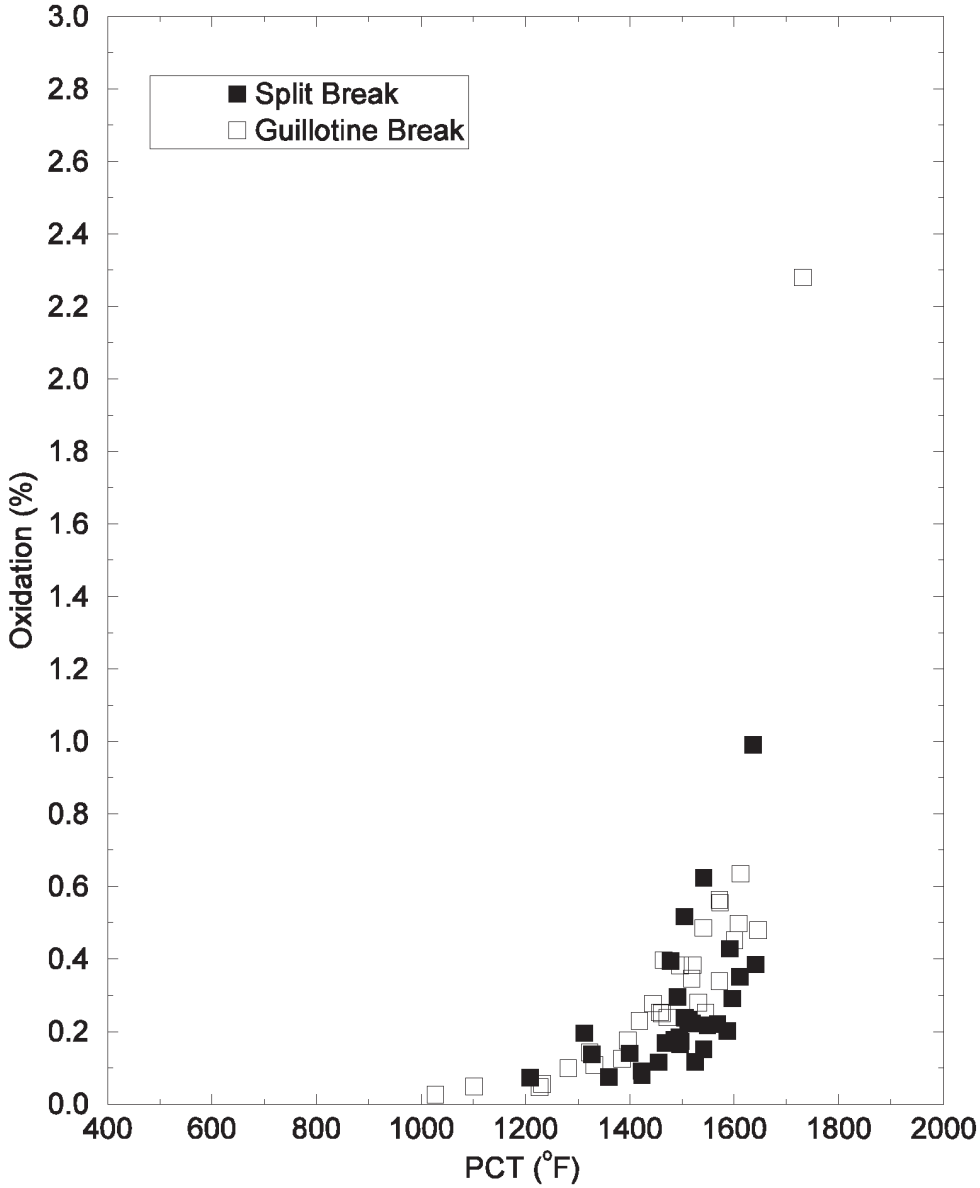

EC287528

FLORIDA POWER & LIGHT COMPANY
ST. LUCIE PLANT UNIT 2

Figure 15.6.5-82
Maximum Oxidation versus PCT Scatter Plot
from 59 Calculations

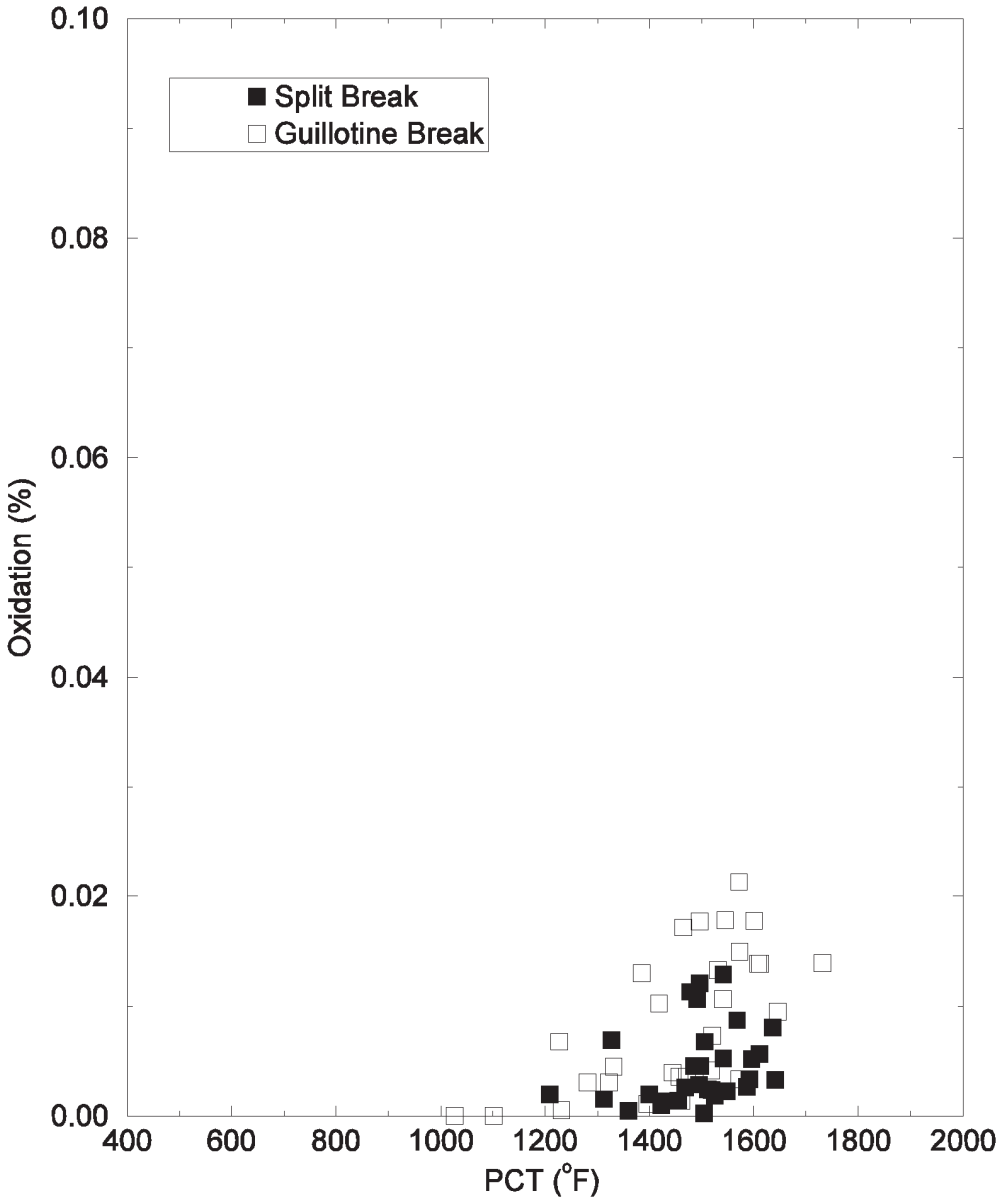

EC287528

FLORIDA POWER & LIGHT COMPANY
ST. LUCIE PLANT UNIT 2

Figure 15.6.5-83
Total Oxidation versus PCT Scatter Plot
from 59 Calculations

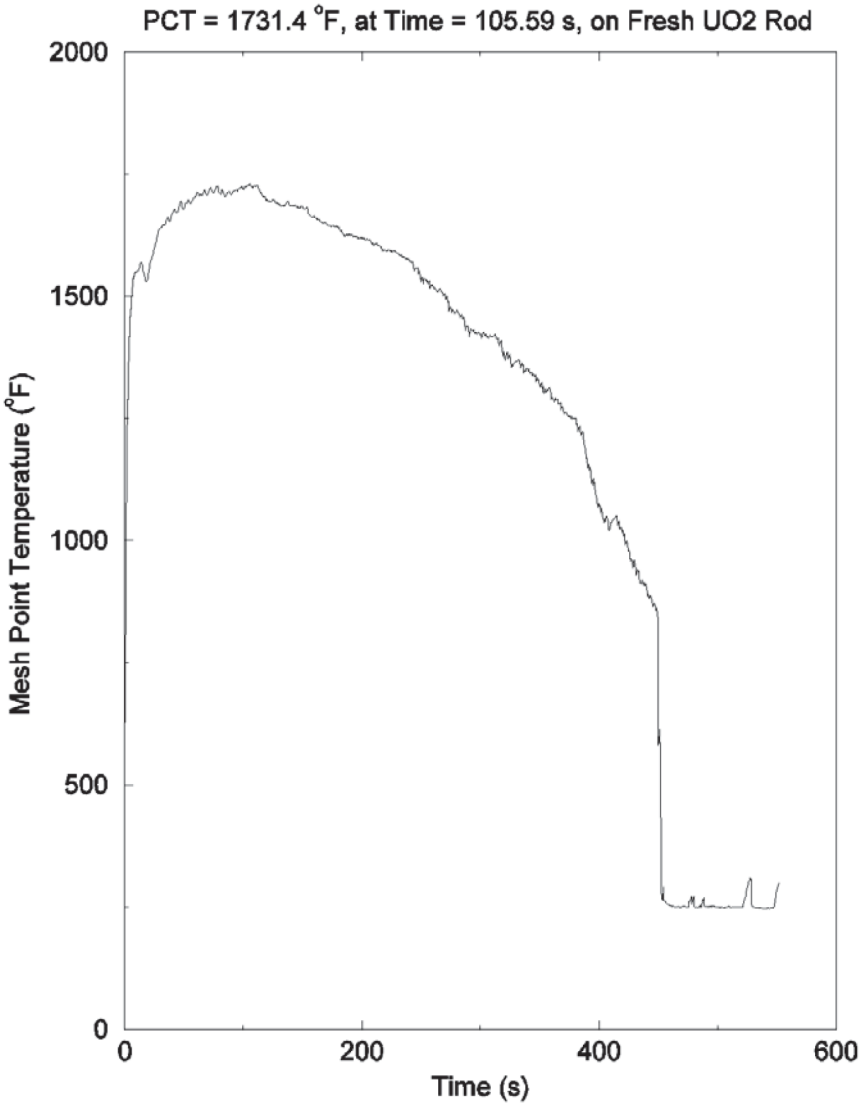

EC287528

FLORIDA POWER & LIGHT COMPANY
ST. LUCIE PLANT UNIT 2

Figure 15.6.5-84
Peak Cladding Temperature (Independent of Elevation) for the Limiting Case

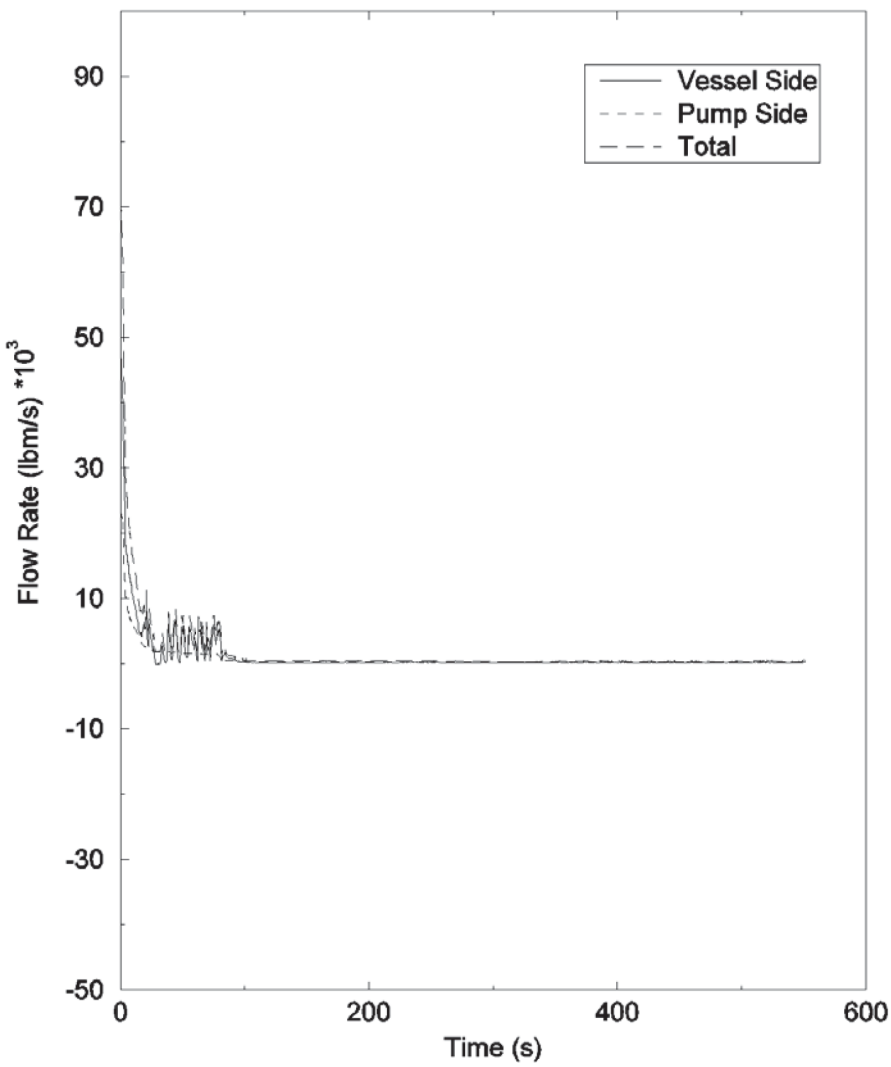

EC287528

FLORIDA POWER & LIGHT COMPANY
ST. LUCIE PLANT UNIT 2

Figure 15.6.5-85
Break Flow for the Limiting Case

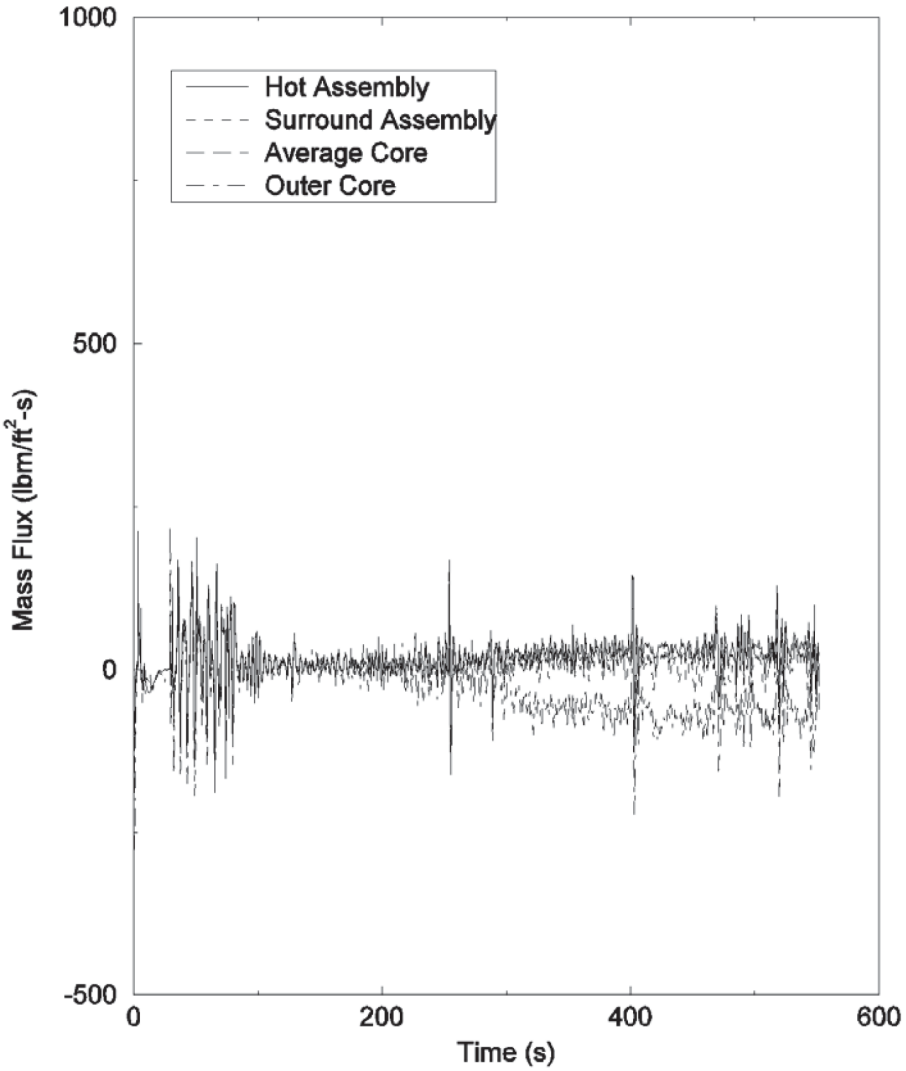

EC287528

FLORIDA POWER & LIGHT COMPANY
ST. LUCIE PLANT UNIT 2

Figure 15.6.5-86
Core Inlet Mass Flux for the Limiting Case

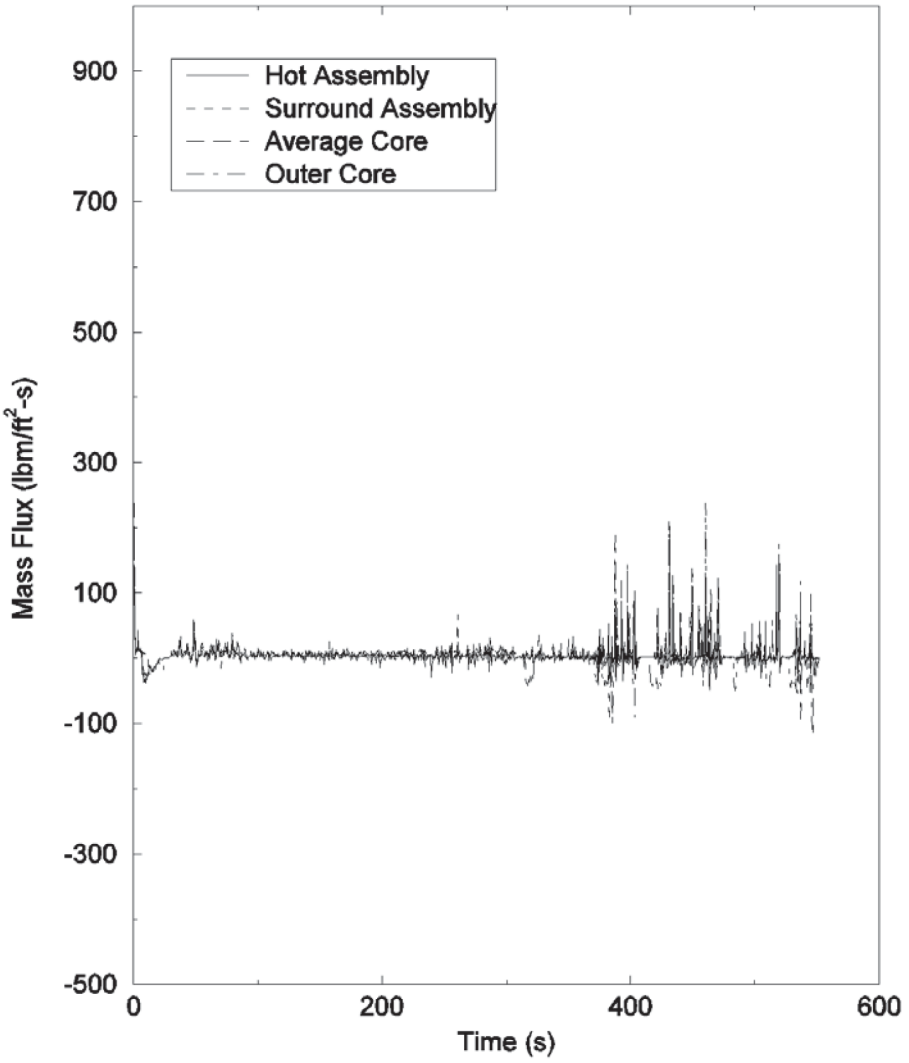

EC287528

FLORIDA POWER & LIGHT COMPANY
ST. LUCIE PLANT UNIT 2

Figure 15.6.5-87
Core Outlet Mass Flux for the Limiting Case

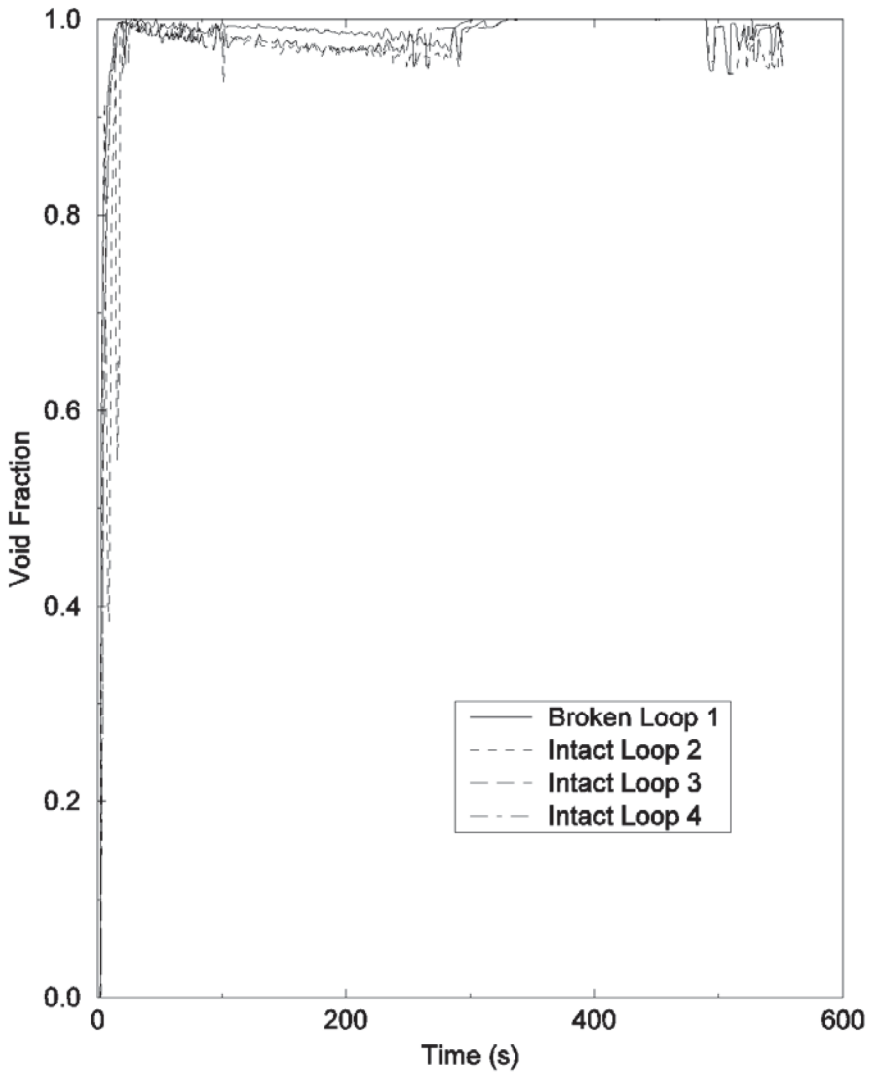

EC287528

FLORIDA POWER & LIGHT COMPANY
ST. LUCIE PLANT UNIT 2

Figure 15.6.5-88
Void Fraction at RCS Pumps
for the Limiting Case

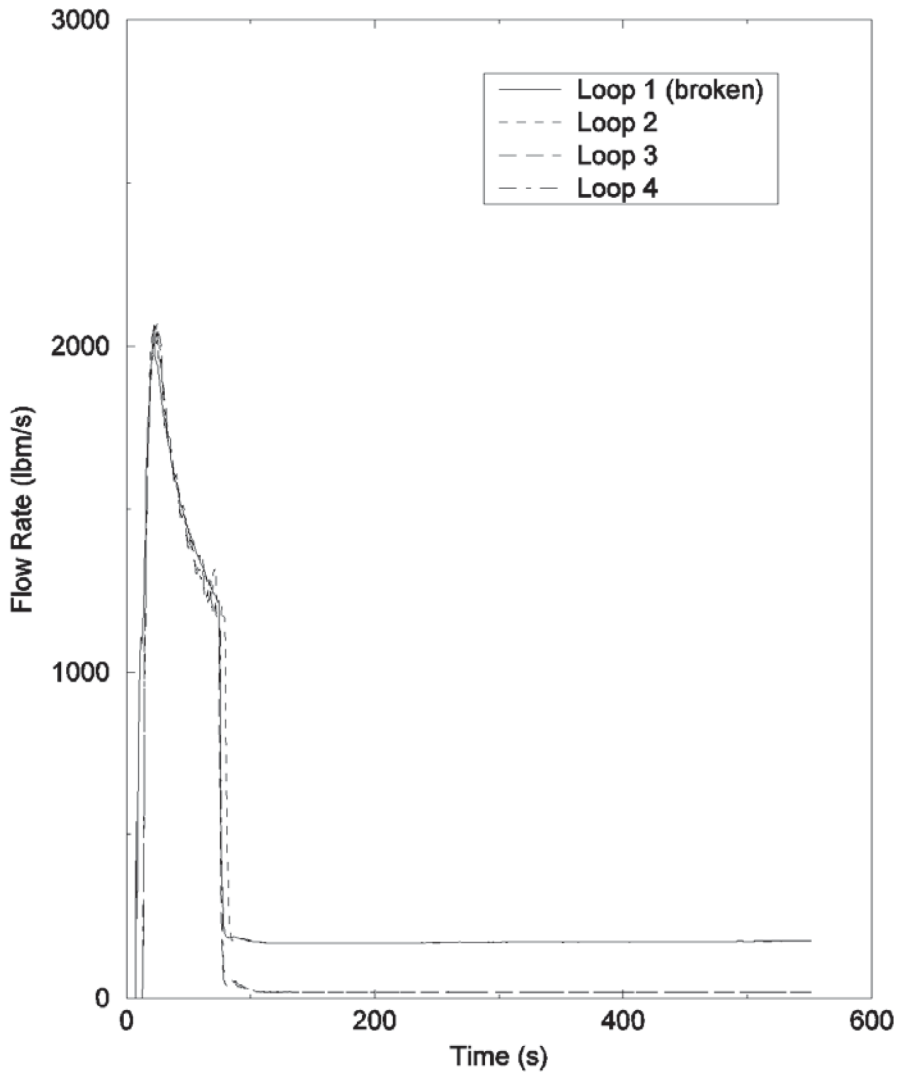

EC287528

FLORIDA POWER & LIGHT COMPANY
ST. LUCIE PLANT UNIT 2

Figure 15.6.5-89
ECCS Flows (Includes SIT, LPSI and HPSI)
for the Limiting Case

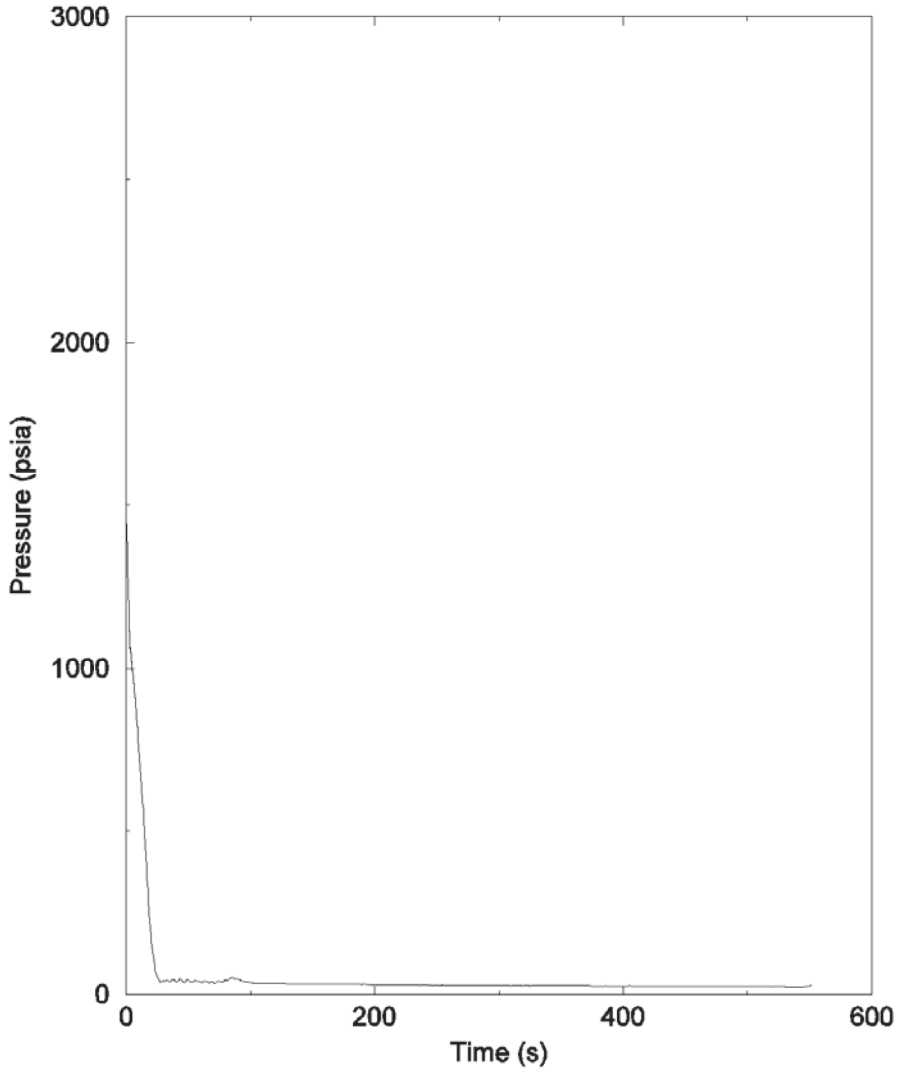

EC287528

FLORIDA POWER & LIGHT COMPANY
ST. LUCIE PLANT UNIT 2

Figure 15.6.5-90
Upper Plenum Pressure for the Limiting Case

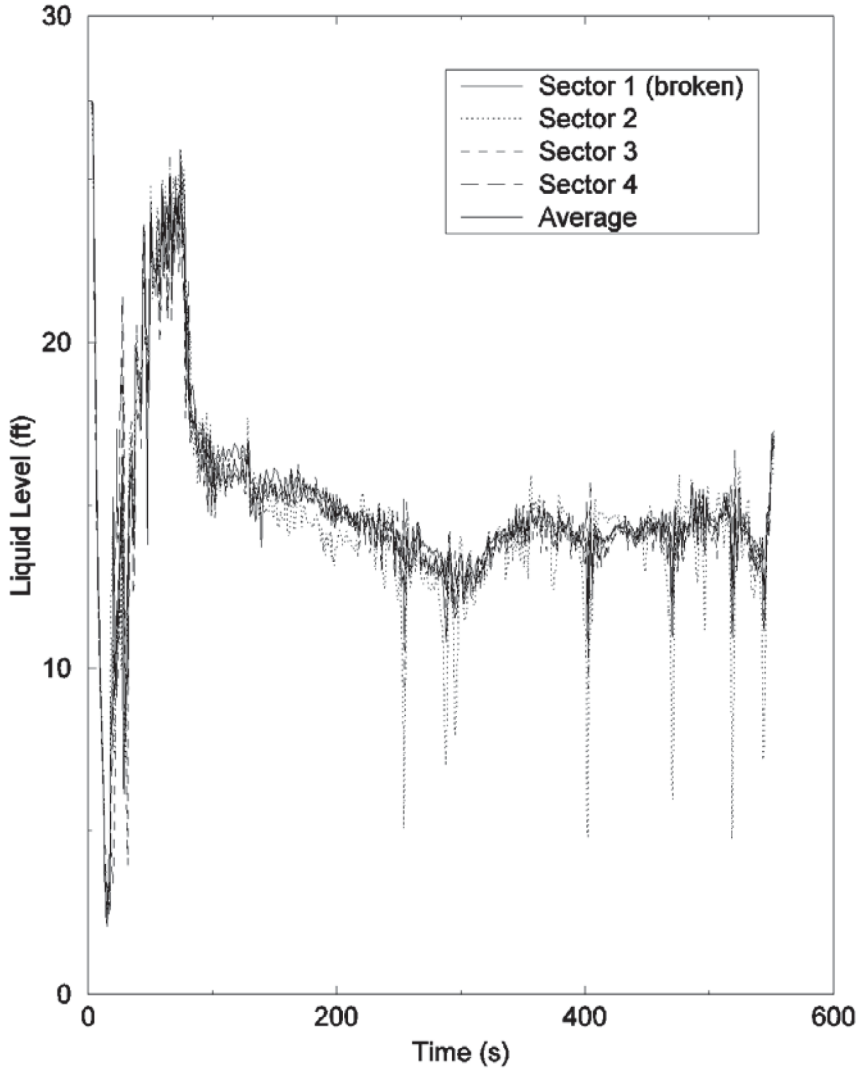

EC287528

FLORIDA POWER & LIGHT COMPANY
ST. LUCIE PLANT UNIT 2

Figure 15.6.5-91
Collapsed Liquid Level in the Downcomer for the Limiting Case

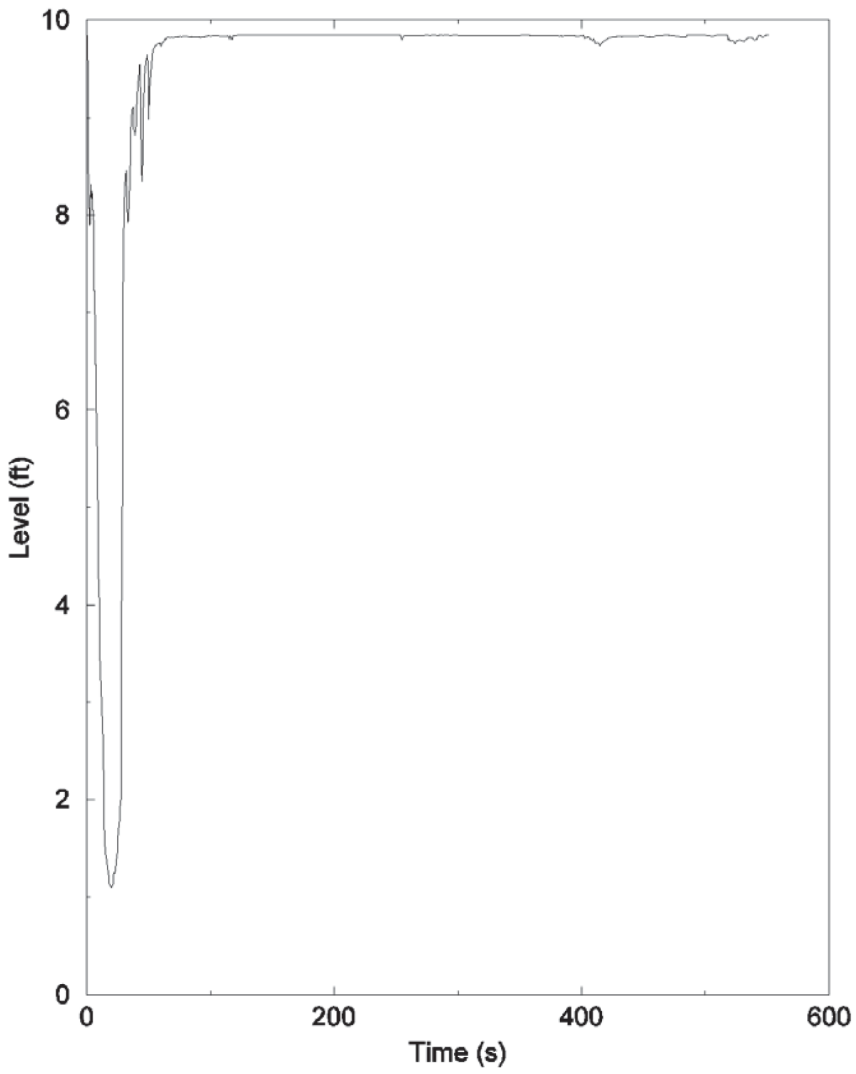

EC287528

FLORIDA POWER & LIGHT COMPANY
ST. LUCIE PLANT UNIT 2

Figure 15.6.5-92
Collapsed Liquid Level in the Lower Plenum for the Limiting Case

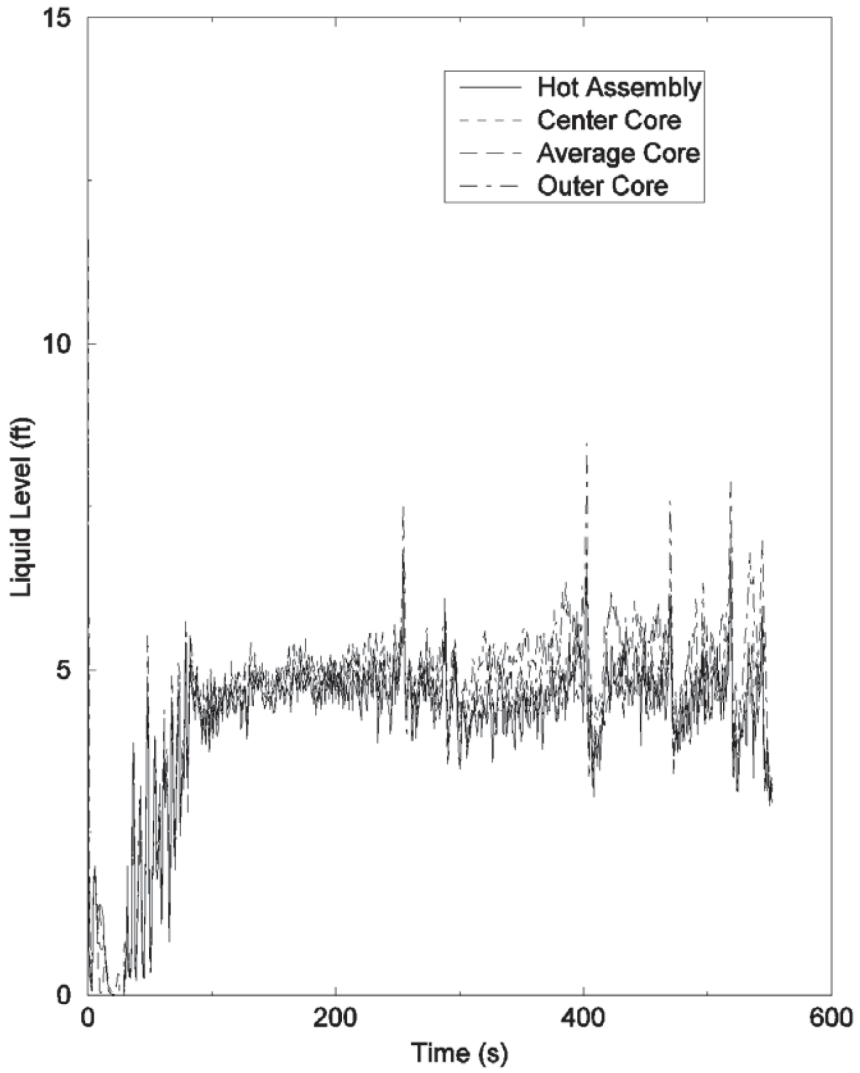

EC287528

FLORIDA POWER & LIGHT COMPANY
ST. LUCIE PLANT UNIT 2

Figure 15.6.5-93
Collapsed Liquid Level in the Core
for the Limiting Case

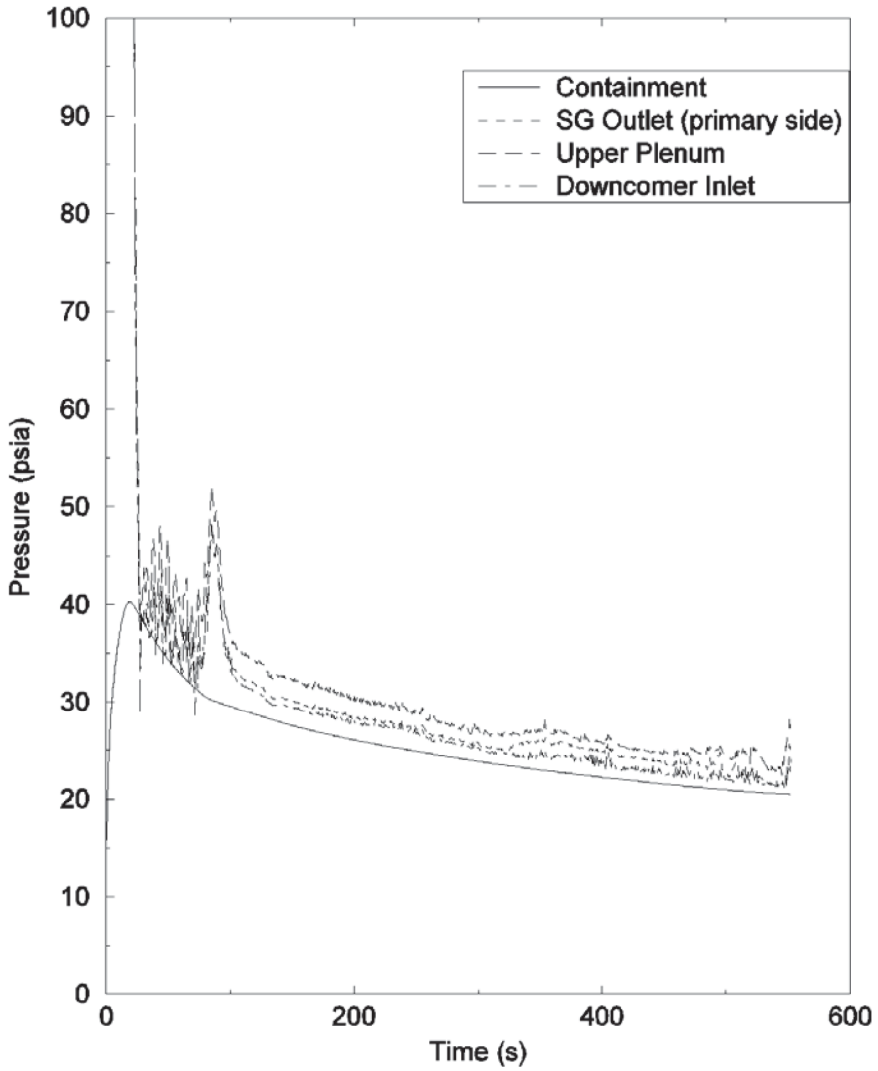

EC287528

FLORIDA POWER & LIGHT COMPANY
ST. LUCIE PLANT UNIT 2

Figure 15.6.5-94
Containment and Loop Pressures
for the Limiting Case

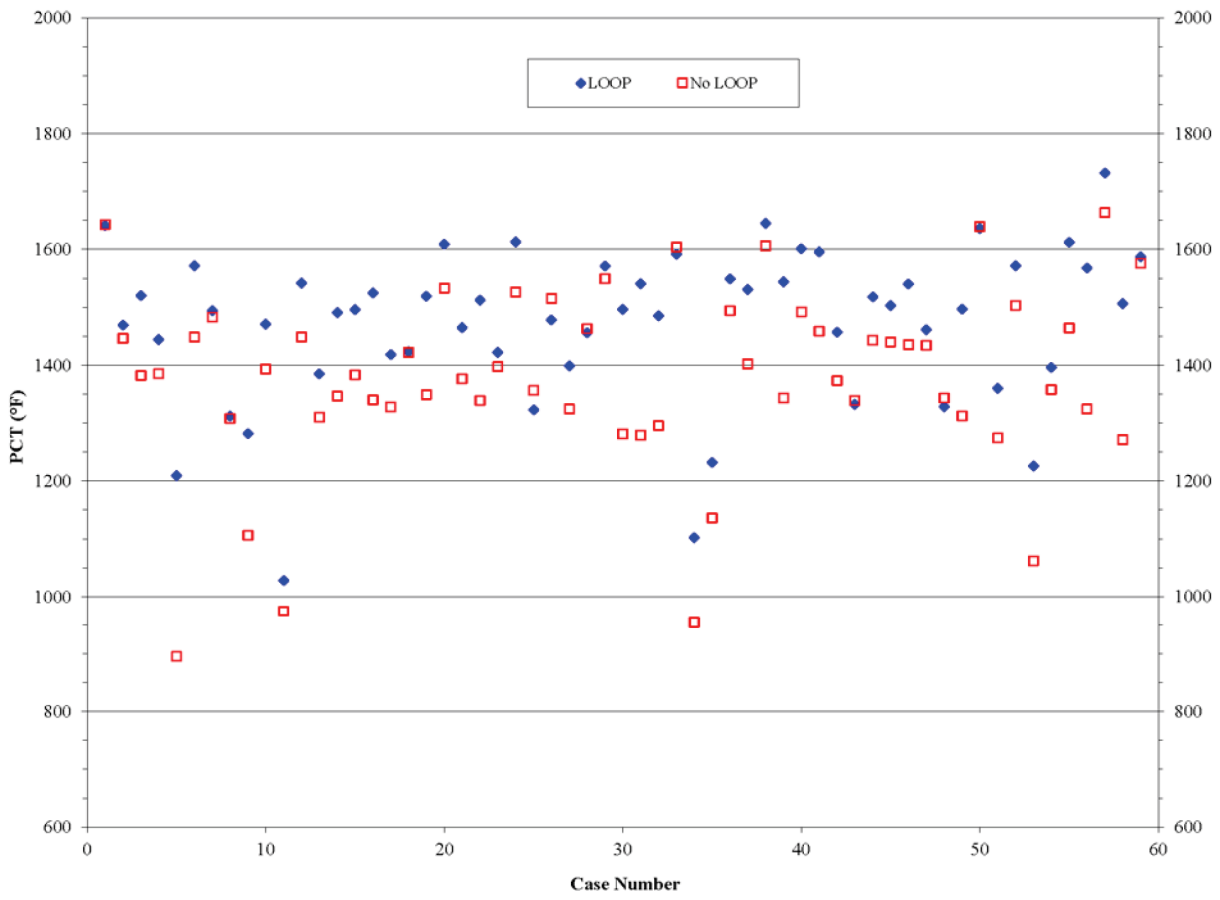

EC287528

FLORIDA POWER & LIGHT COMPANY
ST. LUCIE PLANT UNIT 2

Figure 15.6.5-95
GDC 35 LOOP versus No-LOOP Cases

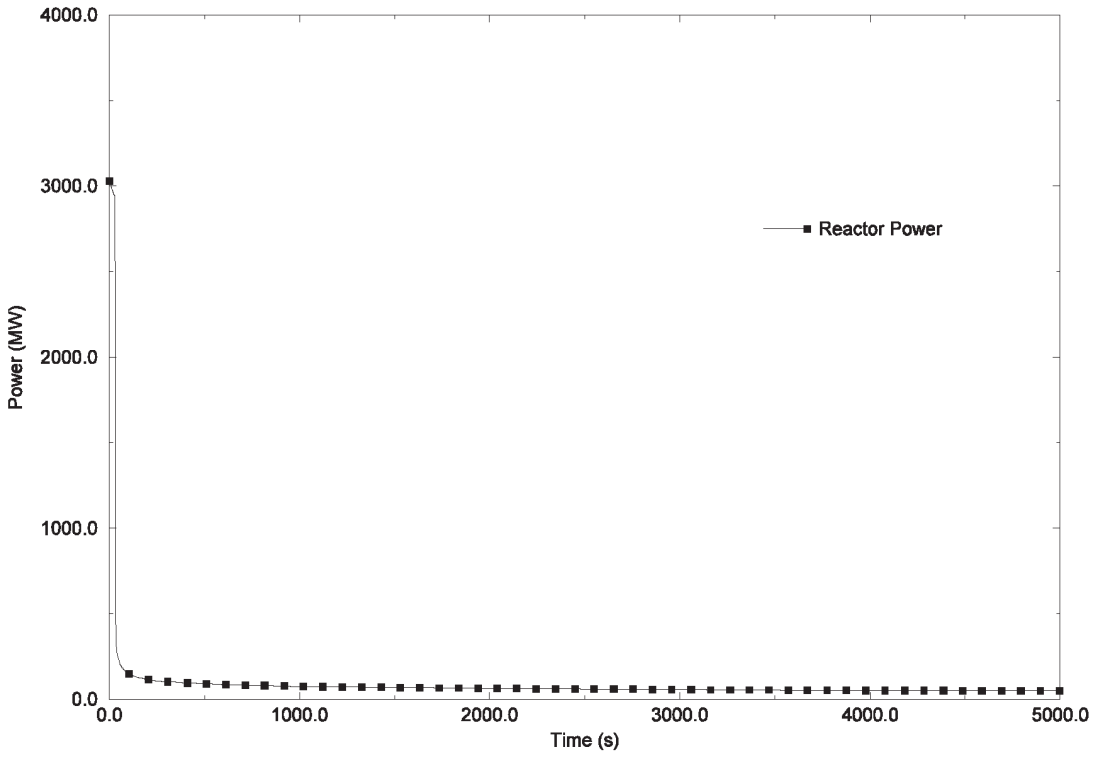

EC287528

FLORIDA POWER & LIGHT COMPANY
ST. LUCIE PLANT UNIT 2

Figure 15.6.5-96
Reactor Power - 2.70 inch Break

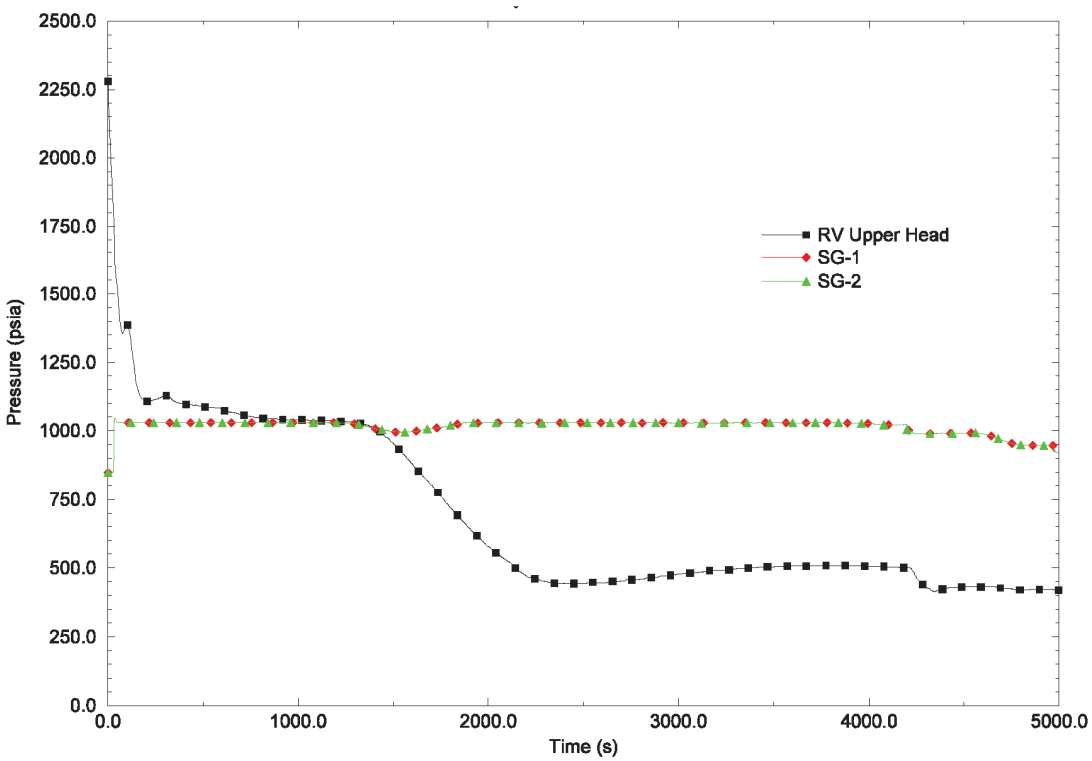

EC287528

FLORIDA POWER & LIGHT COMPANY
ST. LUCIE PLANT UNIT 2

Figure 15.6.5-97
Primary and Secondary System
Pressures - 2.70 inch Break

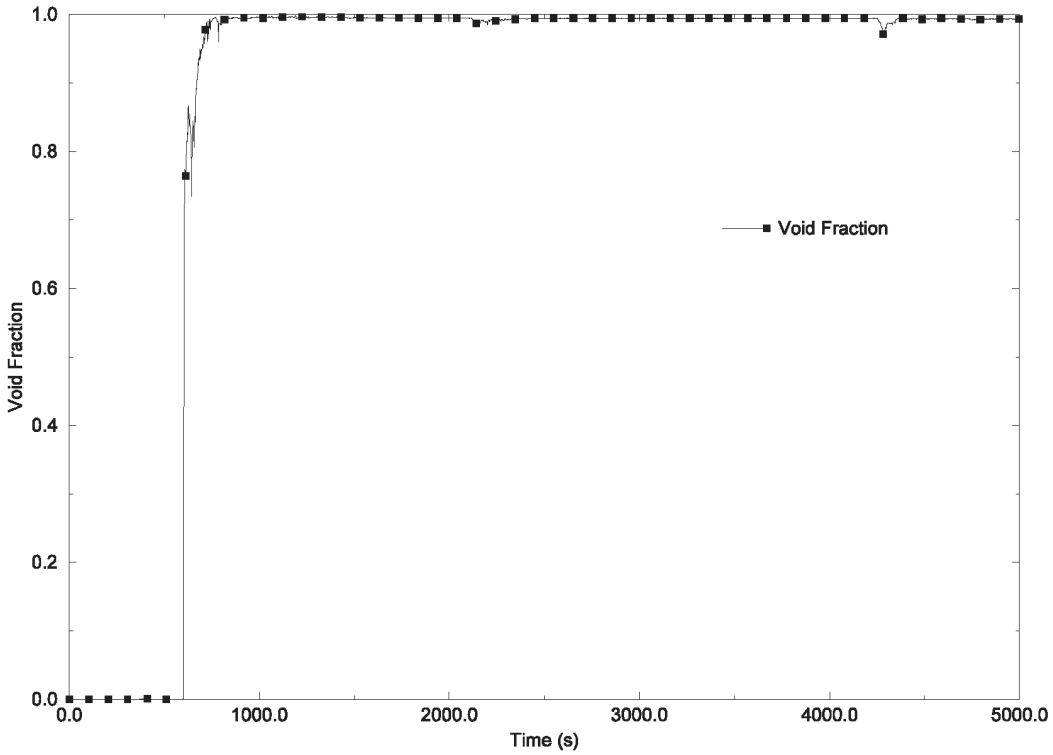

EC287528

FLORIDA POWER & LIGHT COMPANY
ST. LUCIE PLANT UNIT 2

Figure 15.6.5-98
Break Void Fraction - 2.70 inch Break

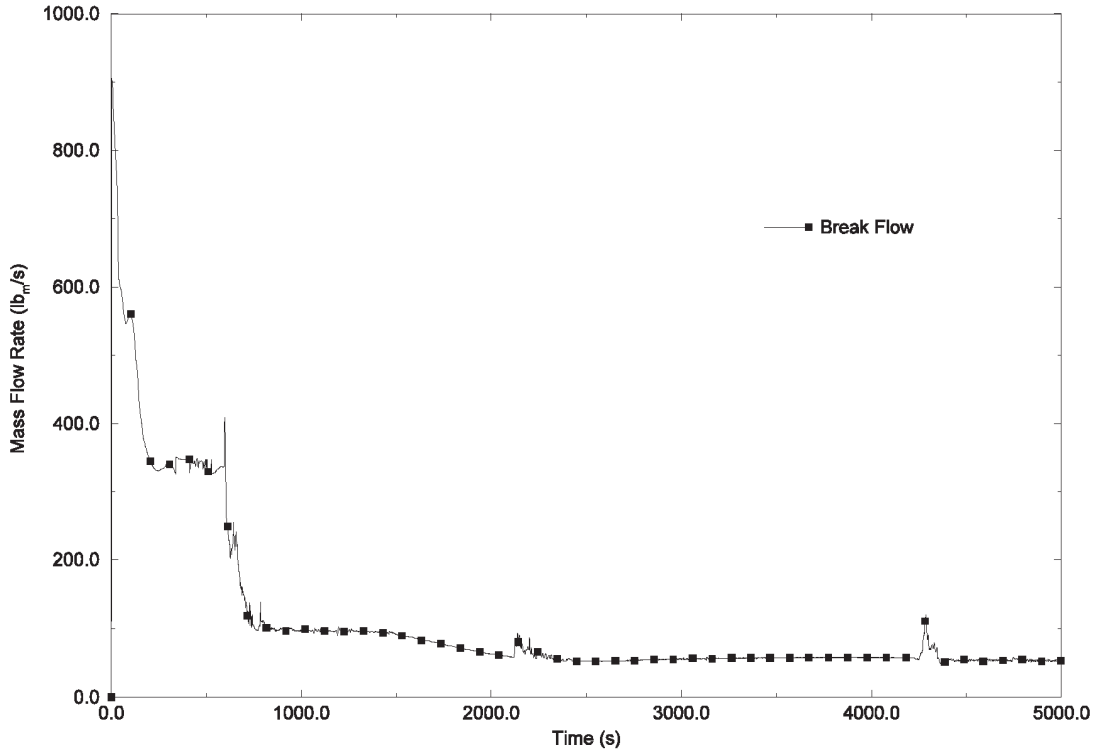

EC287528

FLORIDA POWER & LIGHT COMPANY
ST. LUCIE PLANT UNIT 2

Figure 15.6.5-99
Break Mass Flow Rate - 2.70 inch Break

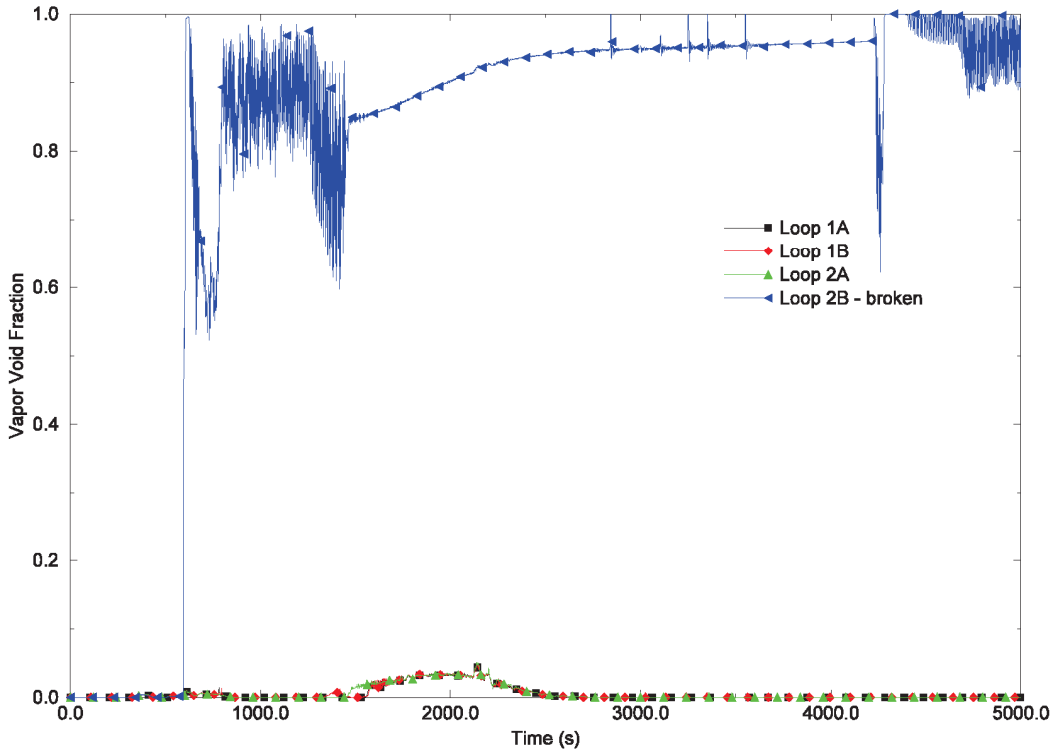

EC287528

FLORIDA POWER & LIGHT COMPANY
ST. LUCIE PLANT UNIT 2

Figure 15.6.5-100
Loop Seal Void Fraction - 2.70 inch Break

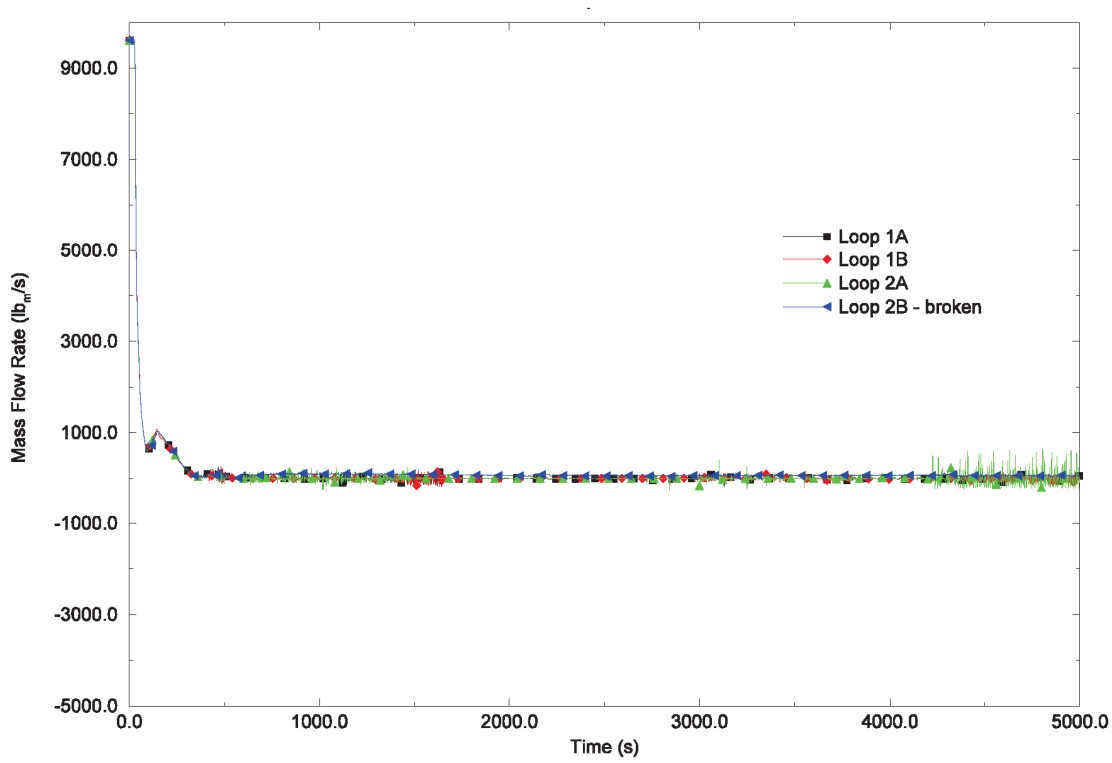

EC287528

FLORIDA POWER & LIGHT COMPANY
ST. LUCIE PLANT UNIT 2

Figure 15.6.5-101
RCS Loop Mass Flow Rate - 2.70 inch Break

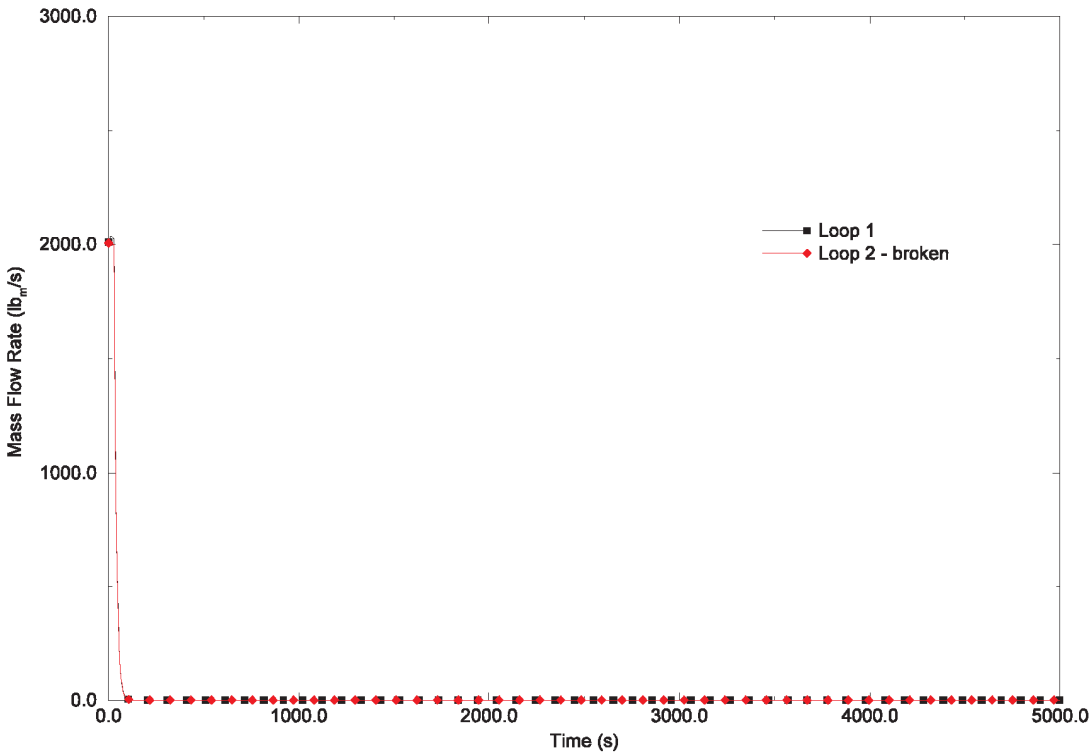

EC287528

FLORIDA POWER & LIGHT COMPANY
ST. LUCIE PLANT UNIT 2

Figure 15.6.5-102
Main Feedwater Mass Flow
Rate - 2.70 inch Break

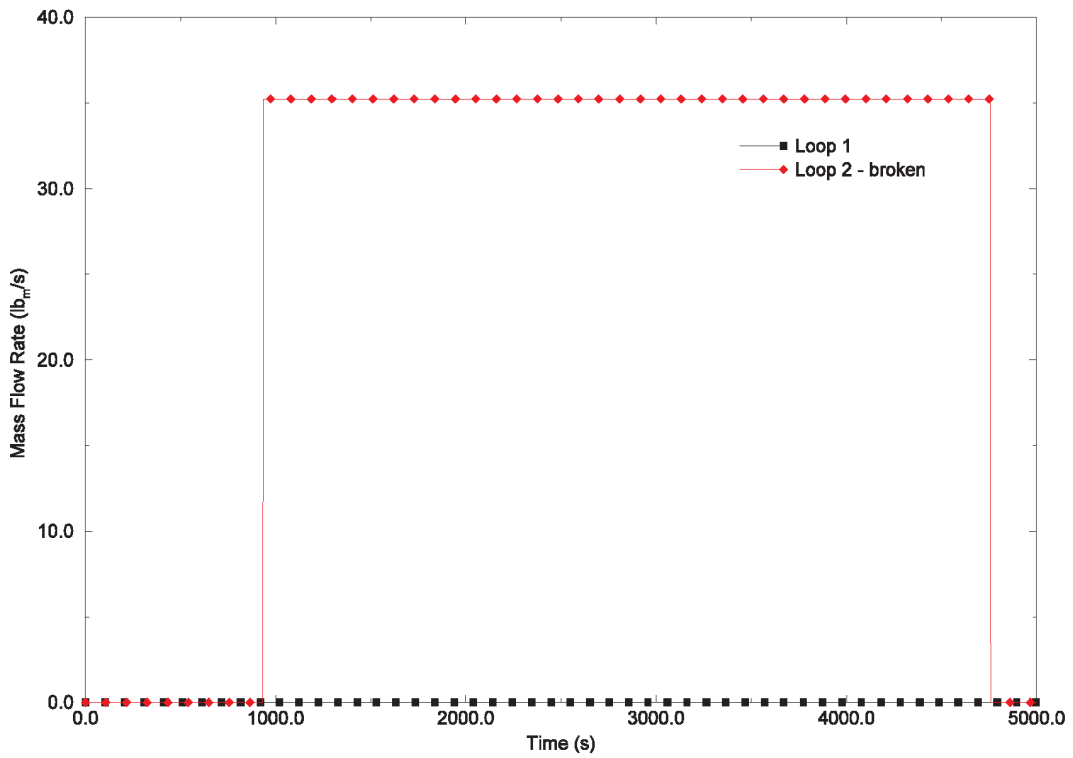

EC287528

FLORIDA POWER & LIGHT COMPANY
ST. LUCIE PLANT UNIT 2

Figure 15.6.5-103
Auxiliary Feedwater Mass Flow
Rate - 2.70 inch Break

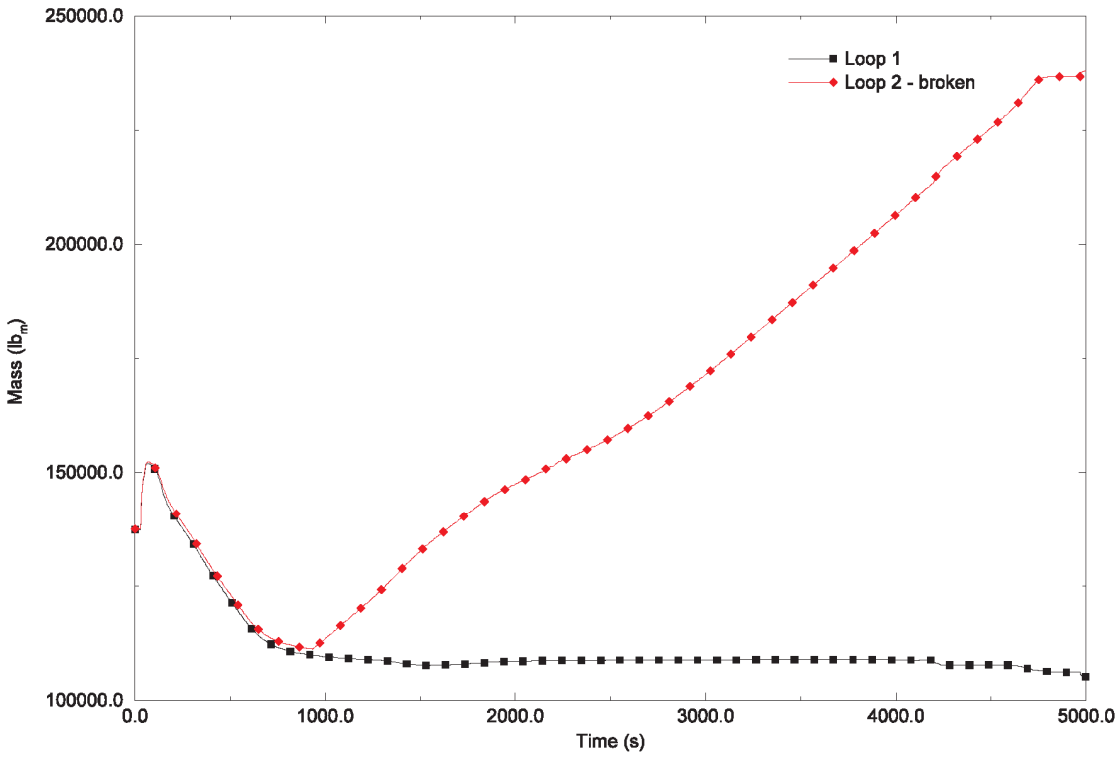

EC287528

FLORIDA POWER & LIGHT COMPANY
ST. LUCIE PLANT UNIT 2

Figure 15.6.5-104
Steam Generator Total
Mass - 2.70 inch Break

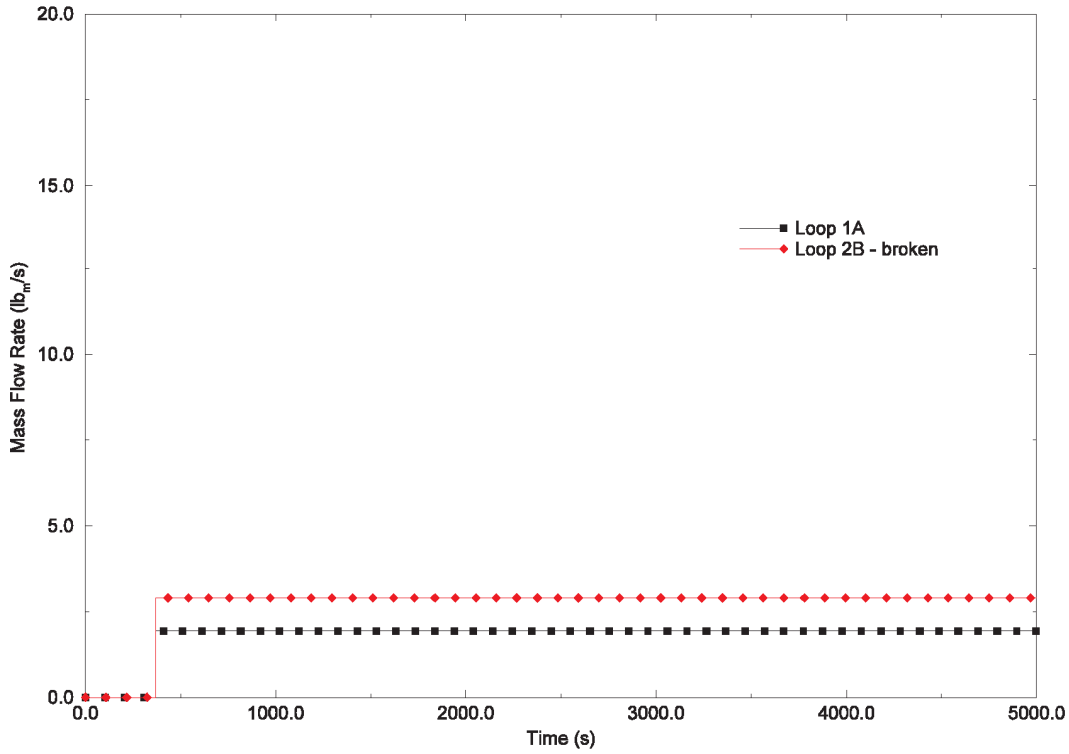

EC287528

FLORIDA POWER & LIGHT COMPANY
ST. LUCIE PLANT UNIT 2

Figure 15.6.5-105
Charging System Mass Flow
Rates - 2.70 inch Break

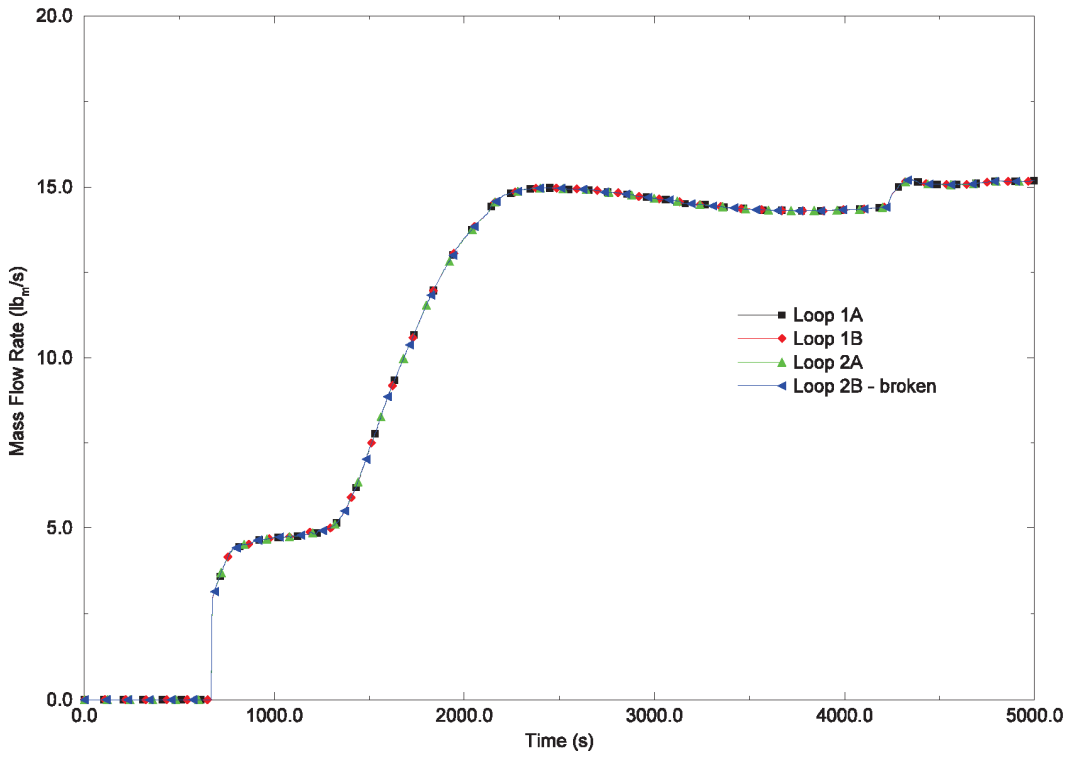

EC287528

FLORIDA POWER & LIGHT COMPANY
ST. LUCIE PLANT UNIT 2

Figure 15.6.5-106
High Pressure Safety Injection Mass Flow Rates - 2.70 inch Break

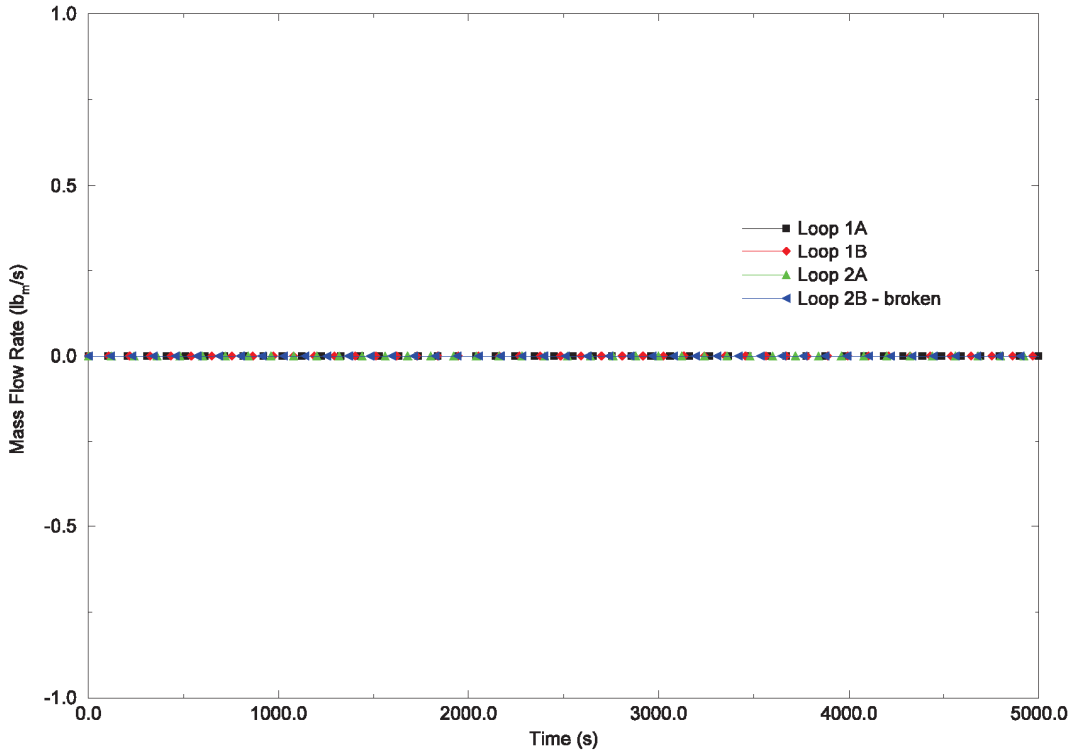

EC287528

FLORIDA POWER & LIGHT COMPANY
ST. LUCIE PLANT UNIT 2

Figure 15.6.5-107
Low Pressure Safety Injection Mass Flow Rates - 2.70 inch Break

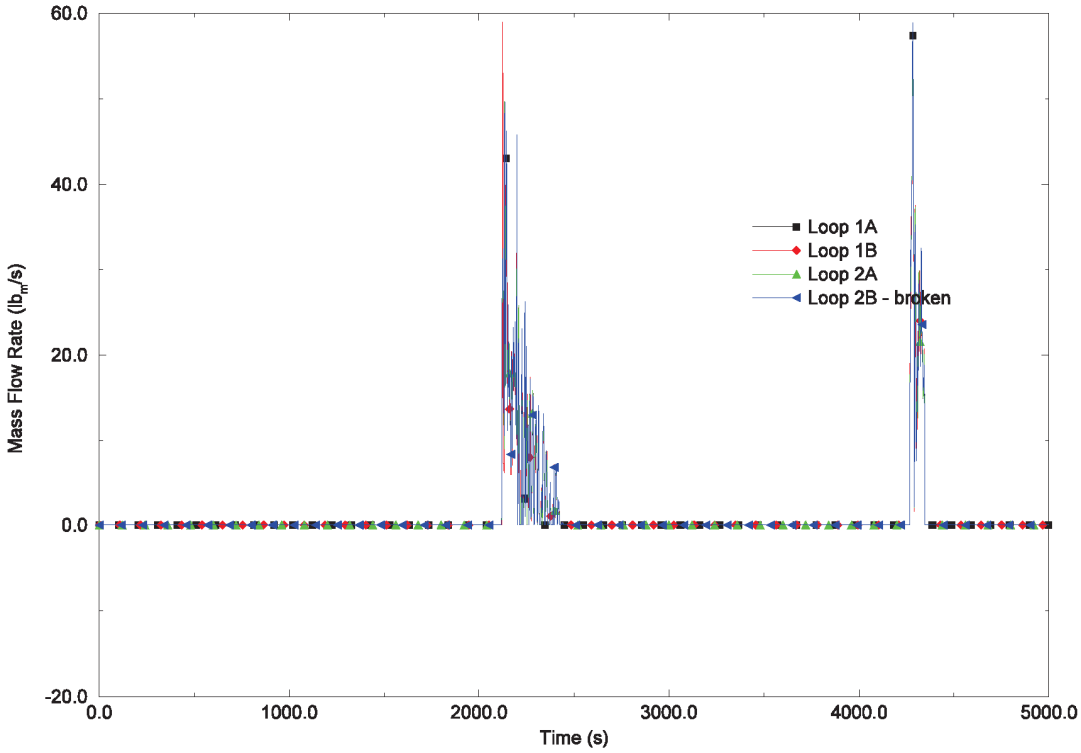

EC287528

FLORIDA POWER & LIGHT COMPANY
ST. LUCIE PLANT UNIT 2

Figure 15.6.5-108
Safety Injection Tank Mass Flow
Rates - 2.70 inch Break

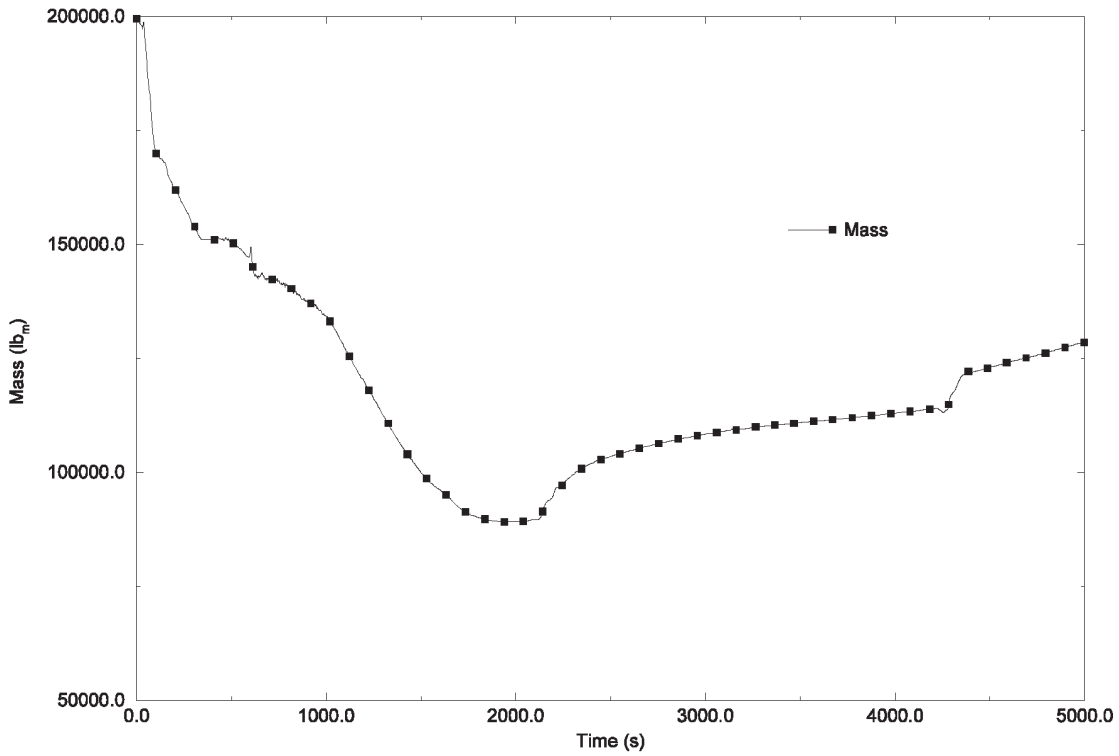

EC287528

FLORIDA POWER & LIGHT COMPANY
ST. LUCIE PLANT UNIT 2

Figure 15.6.5-109
Reactor Vessel Mass
Inventory - 2.70 inch Break

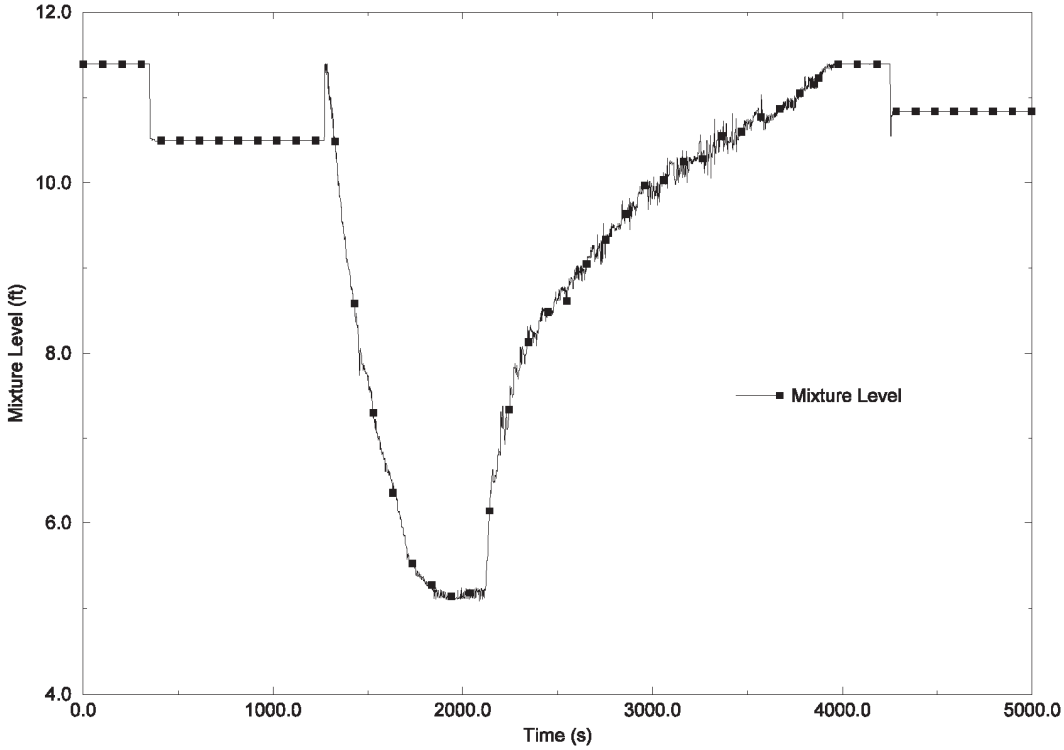

EC287528

FLORIDA POWER & LIGHT COMPANY
ST. LUCIE PLANT UNIT 2

Figure 15.6.5-110
Hot Assembly Mixture
Level - 2.70 inch Break

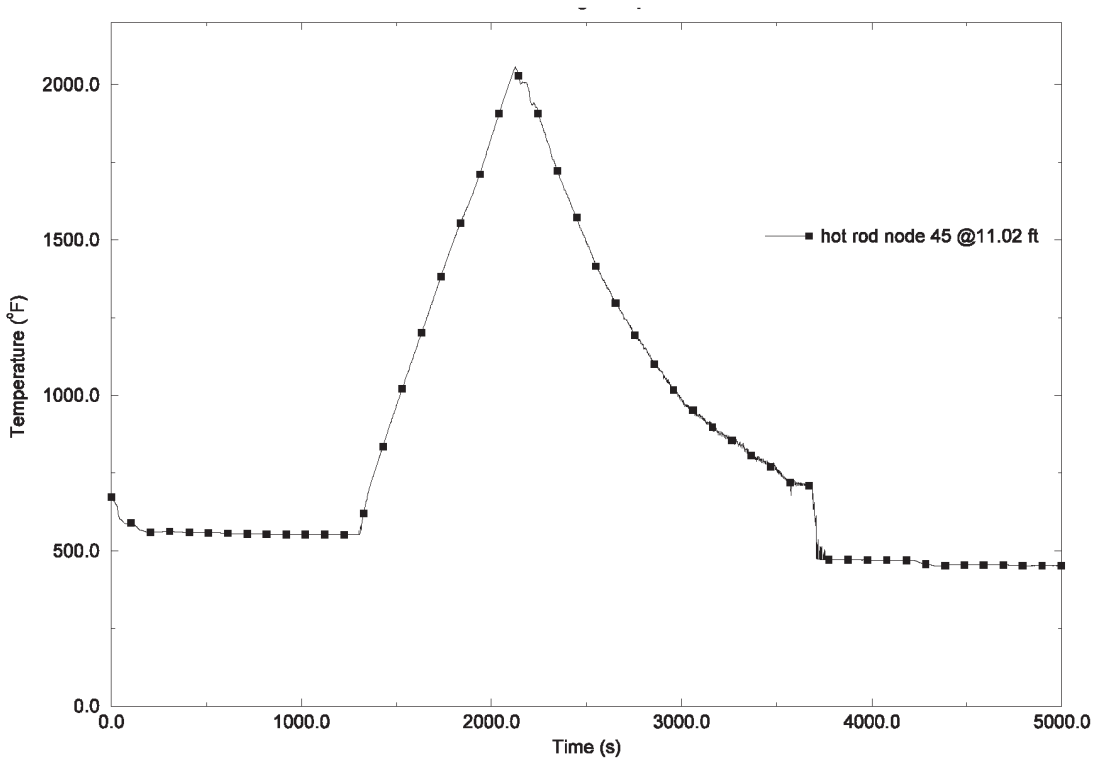

EC287528

FLORIDA POWER & LIGHT COMPANY
ST. LUCIE PLANT UNIT 2

Figure 15.6.5-111
Hot Spot Cladding
Temperature - 2.70 inch Break

15.7 RADIOACTIVE RELEASES FROM A SUBSYSTEM OR COMPONENT

15.7.1 MODERATE FREQUENCY EVENTS

There is no event group in Table 15.0-2 which results in radioactive releases from a subsystem or component and which has an estimated frequency of occurrence which would classify it as a Moderate Frequency event.

15.7.2 INFREQUENT EVENTS

There is no event group in Table 15.0-2 which results in radioactive releases from a subsystem or component and which has an estimated frequency of occurrence which would classify it as an Infrequent Event.

15.7.3 LIMITING FAULT-I EVENTS

15.7.3.1 Limiting Offsite Dose - Radioactive Liquid Waste System Leak or Failure

15.7.3.1.1 Identification of Event and Causes

As discussed in Subsection 2.4.13.3, any type of liquid discharge introduced into the ground at the reactor site would reach the Indian River, where it would be greatly diluted. Because of the proximity and width of the Indian River and the artesian head in the Floridian Aquifer, there is no possibility of contaminating any groundwater withdrawal. Therefore, the failure of a liquid waste holdup tank will not result in radionuclide concentrations in excess of the limits in 10 CFR 20, Appendix B, Table 2, column 2, in the Indian River.

Historical Information

The event groups evaluated and the significance of the exclusion area boundary dose for each event are indicated in Table 15.7.3-1. All of the events indicated as insignificant (I) produce offsite doses well within the acceptance guidelines in Table 15.0-4.

Although liquid waste management tanks are constructed according to strict engineering codes and standards, and are operated at atmospheric pressures and low temperatures, in order to analyze a bounding case, a complete failure of all nonsafety and nonseismic Category I equipment in the Liquid Waste Management System (including boron recovery portion) is assumed.

Such a bounding case as a complete failure of all nonsafety and nonseismic Category I equipment in the Liquid Waste Management System can only be caused by a safe shutdown earthquake. The frequency of an occurrence of a safe shutdown earthquake is less than 10^{-6} per year and as such would cause this event to fall outside the bounds of the categorization vs acceptance guideline scheme in Table 15.0-4. However, the bounding failure case is presented herein.

15.7.3.1.2 Sequence of Events and System Operation

The nonsafety and nonseismic Category I components in the Liquid Waste Management System (including boron recovery portion) are assumed to fail with this bounding case, releasing

their contents in the Reactor Auxiliary Building (RAB). The operator upon receiving the alarms, alerts personnel to evacuate affected areas of the RAB.

15.7.3.1.3 Analysis of Effects and Consequences

A. Mathematical Models

The analysis is based on Standard Review Plan 15.7.2. The models used for evaluation of the radiological doses, are described below.

The thyroid and whole body doses are calculated using the following equations:

Thyroid Dose = $B(\chi/Q)(TDCF)Q$

Whole Body Dose = $(WDCF)(Q)(\chi/Q)$

Where:

Q = Total activity released to the environs [Ci]

χ/Q = Atmospheric Dispersion Factor [sec/m^3]

B = Breathing Rate [m^3/sec]

TDCF = Thyroid Dose Conversion Factor [rem/Ci-inhaled] (See Table 15.7.3.1-4)

WDCF = Whole Body Dose Conversion Factor [rem/Ci-inhaled] (See Table 15.7.3.1-4)

The dose calculation models given above are applicable in the evaluation of exposure in cases involving the instantaneous “puff” release of activity.

The external whole body gamma dose is calculated using semi-infinite cloud assumptions, i.e., the dimensions of the cloud are assumed to be large compared to the distance that the gamma rays travel.

B. Input Parameters and Initial Conditions

It is assumed that the components contain radioactive inventories based on one percent failed fuel as included in Section 12.2. The spilled liquids are contained within the building. The only resultant offsite doses will occur as a consequence of released noble gases and iodines assumed to volatilize from the spilled liquids.

The specific values of parameters used in the analysis are presented in Table 15.7.3.1-1. The assumptions and parameters acceptable for a realistic analysis are also included in Table 15.7.3.1-1 for comparison purposes.

C. Results

The radioactivity released to the environment is presented in Table 15.7.3.1-2. The offsite dose produced is no more than a 0.18 rem two hour inhalation thyroid dose at the exclusion area boundary. The two hour and entire event doses for both thyroid and whole body are shown in Table 15.7.3.1-3.

15.7.3.1.4 Conclusions

This evaluation shows that the plant response to a complete failure of all nonsafety and nonseismic Category I equipment in the Liquid Waste Management System (including boron recovery portion) results in a maximum offsite dose which is well within the acceptance guidelines for the Limiting Fault-1 events in Table 15.0-4.

15.7.3.2 Limiting Reactor Coolant System Pressure Event

None of the Limiting Fault-1 events resulting in a radioactive release from a subsystem or component as shown in Table 15.7.3-1 have an effect on Reactor Coolant System pressure.

15.7.3.3 Limiting Fuel Performance Event

None of the Limiting Fault-1 events, resulting in a radioactive release from a subsystem or component as shown in Table 15.7.3-1 have an effect on fuel performance.

15.7.4 LIMITING FAULT-2 EVENTS

15.7.4.1 Limiting Offsite Dose

The event groups listed in Table 15.7.4-1 are analyzed and presented below. The event groups evaluated and the significance of the exclusion area boundary dose for each are indicated in Table 15.7.4-1. All of the events indicated as insignificant (1) produce offsite doses well within the acceptance guidelines in Table 15.0-4.

15.7.4.1.1 Waste Gas Tank Failure

15.7.4.1.1.1 Identification of Event and Causes

A release of the stored radioactive gases in the gas decay tanks in the Gaseous Waste Management System, described in Section 11.3, as a result of component failure or inadvertent venting is considered improbable. The waste gas decay tanks are not subjected to high pressures or unusual stresses. The radioactive gases stored in the decay tanks consist of fission gases, hydrogen and nitrogen. The nitrogen is added in the various collection and holdup tanks to preclude the possibility of obtaining a flammable mixture of hydrogen gas. Hence, the tank rupture as a result of ignition of hydrogen in the decay tank is remote. A failure probability is further reduced since the design, quality assurance, construction and testing criteria for the GWMS meet or exceed the guidelines of Regulatory Guide 1.143, "Design Guidance for Radioactive Waste Management Systems, Structures, and Components Installed in Light-Water Cooled Nuclear Power Plants," October 1979 (Rev 1), see Section 11.3.

However, the accidental release resulting from such events as failure of gas decay tank or associated piping is analyzed to define the upper limit of a gaseous release that could result from any malfunction in the Gaseous Waste Management System.

15.7.4.1.1.2 Sequence of Events and System Operation

The gas decay tank, which collects gases removed from the Reactor Coolant System is postulated to release its contents in an uncontrolled manner. The releases from the tank would be detected by the area radiation monitor in the area of the tanks. In the event of a high radiation level, an alarm sounds in the control room and personnel are evacuated from the affected area.

15.7.4.1.1.3 Radiological Analysis

15.7.4.1.1.3.1 Applicable Regulatory Guidance

This analysis is performed using the AST consistent with Regulatory Guide 1.183. In addition, the recent NRC guidance given in Regulatory Issue Summary RIS-2006-04 regarding application of the AST to WGDT events is also followed. The RIS-2006-04 guidance specifically endorses BTP 11-5, Rev. 3 from the Standard Review Plan, NUREG-0800.

15.7.4.1.1.3.2 Source Term

The source term released during the failure of a WGDT is comprised of 100% of the equilibrium noble gas activity of the RCS. The source term was derived from the St. Lucie specific core source term and 1% fission product release to coolant inventories using the ORIGEN 2.1 computer code. ORIGEN is an NRC approved methodology for source term development. The resulting WGDT source term is provided in Table 15.7.4.1-2.

15.7.4.1.1.3.3 Acceptance Criteria

The offsite dose acceptance criterion for a WGDT rupture accident of 0.1 rem total effective dose equivalent (TEDE), as specified in BTP 11-5, is chosen to apply to receptors located at the exclusion area boundary (EAB) and the low population zone (LPZ). As noted in UFSAR Section 11.3, the gaseous waste management system is designed to prevent an explosive gas mixture and the WGDTs are seismically designed. Per BTP 11-5, a dose limit of 2.5 rem could be applied. However, the more restrictive dose limit of 0.1 rem TEDE for systems not designed to withstand explosions and earthquakes was applied as a conservative way to establish a restrictive technical specification limit for the contents of the WGDTs. Note that this dose limit applies to the duration of the event (30 days), unlike most AST analyses of doses at the site boundary which typically consider only the worst two hour time period.

The TEDE dose limit for the control room is given as 5.0 rem (TEDE) in 10 CFR 50.67 and GDC-19.

15.7.4.1.1.3.4 Methodology

The radiological consequences of the WGDT Rupture are analyzed using the RADTRAD-NAI code and the inputs/assumptions discussed herein. The St. Lucie EPU dose analysis used one bounding analysis, applicable to both St. Lucie Units. Where necessary, analysis inputs which vary between the units were examined, and a bounding value was selected. The Atmospheric Dispersion Factors for both units' release and receptor points were examined and a conservative selection of the more limiting of the choices available was made. Consistent with Position 1.C of BTP-11-5:

- Only the radioactive noble gases (Xenon and Krypton) are considered.
- A ground level release is assumed.
- No credit for building wake correction factors was assumed.
- A conservative (5%) short term diffusion estimate was applied.

- No deposition was assumed to occur.

For this event, the Control Room ventilation system cycles through three modes of operation:

- Initially the ventilation system is assumed to be operating in normal mode. The air flow distribution during this mode is 920 cfm of unfiltered fresh air and an assumed value of 460 cfm of unfiltered inleakage.

- After the start of the event, the Control Room is isolated due to high radiation signal in the Control Room ventilation system. A 50-second delay is applied to account for diesel generator start time, damper actuation time, instrument delay, and detector response time. After isolation, the air flow distribution consists of 0 cfm of makeup flow from the outside, 460 cfm of unfiltered inleakage, and 1760 cfm of filtered recirculation flow.

- At 1.5 hours into the event, the operators are assumed to initiate makeup flow from the outside to the control room. During this operational mode, the air flow distribution consists of up to 504 cfm of filtered makeup flow, 460 cfm of unfiltered inleakage, and 1256 cfm of filtered recirculation flow.

- The Control Room ventilation filter efficiencies that are applied to the filtered makeup and recirculation flows are 99% for particulate, 95% elemental iodine, and 95% organic iodine. The control room recirculation filtration system will have no effect on the noble gas; therefore, control room recirculation filtration is not modeled.

15.7.4.1.1.3.5. Radiological Consequences

The dose locations were specified for the Exclusion Area Boundary (EAB), the Low Population Zone (LPZ), and the Control Room (CR) based upon the most limiting combinations of release points and receptor locations to bound both Unit 1 and Unit 2 analysis. The atmospheric dispersion factors (χ/Qs) for the EAR are presented in Table 15.7.4.1.-1b. Note that only 0.0 to 2.0 hour χ/Q value is input into RADTRAD-NAI, since this conservatively maximizes the EAB dose for any two hour time period, and has little effect on the 30 day EAB dose for this event. the χ/Qs for the LPZ are presented in Table 15.7.4.1-1c. The breathing rates are from Section 4.1.3 of Regulatory Guide 1.183.

Control Room χ/Qs are presented in Table 15.7.4.1-1d and 15.7.4.1-1e. Control Room breathing rates and occupancy factor are from Regulatory Guide 1.183 Section 4.2.6.

Table 15.2.4-3 presents the results for the WGDT rupture. The control room shine dose included in the summary table conservatively reflects the contribution from the external cloud for the LOCA event. As shown in this table, the results for EAB dose, LPZ dose, and Control Room dose are well within the appropriate regulatory guidance.

An additional output of this calculation is the determination of a candidate Technical Specification limit on Waste Gas Decay Tank inventory of each tank, as described in BTP-11-5 Rev. 3 (March 2007), Position 2.A.iii. The analysis for St. Lucie Units 1 and 2 EPU conditions defines a limit on Waste Gas Decay Tank Inventory of 165,000 Curies (Dose Equivalent Xe-133, as defined by TSTF-490).

15.7.4.1.2 Fuel Handling Accident

15.7.4.1.2.1 Identification of Event and Causes

The possibility of a fuel handling accident is remote because of the many interlocks and administrative controls and physical limitations imposed on the fuel handling operations (refer to Subsection 9.1.4). All refueling operations are conducted in accordance with prescribed procedures under direct surveillance of a supervisor technically trained in nuclear safety and fuel handling.

The fuel handling accident is assumed to occur as a consequence of a failure of the fuel assembly lifting mechanism resulting in the dropping of a raised fuel assembly onto other fuel bundles. The doses from a fuel handling accident occurring inside containment were calculated, assuming no prior isolation, and are bounded by the fuel handling accident presented herein.

15.7.4.1.2.2 Sequence of Events and Systems Operation

The refueling procedure is described in Subsection 9.1.4. The earliest anticipated time at which a spent fuel assembly could be handled is three days (72 hours) after shutdown.

For this evaluation, dropping of a fuel assembly is assumed to occur, breaching the cladding and releasing the volatile fission products in the gas gap of the fuel pins. In addition to the area radiation monitor located in the spent fuel cask area, portable radiation monitors capable of emitting audible alarms are located in this area during fuel handling operations. The containment equipment door and the emergency and personnel airlock doors are assumed closed two hours after the event to maintain controlled leakage characteristics in the reactor containment building. Should a fuel assembly be dropped, the airborne radiation monitors sound an alarm, alerting personnel to the problem. Airborne radiation monitors in the reactor containment building provide a containment isolation signal and automatically initiate the control room filtration subsystem for both unit's controls rooms.

15.7.4.1.2.3 Analysis of Effects and Consequences

15.7.4.1.2.3.1 Background

This event consists of the drop of a single fuel assembly either in the Fuel Handling Building (FHB) or inside of Containment. This analysis considers both a dropped fuel assembly inside the containment with the maintenance hatch open, and an assembly drop inside the FHB. Section 9.4.2.2.2 of the UFSAR identifies that in the event of a high radiation signal in the FHB, the pool area is exhausted to the plant vent via the SBVS filters. However, a more conservative approach is taken for the drop inside in the FHB, and the release is assumed to occur directly from the FHB without filtration. The source term released from the overlying water pool is the same for both the FHB and the containment cases. RG 1.183 imposes the same 2-hour criteria for the direct unfiltered release of the activity to the environment for either location.

A minimum water level of 23 feet is maintained above the damaged fuel assembly for both the containment and FHB release locations. This water level ensures an elemental iodine decontamination factor of 285 per the guidance provided in NRC Regulatory Issue Summary 2006-04 (Reference 15.6.5-29). The St. Lucie 2 AST dose analysis methodology is presented in NAI-1101-044, “AST Licensing Technical Report for St. Lucie Unit 2”.

15.7.4.1.2.3.2 Compliance with RG 1.183 Regulatory Positions

The FHA dose consequence analysis is consistent with the guidance provided in RG 1.183 Appendix B, "Assumptions for Evaluating the Radiological Consequences of a Fuel Handling Accident," as discussed below:

1. Regulatory Position 1.1 - The amount of fuel damage is assumed to be all of the fuel rods in a single fuel assembly.

2. Regulatory Position 1.2 - The fission product release from the breached fuel is based on Regulatory Positions 3.1 and 3.2 of RG 1.183. The gap activity available for release is specified by Table 3 of RG 1.183. This activity is assumed to be released instantaneously.

3. Regulatory Position 1.3 - The chemical form of radioiodine released from the damaged fuel into the spent fuel pool is assumed to be 95% cesium iodide (CsI), 4.85% elemental iodine, and 0.15% organic iodide. The cesium iodide is assumed to completely dissociate in the spent fuel pool resulting in a final iodine distribution of 99.85% elemental iodine and 0.15% organic iodine.

4. Regulatory Position 2 - A minimum water depth of 23 feet is maintained above the damaged fuel assembly. Therefore, a decontamination factor of 285 is applied to the elemental iodine and a decontamination factor of 1 is applied to the organic iodine. As a result, the breakdown of the iodine species above the surface of the water is 57% elemental and 43% organic. Guidance for the use of 285 for the elemental iodine decontamination factor is provided in NRC Regulatory Issue Summary 2006-04, “Experience with Implementation of Alternate Source Terms.”

5. Regulatory Position 3 - All of the noble gas released is assumed to exit the pool without mitigation. All of the non-iodine particulate nuclides are assumed to be retained by the pool water.

6. Regulatory Position 4.1 - The analysis models the release to the environment over a 2-hour period.

7. Regulatory Position 4.2 - No credit is taken for filtration of the release.

8. Regulatory Position 4.3 - No credit is taken for dilution of the release.

9. Regulatory Position 5.1 - The containment maintenance hatch is assumed to be open at the time of the fuel handling accident.

10. Regulatory Position 5.2 - No automatic isolation of the containment is assumed for the FHA.

11. Regulatory Position 5.3 - The release from the fuel pool is assumed to leak to the environment over a two-hour period.

12. Regulatory Position 5.4 - No ESF filtration of the containment release is credited.

13. Regulatory Position 5.5 - No credit is taken for dilution or mixing in the containment atmosphere.

15.7.4.1.2.3.3 Methodology

The input assumptions used in the dose consequence analysis of the FHA are provided in Table 15.7.4.1-4. It is assumed that the fuel handling accident occurs at 72 hours after shutdown of the reactor per TS 3.9.3. 100% of the gap activity specified in Table 3 of RG 1.183 is assumed to be instantaneously released from a single fuel assembly into the fuel pool. A minimum water level of 23 feet is maintained above the damaged fuel for the duration of the event. 100% of the noble gas released from the damaged fuel assembly is assumed to escape from the pool. All of the non-iodine particulates released from the damaged fuel assembly are assumed to be retained by the pool. Iodine released from the damaged fuel assembly is assumed to be composed of 99.85% elemental and 0.15% organic. All activity released from the pool is assumed to leak to the environment over a two-hour period. No credit for dilution in the containment or FHB is taken.

The FHA source term listed in Table 15.7.4.1-5 meets the requirements of Regulatory Position 1 of Appendix B to RG 1.183. The analysis includes a decay time of 72 hours before the beginning of fuel movement. Since the FHA source term presented in Table 15.7.4.1-5 does not include this decay time, it is accounted for in the RADTRAD-NAI model.

For this event, the Control Room ventilation system cycles through three modes of operation:

- Initially the ventilation system is assumed to be operating in normal mode. The air flow distribution during this mode is 1000 cfm of unfiltered fresh air and an assumed value of 395 cfm of unfiltered inleakage.

- After the start of the event, the Control Room is isolated due to a high radiation reading in the Control Room ventilation system. A 30-second delay is applied to account for diesel generator start time, damper actuation time, instrument delay, and detector response time. After isolation, the air flow distribution consists of 0 cfm of makeup flow from the outside, 395 cfm of unfiltered inleakage, and 1760 cfm of filtered recirculation flow.

- At 1.5 hours into the event, the operators are assumed to initiate makeup flow from the outside to the control room. During this operational mode, the air flow distribution consists of up to 504 cfm of filtered makeup flow, 395 cfm of unfiltered inleakage, and 1256 cfm of filtered recirculation flow.

- The Control Room ventilation filter efficiencies that are applied to the filtered makeup and recirculation flows are 99% for particulate, and 95% for elemental iodine, and organic iodine.

15.7.4.1.2.3.4 Radiological Consequences

The Control Room atmospheric dispersion factors (χ/Qs) used for this event are based on the postulated release locations and the operational mode of the control room ventilation system. The release-receptor point locations are chosen to minimize the distance from the release point to the Control Room air intake.

When the Control Room Ventilation System is in normal mode, the most limiting χ/Q corresponds to the worst air intake to the control room. When the ventilation system is isolated, the limiting χ/Q corresponds to the midpoint between the two control room air intakes. The operators are assumed to reopen the most favorable air intake at 1.5 hours. Development of control room atmospheric dispersion factors is discussed in Appendix 2.5D. The χ/Qs for the FHA events are summarized in Table 15.7.4.1-6.

For the EAB dose analysis, the χ/Q factor for the zero to two-hour time interval is assumed for all time periods. Using the zero to two-hour χ/Q factor provides a more conservative determination of the EAB dose, because the χ/Q factor for this time period is higher than for any other time period. The LPZ dose is determined using the χ/Q factors for the appropriate time intervals. These χ/Q factors are provided in Appendix 2.5C.

The radiological consequences of the FHA are analyzed using the RADTRAD-NAI code and the inputs/assumptions previously discussed. As shown in Table 15.7.4.1-7, the results for EAB dose, LPZ dose, and Control Room dose are all within the appropriate regulatory acceptance criteria.

15.7.4.1.3 Spent Fuel Cask Drop Analysis - Deleted

15.7.4.2 Limiting Reactor Coolant System Pressure Event

None of the Limiting Fault-2 events resulting from:

A. waste gas system failure

B. fuel handling accident, or

have an effect on Reactor Coolant System Pressure.

15.7.4.3 Limiting Fuel Performance Event

None of the Limiting Fault-2 events resulting from:

A. Waste gas system failure,

B. Fuel handling accident, or

have an effect on fuel performance.

15.7.5 LIMITING FAULT-3 EVENT

There is no event group in Table 15.0-2 which results in radioactive releases from a subsystem or component and which has an estimated frequency of occurrence which would classify it as a Limiting Fault-3 event.

TABLE 15.7.3-1

LIST OF EVENT GROUPS AND EVENT GROUP COMBINATIONS EVALUATED IN THE LIMITING FAULT-1 CATEGORY - RADIOACTIVE RELEASES FROM A SUBSYSTEM OR COMPONENT

Event Group and Event Group Combination	Acceptance Guidelines		
	Offsite Dose	RCS Pressure	Fuel Performance
1. Radioactive Liquid Waste System Leak or Failure	I	I	I
2. Liquid Containing Tank Failures	I	I	I

I - Insignificant approach to acceptance guideline.

TABLE 15.7.3.1-1

LIQUID RADIOACTIVITY WASTE SYSTEM FAILURE
ASSUMPTIONS TABULATED FOR POSTULATED ACCIDENT ANALYSIS
Historical Information

	Design Basis Assumptions	Realistic Basis Assumptions
1. Data and assumptions used to estimate radioactive sources from postulated accident:		
a. Power Level	2700 MWt	2560 MWt
b. Burnup (anytime during core life)	NA	NA
c. Fuel damaged	1.0%	0.12%
d. Reactor coolant activity before the accident	Table 11.1-2	Table 11.1-2
2. Dispersion Data		
a. EZ/LPZ distance (kilometers)	1.56/1.61	1.56/1.61
b. Assumed release level	Ground	Ground
c. χ/Qs (sec/m^3)		
EAB	1.6 E-04	2.6 E-05
LPZ	7.1 E-05	7.4 E-06
3. Breathing Rate (m^3/sec)		
0-8 hours	3.47 E-04	
8-24 hours	1.75 E-04	
1-30 days	2.32 E-04	
4. Dose Data		
a. Method of dose calculation	Section 15.6.5.5	
b. Dose conversion factor	Section 15.7.3.1.3 Table 15.7.3.1-4	

TABLE 15.7.3.1-2

LIQUID RADIOACTIVITY WASTE SYSTEM FAILURE
(DESIGN BASIS ANALYSIS)

Historical Information

ACTIVITY RELEASE TO ENVIRONMENT (CURIES)

Isotope	Activity
I-131	2.0 E+00
I-132	1.3 E-02
I-133	5.0 E-01
I-134	3.6 E-03
I-135	9.9 E-02
Kr-85m	1.0 E+03
Kr-85	1.2 E+04
Kr-87	2.8 E+02
Kr-88	1.8 E+03
Xe-131m	1.0 E+04
Xe-133	6.0 E+05
Xe-135	4.8 E+03
Xe-138	1.4 E+01

TABLE 15.7.3.1-3

OFFSITE DOSES

Historical Information

	Two Hour Exclusion Area Boundary Dose	Entire Event Low Population Zone Dose
Thyroid	1.8×10^{-1} rem	7.8×10^{-2} rem
Whole Body	8.8×10^{-1} rem	3.8×10^{-1} rem

Table 15.7.3.1-4 Isotope Properties

Historical Information

Isotope	Radioactive Decay Constant (sec^{-1})	Thyroid Conversion Factors (rem/Ci - Inhaled)	Whole Body Dose Conversion Factors (rems - m^3)** (sec -Ci)	Skin Dose Conversion (rems - m^3)** (sec-Ci)
Kr-85m	4.41×10^{-5}	-	3.61×10^{-2}	8.89×10^{-2}
Kr-85	2.21×10^{-9}	-	6.11×10^{-4}	4.44×10^{-2}
Kr-87	1.48×10^{-4}	-	3.61×10^{-1}	7.50×10^{-1}
Kr-88	6.95×10^{-5}	-	4.17×10^{-1}	5.56×10^{-1}
Xe-131m	6.68×10^{-7}	-	7.78×10^{-4}	1.33×10^{-2}
Xe-133	1.52×10^{-6}	-	6.94×10^{-3}	1.92×10^{-2}
Xe-135m	7.40×10^{-4}	-	9.72×10^{-2}	1.39×10^{-1}
Xe-135	2.11×10^{-5}	-	5.83×10^{-2}	1.36×10^{-1}
Xe-138	8.04×10^{-4}	-	3.33×10^{-1}	4.72×10^{-1}
I-131	9.96×10^{-7}	1.48×10^{6}	8.61×10^{-2}	1.36×10^{-1}
I-132*	2.46×10^{-6}	5.35×10^{4}	5.56×10^{-1}	7.50×10^{-1}
I-133	9.20×10^{-6}	4.00×10^{5}	1.22×10^{-1}	2.44×10^{-1}
I-134	2.20×10^{-4}	2.50×10^{4}	5.56×10^{-1}	8.06×10^{-1}
I-135	2.86×10^{-5}	1.24×10^{5}	4.17×10^{-7}	5.56×10^{-1}

* Decay Constant of precursor used.

** Final Environmental Statement Concerning: Numerical Guides for Design Objectives and Limiting Conditions for Operation to Meet the Criterion "As Low as Practicable" For Light-Water-Cooled Nuclear Power Reactor Effluents, Volume 2, Table A-4, Pg. 3, F-53 (July 1973).

TABLE 15.7.4-1

LIST OF EVENT GROUPS AND EVENT GROUP COMBINATIONS EVALUATED IN THE LF-2 - RADIOACTIVE RELEASES FROM A SUBSYSTEM OR COMPONENT

Event Group and Event Group Combination	Acceptance Guidelines		
	Offsite Dose	RCS Pressure	Fuel Performance
1) Waste Gas System Failure	I	I	I
2) Fuel Handling Accidents	I	I	I

S - Significant approach to acceptance guideline.
I - Insignificant approach to acceptance guideline.

TABLE 15.7.4.1-1a
WGDT Rupture - Inputs and Assumptions

Input / Assumption	Value
Core Power Level	3030 MWth (3020 + 0.3%)
Core Average Fuel Burnup	49,000 MWD/MTU
Fuel Enrichment	1.5 - 5.0 w/o
WGDT Activity	Table 15.7.4.1-2
Atmospheric Dispersion Factors Offsite Onsite	 Table 15.7.4.1-1b and 15.7.4.1-1c Table 15.7.4.1-1d and 15.7.4.1-1e
Control Room Ventilation System Time of Control Room Ventilation System Isolation Time of Control room Filtered Makeup Flow Control Room Unfiltered Inleakage	 50 Seconds 1.5 hours 460 cfm
Breathing Rates	RG 1.183 Sections 4.1.3 and 4.2.6
Control Room Occupancy Factor	RG 1.183 Section 4.2.6

TABLE 15.7.4.1-1b
EAB X/Q

Time (hours)	St. Lucie Common EAB X/Q (sec/m^3)
0.0	1.05E-04
720.0	1.05E-04

TABLE 15.7.4.1-1c
LPZ X/Q

Time (hours)	St. Lucie Common LPZ X/Q (sec/m^3)
0.0	1.05E-04
2.0	5.74E-05
8.0	4.32E-05
24.0	2.33E-05
96.0	9.62E-06
720.0	9.62E-06

TABLE 15.7.4.1-1d
Common St. Lucie HVAC X/Q Table

Time (hours)	**Common HVAC X/Q (sec/m^3)**
0	3.770E-03
0.01389	3.770E-03
1.5	3.770E-03
2	3.195E-03
8	1.390E-03
24	1.101E-03
96	8.870E-04
720	8.870E-04

TABLE 15.7.4.1-1e
Common St. Lucie Control Room Unfiltered Inleakage X/Q

Time (hours)	**Unfiltered Inleakage X/Q (sec/m^3)**
0	3.61E-03
2	2.92E-03
8	1.23E-03
24	9.38E-04
96	7.66E-04
720	7.66E-04

TABLE 15.7.4.1-2
WGDT Source Term - 165,000 Curies Xe-133 Equivalent

Isotope	**RCS/WGDT Event Inventory (Ci)**	**Tech Spec Maximum Inventory (Ci)**
Kr-85	41.60	
Kr-85m	1.268	
Kr-87	0.7574	
Kr-88	2.247	
Xe-131m	3.022	
Xe-133	238.1	165,000
Xe-133m	3.479	
Xe-135	9.235	
Xe-135m	0.8553	
Xe-138	0.5168	
Nominal Eq.* Xe-133	90,921.0	165,000
Rounded Down Eq. Xe-133	90,900	
* Analysis Basis (T.S.) Eq. Xe-133		

TABLE 15.7.4.1-3

St. Lucie Units 1 and 2 Waste Gas Decay Tank Failure Consequences

Dose Contribution	**TEDE Dose (rem)**		
	EAB 30 Days	**LPZ 30 Days**	**CR 30 Days**
WGDT Failure	0.055086	0.052967	0.19085
Control Room Cloud Shine	N/A	N/A	0.078
Total	**0.055**	**0.053**	**0.269**
Acceptance Criteria	0.1*	0.1*	5.0**
Control Room Unfiltered Inleakage = 460 cfm			

* The 0.1 REM (TEDE) 30 day dose limit is specified in NUREG-0800, BTP-11-5 Rev. 3 (March 2007) Position B.1.A for the EAB. The LPZ limit is assumed in this calculation to be the same value.

** The 5.0 REM (TEDE) CR limit is not specified in either the BTP or Regulatory Guide 1.183 for this event, but is the specified Control Room limit for all other AST events.

Table 15.7.4.1-4

Fuel Handling Accident (FHA) – Inputs and Assumptions

Input/Assumption	Value
Core Power Level Before Shutdown	3030 MW_{th} (3020 + 0.3%)
Core Average Fuel Burnup	49,000 MWD/MTU
Discharged Fuel Assembly Burnup	45,000 – 62,000 MWD/MTU
Fuel Enrichment	1.5 – 5.0 w/o
Maximum Radial Peaking Factor	1.65
Number of Fuel Assemblies in the Core	217
Number of Fuel Assemblies Damaged	1
Delay Before Spent Fuel Movement	72 hours
FHA Source Term for a Single Assembly	Table 15.7.4.1-5
Water Level Above Damaged Fuel Assembly	23 feet minimum
Iodine Decontamination Factors	Elemental – 285 Organic – 1
Noble Gas Decontamination Factor	1
Chemical Form of Iodine In Pool	Elemental – 99.85% Organic – 0.15%
Chemical Form of Iodine Above Pool	Elemental – 57% Organic – 43%
Atmospheric Dispersion Factors Offsite Onsite	 Appendix 2.5C Table 15.7.4.1-6
Control Room Ventilation System Time of Control Room Ventilation System Isolation Time of Control Room Filtered Makeup Flow Control Room Unfiltered Inleakage	 30 seconds 1.5 hours 395 cfm
Breathing Rates	RG 1.183 Sections 4.1.3 and 4.2.6
Control Room Occupancy Factor	RG 1.183 Section 4.2.6

This page has been intentionally left blank.

Table 15.7.4.1-5

Fuel Handling Accident Source Term

Nuclide	Activities (Curies)	Nuclide	Activities (Curies)	Nuclide	Activities (Curies)
Co-58	0.000E+00	I-135	1.183E+06	Sb-126	1.359E+03
Co-60	0.000E+00	Xe-133	1.260E+06	Te-131	5.853E+05
Kr-85	9.417E+03	Xe-135	3.341E+05	Te-133	7.486E+05
Kr-85m	1.508E+05	Cs-134	2.536E+05	Te-134	9.973E+05
Kr-87	2.864E+05	Cs-136	6.227E+04	Te-125M	3.911E+03
Kr-88	4.026E+05	Cs-137	1.052E+05	Te-133m	4.424E+05
Rb-86	2.142E+03	Ba-139	1.094E+06	Ba-141	9.918E+05
Sr-89	5.521E+05	Ba-140	1.054E+06	Ba-137m	9.973E+04
Sr-90	7.554E+04	La-140	1.101E+06	Pd-109	4.216E+05
Sr-91	6.856E+05	La-141	9.966E+05	Rh-106	7.574E+05
Sr-92	7.494E+05	La-142	9.600E+05	Rh-103m	1.081E+06
Y-90	7.880E+04	Ce-141	1.014E+06	Tc-101	1.117E+06
Y-91	7.212E+05	Ce-143	9.179E+05	Eu-154	1.586E+04
Y-92	7.531E+05	Ce-144	8.526E+05	Eu-155	1.100E+04
Y-93	8.804E+05	Pr-143	9.128E+05	Eu-156	3.622E+05
Zr-95	1.016E+06	Nd-147	4.023E+05	La-143	9.110E+05
Zr-97	1.011E+06	Np-239	1.851E+07	Nb-97	1.021E+06
Nb-95	1.028E+06	Pu-238	4.719E+03	Nb-95m	7.268E+03
Mo-99	1.202E+06	Pu-239	2.911E+02	Pm-147	9.215E+04
Tc-99m	1.052E+06	Pu-240	5.480E+02	Pm-148	1.879E+05
Ru-103	1.200E+06	Pu-241	1.357E+05	Pm-149	4.224E+05
Ru-105	9.714E+05	Am-241	1.532E+02	Pm-151	1.544E+05
Ru-106	6.909E+05	Cm-242	6.798E+04	Pm-148m	2.259E+04
Rh-105	8.747E+05	Cm-244	2.488E+04	Pr-144	8.583E+05
Sb-127	8.842E+04	I-130	5.275E+04	Pr-144m	1.024E+04
Sb-129	2.399E+05	Kr-83m	7.273E+04	Sm-153	5.158E+05
Te-127	8.796E+04	Xe-138	1.004E+06	Y-94	8.931E+05
Te-127m	1.200E+04	Xe-131m	7.470E+03	Y-95	9.671E+05
Te-129	2.361E+05	Xe-133m	4.074E+04	Y-91m	3.980E+05
Te-129m	3.503E+04	Xe-135m	2.671E+05	Br-82	5.881E+03
Te-131m	1.012E+05	Cs-138	1.117E+06	Br-83	7.247E+04
Te-132	9.227E+05	Cs-134m	5.683E+04	Br-84	1.241E+05
I-131	6.654E+05	Rb-88	4.100E+05	Am-242	9.393E+04
I-132	9.425E+05	Rb-89	5.234E+05	Np-238	5.019E+05
I-133	1.255E+06	Sb-124	2.681E+03	Pu-243	8717E+05
I-134	1.358E+06	Sb-125	1.767E+04		

Table 15.7.4.1-6a

Control Room X/Qs for Containment Release

Time (hours)	X/Q (sec/m^3)
0	1.90E-03
72.00833	1.27E-03
73.5	8.28E-04
74	6.57E-04
80	2.92E-04
96	1.93E-04
168	1.76E-04
792	1.76E-04

Table 15.7.4.1-6b

Control Room X/Qs for FHB Release

Time (hours)	X/Q (sec/m^3)
0	4.92E-03
72.00833	3.29E-03
73.5	1.87E-03
74	1.36E-03
80	5.88E-04
96	4.00E-04
168	3.06E-04
792	3.06E-04

Table 15.7.4.1-7

Fuel Handling Accident Dose Consequences

Case	**EAB Dose[1] (rem TEDE)**	**LPZ Dose[2] (rem TEDE)**	**Control Room Dose[2] (rem TEDE)**
FHA Containment Release	0.60	0.58	1.28
FHA Fuel Handling Building Release	0.60	0.58	3.01
Acceptance Criteria	6.3	6.3	5

[1] Worst 2-hour dose
[2] Integrated 30-day dose

15.8 PRIMARY SYSTEM PRESSURE DEVIATION

The fuel design parameters have no significant effect on the pressure increase or decrease of any of the primary system pressure deviation events identified in Section 15.8 of the UFSAR. Also, none of the primary system pressure deviation events identified in this Section (Section 15.8) pose a significant challenge to the DNBR SAFDL. Therefore, none of the events in Section 15.8 of the UFSAR require a re-analysis for the fuel transition. EC287528

15.8.1 MODERATE FREQUENCY EVENTS

There is no event group in Table 15.0-2 which results in a primary system pressure deviation and has an estimated frequency of occurrence which would classify it as a Moderate Frequency event.

15.8.2 INFREQUENT EVENTS

15.8.2.1 Limiting Offsite Dose

None of the Infrequent events resulting in a primary system pressure deviation shown in Table 15.8.2-1 produce a significant offsite dose. The offsite dose which would occur during the most adverse of these events is well within the acceptance guideline in Table 15.0-4.

15.8.2.2 Limiting Reactor Coolant System Pressure Event - (Overpressurization of the Primary System)

None of the Infrequent events resulting in a primary system pressure deviation shown in Table 15.8.2-1 produce a significant approach to the maximum allowable pressure when at a temperature below the minimum pressurization temperature (MPT) from the MPT limit curve that will be presented in the Technical Specifications.

15.8.2.3 Limiting Fuel Performance Event

None of the Infrequent events resulting in primary system pressure deviation shown in Table 15.8.2-1 produce a significant approach to fuel performance limits. The degradation in fuel performance which would occur during the most adverse of these events does not result in a DNBR less than 1.19 and therefore, is well within the acceptance guideline specified in Table 15.0-4.

15.8.3 LIMITING FAULT 1 EVENTS

15.8.3.1 Limiting Offsite Dose Event

None of the Limiting Fault 1 (LF-1) events resulting in primary system pressure deviation shown in Table 15.8.3-1 produce a significant offsite dose. The offsite dose which would occur during the most adverse of these events is well within the acceptance guideline specified in Table 15.0-4.

15.8.3.2 Limiting Reactor Coolant System Pressure Event - Overpressurization of the Primary System with the Failure of One Power Operated Relief Valve to Open

None of the LF-1 events resulting in primary system pressure deviation shown in Table 15.8.3-1 produce a significant approach to the maximum allowable pressure when at a temperature below the minimum pressurization temperature (MPT) from the MPT limit curves that will be presented in the Technical Specifications.

15.8.3.3 Limiting Fuel Performance

None of the LF-1 events resulting in primary system pressure deviation shown in Table 15.8.3-1 produce a significant approach to fuel performance limits. The degradation in fuel performance which would occur during the most adverse of these events does not result in a DNBR less than 1.19 and therefore, is well within the acceptance guidelines specified in Table 15.0-4.

15.8.4 LIMITING FAULT 2 EVENTS

There is no event group in Table 15.0-2, or event group combination, which results in a primary system pressure deviation and has a estimated frequency of occurrence which would classify it as a Limiting Fault 2 event.

15.8.5 LIMITING FAULT 3 EVENTS

There is no event group in Table 15.0-2, or event group combination, which results in a primary system pressure deviation and has an estimated frequency of occurrences which would classify it as a Limiting Fault 3 event.

TABLE 15.8.2-1

LIST OF EVENT GROUPS AND EVENT GROUP COMBINATIONS EVALUATED IN THE INFREQUENT/PRIMARY SYSTEM PRESSURE DEVIATION MATRIX ELEMENT COMPARED TO THE ACCEPTANCE GUIDELINES

	Acceptance Guidelines		
Event Group and Event Group Combination	Offsite Dose	RCS Pres-sure	Fuel Perfor-mance
* 1. Inadvertent generation of a SIAS and safety injection actuation	I	I	I
* 2. Startup of an inactive reactor coolant pump	I	I	I
* 3. Opening a safety injection tank discharge isolation valve	I	I	I
4. Pressurizer pressure signal failed low	I	I	I
5. Depressurization of Primary System	I	I	I

*Events evaluated in Mode 5 (Cold Shutdown)

S - Significant approach to acceptance guideline.
I - Insignificant approach to acceptance guideline.

TABLE 15.8.3-1

LIST OF EVENT GROUPS AND EVENT GROUP COMBINATIONS EVALUATED IN THE LIMITING FAULT 1 PRIMARY SYSTEM PRESSURE DEVIATION MATRIX ELEMENT COMPARED TO THE ACCEPTANCE GUIDELINES

	Acceptance Guidelines		
Event Group and Event Group Combination	Offsite Dose	RCS Pres-sure	Fuel Perfor-mance
* 1. Inadvertent generation of a SIAS and safety injection actuation and Low Probability Independent Occurrence (LPI)	I	I	I
* 2. Startup of an inactive reactor coolant pump + LPI	I	I	I
* 3. Opening a safety injection tank discharge isolation valve + LPI	I	I	I
4. Pressurizer pressure signal failed low + LPI	I	I	I
5. Depressurization of Primary System + LPI	I	I	I

*Events evaluated in Mode 5 (Cold Shutdown)

S - Significant approach to acceptance guideline.
I - Insignificant approach to acceptance guideline.

15.9 ANTICIPATED TRANSIENTS WITHOUT SCRAM (ATWS)

Florida Power & Light Company is part of the Combustion Engineering's (CE) Nuclear Steam Supply System (NSSS) owners group which has provided the NRC Staff generic information regarding the ATWS mitigating capabilities for nuclear power plants using the CE designed NSSS. The information (ATWS Early Verification for CE NSSS's) was transmitted to Dr S H Hanauer (NRC) from C H Poindexter (on behalf of the CE NSSS Owners Group) on November 30, 1979.

Note: the above information is historical. A description of ATWS functions are provided in Subsection 7.6.3.11.

The change in fuel design parameters will have no significant effect on the ATWS analysis described in the UFSAR. Therefore, ATWS is not affected by the fuel transition. EC287528

15.10 STATION BLACKOUT ANALYSIS

The station blackout event is part of the design basis for St. Lucie Unit 2. An analysis was performed as requested by the NRC in response to the decision of ALAB-603. This analysis shows that St. Lucie Unit 2 can successfully endure a complete loss of ac power for at least 4 hours. The acceptability of this approach was reconfirmed in an NRC June 11, 1992 letter, Safety Evaluation for the St. Lucie Units 1 and 2 SBO. However, it is expected that ac power would be restored within 30 minutes to one hour as a result of either one of the following corrective actions:

a. Offsite power is restored;

b. One or both of the St. Lucie Unit 2 diesel generators are started.

Operator action at 30 minutes is credited to open the atmospheric dump valves resulting in the closure of the main steam safety valves. Operator control of the atmospheric dump valves to assure natural circulation by maintaining subcooling in the RCS occurs after 2 hours.

The results of this analysis have shown that:

1. Natural circulation and core cooling can be maintained;

2. The reactor core remains in a subcritical condition;

3. There is no fuel failure;

4. The RCS coolant pressure remains within limits; and,

5. The resulting radiological doses are within limits.

The DC coping capability is further enhanced by ability to provide power to the one division of the Class 1E distribution system from Unit 1 emergency diesel-generator(s). Even though the amount of power available to Unit 2 loads under Station Blackout scenario (only one EDG operational on Unit 1) is limited by plant procedures as not to affect Unit 1 safe shutdown, it can be used to power selected loads, i.e., battery chargers, UPS, certain fans, etc.

Therefore, this analysis shows that St. Lucie Unit 2 can successfully endure a station blackout event. Florida Power and Light implemented operator training and emergency procedures to ensure that plant operators would take appropriate actions to assure maintenance of natural circulation.

15.10.1 IDENTIFICATION OF EVENT AND CAUSES

The Station Blackout event results from a loss of offsite power followed by failure of both standby diesel generators to start.

For Unit 2, this event results in a loss of all onsite ac power except that supplied by inverters from the two safeguards batteries. This provides power to the 120V ac (safeguards) instrument power and other required dc loads. The SBO cross-tie can be used to supply additional power to Unit 2 to power selected equipment, however, there was no credit taken for that in the SBO analysis.

15.10.2 SEQUENCE OF EVENTS AND SYSTEMS OPERATION

Table 15.10-1 shows a chronological list of the timing of systems actions from the initiation of a station blackout event to the time that offsite power is restored (4 hours). A description of the sequence of events* is given below for each safety function:

Reactivity Control:

As a result of the loss of power to the reactor coolant pumps an automatic reactor trip signal is generated by the RPS on low reactor coolant system flow, as measured by steam generator delta-pressure (Δ P). The reactor trip signal interrupts power to the reactor trip switchgear which in turn releases the CEAs to drop into the core. The negative reactivity inserted by the CEAs is sufficient to maintain the core subcritical throughout the rest of the transient.

Reactor Heat Removal:

Following coastdown of the reactor coolant pumps, flow through the reactor is maintained by natural circulation. Heat is transferred to the secondary system through the steam generators.

Primary System Integrity:

The major contributors to reactor coolant inventory loss are the opening of the primary safety valves (PSVs), the power operated relief valves (PORVs), and reactor coolant pump (RCP) seal leakage. The analysis of the SBO event at EPU conditions demonstrates that the primary system pressurizer remains below the opening setpoint of both the PSVs and the PORVs (2370 psia), thereby minimizing any reactor coolant inventory loss via these valves. The major contributor to reactor coolant system (RCS) coolant inventory loss during the SBO event is RCP seal leakage. Letdown is isolated by the closing of the letdown control valve on loss of offsite power. The primary system pressure remains above the maximum safety injection tank (SIT) discharge pressure of 650 psig for the duration of the coping period.

Secondary System Integrity:

A turbine trip signal (TTS) is generated following the loss of offsite power and causes the turbine stop valves to close. The Main Steam Safety Valves (MSSVs) open to limit the pressure increase.

Auxiliary feedwater is automatically actuated on low steam generator level. Flow is provided by the turbine driven pump which derives all its control power from the station batteries. The operator opens the Atmospheric Dump Valves (ADVs) and regulates them from the control room to maintain steam generator pressure below the setpoint of the MSSVs and to reduce the primary system temperature to maintain subcooling in the hot leg.

Control Room Habitability:

The loss of ac power will result in a loss of control room air conditioning. The low initial temperature of the control room and the surrounding heat sinks (floor, walls, etc.,) and the greatly reduced internal heat load due to a loss of power both serve to moderate the temperature rise resulting from the loss of cooling. In addition, certain manual operations can

*Those safety actions necessary to maintain the plant in hot shutdown.

be performed such as opening roof top dampers and exterior doors to establish natural circulation cooling paths. The limited duration of the blackout helps to ensure that the control room remains habitable and that the equipment required for hot standby remains operable during this period.

Restoration of AC power:

Although the analysis which follows shows acceptable results assuming no ac power for 4 hours, in actuality ac power would be restored to the plant prior to this time by either one of the following corrective actions.

a. Offsite power is restored and the onsite buses are manually connected to the startup transformers. Equipment is manually loaded on these buses, according to plant emergency procedures, or,

b. One (or both) Unit 2 diesel generators is started and safeguards loads are sequenced onto its 4.16 kV bus.

c. Power is transferred from a St. Lucie 1 diesel generator set via station blackout cross-tie to operate the selected hot standby loads until the conclusion of the event.

15.10.3 EMERGENCY DC BATTERY - PROFILE DURING STATION BLACKOUT

Two Class 1E batteries, each rated at 2400 ampere-hours (AH), at an eight hour discharge rate, are provided to supply the two Class 1E dc buses 2A and 2B, and the swing bus 2AB. The 2AB bus was assumed to be aligned to the 2B bus, for the purposes of the station blackout study. The 2B bus is the more heavily loaded of 2A and 2B buses. The 2B battery, supplying the 2B and 2AB buses was selected as the most conservative for the purpose of battery capacity analysis.

Specific 125V dc system load scenarios (SBO, SIAS) have been evaluated utilizing industry standard calculation methods and the battery size has been determined to be sufficient to support the “worst-case” system loading. The load profile shown in Figure 15.10-13 103 was established by analysis. For conservatism, a near constant loading has been assumed (i.e., no credit has been taken for manual load shedding performed by a plant operator) and a 1.19 electrolyte temperature correction factor for 10°C has been included in the calculation.

The following demonstrates that the station battery has sufficient capacity to supply the required dc loads for the four hour station blackout scenario.

Using the battery load profile shown on Figure 15.10-103, Table 15.10-5 has been developed.

Referring to the load profile (Figure 15.10-103), from time 0 to one minute, the battery load is comprised of the normal bus loads and the inrush loads associated with valve actuation, relay operation and various control circuit functions which are completed in less than one minute. The time period from one minute to 239 minutes reflects the full accident loading of the 2B and 2AB buses. (Note that at or before 30 minutes the operator can perform the load shedding operations defined in the operating procedures. After 60 minutes the load can be further

reduced, since, in accordance with the NSSS analysis, operation of the PORVs is not required*.) At or before 239 minutes the diesel generator field is flashed and the event is terminated.

The following instrumentation is required to remain functional during a station blackout:

- Pressurizer Pressure: PIA-1102A, B, C & D
- Steam Generator Press: PI-8013 & 8023 A, B, C & D
- Steam Generator Level: LIC-9013 & 9023 A, B, C & D
- AFW System Valve Position Indication
- Power Operated Relief: PORV Position Indication
- Containment Pressure: PIS-07-2A, B, C & D
- Containment Radiation Monitors
- Battery Voltage & Current
- ESFAS
- AFAS
- RPS (Including Hot & Cold Leg Temp, Neutron Flux)

Additional instrumentation, although not required by the station blackout rule, is provided with an uniterruptible power supply and therefore is available to determine system operation status:

- AFW Pump 2C Flow: FR-09-2B/2C
- Pressurizer Pressure: PI-1108-1
- Containment Atmosphere Temperature: TI-07-3A
- Containment Sump Water Temperature: TI-07-5A

The following equipment is required to remain functional during a station blackout:

- CEDMs, CST, SITs
- AFW Pump 2C
- MV-08-12 & 13 (Steam Supply to Turbine)
- MV-09-11 & 12 (AFW Isolation Valves)
- MV-08-18A, 18B, 19A & 19B (ADVs)

---

*This manual load shedding reduces the total load on the battery which will extend useful battery life and increase the margin of safety.

- SE-09-4 & 5 (AFW Isolation Valves)
- V1474 & 1475 (Power Operated Relief Valves)
- Main Steam Safety Relief Valves
- V2515 & 2516 (Letdown Isolation Valves)
- Turbine Stop Valves

During a station blackout at the St. Lucie Site, certain loads that are automatically loaded onto the dc emergency battery can be stripped from the dc battery by the plant operators. Two such load categories that will be stripped are dc lighting and communications. To offset the losses of lighting and communications, the following design modifications have been implemented:

A sound powered jack station is installed on the communication console located in the control room. This enables communications to be maintained from the control room to the main steam trestle area, the emergency switchgear room and the Diesel Generator Building. This system uses voice sound power to generate the communication signal and does not require external power making it immune in the event of loss of all onsite power. Additional dc emergency lighting (battery lighting fixture assemblies) has been added to the main steam trestle area, the emergency switchgear room (to allow for identification and operation of a breaker), and to the Diesel Generator Building (to allow for dg maintenance).

The NRC approved station blackout procedure has been incorporated into the Unit No. 2 plant procedures manual.

15.10.4 ANALYSIS OF EFFECTS AND CONSEQUENCES

a. Mathematical Models

The NSSS response to a Station Blackout was simulated using the RETRAN computer program.

b. Input Parameters and Initial Conditions

The initial conditions assumed for this event are contained in Table 15.10-2. These conditions were chosen to provide the largest and most rapid depletion of RCS inventory and shutdown margin. The major contributors to the RCS depressurization are the pressurizer heat losses and RCS leakage. Maximum values of these parameters were selected based on technical specifications, plant operating data and reactor coolant pump test results. The lowest initial pressurizer water volume minimizes the available RCS inventory. Initial core inlet temperature, core mass flow rate and pressurizer pressure have a negligible impact on the primary system depressurization. The evaluation of shutdown margin depletion was performed using the most negative moderator temperature coefficient and the least negative CEA worth for trip. This minimizes the shutdown margin remaining at the end of the transient.

The disposition of normally operating systems is given on Table 15.10-3. The utilization of safety systems is given on Table 15.10-4.

c. Results

The dynamic behavior of important NSSS parameters following a Station Blackout is presented in Figures 15.10-1 to 15.10-10. Table 15.10-1 summarizes some of the important results of this event and the times at which the minimum and maximum parameter values discussed below occur. The loss of all AC electrical power initiates, among other things, a simultaneous loss of feedwater, loss of load, and loss of forced reactor coolant flow. As indicated in Figure 15.10-1, the core power increases initially due to positive reactivity feedback and reaches a maximum value within a few seconds. Subsequent to loss of power to the reactor coolant pumps, the primary coolant flow decreases and a low flow reactor trip occurs as indicated in Table 15.10-1. Reactor coolant flow vs. time is shown on Figure 15.10-6. Subsequently, due to the insertion of large negative reactivity by the scram rods, the core power decreases very rapidly and approaches the decay heat value. Departure from nucleate boiling is not analyzed in this event as it is bound by the complete loss of flow event.

During the initial few seconds prior to reactor trip, the reduced steam generator heat rejection capability leads to a rapid increase in both the primary and secondary fluid temperatures. The volumetric expansion due to these increases in temperature produces sharp increases in primary and secondary pressures as well as an insurge of primary coolant into the pressurizer. The variations of the primary and secondary pressures are illustrated in Figures 15.10-3 and 15.10-7. The primary pressure does not reach the PORV opening setpoint. The secondary safety valves cycle open and closed until the operator opens the atmospheric dump valves. MSSV and ADV flow vs. time are shown on Figures 15.10-9 and 15.10-10, respectively.

The steam generator liquid level decreases during the transient and reaches a minimum value after auxiliary feedwater flow is automatically actuated using the steam-driven auxiliary feedwater pump. Steam generator level increases until normal water level is reached. The operator subsequently controls auxiliary feedwater to maintain normal level. See Figure 15.10-8.

The RCS pressure and temperature gradually decrease at fairly constant rates in the long term as a result of pressurizer heat loss, RCS leakage, low heat transfer rates at the steam generators, and the operator manually reducing secondary side pressure. Since the RCS pressure decreases at a higher rate than the RCS temperature, the pressure approaches the saturation pressure.

Saturation occurs in the reactor vessel head. Continued primary pressure drop without a significant decrease in primary temperatures would result in saturated conditions in the hot leg. Credit is taken for operator action to maintain at least 10 F subcooling in the hot leg. This is accomplished by further opening the atmospheric dump valves to reduce the secondary system pressure and temperature. The increased heat removal in the steam generators caused by the larger ΔT across the steam generator tubes reduces the primary system temperatures. Voiding is restricted to the vessel head. The maximum void fraction occurs at 4 hours. The size of the void is such that 7.01 ft of water remains above the hot leg. Primary pressure does not depressurize low enough to actuate the Safety Injection Tanks (SITs).

At 4 hours, sufficient AC power is assumed to be restored to provide power to the charging pumps and pressurizer heaters. These will be used to pressurize the RCS and to continue hot leg subcooling.

Operability of the turbine driven auxiliary feedwater pump requires at least 50 psia secondary pressure. At 4 hours after the initiation of the event, the secondary pressure will be greater than 300 psia. Less than 100,000 gallons of auxiliary feedwater are used during the event. The condensate storage tank capacity is greater than 300,000 gallons.

15.10.4.1 This Section has been Deleted

15.10.4.2 Radiological Analysis

15.10.4.2.1 Background

The radiological consequences of the Station Blackout (SBO) are analyzed for Extended Power Uprate (EPU) conditions using NRC Regulatory Guide 1.183 guidance for an acceptable methodology for applying alternative source terms to the calculations of radiological doses for design basis events.

15.10.4.2.2 Compliance with RG 1.183 Regulatory Positions

Regulatory Guide 1.183 does not provide specific guidance for this event; however, the general guidance of the Regulatory Guide was followed and supplemented by the acceptable implementation practices outlined in NRC Regulatory Issue Summary RIS-2006-04.

15.10.4.2.3 Other Assumptions

1. All noble gases are assumed to leak directly to the environment.

2. Radionuclide concentrations in the secondary side fluid of the steam generators assume operator action to maintain a constant secondary mass during periods of steam release.

3. The initial concentration of the iodine on the secondary side was set 0.1 μCi/gm Dose Equivalent I-131 based upon Tech. Spec. LCO 3.7.1.4).

4. The initial steam generator mass is assumed to be equal to the minimum (HFP) value. This is a conservative assumption that maximizes the secondary side nuclide concentration resulting from primary-to-secondary leakage.

5. The tubes on the secondary side of the steam generator are assumed to become uncovered as a result of the steam generator level shrink which occurs at the time of reactor trip. During the time of tube bundle uncovery, a portion of the primary-to-secondary leakage into the steam generators flashes to vapor and is available for release from the steam space. Auxiliary Feedwater is credited with restoration of steam generator level above the top of the tube bundle within 60 minutes from the time of reactor trip.

6. No credit is taken for iodine scrubbing of flashed fluid in the steam generator secondary.

7. Offsite power is restored after four hours; however, the RCS cooldown is assumed to continue by releasing steam until the RCS is cooled to 212°F. A cooldown rate of 20°F/hr conservatively maximizes the steam release.

8. The steam generator tube leakage is assumed to continue until the RCS is cooled to 212°F.

9. The control room ventilation system is assumed to remain in the normal configuration after offsite power is restored.

10. This event does not result in fuel failures.

15.10.4.3.4 Methodology

Steam releases for the first four hours of the St. Lucie Unit 2 SBO event based upon a reactor power level of 2630 MW are directly proportional to reactor power level and have been applied to the development of the EPU steam release rates. In this radiological analysis, the RCS cooldown will be continued beyond four hours until the RCS temperature reaches 212°F. Data for the continued cooldown will be based upon the St. Lucie Unit 2 EPU Steam Generator Tube Rupture event. Due to the nature of the SBO event response, steam releases are calculated for three distinct phases:

1. Event Start to 30 minutes

2. 30 minutes to 4 hours

3. 4 hours until the RCS reaches 212°F

The steam release data is given in units of total mass for selected time intervals. The release rates are applied as constant values over the duration of each period. The steam release rate from the Steam Generators is provided in Table 15.10-10.

For this analysis, tube uncovery coincident with the reactor trip is assumed. Therefore, a portion of the steam generator leakage will flash to vapor. The flashed portion of the tube leakage is assumed to be released directly into the steam generator steam space and does not mix with the fluid in the secondary. The flashed portion of the total leakage flow must be accounted for in determining the flow rate. Information provided for the Steam Generator Tube Rupture event gives a reliable indication of the RCS conditions immediately following a reactor trip to calculate a post-trip flashing fraction of 0.06. Auxiliary Feedwater is credited with restoring water levels in the steam generator secondary to above the top of the tube bundle within 60 minutes. Therefore, the flashed tube leakage rates developed from the post-trip flashing fraction of 6% applied to the values for the first hour are shown in Table 15.10-8. The unflashed SG Tube Leakage is given in Table 15.10-9.

The control room normal ventilation flow rate is listed as 1000 cfm. Since all power is lost at the start of this event, this flow rate is initially set to zero.

Since the control room ventilation system is assumed to remain in the normal configuration, the emergency control room ventilation makeup flow rate is set to zero for the duration of the event.

The unfiltered inleakage was set to 395 cfm. Although forced convection through the control room is unavailable during the first 4 hours of this event, this inleakage is assumed to remain constant during all modes of control room ventilation system operation.

The control room exhaust is equal to the sum of the control room intake and inleakage flows.

It is assumed that control room ventilation will be established in the normal mode when offsite power is restored after 4 hours.

As summary of the radiological consequences is presented in Table 15.10-11.

15.10.5 CONCLUSIONS

The maximum RCS pressure is 2389 2404 psia (including reactor coolant pump and elevation heads). This is well below 110 percent of design pressure.

Natural circulation is maintained for at least the 4 hour period that offsite AC power and diesel generator power are assumed unavailable. During this time voids are restricted to the reactor vessel head and subcooling is maintained in the hot leg.

The radiological consequences due to a Station Blackout are summarized in Table 15.10-12.

The core is determined to be maintained in a subcritical post-trip condition for the SBO event by the fact that the core reactivity never exceeds a total reactivity of -3290 pcm.

No fuel damage occurs during this event.

AREVA Conclusion

Other than the short period before reactor trip, which is bounded by UFSAR event 15.3.2 (Complete Loss of Forced Reactor Coolant Flow), fuel design parameters are not key parameters for this event. Therefore, this event does not require a re-analysis for the fuel transition. EC287528

15.10.6 DELETED

15.10.7 References for Section 15.10

1. FPL letter L-92-106 dated 4/21/92, Bohlke to NRC, "St. Lucie Unit 2, Docket No. 50-389, Prepared License Amendment, Safety Injection Tank Pressure Reduction"

TABLE 15.10-1

SEQUENCE OF EVENTS, CORRESPONDING TIMES AND SUMMARY OF RESULTS FOR THE STATION BLACKOUT EVENT

Time (Sec)	Event	Setpoint or Value
0 – 20.0	Steady State Period	---
20.0	Loss of all on- and offsite AC power and loss of main feedwater	--- ---
21.6	Reactor trip signal on low RCS flow	91.9%
22.3	Maximum core power	102.3%
25.2	Maximum RCS pressure	2404 psia
25.6	Maximum pressurizer pressure	2382 psia
26.8	MSIVs Close	---
27.7	Main steam safety valves open	1000 psia
33.4 1187.6	Maximum secondary system pressure Auxiliary feedwater actuation signal	1015 psia 5% NRS
1517.6	Auxiliary feedwater reaches the steam generators	500 gpm total
1820	Operator opens and controls ADVs Main Steam Safety Valves close Total Main Steam Safety Valve Release	99500 psia 995 psia 314,700 lbm
8620	Operators act to reduce steam pressure to cool the primary RCS via ADV control	---
40	Voiding occurs in reactor vessel upper head Pressurizer is empty Minimum Hot Leg Subcooling Margin	--- --- 26.3°F
14420	1. Operator restores AC power 2. Total atmospheric dump valve release	 418,600 lbm

TABLE 15.10-2

ASSUMED INITIAL CONDITIONS FOR
STATION BLACKOUT ANALYSIS

PARAMETER	ASSUMED VALUE
Initial Core Power Level, MWt	3030
Core Inlet Coolant Temperature, °F	
High Tavg Nominal Value, °F	578.5
Low Tavg Nominal Value, °F	563
Core Volumetric Loop Flow, gpm	187500
Pressurizer Pressure, psia	2250
Initial Pressurizer Water Volume, % Level	63
Steam. Generator Water Level, % of Narrow Range Tap Span	65
Moderator Temperature Coefficient, 10^{-4} Δρ/°F	-0.91
CEA Worth for Trip, 10^{-2} Δρ	-5.20
Primary Coolant Leakage, gpm:	16

TABLE 15.10-3

DISPOSITION OF NORMALLY OPERATING SYSTEM
FOR STATION BLACKOUT

System	Normal Automatic Mode Throughout Transient	Manual Mode Through-Out Transient	Normal Automatic Mode Inoperative on Loss of AC	Manual Mode Inopera-tive on Loss of AC	Failure Assumed Within System	Associated Notes
1. Main Feedwater System			X			
2. Turbine-Generator Control System	X					
3. Steam Bypass Control System				X		
4. Pressurizer Pressure Control System				X		2
5. Pressurizer Level Control System				X		
6. Control Element Drive Mechanism Control System	X					
7. Reactor Regulating System				X		
8. Reactor Coolant Pumps				X		1
9. Chemical and Volume Control System				X		2
10. Condenser Evacuation System				X		
11. Turbine Gland Sealing System				X		
12. Component Cooling Water System						2
13. Turbine Cooling Water System				X		
14. Intake Cooling Water System						2
15. Condensate Transfer System				X		
16. Circulating Water System				X		
17. Spent Fuel Pool Cooling System				X		2
18. AC Power (Nonsafety)			X			
19. AC Power (Safety)					X	3
20. DC Power		X				
21. Power-operated Relief Valves	X					
22. Instrument Air System			X			2
23. Waste Management-Liquid				X		

NOTES:
1. RCP bleedoff is not isolated during this event.
2. Portions of these systems, powered by the safety bus on loss of AC, are not available due to the failure of both diesel generators.
3. Only the AC power supplied through the inverters is available.

TABLE 15.10-4

UTILIZATION OF SAFETY SYSTEMS
FOR STATION BLACKOUT

	Actuated and Required	Actuated But Not Required	Safety Grade Backup To Nonsafety Grade System	Failure Assumed Within System (See Notes)	Associated Notes
1. Reactor Protection System	X				
2. Engineered Safety Features Actuation Systems					2
3. Diesel Generators and Support Systems				X	1
4. Reactor Trip Switchgear	X				
5. Main Steam Safety Valves	X				
6. Pressurizer Safety Valves			X		
7. Main Steam Isolation Valves		X			2
8. Main Feedwater Isolation Valves			X		
9. Auxiliary Feedwater System	X				2,4
10. Safety Injection System					3
11. Shutdown Cooling System (CCW & ICW)					
12. Atmospheric Dump Valve System	X				5
13. Containment Isolation System		X			6
14. Containment Spray System					
15. Iodine Removal System					
16. Containment Combustible Gas Control System					
17. Containment Cooling System					

NOTES:
1. Both diesel generators fail for this event
2. Only those portions powered from the safeguard batteries are available.
3. Safety Injection Tanks are available.
4. Auxiliary Feedwater is automatically actuated. Only the turbine driven pump is available.
5. ADVs can be manually operated from the control room.
6. Portions of this system are actuated on loss of instrument air.

Systems not checked are not utilized during this event.

TABLE 15.10-5

STATION BATTERY LOSS OF AC

1	2	3	4	5	6	7
Profile Internal, n (See Note 1)	Load Supplied (amps) (See Note 1)	Interval Duration (minutes) (See Note 1)	Amp-Hours Consumed Per Interval [A-hr] (See Note 2)	Cumulative Amp-Hours Consumed [A-hr] (See Note 3)	Cumulative Amp-Hour Rating [A-hr] (See Note 4)	Corrected Amp-Hour Rating (apply 1.19 temp correction factor) (See Note 5)
1	598	1	10.0	10.0	50.67	42.6
2	320	238	1269.3	1279.3	2052	1724.4
3	385	1	6.4	1285.7	2052	1724.4

NOTES:

(1) Data taken from battery load profile graph (see Figure 15.10-13).

(2) amp-hours consumed = $\frac{\text{(column \#2 data) x (column \#3 data)}}{\frac{\text{60 min}}{\text{hr}}}$

(3) Cumulative amp-hours consumed = $\sum_{k=1}^{n}$ (column #4 data)$_k$

(4) Cumulative amp-hour rating: manufacturer's specification based on battery discharge to 1.75V per cell. Refer to the latest design margin calculation for current battery discharge results and voltage requirements.

(5) Corrected amp-hour rating = (column #6 data)/1.19
(electrolyte temperature correction for 10°C)

TABLE 15.10-6 HAS BEEN DELETED

TABLE 15.10-7
STATION BLACKOUT EVENT INVENTORY SUMMARY

	PRESS PSIG	INTEGRATED SIT, lbm	INTEGRATED LEAK, lbm	CESEC THERMAL-HYDRAULIC SUMMARY				RCS w/o UPH MASS, lbm	RCS TOTAL MASS, lbm
TIME				PZR MASS, lbm	RCS Inc UPH MASS, lbm	UPPER HEAD MASS, lbm	UPPER HEAD VOID FRACT		
A	B	C	D	E	F	G	H	I	J
12000	632.9	0.0	10215.4	7.5710E+03	4.4990E+05	8.5076E+03	8.7677E-01	441392.4	457471
12200	622.3	0.0	10332.8	8.6070E+03	4.4880E+05	9.0452E+03	8.6696E-01	439754.8	457407
12400	598.2	0.0	10445.4	8.3660E+03	4.4890E+05	9.1083E+03	8.6547E-01	439791.7	457266
12600	559.1	2352.1	10560.8	4.8990E+03	4.5580E+05	8.3772E+03	8.7782E-01	447422.8	460699
12800	549.7	3707.9	10678	6.0010E+03	4.5660E+05	8.7643E+03	8.7086E-01	447835.7	462601
13000	544.5	4411.1	10790.2	7.7420E+03	4.5570E+05	9.2671E+03	8.6196E-01	446432.9	463442
13200	539.1	5226.5	10899.4	9.3640E+03	4.5510E+05	9.7185E+03	8.5398E-01	445381.5	464464
13400	531.5	6259.9	11005.2	1.0760E+04	4.5520E+05	1.0093E+04	8.4734E-01	445107	465960
13600	508.1	9964.3	11115.6	1.0350E+04	4.612E+05	1.0127E+04	8.4657E-01	451073	471550
13800	501.2	11092.6	11226.6	1.1840E+04	4.614E+05	1.0396E+04	8.4185E-01	451004	473240
14000	496.6	11824.4	11333.4	1.3670E-04	4.607E+05	1.0889E+04	8.3328E-01	449811	474370
DIFF		11824.4	1118	6.0990E+03	1.0800E+04	2.3814E+03		8418.6	16899

DESCRIPTION OF COLUMN HEADINGS
A) TIME (SECONDS
B) RCS PRESSURE (PSIG)
C) INTEGRATED SIT DISCHARGE (LBM)
D) INTEGRATED LEAK FROM RCS, TOTALED FOR THE TWO SIMULATED LEAKS (LBM)
E) TOTAL PRESSURIZER MASS. PRESSURIZER LIQUID PLUS STEAM MASS (LBM)
F) MASS OF RCS PLUS SURGE LINE (LBM)
G) MASS IN THE UPPER HEAD (LBM)
H) UPPER HEAD VOID FRACTION
I) MASS IN THE RCS LOOP, EXCLUDING MASS OF PRESSURIZER AND UPPER HEAD (LBM)
OBTAINED BY SUBTRACTING COLUMN G FROM F
J) TOTAL RCS MASS, INCLUDING THE PRESSURIZER AND UPPER HEAD MASSES (LBM)
OBTAINED BY ADDING COLUMNS E AND F
DIFF: THE LAST ROW PROVIDES THE MASS DIFFERENCE BETWEEN 14000 AND 12000 SECONDS FOR EACH PARAMETER

TABLE 15.10-8

Flashed Steam Generator Tube Leakage

Time (hours)	Flow Rate (lb/min)
0.00	0.19
1.00	0.000

TABLE 15.10-9

Unflashed Steam Generator Tube Leakage

Time (hours)	Flow Rate (lb/min)
0	2.95
0.50	2.95
1.00	3.52
4.00	3.46
5.00	3.52
6.00	3.63
8.00	3.73
10.00	3.86
13.00	4.03
17.00	0.00

TABLE 15.10-10

Steam Generator Steam Release

Time (hours)	Flow Rate (lb/min)
0	4479
0.50	1993
1.00	1993
4.00	3402
5.00	3148
6.00	2850
8.00	2559
10.00	2314
13.00	2064
17.00	0.00

TABLE 15.10-11

Control Room X/Qs

Time (hours)	X/Q (sec/m^3)
0	3.13E-03
2	2.51E-03
8	9.06E-04
24	7.50E-04
96	6.24E-04
720	6.24E-04

TABLE 15.10-12

Station Blackout Dose Summary

Dose Contribution	**TEDE Dose (rem)**		
	EAB	**LPZ**	**CR**
Total	4.31E-04	1.30E-03	0.20
Acceptance Criteria	*2.5*	*2.5*	*5*

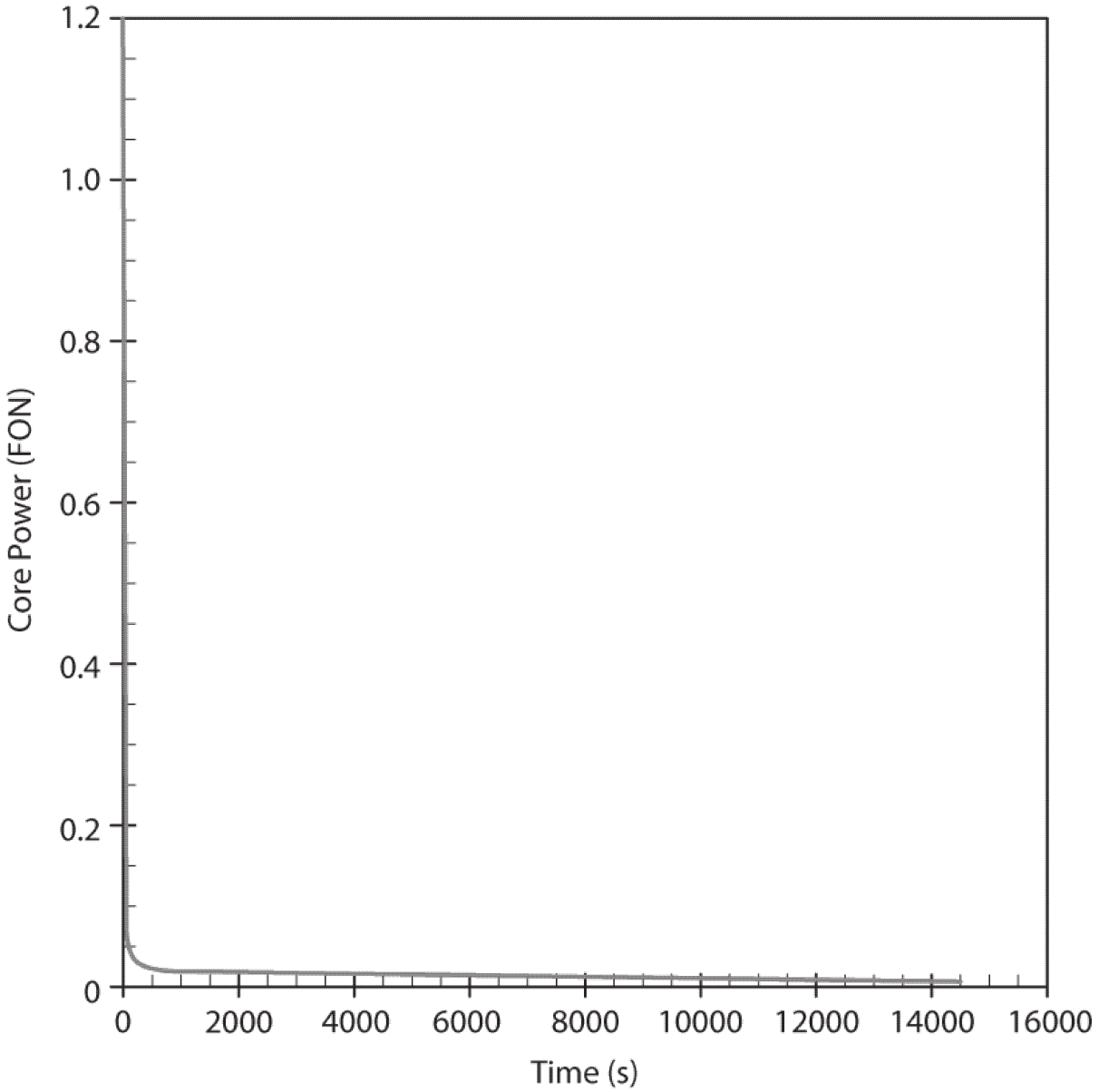

FLORIDA POWER & LIGHT COMPANY
ST. LUCIE PLANT UNIT 2

FIGURE 15.10-1

Station Blackout Event
Core Power versus Time

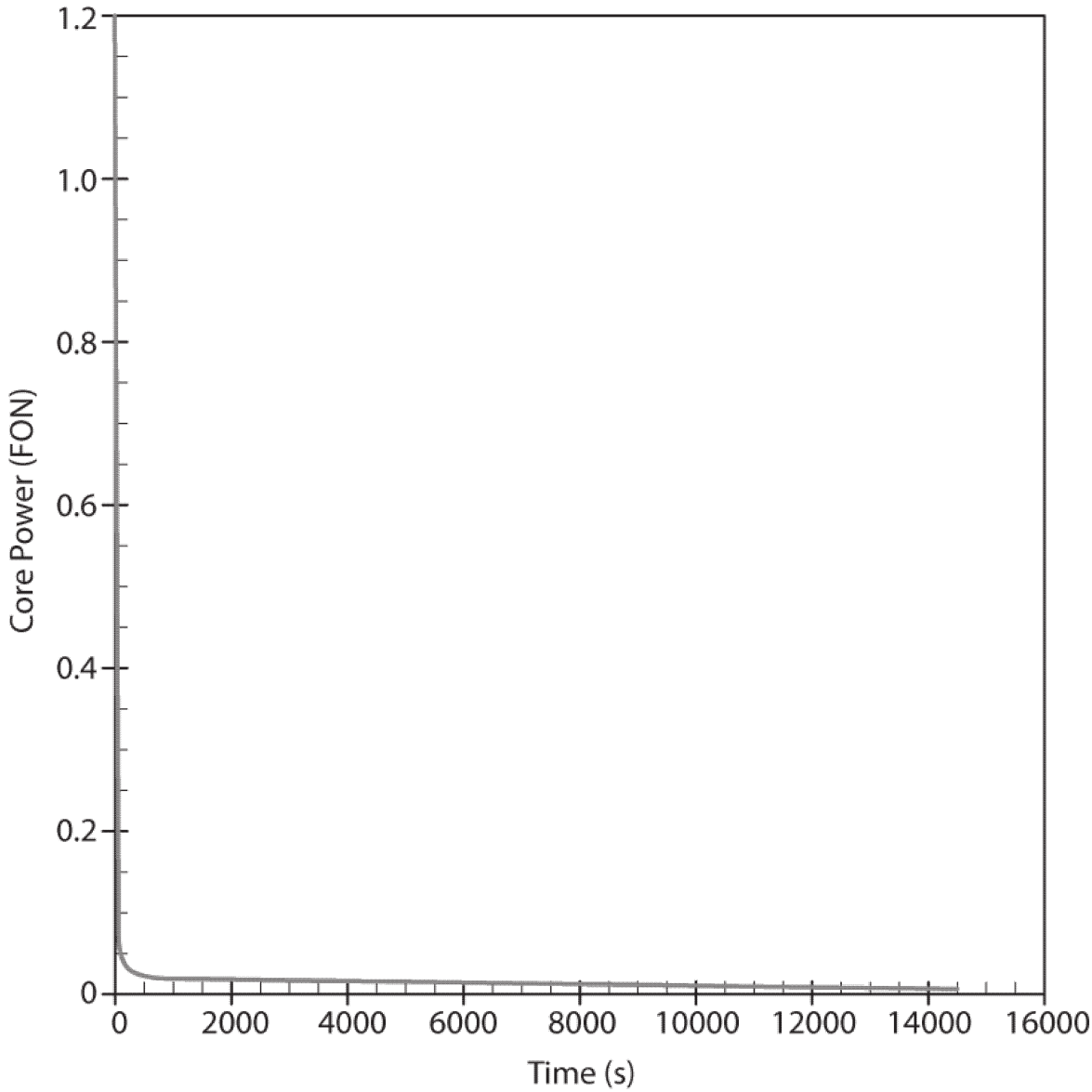

FLORIDA POWER & LIGHT COMPANY
ST. LUCIE PLANT UNIT 2

FIGURE 15.10-2

Station Blackout Event
Core Avg. Heat Flux versus Time

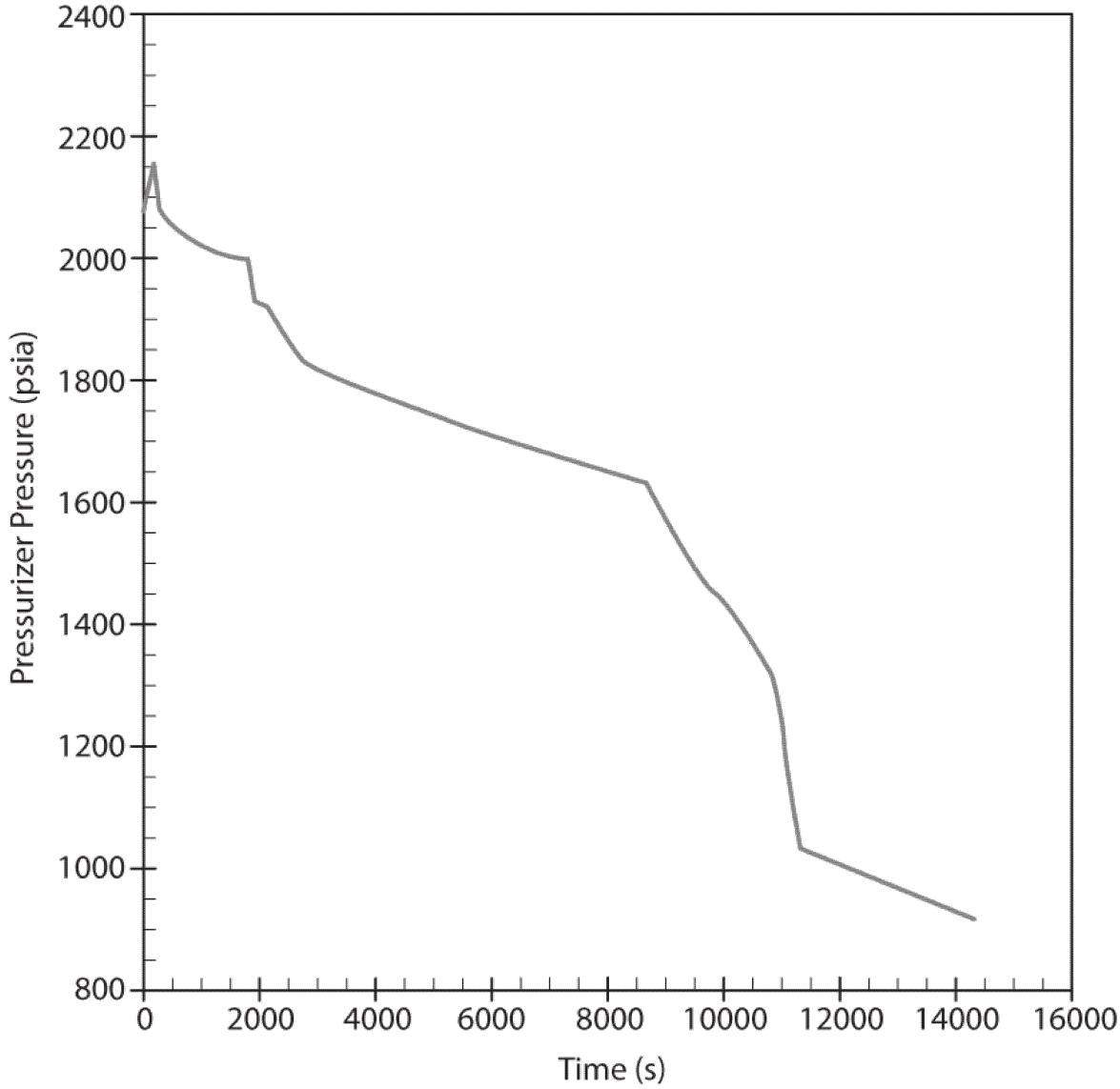

FLORIDA POWER & LIGHT COMPANY
ST. LUCIE PLANT UNIT 2

FIGURE 15.10-3

Station Blackout Event
Pressurizer Pressure versus Time

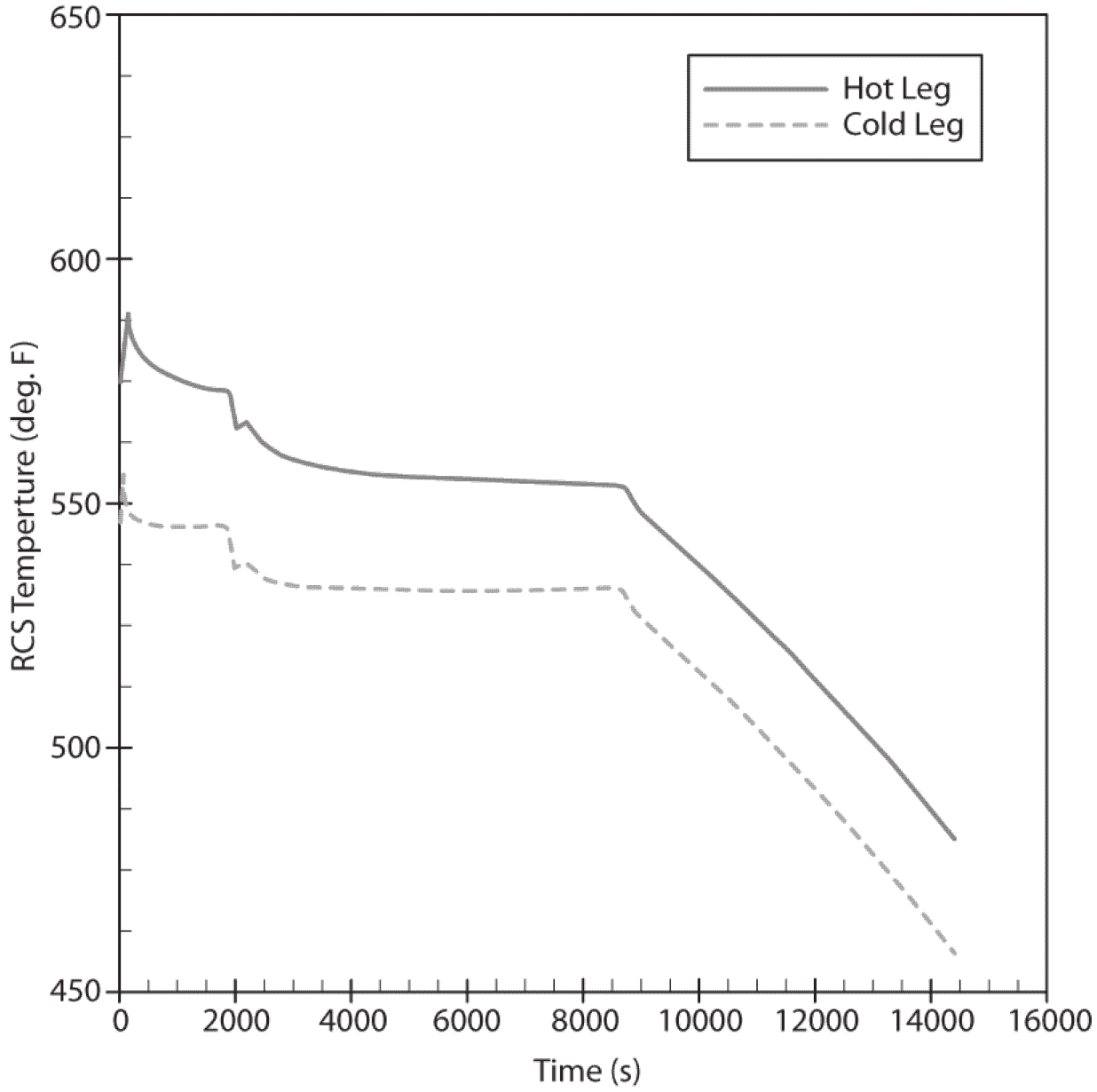

FLORIDA POWER & LIGHT COMPANY
ST. LUCIE PLANT UNIT 2

FIGURE 15.10-4

Station Blackout Event
RCS Temperatures versus Time

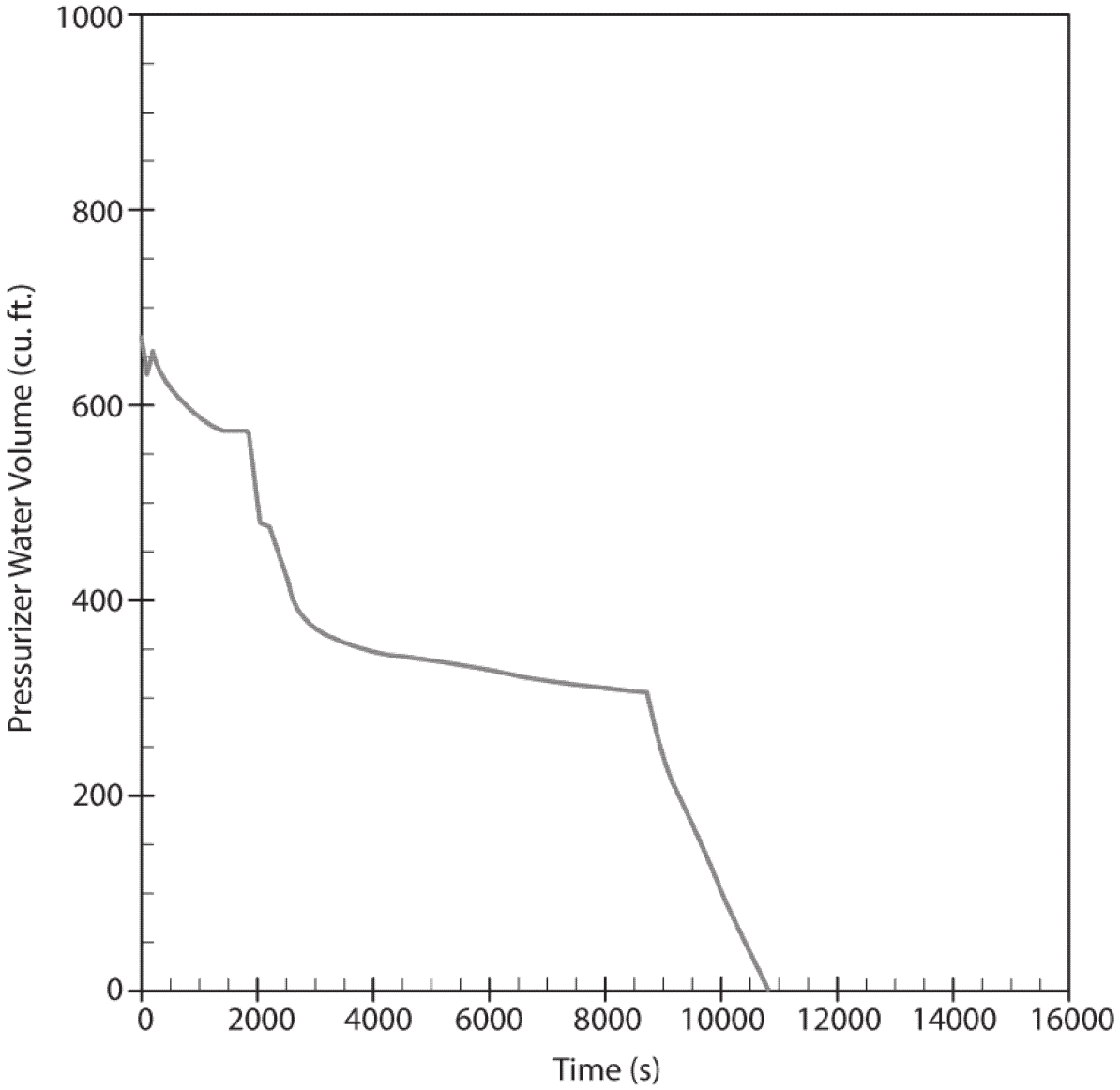

FLORIDA POWER & LIGHT COMPANY
ST. LUCIE PLANT UNIT 2

FIGURE 15.10-5

Station Blackout Event
Pressurizer Water Volume versus Time

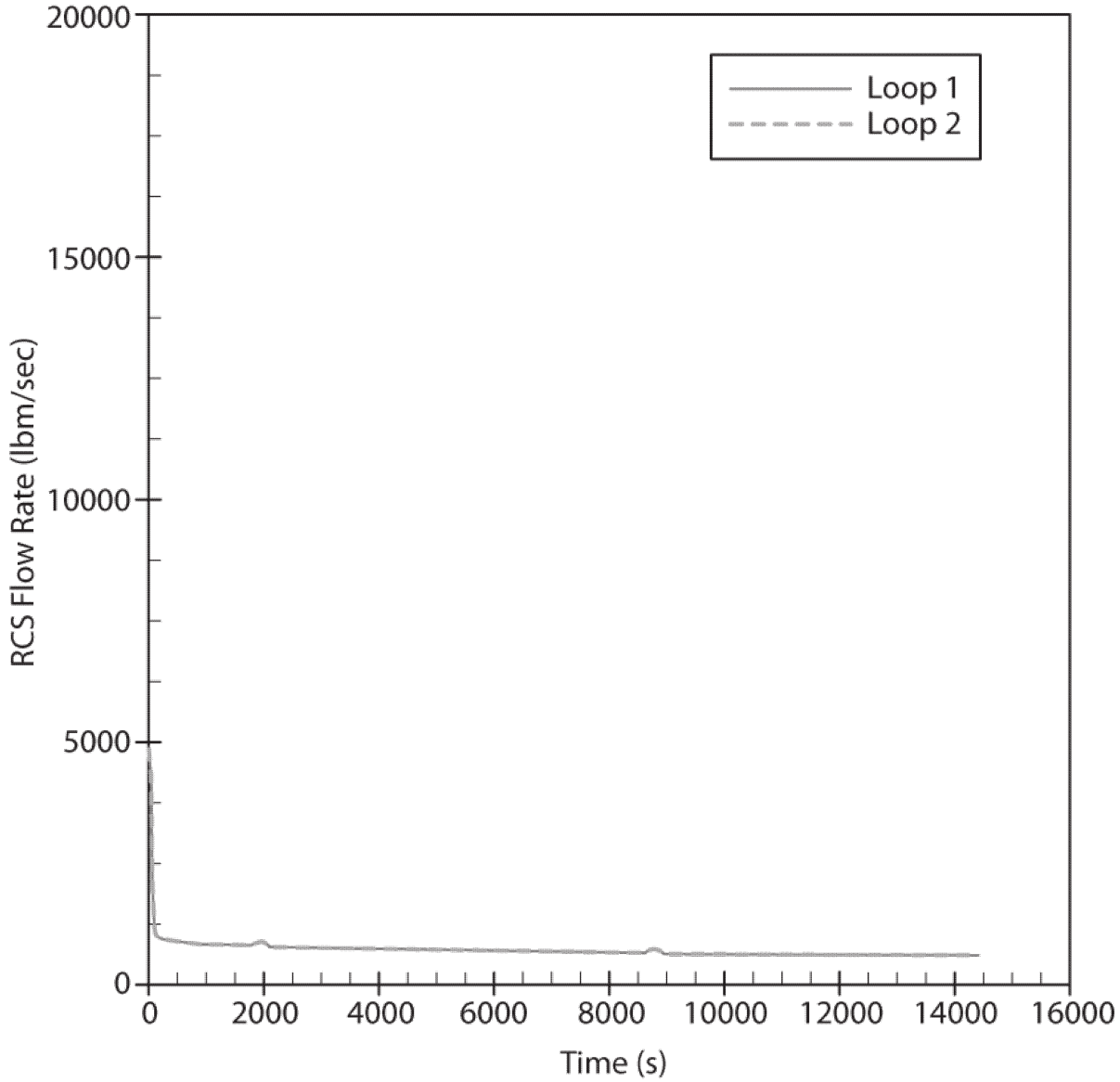

FLORIDA POWER & LIGHT COMPANY
ST. LUCIE PLANT UNIT 2

FIGURE 15.10-6
Station Blackout Event
Reactor Coolant Flow Rate versus Time

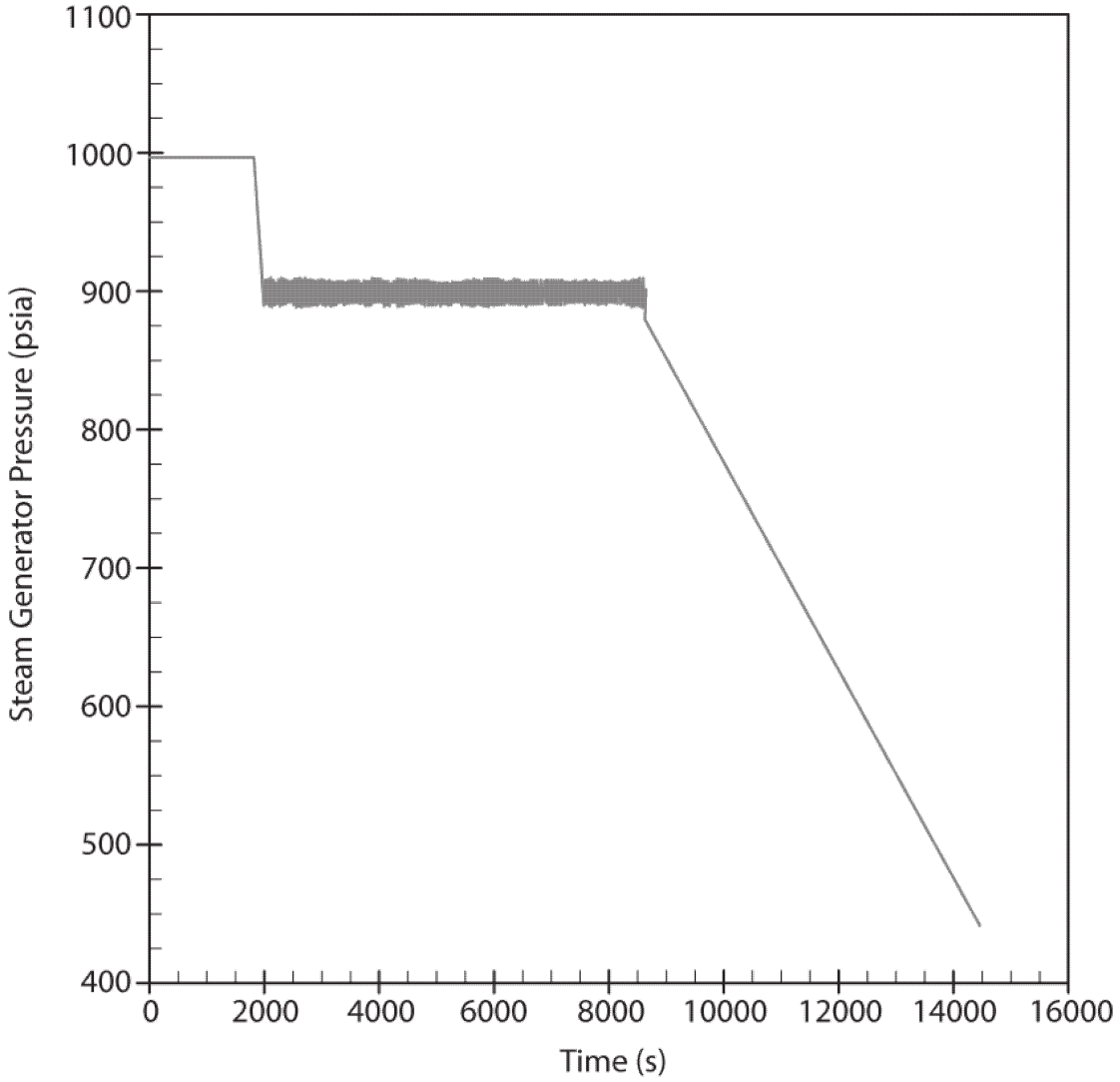

FLORIDA POWER & LIGHT COMPANY
ST. LUCIE PLANT UNIT 2

FIGURE 15.10-7

Station Blackout Event
Steam Generator Pressure versus Time

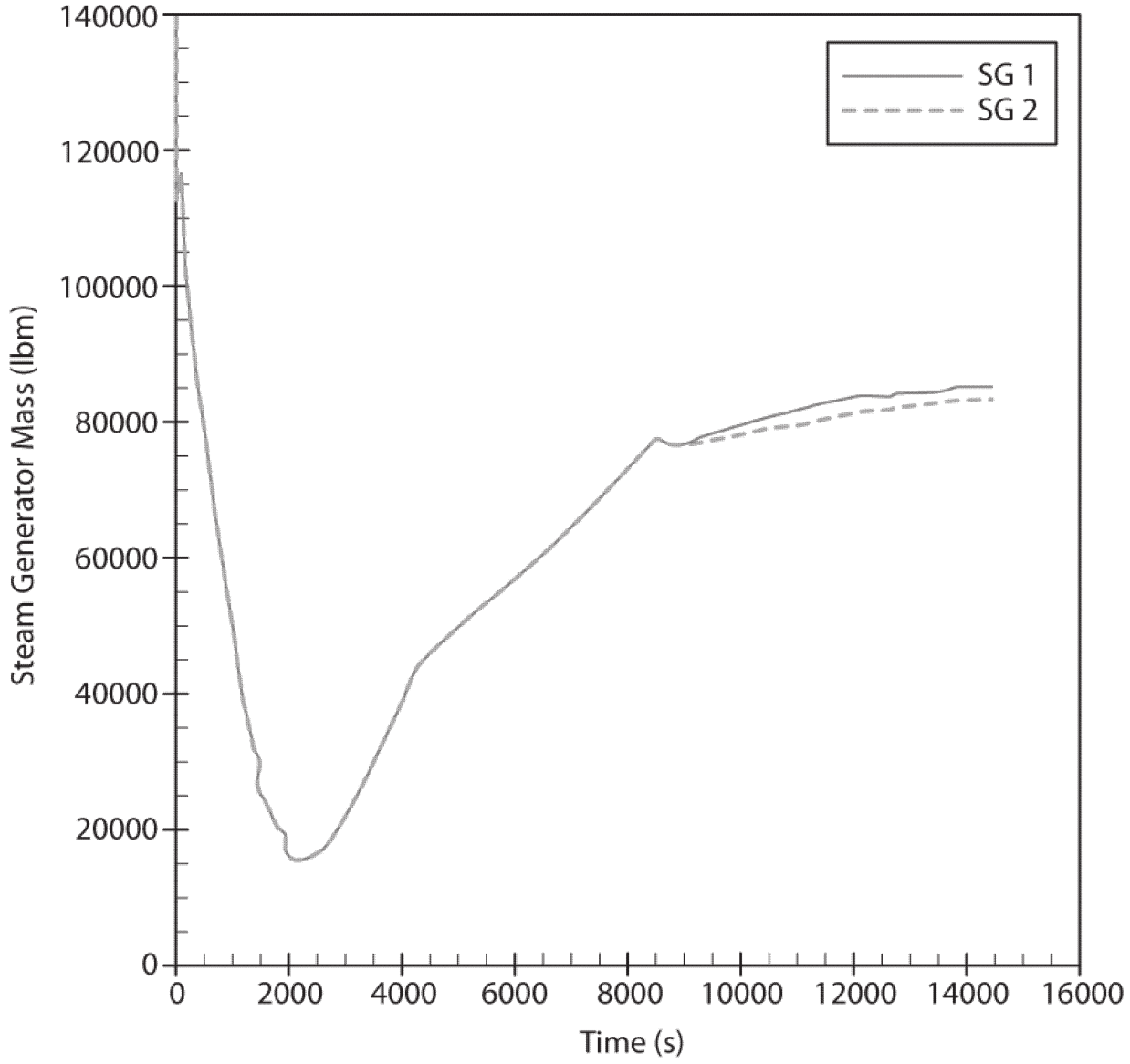

FLORIDA POWER & LIGHT COMPANY
ST. LUCIE PLANT UNIT 2

FIGURE 15.10-8

Station Blackout Event
Steam Generator Water Mass versus Time

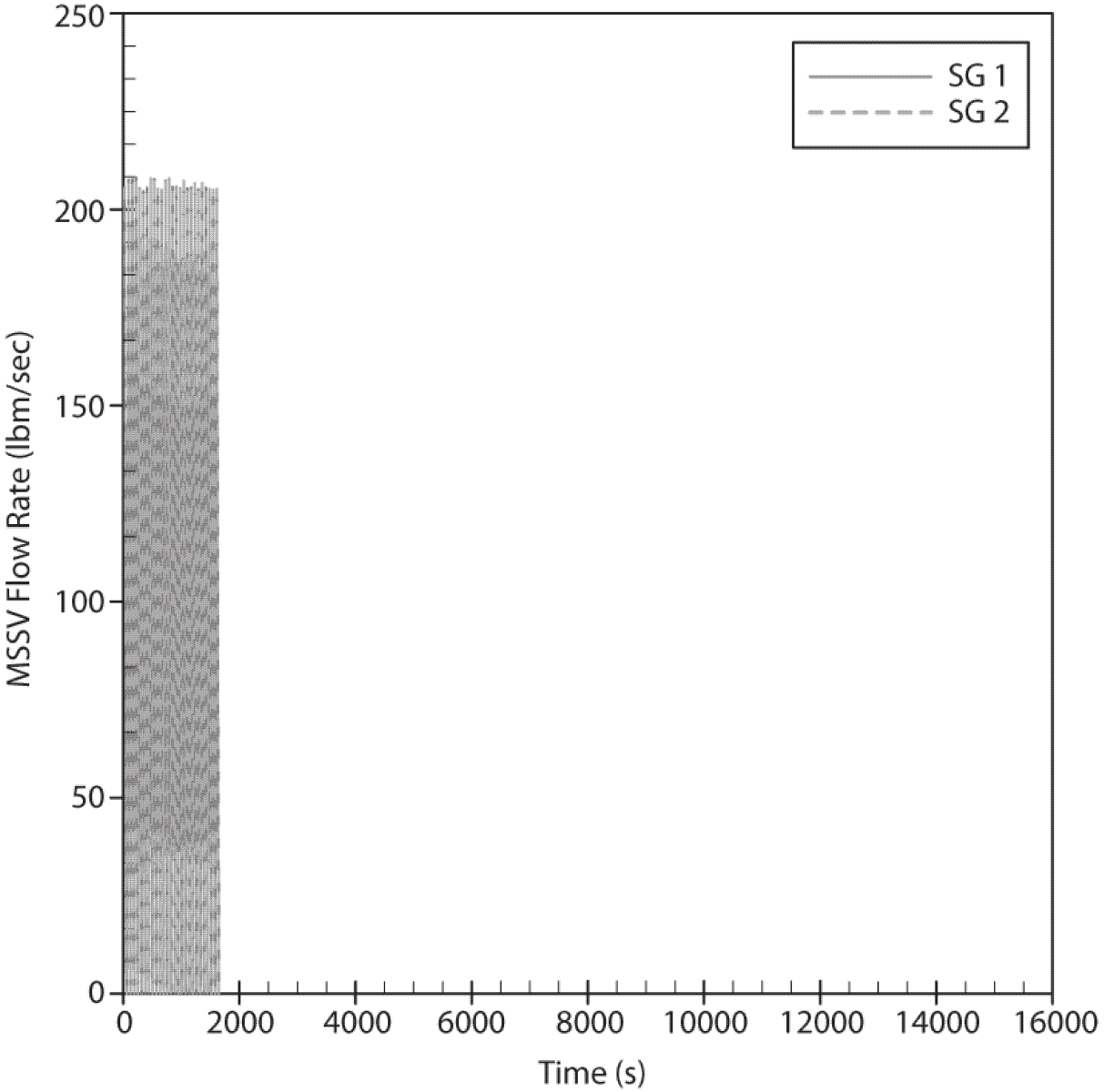

FLORIDA POWER & LIGHT COMPANY
ST. LUCIE PLANT UNIT 2

FIGURE 15.10-9

Station Blackout Event
MSSV Flow Rate versus Time

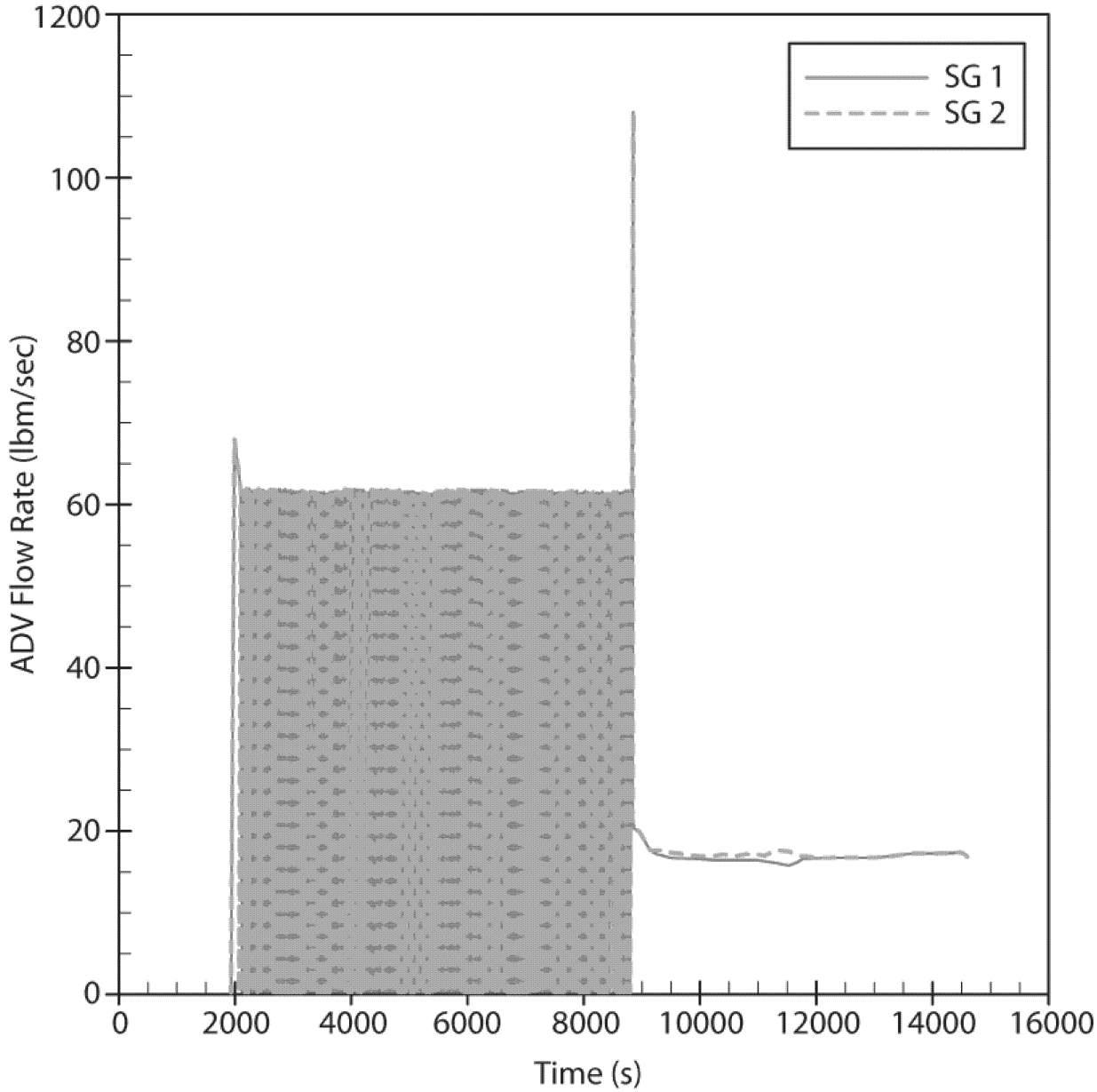

FLORIDA POWER & LIGHT COMPANY
ST. LUCIE PLANT UNIT 2

FIGURE 15.10-10

Station Blackout Event
ADV Flow Rate versus Time

THIS FIGURE HAS BEEN DELETED

THIS FIGURE HAS BEEN DELETED

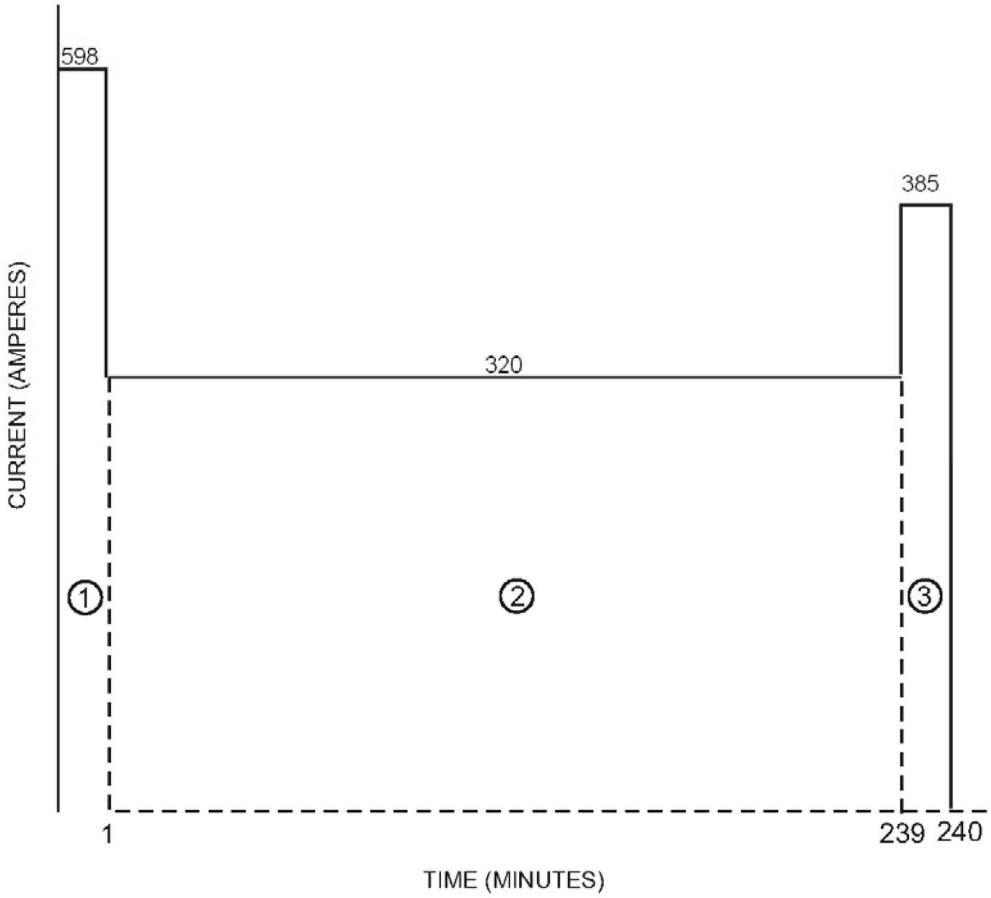

Amendment No. 20 (05/11)

FLORIDA POWER & LIGHT COMPANY
ST. LUCIE PLANT UNIT 2

SAFETY BATTERY LOAD PROFILE

FIGURE 15.10-13

15.11 CESEC CYCLE 1

15.11.1 INTRODUCTION

The CESEC digital computer program[1 to 8] provides for the simulation of a Combustion Engineering Nuclear Steam Supply System (NSSS). The program calculates the plant response for non-LOCA (loss of coolant accident) initiating events for a wide range of operating conditions.

The CESEC program, which numerically integrates the one-dimensional conservation equations, assumes a node/flow-path network to model the NSSS. The primary system components considered in the code include the reactor vessel, the reactor core, the primary coolant loops, the pressurizer, the steam generators, and the reactor coolant pumps (see Figure 15.11-1). The secondary system components, shown on Figure 15.11-2, include the secondary side of the steam generators, the Main Steam System, the Feedwater System, and the various steam control valves. In addition, the program models some of the control and plant protection systems.

The code self-initializes for any given, but consistent, set of reactor power level, reactor coolant flow rate, and steam generator power sharing. During the transient calculation, the time rate of change in system pressure and enthalpy are obtained from the solution of the conservation equations. These derivatives are then numerically integrated in time, under the assumption of thermal equilibrium, to give the system pressure and nodal enthalpies. The fluid states recognized by the code are subcooled and saturated; superheating is allowed in the pressurizer. The fluid in the Reactor Coolant System is assumed to be homogeneous.

In the subsections which follow, a short description of the major code models which comprise the present version of CESEC called CESEC-II is provided. Section 15.11.11 provides a brief description of the models which are specific for the analysis of the steam line break event. These models can be exercised by attaching the steam line break version of CESEC which is referred to as CESEC-SLB.

15.11.2 PRIMARY COOLANT THERMAL-HYDRAULIC MODEL

The CESEC-II code uses a node/flow-path type network to model the Reactor Coolant System. The conservation of mass and energy equations are solved for control volumes or nodes. The steady state form of the conservation of momentum equation is assumed with the further assumption of a uniform pressure around the reactor coolant loops.

The Reactor Coolant System, consisting of two reactor coolant loops, the reactor vessel, and the pressurizer is divided into 16 nodes of constant volume. The nodes are chosen to appropriately simulate the RCS component volumes (see Figure 15.11-3) and, thus, provide an adequate description of the spatial variation of the coolant properties. Node 1, which is the pressurizer node, is subdivided into a steam and a liquid region having variable volumes. The fluid in nodes 2-16 is assumed to be homogeneous and in thermal equilibrium. The conservation of mass and energy equations for a typical constant volume node, i, are provided on Figure 15.11-4. The reactor coolant pump flow is specified by a user input table. The system of equation is solved for the time derivatives of the RCS pressure and the nodal enthalpies, the surge line flow, and the rate of vaporization and/or condensation in the pressurizer. The time derivatives are updated using an explicit forward difference scheme.

15.11.3 PRESSURIZER

The CESEC-II pressurizer model assumes both the steam and the liquid regions to exist for any of the eight thermal-hydraulic states shown in Figure 15.11-5. The model considers such components as sprays, heaters, and relief/safety valves. The Pressurizer Level Control System which controls charging flow and letdown flow by means of pressurizer level setpoints, is also modeled (see Section 15.11.7). The loss of heat through the pressurizer wall is accounted for in the conservation of energy equation.

The mass and energy transport between the two fluid regions is assumed to occur only as a result of liquid vaporization and/or steam condensation. The spray flow which enters the pressurizer is assumed to condense the steam if it is in the saturation state. That is, when the steam region is at saturation, the spray droplets are assumed to reach saturation temperature and will result in bulk condensation of the steam. However, when the steam region is superheated, the spray droplets are assumed to evaporate into the steam region.

The code models two spray operating modes, continuous and proportional. The continuous mode spray is a user input constant flow which is added continuously to the pressurizer. The proportional mode spray flow originates at the pump discharge in the RCS loop and is linked to the pressurizer as shown on Figure 15.11-3. The spray flow for the proportional mode is controlled automatically by two pressure setpoints which turn the spray on and off, respectively. Within these two setpoints, the spray flow increases linearly with the pressurizer pressure.

The code also models two types of heaters located near the bottom of the pressurizer: (1) the proportional heaters which are controlled by the Pressurizer Pressure Control System to generate heat at a rate which decreases linearly with increasing pressure between two pressure setpoints and (2) the backup heaters which turn on and off at two pressure setpoints. In addition, the backup heaters are also controlled by the measured deviation of the pressurizer liquid level from the programmed level. The addition of heat from heaters to the fluid is accounted for in the conservation of energy equation.

CESEC-II models the operation of the pressurizer safety valves. Figure 15.11-6 shows the valve opening and closing characteristics programmed in the code. The input parameters are the opening pressure, the accumulation and blowdown pressures which are input as percent of the opening pressure, and the fractional opening area at the corresponding pressures. Up to five individual valves may be simulated by the code. Various valve failure conditions may be modeled through user options on a per valve basis. When the valve opens, the discharge of the pressurizer fluid, either steam or water, is assumed to be choked. The critical flow is calculated by using the appropriate critical flow calculational model (See Section 15.11.10).

The surge line volume is included in the pressurizer control volume. The surge line flow is solved for when solving the set of equations representing the Reactor Coolant System. This flow is then used to calculate the pressure drop within the surge line due to frictional losses.

15.11.4 REACTOR KINETICS

The energy source in the CESEC-II code is from fission in the fuel. The core is represented by a cylindrical fuel rod located in an average coolant channel. This fission energy consists of two parts, the instantaneous fission power and the decay power released by the fission products. The instantaneous power is determined by solving the standard point kinetics neutron equations

with six delayed neutron groups white the decay power is calculated from an 11 fission product group decay heat model.

The power level is a function of the reactivity term in the point kinetics equation. In CESEC-II, the total reactivity is calculated as the sum of the control rods, moderator, fuel temperature (Doppler), and boron contributions. The code also has an explicit function of time simulating the control rod reactivity insertion. A table of rod reactivity versus time after initiation of scram is user input. The moderator feedback effects considered include the moderator density or the moderator temperature. The moderator and Doppler reactivity feedback terms are calculated at each time step by interpolation of user input tables. The boron reactivity effect includes the contribution from the Safety Injection System and the letdown and charging portions of the Chemical and Volume Control System.

The kinetics equation is solved numerically by a fourth order Runge-Kutta/ Merson method for the power generation at each time step.

15.11.5 HEAT TRANSFER WITHIN THE CORE

The CESEC-II core heat transfer model represents a fuel rod at core average conditions. The cylindrical configuration models the fuel, gap and clad. The fuel rod is divided into three equal-volume radial nodes (see Figure 15.11-7). The third radial node is assumed to contain the outer portion of the fuel, the gap, and the clad. The radial energy equation (see Figure 15.11-7) is formulated for each node with the nodal properties (e.g., specific heat and thermal conductivity of fuel and clad) determined by temperature dependent correlations. The input parameters required by the model include the fractions of power generated within the fuel, the clad, and the moderator respectively, and the gap conductance, which is assumed to be a constant. Within the fuel region, a uniform power distribution is assumed by the code.

The heat transfer at the clad - coolant interface is assumed to be given by the following correlation for all fluid conditions (Reference 6):

$$h = 0.148\,(1+0.01T - 0.00001T^2)\,\frac{V^{0.8}}{D^{0.2}} \qquad (15.11.5.1)$$

Where:

T = fluid temperature

V = fluid velocity

D = channel hydraulic diameter

Initially, the steady state fuel temperature distribution is determined by a scheme which solves the radial energy equation iteratively based on the initial reactor power output, the gap conductance, and the initial coolant condition. The radial energy equation is solved numerically at each time step by a fourth order Runge-Kutta/Merson method.

15.11.6 STEAM GENERATOR MODEL

The CESEC-II steam generator model performs a detailed computation of the overall heat transfer coefficient for each steam generator. The heat transfer correlation used in the primary

side for calculating the film resistance is the same as for the core. The secondary side heat transfer mechanism is pool boiling. The boiling resistance is calculated using the modified Rohsenow pool boiling correlation[6].

$$h_{sec} = K_R \left(\frac{q}{A}\right)^{2/3} \qquad (15.11.6.1)$$

where

q	=	heat rate
A	=	heat transfer area
K_R	=	a constant experimentally determined at CE and is a function of the secondary side pressure

The heat transfer between the primary and secondary sides of the steam generator is calculated using a logarithmic mean temperature difference (see Figure 15.11-8). The overall heat transfer coefficient is determined from the film resistance of the primary and secondary sides, the tube wall resistance, and the tube fouling resistance. The tube wall/fouling resistance is determined initially by the design full power condition and is assumed to be constant thereafter during the transient.

The secondary side of each steam generator is represented by a control volume. The control volume consists of saturated liquid and steam. The fluid properties and mass inventory are determined by solving the conservation of mass and energy equations shown on Figure 15.11-9. The initial conditions of the secondary side of the steam generator are determined by iterating on the secondary pressure given the initial heat flux and power demand as specified by the user. During the transient calculation, the modes of heat transfer are generally valid for all transient conditions and include reverse heat transfer. That is, the condition during which the primary side coolant temperature is lower than the secondary temperature.

The CESEC-II code has an input option which allows the steam generator heat transfer area to be reduced on decreasing secondary water mass. It is assumed in this option that the steam generator area is linearly proportional to the steam generator water mass between two setpoints representing full and zero heat transfer, respectively.

The feedwater flow is optionally determined in CESEC-II by the following three methods: 1) matching the steam flow, 2) input table of flow rate versus time, 3) automatic feedwater control on the steam generator water level. The initial feedwater flow is assumed to match that corresponding to the power level at time zero. The flow during an event is calculated according to the user option selected. The feedwater isolation valves are programmed to close at a specified rate of closure following the main steam isolation signal which is actuated on low steam generator pressure. The feedwater enthalpy can be specified by input tables of enthalpy as a function of either power level or time.

The CESEC-II also models the auxiliary feedwater. Both the feedwater flow rate and enthalpy are specified by input tables as a function of time.

The path of the steam flow from the secondary side of the steam generator is illustrated on Figure 15.11-2. Downstream of the main steam isolation valve, the main steam lines from each steam generator are connected together at a common steam header. At the initial steady state, the steam flow in each steam line is determined consistent with the reactor coolant flow rate in each steam generator loop.

During the transient calculation, the steam flow is determined by the turbine power demand, the operation of the secondary valves, and (for steam line break events) the break flow rate.

The code simulates the turbine stop and admission valves, the steam dump and bypass valves, the main steam safety valves, the atmospheric dump valves, and the main steam isolation valves. The steam flow through each valve is assumed to be choked. Thus, a critical flow correlation (see Section 15.11.10) for steam is used to calculate the flow rate. The control schemes for these valves are briefly described below.

Turbine Admission and Stop Valve

The area of the turbine admission valve is sized at each time step such that the power demand which is input as a tabular function of time is met. At the time of a turbine trip, the valve is closed at a rate specified by a user input to simulate the closing of the turbine stop valves.

Steam Dump and Bypass Valves

The code provides three options for the control of the steam bypass valves:

1. An input table of valve area as a function of time,

2. A proportional-plus-integral-plus derivative (PID) controller model, and

3. A linear control scheme which operates the bypass valves as a function of the steam line header pressure (i.e., the valves start to open when the pressure reaches an input setpoint and then open linearly as the pressure increases). As the pressure drops, the valves will close by following the same path.

Main Steam Safety Valves (MSSVs)

The main steam safety valves are of the accumulation, blowdown type (see Figure 15.11-6). Up to 10 individual banks of valves may be used with associated opening, accumulation, and blowdown pressures. Various types of valve malfunctions, such as valve sticks open, valve sticks closed, and one valve inadvertently opens, can be simulated for each individual valve.

Atmospheric Dump Valves (ADVs)

The operation of the atmospheric dump valves can be simulated by the following four techniques:

1. an input table of valve area as a function of time,

2. a step function control scheme which operates the ADVs as a function of the steam generator pressure and allows the simulation of various types of valves malfunctions

(one valve sticks open, one valve sticks closed, and one valve inadvertently opens initially).

3. a PID controller model, and

4. a control scheme operated on the reactor coolant temperature

Main Steam Isolation Valves (MSIVs)

The code simulates two main steam isolation valves, one for each main steam line. These valves are normally open and do not affect steam generator operation unless the steam generator pressure drops below a specified setpoint. Once this occurs, the MSIVs begin to close after an input delay time. As the MSIVs close, steam flow to the turbine and other downstream components terminates. The steam flow from the main steam safety valves, the atmospheric dump valves, and from a steam line break upstream of the MSIVs is unaffected by MSIV closure.

15.11.7 CHARGING AND LETDOWN

The CESEC-II code provides a model for calculating the charging and letdown flows. The contributions from the charging and letdown flows are included in the conservation of mass and energy equations for the corresponding RCS nodes. Included in the model is a Pressurizer Level Control System which determines the deviation between the measured pressurizer water level and the programmed level. The programmed level is given by an input table as a function of either power or average RCS temperature. The algorithm by which the measured level is calculated is described in Reference 5. The charging flow is provided by a set of constant speed charging pumps, with the charging flow rate automatically controlled by switching each pump on or off at two input level deviation setpoints. The letdown flow control is provided either by a set of letdown control and backpressure valves, with the flow rate either controlled by the opening or the closing of each set of valves at two level deviation setpoints, or by a linear letdown flow control model.

The charging and letdown fluid temperatures are user input. In addition, the letdown fluid temperature can be selected to be that corresponding to the steam generator outlet temperature. The boron concentration from the letdown and charging portion of the Chemical and Volume Control System (CVCS) is only accounted for in CESEC-II when the Safety Injection System is activated. However, the user can optionally turn off the letdown and charging systems and take no credit for the boron reactivity contribution from the letdown and charging systems. The calculation of the boron concentration in the reactor coolant is described in Section 15.11.9.

For a letdown line break event, the code models the heat exchanger between the charging line and the letdown line to obtain the letdown line temperature and the corresponding pressure at the break. Based on this fluid condition, the blowdown rate through the break is determined either by the choked flow model of F J Moody[9] for two-phase flow or by the Bernoulli equation for single phase flow.

15.11.8 REACTOR PROTECTIVE SYSTEM TRIPS

The reactor is shutdown by the insertion of the control element assemblies (CEAs) following the generation of a trip signal. A trip signal is initiated when a certain system parameter reaches a

value which exceeds the corresponding user input trip setpoints. The delay time between the initiation of the trip signal and the start of CEA motion is accounted for in CESEC-II. The CEA motion is represented by an input rod worth versus time table. The following trips are programmed in the CESEC-II code:

1. high power trip,
2. high pressurizer pressure trip,
3. low pressurizer pressure trip,
4. low coolant flow trip,
5. low steam generator pressure trip,
6. low steam generator level trip, and
7. manual trip.

To generate the trip signal on the low steam generator water level, the steam generator water level is determined from a set of steady state input data and the transient inventory in the steam generator. The set of steady state curves relates steam generator water level to secondary water mass and power level. This data is then used in a table look-up routine to obtain the steam generator water level for the purpose of determining the trip signal.

15.11.9 SAFETY INJECTION SYSTEM

The borated safety injection water from the high and low pressure safety injection pumps is injected into each cold leg downstream of the reactor coolant pumps. The borated injection flow rates versus pressure are specified by input tables. The borated safety injection fluid follows a path along the cold leg to the reactor vessel nozzles, the downcomer region, and into the vessel inlet plenum to the reactor core. Once the safety injection flow reaches the cold leg, it is assumed to mix homogeneously with the reactor coolant inventory. The boron is transported through the RCS by solving at each time step the continuity equation for each coolant node for the boron concentration:

$$M \frac{dC}{dt} = W_{in} C_{in} - W_{out} C \qquad (15.11.9)$$

Where:

C is the boron concentration

C_{in} is the inlet boron concentration

W_{in} is the inlet flow rate

W_{out} is the outlet flow rate

M is the mass inventory in the node

The boron concentration for the reactor core node is used to calculate the reactivity contribution due to boron via an input reciprocal boron worth.

A time delay is input to CESEC-II to account for the time required to start the diesel generator and/or to bring the safety injection pumps to full speed. An additional time delay is input to account for the time required for the unborated water in the safety injection line (from the outlet of the safety injection pumps to the injection nozzles) to be swept out before borated water from the refueling water tanks enters the cold legs.

The safety injection tanks are not modeled in CESEC-II.

15.11.10 CRITICAL FLOW MODEL

The CESEC-II code selects the applicable critical flow model depending on the fluid state.

1. For steam, the mass flow rate is calculated from the following empirical critical flow correlation[4]:

$$\frac{W}{A} = 1977.6 \times \frac{P}{h-185.0} \qquad (15.11.10.1)$$

   where:

   W is the mass flow rate, lbm/sec

   A is the effective flow area, ft^2

   P is the steam pressure, Psia

   h is the steam enthalpy, Btu/lbm

2. For subcooled and saturated water (or a water-steam mixture), the code uses an interpolation scheme on a user input table which relates the critical flow rate to the fluid pressure and enthalpy. The Henry-Fauske critical flow data is used for the preparation of this table.

15.11.11 STEAM LINE BREAK VERSION OF CESEC

In order to simulate more realistically the NSSS behavior following the initiation of a steam line break event, the version of CESEC called CESEC-SLB is used. The major model improvements include: 1) a more detailed thermal-hydraulic model of the Reactor Coolant System in order to handle the effect of temperature tilt in the reactor core during an asymmetric transient, 2) an explicit representation of the reactor vessel closure head, 3) a flow model which is able to explicitly calculate the time dependent reactor coolant mass flow rate, 4) an improved primary-to-secondary heat transfer model, and 5) a safety injection tank model, and 6) a 3-D reactivity feedback model.

Each of these models is briefly discussed below

15.11.11.1 RCS Thermal-Hydraulics

The reactor vessel flow in CESEC-II is represented by a single, average flow channel. The coolant is assumed to be perfectly mixed in the reactor vessel lower plenum before entering the core. Thus, when the RCS loops response is non-symmetric, the effect of the radially tilted temperature of the moderator reactivity is accounted for by using the cold leg temperature to calculate the moderator reactivity feedback.

The noding model used in CESEC-SLB is shown on Figure 15.11-10. Each channel represents one half of the reactor vessel inlet downcomer section, the lower plenum, the core region, the bypass flow, and the upper plenum.

These two symmetrical loops are linked by the cross flow at the reactor, vessel inlet and outlet sections and by the flow mixing within the reactor vessel lower and upper plenums. No cross flow is assumed between the parallel regions in the core. The mass flow between the jth and k^{th} node of Figure 15D-10 is denoted by $W_{j,k}$ The mixing flows $W_{2,15}$, $W_{14,3}$, $W_{6,19}$, and $W_{18,7}$, are calculated using constant, experimentally determined mixing parameters, F_I and F_O, defined such that:

$$W_{2,15} = F_I W_{2,3}$$

$$W_{14,3} = F_I W_{14,15}$$

$$W_{6,19} = F_O W_{6,7}$$

and

$$W_{18,7} = F_O W_{18,19}$$

where $W_{2,3}$ $W_{14,15}$, $W_{6,7}$, and $W_{18,19}$ are found from the solution of the time dependent conservation of mass and energy equations.

In CESEC-SLB, the selection of the moderator temperature used for the reactivity calculation is determined by a linear extrapolation based on the two core node temperatures obtained from the solution of the thermal-hydraulic equations.

15.11.11.2 Closure Head Node

During the rapid contraction of the reactor coolant which takes place as a result of a steam line break, the pressurizer empties and voids begin to form in the RCS. Since flow through the closure head is only a small fraction of the RCS flow, the temperatures in the closure head remain high and the voiding first occurs there. To some extent, the closure head itself then begins to perform the function of a pressurizer. Therefore, the reactor vessel closure head region is explicitly modeled in CESEC-SLB, rather than including it in with the outlet plenum. The flow from the region above the core to the closure head node is modeled in CESEC-SLB as a fixed input fraction of the total flow leaving the nodes which represent the region above the core (inactive core region and upstream half of the outlet plenum). This fraction has been obtained from detailed, steady-state calculations of flow distribution in the reactor vessel. The flow between the closure head and the downstream half of the outlet plenum is determined from the solution of the conservation of mass and energy equations with the further constraint that

this flow is equally divided between the two parallel nodes used to model the downstream half of the outlet plenum.

15.11.11.3 Flow Model

The CESEC-SLB flow model calculates the mass flow rate (lbm/sec) at the pump outlet for each Reactor Coolant System steam generator loop. The two pumps in each steam generator loop are modeled as one effective pump. The model includes explicit simulations of the reactor coolant pumps and of the effects of natural circulation flow. The calculation is based on a solution of the one-dimensional momentum equation for each RCS loop. The loops are divided into a number of nodes whose densities, temperatures, and flows are obtained from the CESEC thermohydraulics model.* The flow model utilizes this nodalization of the loop to calculate the sum of the various forces around the loop. The forces acting on the fluid volume consist of (1) gravitational forces due to density and elevation changes around the loop, (2) viscous forces due to wall friction and geometric expansions and contractions of the flow path, and (3) forces due to the RCS pumps. The one-dimensional momentum equation for each closed loop, is written as follows:

$$\frac{dw}{dt} = \frac{g\sum_{i=1}^{n} \rho_i h_i - \sum_{i=1}^{n} w_i^2 \left[\frac{\phi_i f_i R_{fric,i}}{\rho_{is}} + \frac{R_{geo,i}}{\rho_{in}} \right] + \Delta P_{pump}}{\sum_{i=1}^{n} \left(L_i / A_i \right)} \qquad (15.11.11.1)$$

where

w	= mass flow rate at the pump, lbm/sec
w_i	= mass flow rate of ith node, lbm/sec
ρ_{in}	= average fluid density of ith node, lbm/ft^3
ρ_{is}	= single-phase fluid density of ith node, lbm/ft^3
h_i	= $h_{in,i} - h_{out,i}$ = the elevation differences across the ith node, ft
ϕ_i	= Thom two-phase multiplier for the ith node
f_i	= Darcy friction factor for the ith node
L_i	= effective flow path length for the ith node, ft
A_i	= effective cross sectional flow area of ith node, ft^2

and

*The average of the properties and the flows from parallel nodes are used for nodes representing reactor vessel.

$$R_{fric,\,i} = \frac{L_i / D_{e,i}}{2 A_i^2}$$

$$R_{geo,i} = \frac{K_{g,i}}{2 A_i^2}$$

where $D_{e,i}$ = effective diameter of ith node

$K_{g,I}$ = dimensionless geometric proportionality constant

The first term on the right hand side of Equation 15.11.11.1 represents the net pressure change around the loop due to the gravitational force acting on each fluid node. The second term represents the total pressure change around the loop due to the frictional loss and the geometric expansions and contractions. The R factors in the equation are constants and are determined by the initial conditions. The Darcy friction factor, f_r, which is a function of the Reynolds number, Re, is determined by the following correlations:

$f = 64/Re$ $\quad Re < 1250$

$f = (-0.000004)Re+0.056$ $\quad 1250 \le Re < 600$ $\quad$ (15.11.11.2)

$f = 0.184/Re^{0.2}$ $\quad Re \ge 6000$

The third term in Equation 15.11.11.1 represents the pressure difference ΔP_{pump}, across the reactor coolant pump, which is calculated by the dynamic pump model described in the following paragraphs.

The CESEC-SLB pump model calculates the pressure difference across the pump, for use in the conservation of momentum equation. The pressure difference, or pump head, is dependent of the pump speed. The speed is calculated throughout the transient, thus, giving a pump head dependent on transient flow conditions. The pump speed is determined from the following equation:

$$\frac{d\omega}{dt} = \left(T_{el} - T_h - T_{f,\omega}\right)\frac{g_c}{I} \qquad (15.11.11.3)$$

where

ω = angular velocity of the rotating assembly

t = time

T_{el} = electrically induced torque acting on the motor rotor

T_h = hydraulic torque exerted on the fluid by the pump impeller

$T_{f,\omega}$ = torque exerted on the rotating assembly due to bearing friction and windage losses

g_c = gravitational constant

I = moment of inertia of the rotating assembly

The three torques (T_{el}, T_h, and $T_{f,\omega}$) are calculated as follows:

a. The hydraulic torque is calculated from the following equations:

$$T_h = (\beta^2/\alpha^2)\,(\alpha^2)\,(T_R)\,(\rho/\rho_R) \text{ for } /\nu/\alpha/ \leq 1.0$$
$$(\beta/\nu^2)\,(\nu^2)\,(T_R)\,(\rho/\rho_R) \text{ for } /\nu/\alpha/ > 1.0$$

where

β = Ratio of the hydraulic torque to the rated hydraulic torque, β = Th/TR

α = Ratio of the pump speed to the rated pump speed, $\alpha = \omega/\omega_R$

v = Ratio of the volumetric flow rate to the rated volumetric flow rate,

v = Q/QR

ρ = Density of coolant at pump node, lbm/ft^3

ρ_R = Density corresponding to pump rated conditions, lbm/ft^3

The values of β/α^2 and β/v^2 as a function of v /α and α/ v, respectively, are determined from the single phase homologous pump curves (tabular input).

b. The friction and windage torque is calculated from the following equation:

$$T_{f,\omega} = 1/2\,\alpha(1+|\alpha|)T_{fWI} \qquad (15.11.11.5)$$

where T_{fWI} is the input friction and windage torque at rated speed.

c. To solve for the electrical torque, the pump speed from the previous time step is used and an interpolation is done in the table of speed versus electrical torque.

With all quantities known in Equation 15.11.11.3, the change in the pump speed can be calculated. The pump speed is then changed by this amount for the next time step.

The pump head, H, is calculated from the following equation:

$$H = (\alpha^2)\,(H_R)\,(h/\alpha^2) \text{ for } |\nu/\alpha| \leq 1.0$$
$$(\nu^2)\,(H_R)\,(h/\nu^2) \text{ for } |\nu/\alpha| > 1.0 \qquad (15.11.11.6)$$

where

h = Ratio of the pump head to the rated pump head, $h \equiv H/H_R$

H_R = Rated pump head, ft of water

The values of h/α^2 and h/v^2 as a function of v/α and α/v, respectively, are determined from single phase homologous pump curves (tabular input).

The pressure difference across the pump is calculated as follows:

$$\Delta P_{pump} = H\rho g \qquad (15.11.11.7)$$

15.11.11.4 Primary-To-Secondary Heat Transfer

In CESEC-SLB the average primary-to-secondary temperature difference is calculated using algorithms based upon a polynomial spatial variation of the primary side temperature, rather than the logarithmic mean temperature difference used in CESEC-II. In addition, the heat transfer coefficients are calculated on a node-center-to-node-center basis rather than for the steam generator as a whole in CESEC-II.

The polynomial algorithm in CESEC-SLB selects the mid-point temperatures of the nodes simulating the steam generator tubes and the inlet and outlet plenum (Figure 15.11-10) to obtain the spatial variation of the primary side temperature along the steam generator tubes. The difference between this temperature variation and the secondary side temperature is integrated between the node mid-points and divided by the distance between these points to obtain the average primary-to-secondary temperature difference. This temperature difference is then used to calculate the steam generator heat transfer rate on a node-center-to-node-center basis at each time step.

The heat transfer correlations used in CESEC-II (Equations 15.11.5.1 and 15.11.6.1) are also used in CESEC-SLB; however, the heat transfer coefficients are on a node-center-to-node-center basis rather than for the steam generator as a whole. An added constraint in CESEC-SLB is that for low heat flux predictions, secondary-side heat transfer coefficient is limited to a small constant input value, rather than being allowed to go to zero with the heat flux as in Equation 15.11.6.1. This minimum value is also used for the secondary side heat transfer coefficient for conditions of reverse (secondary-to-primary) heat transfer. The primary-side coefficients are calculated using the same correlation (Equation 15.11.5.1) for forward and reverse heat transfer.

To avoid singularities in the solution of the conservation equations shown in Figure 15.11-9a, the minimum liquid inventory in each steam generator is limited by preventing liquid boiloff for steam generator liquid masses less than 2500 lbm. For liquid inventories less than 2500 lbm the product of heat transfer coefficient and heat transfer area, UA, is assumed to be just sufficient to raise the enthalpy of any incoming feedwater to that of saturated liquid. For steam generator liquid inventories greater than 5000 lbm, the total heat transfer area is used together with a primary-to-secondary heat transfer coefficient calculated using the correlations given above. For liquid inventories between 2500 lbm and 5000 lbm the product UA is scaled linearly between values calculated for inventories equal to 2500 lbm and 5000 lbm, respectively. In all cases, steam is allowed to escape through the ruptured steam line with a critical flow velocity as long as the steam pressure is above atmospheric pressure.

15.11.11.5 Safety Injection Tank

CESEC-SLB solves an orifice equation to determine the rate of safety injection flow from the safety injection tank into the RCS as a function of time. The input parameters are the initial nitrogen pressure, volume of water, volume of gas, flow coefficient, flow area, water specific volume, and elevation head of the safety injection tanks. In addition to the nitrogen pressure within the safety injection tank, the static head of fluid within the safety injection piping is considered when calculating the instantaneous pressure difference across the orifice. The nitrogen expansion process is assumed to be isentropic.

In computing the safety injection flow rate by means of an orifice equation, the code takes into account the effect of piping friction, turning losses, and expansion/contraction losses through the use of a single equivalent loss coefficient which is based on the minimum cross-sectional flow area. The instantaneous liquid discharge rate at time t is given by

$$W(T) = A \left(\frac{288\, g_c\, \Delta P(t)}{Kv}\right)1/2 \qquad (15.11.11.8)$$

$$\Delta P(t) = P_G^{(t)} + P_E - P_{RCS}^{(t)} \qquad (15.11.11.9)$$

where

W is the mass flow rate in lbm/sec

A is the flow area of safety injection tank line in ft^2

K is the friction loss coefficient for the flow area

v is the specific volume of liquid in ft^3/lbm

$P_G(t)$ - nitrogen pressure at time t

P_E = elevation head

$P_{RCS}(t)$ - RCS pressure at time t

If ΔP is less than or equal to zero, the code sets this variable equal to zero in order that no liquid mass be ejected from the tank for this condition.

The instantaneous liquid volume V in the tank at time t is then

$$V(t) = v\,(t-\Delta t) - W(t)\Delta t.v \qquad (15.11.11.10)$$

where Δt is the time step interval.

The instantaneous gas volume V_G in the tank at time t is given by

$$V_G(t) = V_G(0) + V(0) - V(t) \qquad (15.11.11.11)$$

where $V_G(0)$ and V (0) are the initial gas volume and liquid volume, respectively.

The instantaneous gas pressure in the tank at time t is given by:

$$P_G(t) - P_G(0) \quad \left(\frac{V_G(0)}{V_G(t)}\right) \quad 1.4 \qquad (15.11.11.12)$$

15.11.11.6 The 3-D Reactivity Feedback Model

CESEC-SLB incorporates a 3-D reactivity feedback model to more accurately represent the post-trip reactivity effects of the temperature distribution at the core inlet plane, the stuck CEA, and changes in the core power distribution. The 3-D reactivity contributions based on neutronic analyses are input into CESEC-SLB as tabular functions of normalized core flow fraction, the normalized fission power to normalized core flow ratio, and temperature tilt (the difference between the hot and cold edge temperatures at the core inlet plane). Table interpolation routines determine the dynamic 3-D feedback from this input data for each time step after CEAs are inserted.

15.11.12 RESPONSE TO NRC QUESTIONS (Historical Information)

15.11.12.1 Question No. 440-67

In light of recent operating experiences (the St. Lucie Unit 1 natural circulation cooldown event of June 11, 1980, and re-analyses of SAR Chapter 15 design bases events by St. Lucie in February 1981) a potential deficiency has been identified with the CESEC computer program and NSSS model. As the pressurizer cools down and the system pressure decreases, steam can form in the reactor vessel upper head due to flashing of the hot coolant in this stagnant region. The steam bubble in the reactor vessel upper head displaces coolant from the reactor vessel into the pressurizer and the steam in the vessel head will determine the system pressure. The CESEC model used for the steam generator tube rupture event does not account for this occurrence. Further, CESEC analyses which predict that the pressurizer will empty, or that the reactor coolant system saturates, do not appear to correctly calculate the system thermal hydraulic response and are not justified for use. These events are to be re-analyzed with a suitable model or additional justification is to be provided for the CESEC analyses to demonstrate that the computer program conservatively accounts for the formation of steam in the reactor coolant system.

Response

The Chapter 15 events performed with CESEC do not explicitly include analyses of natural circulation cooldowns. However, a comparison has been made between CESEC and data from the St. Lucie 1 natural circulation cooldown event. This information is provided in the documentation for the CESEC-III computer code (see Subsection 15.1.5.3.5. Additionally, comparative analyses were performed between CESEC-II and CESEC-III. CESEC analyses have indicated that for the steam generator tube rupture, the letdown line break, and the steam line break events, the pressurizer empties and/or the reactor coolant system (RCS) saturates. Since the steam line break event was analyzed using CESEC-III, no comparative analysis will be performed for this event. The steam generator tube rupture and letdown line break events belong to the decrease in RCS inventory event category. The most limiting event in this category with respect to void formation, the steam generator tube rupture event, will most significantly emphasize differences between CESEC-II and CESEC-III in the calculational results. Conclusions from this analysis bound those which would have been ascertained from a

comparative analysis for the letdown break event. Therefore, qualification of CESEC-II against CESEC-III for the steam generator tube rupture event provides the necessary justification for the acceptability of Chapter 15 analyses conclusions for depressurization events.

For all Chapter 15 events for which the pressurizer fluid is calculated to drain into the hot leg, or the system pressure drops below the saturation pressure of the hottest fluid in the system, the hottest fluid will be located in the relatively stagnant upper head region of the reactor vessel. The CESEC-II code, used in the FSAR Chapter 15 analyses did not explicitly model the steam formation in the reactor vessel upper head (except for steam line break analyses which used CESEC-III) region. The latest version of CESEC, namely CESEC-III, appropriately models steam formation and collapse in the upper head region of the reactor vessel. Heat transfer from metal structures to the reactor coolant system (RCS) fluid is modeled in addition to flashing of the reactor coolant into steam during depressurization of the RCS. Following the reactor coolant pump (RCP) coastdown due to loss of offsite power or manual shutoff following SIAS, thermal-hydraulic decoupling of the upper head region is characterized in CESEC-III by progressively decreasing flow to the upper head from the upper plenum region. Table 15.11-1 summarizes the significant differences between the two CESEC code versions which impact depressurization transients. (Note that the 3-D feedback impacts only the steam line break analyses).

The steam generator tube rupture event presented in the FSAR was reanalyzed, using the CESEC code version known as CESEC-III. The re-analysis of the SGTR event without loss of offsite power indicated the following:

The modeling of the stagnant upper head region with metal structure heat transfer results in the formation of voids in this region. The void volume in the upper head region peaks at about 289 cubic feet during the transient and gradually decreases under the combined action of the HPSI flow and the cooldown at the steam generators. The duration of the voids is a strong function of the rate of cooldown of the primary side and the HPSI flow rate.

Figure 15.11-11 provides a comparison of pressurizer pressures predicted by the CESEC-II and CESEC-III codes. The effect of upper head voids on primary system pressure is illustrated in this figure. It shows similar trends for the RCS pressures during the transient. However, subsequent to reactor trip, the pressure predicted by the CESEC-III code decreases at a lower rate than that predicted by the CESEC-II code. This is due to the formation of voids in the upper head region, which controls the system pressure decay after the emptying of the pressurizer subsequent to reactor trip. The voids in this region are calculated to collapse at about 1700 seconds under the combined effect of charging flow, safety injection flow, reduced primary-to-secondary leak, and cooldown at the steam generators. The CESEC-III code predicts refilling of the pressurizer and repressurization of the RCS as a result of the net mass influx into the RCS, subsequent to collapse of the upper head voids. The CESEC-II code predicts refilling of the pressurizer and RCS repressurization much earlier than CESEC-III, since it does not explicitly account for upper head void formation and collapse.

Figure 15.11-12 shows the behavior of the liquid volume in the reactor vessel above the top of the hot legs for the CESEC-III analysis. The amount of voids predicted is not large enough to expand the steam bubble beyond the upper head region and to the elevation of the hot legs.

Additionally, the prediction of the upper head bubble does not alter the conclusions of the previous CESEC-II analyses. That is, for the SGTR event the major concern is with radiological releases to the environment. A breach of the primary system boundary provides a pathway for radioactive primary coolant release into the secondary side and subsequently into the

atmosphere. The offsite accident dose for a SGTR event is dependent on the integrated primary to secondary leak as well as the total main steam safety valve (MSSV) steam releases. As seen from Table 15.11-2, both CESEC-II and CESEC-III codes predict comparable values for these parameters. The minimum DNBR for both analyses remains above 1.19 for the duration of the event. Thus, from the results of this comparison, it can be concluded that the impact on the offsite doses is insignificant. Additionally, the comparison demonstrated that the plant is maintained in a stable condition by the collapse of the upper head voids due to automatic actions.

Subsequent to operator action, the operator can bring the plant to the shutdown cooling entry conditions, by cooling down the RCS at a prescribed cooldown rate using the intact steam generator, the condenser, and the feedwater system and by following specific plant procedures.

For the steam generator tube rupture with loss of offsite power event (see Subsection 15.6.2.1.5 similar conclusions as for the SGTR event without loss of offsite power can be made. For this case, the operator will not have the condenser available for cooldown, and would use the atmospheric dump valves. Additionally, the RCS will be in a natural circulation cooldown mode as a result of the coastdown of all RCS pumps following loss of offsite power. The analysis demonstrated that natural circulation cooldown of the RCS is not impaired as the amount of voids predicted is not large enough to expand the steam bubble beyond the upper head region and to the elevation of the hot legs.

The conclusions from the comparative analyses for the SGTR event bound the other depressurization events in Chapter 15.6 for which void formation is less limiting and/or non-existent. This is due to slower cooldown rates and higher minimum RCS pressures for these depressurization events. Thus, the qualification of CESEC-II against CESEC-III for the SGTR event provides the necessary justification for the acceptability of the Chapter 15 analyses conclusion for depressurization events.

15.11.12.2 Question No. 440.75

The overcooling transients analyzed in Chapter 15 (excluding the steam line break events) were assessed utilizing the CESEC-II computer program. This program does not properly account for steam formation in the reactor vessel and in the primary system after the pressurizer empties. CESEC-II is also incapable of evaluation asymmetric cooldown (i.e., independent hot leg temperature between the broken and intact loops). Neglecting these effects can result in the improper evaluation of the system pressure and hydraulic behavior. The modeling deficiency in CESEC-II has the potential for providing unacceptable results for depressurizing transients. As such, for transients which empty the pressurizer or result in saturated coolant conditions at other locations in the primary system, the CESEC-II computer program must be verified to correctly calculate system thermalhydraulic responses. The staff requires the applicant to re-analyze these events with a suitable model in order to demonstrate the acceptability of the CESEC-II program to predict thermalhydraulic phenomena in question, and to demonstrate compliance with NRC regulation.

Response

The CESEC model predicts emptying of the pressurizer for the steam generator tube rupture event presented in St. Lucie Unit 2 FSAR Subsection 15.6.2, and, for the letdown line break (outside containment, upstream of the letdown control valve) event presented in Subsection 15.6.5.

The most limiting event with respect to void formation (excluding the steam line break), the steam generator tube rupture event, was re-analyzed using CESEC-III to demonstrate the capability of CESEC-II to correctly calculate the system response for depressurization events. The analysis will also demonstrate that upper head voiding does not cause the calculated DNBR to be much different than that calculated from CESEC-II results for this event. The calculated void formation in the upper head tends to slow the depressurization rate predicted by CESEC-III, thereby maintaining the system pressure slightly higher than that predicted by CESEC-II. Therefore, given essentially the same core heat flux, flow rate, and coolant inlet temperature (other parameters which affect DNBR in addition to pressure), the DNBRs calculated from CESEC-II results are expected to be conservative when compared to those calculated from CESEC-III results. Prior to reactor trip the DNBR is not affected by voiding in the reactor coolant system, since voiding is not calculated to occur until after the reactor has tripped. The saturation temperature (628F) corresponding to a low pressurizer pressure trip (at 1875 psia) is above any transient RCS temperatures. Refer to Subsection 15.11.12.1 for the comparison of the CESEC-II and CESEC-III for depressurization events.

15.11.12.3 Question No. 440-77

Section 15 addresses operator actions required to bring the reactor system to cold shutdown. Based on the experiences learned from the St. Lucie Unit 1 natural circulation cooldown event of 1980, update the operator actions to include any precautions and modifications resulting from the St. Lucie Unit 1 event to prevent voiding in the upper head of the reactor vessel.

Response

A plant cooldown under natural circulation conditions proceeds normally except that sufficient time must be allowed for the water in the upper head to cool. More specifically, the upper head water temperature must be subcooled with respect to shutdown cooling entry pressure when the RCS is depressurized. Best estimate calculations show that the time required for this cooling to occur is 21 hours. Twenty-one hours is predicated on the availability of all safety grade equipment; non-safety grade equipment was not credited in determining this time frame. The St. Lucie 2 SDC entry pressure of 276 psia was also considered. Operators are instructed to conduct natural circulation cooldown as rapidly as possible, subject to Tech Spec limitations, and to depressurize only after 21 hours of elapsed time. Operators are further instructed to recognize voiding by abnormal pressurizer level changes and ineffective depressurization. Should voiding occur, the operator is to repressurize the RCS and wait 2 to 4 more hours before subsequently depressurizing. Finally, operators are instructed to deliberately cool the upper head region via "voiding and filling" if plant conditions (such as available feedwater) do not permit the longer cooling times referenced above. However, as stated in FSAR Subsection 5.4.7.5.E, a cooldown rate more stringent than 75 F/hr is not required to ensure safe cooldown or plant shutdown.

15.11.12.4 Question No. 440.83

Describe in detail the relationship between CESEC-SAR, CESEC-ATWS, CESEC- SLB and CESEC-III with an emphasis on the difference.

Response

The significant differences between various CESEC versions are summarized in Section 18 of Ref. 10 in terms of CESEC-I, CESEC-II, and CESEC-III. CESEC- SAR is a generic term which refers to the version used specifically for a particular safety analysis report.

CESEC-ATWS is essentially the same as CESEC-II, but with additional detail in the steam generator and reactivity feedback models. The CESEC-ATWS steam generator includes a dynamic simulation of the effect of two-phase level on primary to secondary heat transfer during loss of feedwater events. (See Subsection 15.11.12.64). The reactivity model provides explicitly for void reactivity feedback.

CESEC-SLB is essentially the same as CESEC-III. The latter version adds to CESEC-SLB certain user conveniences of CESEC-II and explicitly models all four cold legs and each reactor coolant pump. CESEC-SLB lumps the two cold legs and reactor coolant pumps in each steam generator loop into one cold leg and pump per steam generator.

15.11.12.5 Question No. 440.84

There is no discussion of DNBR calculations. If the code does compute DNBR, provide details.

Response

CESEC-III does not calculate DNBR. Earlier CESEC versions (Ref. 1) calculated DNBR trends. However DNBR values presented in licensing analyses are never those calculated by the CESEC version.

15.11.12.6 Question No. 440.85

Describe the self-initialization procedure.

Response

The subroutine STEADY serves as a calling subroutine which coordinates the self initialization process and input data loading in CESEC-III. The reactor system modules are called to set up their input information and to define their initial conditions at time zero. The CESEC code can be initialized at any combination of reactor power level, Reactor Coolant System flow rate, and steam generator power sharing. Since some of the main steam system parameters are mutually dependent on one another (i.e., PSECR, PSECL, PHEAD, etc.) an iteration process is used among subroutines SGLEQL, SGREQL, and SECEQL to find their equilibrium initial conditions. The calling sequence in STEADY is as follows:

a. Call FLOWQL to define full power symmetric coolant flow, core, inlet temperature at full power, and core inlet temperature at initial power level;

b. Call COREQI to load input data and to initialize the reactor core at specified power level and to find core outlet temperature at full power operating conditions;

c. Call FEEDEQI to find feedwater enthalpy;

d. *Call SGREQI, SGLEQI, and SECEQI to load their input data and evaluate design full power steam generator heat transfer parameters;

e. *Call SGLEQL, SGREQL, and SECEQL to perform power sharing between the two steam generators which equalizes, within a specified convergence criteria, the main steam line header pressure (PHEAD);

f. *Call SGREQS, SGLEQS, and SECEQS to define their initial equilibrium conditions which are consistent with the power sharing found through iteration;

g. Call the initialization section of the rest of the reactor system modules to load input data and to define their initial equilibrium conditions. [FEEDQI, PRESQI, COOLQI, FLOWQI, WALLQI, PROTQI, BOREQI, LAMEQI]

Figure 15.11-13 details the above steps in block diagram form. The loop at the center of this diagram shows the iterative procedure used to arrive at values for power sharing. Steam line pressure loss is accounted for during this iterative procedure for solving for power sharing. The effective flow loss coefficient for the piping modeled in the header simulation equations (see Figure 15-1A of Ref. 10) is used to calculate the header pressure that would result from the pressure in each steam generator and the steam flow from that generator due to the heat transfer from primary to secondary (i.e., power) in that generator. Iteration is continued until the resultant header pressure calculated from the pressure and steam flow of one generator equals that for the other.

Design full power conditions for primary system cold leg temperature, pressure, power, flow rates in each loop, secondary pressure, and steam generator tube heat transfer area are input. Assuming saturation the secondary temperature can be found using the secondary pressure. Knowing these design values of the temperatures of the fluids on both sides of the tubes, the heat transfer area, and heat flux, a resultant value for the overall steam generator tube heat transfer coefficient can be found. Since the primary and secondary side heat transfer coefficients are determined from heat transfer correlations, the only undetermined parameter in this overall heat transfer coefficient is the effective steam generator tube heat transfer resistance. This resistance is thus fixed by this calculation at design conditions and is then held constant and used for the particular case being analyzed with CESEC at the time.

15.11.12.7 Question No. 440.86

How is the closure head bubble modeled?

Response

The thermal hydraulic equations for the upper head region of the reactor vessel are the same as for the other regions of the RCS excluding the pressurizer (see Section 2 and Appendix B of Ref. 10). User input control of the algorithm used to calculate the enthalpy of fluid leaving this upper head node permits simulation of the degree of separation of the liquid and vapor phases in the region. For steam line break and steam generator tube rupture events phase separation and RCS pressure are maximized by causing the enthalpy of fluid leaving the node to be that of saturated liquid when two phases are present. For other transients the enthalpy of fluid leaving the node is the average enthalpy of the fluid in the node. User input control also allows the value

*Figure 15.11-13 is a flow diagram of steps d, e, and f.

of the fraction of flow to the upper head, Fh, to be changed once during the transient. This may be used to simulate a reduction in flow to the upper head due to reactor coolant pump coastdown or due to RCS contraction during severe increase in heat removal events.

15.11.12.8 Question No. 440.87

Does assumption (1) of Appendix B, assuming pressure to be spatially uniform throughout the entire primary coolant system, imply that no differentiation is made between pressurizer pressure and system pressure in the derivation of the T/H equations, Eq. (B-30) through Eq. (B-78)? Where and how is each pressure used?

Response

A distinct differentiation is made between pressurizer pressure and RCS pressure. For all of the equations of the form of Eqn. (B-29), i.e., Eqns. (B-30) through (B-54), the appropriate pressure is the RCS pressure, P_{RCS}. All properties and their derivatives are evaluated at P_{RCS} for these equations. The relationship $P_{RCS} = P_{PRZ} + \Delta P_{ws}$, where P_{PRZ} is the pressurizer pressure and ΔP_{ws} is the surge line pressure drop which is calculated in the code, is used to transform the P of Eqns (B-30) through (B-54) from P_{RCS} to P_{PZR}. As a result, ε_i of Eq. (B-29) contains the term ($-\delta i\ \Delta P_{WS}$), with ΔP_{ws} being determined as described in Chapter 7 of Ref. 13. Thus for Eqns (B-30) through (B-54)

$$\beta_i(\sum W_{\text{int}})_i + \alpha_i(\sum hW_{\text{int}})_i + \delta_i \dot{P}_{PRZ} = \varepsilon'_i$$

and

$$\varepsilon'_i = \varepsilon_i - \delta_i \Delta \dot{P}_{ws} .$$

(See page B-5 of Ref. 10 for definitions of parameters) for Eqns (B-55) through (B-83) P is P_{PRZ}, directly, and all properties and their derivatives are evaluated at the pressurizer pressure. The only exception to the foregoing is that the average of P_{RCS} and P_{PRZ} is used in the determination of the properties of surge line fluid.

15.11.12.9 Question No. 440.88

How are the crossflows, bypass flows, mixing flows, head flows and leak flows incorporated into Eq. (3-1), the equation for the pump flow?

Response

All flows mentioned, except the leak flows are directly incorporated into Eq. (3-1) of Ref. 10 according to the definition of the flow model nodal flow as being the arithmetic mean of sums of internodal flows entering the node and internodal flows leaving the node.

$$W_i = \frac{1}{2}\left[\sum_j W_{in,j} + \sum_j W_{out,j}\right]_i$$

The leak flows are not directly incorporated into Eq. (3-1), however, they are accounted for in the thermal-hydraulic (T-H) model as external flows. The solution of the T-H equation system

gives the internodal flows used in determination of the flow model nodal flows as described above.

The T-H equation system assumes one dimensional flow and does not consider the effect of momentum flux in the solution. Momentum flux terms are negligible for the transients analyzed by CESEC-III and small break LOCAs. Only large break LOCA methods consider the effect of momentum flux in the T-H solution.

15.11.12.10 Question No. 440.89

How does the inertia term in Eq. (3-1) take account of the flow split for parallel pumps?

Response

The flow model calculates the mass flow rate through each of four reactor coolant pumps using Eq. (3-1) of Ref 10. The term "loop" in the description should be understood as four separate loops consisting the specified series of nodes following (refer to Fig. 3-1 of Ref. 10):

Pump Loop 1:	nodes 1, 2, 3 through 12	Right Hand (RH) loops
Pump Loop 3:	nodes 13, 14, 3 through 12	
Pump Loop 2:	nodes 15, 16, 17 through 26	Left Hand (LH) loops
Pump Loop 4:	nodes 27, 28, 17 through 26	

The inertia term (denominator) in Eq. (3-1) is defined as a sum of terms L_i/A_i around each of these four loops.

15.11.12.11 Question No. 440.90

Justify the use of the Semiscale degraded two phase pump data to model CE pumps.

Response

The appropriateness of the Semiscale degraded two phase pump data for modeling of CE pumps has been accepted by the NRC (Section III.C.6 of Ref. 11 and Section III.8.17 of Ref. 12) which utilizes the model.

15.11.12.12 Question No. 440.91

Describe how the level in the pressurizer is determined and how the external heat transfer/mass flow terms are divided between the steam region and the liquid region.

Response

Pressurizer liquid level is determined by dividing the volume of liquid in the pressurizer by the cross sectional area of the pressurizer. Complete separation of the vapor and liquid phases, or an effectively infinite bubble rise velocity, is assumed. The measured liquid level is determined as described in Subsection 4.3.1 of Ref. 5. The external heat transfer/mass flow terms are divided between the steam region and the liquid region as described in Subsections 4.3.2 through 4.3.4 of Ref. 5.

15.11.12.13 Question No. 440.92

Why does the gravity term in the surge line momentum equation, Eq. (7.1) contain expressions for the pressurizer when the inertia term is written only for the surge line?

Response

The surge line momentum equation can be written as (See Figure 15.11-14).

$$P_1 - P'_2 = \frac{\left(\frac{L}{A}\right)}{144g}\frac{dW}{dt} + \frac{f(L/De)|W|W}{288pgA^2}\phi$$

$$+ \frac{Kg|W|W}{288\bar{\rho}A^2} + \frac{\bar{\rho}(Z_a - Z_2)}{144}$$

The static pressure balance inside the pressurizer yields

$$P'_2 - P_2 = \frac{\rho_w}{144}(Z_w - Z_a) + \frac{\rho_s}{144}(Z_p - Z_w)$$

Therefore, substituting Equation (2) into Equation (1) for P'_2 yields Equation (7.1).

The (L/A) in the inertia term is written in terms of the surge line since the L/A for the pressurizer is small compared with the L/A for the surge line.

15.11.12.14 Question No. 440.93

Show the table of f values used in Eq. (7-1) when Re > 15000.

Response

The table of f values used in Eq. (7-1) when Re > 15000 is as follows:

Re	$1.5x10^4$	$1.0x10^5$	$4.0x10^5$	$1.0x10^6$	$4.0x10^6$	$1.0x10^7$	$4.0x10^7$	$1.0x10^8$	$1.0x10^{14}$
f\	.0275	.018	.0139	.0122	.0103	.0095	.009	.0088	.0088

See Subsection 4.4.5 of Ref. 5.

15.11.12.15 Question No. 440.94

Why is the pressurizer pressure time derivative and not the RCS pressure time derivative used in Eq. (8-1)?

Response

See Subsection 15.11.12.8.

15.11.12.16 Question No. 440.95

Are the 13 nodes referred to in the wall heat transfer model radial nodes? Provide a figure for the model to illustrate it.

Response

The 13 nodes are referred to in the wall heat transfer model are radial nodes. Figure 15.11-15 presents the basic geometry of the wall heat model in the thermal hydraulic node.

15.11.12.17 Question No. 440.96

How is heat conduction through the steam generator tubes modeled? Response

Heat conduction through the steam generator tubes is modeled by two equations-- one for conducted heat, $Q_{c,n}$ and one for stored heat,$Q_{s,n}$.

$$Q_{c,n} = U_n A_n (T_{pri_n} - T_{\sec})$$

(This is Eq. 13-1 of Ref 10; the notation is the same as defined there.)

$$Q_{s_{n,i+1}} = C_n (T_{pri_{n,i+1}} - T_{pri_{n,i}}) / \Delta t,$$

where, additionally,

C_n = heat capacity of steam generator tubes in node n (BTU/F),

i = time step number, and

Δt = time step size (sec).

This assumes that the tube walls essentially follow the temperature of the primary coolant, rather than the secondary fluid. This is consistent with the small time constant (on the order of one second) for heat transfer to the tube walls.

The source term for net heat rate into the thermal hydraulic equation, Eq. 2-1 of Ref. 10) for the steam generator tube node is then

$$Q_n = - (Q_{c,n} + Q_{s,n})$$

15.11.12.18 Question No. 440.97

Is Eq. (9-2) for the shroud heat capacity solved simultaneously with the thermal hydraulic equations of Appendix B?

Response

Eq. (9-2) of Ref. 10 for the shroud heat capacity is not solved simultaneously with the thermal hydraulic equations of Appendix B of Ref. 10. The time constant for heat transfer to the shrouds is of the order of one second. Time step sizes are typically small fractions of a second.

Therefore, no large change in heat transfer to the relatively thin walled shrouds would be expected from one time step to another.

15.11.12.19 Question No. 440.98

For the Doppler and the moderator reactivity feedback calculation does the core have only one axial node? How is the split core accounted for?

Response

Present applications of the CESEC code utilize only one axial node.

The Doppler reactivity is determined from a tabular input function of reactivity versus fuel temperature with the fuel temperature calculated as specified in Subsection 15.11.12.21. The coolant temperature utilized in the fuel temperature calculation is the arithmetic average of the coolant temperatures associated with the core thermal-hydraulic nodes.

Moderator reactivity is determined from either a tabular input function of reactivity versus moderator temperature or moderator density. The arithmetic average of the coolant temperatures associated with core thermal-hydraulic nodes is used for the moderator temperature. Except for steam line break applications, when the density function is specified, the moderator density is based on the arithmetic average of the coolant specific volumes associated with the core thermal-hydraulic nodes. For steam line break applications, the moderator density is computed from the cold edge enthalpy and steam pressure as described in Subsection 15.11.12.66.

15.11.12.20 Question No. 440.99

How is the moderator temperature/density calculated for the reactivity feedback?

Response

See Subsection 15.11.12.19.

15.11.12.21 Question No. 440.100

How is the fuel temperature for the Doppler feedback calculated?

Response

The fuel rod temperature is calculated using the model presented in Section 10 of Reference 10. The temperatures calculated for the three radial nodes are then used for the Doppler feedback calculations. This is done by calculating the Doppler feedback for each of the three fuel rod node temperatures and averaging the reactivities. This average is then used in the kinetics calculations.

15.11.12.22 Question No. 440.101

Describe in detail the 3-D reactivity feedback model used for steam line breaks.

Response

The 3-D reactivity contributions used in the CESEC code for steam line break analysis (pp. 10-1, 2 of Ref. 10) are calculated via the HERMITE code. The majority of the physical models within the current version of the HERMITE code are described in Reference 37 The only portion of that code in which the physical model has changed is in the area of the code thermal hydraulic calculation. There, the closed channel model described in Reference 37 has been replaced with the same core-wide open channel model described in the TORC code (References 13, 14). Cross sections are generated via the DIT code (Reference 15).

A three-dimensional quarter-core HERMITE model is assembled and depleted to the end of au equilibrium cycle. This model is then expanded to full core geometry and a series of return-to-power eigenvalue calculations are performed. The most adverse control rod in assumed to be stuck in the fully withdraws position in all return-to-power cases.

The reactivity insertion from hot full power to each return-to-power condition in then computed. A corresponding reactivity insertion is computed via traditional steam line break methods, using isothermal two dimensional HERMITE calculations. A best estimate reactivity credit is defined as the difference between the standard 2D reactivity insertion and the more precise 3-D reactivity insertion. A multiplicative conservatism factor is then applied within the CESEC code.

As described on page 10-2 of Ref. 10, these reactivity credits are input to CESEC as tabular functions of normalized core flow fraction, normalized fission power to normalized core flow ratio, and temperature tilt. In the dynamic calculation the normalized flow and fission power are calculated by dividing core flow and fission power by the flow and fission power values, respectively, that were used to normalize the results of the HERMITE calculations. The temperature tilt is the difference between the how and cold edge temperatures at the core inlet plane. Test results (Ref. 16) indicate that the temperature of the fluid at the very edge of the core directly under one steam generator loop would have very little contribution from the fluid of the opposite loop. Therefore, the temperature tilt is calculated using an algorithm which factors out the effect of reactor vessel inlet mixing:

Temperature tilt $T(h_H, P) - T(h_c, P)$,

where =

$$h_H = \frac{h_3 + h_{15}}{2} + \left(\frac{1+F_I}{1-F_I}\right)\left(\frac{h_{15} - h_3}{2}\right)$$

and

$$h_c = \frac{h_3 + h_{15}}{2} - \left(\frac{1+F_I}{1+F_I}\right)\left(\frac{h_{15} - h_3}{2}\right),$$

all notation being the same as that of Section 2 of Reference 10. Table interpolation routines use dynamically calculated values of normalized core flow fraction, normalized fission power to normalized core flow ratio, and temperature tilt to obtain the dynamics 3-D feedback from the input tables of reactivity credits as a function of these three parameters. This 3-D feedback is added to the other feedback reactivities (moderator, Doppler, etc.) after multiplication by the

conservatism factor mentioned above. An input option allows the user to activate the 3-D feedback calculation for the analyses to which 3-D feedback is appropriate.

15.11.12.23 Question No. 440.102

Explain the homogenization procedure for the third radial node of the fuel rod heat conduction model.

Response

The homogenization procedure for the parameters for the third radial node of the rod heat conduction model is described in Section 1.3 of Reference 6, in the response to Question 240.22 and 240.23 of Reference 4, and in Subsection 2.2.2 of Reference 1. The temperature of each radial fuel rod is taken to be the temperature of the fuel at a reference radius for that node. For the first and second nodes this reference radius is the average of the radii of the boundaries of the nodes. For the third node the reference radius is the average of the radius at the boundary of the second radial node and the radius of the fuel pellet. The effective thermal conductance* between the second and third node, K23, is calculated between the reference radii for these nodes. This conductance includes the effect of cylindrical geometry, assuming a uniform heat source within the fuel pellet, and accounts for the temperature dependence of the thermal conductivity of the fuel.

$$K_{23}=\frac{16\pi\ R_2^2\ \ell K_F\ (T_{F3})}{(R_2+R_F)^2-(R_1+R_2)^2}$$

where:

$K_F(T_{F3})$ = thermal conductivity of fuel at the temperature of the fuel in node 3, T_{F3}

ℓ = length of axial node

R_1 = radius of boundary between nodes 1 and 2

R_2 = radius of boundary between nodes 2 and 3

R_F = radius of fuel pellet

The effective thermal conductance between the third node and the reactor coolant, K_{3w}, is calculated between the reference radius of the third node and the coolant. This conductance includes the conductance of the fuel from the reference radius to the pellet surface, based on the same assumptions used for the conductance between the second and third nodes, and the conductances of the gas gap, the clad, and the fluid film on the clad surface.

*See Figure 10-6 of Ref. 10.

$$K_{3W}\left\{=\frac{4R_F^2-(R_2+R_F)^2}{\pi\ell(R_2+3R_F)^2K_F(T_{F3})}+\frac{1}{2\pi R_F\ell h_G}\right.$$

$$+\frac{\ln\left[R_3/(R_3-\delta_c)\right]}{2\pi\ell K_c(T_c)}$$

$$\left.+\frac{1}{2\pi R_3\ell h_W(T_W,W)}\right\}^{-1}$$

where in addition to the parameters defined earlier:

h_G = gap conductance

R_3 = radius of fuel pin

$K_c(T_c)$ = thermal conductivity of clad at clad temperatures Tc

δ_c = clad thickness

$h_W(T_W,W)$ = film heat transfer coefficient of clad to coolant interface evaluated at the temperature, T_W, and mass flow rate, W, of the coolant

The clad temperature, T_c, is calculated using T_W, the thermal resistance between the coolant and the clad, and the heat flux at the surface of the fuel pin.

The heat capacity of the third node, $(MC)_3$, is the heat capacity of the volume of fuel pellet in this node plus the product of the heat capacity of the clad with the ratio of the clad temperature to the temperature of the third fuel rod node.

$$(MC)_3 = V_{F3}\ \rho_F(T_{F3})C_F(T_{F3}) + V_c\ \rho_c(T_c)C_c(T_c)\frac{T_c}{T_{F3}}$$

where in addition to the parameters defined above:

V_{F3} = volume of fuel pellet portion of node 3

V_c = volume of clad

$\rho_F(T_{F3})$ = density of fuel at temperature of fuel in node 3

$\rho_c(T_c)$ = density of clad at clad temperature

$C_F(T_{F3})$ = specific heat of fuel at temperature of fuel in node 3

$C_c(T_c)$ = specific heat of clad at temperature of clad

15.11.12.24 Question No. 440.103

Is the heat transfer correlation given by Eq. (10-1), for the clad-coolant interface, actually used for all pressures and temperatures.

Response

Eq. (10-1) is used for calculating the heat transfer coefficient for forced convection flow of sub-cooled liquid. Calculations show that values calculated using Eq. (10-1) differ from those obtained using the Dittus-Boelter correlation (Ref. 17), by less than 4 percent over the pressure range from atmospheric pressure to 3200 psia for temperatures from 200F to a temperature just below saturation.

15.11.12.25 Question No. 440.104

What is the difference between T_w and T_{wl} in Fig. 10-6?

Response

The equation for heat to water in Fig. 10-6 should read as follows:

$Q_w = K_{3w} (T_{F3} - T_w) - C_w P$

15.11.12.26 Question No. 440.105

Is Q_w in Fig. 10-6 the source term used in the thermal-hydraulic equations of Appendix B?

Response

The Qw in Fig. 10-6 is the source term used in the thermal-hydraulic equation of Appendix B:

$Q_5 = Q_{17} = 0.5\ Q_w$

15.11.12.27 Question No. 440.106

Is the letdown fluid temperature at the heat exchanger user input as stated by Section 11.0 or calculated in accordance with Eq. (F-3)?

Response

For analyzing letdown line break events, the mathematical model described in Appendix F is employed. For these events the letdown fluid temperature at the regenerative heat exchanger (RHX) exit is calculated using Eq. (F-3).

Under normal operating conditions the charging and letdown temperatures are selected to be those corresponding to the steam generator outlet temperature. The letdown flow rate (gpm) is a user input quantity. The user input temperature referred to in Section 11.0 is the temperature at which this letdown flow is measured.

15.11.12.28 Question No. 440-107

In the iterative procedure described in Appendix F is the critical flow set equal to the Darcy flow? Why assume saturation at the RHX exit?

Response

In the procedure described in Appendix F the Darcy flow in the letdown line and the critical flow rate at the break are iteratively calculated until these two values agree within a specified criterion.

The model does not assume that the letdown fluid is saturated at the RHX exit. However, the fluid enthalpy at the RHX exit is assumed to be equal to the saturation liquid enthalpy corresponding to the RHS exit temperature (from eq. (F-3)). If the fluid is, in fact, subcooled at the RHX exit, the above assumption would have a negligible effect on the results.

If the fluid is in a two-phase state, the above assumption yields conservative results, since the assumption of a lower enthalpy (i.e., saturated liquid enthalpy) results in a higher calculated critical flow rate at the break.

15.11.12.29 Question No. 440.108

What is the data base for the heat transfer correlation given by Eq. (F-4)?

Response

The overall heat transfer coefficient U is dependent on the letdown and charging flow rates. UA is given by the CE generated (Ref. 10) empirical equation (F-4) shown below.

$$(UA)^{-1} = X \ . \ G_1{}^{-0.8} + Y \ . \ G_c{}^{-0.8} + Z$$

where,

U is the overall heat transfer coefficient, Btu/hr-ft^2 -°F,

A is the heat transfer area, ft^2

G_1 and G_c are the letdown and charging flows in gallons/minute, and

X, Y, and Z are constants dependent on the design of the regenerative heat exchanger (RHX).

The constants X, Y, and Z for the System 80 RHX were calculated using the RHX performance data shown in Table 15.11-3. The date was extracted from the general specification for the RHX for the System 80 standard design provided in Table 15.11-5.

UA is calculated using the data shown in Table 15.11-3 and the following equation:

$$UA = \frac{\left(\dot{M}_c\right)\left(C_{pc}\right)\left(t_{co} - \left(t_{ci}\right)\right.}{\Delta t_{lm}} \qquad (2)$$

where,

$$\Delta t_{lm} = \frac{\left(t_{li} - t_{co}\right) - \left(t_{lo} - t_{ci}\right)}{\ln \frac{\left(t_{li} - t_{co}\right)}{\left(t_{lo} - t_{ci}\right)}}$$

$\dot{M}_c$ is the charging flow rate, lbm/hr,

C_{pc} is the average specific heat for the charging fluid, Btu/lbm - F,

t_{li} and t_{lo} are the temperatures of the letdown fluid at the RHX inlet and outlet, F, and

t_{ci} and t_{co} are the temperatures of the charging fluid at the RHX inlet and outlet, F.

The values of UA generated from Equation 2 are employed in Equation 1 to calculate the constants X, Y, and Z. For the System 80 RHX, the constants are:

X = 7.2160 X 10^{-5}

Y = 6.3085 X 10^{-5}

and Z = 1.0800 x 10^{-5}

These constants are input into the CESEC code to calculate UA for different letdown and charging flow rates. The CESEC calculated values of UA are then employed in Equation (F-3) to calculate the temperature of the letdown fluid at the RHX exit, t_{lo} (Ref. 10).

$$t_{lo} = \frac{tci\left\{1 - \exp\frac{\left[UA(1-R)\right]}{\dot{M}_l C_{P_l}}\right\} - t_{li}\ (1-R)}{R - \exp\frac{UA(1-R)}{\dot{M}_l C_{P_l}}} \qquad (3)$$

(eqn. F(3) of Ref. 10)

where,

$$R = \frac{\dot{M}_l\ C_{pl}}{\dot{M}_C\ C_{pc}}$$

$\dot{M}_l$, $\dot{M}_c$ are letdown and charging flow rates, lbm/hr

C_{pl}, C_{pc} are the average specific heats of letdown and charging fluids Btu/lbm - °F

In order to assess the accuracy of the empirical correlation provided as Equation (F-4), calculated values of t_{lo} (using Equation F-3) for various flow rates and inlet temperatures are compared in Table 15.11-4 with measured values of t_{lo}. The flow rates and temperatures in Table 15.11-4 are extracted from the general specification and the project specification for the RHX for the System 80 standard design (Tables 15.11-5 and 15.11-6).

The comparisons provided in Table 15.11-4 indicate that the calculated values of t_{lo} agree very well with the measured steady-state values (see sample calculation).

Sample Calculation:

Calculation of t_{lo} for case 3 of Table 15.11-4 is shown below.

Equation (3) uses the average specific heats of the charging and letdown fluids, i.e., specific heats at the average temperature, $(t_{li} + t_{lo})/2$ and $(t_{ci} + t_{co})/2$. Since, at the start of the computation t_{lo} and t_{co} are not known, assumed values of C_{pl} and C_{pc} are used in the beginning and Equation 3 is used iteratively to compute the value of t_{lo}.

In the sample calculation below, since measured values of t_{lo} and t_{co} are known, C_{pl} and C_{pc} at the average of the measured temperatures are used. The need for an iterative procedure is thus avoided.

Data (measured values):

G_c = 92 GPM	G_l	= 135 gpm
T_{ci} = 130F	T_{li}	= 564.5F
T_{co} = 419F	T_{lo}	= 382F

Calculation:

Average Temperatures:

T_c = 274.5F T_l = 473.3F

Specific heats at the average temperatures and assumed pressure of 2000 psia are obtained from Ref. 18.

C_{pc} = 1.0091 Btu/lbm°F

C_{pl} = 1.1235.8 Btu/lbm°F

From Equation (1)

(UA)-1 = 1.3920 X 10^{-5}

or UA = 7.1839 X 10^4 Btu/hr - °F

$$R = \frac{\dot{M}_1 C_{p1}}{\dot{M}_c C_{pd}} = \frac{G_1}{G_c}\frac{C_{p1}}{C_{pc}} = \frac{1.6337}{}$$

$\dot{M}_1$ = 67,242.7 lbm/hr (using ρ = 62.104 lbm/ft^2) (Ref. 18).

Using UA, R and $\dot{M}_1$ in Equation (3) we obtain t_{1o} = 383.4°F which agrees well with the measured t_{1o} of 382°F.

15.11.12.30 Question No. 440.109

a. Why does the suppression factor S, given by Eq. (13-9) not correspond with the formula given in Table 2 of the Hoeld* paper referenced?

b. Provide references/explanation for the difference in functional dependence between Chen's suppression factor† $f(Re_R F^{1.25})$ and Hoeld's expression $f(1 - x)Re\ R^{F-1.25}$.

c. Justify the choice of Hoeld's formula for the Reynold's number factor, F, Eq. (13-8) over the original Chen values.

Response

The suppression factor S introduced in Chen's correlation for the two-phase flow is a function of Re_b – $F^{1.25}$ (Reference 36). In the Hoeld paper (Ref. 20), he formulated the factor as

$s = 1/[1+(1.63)(10^{-5})(1-X)\ Re_b\ F^{1.25}]$

Note that the exponential 1.25 was misprinted as -1.25. The (1-X) term is accounted for a mixture. If the mixture quality equals 0, F=1.

The CESEC code uses this formula for calculating the primary side heat transfer for a condition of two-phase flow with boiling (reverse heat transfer). CESEC will be modified as indicated above. However, no significant differences are expected in the consequences of transients analyzed with the incorrect exponent, since boiling occurs in the primary side of the steam generator tubes for only a very limited portion of a few transients analyzed with CESEC.

In order to solve for the heat transfer coefficient using the Chen correlation it is necessary to determine the Reynolds-number Factor, F. The open literature prior to the Hoeld paper

---

*A. Hoeld, "A Theoretical Model for the Calculation of Large Transients in Nuclear Natural Circulation U-Tube Steam Generators (Digital Code UTSG)," Nuclear Eng. and Design, 47, pp-1-23, 1978.

†J. C. Chen, "Correlation for Boiling Heat Transfer to Saturated Fluids in Convection Flow," I&EC Process Design and Development, 5, pp. 322-329

recommended a lookup of the value from a graph or table. Since Hoeld was generating a digital computer code, it was more practical to use a fit to Chen's data for use in the code. The Hoeld paper provides a fit to the Chen data for the Reynolds-number factor as a function of the Martinelli parameter, X_{tt}. It is of the form

$F = 1.0 + 1.6 (1/ X_{tt}) 0.8174$

When the Hoeld functional fit is compared to the Chen data (Reference 19), reasonable agreement is observed (See Figure 15.11-16). For these reasons the Hoeld expression for the Reynolds-number factor is used in the CESEC-III code.

15.11.12.31 Question No. 440.110

Justify the use of the Dittus-Boelter correlation, Eq. (13-3) for film heat transfer.

Response

Equation (13-3), the Dittus-Boelter correlation is used during subcooled flow to calculate the heat transfer coefficient. The correlation is not used during film boiling heat transfer.

The physical properties of water required for all of the heat transfer correlations used in CESEC are obtained using the relationships given in Reference 21.

15.11.12.32 Question No. 440.111

a. Justify the assumption of two phase flow with condensation in the steam generator primary for all cases of forward heat transfer.

b. Explain why the extrapolation of the Akers, Deans, and Crosser correlation to the water system is valid.

Response

a. CESEC uses the correlation for two-phase flow with condensation, Equation (13-4), for heat transfer from the reactor coolant to the steam generator tubes (forward heat transfer only) whenever the reactor coolant in the steam generator tubes is saturated.* Under such conditions heat transfer can be expected to involve a condensation component, since in order for heat transfer to take place in the forward direction the tube walls and any liquid film on the inside surface of the tube walls must be at a lower temperature than that of vapor phase present in the node, which will be saturated and at the bulk fluid temperature.

b. The Akers, Deans, and Crosser correlations has been demonstrated by CE in Reference 28, Section 3.5, to be valid in the water system.

*See Section 13 of Ref. 10 for a discussion of the correlations used for other conditions.

15.11.12.33 Question No. 440.112

a. Present the database for CE's modification of the Rohsenow pool boiling correlation, Eq. (13-10), and discuss the range of validity.

b. Should the term (P-800) be (P_{sec} - 800) in the second expression for K_R on page 13-5?

Response

a. The modified Rohsenow pool boiling correlation (Equation 13-10, Reference 10) is used in the calculation of the secondary side heat transfer coefficient during forward heat transfer. The coefficient K_r in the correlation is a function of the pressure on the secondary side of the steam generator.

For pressures less than 800 psia, K_r has been compared to the experimental data from which it was generated using Equation 1.

$$E = \left[\frac{1}{N-K-1} \sum_{x-1}^{N} \left(\frac{K_{\exp} - K_{cor}}{K_{cor}} \right)^2 \right]^{1/2} \qquad (1)$$

where:

E = Difference between correlation and experiment, percent
N = Number of data points
K = Number of undetermined coefficients in correlation
K_{exp} = Experimental data point
K_{cor} = Coefficient as calculated from correlation

The difference between the correlation for Kr and the experimental data using Equation 1 was 7.2 percent for data taken over the following ranges.

Pressure 300 - 900 psia
Heat Flux 30,000 to 52,000 Btu/hr-ft^2

The correlation for K_r which is used for pressures greater than 800 psia was based on preliminary results from experiments performed at CE. When the correlation is compared to a more reliable set of CE data, a 30.4% difference between the correlation and the experimental data using Equation 1 results. The experimental database for this comparison has the following ranges.

Pressure 800 - 1200 psia
Heat Flux 27,000 - 86,000 Btu/hr-ft^2

Although both correlations differ from the experimental data, the differences are accounted for in the initialization scheme by adjusting tube resistance and wall fouling resistance term in the calculation of the overall heat transfer coefficient.

b. The term (P-800) should be (P_{sec} - 800).

15.11.12.34 Question No. 440.113

Justify the assumption of free convection in the steam generator secondary during reverse heat transfer.

Response

If the temperature of the secondary side exceeds that of the primary side, then reverse heat transfer (secondary to primary) exists. During this mode of heat transfer, free convection on the secondary side is assumed to exist. The appropriateness of this assumption has been established by the NRC acceptance of the model used for small break LOCA analysis (References 22 & 23) and of the CEFLASH-4AS computer code (References 24 & 25) which utilizes the model. The McAdams correlation used in CESEC (Eq. 13-11 of Ref. 10) for this heat transfer mode is the same as the correlation used in CEFLASH-4AS (Section 2.2 of Ref. 25), as approved by the NRC.

15.11.12.35 Question No. 440.114

Is flow through the valves of the steam system assumed to be choked even when the sink pressure is higher than the throat pressure?

Response

When the sink pressure is higher than the throat pressure, the flow through the valves of the steam system is not assumed to be choked and the orifice equation is used to calculate the mass flow rate. The throat pressure is determined from correlations appropriate to the critical flow correlation used. The turbine is represented by an effective flow area with critical flow and zero sink pressure. When the turbine is tripped the effective flow area is zero.

For steam generator tube rupture events flow rate is calculated using the appropriate correlation. The mass and energy removal from the primary coolant due to this flow is accounted for in the external flow terms of the thermal hydraulic equations (Eq. B-28 of Ref. 10) for the steam generator tube nodes. The addition of this mass and energy to the secondary is accounted for in the "leakage" terms, W_L and h_L, of the steam generator shell side mass and energy balance equations (Figure 13-1 of Ref. 10). It should be noted that 1 these "leakage" terms are specifically for the steam generator tube rupture event. Ordinary operational steam generator tube leakage up to the Technical Specification limit is neglected in analyses done with CESEC (p. 16-4 of Ref. 10).

15.11.12.36 Question No. 440.115

Justify the expression for A_{TUB} in Fig. 15-1A.

Response

All flow processes in the secondary system header simulator of Fig. 15-1A (of Ref. 10) are assumed to be isenthalpic. The steam flow through the turbine is

$$W_{TUB} = A_{TUB}\, P_{HEAD} \quad \frac{1977.6}{h_g - 185}$$

Turbine power is W_{TUB} x (h_g - h ℓ),

where h ℓ = effective enthalpy of fluid leaving turbine. Turbine power, P_{TBD} f'_D (t), at time t equals the steam power.

Therefore P_{TBD} f'_D (t) = W_{TUB} (Hg - h ℓ)

$$= \quad A_{TUB}\, P_{HEAD} \frac{1977.6}{h_g - 185} \quad (h_g - h_\ell)$$

This yields A_{TUB} = $$\frac{P_{TBD}}{\frac{1977.6}{h_g - 185} P_{HEAD}\, h_g} \left[\frac{h_g}{h_g - h_\ell} \quad f'_D(t)\right]$$

The time function power demand fraction, F_D (t), in Fig. 15-1A is therefore equal to $\left[\frac{h_g}{h_g - h_\ell} f'_D(t)\right]$.This quantity is input to the code as a table.

15.11.12.37 Question No. 440.116

Correct the equation for W_{gL} in Fig. 15-1A.

Response

The equation for W_{gL} in Fig. 15-1A should read

$$W_{gL} = F_{RC}\left(\frac{P_{SECL} - P_{HEAD}}{v_L}\right)^{1/2}$$

15.11.12.38 Question No. 440.117

Justify the use of CRITCO for steam discharge flow when the reference* quoted in the CESEC report is for two phase mixtures.

Response

---

*A. N. Nahavandi and H. Rashevsky, "Computer Program for Critical Flow Discharge of Two Phase Steam-Water Mixtures," CVNA-128, February, 1962.

Calculations were done to show the correlation between the Darcy formulation for critical flow (last equation on p. 2-15 of Ref. 26) and the CRITCO (Ref. 27) formulation over the pressure range of interest (100-1000 psia) for the steam line break incident. With an average deviation between the Darcy and CRITCO formulations of about 1.7 percent over the pressure of interest, these two formulas correlate closely. In this comparison for the steam line break incident, the flow path geometry was used to determine the critical flow constants in the Darcy formulation.

For flow through valves the flow path geometry is accounted for by a normalization during code initialization. The code calculates an effective, full-open design valve flow area based on full-open design steam flow at design pressure. Then during the dynamic calculation, the steam flow rate is determined using this area, the pressure, and the fractional valve opening.

15.11.12.39 Question No. 440.118

Is an orifice coefficient used in Eq. (16-4) only when the steam generator tube rupture option is selected?

Response

The orifice equation, (16-4) is of the following form:

$G = (C\ \Delta P\ \rho)^{1/2}$

where,

G = Mass flow rate per unit area (lbm/sec/ft^2)

C = 2 X acceleration due to gravity = 64.4 $\left(\frac{\ell bm - ft}{\ell bf - \sec^2}\right)$

ΔP = source to sink pressure drop (lb/ft^2)

ρ = fluid density (lbm/ft^3)

When the steam generator tube rupture option is selected the right hand side of the above equation is multiplied by a coefficient which accounts for the friction and geometric losses. For other options such as the steam line break option, this coefficient is assumed to be unity. (See page 16-3 of Ref. 10).

15.11.12.40 Question No. 440.119

Show why the steam generator load dependency of the steam generator water level, required in the steady-state situation, is not needed to determine level during transients.

Response

The downcomer water level for the steam generator is calculated during the transient using the load dependent model described in Section 17 of Reference 10. The model is used only for the determination of the low water level trip and is valid for steady state or near steady-state conditions on the load demand. Since the model is not valid during periods of rapidly changing

load demands, the low-level trip is not, in general, used as the primary trip for core protection. Other trips such as high pressurizer pressure or low DNBR are the primary trips credited for Chapter 15 analysis. When the low-level trip is credited, the setpoint for the trip is conservatively selected.

15.11.12.41 Question No. 440.120

Equations (B-31), (B-33), (B-35) and (B-54) should be corrected.

Response

(B-31)

$$(\beta_2 + \alpha_2 h_2^1)\, W_{1,2} - (\beta_2 + \alpha_2 h_2)\,(1 + F_I)\, W_{2,3} + (\beta_2 + \alpha_2 h_2^{14})\, W_{14,2}$$

$$\underline{+\delta_2 \dot{P} = \varepsilon_2}$$

$$\downarrow$$

(a second line which ends Eq. (B-31) was missing)

(B-33)

$$-(\beta_4 + \alpha_4 h_4)_2 W_{\underset{\downarrow}{4,2}} + \delta_4 \dot{P} = \varepsilon_4 - (\beta_4 + \alpha_4 h_4^{12}) W_{P^2}^{R}$$

(error in first term: Was W4,12, should be W4,2)

(B-35)

$$(\beta_6 + \alpha_6 h_5^{,}\, W_{5,6} + (\beta_6 + \alpha_6 h_3) \underset{\downarrow}{F_B}\, W_{3,5} - (\beta_b + \alpha_6 h_6)\,(1 + F_o + F_H)\, W_{6,7}$$

$$+\delta_6 \dot{P} = \varepsilon_6$$

(error, was FR, should be FB)

(B-54)

$$(\beta_{25} + \alpha_{25} h_{25}^{6})\, F_H\, W_{\underset{\downarrow}{6,7}} + (\beta_{25} + \alpha_{25} h_{25}^{18})\, F_H\, W_{18,19} - (\beta_{25} + \alpha_{25} h_{25})\, W_{25}$$

$$+\delta_{25} \dot{P} = \varepsilon_{25}$$

(error in second term: was W6,25, should be W6,7)

15.11.12.42 Question No. 440.121

Is reverse flow allowed in the core?

Response

The CESEC code does not allow reverse flow in the core.

15.11.12.43 Question No. 440.122

Is $W_{25} = 2W_{25,7}$?

Response

$W_{25,7} = W_{25,19} = 0.5W_{25}$

15.11.12.44 Question No. 440.123

Describe the algorithm CESEC uses to trace the state of the pressurizer and to maintain continuity as the state changes. Is there an automatic time step adjuster?

Response

The continuity of the state changes of the pressurizer fluid is controlled using the algorithms described in Subsection 4.2.5.3 of Reference 5. There is no automatic time step adjustment due to the pressurizer status change in CESEC. The user is furnished at each major edit with a print-out of the accumulated non-conservation of mass and energy in the pressurizer (and in the RCS) up to that time. If the small discontinuities which may result from state changes cause significant non- conservations of mass and/or energy, the user can re-run the case with smaller time steps.

The initially pre-determined values of fluid mass and enthalpy are associated with the pressurizer fluid status defined as saturated liquid and vapor.

At the beginning of each time step the actual fluid mass and enthalpy values are updated based on the pressurizer status, i.e., the status determined at the end of the previous time step.

At the end of each time step the pressurizer status is determined based on the vapor and liquid mass and enthalpy check. If the current status differs from that determined at the end of the previous time step, the necessary adjustment takes place and an appropriate message is given to the user. The adjustment is performed in order to maintain the continuity of the pressurizer status throughout the transient.

15.11.12.45 Question No. 440.124

Justify the identification, in state 8, of W_B with the vapor portion of the critical flow through the pressurizer valve. How is this consistent with the absence of W_B in state 7?

Response

No boiling is assumed for pressurizer state 7 which is defined as subcooled liquid without presence of a steam region. However, when the pressurizer state ischecked (at the end of each

time step) boiling can appear (see Subsection 15.11.12.44) in which case the pressurizer state is changed to 8 if $W_B \leq W_{valve}$ or to 4 if $W_B > W_{valve}$. Since the valves are located near the top of the pressurizer, for the condition $W_B \leq W_{valve}$,it is assumed that all steam generated from boiling is removed through the valves. Therefore, the boiling flow in state 8 is identified with the vapor portion of the valve flow at the valve entrance. Note that this is used to determine the enthalpy of the fluid entering the valves, not the vapor fraction directly. Flashing in the valves will in general increase the vapor fraction in the flow exiting the valves.

15.11.12.46 Question No. 440.125

Provide references for the two phase pressure drop correlations Eqs. (C-1) - (C-5) and a comparison with the Barcozy* or Chisholm† correlation.

Response

Equations (C-1) through (C-5) provide the two-phase multiplier for the frictional pressure drop term for pressures less than 250 psia. The appropriateness of these equations has been established by the NRC acceptance of the model (Section III. C.2.b of Ref. 11) and of the CEFLASH-4A computer code (Section III. B.18 and Appendix N, of Ref. 12) which utilizes the model.

15.11.12.47 Question No. 440.126

Are the CEFLASH-4A water properties applicable to the supercritical region? Provide a copy of the report.‡

Response

The McClintock and Silvestri routines (Ref. 21) are used to determine water properties in CESEC (p. 8-1, Ref. 10). Water property derivatives are determined using CEFLASH-4A routines (p. 8-2, Ref. 10). The CEFLASH-4A water property derivatives are limited to subcritical pressure regions. The transients which are studied in the safety analysis reports stay within the applicable pressure range. ATWS transients, which may go beyond this range, would bear further investigation to determine the errors encountered by use of the CEFLASH-4A water property derivatives. However, significant errors are not expected, even for ATWS transients. At the present time there is no ATWS licensing requirements. CESEC-III is not being used for ATWS evaluations.

A copy of the requested document* has been transmitted.

---

*C. J. Barcozy, "A System Correlation for Two Phase Pressure," AIChE reprint #37. Paper presented at the 8th Nat. Heat Transfer Conf., Los Angeles, Aug., 1965.
†D. Chisholm, "The Influence of Mass Velocity on Frictional Pressure Gradients During Steam-Water Flow," Paper 35 presented at the 1968 Thermodynamics and Fluid Mechanics Convention, Bristol, 1968.

‡CENPD-133, "CEFLASH-4A, A FORTRAN IV Digital Computer Program for Blowdown Analysis," August, 1974.

15.11.12.48 Question No. 440.127

Explain why Eq. (D-12A) can be neglected.

Response

The set of equations which appear in Section 5.0 and Appendix D of the CESEC report have been approved by the NRC for usage in CEFLASH-4A (Reference 12). These equations appear, respectively, in Section III.B.3 and Appendix I of Ref. 12.

Equation D-11 as explained in Ref. 12 and Appendix D of the CESEC report can be rewritten in terms of two linear differential equations of the first order. The solution of these equations then represents the total solution to Equation D-11. Equation D-12B relates the exit fluid conditions of the node to the nodal average fluid conditions, while Equation D-12A yields the relationship between inlet and average node enthalpies. The solution of Equation D-12A provides numerically for the proper heating of the fluid as it exits the node for steady-state and transient conditions. Therefore, Equation D-12A may be neglected from a numerical standpoint.

15.11.12.49 Question No. 440.128

a. How is the reference exit temperature in the steam generator node calculated and how is it used?

b. How is the exiting enthalpy computed?

Response

a. The reference exit temperature used in CESEC is Tsec, the temperature of fluid in the secondary side of the steam generator. This reference temperature is applied to ensure that the heat transfer between the primary and secondary sides has not violated the second law of thermodynamics. In other words, it is used as a physical bound for the calculated exiting temperature of the primary side. For example, in the situation of heat transfer from primary to secondary, the exiting temperature of the primary side must be greater than or equal to Tsec. For the situation of reverse heat transfer, secondary to primary, the exiting temperature of the primary side must be less than or equal to Tsec. Upon violation of the 2nd law of thermodynamics, the exiting enthalpy is set equal to the node enthalpy (see Equation (D-15)). This updated value of exiting enthalpy is then used in either Equation (D-13) or (D-14), depending on the flow condition, to solve for the corrected heat transfer rate between primary and secondary, Q. At this point, the newly calculated heat transfer rate is compared to the original which is calculated by the steam generator algorithm (see Equation (13-1)). If the direction of heat transfer predicted by both calculations is the same, then the corrected heat transfer rate and the updated exiting enthalpy (node enthalpy) will be used for that time step. If the direction of heat transfer predicted by both calculations is not the same, then the heat transfer rate is set equal to zero for that time step. These steps are presented in outline form in the detail at step G(8) of Table 15.11-7.

b. The exiting enthalpy is calculated by using either Equation (D-13) or (D-14).

15.11.12.50 Question No 440.129

Prove that Eq. (E-4) converges. Response

Convergence of Equation (E-4) is a necessary condition for the execution of CESEC. The equation is known to converge within the upper limit specified within the code on the number of iterations. If this limit is exceeded, code execution is terminated.

15.11.12.51 Question No. 440.130

How is the moderator feedback divided between the void feedback and the density feedback?

Response

Void formation is not a significant concern in non-ATWS events. In ATWS calculations, the void contribution to moderator reactivity is separated from the density contribution as follows.

When there is significant void formation in the core, the density contribution to moderator reactivity is evaluated at the core average two-phase density of the coolant under saturated conditions at the given pressure (P) and temperature (T). An input table of moderator reactivity vs. moderator density is interpolated for this purpose.

The method of estimating the void contribution consists of (1) calculating the void distribution throughout the core, and (2) flux and volume weighting the point-wise reactivity contributions to obtain the core average void reactivity. With a knowledge of void distribution and hence the density distribution in the core, spatially dependent void reactivity R(z) is given by the relation:

$R(Z)_{void} = R\ [\ D\ (Z)_{P,T}) - (D_p,T)$

where:

P = system pressure (psia)

T = saturation temperature at pressure P (F)

$D_{P,T}$ = core-average two-phase density when coolant is saturated at pressure P and temperature T.

$\rho(D_{P,T})$ = reactivity contribution due to the core-average two-phase moderator density.

$D(Z)_{P,T}$ = local two-phase fluid density corresponding to the given P, T and the local void fraction.

R[D(Z)]= local point-wise reactivity interpolated from an input table density D (Z).

The above formula is flux and volume integrated over the core to obtain the core average void reactivity ρ_V. (Ref. 2, Section 2.3 and Ref 6, Section 1.4).

15.11.12.52 Question No. 440.131

a. Provide additional information about the core coolant flow and temperature calculation as the connection between COREQ and LOOPEQ is not clear. Which moderator temperature and density is used for the reactivity feedback?

b. What fraction of instantaneous core power is absorbed by the coolant?

Response

a. COREQ is the CESEC-ATWS routine responsible for reactor kinetics and fuel heat transfer calculations. Briefly, it solves the point kinetic equations, and performs decay heat calculations to arrive at the toal core power. Alternatively, core pwer can be specified as an input function of time, and the ANS decay heat curve option is available after long term operation.

   In the heat transfer part of COREQ the standard heat conduction equation for the core average channel is solved to obtain the temperature distribution and core heat flux at each time step. The heat conduction model uses three equal volume radial nodes in the fuel road, and one node in the coolant channel. Core coolant flow is an input constant to this calculation (Ref. 6, Section 1.3).

   LOOPEQ does not perform any calculations in CESEC-ATWS. This routine was retained for initializing certain parameters such as RCS temperatures and flows. There is no direct connection between COREQ and LOOPEQ.

   Moderator reactivity is determined in the code at core-average moderator temperature and density by interpolating input reactivity tables.

b. The fraction of instantaneous core power liberated in the moderator is a plant specific input parameter. Typically for a PWR, the value is around 2.5 percent.

15.11.12.53 Question No. 440.132

Justify the reactivity flux weighting method (i.e., flux or flux **2).

Response

Although provision for reactivity flux weighting exists in the void reactivity model, this option has not been utilized. In analyses performed to date, only one axial node is specified for the core in the input, and as such flux weighting is immaterial.

15.11.12.54 Question No. 440.133

Why does the void reactivity calculation employ static quality when the Martinelli- Nelson correlation* referred to uses flowing quality?

---

*N. C. Sher, "Review of Martinelli-Nelson Pressure Drop Correlation," Westinghouse Electric Corp., Report WAPD-TH-219 (July 1956).

Response

The void reactivity calculation option has not been exercised in CESEC-III. It has been used only in ATWS analyses.

Martinelli-Nelson correlation is used to estimate the void fraction when system pressure falls below 1850 psia. At pressures of 1850 psia and higher, the void formation is simply given by the homogeneous model based on static quality.

In ATWS events the critical parameter is the RCS peak pressure which is in the region of 2900-4000 psia for CE plants. Thus, Martinelli-Nelson correlation is of no concern in predicting the severity of ATWS events. The correlation comes into play only during the depressurization phase when system pressures are below 1850 psia and power levels are low (< 10% design).

The question of static vs. flowing quality in Martinelli-Nelson correlation has no effect on the conclusions of the safety analysis. Therefore, the use of static quality derived from the enthalpy distribution throughout the calculation is a simplifying assumption which is entirely adequate. Additionally, a comparison of total reactivity for a range of representative cases shows good agreement between CESEC and PDQ-TH which is the industry-wide production code for reactor physics calculations. This comparison confirms the adequacy of using static quality throughout the void reactivity calculations. (See Section 2.0, Reference 6.)

15.11.12.55 Question No. 440.134

a. Is the quantity Q used in T_{eff} for the Doppler an input constant.

b. How is it detemined?

Response

a. Doppler reactivity is interpolated from an input table of reactivity vs effective fuel temperature T_{eff}. The quantity Q used in the expression for T_{eff} is not an input constant. It is defined as the ratio

$$Q = \frac{\text{Core heat flux (t)}}{\text{Design power}}$$

Design power is an input to the code, while core heat flux is calculated at each time step.

b. Average core heat flux is computed in CESEC by solving the heat conduction equation for an average fuel rod surrounded by moderator. In the steady state, core heat flux equals the total fission power (Mwt), and Q is a constant. In a power transient, however, the heat flux from the fuel lags behind the total fission power, and Q, the core heat flux expressed as a fraction of input design power becomes time-dependent. Details of the fuel heat conduction model are found in Ref. 6, Section 1.3 and related references.

15.11.12.56 Question No. 440.135

Justify the CESEC/PDQ-TH calibration scheme for weighting factors.

Response

A comparison of total reactivity as calculated by CESEC-ATWS and PDQ-TH for several realistic cases, shows that there is good agreement between the two codes, and hence, demonstrates the adequacy of the CESEC reactivity model. Thus, weighting factors to adjust reactivities are no longer used (Ref. 6, Section 2.0).

15.11.12.57 Question No. 440.136

Explain why in the formulation of the T/H nodal equations the pressure p is used but in the determination of water properties the pressure $p + \Delta\rho$ surge is utilized.

Response

Although for a different number of nodes, the CESEC-ATWS code uses the same thermal-hydraulic formulation as the CESEC-III version. Therefore, refer to Subsection 15.11.12.8 for the response to this question.

15.11.12.58 Question No. 440.137

Present the derivation/assumptions used to reduce the T/H nodal equations to a 19 equation set.

Response

The derivation for the 19 equation set utilizes the same assumptions as are used for CESEC-III, but with different variable names. The derivation for the 19 equation set is presented in Section 4.2 of Reference 5.

15.11.12.59 Question No. 440.138

In the T/H model is the instantaneous core power entirely absorbed by the coolant with no heating of the fuel?

Response

The CESEC-ATWS code used the same formulation as the CESEC-III version. The instantaneous core power is used in the solution of the heat conduction equation for the fuel rod. A discussion of the solution model is presented in Section 10.2 of Reference 10.

15.11.12.60 Question No. 440.139

Are the sprays 100 percent efficient?

Response

The pressurizer sprays are 100 percent effective in the CESSAR-ATWS code.

15.11.12.61 Question No. 440.140

Discuss the DNBR calculation in more detail; in particular the open/closed channel aspect.

Response

The CESEC-ATWS code had the capability of calculating DNBR. This calculation is used only to determine trends in DNBR and not for safety analysis. Refer to Subsection 15.11.12.5 for the details of the DNBR methodology.

15.11.12.62 Question No. 440.141

Describe the modeling of the steam bubble. What effect does the assumption of a uniform RCS pressure have?

Response

The CESEC-ATWS code does not explicitly model the formation of voids in the upper head region which may occur during events with rapid primary system depressurization or overcooling.

SAR Chapter 15 depressurization and overcooling transients, which have a potential for causing void formation due to pressurizer drain, or depressurization to saturation conditions, are increased heat removal by the secondary system events (e.g., steam line break) and the decrease in primary system inventory events (e.g., steam generator tube rupture). Analyses of these transients have been conducted (Ref.30) to evaluate the impact of void formation in the reactor vessel upper head region on system response and in terms of meeting criteria as specified by the SRP guidelines.

The limiting Chapter 15 accident with respect to void formation for the increase in heat removal events is the steam line break. For the decrease in inventory events the steam generator tube rupture is limiting. The limiting anticipated operational occurrence (AOO) is the inadvertent opening of an atmospheric dump valve with loss of offsite power (limiting single failure). Conclusions from these analyses, for which the most severe depressurization is predicted, bound the rest of the SAR Chapter 15 depressurization and overcooling events.

The SAR analyses performed with vessel head voiding indicate that voiding is not extensive enough to initiate the uncovery of the reactor vessel hot legs. Additionally, these analyses conclude that voiding does not result in violation of the SRP requirements for CE plants. The main impact of the vessel upper head void is a slower pressure response; since once this relatively stagnant region reaches saturation, it acts like a pressurizer. The slower pressure response can hold up the pressure for steam generator tube rupture and steam line break events. This will increase the primary to secondary leakage during a steam generator tube rupture event and reduce the safety injection flow during a main steam line break event. However, the impact of these effects does not result in a violation of the criteria specified by the SRP guidelines, even though upper head voiding has an impact upon transient values of plant parameters.

See Subsection 15.11.12.7 for assumption of a uniform RCS pressure.

15.11.12.63 Question No. 440.142

Is there only boiling heat transfer on the secondary side of the steam generator and only film heat transfer on the primary side?

Response

In the CESEC-ATWS code, boiling heat transfer is assumed to exist in the secondary side until the quality exceeds 90 percent. At qualities greater than 90 percent no heat transfer is assumed to exist. See Subsection 15.11.12.64 for the 1 details of the tube bundle quality calculations.

On the primary side of the tube bundle, only film heat transfer is assumed to exist.

15.11.12.64 Question No. 440.143

a. Explain the steam generator dryout heat transfer criterion and the calculation of UA.

b. How is the steam flow calculated?

c. How is tube heat transfer area related to the mass inventory, the recirculation flow, and the quality calculation?

d. How is quality calculated?

Response

a. Refer to Part C.

b. The steam flow from the secondary side of the steam generator is determined as described in Section 15.0 of Reference 10.

c. A model is provided in the CESEC-ATWS code to calculate the steam quality in the tube bundle region, the downcomer level, and the effective heat transfer area, for each of the two steam generators. The calculations are performed consistent with the assumptions of saturated conditions in the steam generator. For this calculation, the liquid inventory, the steam inventory, the secondary pressure, the fluid specific volume, the steam specific volume, the feedwater flow, the steam flow, and the time increment, are the independent variables. The model calculates the steam generator downcomer level, and the fraction of total tube bundle area, which is effective in providing heat transfer.

   The steam generator is divided into five basic regions, the downcomer, the steam drum, a riser region with a perfect steam separator, a non-boiling region of the tube bundle, and a boiling region of the tube bundle. During conditions where effective heat transfer exists over the entire length of the tube bundle, the boundary between the non-boiling and boiling regions of the tube bundle and the tube bundle exit quality are calculated consistent with the total liquid and steam inventory in the steam generator. Two basic assumptions made in this calculation are the existence of saturated conditions (for both water and steam) and a linear variation of quality with height in the boiling region of the tube bundle. Although

the option of specifying a non-boiling region exists, the option was never exercised. The non-boiling region terms, however, are included here for completeness.

The downcomer level is determined from hydraulic and momentum balance around the internal circulation loop of the steam generator, which is described by:

DCL = (H1*1./VF-1./VR) + H2*(1./VB-1./VR) + HRISER*
((1./VR-1./VG)

+ HTUBE*((1./VR-1./VG) + DP*144)/(1.VF-1./VG)

where:

DCL = water level in the downcomer region

H1 = height of the non-boiling region of the tube bundle

H2 = height of the boiling region of the tube bundle

VF = specific volume of saturated liquid

VG = specific volume of saturated steam

HTUBE= height of the tube bundle

VB = average specific volume of the tube bundle boiling region assuming a linear variation in quality.

calculated by

1.0/((1.0/(VFG*XR)))*ALØG(((VF+VFG*XR)/VF)))

XR = tube bundle exit quality

VFG = VG - VF

HRISER= height of the riser region

VR = average specific volume of the riser region

calculated by

VF + VFG * XR

DP = momentum pressure drop

In establishing the initial steady-state conditions, the downcomer level is input, the tube bundle exit quality is calculated and Equation 1 is solved for the balancing pressure drop.

During steam generator operation in the absence of any decrease in the effective heat transfer area, the total fluid mass in the steam generator (TØTFM) is given by:

TØTFM = DCM + SCM + BØILM + RISEM

where:

DCM = fluid mass in the downcomer region

= VDC/VF and VDC is the volume of the downcomer region calculated as a function of downcomer fluid level.

SCM = fluid mass in the non-boiling region of the tube bundle.

= ATUBE*H1/VF where ATUBE is the cross-sectional area of the tube bundle.

BØILM = fluid mass in the boiling region of the tube bundle

= (ATUBE*H2/(VFG*XR)*((VG/VFG)*ALØG((VF+VFG*XR)(/VF)-XR)

RISEM = fluid mass in the riser region

= ARISER*HRISER* (1.-XR)/(VF+VFG*XR)

The total steam mass in the steam generator (MSTØT) is given by:

MSTØT= BØILS + RISES + DRUMM

where:

BØILS = steam mass in the tube bundle

RISES = steam mass in the riser region

DRUMM= steam mass in the drum region

Steam masses are determined from similar equations involving the appropriate volumes, qualities and specific volumes, as are the fluid masses.

The two transcendental equations, 2 and 3 are solved iteratively for XR and DCL until the total steam and fluid masses converge to the total steam and fluid masses determined by mass and energy balance for the secondary side.

For those transients in which the steaming rate exceeds the feedwater flow rate: as the inventory of the steam generator is depleted and the total energy input to the steam generator is sufficient to increase the quality in the steam generator, secondary side bundle. A tube bundle exit quality will eventually be reached above which a mode is switched where the exit quality is kept constant at XDNB and H2 determined from Equations 2 and 3 to define the location where XDNB was first achieved (see Figure 15.11.17).

A heat transfer area degradation factor is then calculated by:

ARATIO = H2/HTUBE

where ARATIO is the ratio of the tube bundle height over which effective heat transfer is maintained to the total tube bundle height. This ratio is then used to

modify the effective heat transfer area in the overall heat transfer coefficient calculation. Thus, the overall heat transfer is calculated as

$U_D A_D - U_D * A_{HTUBE} * ARATIØ.$

where:

U_D = Dynamic overall heat transfer coefficient, Btu/hr-ft-F

A_D = Effective heat transfer area, ft

A_{HTUBE} = Total heat transfer area, ft

Further information on the steam generator model in the CESEC-ATWS code is presented in Section 3.2 of Reference 2. Section 3.3 of Reference 5, and Section 4.2 of Reference 6.

d. Refer to Part C.

15.11.12.65 Question No. 440.144

Is it correct that the heat transfer in the steam generator is

$$Q = \begin{cases} \dfrac{UA(T_i - T_s)}{\ell n \dfrac{(T_i - T_s)}{(T_o - T_s)}} \\ \\ \dfrac{UA(T_i + T_o - T_s)}{2} \end{cases}$$

UA = 1.0 UA forward transfer

= input reverse transfer

when $T_i > T_s$ and $T_o < T_{-s}$

with UA = 0.8 UA of previous timestep

where

UA = overall heat transfer coefficient

T_i = primary side inlet temperature

T_o = primary side outlet temperature

T_s = secondary side temperature

Response

Yes, the heat transfer in the steam generator is governed by these equations in the CESEC-ATWS version of the code.

15.11.12.66 Question No. 440.145

a. Does the code use the cold edge temperature or the cold leg temperature for the moderator feedback?

b. How is the cold edge temperature calculated?

Response

a. For conservatism in the analysis of steam line break initiated events, the code has an option which allows the user to specify that the cold edge density will be used for moderator feedback calculations.

b. The cold edge density is determined from the RCS pressure and the cold edge enthalpy, h_{edge}. The cold edge enthalpy is defined as the enthalpy of the fluid from the cold legs of the loop with the ruptured steam generator, with the addition of core heat up to the core axial midplane, and without the effect of mixing with fluid from the other loop. Using the notation used in Section 2 of Ref. 10,* and choosing SG2 as the steam generator with the ruptured steam line, an expression for h_{edge} can be written for steady-state:

*See also Figure 15.11-18

$$h_{edge} = h_1 + \frac{Q}{4W_{3,5}}, \qquad (15.11.12.66\text{-}1)$$

where Q is the total core heat generation rate and where it is assumed that $h_1 = h_4$ due to steady-state conditions.

The following also hold true at steady-state:

$W_{16,14} = W_{13,14} = W_{1,2} = W_{4,2}$, $W_{14,15} = W_{2,3}$,
$W_{15,17} = W_{3,5}$, and $h_{13} = h_{16}$.

Mass and energy balances can be written on nodes 3 and 15 and solved using the foregoing steady-state relationships together with the coolant heatup from node 3 to 5 and from node 15 to 17, to yield the enthalpies at nodes 5 and 17:

$$h_5 = \frac{h_1 + h_{13} F_1}{1 + F_1} + \frac{Q}{4W_{3,5}} \qquad (15.11.12.66\text{-}2)$$

$$h_{17} = \frac{h_{13} + h_1 F_1}{1 + F_1} + \frac{Q}{4W_{3,5}} \qquad (15.11.12.66\text{-}3)$$

Simultaneous solution of Eqns. (15.11.12.66-1), (15.11.12.66-2) and (15.11.12.66-3) yields the algorithm used in CESEC to calculate cold edge enthalpy:

$$h_{edge} = \frac{h_5 - h_{17} F_1}{1 - F_1} = \frac{h_5 + h_{17}}{2} - \frac{(1 + F_1)}{(1 - F_1)} \left[\frac{h_{17} - h_5}{2} \right] \qquad (15.11.12.66\text{-}4)$$

15.11.12.67 Question No. 440.146

Is there an iteration between the pump flow calculation and the energy/mass balance calculations?

Response

There is no iteration between the pump flow calculation and the thermal hydraulic equations.

15.11.12.68 Question No. 440.147

a. How is the input flow fraction for the outlet plenum to closure head flow determined?

b. Are the plena crossflows or the bypass flows user specified? If so what is the basis for the input values?

Response

a. The method used to determine the fraction of flow from the outlet plenum to the closure head, F_H, is based on flow net calculations. All possible flow paths are

determined and the loss coefficients for each component in each flow path is calculated. The loss coefficient calculations are generally based on published experimental data. Invoking conservatism of momentum and mass, the flow net equations are solved for each node. The results of these flow net calculations are mainly used for ECCS analysis and are quite detailed. All the fractions of flow from all flow paths leading from the outlet plenum to the upper head are summed to produce the input value of F_H for CESEC.

b. Certain plena crossflows and the bypass flows are calculated using input flow fractions. The plena crossflows $W_{2,14}$ and $W_{7,19}$ (see footnote on page 2-2 and Figure 2-1 of Ref. 10) are determined directly from the solution of the thermal hydraulic equations. The other plena crossflows are determined as described on page 2-2 of Reference 10, with the factors F_I and F_o being user specified values which are determined as described in response to Question 15.11.12.71 bypass flows are calculated using the input flow fraction F_B:

$W_{3,6} = F_B W_{3,5}$

$W_{15,18} = F_B W_{15,17}$

The bypass fraction, F_B, used for CESEC calculation is taken to be equal to the design value. However, bypass flows are calculated in considerable detail, using methods similar to those used to calculate F_H, to ascertain that the total bypass flow does not exceed the design value.

15.11.12.69 Question No. 440.148

How is the UA parameter used in the steam generator heat transfer determined at the minimum mass inventory (for CESEC-SLB)?

Response

UA is set equal to a value sufficient to transfer enough heat to raise any incoming feedwater to saturation enthalpy at the minimum mass inventory in CESEC-SLB.

15.11.12.70 Question No. 440.149

It is our intent that CESEC-III be used for future analyses instead of CESEC-I or CESEC-II. Please demonstrate that CESEC-III is capable of performing the required analyses by submitting an analysis of the following transients for the CESSAR design using CESEC-III:

a. steamline break,

b. feedwater line break,

c. loss of feedwater ATWS, and

d. steam generator tube rupture.

The results obtained with CESEC-III should be overlaid with the results obtained with CESEC-I and CESEC-II.

Response

a. Comparisons of CESEC-I, CESEC-II, and CESEC-III for Steam Line Break Analyses.

Introduction

Comparisons of results obtained using CESEC-I, CESEC-II, and CESEC-III for a full power large steam line break (SLB) with concurrent loss of offsite power are presented on Figures 15.11-19 through 15.11-30. The comparisons between CESEC-I and CESEC-III have been made for Waterford Unit 3 and are shown on Figures 15.11-19 through 15.11-24. Table 15.11-8 presents the initial conditions and Table 15.11-9 presents the sequence of events for this CESEC-I/CESEC-III comparison. The CESEC-I results presented here are the same as those given in the Waterford Unit 3 FSAR. Figures 15.11-25 through 15.11-30 present comparisons between CESEC-II and CESEC-III for System 80. Table 15.11-10 presents the initial conditions and Table 15.11-11 presents the sequence of events for this CESEC-II/CESEC-III comparison. The results obtained using CESEC-III are those presented in CESSAR-F. For each case, plots of reactivity, core power, RCS pressure, reactor coolant temperatures, reactor coolant flow rate, and minimum post-trip DNBR are presented versus time. The first five of these parameters are calculated directly by CESEC. A separate calculation, using CESEC output is used to determine DNBR.

The differences between results obtained using CESEC-III compared with those obtained using CESEC-I or CESEC-II are due to the presence of improved models in CESEC-III. For these SLB transients the most important effects are due to the improved/new models for

- reactor coolant pumps/flow
- reactor vessel upper head
- 3D reactivity feedback
- heat transfer from the metal walls of the RCS

The effect of each of these models upon the transient results will be discussed first with respect to comparison of CESEC-I with CESEC-III for Waterford and then with respect to the comparison of CESEC-II with CESEC-III for System 80.

CESEC-I/CESEC-III Comparison

The major reason for those differences which exist between the CESEC-I and CESEC-III results for Waterford are due to the differences in reactor coolant flow. CESEC-I uses an input table of flows. CESEC-III uses the pump/flow models to calculate flow. This model has been shown to yield very good agreement with test results (Fig. I-2 of Ref. 10). The initially higher loop flows in CESEC-I analysis causes a more rapid transport of the effect of the cooldown to the moderator density. This results in an early return-to-power in the CESEC-I analysis. The associated fluid heating, together with reactor coolant flows which

by this time are lower than those calculated by CESEC-III, results in a marked increase in reactor average and outlet temperatures. CESEC-III shows lower core inlet -- and consequently average and outlet -temperatures due to the appreciable higher flow rate from the loop with the affected steam generator compared with that from the other (hotter) loop. Overall moderator reactivity values are very similar for both code versions since both base moderator reactivity on a cold edge density. CESEC-III calculates this density as described in Subsection 15.11.12.66. The method for determination of cold edge density in CESEC-I is presented in Subsection 2.2.9.3 of Ref. 1.

The RCS pressure decrease with NSSS cooldown calculated by CESEC-III shown the effect of upper head voiding. The CESEC-I and CESEC-III pressure transients are essentially identical until flashing begins in the upper head node of the CESEC-III model. Without the influence of an upper head model RCS pressure, as calculated by CESEC-I, continues to fall until the pressurizer empties and hot leg saturation occurs. Thereafter the RCS pressure in CESEC-I follows the hot leg saturation temperature until pressurizer level is re-established.

The Waterford CESEC-III analysis illustrates the 3D reactivity results upon an SLB transient. As the power-to-flow ratio and the temperature tilt across the core (see Subsection 15.11.12.22) increase during the cooldown/return-to-power portion of the transient, 3D effects contribute a small amount of negative reactivity to help reduce the return-to-power.

For the analysis presented here wall heat transfer effects were included mainly in the upper head node of the reactor vessel. This increased the amount of void formation in the upper head and reduced the rate of decrease of RCS pressure. For the balance of the RCS only those components which could contribute to heating of the RCS over very long time periods were included. The effect upon the SLB transient of this heating over the time span shown here was small.

The minimum post-trip DNBR is affected by core power, core flow, core inlet temperature, and RCS pressure. Due to the very large radial neutron power peaking factors associated with the DNBR analyses for the post-trip portion of SLB events with an assumed stuck CEA, the most important parameter for these analyses is usually the core power at time of return to power. The lower return-to-power is the major factor in the higher DNBR calculated from the CESEC-III results. The slightly higher core flow and lower core inlet temperature had a smaller contribution. The effect of RCS pressure was negligible.

CESEC-II/CESEC-III Comparison

Similar to the comparison between CESEC-I and CESEC-III for Waterford, a significant reason for differences between CESEC-II and CESEC-III results for System 80 is the difference between reactor coolant flow in the two analyses. However, both the effect of the upper head model and the wall heat model are more evident for System 80, the upper head model having the most significant effect. The 3D reactivity model was not used in this analysis.

CESEC-II uses in an input table of flows, as does CESEC-I. The effect of the large natural circulation driving heads caused by the cooldown is to produce higher core flow in the CESEC-III results after reactor coolant pump coastdown. This causes a lower core T and a more rapid cooldown with earlier steam generator dryout. The presence of heat from the walls of the RCS compensates for the more rapid cooldown due to the higher natural circulation flow to yield a net cooldown rate which is slightly less than that calculated using CESEC-II. Further, this wall heat yields minimum transient temperatures from CESEC-III which are somewhat greater than those determined by CESEC-II.

The effect of the upper head node upon RCS pressure is much more pronounced for System 80 due to the much larger upper head volume than that present in other CE NSSS's. The marked reduction in rate of depressurization at the point of initiation of void formation in the upper head model of CESEC-III yields a safety injection flow which is both delayed in time and reduced in amount compared with that calculated by CESEC-II. This causes a larger calculated post-trip total reactivity and resulting return-to-power for CESEC-III than for CESEC-II.

As for the Waterford analysis the major effect upon the calculated post-trip minimum DNBR for System 80 is the core power. The impact of the other relevant parameters is small due to the lack of a return-to-power in the CESEC-II analyses.

Summary

The CESEC-I/CESEC-III comparison and the CESEC-II/CESEC-III comparison demonstrate that CESEC-III models important effects for SLBs more completely than did either CESEC-I or CESEC-II. Further the CESEC-I/CESEC-III comparisons demonstrates that the conclusions reached in SLB analyses done using CESEC-I would not be changed by analyses done with CESEC-III. No FSAR analysis uses CESEC-II for SLB events.

b. Of all the decreased heat removal events analyzed in Section 15.2 of the FSAR, the feedwater line break event is limiting in terms of primary overpressurization. Combustion Engineering's Chapter 15 feedwater line break analyses used either the CESEC-II or the CESEC-III codes. CESEC-I was not used to analyze feedwater line break transients. Therefore, in response to this event or section only the results of the CESEC-II and CESEC-III codes are compared.

A comparison of these two codes was made with the basis being the feedwater line break transient for a System 80 plant. The limiting case feedwater line break for the System 80 plants is found in 15.6.6 of the CESSAR FSAR. 15.6.6 results were obtained using the CESEC II computer code, and are provided as the CESEC II portion of this question response.

The CESEC-III code was run using the initial conditions listed in Table 15.11-12. The resulting sequence of events for the two codes are provided for comparison in Table 15.11-13.

Figures 15.11-31 through 15.11-38 show the results of the analyses over the time frame of maximum RCS pressurization.

The results presented show very good agreement between the CESEC-II and CESEC-III computer codes. A discussion of the differences in the results of the codes follows.

There is a small difference between the two codes in terms of RCS pressure vs time (Fig. 15.11-31). CESEC-II does not model the elevation pressure drop between the pressurizer and the hot leg centerline, while CESEC-III does. This accounts for approximately a 10 psia difference in RCS pressure, with the CESEC- III results being higher. In neither the CESEC-II or CESEC-III curve of RCS pressure vs time is the reactor coolant pump head included. However, these effects are accounted for separately in the results specified in Table 15.11-13.

A slight difference between the two codes occurs in the plots of steam generator pressure vs time (Figures 15.11-37 and 15.11-38). These differences can be attributed to the slightly higher primary flow rate calculated in the CESEC-III code than was input into the CESEC-II code. The differences can also be attributed in part to the modeling of the primary to secondary heat transfer rate. These phenomena cause the steam generator pressure to be initialized at a value about 15 psia greater in CESEC-III than in CESEC-II. The differences in the plot of steam generator pressure vs time occurring beyond 45 seconds in the transient can be attributed to the differences in secondary safety valve modeling of the two codes, although the averaged responses are nearly identical.

A small difference in the RCS temperature vs time plot exists (Figure 15.11-33). This is due to the slight differences in primary coolant flow rate. The CESEC-III code's pump model predicts slightly higher flow rates than were input into the CESEC-II code. This causes the initial temperature rise across the core to be lower for the CESEC-III code.

As demonstrated by the figures provided, the CESEC-II and CESEC-III feedwater line break predictions are in very good agreement.

c. At the present time, there is no ATWS licensing requirement. CESEC-III is not used for ATWS evaluation.

d. For all decrease in primary system inventory events, Chapter 15.6 events, for which the pressurizer fluid is calculated to drain into the hot leg, or the system pressure drops below the saturation pressure of the hottest fluid in the system, the hottest fluid will be located in the relatively stagnant upper head region of the reactor vessel. The CESEC-I code, used in the Waterford Unit 3 FSAR Chapter 15.6 analyses, did not explicitly model the steam formation in the reactor vessel upper head region. The CESEC-II code, used in the FSARs for St. Lucie Unit 2 and CESSAR-F SARs Chapter 15.6 analyses also did not explicitly model the steam formation in the reactor vessel upper head region. The latest version of CESEC, namely CESEC-III, appropriately models steam formation and collapse in the upper head region of the reactor vessel. Heat transfer from metal

structures to the reactor coolant system (RCS) fluid is modeled in this region in addition to flashing of the reactor coolant into steam during the depressurization of the RCS. Following the reactor coolant pump (RCP) coastdown due to loss of offsite power or manual shutdown following SIAS, thermal hydraulic decoupling of the upper head region is characterized in CESEC- III by progressively decreasing flow to the upper head from the upper plenum region.

The limiting event with respect to void formation in the decrease in primary system inventory event category is the steam generator tube rupture event. The effect of upper head voiding on the consequences of this event has been evaluated in support of the Waterford Unit 3, St. Lucie Unit 2, and CESSAR-FSARs. Analyses for this event bound all other events for which void formation is less limiting and/or non-existent in the above event category. This is due to slower cooldown rates, RCS pumps on, and/or higher minimum RCS pressures for the other events in the category. The major concern for this event is the primary to secondary leakage and, consequently, the secondary side activity releases.

The loss of primary coolant for a double-ended tube rupture results in a steady decline in RCS pressure. This steady pressure decline continues until the reactor trips (e.g., low pressurizer pressure). Subsequent to reactor trip the RCS pressure drops very quickly and the pressurizer empties. Voids due to flashing begin to form in the reactor vessel upper head region after the RCS pressure reaches the saturation temperature of the fluid. The RCPs are shutoff subsequent to a SIAS. The thermal hydraulic decoupling of the upper head from the rest of the RCS subsequent to the RCPs shutoff and the effect of the metal structure heat transfer from the reactor vessel walls and internals, enhances the void formation in the upper head regions through boiloff.

The analyses presented for the double-ended break of a steam generator tube event assume initiation from a full power condition with the assumptions of loss of offsite power subsequent to generator trip, one percent of the full power core/upper plenum flow into the upper head up to the time that the RCPs are shutoff, RCPs shutoff coincident with loss of offsite power, and the most reactive CEA in its fully withdrawn position.

The effect of the reactor vessel upper head voiding upon the system response is illustrated on Figures 15.11-39 through 15.11-42. Figures 15.11-39 and 15.11-40 show the results for the Waterford plant and Figures 15.11-41 and 15.11-42 show the results for System 80. The solid lines and dashed lines represent, respectively, the case for which the reactor vessel upper head fluid is explicitly modeled (CESEC-III) and the case for which the upper head region is mixed completely with that of the reactor vessel outlet plenum (CESEC-I and CESEC-III). The maximum allowable initial pressurizer liquid volume was assumed for these analyses. The radiological consequences of the steam generator tube rupture event are more adverse when maximizing this parameter. However, they still satisfy the SRP guidelines.

Figures 15.11-40 and 15.11-42 illustrate the reactor vessel upper head response. The amount of voids formed is definitely not large enough to expand the steam bubble beyond the top elevation of the hot legs. The duration of the voids will be a function of the rate of RCS cooldown and the safety injection flow rate. The slower RCS pressure decay for the case for which the upper head is explicitly modeled (see Figures 15.11-39 and 15.11-41) results in a delayed SIAS and a corresponding delay in the time at which delivery of the HPSI flow begins. The slower pressure decay for this case is caused by the voids as after the pressurizer empties, the reactor vessel upper head behaves as a pressurizer. For System 80 with the upper head not modeled the relatively large amount of HPSI flow results in the crossing of the RCS pressures late in the transient as shown on Figure 15.11-41. For this plant class the HPSI shutoff head is higher than for the 3410 plant class which causes this dissimilarity in behavior.

Tables 15.11-14 and 15.11-15 summarize the integrated primary to secondary leakages the integrated releases through the main steam safety valves (MSSVs), and the trip times for the cases analyzed. When the upper head region is explicitly modeled, the results are more adverse. However, the radiological consequences satisfy the SRP acceptance criteria. The more adverse results are due to the relatively higher RCS pressures and primary to secondary heat transfer for the case the upper head region is explicitly modeled.

In summary, void formation in the upper head will occur for the SGTR event. However, the consequences of a steam generator tube rupture as demonstrated in the Waterford Unit 3, St. Lucie Unit 2, and CESSAR-F SARs satisfy the SRP acceptance criteria when the reactor vessel upper head region is explicitly modeled.

15.11.12.71 Question No. 440.150

In general, it is our impression that the data* presented by FP&L is sufficient to support a general mixing model since only one flow condition was measured. Furthermore, the particular flow condition chosen has a Reynolds number nearly one full order of magnitude below operating conditions.

The experiment represented each core assembly by a single flow tube and used air as its simultant fluid. $S0_2$ was injected into the air flow of one (of four) reactor vessel inlet nozzles on a roughly 1/4 scale model. The $S0_2$ concentration was reassured at the exit of each of the "core tubes" and in each of the two reactor vessel outlet nozzles. Although the method appears reasonable for obtaining information on reactor vessel outlet flow, unfortunately, data is presented for only one operating condition. Furthermore, we are concerned about the impact of constraining the core flow in tubes when substantial cross flow is to be expected.

Thus, it is our general opinion that this single data point is not an adequate basis upon which to build a computer code model intended to model a wide range of flow conditions. The following specific questions should be addressed by the applicant.

---

*"Test Report on Fluid Mixing in a Scaled Reactor Vessel Flow Model, "CEN-169(L)-P, July, 1981, Combustion Engineering.

a. This data is only for one Reynolds number, representing only one operating condition. Upon what grounds does CE utilize this data for other flow conditions such as pump coastdown or loss of one pump.

b. How was this data implemented in the CESEC computer codes, justify and explain in depth.

c. Discuss the impact of having done these experiments in a geometry which prohibits cross flow between assemblies. How is the cross flow expected to impact the flow split in the exit nozzles. Furthermore, how does this lack of cross flow impact the accuracy of simulation of core moderator temperature during a return to power?

d. Discuss accuracy of the experiments - what are the fractional errors in the percent of flow through the various "core tubes"? The total percent of flow going into the two outlet nozzles is (38% + 14% = 52% - why is it not 50%)? What were the experimental errors?

Response

The purpose of Reference 16 is to use mixing data obtained at an appropriate Reynolds number and in a scaled geometry typical of CE NSSS's to determine mixing factors which can be used to simulate the amount of mixing in the reactor vessel downcomer/lower region and in the outlet plenum region in CE NSSS's. It is not the intention of this reference to support a general mixing model with data from only one set of flow conditions, but rather to quantify mixing in a very particular geometry. The specific items, asked as subsections of question are responded to by item as follows:

a. For Reynolds numbers greater than about 10^4, momentum transfer for mixing phenomena is substantially independent of the Reynolds number (e.g., Reference 31). This is due to the fact that in highly turbulent flows mixing is mainly due to vortex mixing, rather than diffusion type mixing. The vortex decay is largely independent of the Reynolds number. The test reported in Reference 16 was conducted at a Reynolds number of approximately 6×10^5, therefore the results of this test should be very nearly independent of the Reynolds number, since it is much greater than 10^4. Typical Reynolds numbers in CE reactor vessels at 100 percent flow are of the order of 5×10^7. A Reynolds number of 10^4 would occur at less than 0.1 percent flow.

   The mixing factors used in CESEC are cross flow terms normalized with the mass flow in that branch of the flow net from which the cross flow leaves. For a wide variety of geometries and flow conditions, see Table 4 of Reference 32, mixing correlations are cited typically showing a Reynolds number dependency of approximately Re^1. If these mixing terms are expressed as non-dimensional ratios of mass flow (mass flow varies approximately as Re^1) one finds that this normalized mixing factor is only weakly dependent on the Reynolds number as shown in Figure 8 of Reference 32 or Figures 11 and 12 of Reference 33. The weak dependencies of mixing on the Reynolds number is evident from Figure 9 of Reference 32, which covers a range of geometries, sizes, and flow conditions.

Further substantiation for the weak dependence of the mixing factor on the Reynolds number is shown in Reference 34 in terms of the mixing length vs the Reynolds number. The geometry involved in one where dye is injected into a pipe flow. A geometric effect is noted in that reference, stating that injection through only one nozzle exhibits a more pronounced Reynolds number dependency, whereas in the case of multiple injection paths (more symmetrical situation than with only one nozzle) only a weak dependence of the mixing length on the Reynolds number exists.

It is, therefore appropriate to use the mixing factors obtained at a Reynolds number corresponding to approximately one percent flow for flows up to 100 percent flow with the understanding that they may underpredict the amount of mixing to a small degree due to the lack of mixing in the reactor core of the scale model test and due to the (weak) increase in the mixing factors which could be expected to occur with increasing flow. For small asymmetries in the flow pattern small increases or decreases in the mixing factors could be expected. For marked asymmetries the values of the mixing factors obtained from the symmetric scale model test reported in Reference 16 could be expected to be inappropriate.

b. The data of Reference 16 is used to calculate the factors F_I and F_o (see page 2-2 of Reference 5). The fraction f_1, of the flow from loops 2A and 2B which reaches loop 1 is (refer to Figure 4-1 of Reference 16).

$$f_1 = \frac{\text{fraction of flow from loop 2A reaching loop 1}}{\text{total fraction of flow in loops 1 and 2 which comes from loop 2A}}$$

The fraction, f_2, of the flow from loops 2A and 2B which reaches the opposite half of the core is determined from the average of the fractions of flow in the core tubes on the half of the opposite loop 2, which are supplied from the traced inlet (loop 2A). F_I and F_o are related to f_1 and f_2 by

$$F_I = \frac{f_2}{1 - f_2}$$

$$F_O \cong \frac{f_1 - f_2}{1 - (f_2 + f_1)}$$

Figure 15.11-43 illustrates the flow paths in the CESEC model for the reactor vessel region. This figure is the same as the reactor vessel region of Figure 2-1 of the CESEC Report (Reference 5). The following discussion will focus on the "cross flows," $W_{14,2}$ and $W_{19,7}$ (or "density driven terms") and on the "mixing flows," $W_{2,15}$, $W_{14,3}$ $W_{6,19}$, and $W_{18,7}$ (or "hardwired terms"). The "cross flows," $W_{14,2}$ and $W_{19,7}$, are determined by direct solution of the thermal hydraulic equations (Equations 2-1 and 2-2 of Reference 5). The "mixing flows" are calculated as described on page 2-2 of Reference 5 using experimentally determined mixing factors, F_I and F_o:

$W_{2,15} = F_I\ W_{2,3}$

$W_{14,3} = F_I\ W_{14,15}$

$W_{6,19} = F_o W_{6,7}$

and

$W_{18,7} - F_o W_{18,19}$

where $W_{2,3}$, $W_{14,15}$, $W_{6,7}$, and $W_{18,19}$ are found from the solution of Eqns. 2-1 and 2-2 of Ref. 5.

This model represents the flow paths internal to the reactor vessel in much more detail than did previous models. CESEC-II, for example, represented the reactor vessel by only three nodes: one equivalent to nodes 2, 3, 14, and 15 of CESEC-III, a second equivalent to nodes 5 and 17, and a third equivalent to nodes 6, 7, 18, 19, and 25. In CESEC-II the flow from all four cold legs was mixed completely in the first reactor vessel node.

c. CESEC does not model cross flow in the core. The effect of cross flow is included in the 3D reactivity feedback only as described in Subsection 15.11.12.22. Moderator reactivity feedback, other than the 3D feedback, conservatively factors out the effect of mixing to use the density on the cold edge of the core, as described in Subsection 15.11.12.66.

The transient which produced the greatest asymmetry in loop flows and which is at the same time affected by these asymmetries is the main steam line break (SLB) with concurrent loss of offsite power. The algorithm for h_{edge} (see Subsection 15.11.12.66) factors out the effect of the mixing between the reactor vessel inlet nozzle and the core inlet plane flows to yield a conservatively low enthalpy for the moderator reactivity calculation, thus eliminating the direct effect of mixing on moderator reactivity. However, this calculation is based on current values of core enthalpies and does not factor out the indirect effect of mixing which may have occurred during previous loop cycles. An increase in mixing in the reactor vessel will cause an increase in the enthalpy of the fluid entering the hot leg of the loop with the ruptured steam generator. This in turn will cause an increase in the enthalpy of the fluid reaching the core from this loop after sufficient time has elapsed for this fluid to be transported around the loop and back into the reactor vessel. An examination of the results of steam line break transients and of the sensitivity of their consequences to the mixing shows that this indirect effect does not have a significant effect on these consequences.

Figures 15.11-44 through 15.11-48 present the flow distributions in the reactor vessel region at important times during the most limiting full power main steam line break with concurrent loss of offsite power event analyzed for System 80. Flow distributions are shown four times after event initiation of 1, 60, 120, 140, and 270 seconds. The first of these timer is chosen to illustrate the flow distributions at the very beginning of the event. At one minute into the transient the asymmetry of the loop flows is approximately 7 percent. By two minutes this asymmetry is 13 percent. The maximum post-trip reactivity occurs at approximately 260 seconds; the maximum post-trip power occurs shortly after 270 seconds into the transient, with minimum post-trip DNBR at 277 seconds. At the flow rates present during these parts of the transient, fluid reaching the

reactor core at the time of the maximum post-trip reactivity cannot have left the reactor vessel later than approximately two minutes into the transient. The fluid present in the core at the time of minimum DNBR had to have left the reactor vessel prior to 140 seconds into the transient. At 140 seconds the vessel flow asymmetry is 15 percent, by 270 seconds it is still only 25 percent. In all of this period the total vessel flow is well above the 1 percent value at which the mixing factors were measured.

The cross flows serve to balance the difference in contractions of the fluids in the two steam generator loops and to redistribute the unequal loop flows into nearly equal flows through the two halves of the core. For example, at 1 second, the net cross flow is from the loop with the pressurizer to the other loop, since pressurizer outsurge is compensating for contraction in both loops. At 60 seconds net cross flow is to the loop with the ruptured steam generator. By 270 seconds a small net cross flow to the loop with the unaffected steam generator exists: the ruptured steam generator has dried out, while the intact steam generator is being cooled by auxiliary feedwater.

If it is assumed that an increasing asymmetry decreases mixing and that this decrease is of the order of the asymmetry, then it could be estimated that over the period of the transient between one and two minutes an approximately 10 percent reduction in mixing might be expected. Since during the first minute of the transient, when the cooldown rate and its effect upon reactivity is greatest, there is much less asymmetry, the overall effect should be much less than of the order of 10 percent. It is possible that this is less than the amount by which the mixing factors used are too low due to the experimental configuration.

Figures 15.11-49 and 15.11-50 show the sensitivy of the results of this SLB to variations in the assumed mixing factors. Figure 15.11-49 shows the sensitivity of maximum post-trip fission power to mixing. The sensitivity of minimum post-trip DNBR is presented on Figure 15.11-50. The abscissa for both of these figures is a mixing factor multiplier. This multiplier was used to reduce or increase both F_I and F_o by a fixed factor for an entire transient. Thus a mixing factor multiplier of 1.2 corresponds to a 20 percent increase in both F_I and F_o over the values normally used.

A reduction in mixing of the order of 10 percent for this transient would yield an increase in maximum post-trip fission power of less than 10 MW out of a total of 100 MW and a reduction in minimum post-trip DNBR of less than 0.2 out of a total of 2.7. Since actual mixing may be higher, rather than lower, than the values used, the consequences of this event could be less adverse by similar small amounts.

d. The accuracy of the mixing data reported in Reference 1 is ± 3 percent.

In summary, the mixing factors obtained from Reference 11 used together with the CESEC-III model of the flow paths in the reactor vessel yield transient results which are much more realistic than those available from earlier models. The results obtained from Ref. 16 are applicable for use in the transient analyses for

which CESEC is used. The effect of possible uncertainties, or flow asymmetry dependencies, in the mixing factors is not of sufficient magnitude to alter the conclusions of any FSAR analysis. This is demonstrated by a sensitivity study using the main steam line break with concurrent loss of offsite power, which is the event that is most sensitive to uncertainties in the dependency of the mixing on flow asymmetry.

15.11.13 REFERENCES: SECTION 15.11

1. CENPD-107, "CESEC-Digital Simulation of a Combustion Engineering Nuclear Steam Supply System," C-E Proprietary Report (April, 1974).

2. CENPD-107, Supplement 1, "ATWS Model Modifications to CESEC," C-E Proprietary Report (September, 1974).

3. CENPD-107, Supplement 2, "ATWS Models for Reactivity Feedback and Effect of Pressure on Fuel," C-E Proprietary Report, (September, 1974).

4. CENPD-107, Supplement 3, "ATWS Model Modifications to CESEC," C-E Non-Proprietary Report (August, 1975).

5. CENPD-107 Supplement 1, Amendment 1-P. "ATWS Model Modifications to CESEC," C-E Proprietary Report (November, 1975).

6. CENPD-107, Supplement 4, "ATWS Model Modifications to CESEC," C-E Proprietary Report (December, 1975).

7. CENPD-107, Supplement 5, "ATWS Model Modifications to CESEC," C-E Proprietary Report (June, 1976).

8. CENPD-107, Supplement 6, "CESEC - Digital Simulation of a Combustion Engineering Nuclear Steam Supply System," C-E Non-Proprietary Report (August, 1978).

9. F. J. Moody, "Maximum Two-Phase Vessel Blowdown From Pipes," APED-4827, (April 20, 1965).

10. Enclosure 1-P to LD-82-001, January 6, 1982, "CESEC Digital Simulation of a Combustion Engineering Nuclear Steam Supply System" Combustion Engineering, Inc., Proprietary Report (December 1981).

11. CENPD-132, "Calculative Methods for the CE Large Break LOCA Evaluation Model," (Vol.1, August 1974).

12. CENPD-133, "CEFLASH-4A, A Fortran IV Digital Computer Program for Reactor Blowdown Analysis," (August 1974).

13. CENPD-161-P, "TORC: A Computer Code for Determining the Thermal Margin of a Reactor Core," CE Proprietary Report (July 1975).

14. CENPD-206-P, "TORC Code Verification and Simplified Modeling Methods," CE Properietary Report (January 1977).

15. CENPD-266-P, "The ROCS and DIT Computer Codes for Nuclear Design, CE Proprietary Report (December 1981).

16. CEN-169(L)-P, "Test Report on Fluid Mixing in a Scaled Reactor Vessel Flow Model, " Combustion Engineering, Inc., Proprietary Report (July 1981).

17. Dittus, F W, and Boelter, L M K, "Heat Transfer in Automobile Radiators, of the Tubular Type, " Pub. in Eng., Vol. 2, n. 13, Univ. of California, pp. 443-461, 1930.

18. M M El-Wakil, Nuclear Heat Transport, (Table E-1), International Text Book Company, 1971.

19. Chen, John C, "A Correlation for Boiling Heat Transfer to Saturated Fluids in Convection Flow," ASME Paper 63-HT-34, 1963.

20. A Theoretical Model for the Calculation of Large Transients in Nuclear Natural Circulation U-Tube Steam Generator, A. Hoeld Nuclear Engineering and Design 47 (1978).

21. McClintock, R S, and Silvestri, G J, "Formulations and Interactive Procedures for the Calculation of Properties of Steam," ASME Publication H-17, 1967.

22. CENPD-137 P, "Calculative Methods for the CE Small Break LOCA Evaluation Model," August 1974.

23. CENPD-137, Supplement 1-P, "Calculative Methods for the CE Small Break LOCA Evaluation Model," January 1977.

24. CENPD-133 P, Supplement 1, "CEFLASH-4AS, A Computer Program for the Reactor Blowdown Analysis of the Small Break Loss-of-Coolant Accident," August 1974.

25. CENPD-133 P, Supplement 3, "CEFLASH-4AS, A Computer Program for the Reactor Blowdown Analysis of the Small Break Loss-of-Coolant Accident," January 1977.

26. "Flow of Fluids," Tech. Paper No. 41, Crane Co., 1957.

27. Nahavandi, A N, and M Rashevsky, "Computer Program for Critical Flow Discharge of Two Phase Steam-Water Mixtures," CVNA-128, February 1962.

28. CEN-114-P, Amendment 1-P, "Review of Small Break Transients in Combustion Engineering Nuclear Steam Supply Systems," July 1979.

29. Lance, G N, "Numerical Methods for High-Speed Computers", to ILIFFE & Sons, Ltd., London (1960) pp. 54-57.

30. CEN-199, "Effects of Vessel Head Voiding During Transients and Accidents in CE NSSS's, March 1982.

31. Johnstone, R E, and Thring, M W, Pilot Plants, Models, and Scale-Up, Methods in Chemical Engineering, McGraw-Hill Book Co., New York (1957), pp. 115-116.

32. Galbraith, K P, and Knudsen, J G, "Turbulent Mixing Between Adjacent Channels for Single Phase Flow in a Simulated Rod Bundle," AICHE SYMPOS. Series 68 (118), 1972, pp. 20-100.

33. Rowe, D S, and Angle, C W, "Cross Flow Mixing-Between Parallel Flow Channels During Boiling," Part III, EFFECT OF SPACERS ON MIXING BETWEEN TWO CHANNELS, BNWL-371, PT 3, UC-80 Reactor Technology.

34. Clayton, C G, Ball, A M, and Spackman, R, "Dispersion and Mixing During Turbulent Flow of Water in a Circular Pipe," UKAEA, MA, 1968, AERE-R-5569.

35. "Response to Questions on CESEC," Combustion Engineering, Inc., CEN-225(L)-P, October 1982.

36. An Analytical representation of convection-boiling function by S Edelstein, A Perez, J C Chen, Dept. of Chemical Engineering, Lehigh University.

37. CENPD-188-A - "Hermits: A Multidimensional Space Time Kinetics Code for PWR Transients." CE Proprietary Report, July 1976.

TABLE 15.11-1

SUMMARY OF SIGNIFICANT DIFFERENCES
BETWEEN CESEC-II AND CESEC-III

MODEL	CESEC-III	CESEC-II
Thermal Hydraulic	26 Nodes, Upper Head Explicitly Modeled	16 Nodes
RCS Flow	Explicitly Modeled	Input Table
RCPs	Four, Explicitly Modeled	Two
Wall Heat	Explicitly Modeled	None
SGTR Option	Critical Flow Check	Darcy Equation
Mixing In RV	Asymmetric Response Explicitly Modeled	Asymmetric Response Included In Reactivity Calculation For SLB
3-D Reactivity Feedwater	Yes(1)	No

(1)For steam line break analysis only.

TABLE 15.11-2

COMPARISON OF RESULTS

FOR THE STEAM GENERATOR TUBE RUPTURE

WITHOUT LOSS OF OFFSITE POWER

	CESEC-II	CESEC-III
Primary-Secondary Integrated Leak (lbm) At 1800 Seconds	61,480	61,010
Integrated MSSV Steam Release (lbm) At 1800 Seconds	76,370	69,470
Minimum DNBR	>1.19	>1.19

TABLE 15.11-3

DATA BASE USED IN CALCULATING
THE VALUES OF X, Y, AND Z

	CHARGING (SHELL SIDE)			LETDOWN (TUBE SIDE)		
Case No.	Flow G_c (gpm @ 120°F)	Inlet Temp t_{ci} °F	Outlet Temp T_{co} °F	Flow G_1 (gpm @ 120F)	Inlet Temp t_{li} (°F)	Outlet Temp t_{lo}(°F)
1	61.6	120	445	72.4	564.5	310
2	61.6	120	488	135	564.5	414
3	105.6	120	348	72.4	564.5	258

TABLE 15.11-4

COMPARISON OF MEASURED AND CALCULATED

VALUES OF t_{lo}

Case No.	G_c (gpm @ 120F)	G_1 (gpm @ 120F)	RHX Operating Parameters (Measured) t_{ci} (°F)	t_{co} (°F)	t_{li} (°F)	t_{lo} (°F)	Calculated Value Using Equation (F-3) t_{lo} (°F)
1**	44	30	120	395	564.5	185	184
2*	61.6	72.4	120	445	564.5	310	311
3**	92	135	130	419	564.5	382	383
4*	105.6	135	40	373	564.5	330	329

* From Attachment 1

** From Attachment 2

TABLE 15.11-5

STEADY STATE PERFORMANCE DATA* FOR SYSTEM 80 RHX

4.1.2 Operating Modes

Tube side letdown and shell side charging flows are controlled to satisfy operating conditions. Typical flow combinations listed below include Mode [13] which is the thermal sizing condition and Mode [3] which is the normal operating condition.

Mode No.	Shell Side (Charging)				Tube Side (Letdown)			
	Flow	Temperature °F		ΔP,	Flow	Temperature °F		ΔP,
	Gpm @ 120°F	In	Out	psi	gpm@120°F	In	Out	psi
1	61.6	120	328	8.5	30	564.5	163	2.6
2	61.6	130	334	8.5	30	564.5	172	2.6
3	61.6	120	445	8.6	72.4	564.5	310	13.3
4	61.6	130	447	8.6	72.4	564.5	315	13.3
5	61.6	120	488	8.7	135	564.5	414	44.1
6	61.6	130	489	8.7	135	564.5	417	44.1
7	105.6	120	348	24.2	72.4	564.5	258	13.2
8	105.6	130	353	24.2	72.4	564.5	264	13.2
9	105.6	40	373	24.3	135	564.5	330	42.8
10	105.6	120	248	24.2	30	564.5	145	2.6
11	44	120	385	4.4	28.4	564.5	178	2.4
12	44	40	351	4.5	28.4	564.5	110	2.4

* Extracted from General Specification for RHX

TABLE 15.11-6

STEADY STATE PERFORMANCE DATA* FOR SYSTEM 80 RHX

4.1.2 Operating Modes

Tube side letdown and shell side charging flows are controlled to satisfy operating conditions. Typical flow combinations listed below include Mode 1 which is the thermal sizing condition and Mode 5 which is the normal operating condition.

Mode No.	Shell Side (Charging)				Tube Side (Letdown)			
	Flow Gpm @ 120°F	Temperature, °F In	Temperature, °F Out	ΔP, psi	Flow gpm@120°F	Temperature, °F In	Temperature, °F Out	ΔP, psi
1	44	130	525	5.2	135	564.5	450 Max.	48.1
2	48	130	520	6.2	135	564.5	441	47.9
3	92	130	419	22.4	135	564.5	382	46.8
4	44	120	508	5.2	84	564.5	379	19.3
5	48	120	496	6.2	84	564.5	368	19.2
6	92	120	389	21.9	84	564.5	295	18.8
7	44	120	440	5.2	40	564.5	233	4.75
8	44	40	415	5.2	40	564.5	177	4.75
9	48	120	422	6.1	40	564.5	225	4.75
10	92	120	301	21.8	40	564.5	176	4.75
11	44	120	395	5.2	30	564.5	185	2.8
12	92	120	266	21.9	30	564.5	148	2.8

*Extracted from Project Specification for RHX

TABLE 15.11-7

CESEC DYNAMIC CALCULATION SEQUENCE

A. Determine time step size.

B. Calculate parameters for Runge-Kutta-Merson (Ref. 35) integration in the interval between t - Δt and t for

- fuel temperature
- steam generator secondary parameters
- reactor kinetics

C. Calculate reactivity at time t

D. Integrate pump and flow model equations over interval from t- Δt to t

E. Calculate values of parameters at time t for

- pressurizer
- feedwater system
- steam system

F. Determine values of parameters and their derivatives at time t (complete Runge-Kutta-Merson integration) for

- fuel temperature
- steam generator secondary parameters
- reactor kinetics

G. Integrate RCS thermal hydraulics equations

(1) calculate values of coefficients and right-hand side of thermal hydraulics equations

(2) solve thermal hydraulic equations for flows and rate of change of pressurizer pressure

(3) if surge line pressure drop iteration scheme is not converged return to (1) and repeat, otherwise calculate surge line pressure drop and continue with (4)

TABLE 15.11-7 (Cont'd)

(4) use flows and rate of change of pressurizer pressure to determine rates of change of enthalpies

(5) use Euler integration to determine pressurizer pressure and enthalpies at $t + \Delta t$

(6) calculate RCS pressure from pressurizer pressure and surge line pressure drop

(7) calculate other thermodynamic properties from pressures and enthalpies

(8) calculate the exiting enthalpy for reactor core and steam generator tube nodes

(a) use enthalpy transport algorithm to calculate exiting enthalpies

(b) check for 2nd law violation for steam generator tube nodes, if none, continue with step (f), otherwise continue with step (c)

(c) set exit enthalpy equal to node average enthalpy

(d) calculate a primary to secondary heat transfer rate which is consistent with exit enthalpy

(e) check for inconsistency in heat transfer direction, if consistent continue with step (f), otherwise set heat transfer rate equal to zero before continuing with step (f)

(f) integration of thermal hydraulics is complete and main calculation is continued at step H.

H. Integrate wall heat equations

I. Calculate reactor protective system trip action times

J. Integrate boron transport equations

K. Print minor or major edit if called for at this time

L. Continue at A unless time equals the run end time

TABLE 15.11-8

CESEC-I/CESEC-III COMPARISON
WATERFORD UNIT 3
ASSUMPTIONS FOR A STEAM LINE BREAK AT FULL POWER INSIDE CONTAINMENT WITH DOUBLE ENDED RUPTURE OF THE STEAM LINE

Parameter	Assumptions
Initial core power level, Mwt	3478
Core inlet coolant temperature, F	560
Core mass flow rate, 10^6 lbm/hr	124.3
Reactor coolant system pressure, psia	2000
One pin radial peaking factor, with uncertainty	1.3
Initial core minimum DNBR	1.29
Steam generator pressure, psia	962.4
Doppler coefficient multiplier	1.15
Moderator coefficient multiplier	1.10
CEA worth for trip, $10^{-2}\Delta\rho$	-8.55
Steam bypass control system	Inoperative
Pressurizer pressure control system	Inoperative
High pressure safety injection pumps	One pump inoperative
Core burnup	End of first cycle
Blowdown fluid	100% steam
Break area, ft^2	7.88

TABLE 15.11-9

CESEC-I/CESEC-III COMPARISON
WATERFORD UNIT 3
SEQUENCE OF EVENTS FOR A STEAM LINE BREAK AT FULL POWER
INSIDE CONTAINMENT WITH DOUBLE ENDED RUPTURE OF THE STEAM
LINE AND CONCURRENT LOSS OF OFFSITE POWER

Time (Sec)		
CESEC-I	CESEC-III	Event
0.0	0.0	Steam line break upstream of the main steam isolation valve initiated; loss of offsite ac power occurs
2.06	2.10	Low steam generator pressure trip signal and MSIS initiated; main steam isolation valve begin to close; feedwater isolation valves begin to close
5.06	5.10	MSIVs closed
14.9	30.4	Pressurizer empties
16.2	19.2	Low RCS pressure initiates SIAS
22.1	22.1	MFIVs closed
34.2	37.2	High-pressure safety injection pump reaches full speed
99.7	110.0	Affected steam generator empties
255.9	237.5	Safety injection boron begins to reach core
337.4	147.5	Pressurizer liquid level re-established

TABLE 15.11-10

CESEC-II/CESEC-III COMPARISON
SYSTEM 80
ASSUMPTIONS AND INITIAL CONDITIONS FOR A LARGE STEAM LINE BREAK DURING FULL POWER OPERATION WITH CONCURRENT LOSS OF OFFSITE POWER

Parameter	Assumed Value
Initial Core Power Level, MWt	3876
Initial Core Inlet Coolant Temperature, °F	570
Initial Core Mass Flow Rate, 10^6 lbm/hr	148.8
Initial Pressurizer Pressure, psia	2400
Initial Pressurizer Water Volume, ft^3	1100
Doppler Coefficient Multiplier	1.15
Moderator Coefficient Multiplier	1.10
Axial Shape Index	+.3
CEA Worth for Trip, $10^{-2}\Delta\rho$	-8.8
Initial Steam Generator Inventory, lbm affected	182000
intact	148000
One High Pressure Safety Injection Pump	Inoperative
Core Burnup	End of Cycle
Blowdown Fluid	Saturated Steam
Blowdown Area for Each Steam Line, ft^2	1.283

TABLE 15.11-11

CESEC-II/CESEC-III COMPARISON
SYSTEM 80
SEQUENCE OF EVENTS FOR A LARGE STEAM LINE BREAK DURING FULL POWER OPERATION WITH CONCURRENT LOSS OF OFFSITE POWER

Time (Sec)			Setpoint or Value	
CESEC-II	CESEC-III	Event	CESEC-II	CESEC-III
0.0	0.0	Steam Line Break and Loss of Offsite Power Occur	--	
0.6	0.6	Low DNBR Trip Condition Occurs, Projected DNBR	1.19	
0.75	0.75	Trip Breakers Open	--	
1.09	1.09	CEAs Begin to Drop	--	
*	8.0	Voids Begin to Form in RV Upper Head	--	
8.2	8.3	Main Steam Isolation Signal, psia	810	
13.2	13.3	MFIVs Close Completely	--	
13.2	13.3	MSIVs Close Completely	--	
13.2	13.3	EFW Initiated to Intact Steam Generator	--	
18	120	Pressurizer Empties	--	
19	178	Safety Injection Actuation Signal psia	1600	
49	208	Safety Injection Flow Begins	--	
390	237	Affected Steam Generator Empties	--	
211	259	Maximum Transient Reactivity, $10^{-2}\Delta\rho$	-0.02	+0.09
**	277	Minimum Post-Trip DNBR	**	2.7
80	280	Safety Injection Boron Begins to Reach Reactor Core	--	

* No upper head node in CESEC-II
** No minimum, see Figure 440.149a-12

TABLE 15.11-12

INITIAL CONDITIONS FOR THE LIMITING CASE
LOSS FEEDWATER INVENTORY EVENT

Parameter	Value
Initial Core Power, Mwt	3876
Initial Core Inlet Temperature, F	560
Initial Reactor Vessel Flow, gpm	446,000
Initial Pressurizer Pressure, psia	1920
Fuel Gas Gap Heat Transfer Coefficient Btu/hr-ft^2 - F	540
Doppler Coefficient Multiplier	1.0
Pressurizer Safety Valves Rated Flow, lbm/hr/valve	460,000
Initial Pressurizer Liquid Volume, ft^3	1120
Initial Steam Generator Inventory, lbm	173,000
Initial Feedwater Enthalpy, Btu/lbm	376
Steam Bypass Control System Mode	Manual
Normal Onsite or Offsite Electrical Power After Turbine Trip	Unavailable
Feedwater Pipe Break Area, ft^2	0.2
CEA Worth at Trip, 10^{-2}	-10.0

TABLE 15.11-13

COMPARISON OF THE
SEQUENCE OF EVENTS FOR THE LIMITING CASE LOSS
OF FEEDWATER INVENTORY EVENT
SYSTEM 80

Time (Sec)			Setpoint or Value	
CESEC-II	CESEC-III	Event	CESEC-II	CESEC-III
0.0	0.0	Break in the Main Feedwater Line	0.2 ft^2	0.2 ft^2
0.0	0.0	Instantaneous Loss of All Feedwater Flow to Both Steam Generators		
0.0	0.0	Instantaneous Development of Critical Flow from the Ruptured Steam Generator to the Break		
33.8	33.3	Instantaneous Loss of All Heat Transfer to the Ruptured Steam Generator		
34.4	34.1	High Pressurizer Pressure Trip Signal	2475 psia	2475 psia
34.6	33.9	Pressurizer Safety Valves Open	2525 psia	2525 psia
38.2	38.3	Maximum Reactor Coolant Pressure	2843 psia	2850 psia
40.5	38.9	Main Steam Safety Valves Open	1282 psia	1282 psia
44.8	42.4	Maximum Steam Generator Pressure	1318 psia	1319 psia
45.4	43.5	Pressurizer Safety Valves Close	2525 psia	2460 psia
73.8	60.6	Main Steam Safety Valves Close	1218 psia	1218 psia

TABLE 15.11-14

COMPARISON OF RESULTS,
STEAM GENERATOR TUBE RUPTURE WITH
LOSS OF OFFSITE POWER

WATERFORD

	CESEC-I	CESEC-III
Primary-Secondary Integrated Leak (LBM) at 1800 secs.	60,739	65,300
Integrated MSSV Steam Release (LBM) at 1800 secs.	78,300	85,100
Trip Time (Sec)	843	940

TABLE 15.11-15

COMPARISON OF RESULTS
STEAM GENERATOR TUBE RUPTURE WITH
LOSS OF OFFSITE POWER

SYSTEM 80

	CESEC-I	CESEC-III
Primary-Secondary Integrated Leak (LBM) at 1800 secs.	75,400	80,300
Integrated MSSV Steam Release (LBM) at 1800 secs.	95,800	110,100
Trip Time (Sec)	1125	1188

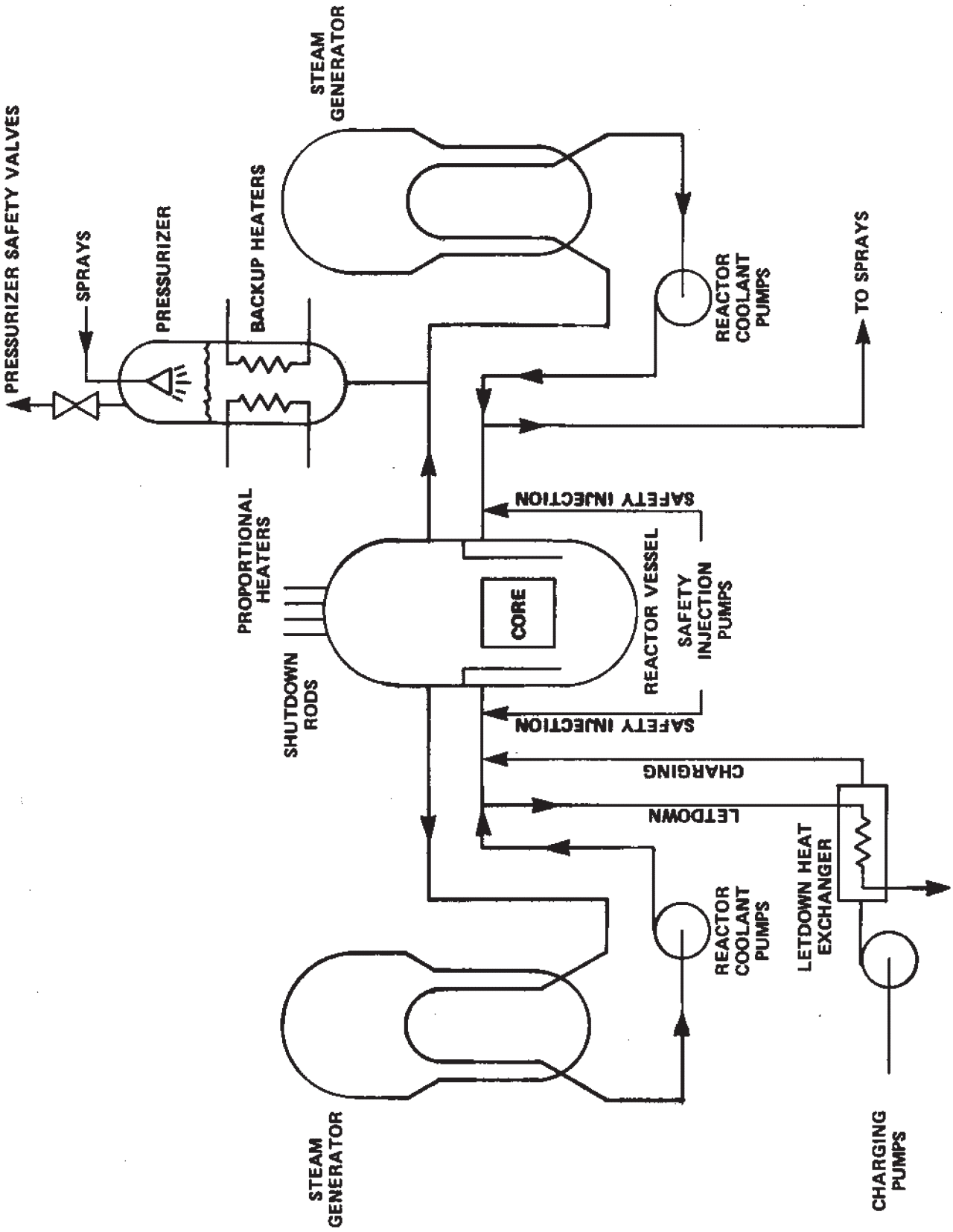

AMENDMENT NO. 1 (4/86)

FLORIDA POWER & LIGHT COMPANY
ST. LUCIE PLANT UNIT 2

THE PRIMARY SYSTEM AND CVCS COMPONENTS CONSIDERED IN CESEC-11

FIGURE 15.11-1

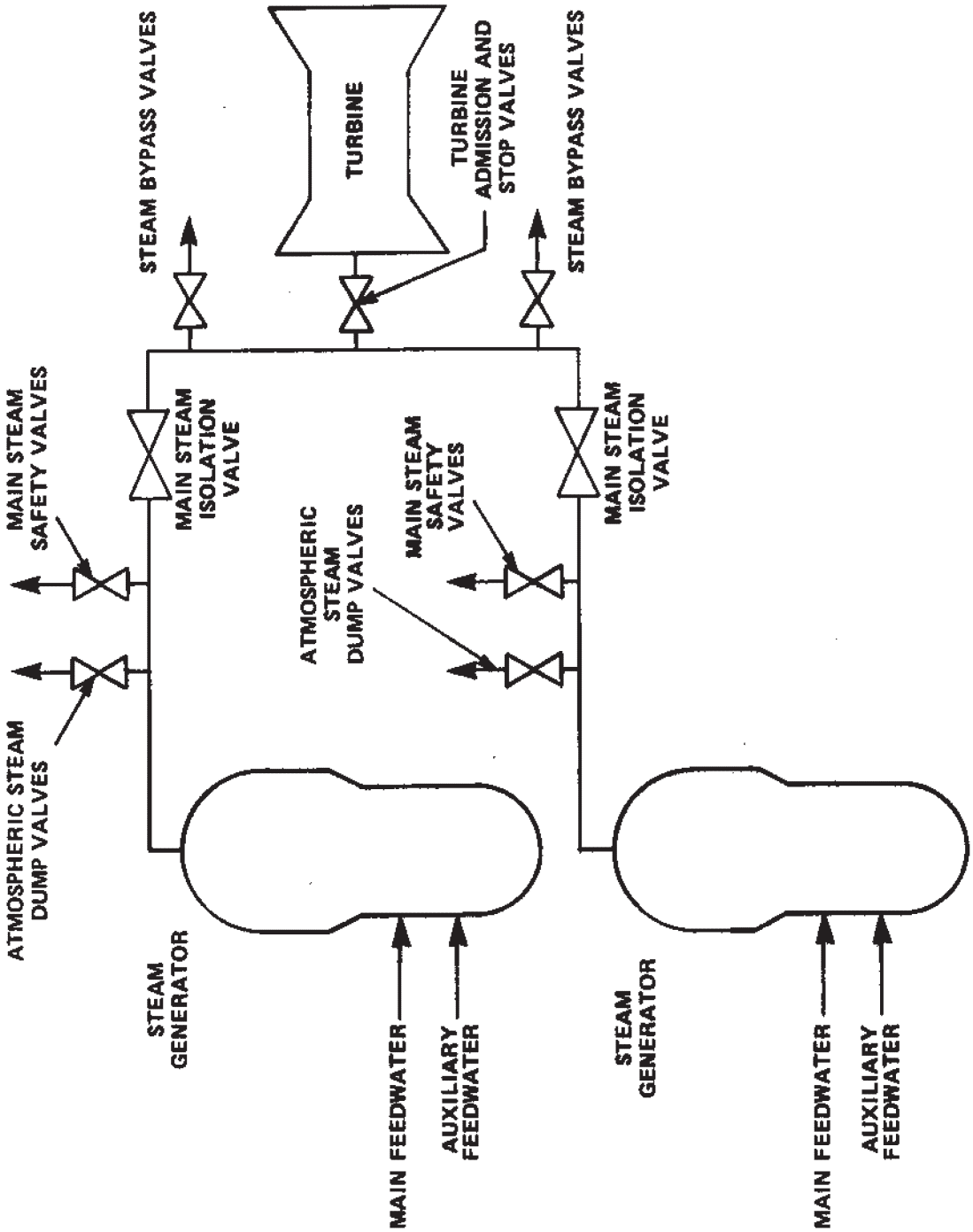

AMENDMENT NO. 1 (4/86)

FLORIDA POWER & LIGHT COMPANY
ST. LUCIE PLANT UNIT 2

THE SECONDARY SYSTEM COMPONENTS CONSIDERED IN CESEC-11

FIGURE 15.11-2

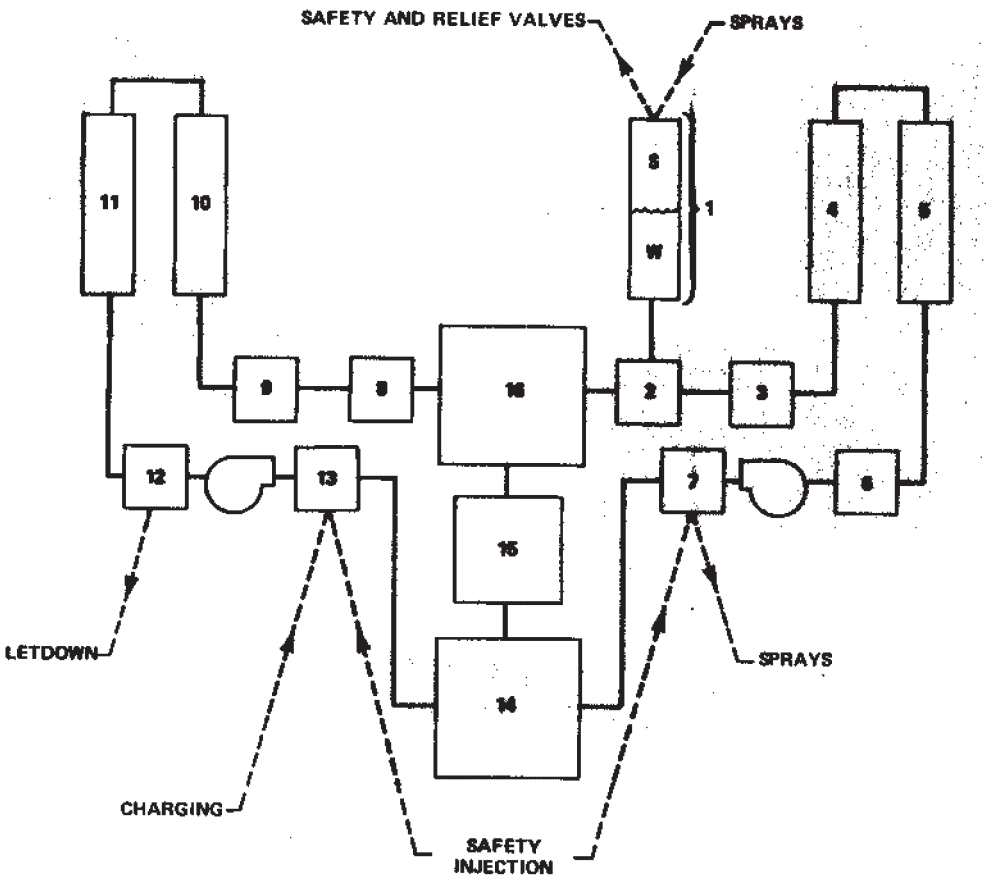

NODE	PHYSICAL DESCRIPTION
1	PRESSURIZER
S	STEAM REGION IN PRESSURIZER (IF PRESENT)
W	LIQUID REGION IN PRESSURIZER (IF PRESENT)
2	UPSTREAM HALF OF HOT LEGS
3	DOWNSTREAM HALF OF HOT LEGS
4	STEAM GENERATOR INLET PLENUM PLUS UPSTREAM HALF OF TUBES
5	STEAM GENERATOR OUTLET PLENUM PLUS DOWNSTREAM HALF OF TUBES
6	UPSTREAM HALF OF COLD LEGS
7	DOWNSTREAM HALF OF COLD LEGS
8	SAME AS 2 IN OTHER RCS LOOP
9	SAME AS 3 IN OTHER RCS LOOP
10	SAME AS 4 IN OTHER RCS LOOP
11	SAME AS 5 IN OTHER RCS LOOP
12	SAME AS 6 IN OTHER RCS LOOP
13	SAME AS 7 IN OTHER RCS LOOP
14	REACTOR VESSEL INLET PLENUM
15	CORE
16	REACTOR VESSEL OUTLET PLENUM

AMENDMENT NO. 1 (4/86)

FLORIDA POWER & LIGHT COMPANY
ST. LUCIE PLANT UNIT 2

SCHEMATIC DIAGRAM OF PRIMARY COOLANT NODES USED IN CESEC-II MODEL

FIGURE 15.11-3

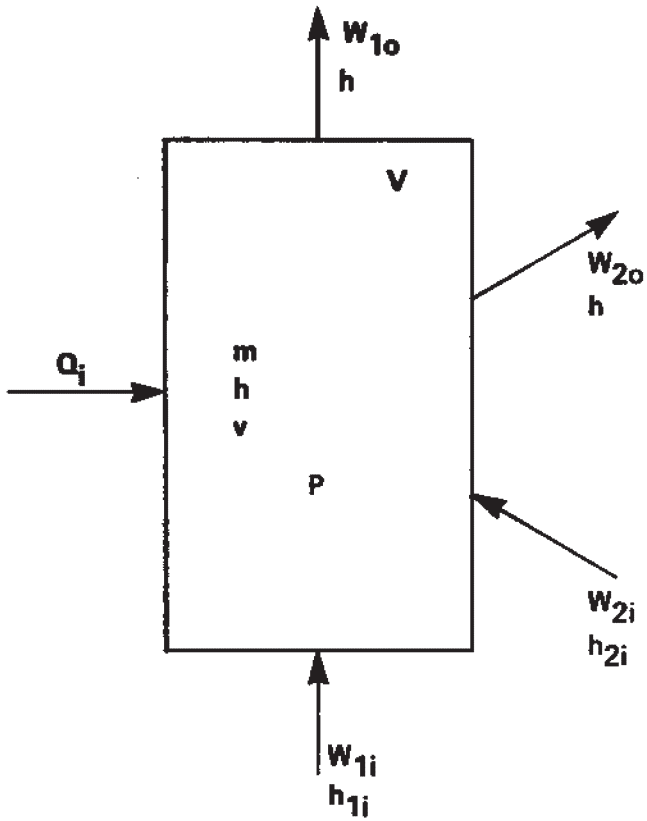

ENERGY EQUATION

$$\frac{d}{dt}(m\,h) - V\frac{dP}{dt} = Q + \sum_j W_{ji}\,h_{ji} - \sum_j W_{jo}\,h$$

MASS BALANCE

$$\frac{dm}{dt} = \sum_j W_{ji} - \sum_j W_{jo}$$

CONSTANT VOLUME

$$\frac{d\,(m\,v)}{dt} = 0.0$$

m = NODE TOTAL MASS

h = NODE AVERAGE ENTHALPY

V = NODE TOTAL VOLUME

v = NODE SPECIFIC VOLUME

Q = NODE HEAT RATE

W_{ji} = NODE INLET FLOWS, i DENOTES INLET

W_{jo} = NODE EXIT FLOWS, o DENOTES EXIT

h_{ji} = NODE INLET FLOW ENTHALPIES

P = COOLANT PRESSURE

AMENDMENT NO. 1 (4/86)

FLORIDA POWER & LIGHT COMPANY
ST. LUCIE PLANT UNIT 2

GENERAL COOLANT NODE EQUATIONS

FIGURE 15.11-4

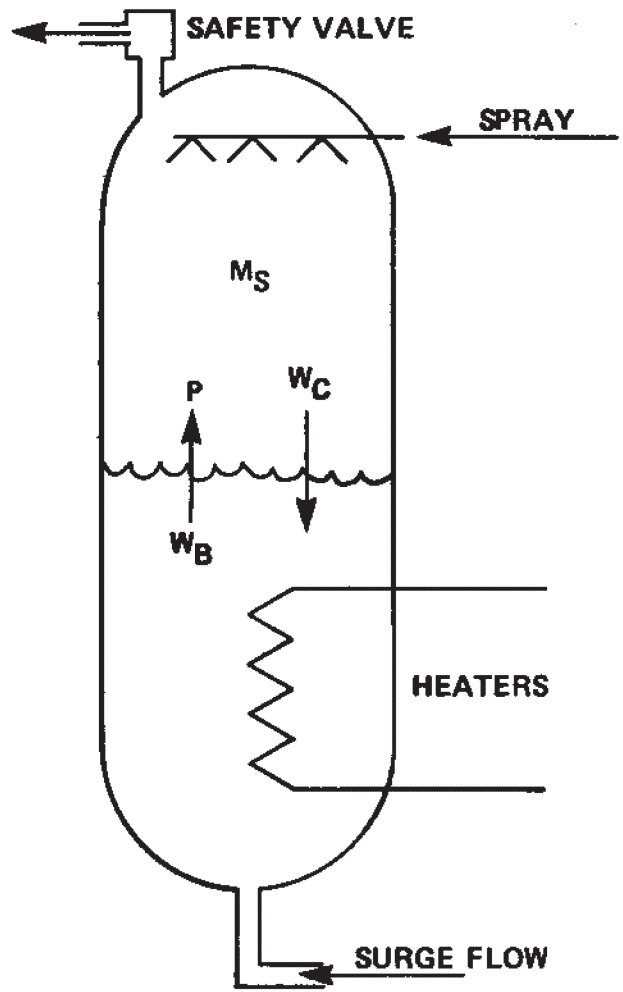

PRESSURIZER

TWO VOLUMES (STEAM AND WATER)

CONSTANT VOLUME CONSTRAINT

$M_S \; v_S + M_W \; v_W = V_P = \text{CONSTANT}$

M_S = TOTAL MASS OF STEAM

v_S = SPECIFIC VOLUME OF STEAM

M_W = TOTAL MASS OF WATER

v_W = SPECIFIC VOLUME OF WATER

V_P = TOTAL VOLUME OF PRESSURIZER

INTERFACE FLOWS

W_B = BOILING FLOW RATE

W_C = CONDENSATION FLOW RATE

CONDITIONS	WATER	STEAM
1	SUBCOOLED	SUPERHEATED
2	SATURATED	SUPERHEATED
3	SUBCOOLED	SATURATED STEAM
4	SATURATED	SATURATED STEAM
5	NONE	SUPERHEATED
6	NONE	SATURATED STEAM
7	SUBCOOLED	NONE
8	SATURATED	NONE

AMENDMENT NO. 1 (4/86)

FLORIDA POWER & LIGHT COMPANY
ST. LUCIE PLANT UNIT 2

PRESSURIZER MODEL IN CESEC-II

FIGURE 15.11-5

A. PRESSURE REACHES P_{ACC}

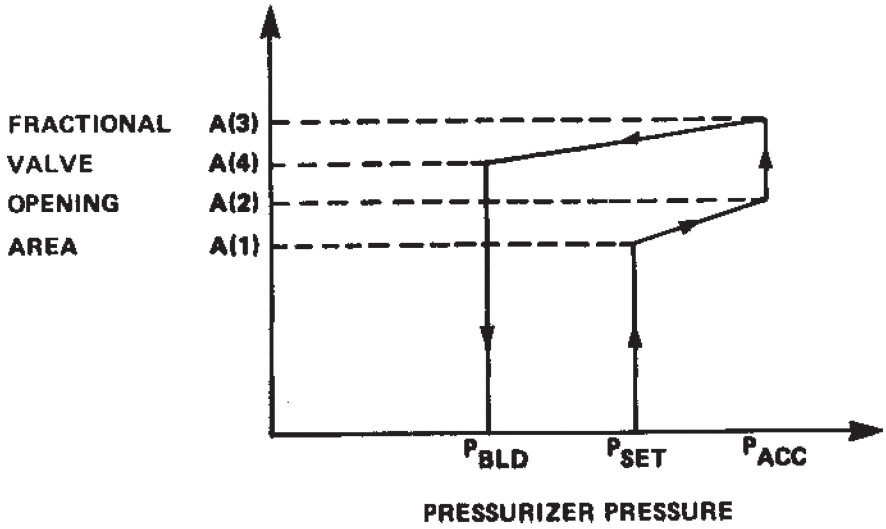

B. PRESSURE DOES NOT REACH P_{ACC}

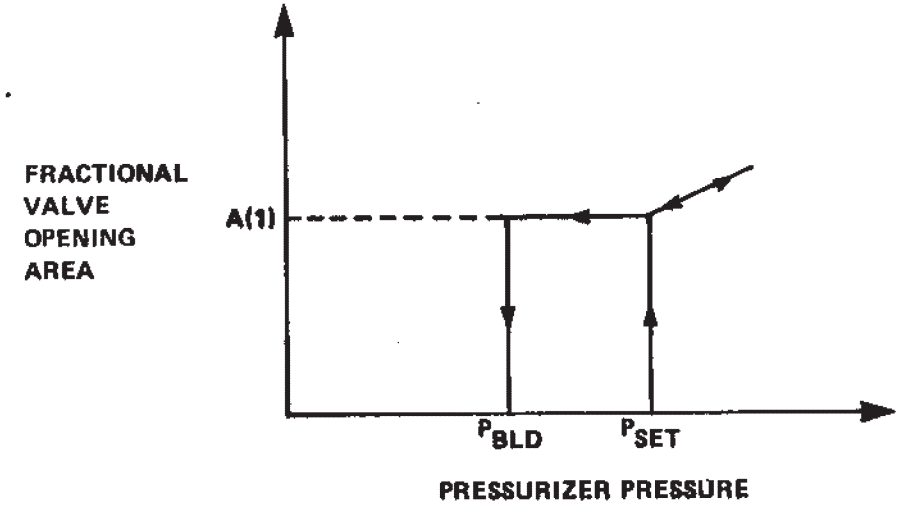

P_{ACC} = ACCUMULATED PRESSURE AT WHICH VALVE FULLY OPENS

P_{SET} = SET PRESSURE AT WHICH VALVE STARTS TO OPEN

P_{BLD} = BLOWDOWN PRESSURE AT WHICH VALVE CLOSES

AMENDMENT NO. 1 (4/86)

FLORIDA POWER & LIGHT COMPANY
ST. LUCIE PLANT UNIT 2

PRESSURIZER SAFETY VALVE OPERATING CHARACTERISTICS USED IN CESEC-II

FIGURE 15.11-6

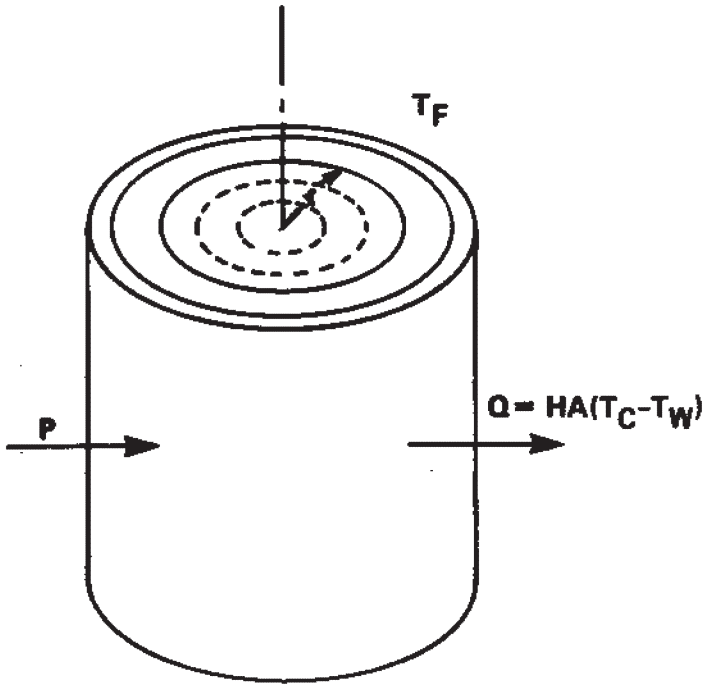

P = HEAT GENERATED IN FUEL

Q = HEAT TRANSFERED TO FLUID

T_c = CLAD SURFACE TEMPERATURE

T_w = FLUID TEMPERATURE

H = HEAT TRANSFER COEFFICIENT

A = SURFACE AREA

HEAT FLOW EQUATION

$$\rho C \frac{\partial T_F}{\partial t} = K\left[\frac{\partial^2 T_F}{\partial r^2} + \frac{1}{r}\frac{\partial T_F}{\partial r}\right] + \frac{\partial K}{\partial r} \bullet \frac{\partial T_F}{\partial r} + q(r,P)$$

ρ = FUEL DENSITY

C = FUEL SPECIFIC HEAT

T = FUEL TEMPERATURE AT RADIUS r

r = RADIUS

K = FUEL THERMAL CONDUCTIVITY

t = TIME

q(r,P) = SPECIFIC HEAT GENERATION DEPENDING ON RADIUS AND THE REACTOR KINETICS POWER

SPATIAL FINITE DIFFERENCE METHODS REDUCE THE ABOVE EQUATION TO:

$$(MC)_n \frac{dT_{Fn}}{dt} = C_1 P + C_2 \left(T_{F_{n-1}} - T_{F_n}\right) - C_3 \left(T_{F_{n+1}} - T_{F_n}\right)$$

$(MC)_n$ = THERMAL CAPACITY OF NODE n

C_1 = HEAT GENERATION FRACTION IN THE NODE

C_2 = EFFECTIVE THERMAL CONDUCTANCE BETWEEN NODES

C_3 = EFFECTIVE THERMAL CONDUCTANCE (HA FOR EDGE NODE)

T_{F_n} = AVERAGE NODE TEMPERATURE

$T_{F_{n-1}}$ = AVERAGE NODE TEMPERATURE FOR NODE NEARER ℄

$T_{F_{n+1}}$ = AVERAGE NODE TEMPERATURE FOR NODE AWAY FROM ℄

AMENDMENT NO. 1 (4/86)

FLORIDA POWER & LIGHT COMPANY
ST. LUCIE PLANT UNIT 2

FUEL ELEMENT TEMPERATURE EQUATIONS

FIGURE 15.11-7

STEAM GENERATOR

HEAT BALANCE

$$Q = UA \frac{(T_{IN} - T_{OUT})}{LN\left(\frac{T_{IN} - T_S}{T_{OUT} - T_S}\right)}$$

UA = 1.0* UA FOR FORWARD HEAT TRANSFER
UA = INPUT U*A FOR REVERSE HEAT TRANSFER

$$Q = UA \left(\frac{T_{IN} + T_{OUT}}{2} - T_S\right)$$

FOR THE CONDITION WHEN $T_{IN} > T_S$ AND $T_{OUT} < T_S$
UA = 0.8* UA (OF PREVIOUS TIME STEP)

UA = OVERALL HEAT TRANSFER COEFFICIENT (FUNCTION OF PRIMARY SIDE RESISTANCE, SECONDARY SIDE RESISTANCE, WALL/FOULING)

A = OUTSIDE SURFACE TUBE HEAT TRANSFER AREA

T_{IN} = COOLANT TEMPERATURE OF HOT SIDE OF STEAM GENERATOR PRIMARY SIDE

T_{OUT} = COOLANT TEMPERATURE OF COLD SIDE OF STEAM GENERATOR PRIMARY SIDE

T_S = SECONDARY SIDE TEMPERATURE

AMENDMENT NO. 1 (4/86)

FLORIDA POWER & LIGHT COMPANY
ST. LUCIE PLANT UNIT 2

HEAT TRANSFER BETWEEN PRIMARY AND SECONDARY SIDE OF STEAM GENERATOR

FIGURE 15.11-8

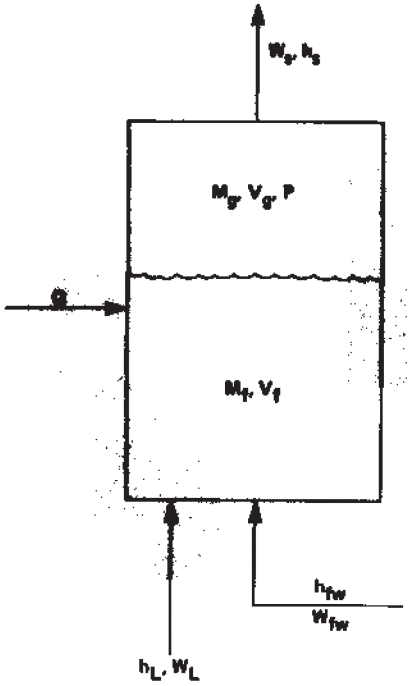

STEAM GENERATOR
SHELL SIDE

MASS BALANCE

$$\frac{dM_g}{dt} + \frac{dM_f}{dt} = W_{fw} + W_L - W_S$$

VOLUME BALANCE

$$\frac{d(M_g V_g)}{dt} + \frac{d(M_f V_f)}{dt} = \frac{dV}{dt} = 0$$

ENERGY BALANCE

$$\frac{d(M_f h_f)}{dt} + \frac{d(M_g h_g)}{dt} = Q + 144\,\frac{V}{J}\,\frac{dP}{dt} + W_{fw}h_{fw} + W_L h_L - W_s h_s$$

STATE: SATURATION

- P = STEAM GENERATOR SECONDARY PRESSURE
- M_g = TOTAL STEAM MASS IN STEAM GENERATOR
- V_g = SPECIFIC VOLUME OF STEAM
- M_f = TOTAL WATER MASS IN STEAM GENERATOR
- V_f = SPECIFIC VOLUME OF WATER
- W_{fw} = MASS FLOW RATE OF FEEDWATER
- h_{fw} = ENTHALPY OF FEEDWATER
- W_s = MASS FLOW RATE OF STEAM LEAVING STEAM GENERATOR
- h_s = ENTHALPY OF STEAM FLOW
- W_L = MASS FLOW RATE OF WATER LEAKING OUT OF STEAM GENERATOR TUBES
- h_L = ENTHALPY OF LEAK FLOW
- Q = HEAT RATE
- V = TOTAL VOLUME
- J = CONVERSION FACTOR

AMENDMENT NO. 1 (4/86)

FLORIDA POWER & LIGHT COMPANY
ST. LUCIE PLANT UNIT 2

CONSERVATION EQUATIONS FOR THE STEAM GENERATOR SHELL SIDE

FIGURE 15.11-9

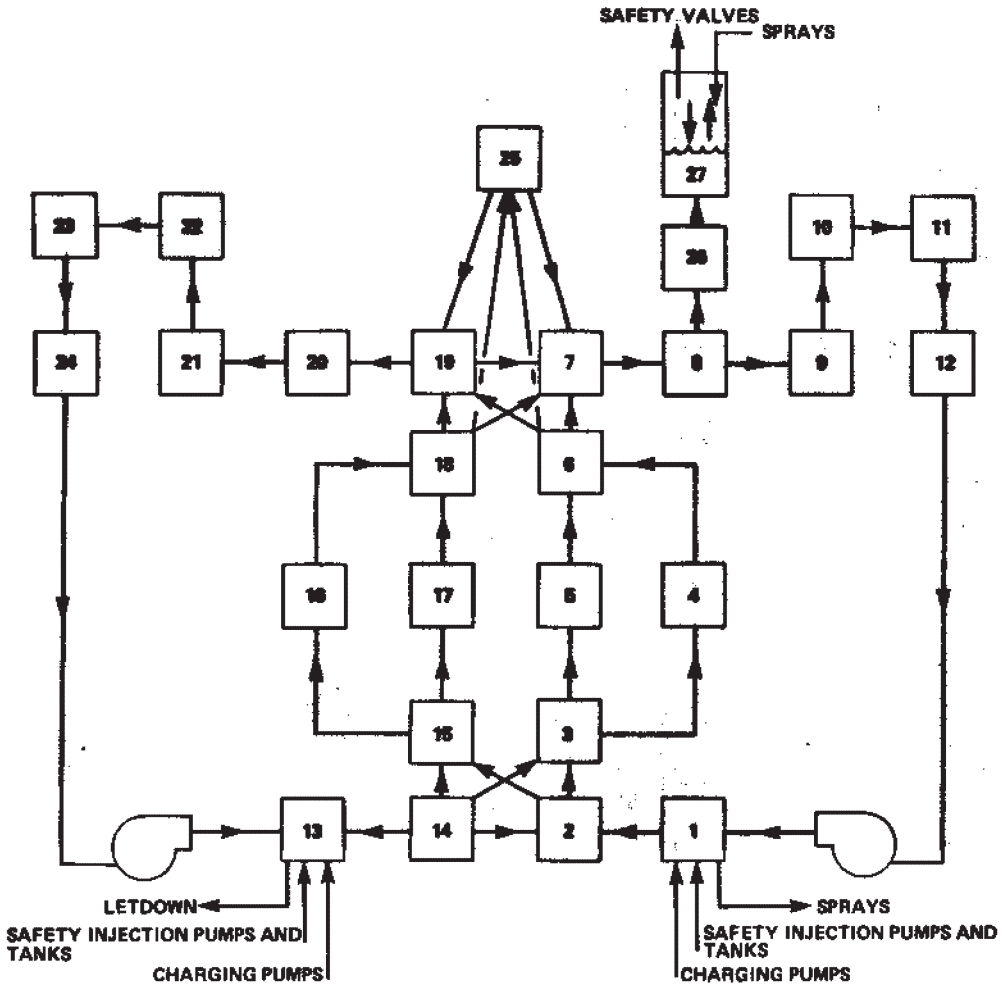

NODE	PHYSICAL DESCRIPTION
1	COLD LEG
2	UPSTREAM HALF OF INLET PLENUM (BEFORE FLOW MIXING)
3	DOWNSTREAM HALF OF INLET PLENUM (AFTER FLOW MIXING)
4	BYPASS FLOW
5	CORE
6	UPSTREAM HALF OF OUTLET PLENUM
7	DOWNSTREAM HALF OF OUTLET PLENUM
8	HOT LEG
9	STEAM GENERATOR INLET PLENUM
10	UPSTREAM HALF OF STEAM GENERATOR TUBES
11	DOWNSTREAM HALF OF STEAM GENERATOR TUBES
12	STEAM GENERATOR OUTLET PLENUM
13	SAME AS 1 IN OTHER STEAM GENERATOR LOOP
14	SAME AS 2 IN OTHER STEAM GENERATOR LOOP
15	SAME AS 3 IN OTHER STEAM GENERATOR LOOP
16	SAME AS 4 IN OTHER STEAM GENERATOR LOOP
17	SAME AS 5 IN OTHER STEAM GENERATOR LOOP
18	SAME AS 6 IN OTHER STEAM GENERATOR LOOP
19	SAME AS 7 IN OTHER STEAM GENERATOR LOOP
20	SAME AS 8 IN OTHER STEAM GENERATOR LOOP
21	SAME AS 9 IN OTHER STEAM GENERATOR LOOP
22	SAME AS 10 IN OTHER STEAM GENERATOR LOOP
23	SAME AS 11 IN OTHER STEAM GENERATOR LOOP
24	SAME AS 12 IN OTHER STEAM GENERATOR LOOP
25	REACTOR VESSEL CLOSURE HEAD
26	SURGE LINE
27	PRESSURIZER

AMENDMENT NO. 1 (4/86)

FLORIDA POWER & LIGHT COMPANY
ST. LUCIE PLANT UNIT 2

SCHEMATIC DIAGRAM OF PRIMARY COOLANT NODES FOR CESEC-SLB

FIGURE 15.11-10

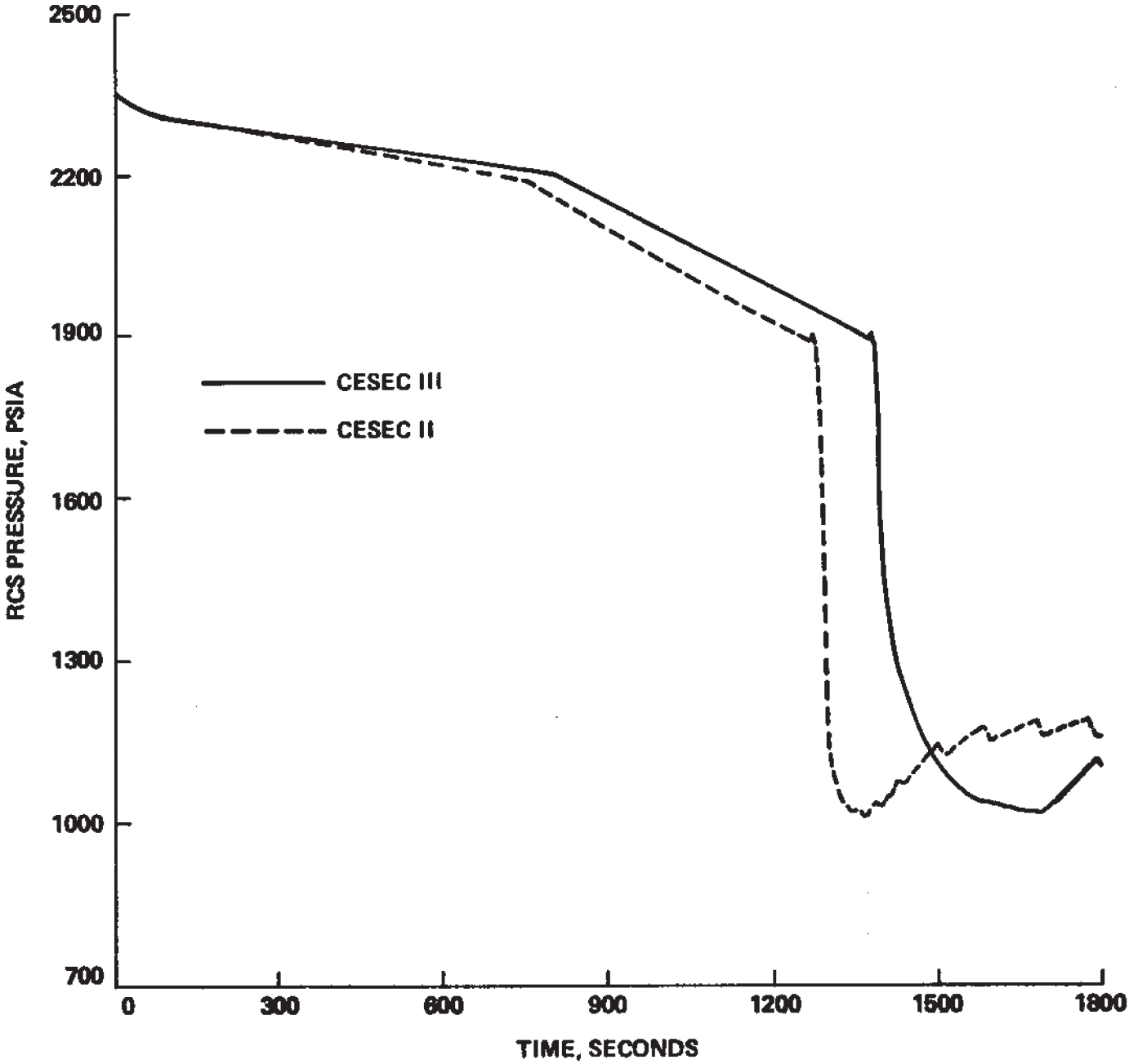

AMENDMENT NO. 1 (4/86)

FLORIDA POWER & LIGHT COMPANY
ST. LUCIE PLANT UNIT 2

STM. GEN. TUBE RUPTURE FOR ST. LUCIE 2 WITHOUT LOSS OF OFFSITE PWR.-REACTOR COOLANT SYSTEM PRESSURE VS. TIME

FIGURE 15.11-11

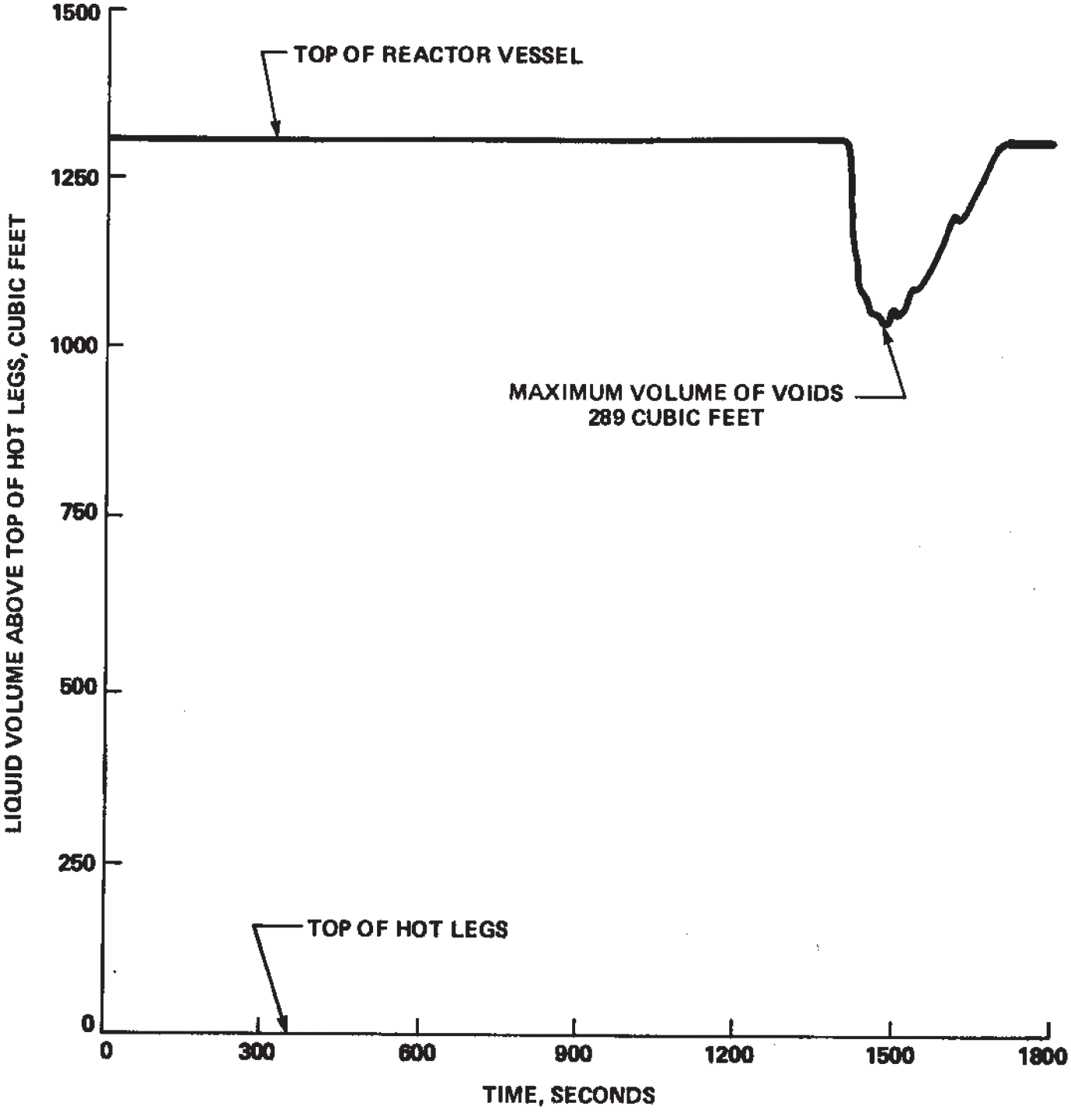

AMENDMENT NO. 1 (4/86)

FLORIDA POWER & LIGHT COMPANY
ST. LUCIE PLANT UNIT 2

STM. GEN. TUBE RUPTURE FOR ST. LUCIE 2 WITHOUT LOSS OF OFFSITE PWR.-VOID FORMATION IN TOP OF REACTOR VESSEL

FIGURE 15.11-12

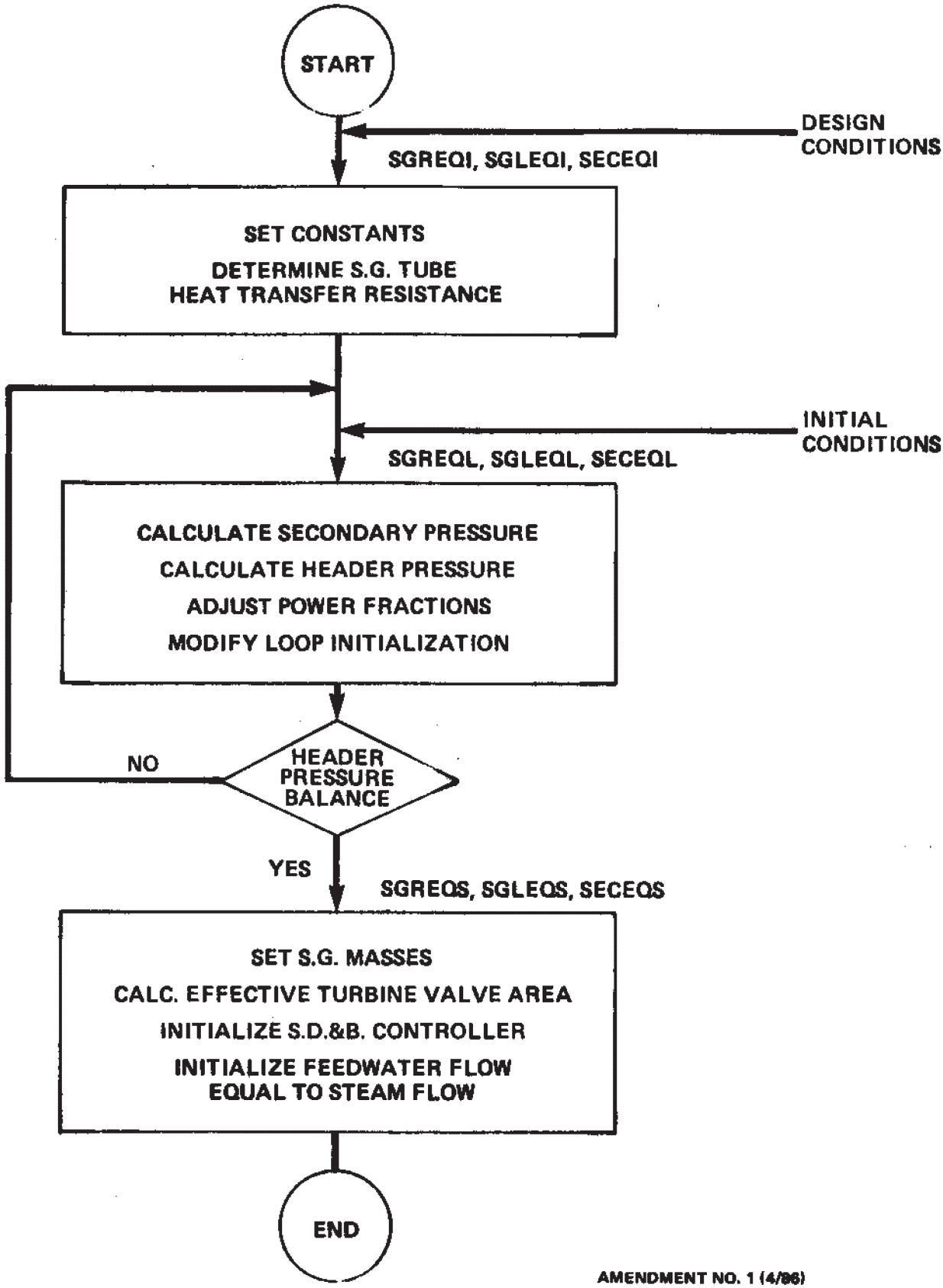

AMENDMENT NO. 1 (4/86)

FLORIDA POWER & LIGHT COMPANY
ST. LUCIE PLANT UNIT 2

STEAM GENERATOR INITIALIZATION
FIGURE 15.11-13

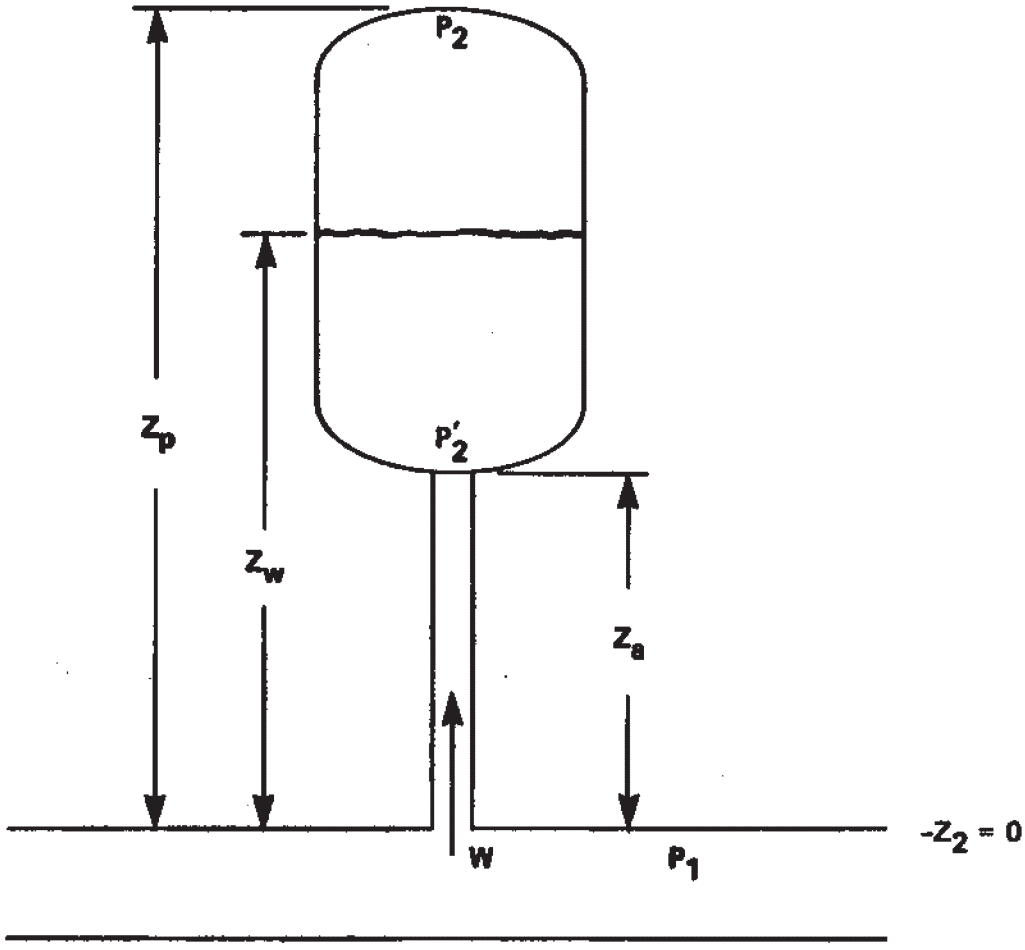

AMENDMENT NO. 1 (4/86)

FLORIDA POWER & LIGHT COMPANY
ST. LUCIE PLANT UNIT 2

SURGE LINE MOMENTUM

FIGURE 15.11-14

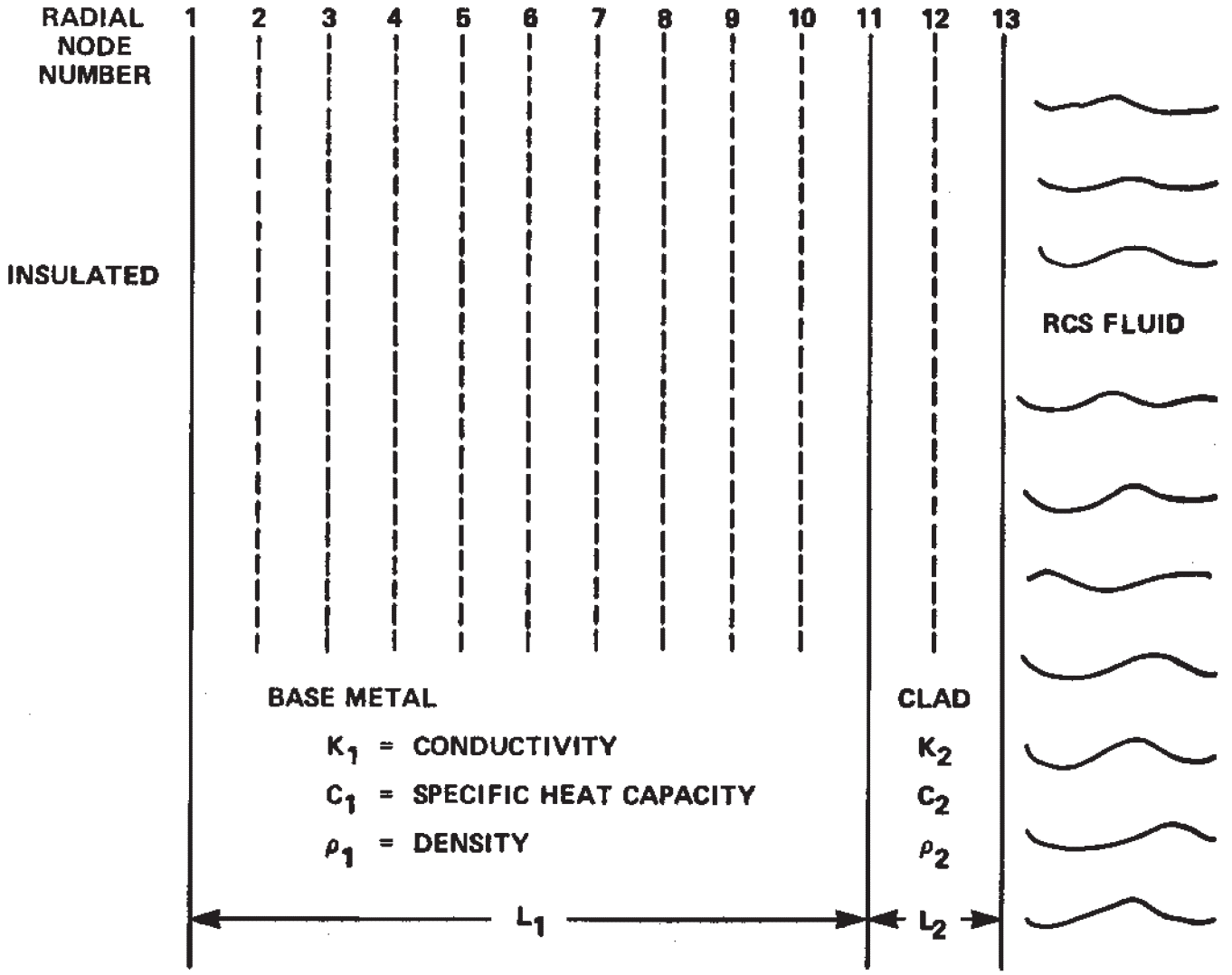

AMENDMENT NO. 1 (4/86)

FLORIDA POWER & LIGHT COMPANY
ST. LUCIE PLANT UNIT 2

BASIC GEOMETRY OF WALL HEAT MODEL

FIGURE 15.11-15

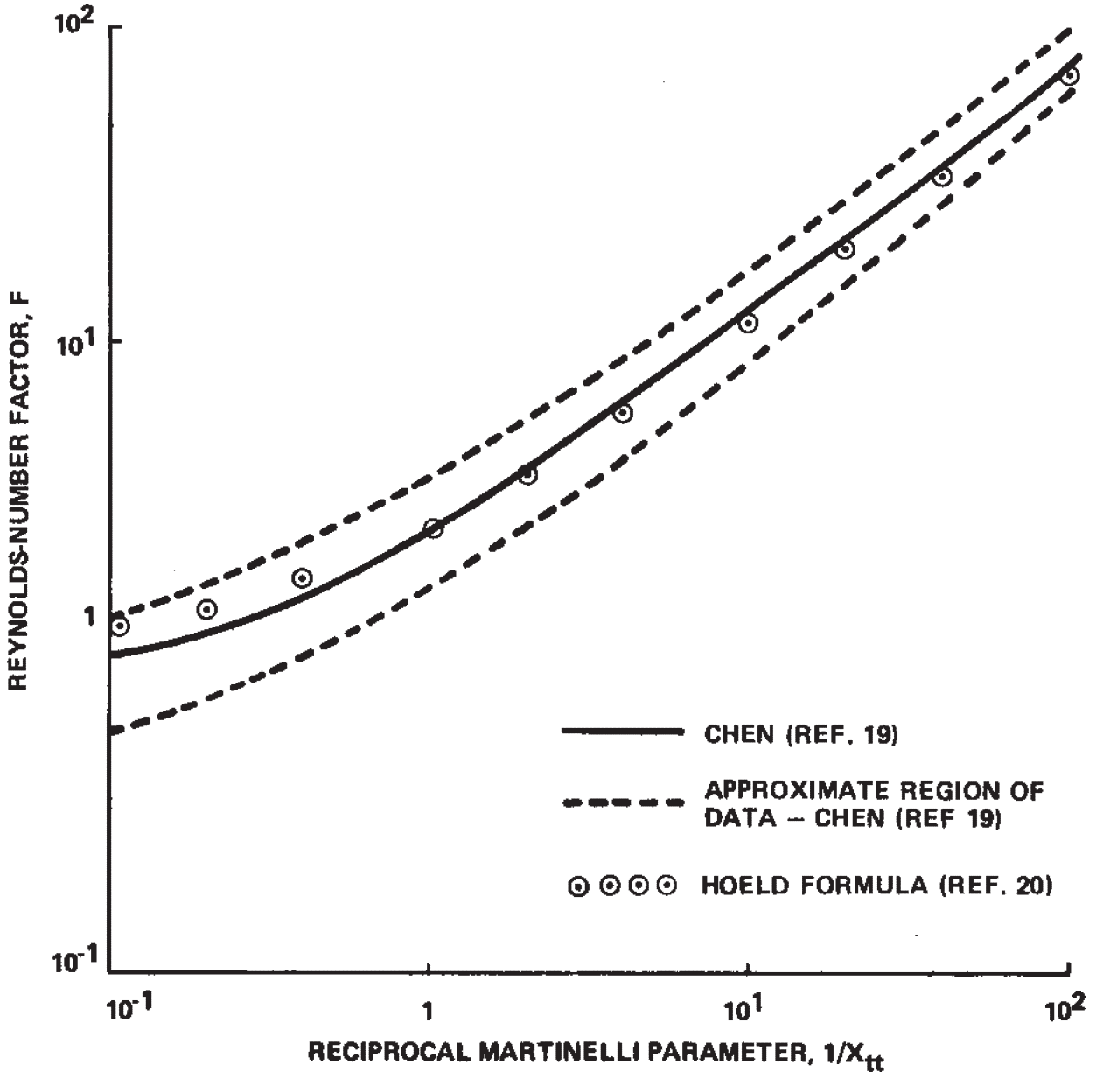

AMENDMENT NO. 1 (4/86)

FLORIDA POWER & LIGHT COMPANY
ST. LUCIE PLANT UNIT 2

REYNOLDS–NUMBER FACTOR
VS
RECIPROCAL MARTINELLI PARAMETER
FIGURE 15.11-16

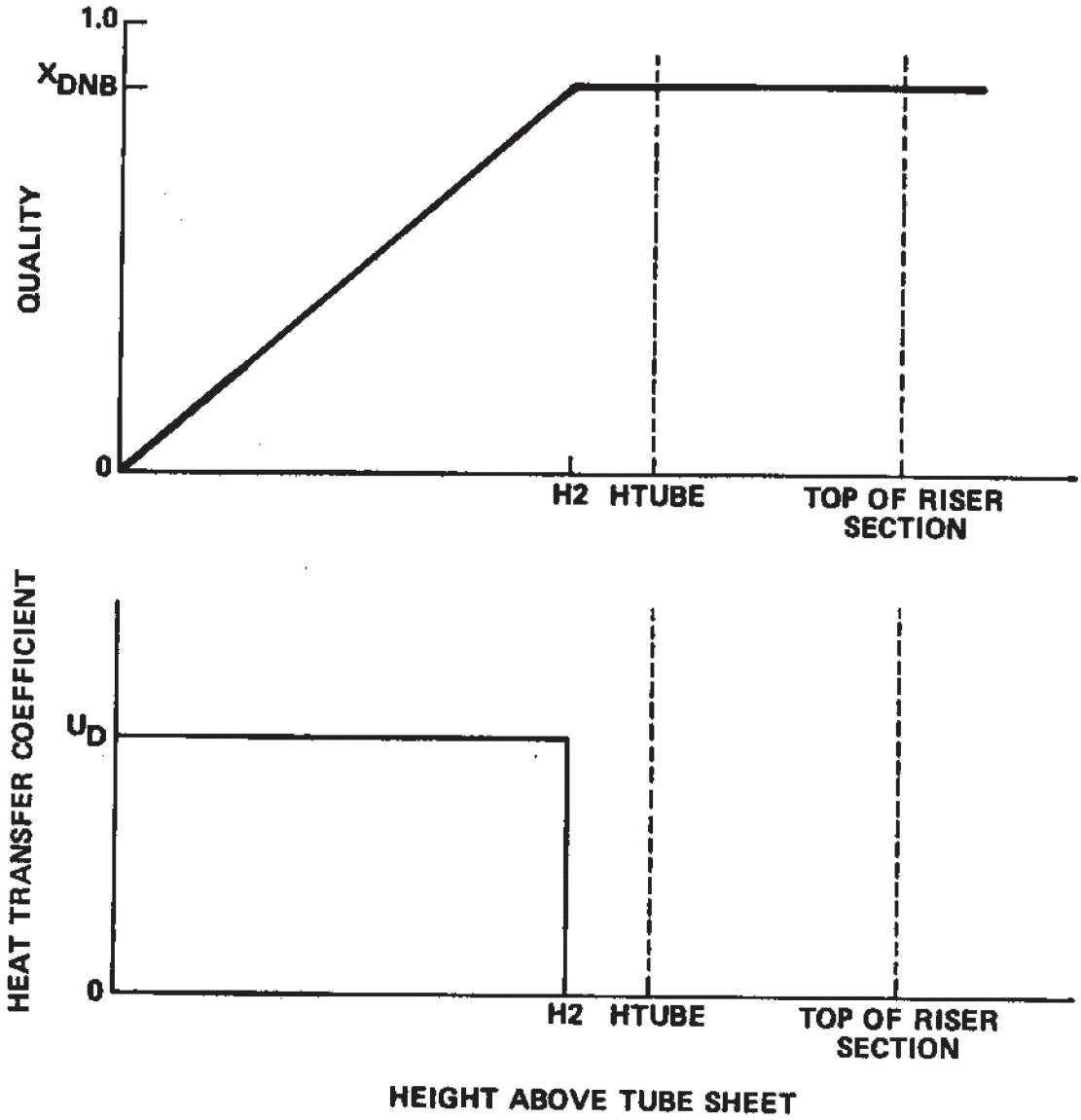

AMENDMENT NO. 1 (4/86)

FLORIDA POWER & LIGHT COMPANY
ST. LUCIE PLANT UNIT 2

QUALITY AND HEAT TRANSFER PROFILE DURING SECONDARY SIDE DRYOUT

FIGURE 15.11-17

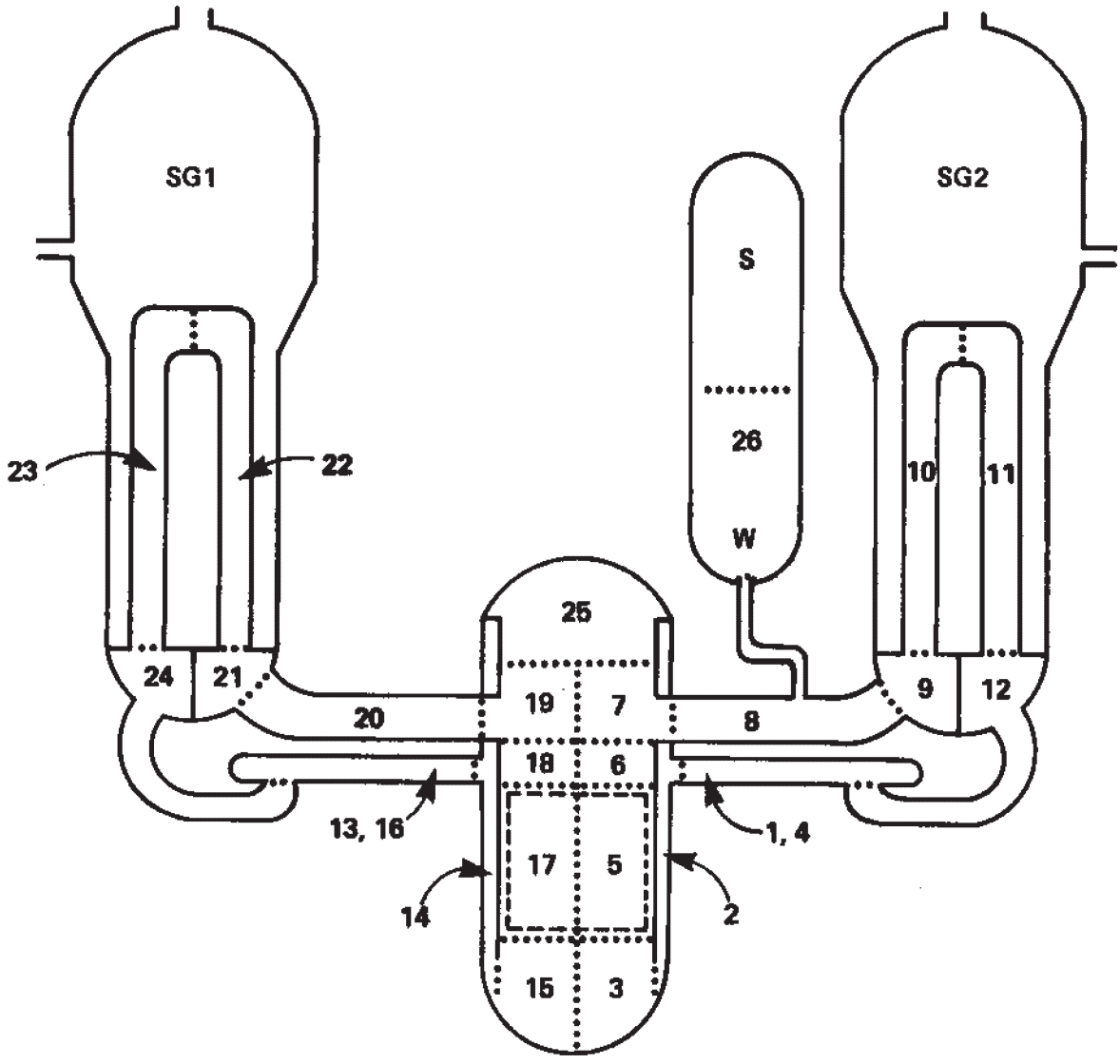

AMENDMENT NO. 1 (4/86)

FLORIDA POWER & LIGHT COMPANY
ST. LUCIE PLANT UNIT 2

SCHEMATIC OF C-E NSSS SHOWING
APPROXIMATE CESEC NODALIZATION

FIGURE 15.11-18

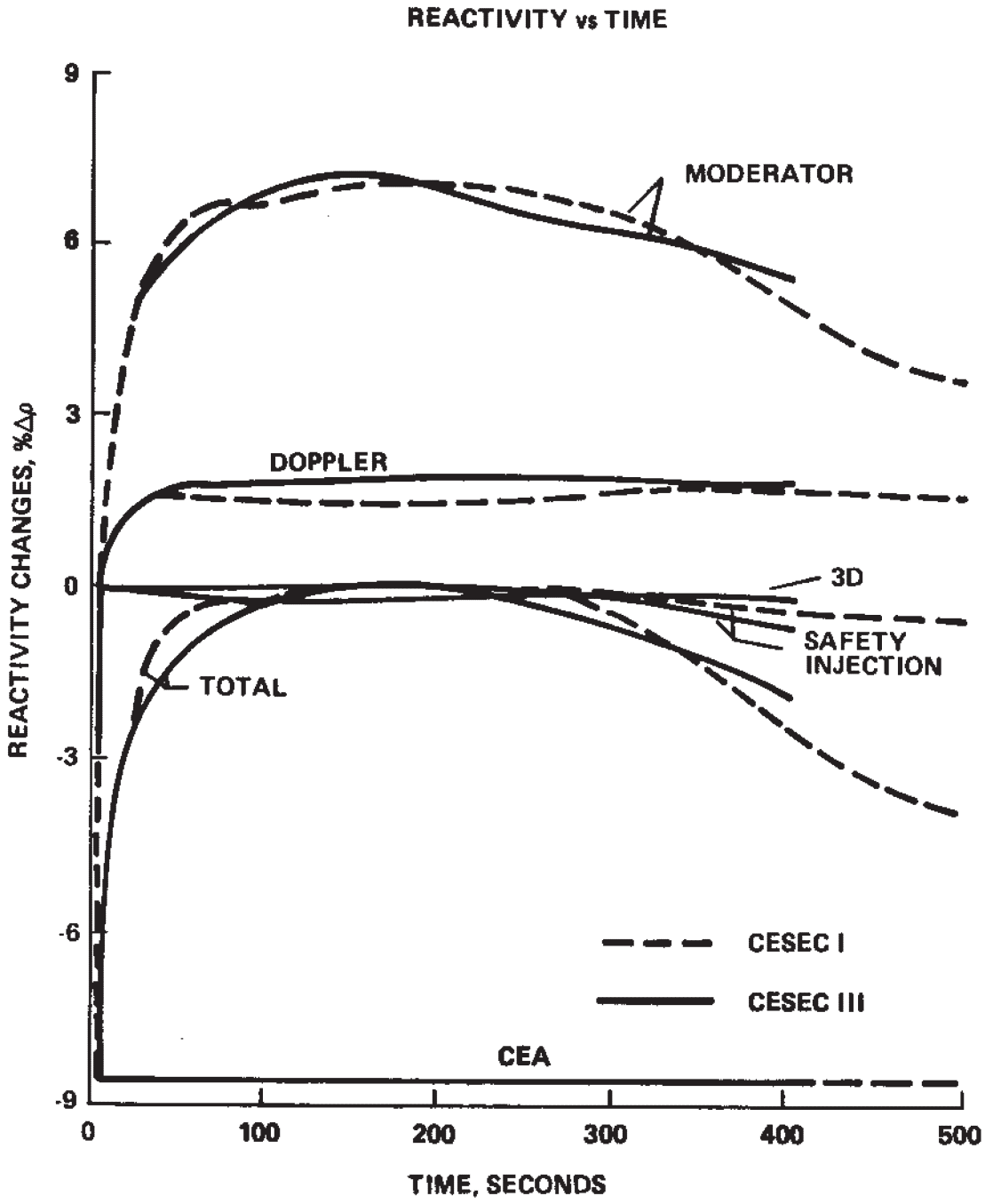

AMENDMENT NO. 1 (4/86)

FLORIDA POWER & LIGHT COMPANY
ST. LUCIE PLANT UNIT 2

FULL POWER LARGE STEAM LINE BREAK WITH CONCURRENT LOSS OF OFFSITE POWER

FIGURE 15.11-19

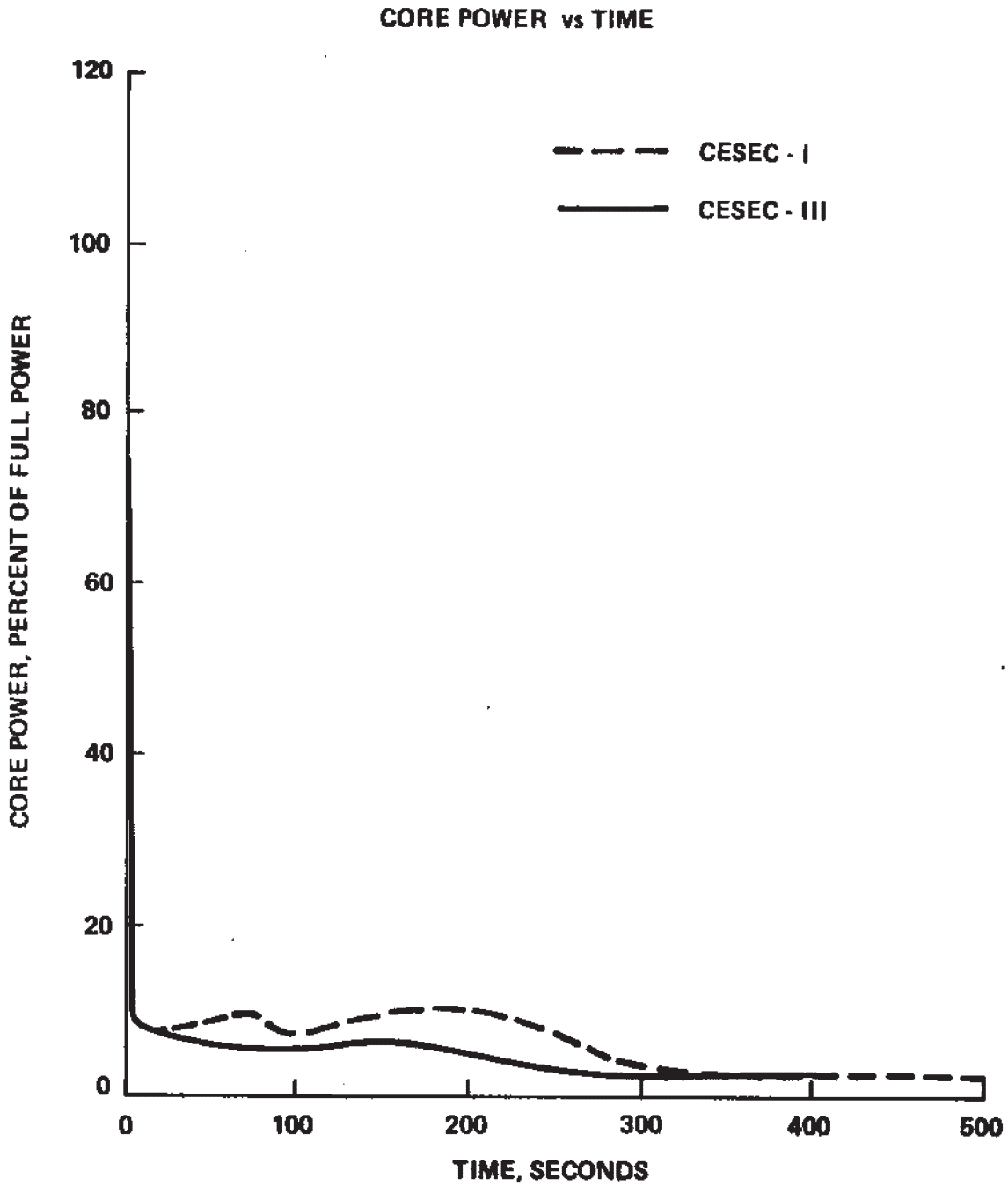

AMENDMENT NO. 1 (4/86)

FLORIDA POWER & LIGHT COMPANY
ST. LUCIE PLANT UNIT 2

FULL POWER LARGE STEAM LINE BREAK WITH CONCURRENT LOSS OF OFFSITE POWER

FIGURE 15.11-20

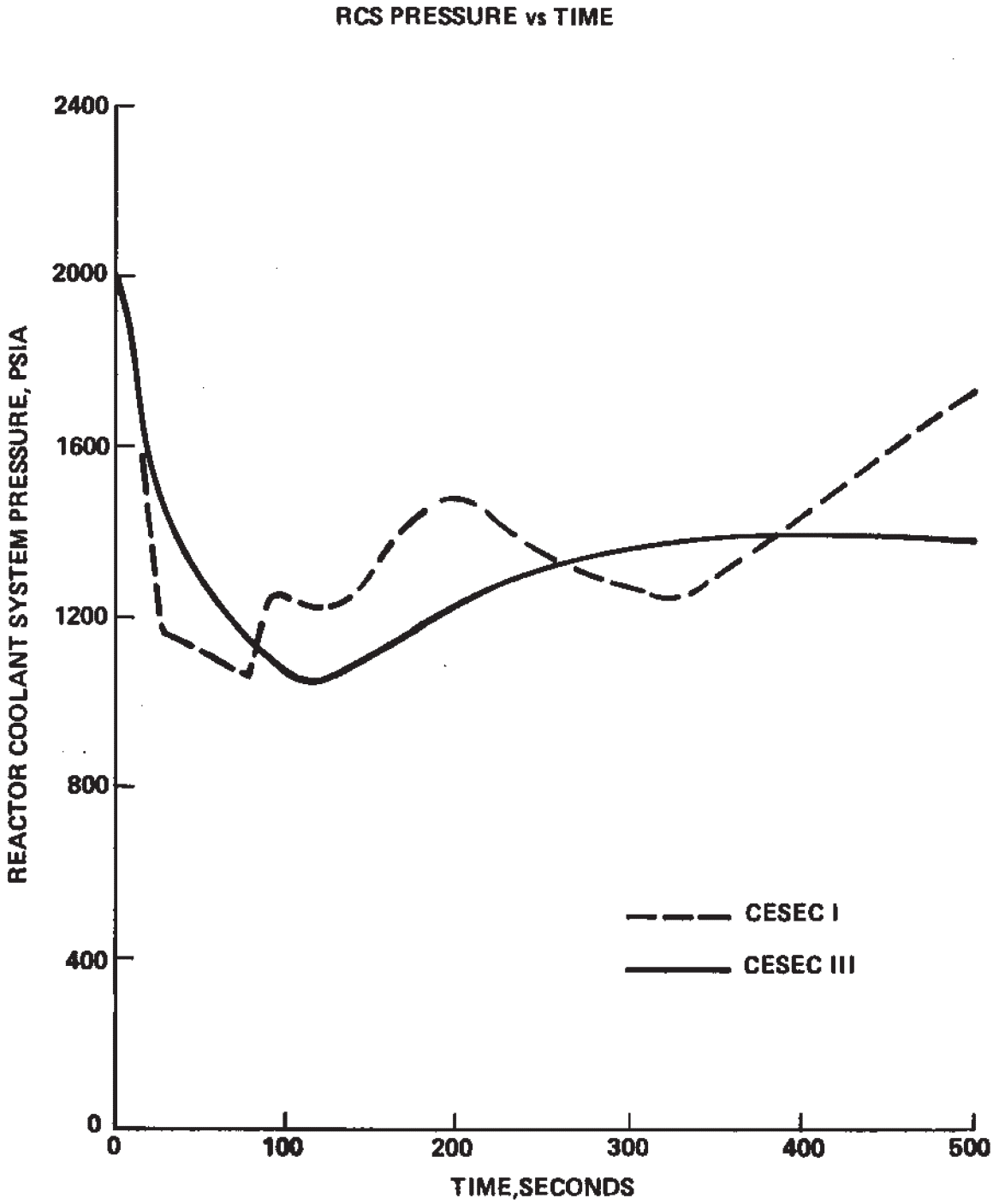

AMENDMENT NO. 1 (4/86)

FLORIDA POWER & LIGHT COMPANY
ST. LUCIE PLANT UNIT 2

FULL POWER LARGE STEAM LINE BREAK WITH CONCURRENT LOSS OF OFFSITE POWER

FIGURE 15.11-21

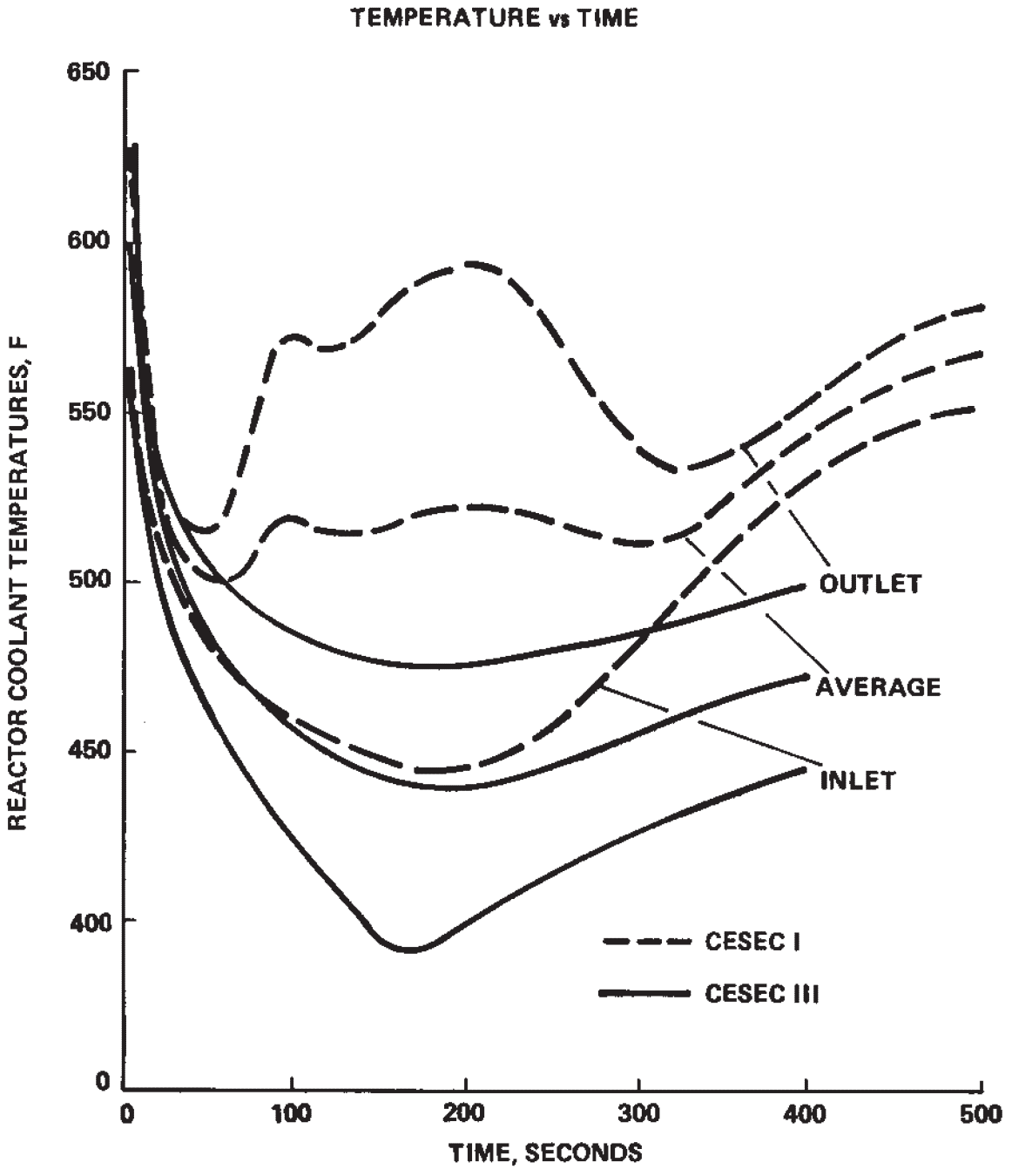

AMENDMENT NO. 1 (4/86)

FLORIDA POWER & LIGHT COMPANY
ST. LUCIE PLANT UNIT 2

FULL POWER LARGE STEAM LINE BREAK
WITH CONCURRENT LOSS OF OFFSITE POWER

FIGURE 15.11-22

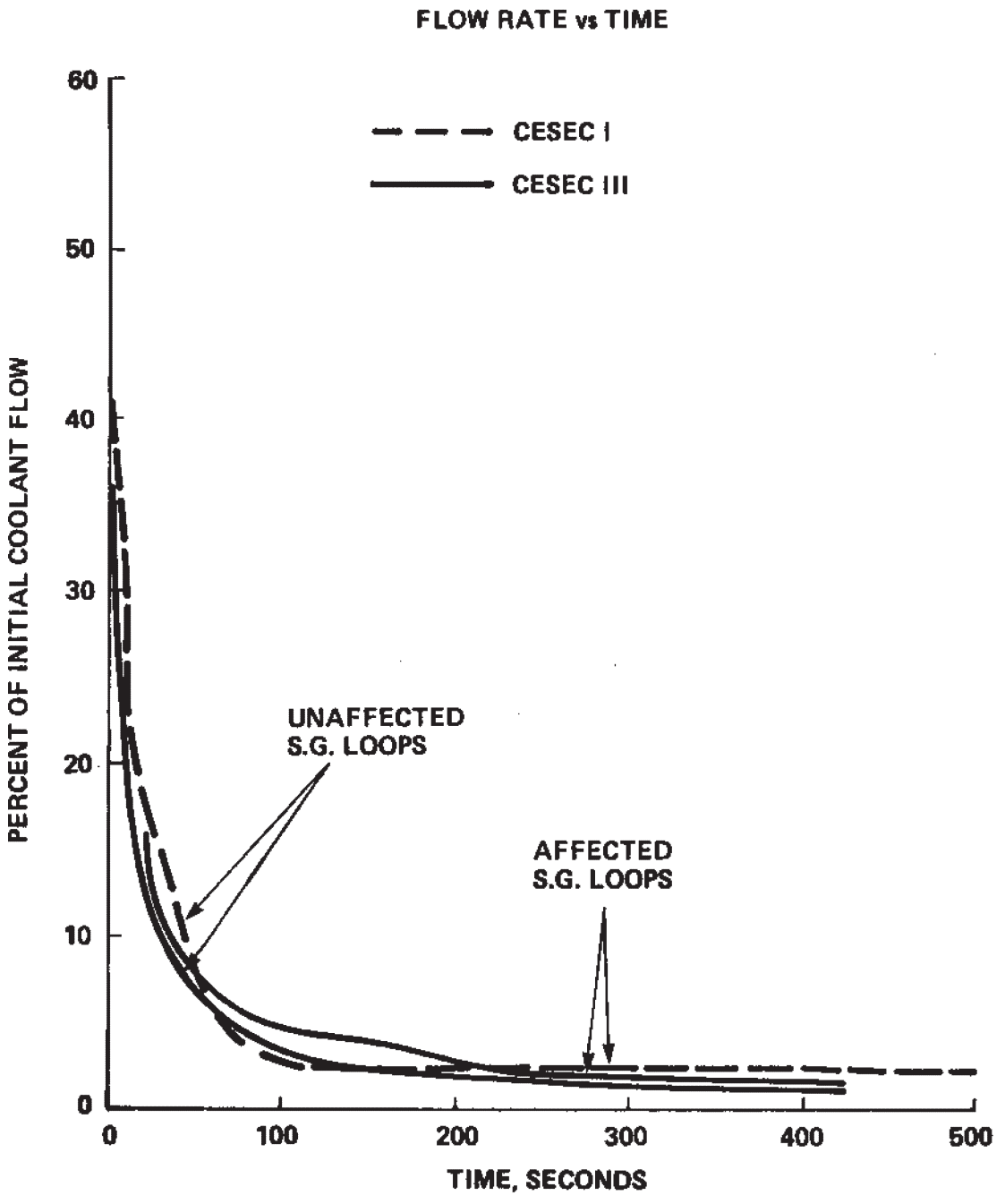

AMENDMENT NO. 1 (4/86)

FLORIDA POWER & LIGHT COMPANY
ST. LUCIE PLANT UNIT 2

FULL POWER LARGE STEAM LINE BREAK
WITH CONCURRENT LOSS OF OFFSITE POWER

FIGURE 15.11-23

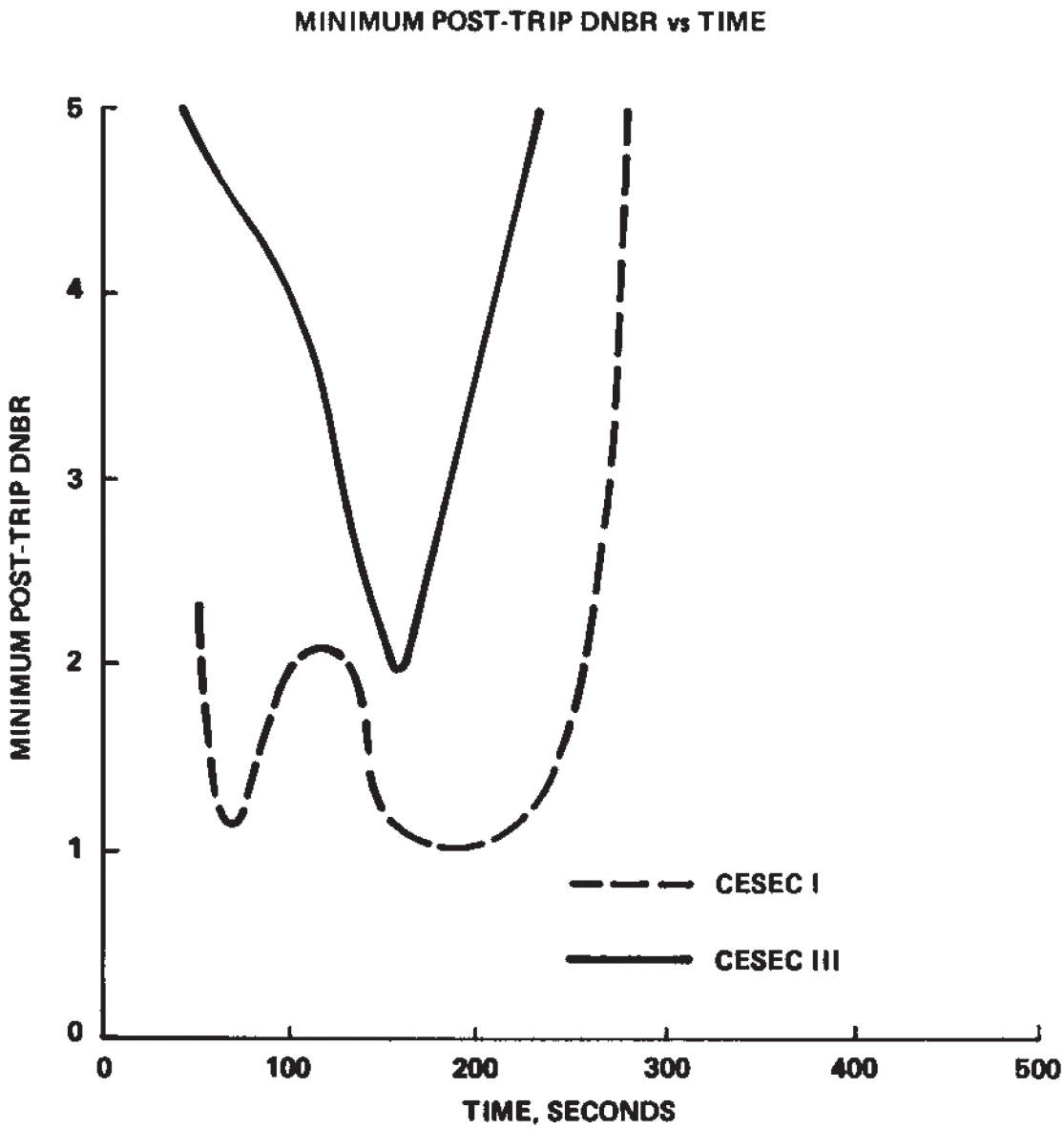

AMENDMENT NO. 1 (4/86)

FLORIDA POWER & LIGHT COMPANY
ST. LUCIE PLANT UNIT 2

FULL POWER LARGE STEAM LINE BREAK
WITH CONCURRENT LOSS OF OFFSITE POWER

FIGURE 15.11-24

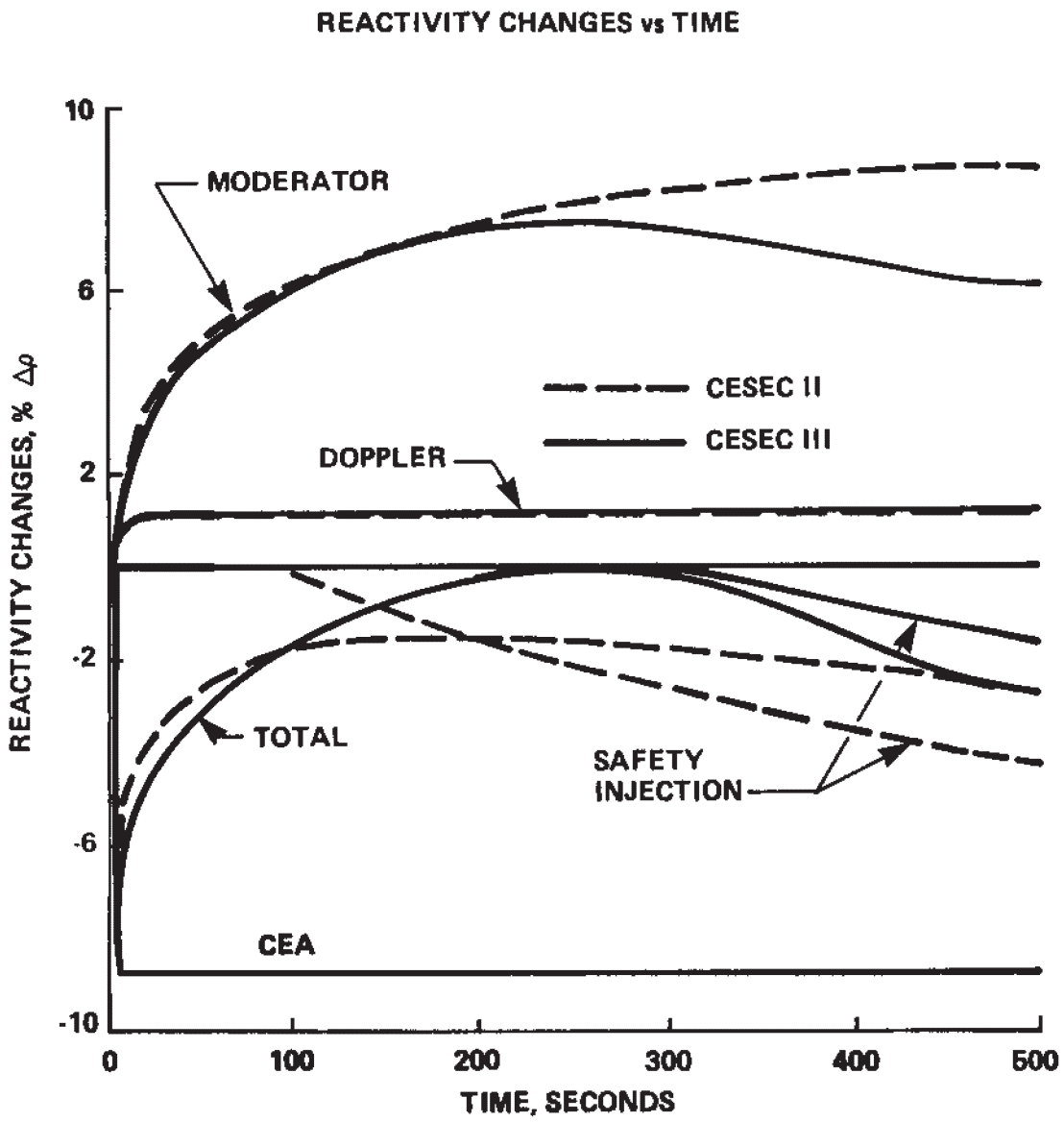

AMENDMENT NO. 1 (4/86)

FLORIDA POWER & LIGHT COMPANY
ST. LUCIE PLANT UNIT 2

FULL POWER LARGE STEAM LINE BREAK
WITH CONCURRENT LOSS OF OFFSITE POWER

FIGURE 15.11-25

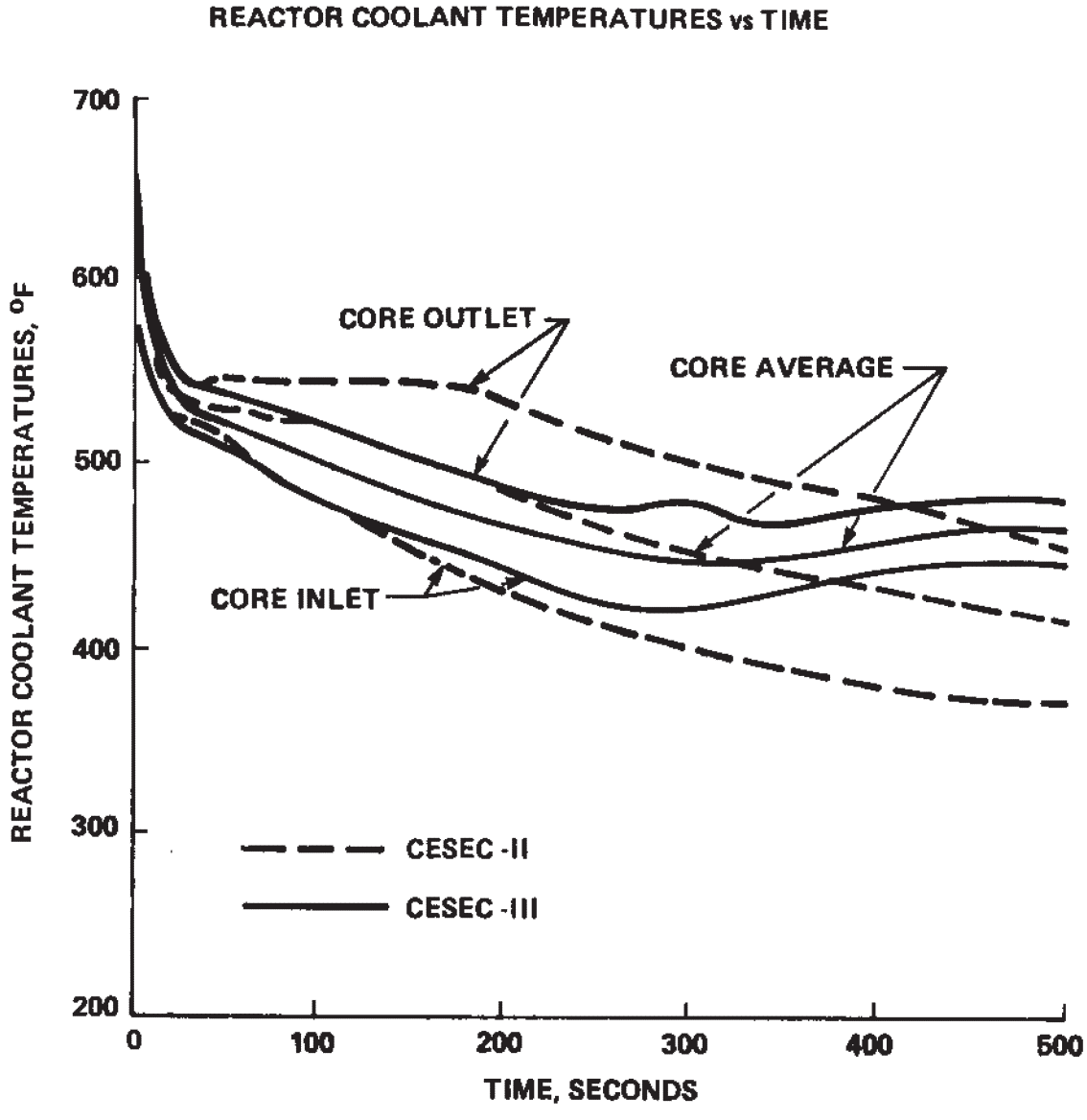

AMENDMENT NO. 1 (4/88)

FLORIDA POWER & LIGHT COMPANY
ST. LUCIE PLANT UNIT 2

FULL POWER LARGE STEAM LINE BREAK WITH CONCURRENT LOSS OF OFFSITE POWER

FIGURE 15.11-26

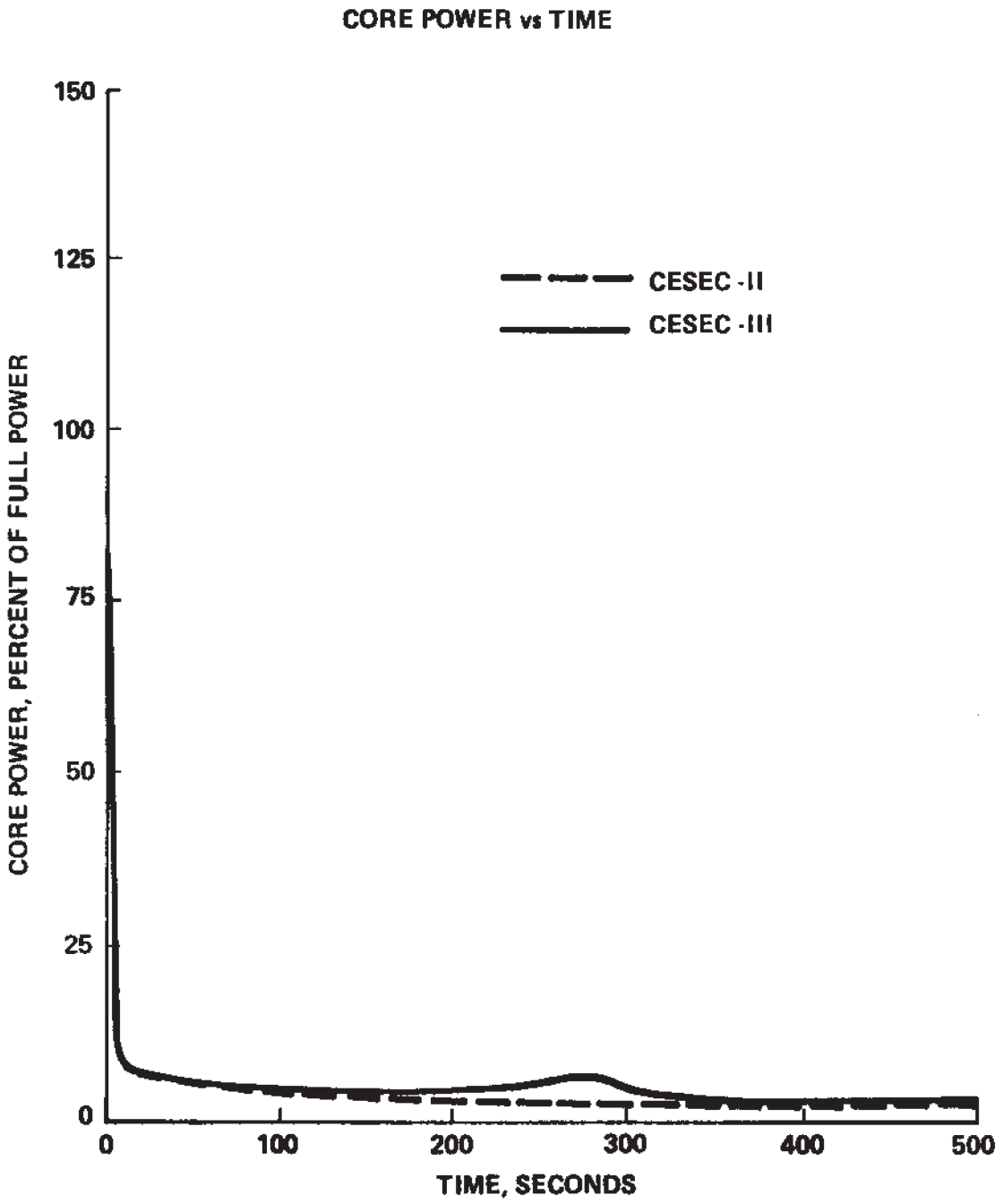

AMENDMENT NO. 1 (4/86)

FLORIDA POWER & LIGHT COMPANY
ST. LUCIE PLANT UNIT 2

FULL POWER LARGE STEAM LINE BREAK
WITH CONCURRENT LOSS OF OFFSITE POWER

FIGURE 15.11-27

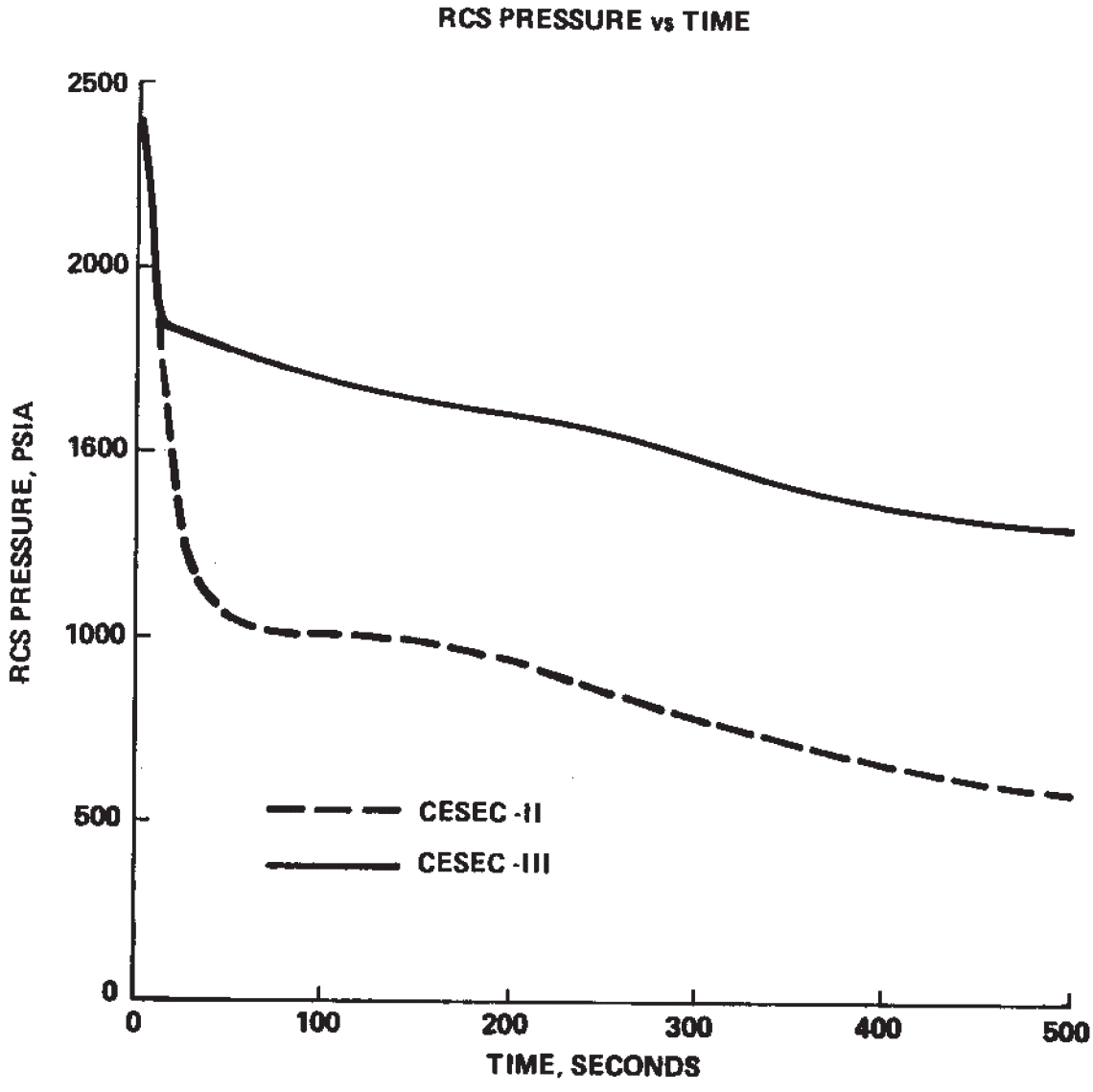

AMENDMENT NO. 1 (4/86)

FLORIDA POWER & LIGHT COMPANY
ST. LUCIE PLANT UNIT 2

FULL POWER LARGE STEAM LINE BREAK WITH CONCURRENT LOSS OF OFFSITE POWER

FIGURE 15.11-28

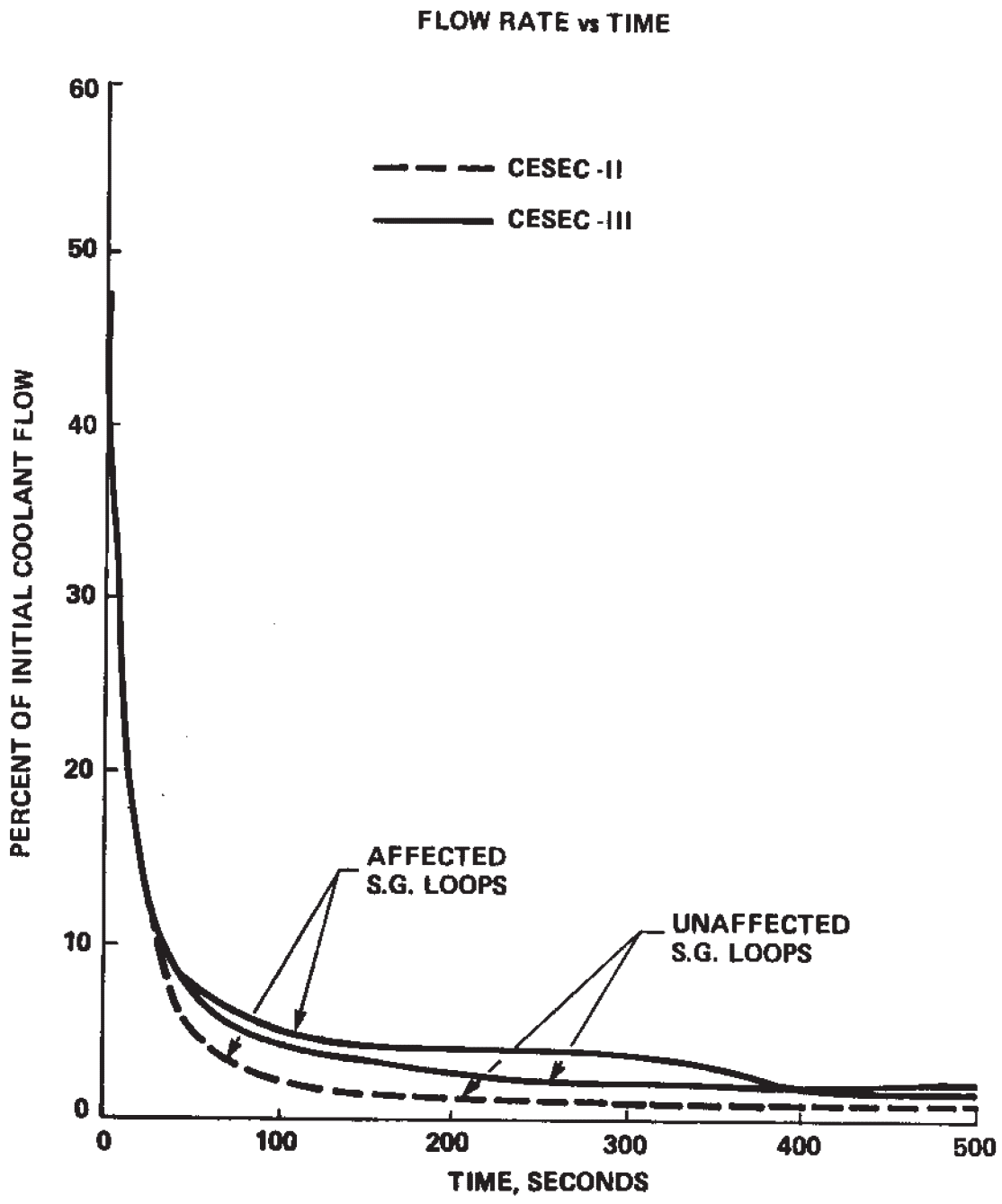

AMENDMENT NO. 1 (4/86)

FLORIDA POWER & LIGHT COMPANY
ST. LUCIE PLANT UNIT 2

FULL POWER LARGE STEAM LINE BREAK WITH CONCURRENT LOSS OF OFFSITE POWER

FIGURE 15.11-29

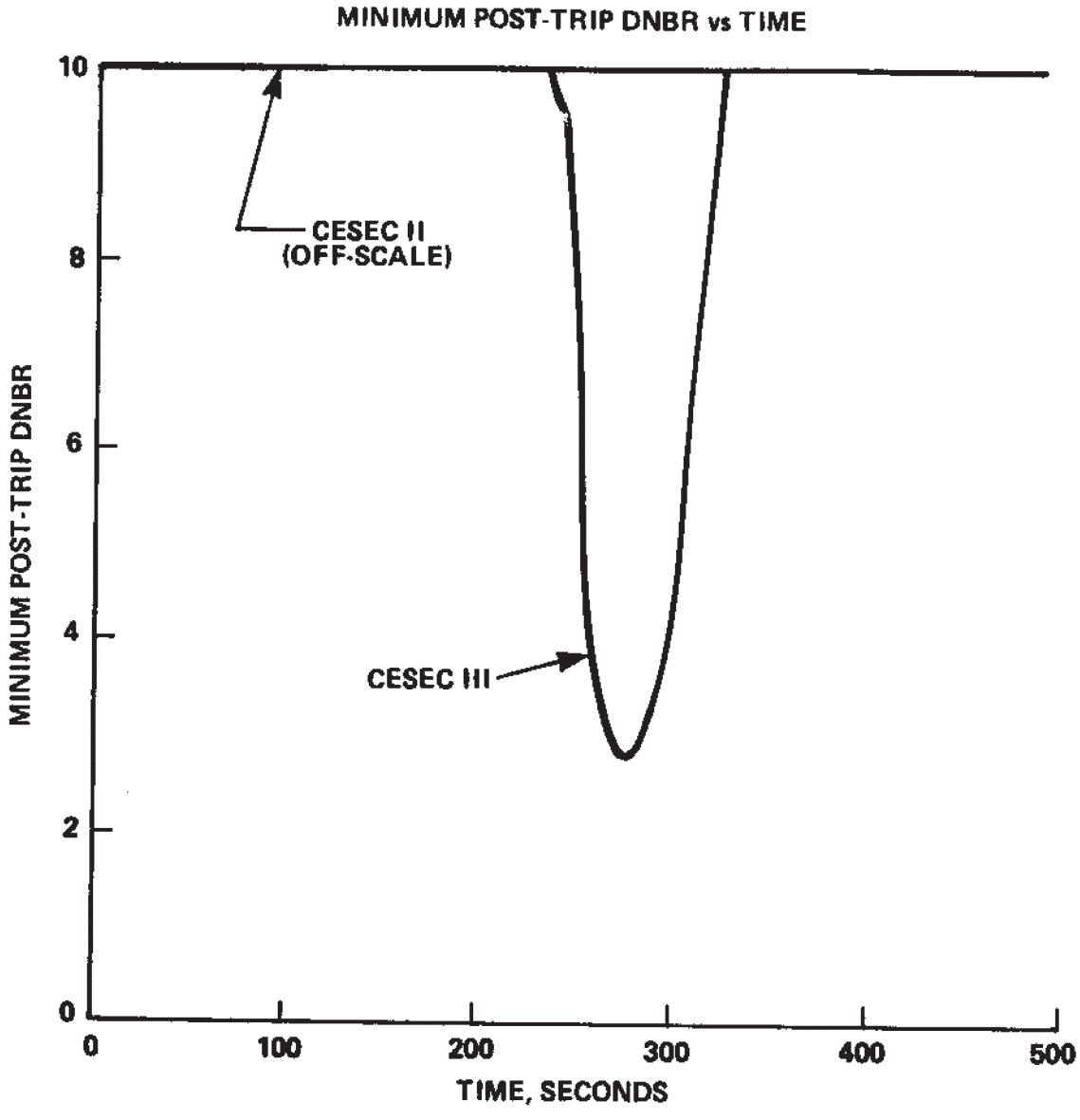

AMENDMENT NO. 1 (4/86)

FLORIDA POWER & LIGHT COMPANY
ST. LUCIE PLANT UNIT 2

FULL POWER LARGE STEAM LINE BREAK WITH CONCURRENT LOSS OF OFFSITE POWER

FIGURE 15.11-30

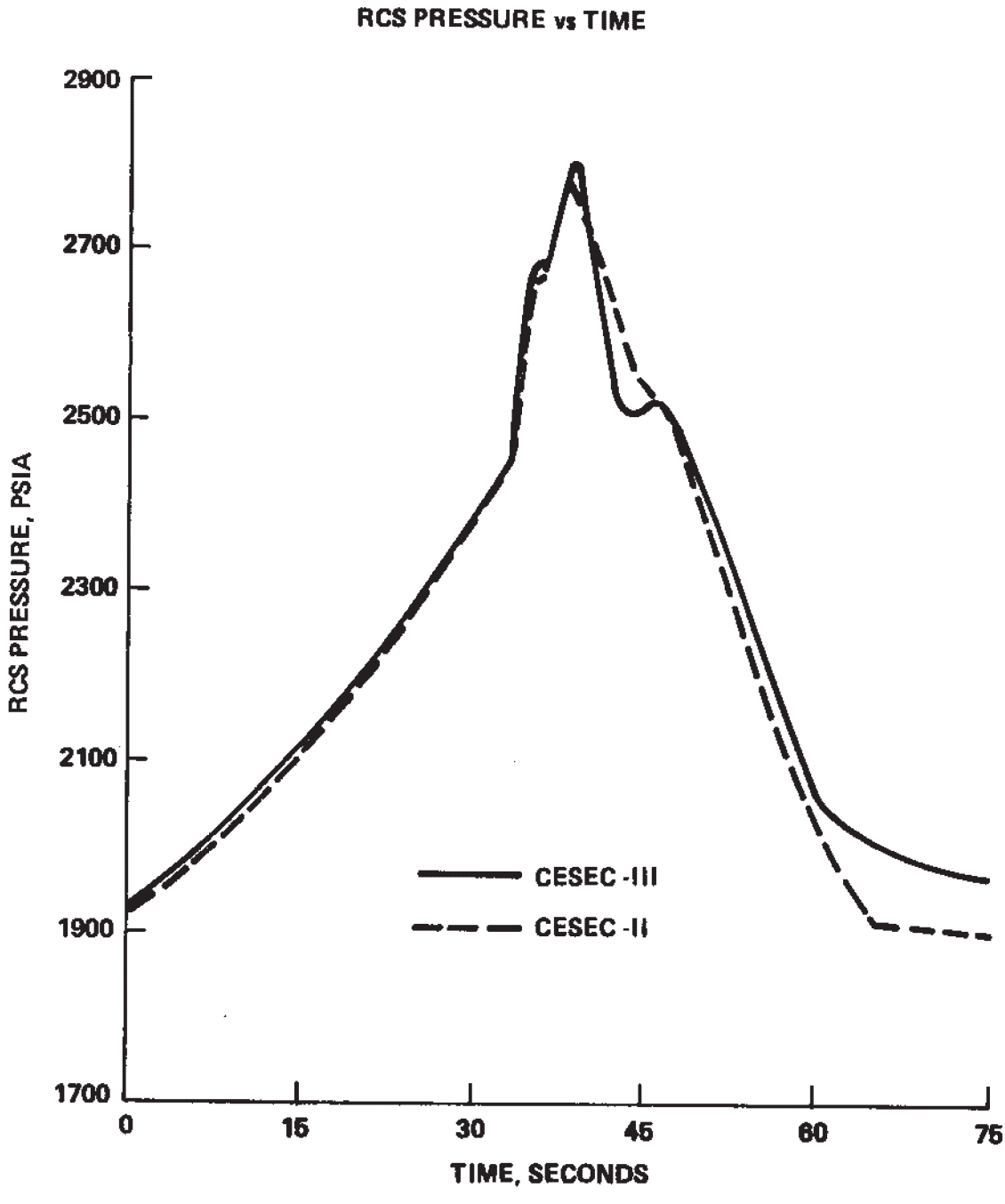

AMENDMENT NO. 1 (4/86)

FLORIDA POWER & LIGHT COMPANY
ST. LUCIE PLANT UNIT 2

LOSS OF FEEDWATER INVENTORY
SYSTEM 80

FIGURE 15.11-31

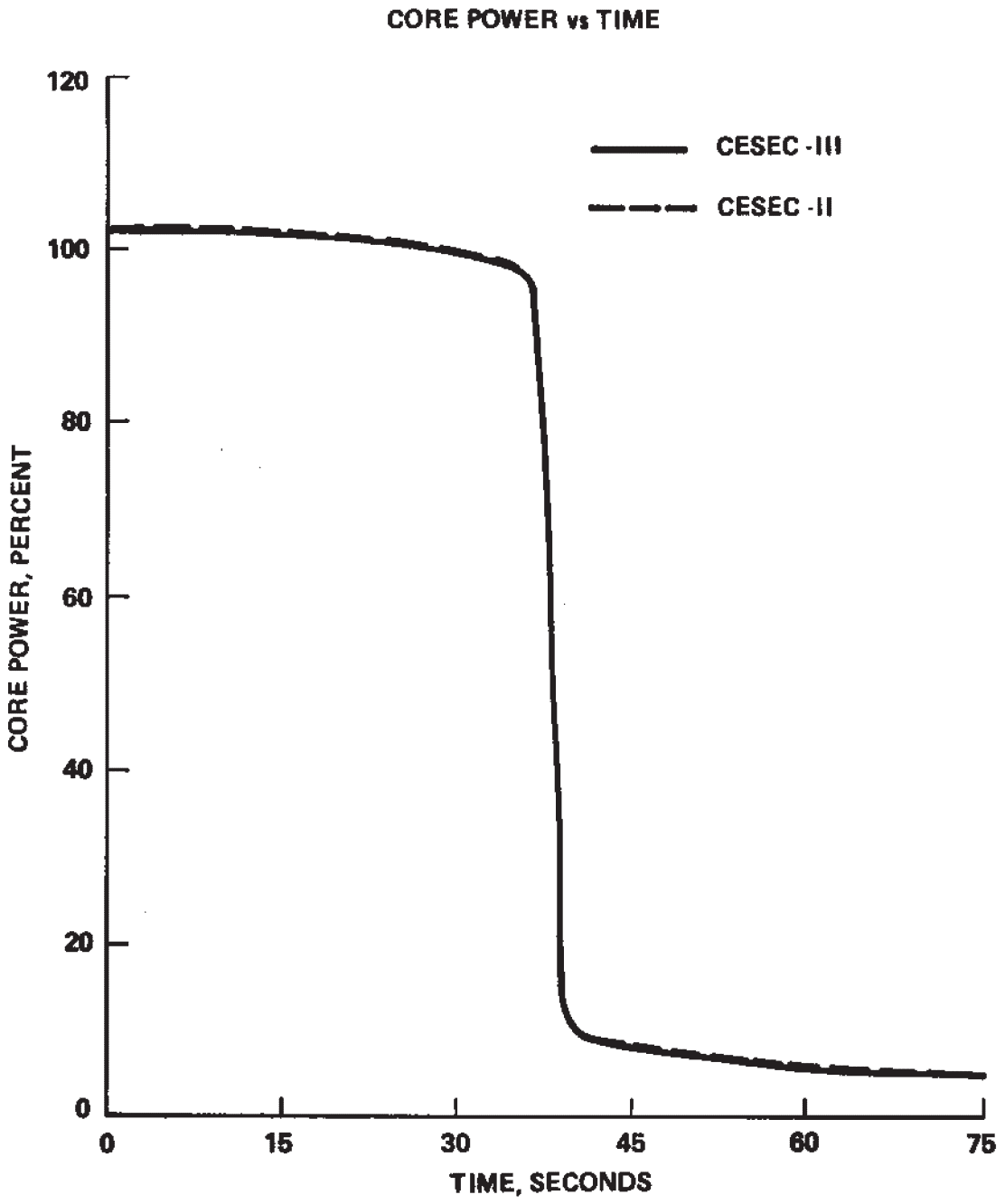

AMENDMENT NO. 1 (4/86)

FLORIDA POWER & LIGHT COMPANY
ST. LUCIE PLANT UNIT 2

LOSS OF FEEDWATER INVENTORY
SYSTEM 80

FIGURE 15.11-32

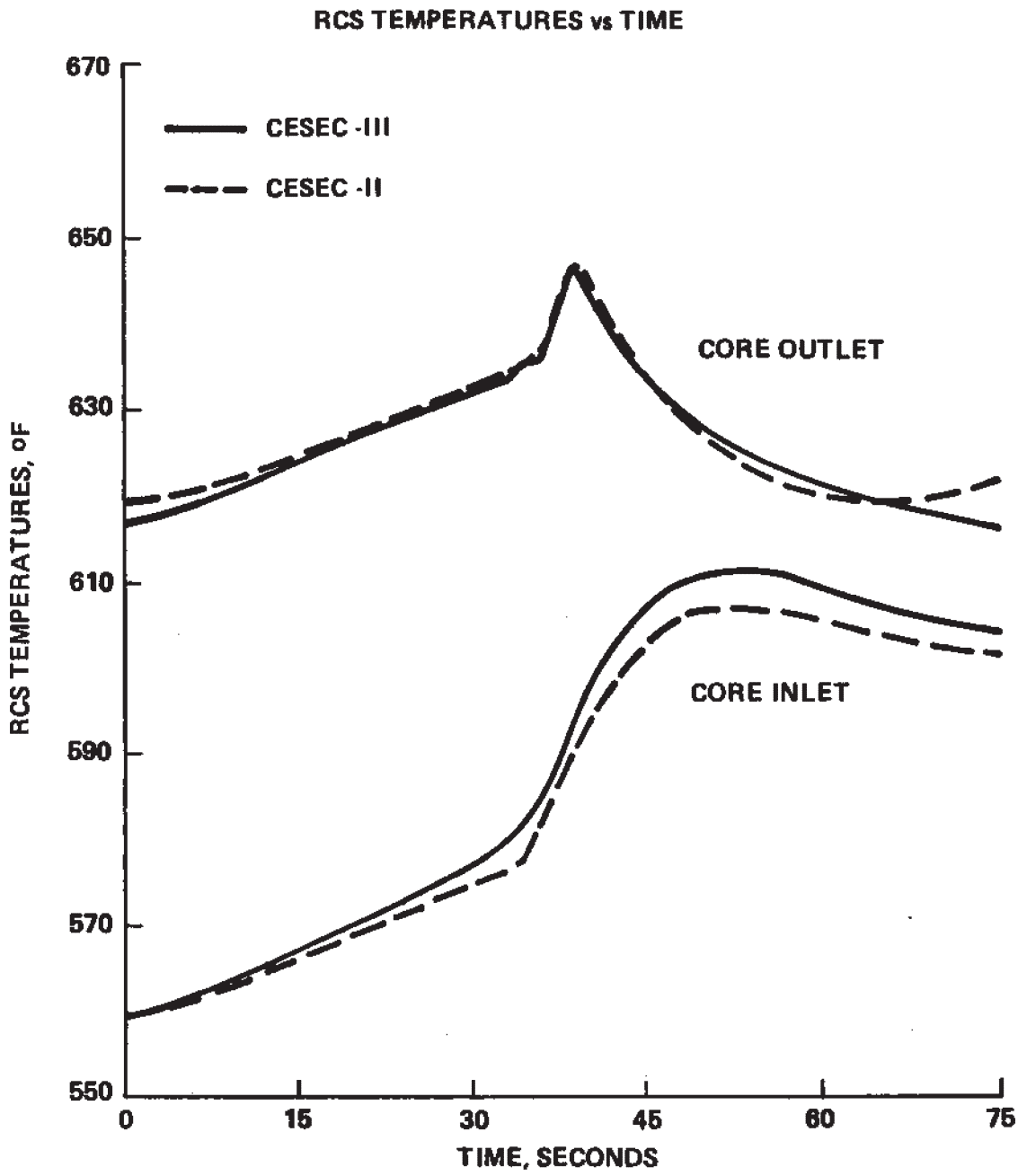

AMENDMENT NO. 1 (4/86)

FLORIDA POWER & LIGHT COMPANY
ST. LUCIE PLANT UNIT 2

LOSS OF FEEDWATER INVENTORY
SYSTEM 80

FIGURE 15.11-33

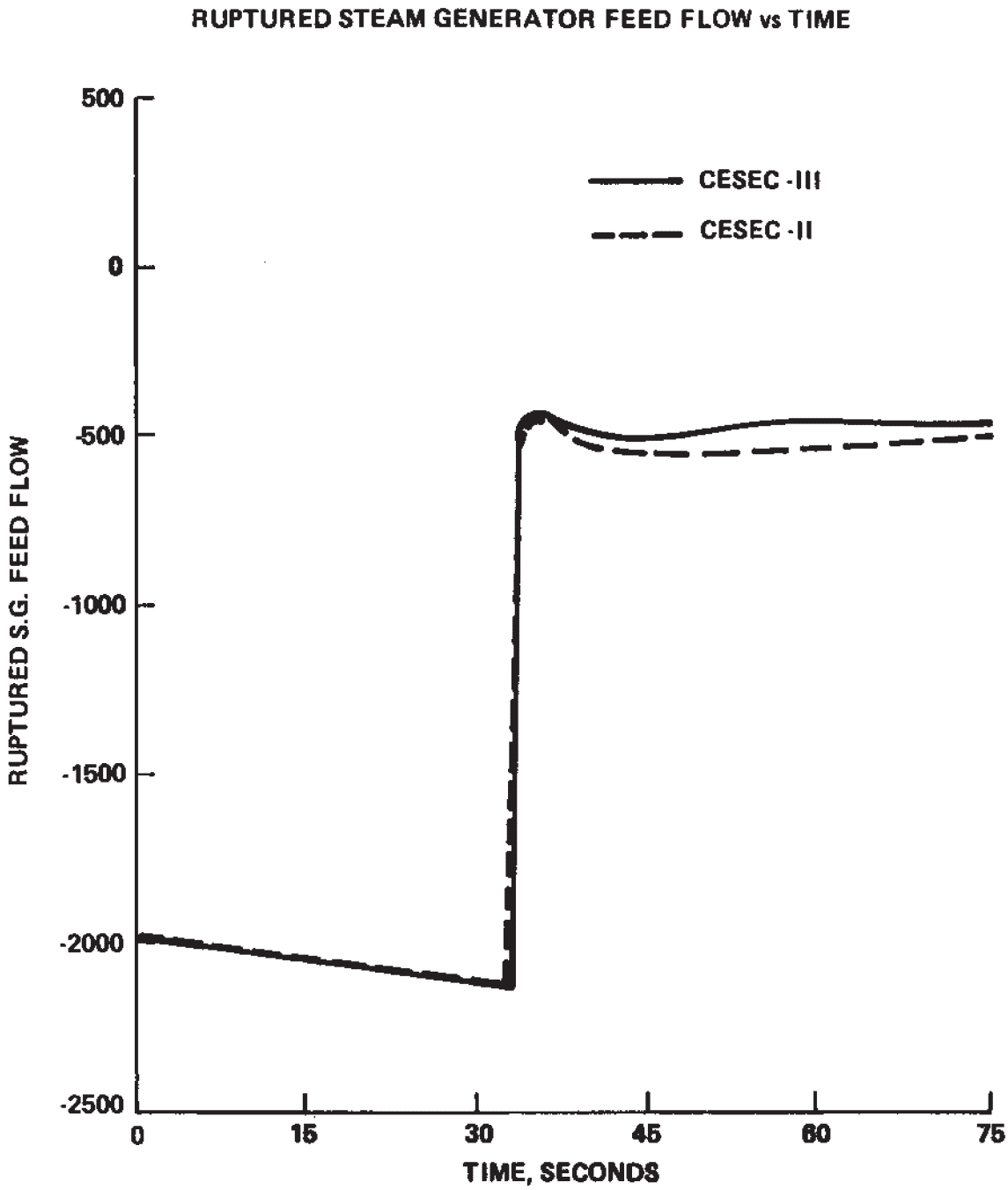

AMENDMENT NO. 1 (4/88)

FLORIDA POWER & LIGHT COMPANY
ST. LUCIE PLANT UNIT 2

LOSS OF FEEDWATER INVENTORY
SYSTEM 80

FIGURE 15.11-34

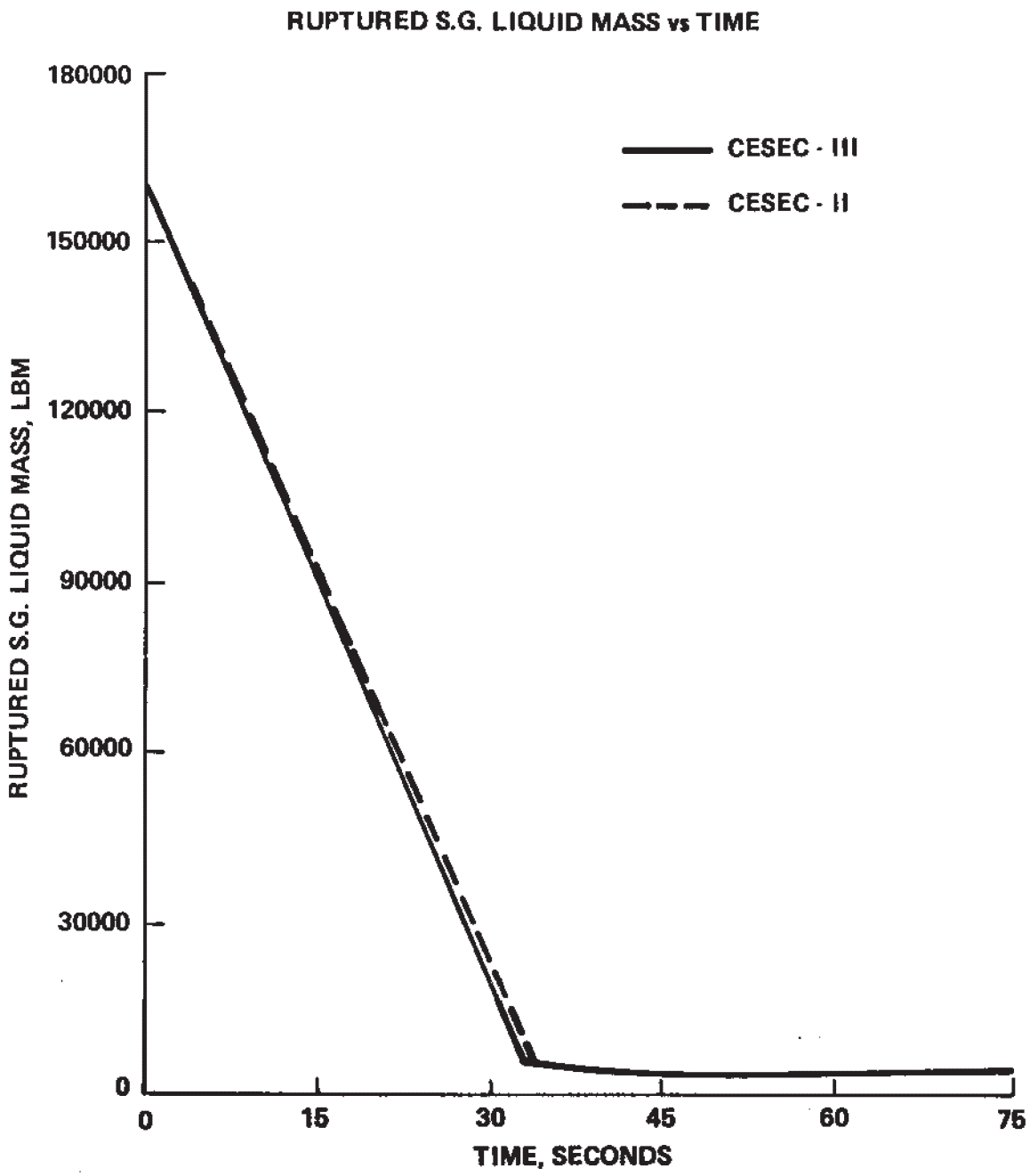

AMENDMENT NO. 1 (4/86)

FLORIDA POWER & LIGHT COMPANY
ST. LUCIE PLANT UNIT 2

LOSS OF FEEDWATER INVENTORY
SYSTEM 80

FIGURE 15.11-35

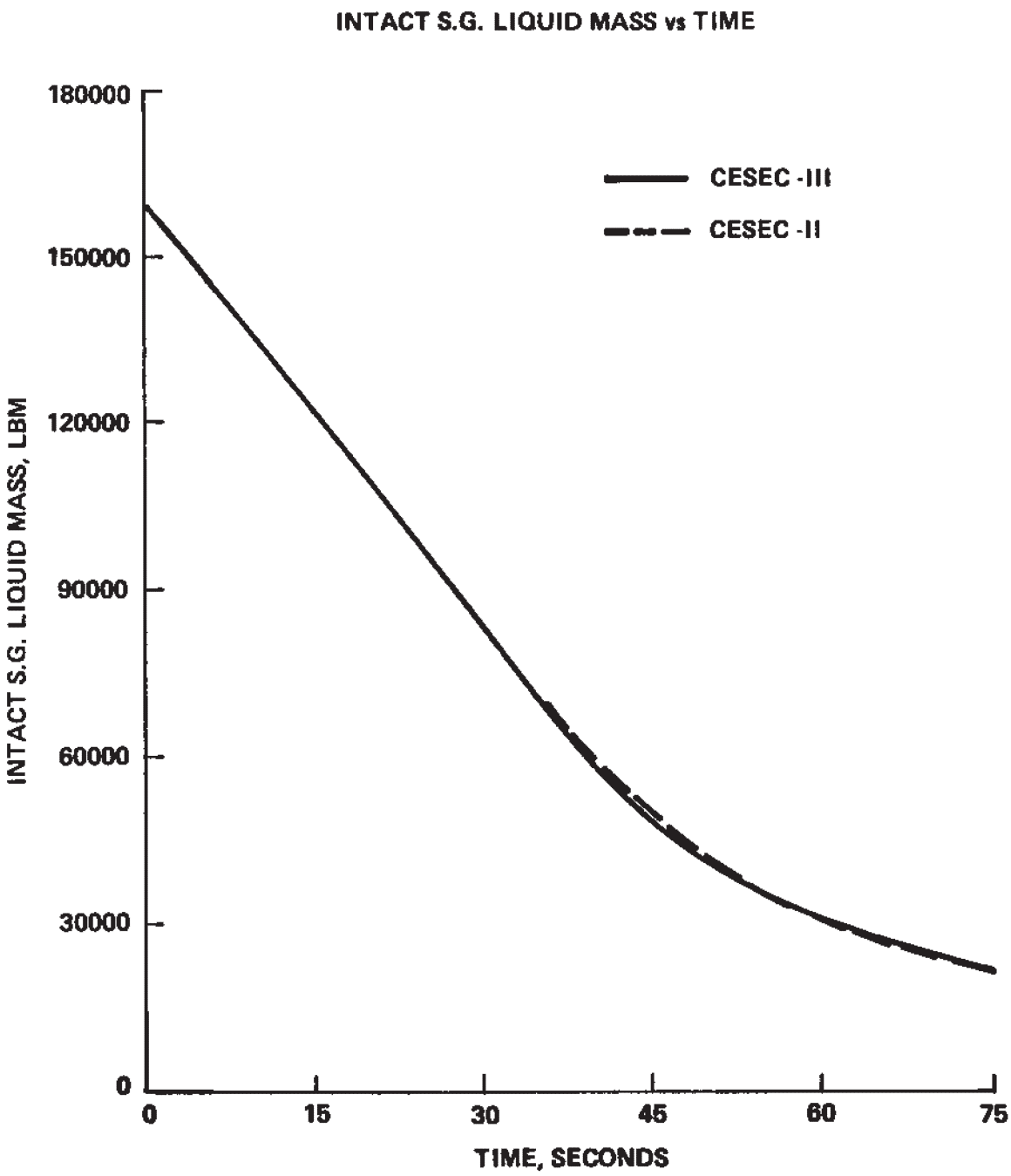

AMENDMENT NO. 1 (4/86)

FLORIDA POWER & LIGHT COMPANY
ST. LUCIE PLANT UNIT 2

LOSS OF FEEDWATER INVENTORY
SYSTEM 80

FIGURE 15.11-36

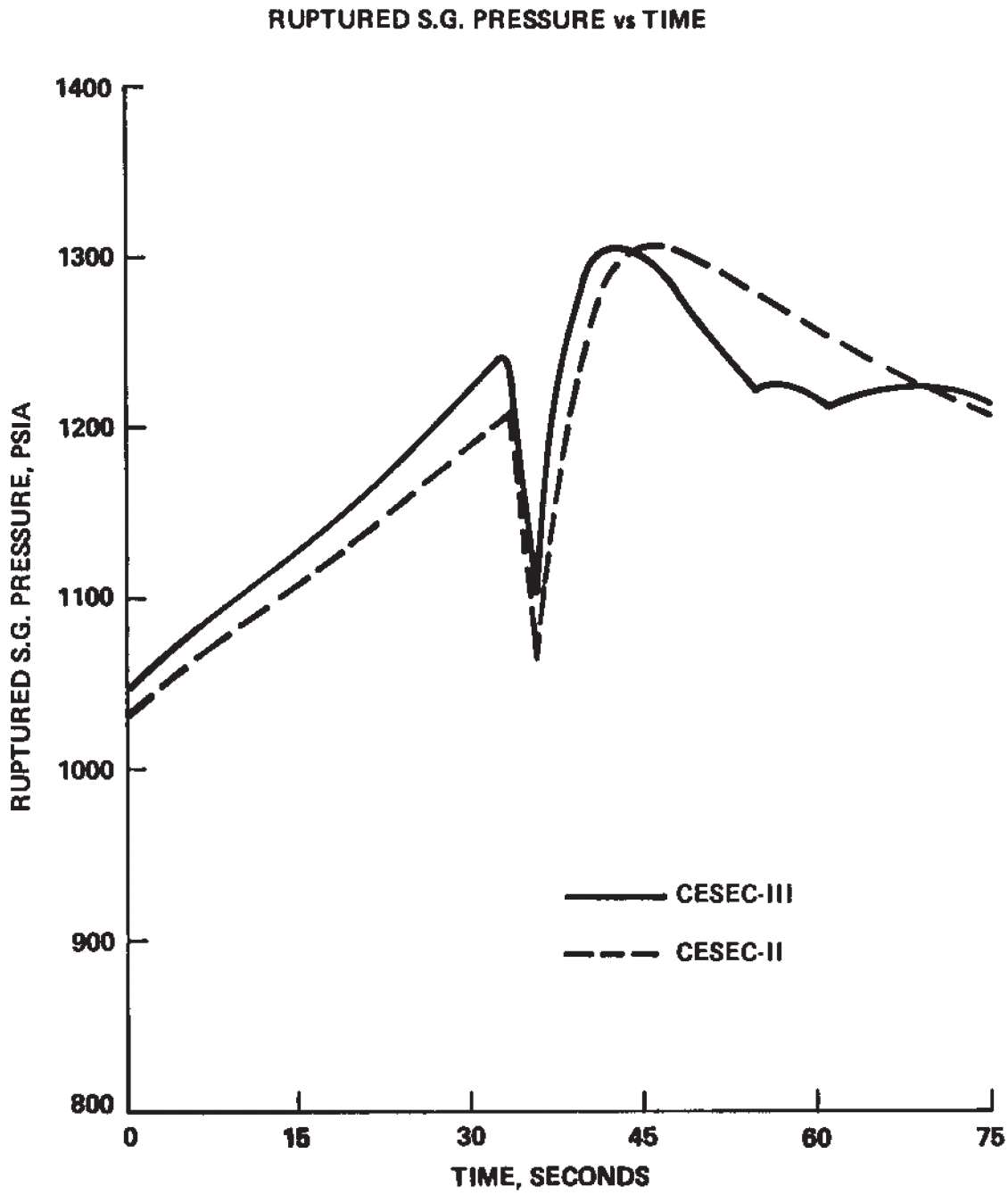

AMENDMENT NO. 1 (4/86)

FLORIDA POWER & LIGHT COMPANY
ST. LUCIE PLANT UNIT 2

LOSS OF FEEDWATER INVENTORY
SYSTEM 80

FIGURE 15.11-37

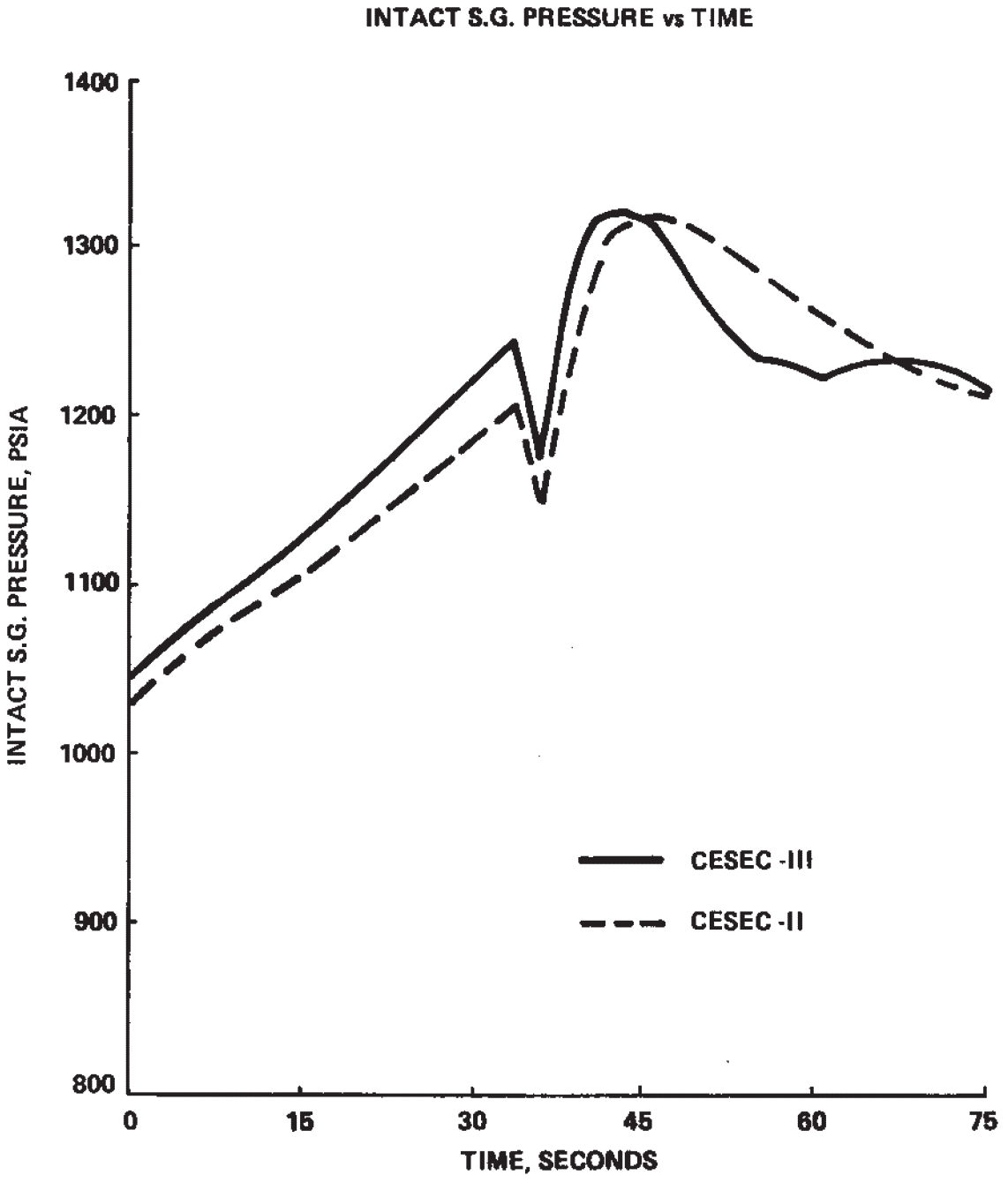

AMENDMENT NO. 1 (4/86)

FLORIDA POWER & LIGHT COMPANY
ST. LUCIE PLANT UNIT 2

LOSS OF FEEDWATER INVENTORY
SYSTEM 80

FIGURE 15.11-38

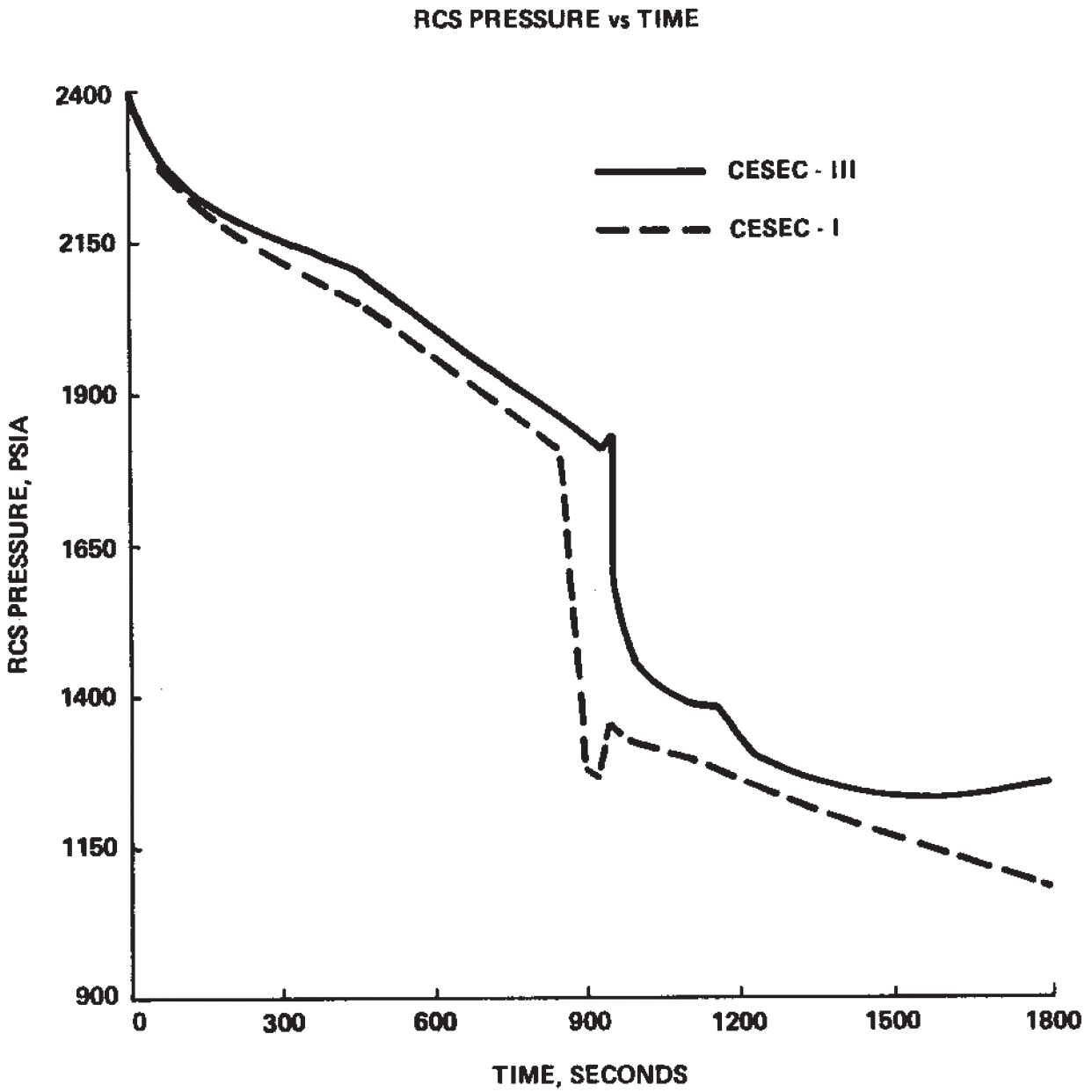

AMENDMENT NO. 1 (4/86)

FLORIDA POWER & LIGHT COMPANY
ST. LUCIE PLANT UNIT 2

STEAM GENERATOR TUBE RUPTURE WITH LOSS OF OFFSITE POWER

FIGURE 15.11-39

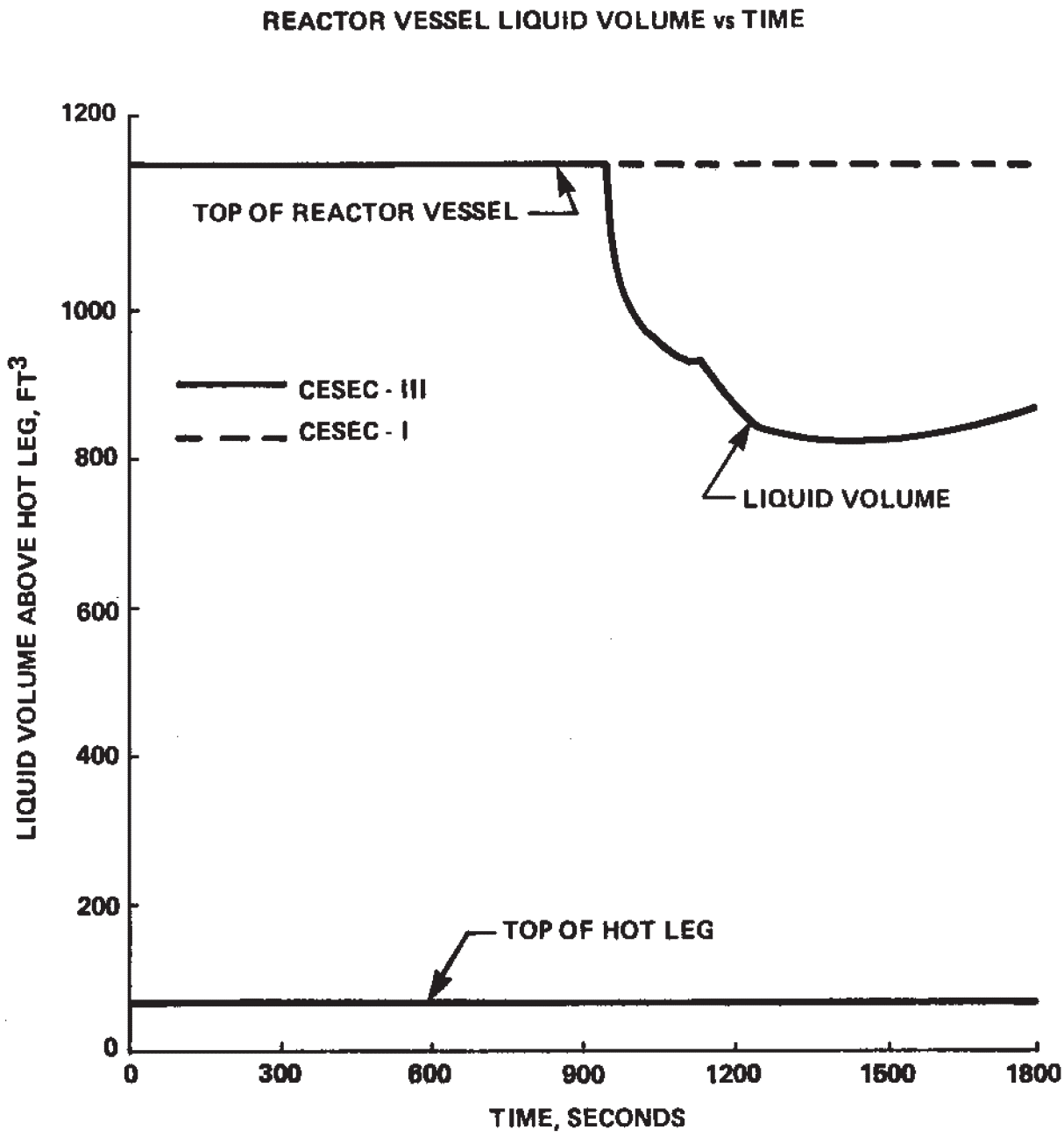

AMENDMENT NO. 1 (4/88)

FLORIDA POWER & LIGHT COMPANY
ST. LUCIE PLANT UNIT 2

STEAM GENERATOR TUBE RUPTURE
WITH LOSS OF OFFSITE POWER

FIGURE 15.11-40

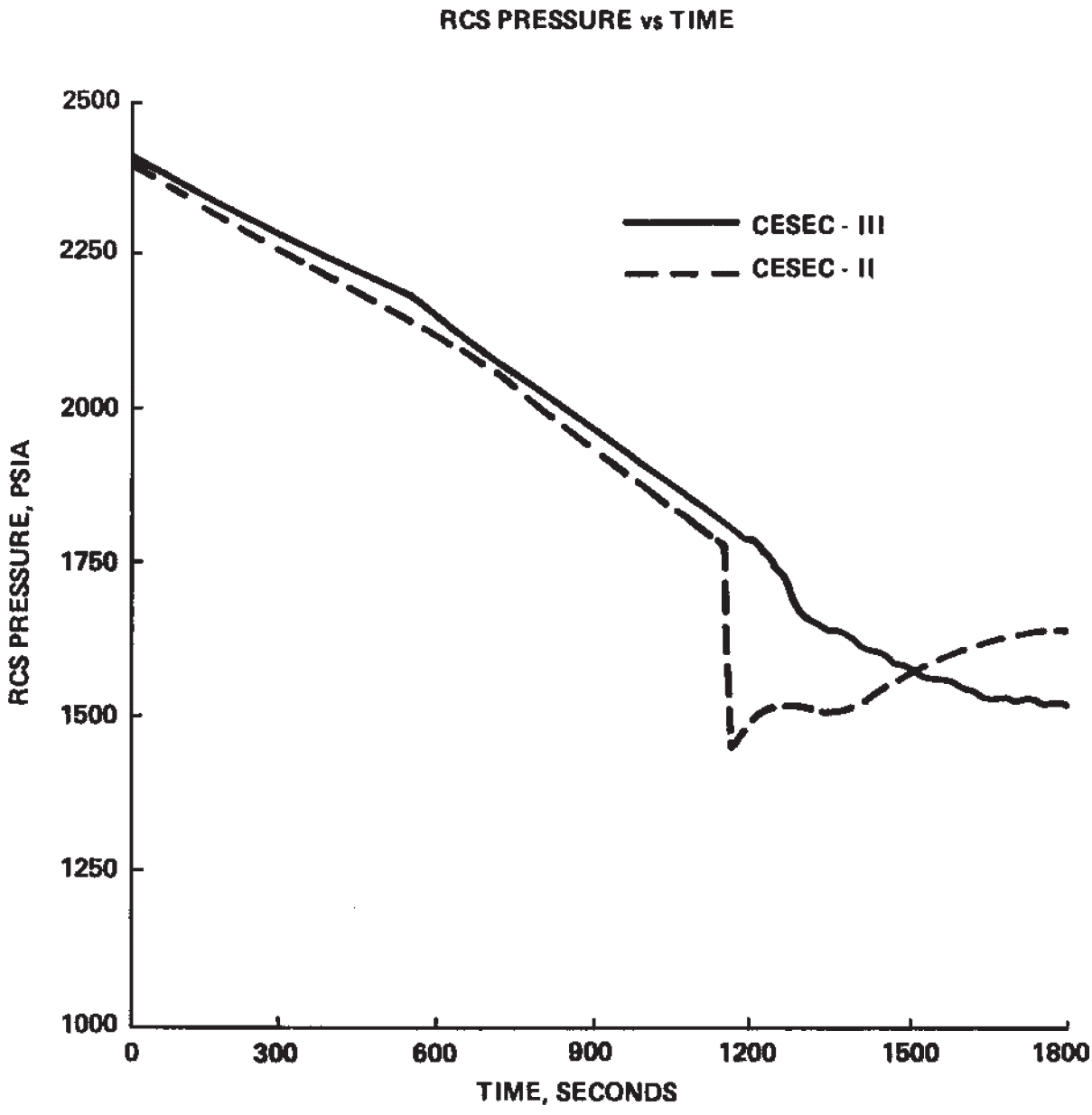

AMENDMENT NO. 1 (4/86)

FLORIDA POWER & LIGHT COMPANY
ST. LUCIE PLANT UNIT 2

STEAM GENERATOR TUBE RUPTURE WITH LOSS OF OFFSITE POWER SYSTEM 80

FIGURE 15.11-41

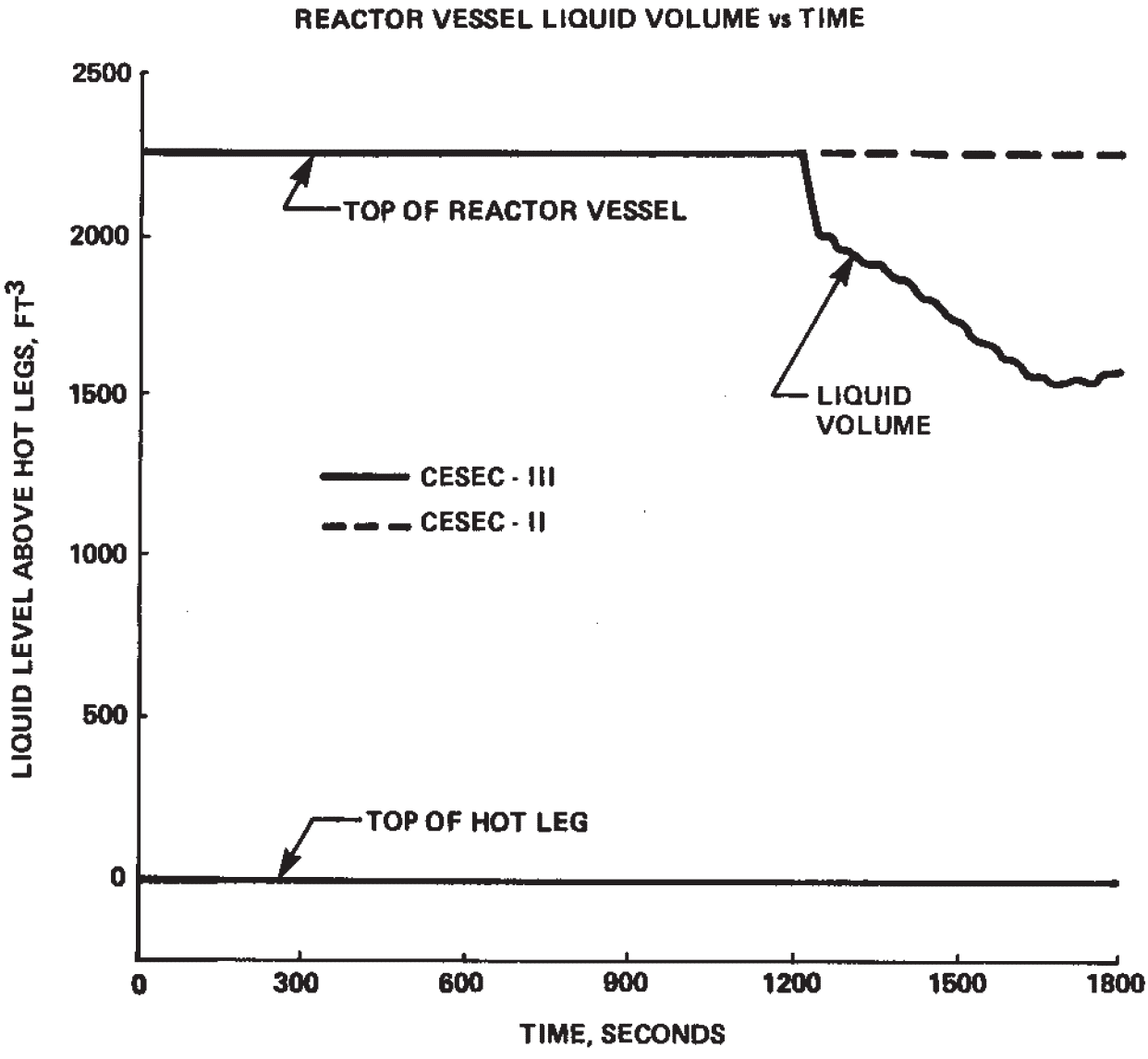

AMENDMENT NO. 1 (4/86)

FLORIDA POWER & LIGHT COMPANY
ST. LUCIE PLANT UNIT 2

STEAM GENERATOR TUBE RUPTURE WITH LOSS OF OFFSITE POWER SYSTEM 80

FIGURE 15.11-42

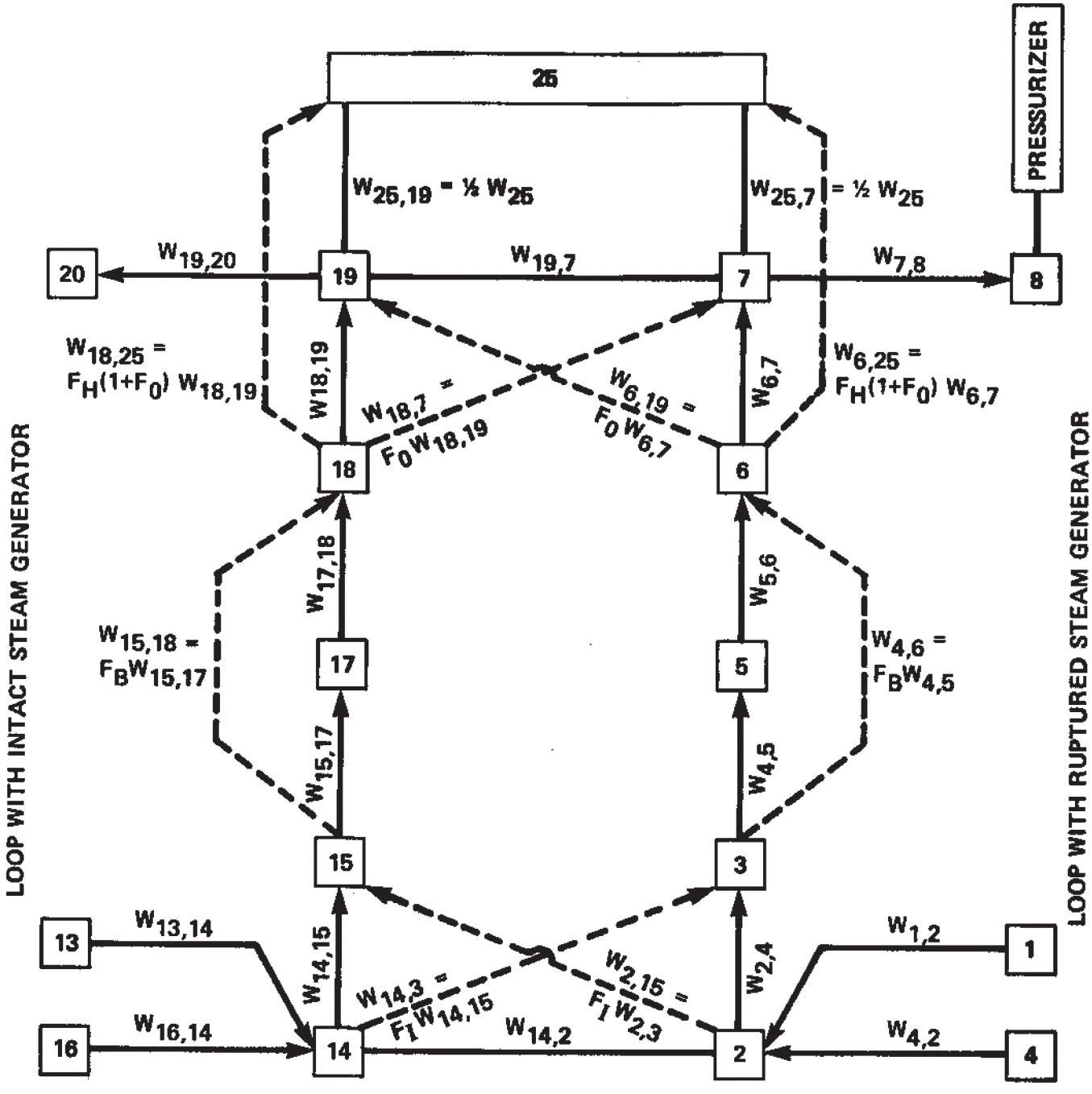

(NOTE: F_H SET EQUAL ZERO AT BEGINNING OF SLB TRANSIENT TO MAXIMIZE RCS PRESSURE THUS MINIMIZING SI REACTIVITY)

AMENDMENT NO. 1 (4/86)

FLORIDA POWER & LIGHT COMPANY
ST. LUCIE PLANT UNIT 2

CESEC FLOW PATHS FOR
REACTOR VESSEL REGION

FIGURE 15.11-43

FIGURES 15.11-44 THROUGH 15.11-48

ARE PROPRIETARY (REFERENCE 35)

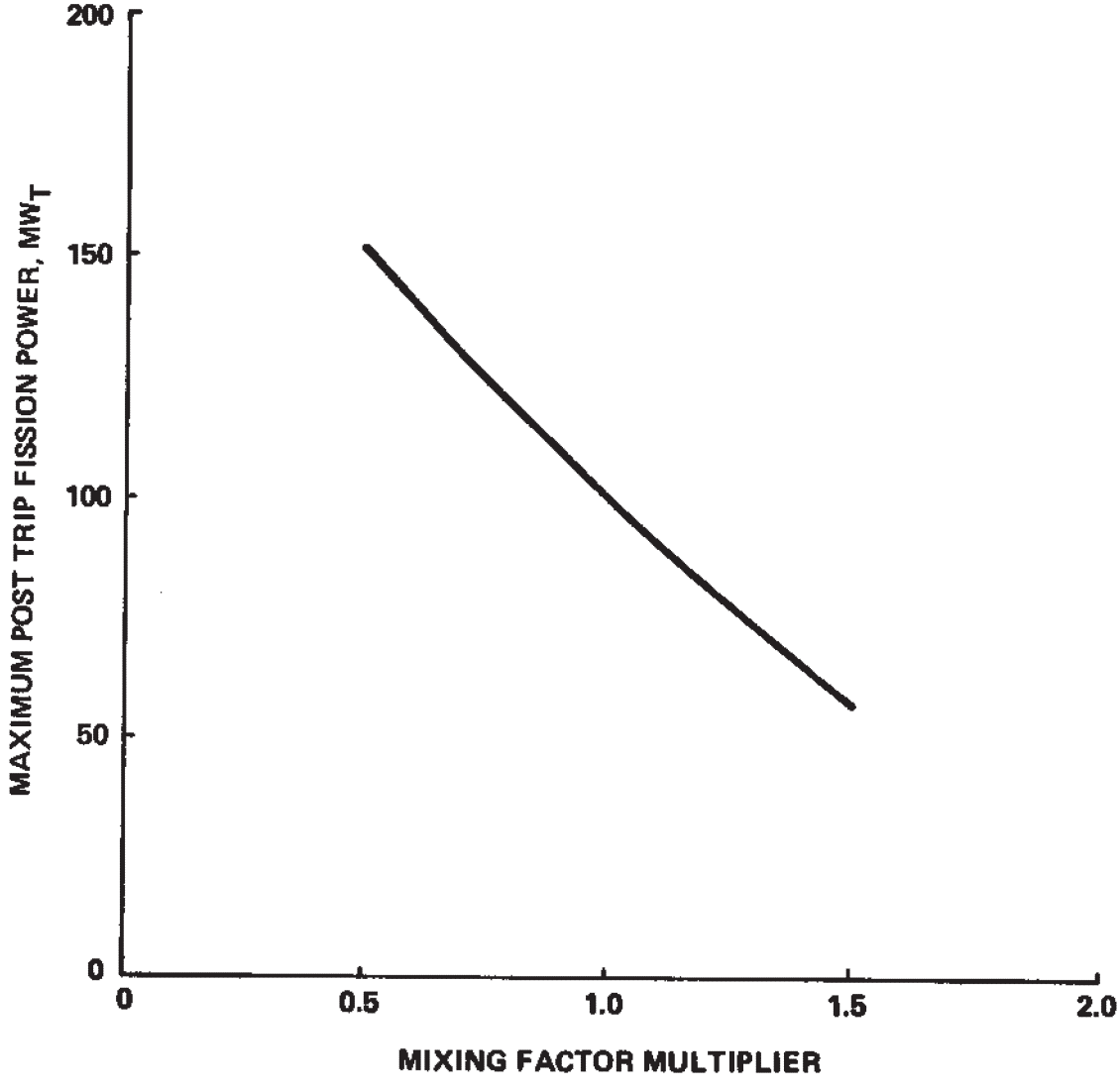

AMENDMENT NO. 1 (4/86)

FLORIDA POWER & LIGHT COMPANY
ST. LUCIE PLANT UNIT 2

SENSITIVITY OF MAXIMUM POST-TRIP FISSION POWER TO MIXING IN REACTOR VESSEL

FIGURE 15.11-49

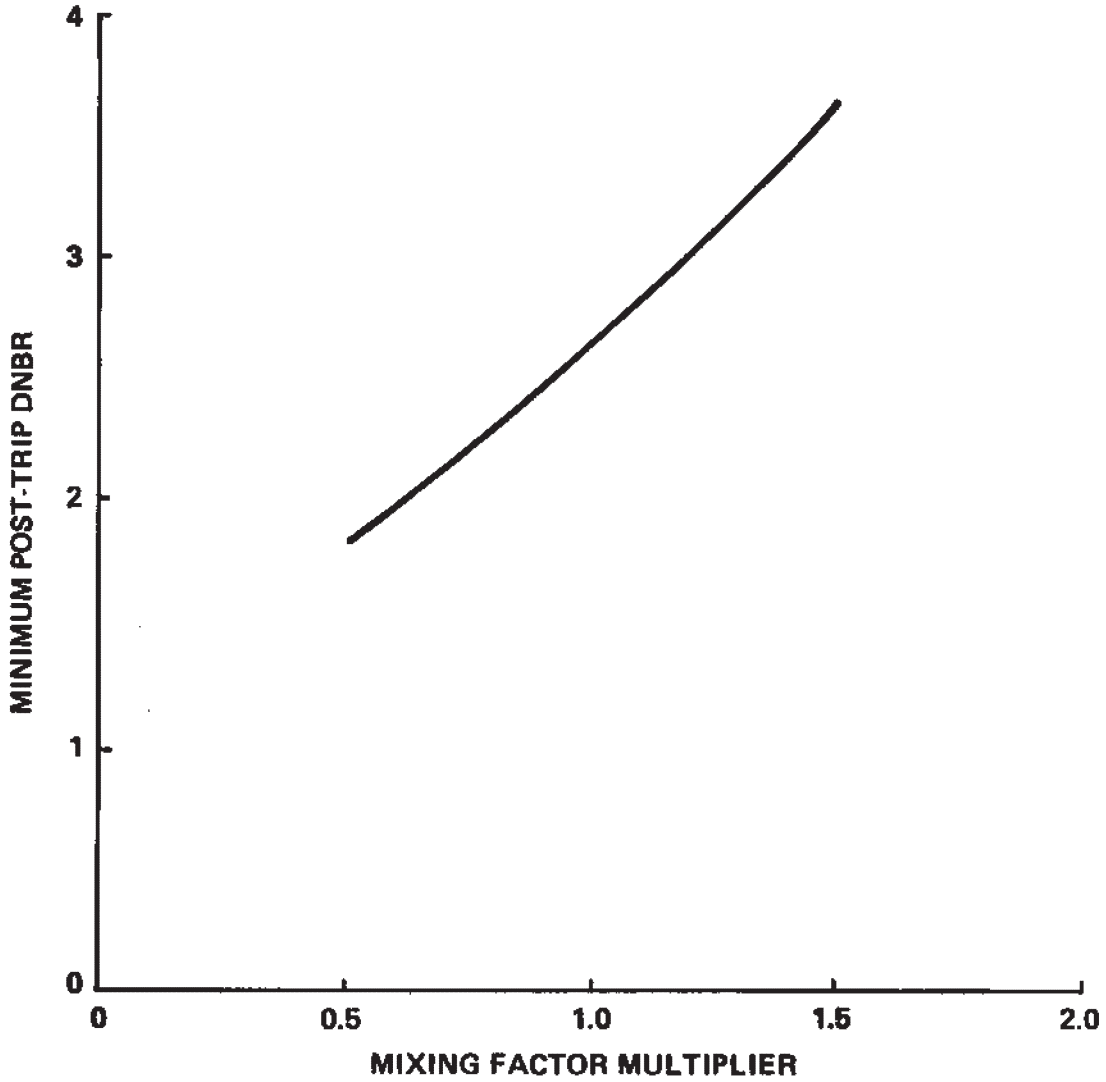

AMENDMENT NO. 1 (4/86)

FLORIDA POWER & LIGHT COMPANY
ST. LUCIE PLANT UNIT 2

SENSITIVITY OF MINIMUM POST-TRIP DNBR TO MIXING IN REACTOR VESSEL

FIGURE 15.11-50